CHEM 230: ESSENTIAL INORGANIC CHEMISTRY



LibreTexts™

Essential Inorganic Chemistry

Chem 230

This text is disseminated via the Open Education Resource (OER) LibreTexts Project (https://LibreTexts.org) and like the thousands of other texts available within this powerful platform, it is freely available for reading, printing, and "consuming."

The LibreTexts mission is to bring together students, faculty, and scholars in a collaborative effort to provide an accessible, and comprehensive platform that empowers our community to develop, curate, adapt, and adopt openly licensed resources and technologies; through these efforts we can reduce the financial burden born from traditional educational resource costs, ensuring education is more accessible for students and communities worldwide.

Most, but not all, pages in the library have licenses that may allow individuals to make changes, save, and print this book. Carefully consult the applicable license(s) before pursuing such effects. Instructors can adopt existing LibreTexts texts or Remix them to quickly build course-specific resources to meet the needs of their students. Unlike traditional textbooks, LibreTexts' web based origins allow powerful integration of advanced features and new technologies to support learning.



LibreTexts is the adaptable, user-friendly non-profit open education resource platform that educators trust for creating, customizing, and sharing accessible, interactive textbooks, adaptive homework, and ancillary materials. We collaborate with individuals and organizations to champion open education initiatives, support institutional publishing programs, drive curriculum development projects, and more.

The LibreTexts libraries are Powered by NICE CXone Expert and was supported by the Department of Education Open Textbook Pilot Project, the California Education Learning Lab, the UC Davis Office of the Provost, the UC Davis Library, the California State University Affordable Learning Solutions Program, and Merlot. This material is based upon work supported by the National Science Foundation under Grant No. 1246120, 1525057, and 1413739.

Any opinions, findings, and conclusions or recommendations expressed in this material are those of the author(s) and do not necessarily reflect the views of the National Science Foundation nor the US Department of Education.

Have questions or comments? For information about adoptions or adaptions contact info@LibreTexts.org or visit our main website at https://LibreTexts.org.

This text was compiled on 01/08/2026

TABLE OF CONTENTS

Licensing

1: Atomic Properties and Periodicity

- 1.1: Quantum Mechanics for Orbital Shapes and Energies
  - 1.1.1: Quantum Numbers
  - 1.1.2: Probability Density and Nodes
  - 1.1.3: Representations of Atomic Orbitals
  - 1.1.4: Energies of Atomic Orbitals
- 1.2: Ground State Electron Configurations
  - 1.2.1: Writing Ground State Electron Configurations
  - 1.2.2: Magnetic Properties
- 1.3: Periodic Properties of the Periodic Table
  - 1.3.1: Atomic Radius
  - 1.3.2: Ionization Energy
  - 1.3.3: Electron Affinity
  - 1.3.4: Electronegativity --- a molecular property
- 1.4: Effective Nuclear Charge (Zeff) and Shielding (S); the Reason for Periodicity
  - 1.4.1: Slater's Rules
  - 1.4.2: Periodic Trends of Zeff
  - 1.4.3: Zeff Controls "Exceptions" to Periodic Trends

2: Bonding Theory Overview

- 2.1: Covalent- Lewis Octet
  - 2.1.1: Lewis- Formal Charge
  - 2.1.2: Lewis- Expanded Octet
  - 2.1.3: Lewis- Resonance
  - 2.1.4: Lewis- Electron-Deficient "Octets" of B and Be
  - 2.1.5: Molecule Shape from Valence Shell Electron Repulsion Theory (VSEPR)
  - 2.1.6: Shape Change from Lone Pairs
  - 2.1.7: Shape Change from Double and Triple Bonds
- 2.2: Covalent- Molecular Orbital Theory
  - 2.2.1: MO- s orbital MOs
  - 2.2.2: MO- p orbital MOs
  - 2.2.3: MO- d orbital MOs
  - 2.2.4: MO- Nonbonding MOs
  - 2.2.5: MO- MO Diagram Features
  - 2.2.6: MO- MO Diagrams of 1st and 2nd row diatomic molecules
  - 2.2.7: MO- MO Diagrams of Heteronuclear Diatomics
- 2.3: Metallic- Sea of Electrons and the van Arkel-Ketelaar Triangle
- 2.4: Structures of Metals and Ionic Compounds
- 2.5: Ionic- Charge and Size Determine Ionic Bonding
  - 2.5.1: Ionic- Measurement of Ionic Bond Strength
  - 2.5.2: Ionic- Examples of Ionic Structures

- 2.5.2.1: Ionic- Rock Salt
- 2.5.2.2: Ionic- Cesium Chloride (CsCl)
- 2.5.2.3: Ionic- Fluorite and Anti-Fluorite
- 2.5.2.4: Ionic- Zinc Blende (ZnS)
- 2.5.3: Predicting Ionic Structure Type

3: Oxidation and Reduction of Elements

- 3.1: Redox Reactions
- 3.2: Balancing Redox Reactions
- 3.3: Electrochemical Cells
- 3.4: Standard Reduction Potentials
- 3.5: Thermodynamic Considerations
- 3.6: General Trends in Reactivity
- 3.7: Latimer Diagrams
- 3.8: Frost Diagrams
- 3.9: Pourbaix Diagrams
- 3.10: Corrosion

4: Inorganic Acids and Bases

- 4.1: Overview
- 4.2: Arrhenius/Bronsted and Lowry
  - 4.2.1: Trends of Binary Acids
  - 4.2.2: Trends of Oxyacids
  - 4.2.3: Trends in Metal Hydroxide Basicity/Solubility
- 4.3: Lewis Acids and Bases
  - 4.3.1: Conjugate Acids of Lewis Bases are Bronsted Acids
  - 4.3.2: Acidity of Metal Ions in Water
  - 4.3.3: Hard-Soft Designation of Lewis Acids and Bases

5: Coordination Chemistry Introduction

- 5.1: Ligands
- 5.2: Electron Configuration of Gas-Phase Metal Ions
- 5.3: Crystal Field Theory, d orbital splitting in presence of ligands
- 5.4: Crystal Field Electron Configuration
- 5.5: Crystal Field Stabilization Energy
- 5.6: Thermodynamic and Structure Consequences of d orbital splitting
- 5.7: Ligand Exchange Reactions and Affinity Determination
- 5.8: Ligand Binding Thermodynamics and the Chelate Effect
- 5.9: Hard and Soft Ligands and Metal Ions
- 5.10: Potential Isomers of Complex Ions

6: Molecular Orbital Theory

- 6.1: Overview of Colors from Transition Metal Ions
- 6.2: Symmetry and Symmetry Operations
- 6.3: Molecule Shapes (Point Groups)
- 6.4: Point Group Assignment
- 6.5: Overview of Classifying Bonding Orbitals in a Molecule
- 6.6: MO Diagram Construction of CO2

- 6.7: MO Diagram Construction of H2O
- 6.8: MO Diagram Construction of NH3
- 6.9: MO Construction of BF3
- 6.10: Lewis Acid-Base Dative Bond and MO Diagrams
- 6.11: MO Diagram for bonding in [M(NH3)6]n+
- 6.12: MO Diagram for bonding in [M(H2O)6]n+
- 6.13: Spectrochemical Series for Ligands
- 6.14: Spectrochemical Series for Metal ions

7: Why is Carbon Monoxide Poisonous?

- 7.1: Pi-Acid Ligands
- 7.2: [Fe(CO)6]2+ MO Diagram
- 7.3: Revisit Octahedral Metal Ion Electron Configurations
- 7.4: Magnetic Moments for Spin State Determination
- 7.5: LFSE/CFSE Calculations Again
- 7.6: Spectrochemical Series of Ligands (Again)
- 7.7: Exchange Inertness of d3, d4(LS), d5(LS), d6(LS), and d8(SQP)
- 7.8: O2 Reduction, since CO displaces O2
- 7.9: Bonding in Carbonmonoxy-myoglobin [Fe(CO)]2+
- 7.10: Active Site of Cytochrome c Oxidase
- 7.11: Cyanide is also a poison (affinity data)
- 7.12: Cyanide is also a poison (spectrocopic data)

8: What Happens "Above The Arrow" in Organic Chemistry

- 8.1: Metal-Pi System Ligands (e.g. ferrocene)
- 8.2: 18 Electron Rule
- 8.3: Organometallic Reaction Types
- 8.4: Organometallic Catalysts
- 8.5: Suzuki-Miyara Coupling

9: Why is Cisplatin "King of the Chemotherapeutic Drugs?"

- 9.1: Jahn-Teller Distortions
- 9.2: d8 Low-Spin Preference for Square Planar Geometry
- 9.3: Trans Effect
- 9.4: Cisplatin Discovery and Mode of Action

Index

Glossary

Detailed Licensing

Detailed Licensing

Licensing

*A detailed breakdown of this resource's licensing can be found in **Back Matter/Detailed Licensing**.*

CHAPTER OVERVIEW

1: Atomic Properties and Periodicity

1.1: Quantum Mechanics for Orbital Shapes and Energies

1.1.1: Quantum Numbers

1.1.2: Probability Density and Nodes

1.1.3: Representations of Atomic Orbitals

1.1.4: Energies of Atomic Orbitals

1.2: Ground State Electron Configurations

1.2.1: Writing Ground State Electron Configurations

1.2.2: Magnetic Properties

1.3: Periodic Properties of the Periodic Table

1.3.1: Atomic Radius

1.3.2: Ionization Energy

1.3.3: Electron Affinity

1.3.4: Electronegativity --- a molecular property

1.4: Effective Nuclear Charge (Zeff) and Shielding (S); the Reason for Periodicity

1.4.1: Slater's Rules

1.4.2: Periodic Trends of Zeff

1.4.3: Zeff Controls "Exceptions" to Periodic Trends

1: Atomic Properties and Periodicity is shared under a not declared license and was authored, remixed, and/or curated by LibreTexts.

1.1: Quantum Mechanics for Orbital Shapes and Energies

Estimated Time to Read: 6 min

Quantum Mechanics

Electrons and other subatomic particles behave as both particles and waves. An individual particle like an electron has mass, but it is spread out, not located in one position, and it has a wavelength. The wavelike nature of electrons and other subatomic particles, as well as the paradox described by Heisenberg's uncertainty principle, made it impossible to use the equations of classical physics to describe the motion of electrons in atoms. Scientists needed a new approach that took the wave behavior of the electron into account.

In 1926, an Austrian physicist, Erwin Schrödinger (1887–1961; Nobel Prize in Physics, 1933), developed *wave mechanics*, a mathematical technique that describes the relationship between the motion of a particle that exhibits wavelike properties and its allowed energies. Schrödinger's wave equation allowed scientists to make predictions about the electronic structure of atoms. Where are the electrons found? What is their energy?

Although quantum mechanics uses sophisticated mathematics, you do not need to understand the mathematical details to follow our discussion of its general conclusions. We focus on the properties of the *wavefunctions* that are the solutions of Schrödinger's equations.

Erwin Schrödinger (1887–1961)

Schrödinger's unconventional approach to atomic theory was typical of his unconventional approach to life. He was notorious for his intense dislike of memorizing data and learning from books. When Hitler came to power in Germany, Schrödinger escaped to Italy. He then worked at Princeton University in the United States but eventually moved to the Institute for Advanced Studies in Dublin, Ireland, where he remained until his retirement in 1955.

Wavefunctions

A wavefunction (Ψ) is a mathematical function that relates the location of an electron and the energy of the electron. A wavefunction uses three variables to describe the position of an electron in space (as with the Cartesian coordinates *x*, *y*, and *z*). A fourth variable specifies the time at which the electron is at the specified location.

By analogy, if you were the captain of a ship trying to intercept an enemy submarine, you would need to know its latitude, longitude, and depth, as well as the time at which it was going to be at this position (Figure **1.1.1**). For electrons, we can ignore the time dependence because we will be using standing waves, which by definition do not change with time, to describe the position of an electron.

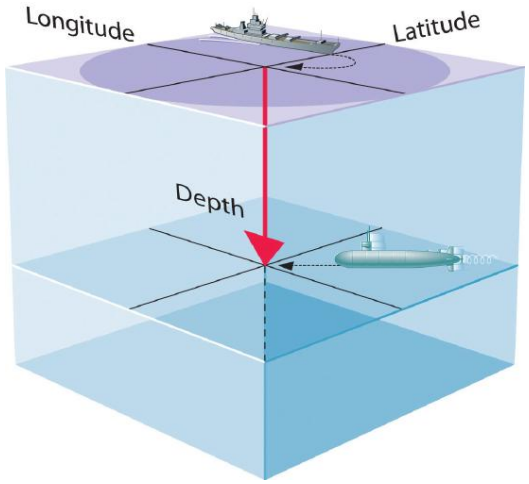


Figure 1.1.1: The Four Variables (Latitude, Longitude, Depth, and Time) required to precisely locate an object

The magnitude of the wavefunction at a particular point in space is proportional to the amplitude of the wavefunction at that point. Many wavefunctions are complex functions, which means that they contain $\sqrt{-1}$, represented as i. Hence the amplitude of the wave has no real physical significance.

In contrast, the sign of the wavefunction (either positive or negative) corresponds to the phase of the wave, which will be important in our discussion of chemical bonding. The sign of the wavefunction should *not* be confused with a positive or negative electrical charge.

The square of the wavefunction at a given point in space is proportional to the probability of finding an electron at that point in space. (The square of the wavefunction (Ψ^2) is always a real quantity [recall that that $\sqrt{-1}^2 = -1$]) The probability of finding an electron at any point in space depends on several factors, including the distance from the nucleus and, in many cases, the atomic equivalent of latitude and longitude. One way of graphically representing the probability distribution is demonstrated in Figure **1.1.2** for a hydrogen atom. The probability of finding an electron is indicated by the density of colored dots.

Schrödinger's approach treats electrons as three-dimensional standing waves. It is a requirement of standing waves that they be in phase with one another to avoid cancellation; this results in a limited number of solutions (wavefunctions), each of which is associated with a particular energy. As in Bohr's model, the energy of an electron in an atom is quantized; it can have only certain allowed values, which are specified by the quantum numbers. Quantum numbers define solutions to the Schrödinger equation. The major difference between Bohr's model and Schrödinger's approach is that Bohr had to impose the idea of quantization arbitrarily, whereas in Schrödinger's approach, quantization is a natural consequence of describing an electron as a standing wave.

Adrien Legendre (1752–1783)

As you might expect, the patterns of three-dimensional standing waves are complicated. However, in the 18th century a French mathematician, Adrien Legendre (1752–1783), developed a set of equations to describe the motion of tidal waves on the surface of a flooded planet. Schrödinger incorporated Legendre's equations into his wavefunctions.

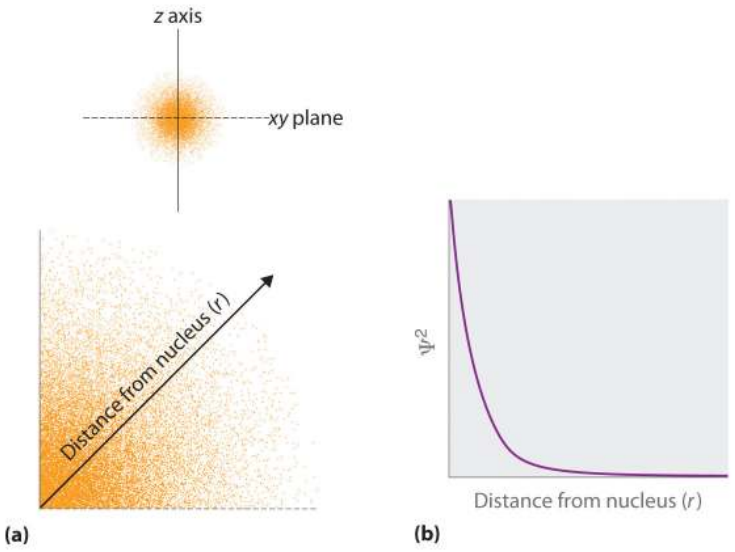


Figure 1.1.2: Probability of Finding the Electron in the Ground State of the Hydrogen Atom at Different Points in Space. (a) The density of the dots shows electron probability. (b) In this plot of Ψ^2 versus r for the ground state of the hydrogen atom, the electron probability density is greatest at $r = 0$ (the nucleus) and falls off with increasing r. Because the line never actually reaches the horizontal axis, the probability of finding the electron at very large values of r is very small but *not* zero.

The *wavefunction* is a mathematical expression that describes the electron. It can be plotted as a three-dimensionional graph. The three-dimensional plot of the wavefunction is sometimes called an *orbital*. Often, chemists find it useful to look at pictures of orbitals in order to gain some sense of where electrons may be and how they may behave. In another sense, orbitals are probability maps that reveal the probability of an electron being located at a particular position in space.

Suppose you could take a series of photos of an electron and superimpose all of those pictures, like time-lapse photography. The result might look something like the drawing in Figure **1.1.2**, in which every dot represents where the electron showed up in one of the photos. It's impossible to predict exactly where the electron would show up in the next photo, but it would be a pretty good guess that it would show up somewhere in the same rough circle as it did all of the other times.



1s

Figure 1.1.3: Probability map, or orbital, of a wavefunction. Each dots represents the probability of an electron being located at that point in space at a moment in time. (https://employees.csbsju.edu/cschall...tomnumbers.htm; Chris Schaller)

In three-dimensional space, the probability map (or *orbital)* shown in Figure **1.1.3** would be a sphere instead of a circle. The probability map shown can be interpreted as a thin slice through the middle of the probability sphere. The orbital shown is specifically an s orbital. In the very center of the sphere, is the nucleus of the atom. The electron is found within a certain distance of the nucleus, but it can be found in any direction. Other electrons will have different distributions about the nucleus of the atom, resulting in other orbital shapes in three-dimensional space. Quantum numbers will be used to describe the various orbitals, the probability of finding an electron at a point in space and roughly how much energy the electron has.

1.1: Quantum Mechanics for Orbital Shapes and Energies is shared under a not declared license and was authored, remixed, and/or curated by LibreTexts.

- **6.5: Quantum Mechanics and Atomic Orbitals** is licensed CC BY-NC-SA 3.0.
- **1.4: Quantum Numbers** by Chris Schaller is licensed CC BY-NC 3.0. Original source: https://employees.csbsju.edu/cschaller/structure.htm.

1.1.1: Quantum Numbers

Estimated Time to Read: 7 min

Quantum Numbers

Schrödinger's approach uses four quantum numbers (n, l, m_l, and m_s) to specify any wavefunction. The first three quantum numbers (n, l, and m_l) provide information about the spatial distribution of an electron. Although n can be any positive integer, only certain values of l, m_l, and m_s are allowed for a given value of n.

The Principal Quantum Number

The **principal quantum number** (n) tells the average relative distance of an electron from the nucleus. Its value can be any positive integer:

$$n = 1, 2, 3, 4, \ldots \tag{1.1.1.1}$$

As n increases for a given atom, so does the average distance of an electron from the nucleus. A negatively charged electron that is, on average, closer to the positively charged nucleus is attracted to the nucleus more strongly than an electron that is farther out in space. This means that electrons with higher values of n are easier to remove from an atom. All wavefunctions that have the same value of n are said to constitute a principal shell because those electrons have similar average distances from the nucleus. The principal quantum number n corresponds to the n used by Bohr to describe electron orbits and by Rydberg to describe atomic energy levels.

The Angular Momentum (or Azimuthal) Quantum Number

The **angular momentum quantum number** (l) describes the shape of the region of space occupied by the electron. The allowed values of l depend on the value of n and can range from 0 to $n - 1$:

$$l = 0, 1, 2, \ldots, n - 1 \tag{1.1.1.2}$$

For example, if $n = 1$, l can be only 0; if $n = 2$, l can be 0 or 1; and so forth.

For a given atom, all wavefunctions that have the same values of both n and l form a subshell. The regions of space occupied by electrons in the same subshell usually have the same shape, but they are oriented differently in space.



Principal quantum number (n) and angular momentum (l): The Orbital Subshell: Principal quantum number (n) and angular momentum (l): The Orbital Subshell [youtu.be]

The Magnetic Quantum Number

The **magnetic quantum number** (m_l) describes the *orientation* of the region in space occupied by an electron with respect to an applied magnetic field. The allowed values of m_l depend on the value of l: m_l can range from $-l$ to l in integral steps:

$$m_l = -l, -l + 1, \ldots, 0, \ldots, l - 1, l \tag{1.1.1.3}$$

For example, if $l = 0$, then m_l can be only 0; if $l = 1$, m_l can be −1, 0, or +1; and if $l = 2$, m_l can be −2, −1, 0, +1, or +2.

Each wavefunction with an allowed combination of n, l, and m_l values describes an atomic *orbital*, a particular spatial distribution for an electron. For a given set of quantum numbers, each principal shell has a fixed number of subshells, and each subshell has a fixed number of orbitals.

The Spin Quantum Number

Scientists analyzed the emission and absorption spectra of the elements closely and saw that for elements having more than one electron, nearly all the lines in the spectra were actually *pairs* of very closely spaced lines. Each line in the spectra represents an energy level available to electrons in the atom; pairs of lines resulted in twice as many energy levels as would be predicted solely based on the quantum numbers n, l, and m_l. Scientists also discovered that applying a magnetic field caused the lines in the pairs to split farther apart. In 1925, two graduate students in physics in the Netherlands, George Uhlenbeck (1900–1988) and Samuel Goudsmit (1902–1978), proposed that the splittings were caused by an electron spinning about its axis, much as Earth spins about its axis. When an electrically charged object spins, it produces a magnetic moment parallel to the axis of rotation, making it behave like a magnet. Although the electron cannot be viewed solely as a particle, spinning or otherwise, it is indisputable that it does have a magnetic moment. This magnetic moment is called **electron spin**.

In an external magnetic field, the electron has two possible orientations (Figure Figure **1.1.1.1**). It can align with the magnetic field or against it. These orientations are described by the **spin quantum number**, m_s, which can have a value of +½ (spin up) and −½ (spin down) to indicate that the two orientations are opposites. The value of m_s does not depend on the other three quantum numbers. Spin is significant in that it allows two electrons to occupy the same orbital. Two electrons can have the same values for n, l, and m_l but opposite spin values that allow them to occupy the same orbital. Thus, each orbital can hold one pair of electrons, each with a different spin quantum number value. Every electron in an atom must have a unique set of quantum number. If n, m, and l are the same for two electrons, then m_s must be different.

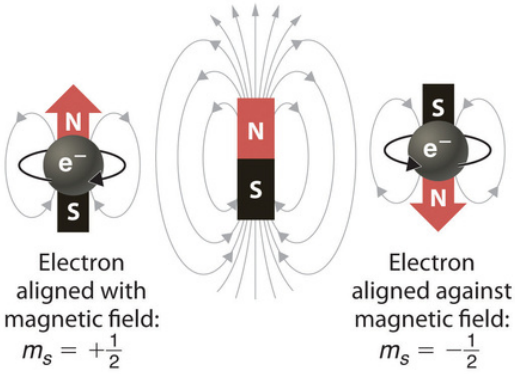


Figure 1.1.1.1: Electron Spin. In a magnetic field, an electron has two possible orientations with different energies, one with spin up, aligned with the magnetic field, and one with spin down, aligned against it. All other orientations are forbidden.



Magnetic Quantum Number (m_l) & Spin Quantum Number (m_s): Magnetic Quantum Number (ml) & Spin Quantum Number (ms) [youtu.be]

Exercise 1.1.1.1: n = 3 Shell Structure

How many subshells are contained within the principal shell with $n = 3$?

Hint

Given $n = 3$, calculate the allowed values of l. From these allowed values, count the number of subshells.

Answer

If $n = 3$, then l can equal 0, 1, or 2. Because the shell has four values of l, it has three subshells.

Exercise 1.1.1.2: n = 3 Shell Structure

How many orbitals are contained within the principal shell with $n = 3$?

Hint

For each allowed value of l, calculate the allowed values of m_l. The sum of the number of orbitals in each subshell is the number of orbitals in the principal shell.

Answer

If $n = 3$, then l can equal 0, 1, or 2.

When $l = 0$, then m_l can be only 0. Thus, the $l = 0$ subshell has only one orbital.

When $l = 1$, then m_l can be 0 or ±1. The $l = 1$ subshell has three orbitals.

When $l = 2$, then m_l can be 0, ±1, or ±2. The $l = 2$ subshell has five orbitals

The total number of orbitals in the $n = 3$ principal shell is the sum of the number of orbitals in each subshell (1 + 3 + 5 = 9).

The total number of orbitals is equal to n^2 ($3^2 = 9$).

Exercise 1.1.1.3: n = 4 Subshell Structure

How many orbitals are contained within the principal shell with $n = 4$?

Hint

For each allowed value of l, calculate the allowed values of m_l. The sum of the number of orbitals in each subshell is the number of orbitals in the principal shell.

Answer

If $n = 4$, then l can equal 0, 1, 2, or 3.

When $l = 0$, then m_l can be only 0. Thus, the $l = 0$ subshell has only one orbital.

When $l = 1$, then m_l can be 0 or ±1. The $l = 1$ subshell has three orbitals.

When $l = 2$, then m_l can be 0, ±1, or ±2. The $l = 2$ subshell has five orbitals

When $l = 3$, then m_l can be 0, ±1, ±2, or ±3. The $l = 3$ subshell has seven orbitals.

The total number of orbitals in the $n = 4$ principal shell is the sum of the number of orbitals in each subshell (1 + 3 + 5 + 7 = 16) and is also equal to n^2 ($4^2 = 16$)

? Exercise 1.1.1.4: l = 5 Shell Structure

How many orbitals are contained within the subshell with $l = 5$?

Hint

For the specified value of l, calculate the allowed values of m_l.

Answer

If $l = 5$, then m_l can equal 0, ±1, ±2, ±3, ±4, ±5. Thus, the $l = 5$ subshell has eleven orbitals.

The total number of orbitals is equal to $2l + 1$ ((2 x 5) + 1 = 11).

Describing an Orbital

Each orbital in an atom is described by a set of three values for n, l, and m_l. Typically when defining an orbital scientists will use an abbreviated system to refer to an orbital or subshell, rather than specifying the values of n, l , and m_l.

In this system, the principal quantum number n is named first and is followed by a lowercase letter to denote the value of the angular momentum quantum number l (Table **1.1.1.1**) (These orbital designations are derived from historical terms for corresponding spectroscopic characteristics: *s*harp, *p*rinciple, *d*iffuse, and *f*undamental.)

Table **1.1.1.1**: Values of angular momentum quantum number, l, and corresponding abbreviations.

l	0	1	2	3
abbreviation	s	p	d	f

A 2*p* subshell has $n = 2$ and $l = 1$. A 2*p* subshell has three orbitals, which correspond to $m_l = -1$, 0, and +1. In the abbreviatiod system, the three orbitals are denoted with a subscript lower case letter that represents an orientation in space (Table **1.1.1.2**). For a 2*p* subshell, the three orbitals are denoted as $2p_x$, $2p_y$, and $2p_z$. The correlation between m_l and a specific orientation in space is beyond the scope of this course.

Table **1.1.1.2**: Values of magnetic quantum number, m_l, and corresponding abbreviations.

l	m_l	abbreviation
2 (*p*)	0, ±1	*x*, *y*, z
3 (*d*)	0, ±1, ±2	*xz*, *yz*, *xy*, x^2-y^2, z^2

Summary

Each principal shell has *n* subshells

For $n = 1$, only a single subshell is possible (1*s*). For $n = 2$, there are two subshells (2*s* and 2*p*). For $n = 3$, there are three subshells (3*s*, 3*p*, and 3*d*).

Every shell has an *ns* subshell. Any shell with $n \geq 2$ also has an *np* subshell, and any shell with $n \geq 3$ also has an *nd* subshell.

Each subshell has 2*l* + 1 orbitals

All *ns* subshells contain a single *s* orbital, all *np* subshells contain three *p* orbitals, all *nd* subshells contain five *d* orbitals, and all *nf* subshells contain seven *f* orbitals.

✓ Example 1.1.1.5

List all the allowed combinations of the four quantum numbers (n, l, m_l, m_s) for electrons in a 2*p* orbital and predict the maximum number of electrons the 2*p* subshell can accommodate.

Hint

List the quantum numbers (n, l) that correspond to an $n = 2p$ orbital. Then list the allowed combinations of n, l, and m_l. Use the allowed values of m_s to determine the maximum number of electrons in each $2p$ subshell.

Answer

For a $2p$ orbital, we know that $n = 2$, $l = 1$, and $m_l = -l, (-l + 1), \ldots, (l - 1), l$. There are only three possible combinations of (n, l, m_l): (2, 1, 1), (2, 1, 0), and (2, 1, −1). Because m_s is independent of the other quantum numbers and can have values of only +½ and −½, there are six possible combinations of (n, l, m_l, m_s): (2, 1, 1, +½), (2, 1, 1, −½), (2, 1, 0, +½), (2, 1, 0, −½), (2, 1, −1, +½), and (2, 1, −1, −½). Hence the $2p$ subshell, which consists of three $2p$ orbitals ($2p_x$, $2p_y$, and $2p_z$), can contain a total of six electrons, two in each orbital.

? Exercise 1.1.1.6

List all the allowed combinations of the four quantum numbers (n, l, m_l, m_s) for a $6s$ orbital, and predict the total number of electrons it can contain.

Hint

List the quantum numbers (n, l) that correspond to an $n = 6s$ orbital. Then list the allowed combinations of n, l, and m_l. Use the allowed values of m_s to determine the maximum number of electrons in each $6s$ subshell.

Answer

For a $6s$ orbital, we know that $n = 6$, $l = 0$, and $m_l = -l, (-l + 1), \ldots, (l - 1), l$. There is only one possible combinations of (n, l, m_l): (6, 0, 0)Because m_s is independent of the other quantum numbers and can have values of only +½ and −½, there are two possible combinations of (n, l, m_l, m_s): (6, 0, 0, +½) and (6, 0, 0, −½). Hence the $6s$ subshell, which consists of one $6s$ orbital and can contain a total of two electrons.

1.1.1: Quantum Numbers is shared under a CC BY-NC-SA 4.0 license and was authored, remixed, and/or curated by Kathryn A. Newton, Northern Michigan University.

- **6.5: Quantum Mechanics and Atomic Orbitals** is licensed CC BY-NC-SA 3.0.
- **6.7: Many-Electron Atoms** is licensed CC BY-NC-SA 3.0.

1.1.2: Probability Density and Nodes

Estimated Time to Read: 6 min

Atomic orbitals are mathematically derived regions of space with different probabilities of containing an electron. An orbital can be viewed as a probability map of finding an electron at a specific point in space.

Probability Density

One way of representing electron probability distributions was illustrated previously for the 1*s* orbital of hydrogen. Ψ^2 gives the probability of finding an electron in a given volume of space, and a plot of Ψ^2 versus distance from the nucleus (r) is a plot of the *probability density*. The 1*s* orbital is spherically symmetrical so the probability of finding a 1*s* electron at any given point depends only on its distance from the nucleus. The probability density is greatest at $r = 0$ (at the nucleus) and decreases steadily with increasing distance. At very large values of r, the electron probability density is very small but is not equal to zero.

Radial Probability Density

The *radial probability density* is the probability of finding an electron at a distance r from the nucleus. It is calculated by adding together the probabilities of an electron being at all points on a series of spherical shells of radius r_1, r_2, r_3,…, r_{x-1}, r_x. In effect, the atom is divided into very thin concentric shells, much like the layers of an onion (Figure **1.1.2.1*a***), and the radial probability density calculates the probability of finding an electron on each spherical Layer. Although the electron probability density is greatest at r = 0 (Figure **1.1.2.1*b***), is lowest at r = 0(Figure **1.1.2.1*c***). The surface area of the spherical shells increases more rapidly with r than the electron probability density decreases; therefore, the plot of radial probability has a maximum at a particular distance (Figure **1.1.2.1*d***).

> Overall, when r is very small, the surface area of a spherical shell is so small that the total probability of finding an electron close to the nucleus is very low; at the nucleus, the electron probability vanishes (Figure **1.1.2.1*d***).

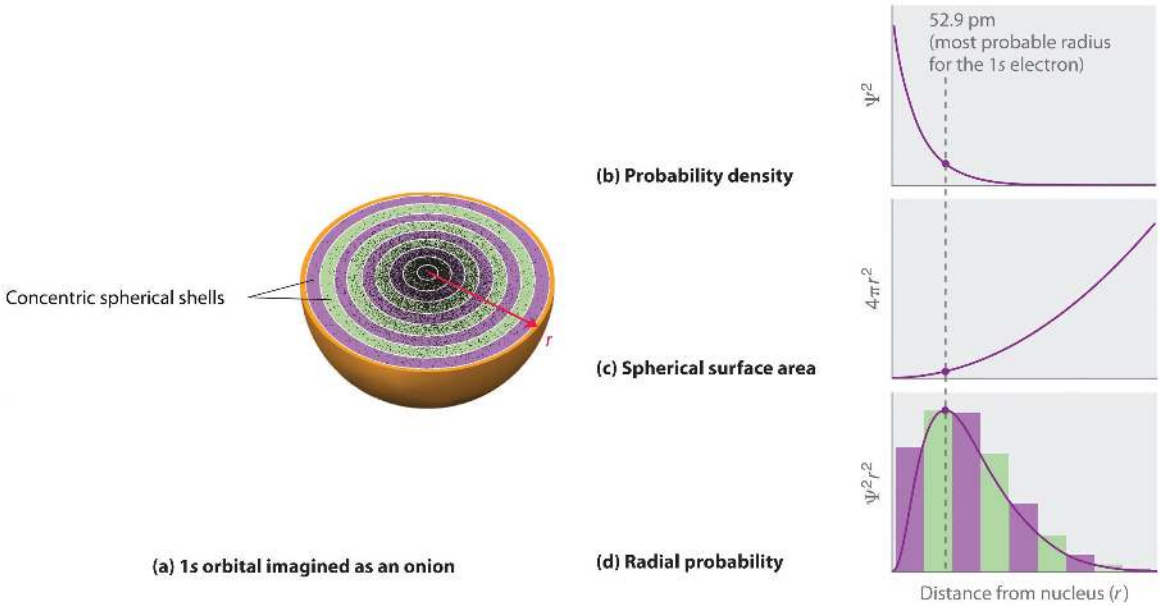


Figure 1.1.2.1: Most Probable Radius for the Electron in the Ground State of the Hydrogen Atom. (a) Imagine dividing the atom's total volume into very thin concentric shells as shown in the onion drawing. (b) A plot of electron probability density Ψ^2 versus r shows that the electron probability density is greatest at r = 0 and falls off smoothly with increasing r. The density of the dots is therefore greatest in the innermost shells of the onion. (c) The surface area of each shell, given by $4\pi r^2$, increases rapidly with increasing r. (d) If we count the number of dots in each spherical shell, we obtain the total probability of finding the electron at a given value of r. Because the surface area of each shell increases more rapidly with increasing r than the electron probability density decreases, a plot of electron probability versus r (the *radial probability density* plot) shows a peak. This peak corresponds to the most probable radius for the electron, 52.9 pm, which is exactly the radius predicted by Bohr's model of the hydrogen atom.

For the hydrogen atom, the peak in the radial probability plot occurs at r = 0.529 Å (52.9 pm), which is exactly the radius calculated by Bohr for the n = 1 orbit. Thus the most probable radius obtained from quantum mechanics is identical to the radius calculated by classical mechanics. In Bohr's model, however, the electron was assumed to be at this distance 100% of the time, whereas in the Schrödinger model, it is at this distance only some of the time. The difference between the two models is attributable to the wavelike behavior of the electron and the Heisenberg uncertainty principle.

Nodes

Radial Nodes

Figure **1.1.2.2** compares the electron probability densities for the hydrogen 1*s*, 2*s*, and 3*s* orbitals. Note that all three are spherically symmetrical. Figure **1.1.2.2*c*** shows that the 2*s* and 3*s* orbitals, the radial probability density does not fall off smoothly with increasing *r*. Instead, a series of minima and maxima are observed in the radial probability plots. The minima correspond to spherical *nodes*, which are regions with zero electron probability that alternate with spherical regions of nonzero electron probability. The existence of these nodes is a consequence of changes of wave *phase* in the wavefunction Ψ. These spherical nodes, which separate electron shells, are known as *radial nodes*. The number of *radial nodes* depends on the energy level of the orbital (n) and on the shape of the orbital (l). The number of radial nodes is equal to $n - l - 1$.

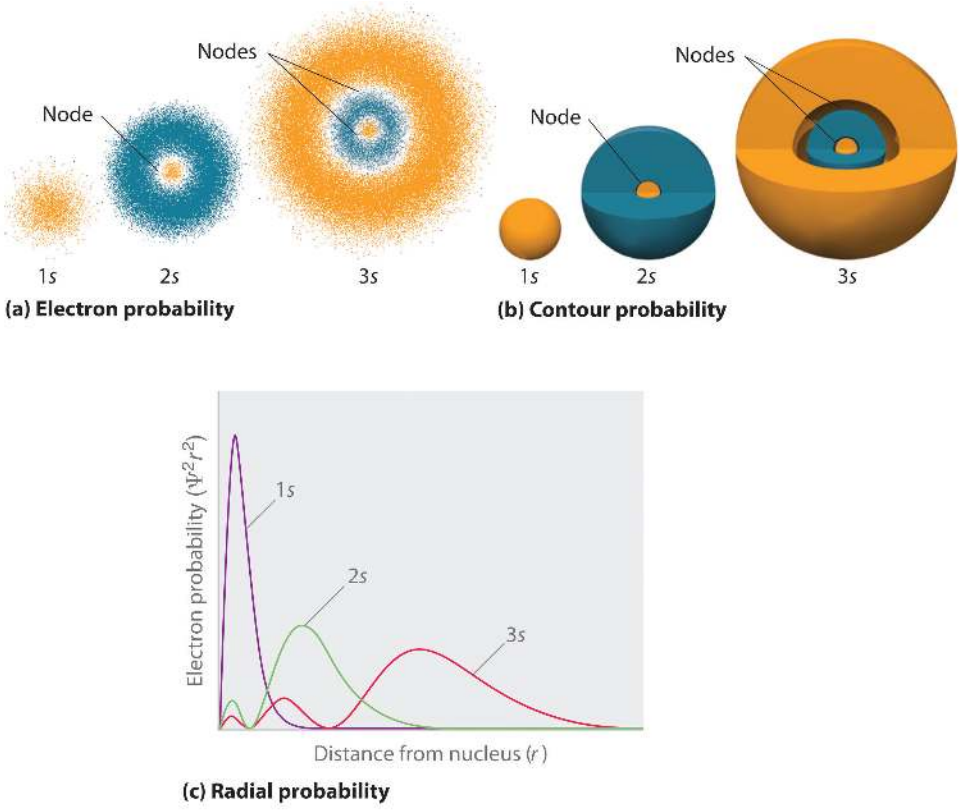


Figure 1.1.2.2: Probability Densities for the 1**s**, 2**s**, and 3**s** Orbitals of the Hydrogen Atom. (a) The electron probability density in any plane that contains the nucleus is shown. Note the presence of circular regions, or nodes, where the probability density is zero. (b) Contour surfaces enclose 90% of the electron probability, which illustrates the different sizes of the 1**s**, 2**s**, and 3**s** orbitals. The cutaway drawings give partial views of the internal spherical nodes. The orange color corresponds to regions of space where the phase of the wave function is positive, and the blue color corresponds to regions of space where the phase of the wave function is negative. (c) In these plots of electron probability as a function of distance from the nucleus (**r**) in all directions (radial probability), the most probable radius increases as **n** increases, but the 2**s** and 3**s** orbitals have regions of significant electron probability at small values of r.

Angular Nodes

Angular nodes are planar nodes that are a result of the shape of an orbital. The number of angular nodes in any orbital is equal to l. For s-orbitals ($l = 0$) so they have zero angular nodes. For p-orbitals ($l = 1$) so they have one angular node, and for d-orbitals ($l = 2$)

so they have two angular nodes. Planar nodes can be flat planes (like the nodes in all p orbitals) or they can have a conical shape, like the two angular nodes in the d_{z^2} orbital. Angular nodes in some p and d orbitals are shown in Figure **1.1.2.3**.

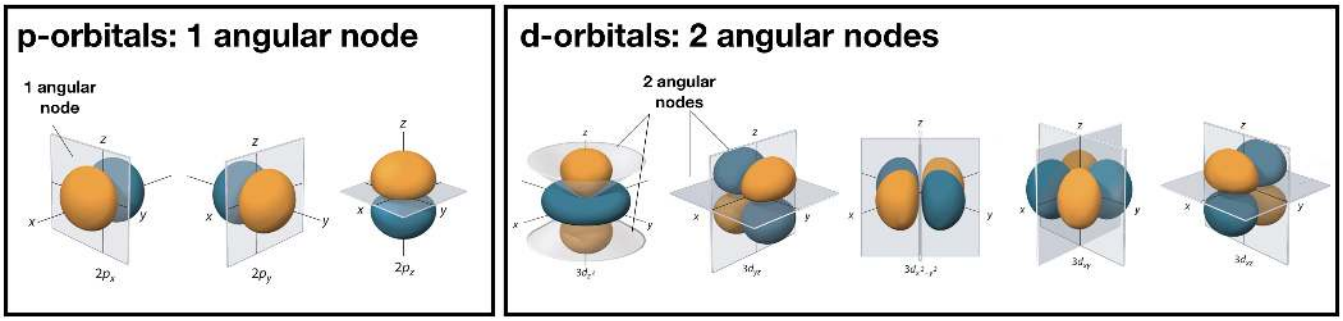


Figure 1.1.2.3: The angular nodes in p-orbitals and d-orbitals. Every p orbital has one angular node, and every d orbital has two angular nodes. The number of angular nodes in any orbital is equal to the value of the quantum number, l. (CC BY-NC-SA; anonymous by request)

? Exercise 1.1.2.1

How many radial nodes are in the s, p, d, and f orbitals in the first four shells? $n = 1, 2, 3, 4$? Do you notice any patterns in your answers?

Hint

You can use the mathematical relationship between the number of radial nodes and the values of n and l: number of radial nodes is $n - 1 - l$.

Answer: s orbitals

1s: $n - 1 - l = 1 - 1 - 0 = 0$, zero radial nodes

2s: $n - 1 - l = 2 - 1 - 0 = 1$, one radial node

3s: $n - 1 - l = 3 - 1 - 0 = 2$, two radial nodes

4s: $n - 1 - l = 4 - 1 - 0 = 3$, three radial nodes

Answer: p orbitals

2p: $n - 1 - l = 2 - 1 - 1 = 0$, zero radial nodes

3p: $n - 1 - l = 3 - 1 - 1 = 1$, one radial node

4p: $n - 1 - l = 4 - 1 - 1 = 2$, two radial nodes

Answer: d orbitals

3d: $n - 1 - l = 3 - 1 - 2 = 0$, zero radial nodes

4d: $n - 1 - l = 4 - 1 - 2 = 1$, one radial nodes

Answer: f orbitals

4f: $n - 1 - l = 4 - 1 - 3 = 0$, zero radial nodes

Answer: patterns

You may notice the pattern that the first orbital of any type (1s, 2p, 3d...) has zero radial nodes, the second orbital of a type (2s, 3p, 4d...) has one radial node, the third orbital of a type has two radial nodes (3s, 4p, 5d...)...etc.

Contributors and Attributions

- Modified by Joshua Halpern (Howard University)

1.1.2: Probability Density and Nodes is shared under a CC BY-NC-SA 4.0 license and was authored, remixed, and/or curated by Kathryn A. Newton, Northern Michigan University.

- **6.6: 3D Representation of Orbitals** is licensed CC BY-NC-SA 3.0.
- **2.2.2: Quantum Numbers and Atomic Wave Functions** by Kathryn Haas is licensed CC BY-NC-SA 4.0.

1.1.3: Representations of Atomic Orbitals

Estimated Time to Read: 5 min

Atomic Orbitals

Three things happen to atomic orbitals as *n* increases:

1. They become larger, extending farther from the nucleus.
2. They become higher in energy because of their increased distance from the nucleus.
3. They contain more radial nodes.

s Orbitals (l=0)

s orbitals are spherically symmetrical. They have no angular nodes but may have radial nodes.

Orbitals are generally drawn as three-dimensional surfaces that enclose 90% of the electron density, as was shown for the hydrogen 1*s*, 2*s*, and 3*s* orbitals in Figure 1.3.2b. Although such drawings show the relative sizes of the orbitals, they do not normally show the spherical nodes in the 2*s* and 3*s* orbitals because the spherical nodes lie inside the 90% surface.

p Orbitals (l=1)

As the value of *l* increases, the number of orbitals in a given subshell increases, and the shapes of the orbitals become more complex. p orbitals have a two-lobed shape split by an angular nodal plane. p orbitals may have radial nodes, depending on the value of *n*.

For the 2*p* subshell $l = 1$, so there are three values of m_l (−1, 0, and +1), and there are three 2*p* orbitals. Figure **1.1.3.1** depicts a 2*p* orbital.Because this orbital has two lobes of electron density arranged along the *z* axis, with an electron density of zero in the *xy* plane (i.e., the *xy* plane is a nodal plane), it is a $\mathbf{2p_z}$ orbital.

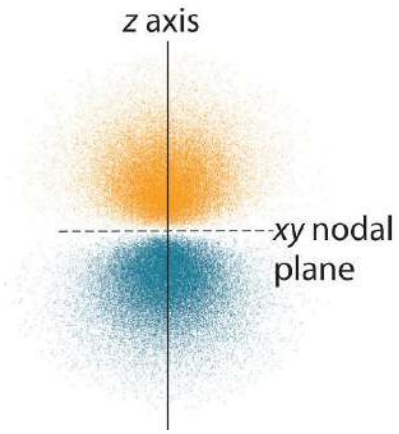


Figure 1.1.3.1: Electron probability distribution for a 2*p* Orbital. The nodal plane of zero electron density separates the two lobes of the 2*p* orbital. The colors correspond to regions of space where the phase of the wave function is positive (orange) and negative (blue).

Figure **1.1.3.2** shows the contour surfaces, which enclose 90% of the total electron probability, for all three 2*p* orbitals. All orbitals have identical shapes just one nodal plane. In each case, the phase of the wave function for each of the 2*p* orbitals is positive for the lobe that points along the positive axis and negative for the lobe that points along the negative axis. It is important to emphasize that these signs correspond to the phase of the wave that describes the electron motion, not to positive or negative charges. Each orbital is oriented along the axis indicated by the subscript, and the nodal plane that is perpendicular to that axis bisects each 2*p* orbital. The shapes of the 90% probability surfaces of the 3*p*, 4*p*, and higher-energy *p* orbitals are essentially the same as those shown in Figure **1.1.3.2**.

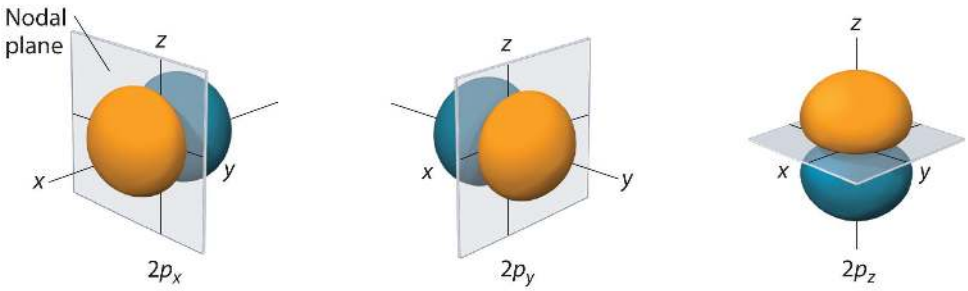


Figure 1.1.3.2: Three equivalent 2*p* orbitals of the hydrogen atom. The surfaces shown enclose 90% of the total electron probability for the three hydrogen 2p orbitals. These three orbitals have the same shape but different orientations. Each orbital consist of two lobes arranged along an axis that is bisected by a perpendicular nodal plane. The colors correspond to regions of space where the phase of the wave function is positive (orange) and negative (blue).

d Orbitals (l=2)

Subshells with $l = 2$ have five *d* orbitals; the first principal shell to have a *d* subshell corresponds to $n = 3$. The five *d* orbitals have m_l values of −2, −1, 0, +1, and +2.

The hydrogen 3d orbitals, shown in Figure **1.1.3.3**, have more complex shapes than the 2p orbitals. All five 3d orbitals contain two nodal surfaces, as compared to one for each p orbital and zero for each s orbital. For three of the d orbitals, the lobes of electron density are oriented between the xy, xz, and yz planes; these orbitals are referred to as the $3d_{xy}$, \)3d_{xz}\), and $3d_{yz}$ orbitals, respectively. A fourth d orbital has lobes lying along the x and y axes; this is the $3d_{x^2-y^2}$ orbital. The fifth 3d orbital, called the $3d_{z^2}$ orbital, has a unique shape: it looks like a $2p_z$ orbital combined with an additional doughnut of electron probability lying in the xy plane. Despite its peculiar shape, the $3d_{z^2}$ orbital is mathematically equivalent to the other four and has the same energy. In contrast to p orbitals, the phase of the wave function for d orbitals is the same for opposite pairs of lobes. For the (dz^2\) orbital, the phase of the wave function is positive for the two lobes that lie along the z axis, and the phase of the wave function is negative for the doughnut of electron density in the xy plane. Like the s and p orbitals, as n increases, the size of the d orbitals increases, but the overall shapes remain similar to those depicted in Figure **1.1.3.3**.

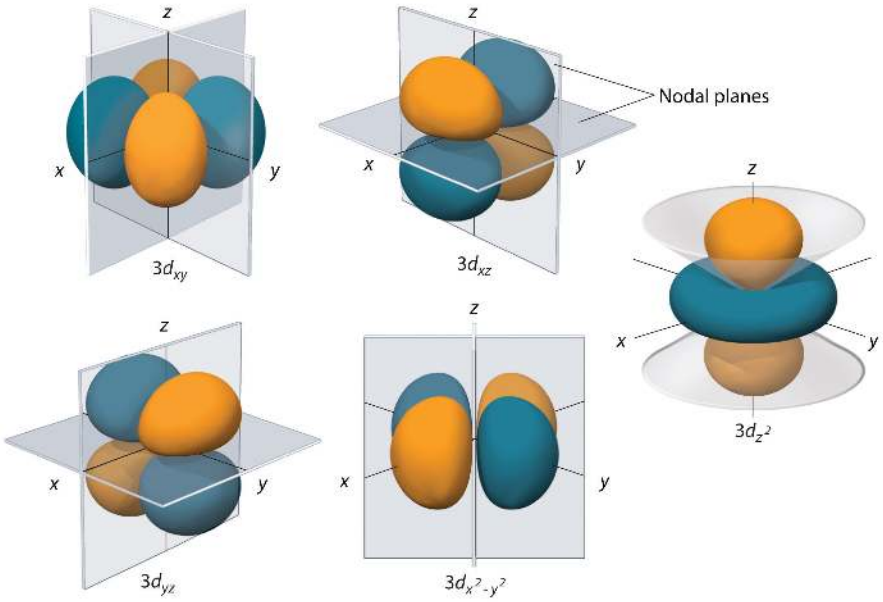


Figure 1.1.3.3: Five equivalent 3d orbitals of the hydrogen atom. The surfaces shown enclose 90% of the total electron probability for the five hydrogen 3d orbitals. Four of the five 3d orbitals consist of four lobes arranged in a plane that is intersected by two perpendicular nodal planes. These four orbitals have the same shape but different orientations. The fifth 3d orbital, $3d_{z^2}$, has a distinct shape even though it is mathematically equivalent to the others. The colors correspond to regions of space where the phase of the wave function is positive (orange) and negative (blue).

f Orbitals (l=3)

Principal shells with $n = 4$ can have subshells with $l = 3$ and m_l values of −3, −2, −1, 0, +1, +2, and +3. These subshells consist of seven f orbitals. Each f orbital has three nodal surfaces, so their shapes are complex. Because f orbitals are not particularly important for our purposes, we do not discuss them further, and orbitals with higher values of l are not discussed at all.

Contributors and Attributions

- Modified by Joshua Halpern (Howard University)

1.1.3: Representations of Atomic Orbitals is shared under a CC BY-NC-SA 4.0 license and was authored, remixed, and/or curated by Kathryn A. Newton.

- **6.6: 3D Representation of Orbitals** is licensed CC BY-NC-SA 3.0.

1.1.4: Energies of Atomic Orbitals

Estimated Time to Read: 4 min

Single-Electron Atoms

Although we have discussed the shapes of orbitals, we have said little about their comparative energies. We begin our discussion of orbital energies by considering atoms or ions with only a single electron (such as H or He^+).

The relative energies of the atomic orbitals with $n \leq 4$ for a hydrogen atom are shown in Figure **1.1.4.1**. Note that the orbital energies depend on only the principal quantum number *n*. Consequently, the energies of the 2*s* and 2*p* orbitals of hydrogen are the same; the energies of the 3*s*, 3*p*, and 3*d* orbitals are the same; and so forth. Quantum mechanics predicts that in the hydrogen atom, all orbitals with the same value of *n* (ex. the three 2*p* orbitals) are *degenerate*, meaning that they have the same energy.

The orbital energies obtained for hydrogen using quantum mechanics are exactly the same as the allowed energies calculated by Bohr. In contrast to Bohr's model, however, which allowed only one orbit for each energy level, quantum mechanics predicts that for the $n = 2$ shell there are 4 orbitals with different electron density distributions (one 2*s* and three 2*p* orbitals). Likewise, for the $n = 3$ principal shell there are 9 orbitals (one 3*s*, three 3*p*, and five 3*d* orbitals), and for the $n = 4$ shell there are 16 orbitals (one 4*s*, three 4*p*, five 4*d*, and seven 4*f* orbitals). Figure **1.1.4.1** shows that the energy levels become closer and closer together as the value of *n* increases, as expected because of the $1/n^2$ dependence of orbital energies.

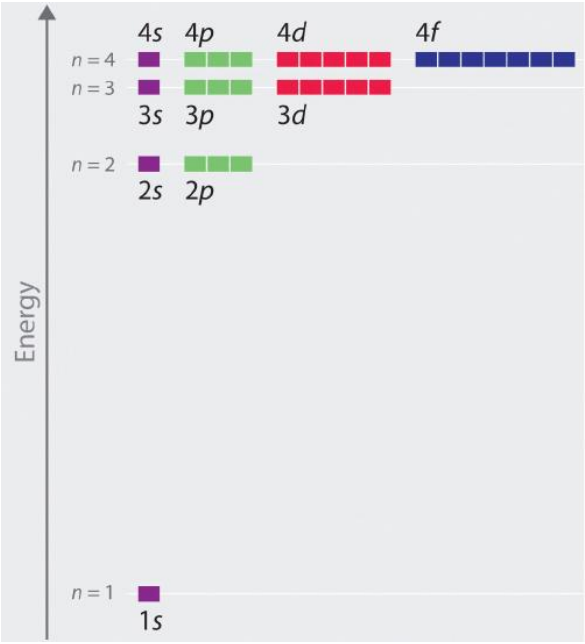


Figure 1.1.4.1: Orbital energy level diagram for the hydrogen atom with a single electron. Each box corresponds to one orbital. Note that the difference in energy between orbitals decreases rapidly with increasing values of *n*.

The energies of the orbitals in any species with only one electron can be calculated by a minor variation of Bohr's equation, which can be extended to other single-electron species by incorporating the nuclear charge Z (the number of protons in the nucleus):

$$E = -\frac{Z^2}{n^2} Rhc \tag{1.1.4.1}$$

In general, both energy and radius decrease as the nuclear charge increases. Thus the most stable orbitals (those with the lowest energy) are those closest to the nucleus. For example, in the ground state of the hydrogen atom, the single electron is in the 1s orbital, whereas in the first excited state, the atom has absorbed energy and the electron has been promoted to one of the n = 2 orbitals. In ions with only a single electron, the energy of a given orbital depends on only *n*, and all subshells within a principal shell, such as the p_x, p_y, and p_z orbitals, are degenerate.

Multi-Electron Atoms

Unlike in hydrogen-like atoms with only one electron, in multielectron atoms the values of quantum numbers *n and l* determine the energies of an orbital. The energies of the different orbitals for a typical multielectron atom are shown in Figure **1.1.4.21**. Within a given principal shell of a multielectron atom, the orbital energies increase with increasing *l*. An *ns* orbital always lies below the corresponding *np* orbital, which in turn lies below the *nd* orbital.

These energy differences are caused by the effects of *shielding* and *penetration*, the extent to which a given orbital lies inside other filled orbitals. For example, an electron in the 2*s* orbital penetrates inside a filled 1*s* orbital more than an electron in a 2*p* orbital does. Since electrons, all being negatively charged, repel each other, an electron closer to the nucleus partially *shields* an electron farther from the nucleus from the attractive effect of the positively charged nucleus. Hence in an atom with a filled 1*s* orbital, the effective nuclear charge (Z_{eff}) experienced by a 2*s* electron is greater than the Z_{eff} experienced by a 2*p* electron. Consequently, the 2*s* electron is more tightly bound to the nucleus and has a lower energy, consistent with the order of energies shown in Figure **1.1.4.2**. We will discuss *shielding* and *penetration* in more detail in a later section. For now, you should note that the energies of different orbitals in the same shell varies depending on the shapes of the orbitals. As the shapes become more complex, they allow less electron density near the nucleus, which destabilizes the electrons, and increases the energy of the orbital.

Notice in Figure **1.1.4.2** that the difference in energies between subshells can be so large that the energies of orbitals from different principal shells can become approximately equal. For example, the energy of the 3*d* orbitals in most atoms is actually *between* the energies of the 4*s* and the 4*p* orbitals.



Figure 1.1.4.2: Orbital energy level diagram for a typical multielectron atom. Each box corresponds to one orbital.

1.1.4: Energies of Atomic Orbitals is shared under a CC BY-NC-SA 4.0 license and was authored, remixed, and/or curated by Kathryn A. Newton, Northern Michigan University.

- **6.6: 3D Representation of Orbitals** is licensed CC BY-NC-SA 3.0.
- **6.7: Many-Electron Atoms** is licensed CC BY-NC-SA 3.0.

1.2: Ground State Electron Configurations

Estimated Time to Read: 4 min

Introduction

In addition to having different energy levels, orbitals also have different shapes and orientations, and each can be occupied by two electrons. For each principal quantum number, *n*, there is up to one *s* orbital, three *p* orbitals, five *d* orbitals and seven *f* orbitals. Each orbital can hold up to two electrons of different spin (m_s = +1/2, -1/2); therefore, the *s* subshell can hold two electrons, the *p* subshell can hold six electrons, the *d* subshell can hold ten electrons, and the *f* subshell can hold 14 electrons.

The ground state electron configuration specifies the lowest-energy arrangement of electrons into subshells for a given element. Ground state electron configurations are the foundation for understanding molecular bonding, properties, and structures. The following rules explain how to determine the lowest energy arrangement of electrons into the orbitals. The ground state electron configurations contribute to a fundamental understanding of the periodic table and will later be used to understand different atomic properties.

The Aufbau Principle

The *Aufbau Principle* (also called the *building-up principle* or the *Aufbau rule*) states that, in the ground state of an atom or ion, electrons fill atomic orbitals of the lowest available energy level before occupying higher-energy levels Figure **1.2.1**. In general, an electron will occupy an atomic orbital with the lowest value of n, l, m_l, in that order of priority.

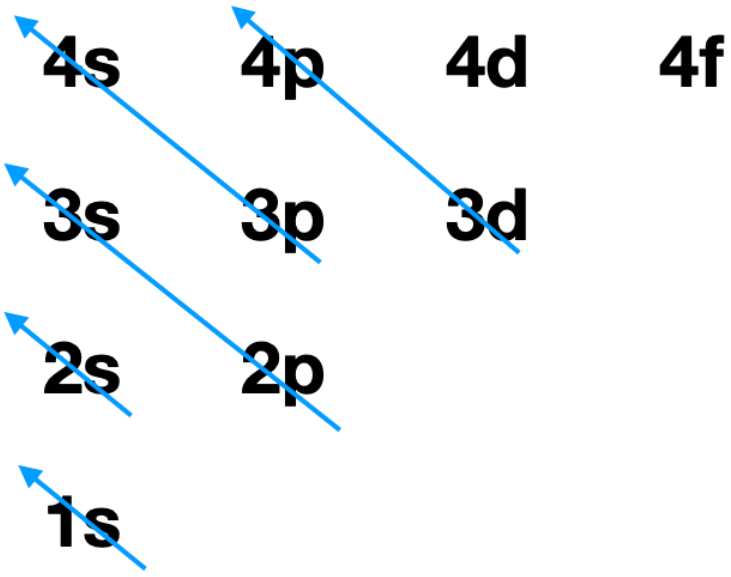


Figure 1.2.1: The order of filling of ground state electron orbitals is 1s, 2s, 2p, 3s, 3p, 4s, 3d, 4p, etc... (CC-BY-NC-SA; Kathryn Haas)

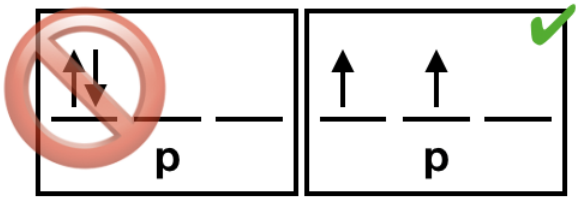
> Electrons will occupy the lowest energy orbitals in order to minimize the total energy. The two quantum numbers that are related to energy in multi-electron atoms are n, and l. Thus, orbitals with the lowest values of n and l will fill first.

Hund's Rule of Maximum Multiplicity

When electron fill into orbitals, the *multiplicity* refers to the number of unpaired electrons. *Multiplicity* is calculated as *n* + 1, where *n* is the number of unpaired electrons. *Hund's Rule of Maximum Multiplicity* states that for a given electron configuration, the lowest energy arrangement of electrons in degenerate orbitals is the arrangement with the greatest multiplicity (or the greatest number of unpaired electrons). This rule is used to predict the ground state of an atom or molecule with one or more open electronic shells.

Hund's rule is based on empirical observation of atomic spectra, and it is a consequence of the energy required to pair two electrons in the same orbital. This energy of repulsion between two electrons in the same orbitals is a Coulombic energy of repulsion, Π_c, caused by two electrons with like charge sharing the same area of space (an orbital). When more than one electron occupies a set of degenerate orbitals, the most favorable arrangement is one where the number of paired electrons is minimized.

A simplified definition of Hund's rule is that the lowest energy arrangement is the one with the greatest number of unpaired electrons. This implies that if two or more orbitals of equal energy are available, electrons will occupy them singly before filling them in pairs. Examples of ground state arrangements of electrons in three degenerate p-orbitals is given in Figure 1.2.2.



# of electrons in a p-subshell	Arrangement (unpaired electrons, n)	Spin Multiplicity (n + 1)
1	(n = 1)	2
2	(n = 2)	3
3	(n = 3)	4
4	(n = 2)	3
5	(n = 1)	2
6	(n = 0)	1

Figure 1.2.2: Hund's rule is that the number of unpaired electrons (*multiplicity*) must be maximized in the ground state. (CC-BY-NC-SA; Libretexts)

The Pauli Exclusion Principle

The Pauli exclusion principle states that it is impossible for two electrons of a multi-electron atom to have the same set of values for all four quantum numbers. Two electrons in different orbitals will have a different set of n, l, and m_l values. When two electrons reside in the same orbital, they posses the same n, l, and m_l values, therefore their m_s must be different. Thus, two electrons in the same orbital must have opposite spin values of $+\frac{1}{2}$ and $-\frac{1}{2}$. The value of m_s for an unpaired electron is conventionally assigned a value of $+\frac{1}{2}$.

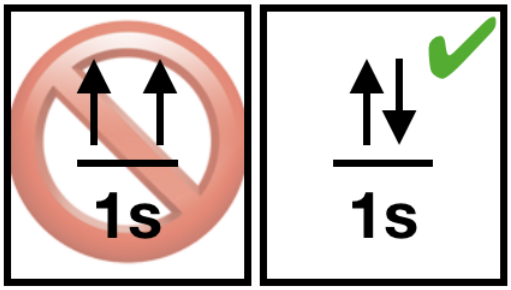


Figure 1.2.3: Pauli's principle tells us that paired electrons must have opposite spin. CC-BY-NC-SA; Libretexts)

References

1. Miessler, Gary L., and Donald A. Tarr. *Inorganic Chemistry*. Upper Saddle River, NJ: Pearson Prentice Hall, 2010. Print.
2. Brown, Ian David. *The Chemical Bond in Inorganic Chemistry the Bond Valence Model*. Oxford: Oxford UP, 2006. Print.

1.2: Ground State Electron Configurations is shared under a not declared license and was authored, remixed, and/or curated by LibreTexts.

- **2.2.3: Aufbau Principle** by Kathryn Haas is licensed CC BY-NC-SA 4.0.
- **1.9A: Ground State Electronic Configurations** by Olivia Allsman is licensed CC BY-NC-SA 4.0.

1.2.1: Writing Ground State Electron Configurations

Estimated Time to Read: 5 min

Basic Steps

Electron configurations list every subshell for an atom or ion and how many electrons are in each subshell. Subshells are described by writing the principal quantum number *n* followed by the symbol for the angular momentum quantum number *l* (s, p, d, or f). The the total number of electrons in each subshell is written as a superscript. The lowest energy subshell is written first, and additional subshells are written in order of increasing energy.

Example 1.2.1.1

Write the ground state electron configuration for sodium, Na.

Solution: Method 1

1. Find the number of electrons in the atom: Sodium has 11 electrons.
2. List the subshells following the model shown in Figure 1.6.3: 1s 2s 2p 3s
3. Fill the subshells until all electrons have been accounted for. Remember: each *s* subshell can hold 2 electrons, each *p* subshell can hold six electrons, each *d* subshell can hold 10 electrons, and each *f* subshell can hold 14 electrons: $1s^2\ 2s^2\ 2p^6\ 3s^1$

Solution: Method 2

1. Locate the atom on the periodic table.

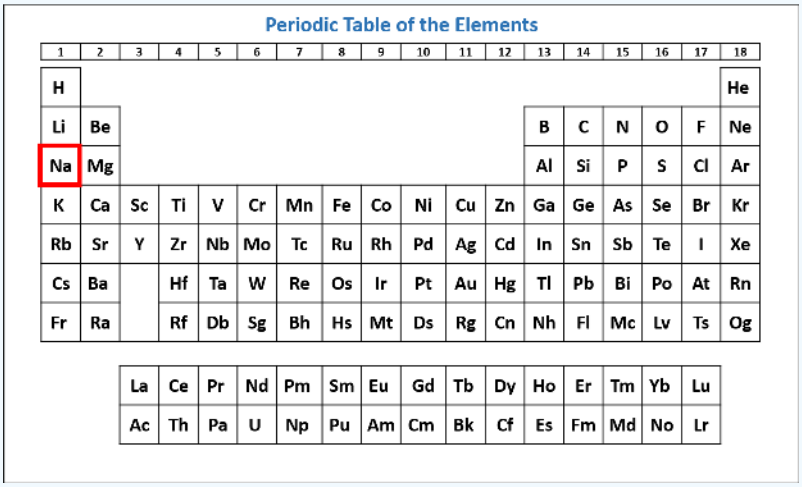


Figure 1.2.1.1: Periodic table of the elements with the location of sodium (Na) highlighted. (CC-BY-NC-SA; Kathryn A. Newton)

2. Starting at hydrogen and the 1s subshell, read across each row of the periodic table until you get to your chosen element. As you read across each row, list each subshell and the number of electrons in the subshell.

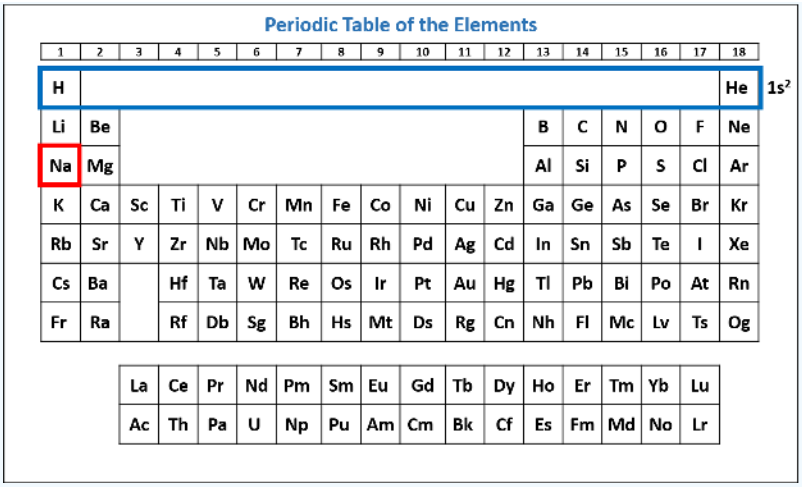


Figure 1.2.1.2: Periodic table of the elements with the $1s^2$ subshell highlighted. Na has two electrons in the 1s subshell. (CC-BY-NC-SA; Kathryn A. Newton)

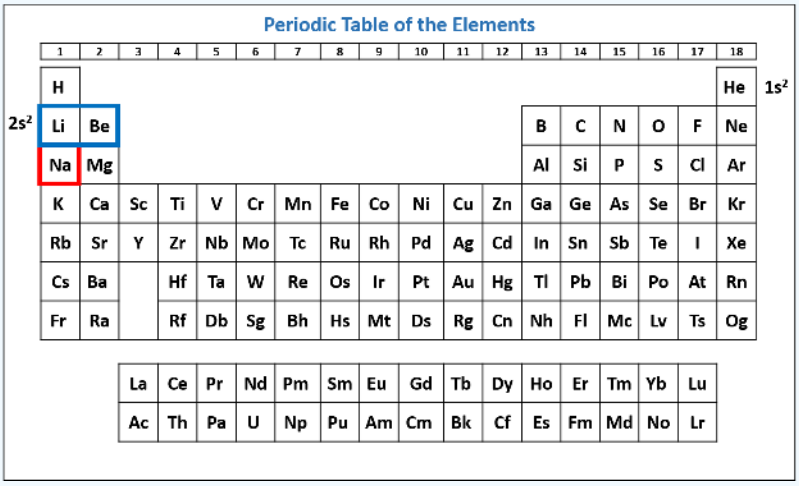


Figure 1.2.1.3: Periodic table of the elements with the $2s^2$ subshell highlighted. Na has two electrons in the 2s subshell. (CC-BY-NC-SA; Kathryn A. Newton)

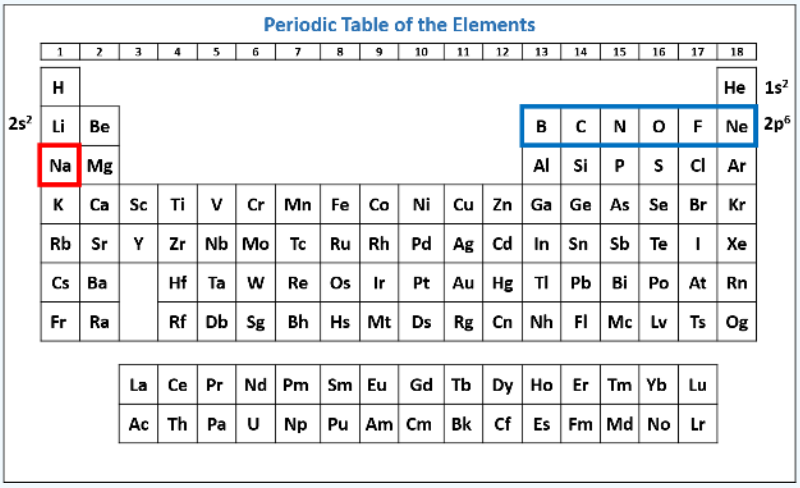


Figure 1.2.1.4: Periodic table of the elements with the $2p^6$ subshell highlighted. Na has six electrons in the 2p subshell. (CC-BY-NC-SA; Kathryn A. Newton)

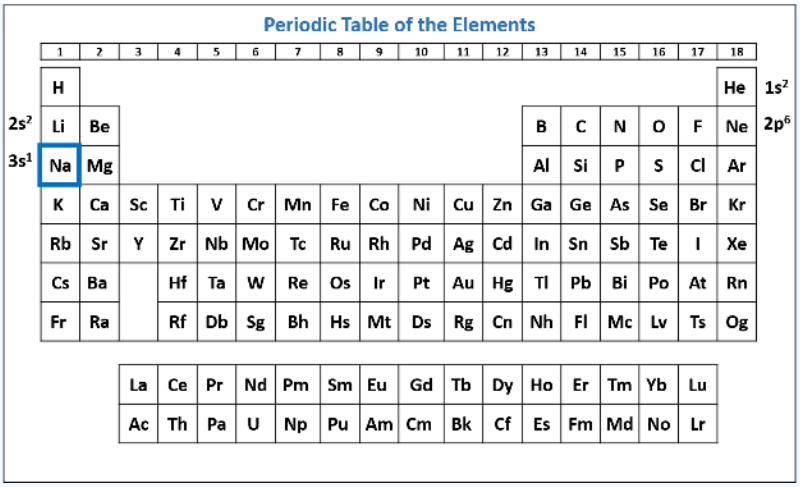


Figure 1.2.1.5: Periodic table of the elements with the $3s^1$ subshell highlighted. Na has one electron in the 3s subshell. (CC-BY-NC-SA; Kathryn A. Newton)

3. Combine the list into a single electron configuration. Na's electron configuration is $1s^2\ 2s^2\ 2p^6\ 3s^1$.

Noble Gas Configurations

Because writing the entire electron configuration can become cumbersome, there is a shorthand option. It is done by using the symbol of the noble gas in the period above the element to represent the electron configuration before it.

Example 1.2.1.2

Write the noble gas electron configuration for sodium (Na).

Solution

1. Locate the atom on the periodic table.

2. Locate the noble gas element in the period above the element of interest.

3. Continue the electron configuration from the noble gas until you reach the element of interest.

4. Put the noble gas in brackets and write the remainder of the electron configuration.

Na has the same electron configuration as Ne with the addition of $3s^1$.

Na's noble gas configuration is $[Ne]3s^1$.

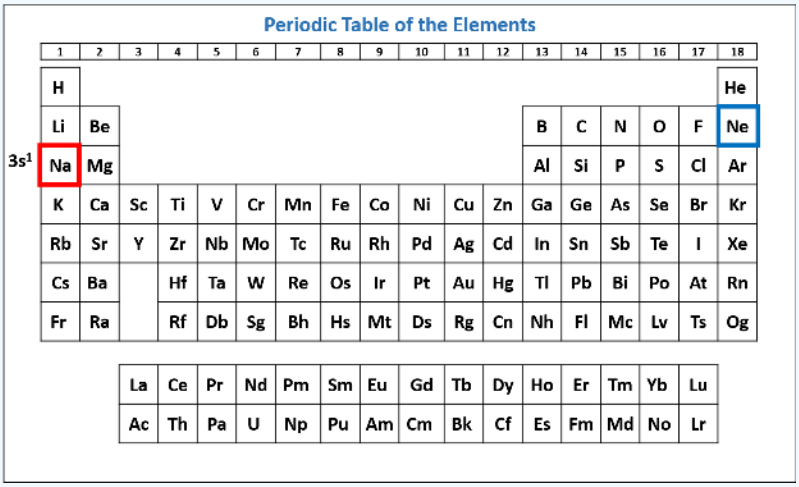


Figure 1.2.1.6: Periodic table of the elements with the locations of sodium (Na) and neon (Ne) highlighted. (CC-BY-NC-SA; Kathryn A. Newton)

Ion Configurations

Cations

Cations are formed when a neutral atom loses electrons. To write an electron configuration for a cation, start by writing the electron configuration for the neutral atom. Then determine the number of electrons that were lost to form the cation. (The loss of a single electron results in a +1 charge, the loss of two electrons results in a +2 charge, and so on.) Subtract the number of lost electrons from the highest energy shell in the neutral configuration. When there is more than one orbital with the same principal quantum number, the electrons will be removed from the *d* subshell before any are removed from the *p* subshell and will be removed from the *p* subshell before any are removed from *s* subshell.

Example 1.2.1.3

Write the electron configuration for Si^{4+}.

Solution

1. Write the configuration of the neutral atom. Si: $1s^2\ 2s^2\ 2p^6\ 3s^2\ 3p^2$

2. Determine how many electrons were lost. Si^{4+} was formed by the loss of four electrons.

3. Remove electrons from the highest shell, starting with the highest energy subshell.

   Si^{+}: $1s^2\ 2s^2\ 2p^6\ 3s^2\ 3p^{\mathbf{1}}$

   Si^{2+}: $1s^2\ 2s^2\ 2p^6\ 3s^2\ 3p^{\mathbf{0}}$

   Si^{3+}: $1s^2\ 2s^2\ 2p^6\ 3s^{\mathbf{1}}$

   Si^{4+}: $1s^2\ 2s^2\ 2p^6\ 3s^{\mathbf{0}}$, which is typically written as $1s^2\ 2s^2\ 2p^6$ or as [Ne]

Anions

Anions are formed when a neutral atom gains electrons. To write the electron configuraiton for a cation, start by writing the electron configuration for the neutral atom. Then determine the number of electrons that were added to form the anion. (The addition of a single electron results in a -1 charge, the addition of two electrons results in a -2 charge, and so on.) Add the additional electrons to the highest energy shell in the neutral configuration. When there is more than one orbital with the same principal quantum number, the electrons will be added to any partially filled subshells first, and any remaining electrons will be added to the *s* subshell before the *p* subshell before the *d* subshell.

Example 1.2.1.4

Write the electron configuration for As^{3-}.

Solution

1. Write the configuration of the neutral atom. As: $1s^2\ 2s^2\ 2p^6\ 3s^2\ 3p^6\ 4s^2\ 3d^{10}\ 4p^3$

2. Determine how many electrons were gained. As^{3-} was formed by the addition of three electrons.

3. Add electrons from the highest shell, starting with any partially filled subshells.

   As^{-}: $1s^2\ 2s^2\ 2p^6\ 3s^2\ 3p^6\ 4s^2\ 3d^{10}\ 4p^4$

   As^{2-}: $1s^2\ 2s^2\ 2p^6\ 3s^2\ 3p^6\ 4s^2\ 3d^{10}\ 4p^5$

   As^{3-}: $1s^2\ 2s^2\ 2p^6\ 3s^2\ 3p^6\ 4s^2\ 3d^{10}\ 4p^6$ or [Kr]

Problems

? Exercise 1.2.1.1

Write the expanded and shortened ground state electron configuration for Cl.

Answer

Expanded: $1s^2\ 2s^2\ 2p^6\ 3s^2\ 3p^5$

Noble Gas: [Ne] $3s^2\ 3p^5$

? Exercise 1.2.1.2

Write the ground state electron configuration for P^{3-}.

Answer

Expanded: $1s^2\ 2s^2\ 2p^6\ 3s^2\ 3p^3$

Noble Gas: [Ar]

References

1. Housecroft, Catherine E. and Alan G. Sharpe, “Inorganic Chemistry,” 3rd ed. England: Pearson Education Limited: 2008.
2. Tro, Nivaldo J. “Chemistry: A Molecular Approach,” 8th ed. Upper Saddle River, New Jersey: Prentice Hall: 2007.
3. Silberberg, Martin S. "Chemistry: The Molecular Nature of Matter and Change," 4th ed. Boston: McGraw Hill: 2006.

1.2.1: Writing Ground State Electron Configurations is shared under a CC BY-NC-SA 4.0 license and was authored, remixed, and/or curated by Kathryn A. Newton, Northern Michigan University.

- **1.9A: Ground State Electronic Configurations** by Olivia Allsman is licensed CC BY-NC-SA 4.0.

1.2.2: Magnetic Properties

Estimated Time to Read: 5 min

The magnetic moment of a system measures the strength and the direction of its magnetism. The term itself usually refers to the magnetic dipole moment. Anything that is magnetic, like a bar magnet or a loop of electric current, has a magnetic moment. A magnetic moment is a vector quantity, with a magnitude and a direction. An electron has an electron magnetic dipole moment, generated by the electron's intrinsic spin property, making it an electric charge in motion. There are many different magnetic forms: including paramagnetism, diamagnetism, ferromagnetism, and anti-ferromagnetism. Only paramagnetism and diamagnetism are discussed here.

Paramagnetism

Paramagnetism refers to the magnetic state of an atom with *one or more unpaired electrons*. The unpaired electrons are attracted by a magnetic field due to the electrons' magnetic dipole moments. Hund's Rule states that electrons must occupy every orbital singly before any orbital is doubly occupied. This may leave the atom with many unpaired electrons. Because unpaired electrons can orient in either direction, they exhibit magnetic moments that can align with a magnet. This capability allows paramagnetic atoms to be attracted to magnetic fields. Diatomic oxygen, O_2, is paramagnetic; it is attracted to the magnet. In contrast, molecular nitrogen, N_2, has no unpaired electrons and is diamagnetic (discussed below); it is therefore unaffected by the magnet.The following video shows liquid oxygen attracted into a magnetic field created by a strong magnet.



Liquid Oxygen is attracted to a magnetic field: Paramagnetism of Liquid Oxygen, YouTube(opens in new window) [youtu.be]

> Paramagnetism is a form of magnetism whereby materials are attracted to an externally applied magnetic field. Paramagnetic species have one or more unpaired electrons.

Diamagnetism

Diamagnetic species are characterized by paired electrons; they have *no unpaired electrons*. According to the Pauli Exclusion Principle which states that no two identical electrons may take up the same quantum state at the same time, the electron spins are oriented in opposite directions. This causes the magnetic fields of the electrons to cancel out. Thus, there is no net magnetic moment, and the atom cannot be attracted into a magnetic field. In fact, diamagnetic substances are weakly *repelled* by a magnetic field as demonstrated with the pyrolytic carbon sheet in Figure **1.2.2.1**. Diamagnetism, to some degree, is a property of all materials and always makes a weak contribution to the material's response to a magnetic field. For materials that show other form of magnetism (such paramagnetism), the diamagnetic contribution becomes negligible.

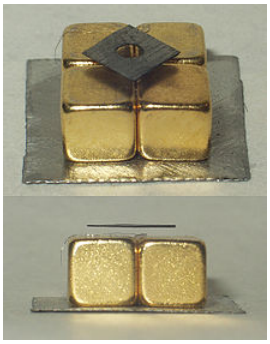


Figure 1.2.2.1: Levitating pyrolytic carbon: A small (~6 mm) piece of pyrolytic graphite levitating over a permanent neodymium magnet array (5 mm cubes on a piece of steel). Note that the poles of the magnets are aligned vertically and alternate (two with north facing up, and two with south facing up, diagonally). [Wikipedia]

Diamagnetic materials are repelled by an applied magnetic field. Diamagnetic species have no unpaired electrons.

How to determine if a substance is paramagnetic or diamagnetic

The magnetic form of a substance can be determined by examining its electron configuration. If it includes unpaired electrons, then the substance is paramagnetic. If all electrons are paired, then the substance is diamagnetic. This process can be broken into four steps:

1. Write the electron configuration
2. Draw the energy diagram for the valence orbitals by applying Hund's Rule
3. Look for unpaired electrons
4. Decide if the substance is paramagnetic (one or more electrons unpaired) or diamagnetic (all electrons paired)

Example 1.2.2.1: Chlorine

Are chlorine atoms paramagnetic or diamagnetic?

Solution

1. Write the electron configuration. Cl: $1s^2\ 2s^2\ 2p^6\ 3s^2\ 3p^5$
2. Draw the energy diagram for the valence orbitals.

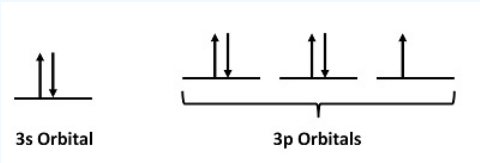


Figure 1.2.2.2: Energy diagram showing the valence orbitals of a Cl atom.

3. Look for unpaired electrons.
4. Determine whether the substance is paramagnetic or diamagnetic. Since there is an unpaired electron, the Cl atom is paramagnetic.

Example 1.2.2.2: Zinc

Are zinc atoms paramagnetic or diamagnetic?

Solution

1. Write the electron configuration. Zn: $1s^2\ 2s^2\ 2p^6\ 3s^2\ 3p^6\ 4s^2\ 3d^{10}$
2. Draw the energy diagram for the valence orbitals.

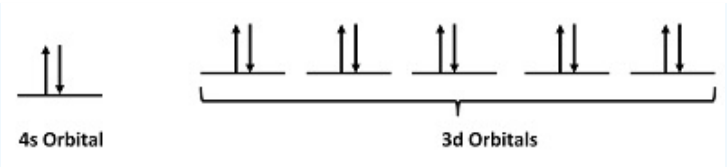
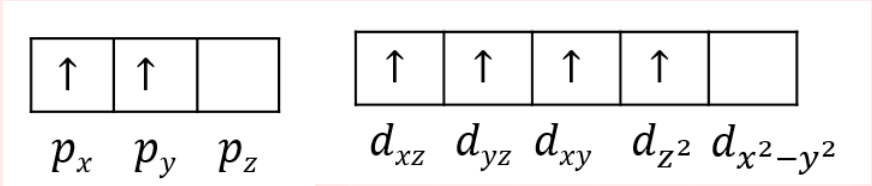


Figure **1.2.2.3**: Energy diagram showing the valence orbitals of a Zn atom.

3. Look for unpaired electrons.
4. Determine whether the substance is paramagnetic or diamagnetic. Since there is are no unpaired electrons, the Zn atom is diamagnetic.

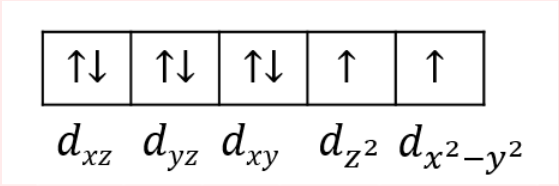
Caution

Having an even number of electrons in a subshell does not mean that all electrons in the subshell are paired! According to Hund's rule, no electrons will be paired until all orbitals in a subshell have at least one unpaired electron.



p^2 configuration

d^4 configuration



d^8 configuration

Figure **1.2.2.4**: Energy diagrams showing diamagnetic electron configurations with even numbers of electrons in the subshell: p^2, d^4, d^8. (CC-BY-NC-SA; Kathryn A. Newton)



Determining Magnetic Properties from Orbital Diagrams, YouTube(opens in new window) [youtu.be]

Problems

Exercise 1.2.2.1

Decide if a boron atom is paramagnetic or diamagnetic.

Answer

B: $1s^2\ 2s^2\ 2p^1$

This configuration has one unpaired electron in the 2p subshell.Because it has one unpaired electron, it is paramagnetic

Exercise 1.2.2.2

Decide if a fluoride ion is paramagnetic or diamagnetic.

Answer

F: $1s^2\ 2s^2\ 2p^5$

F^-: $1s^2\ 2s^2\ 2p^6$

This configuration has no unpaired electrons. Because it has no unpaired electrons, it is diamagnetic.

Exercise 1.2.2.3

Decide if a bromine atom is paramagnetic or diamagnetic.

Answer

Br: [Ar] $4s^2\ 3d^{10}\ 4p^5$

This configuration has one unpaired electron in the 2p subshell (and four paired electrons). Because it has one unpaired electron, it is paramagnetic.

Exercise 1.2.2.1

Decide if Fe^{2+} is paramagnetic or diamagnetic.

Answer

Fe: [Ar] $4s^2\ 3d^6$

Fe^{2+}: [Ar] $3d^6$

This configuration has two paired electrons and four unpaired electrons in the 3d subshell. Because it has at least one unpaired electron, it is paramagnetic.

References

1. Pettrucci, Ralph H. General Chemistry: Principles and Modern Applications. 9th. Upper Saddle River: Pearson Prentice Hall, 2007
2. Sherman, Alan, Sharon J. Sherman, and Leonard Russikoff. Basic Concepts of Chemistry Fifth Edition. Boston, MA: Houghton Mifflin Company, 1992. Print.

1.2.2: Magnetic Properties is shared under a CC BY-NC-SA 4.0 license and was authored, remixed, and/or curated by Kathryn A. Newton, Northern Michigan University.

- **9.6: Magnetic Properties** is licensed CC BY-NC-SA 4.0.

1.3: Periodic Properties of the Periodic Table

Estimated Time to Read: 5 min

The Periodic Table

The Periodic Table of Elements categorizes like elements together. Dmitri Mendeleev, a Russian scientist, was the first to create a widely accepted arrangement of the elements in 1869. Mendeleev believed that when the elements are arranged in order of increasing atomic mass, certain sets of properties recur periodically. Although most modern periodic tables are arranged in eighteen groups (columns) of elements, Mendeleev's original periodic table had the elements organized into eight groups and twelve periods (rows).

On the periodic table, elements that have similar properties are in the same groups (vertical). From left to right, the atomic number (z) of the elements increases from one period to the next (horizontal). The groups are numbered at the top of each column and the periods on the left next to each row. The main group elements are groups 1,2 and 13 through 18. These groups contain the most naturally abundant elements, and are the most important for life. The elements shaded in light pink in the table above are known as transition metals. The two rows of elements starting at z=58, are sometimes called inner transition metals and have that have been extracted and placed at the bottom of the table, because they would make the table too wide if kept continuous. The 14 elements following lanthanum (z=57) are called lanthanides, and the 14 following actinium (z=89) are called actinides.

Elements in the periodic table can be placed into two broad categories, metals and nonmetals. Most metals are good conductors of heat and electricity, are malleable and ductile, and are moderate to high melting points. In general, nonmetals are nonconductors of heat and electricity, are nonmalleable solids, and many are gases at room temperature. Just as shown in the table above, metals and nonmetals on the periodic table are often separated by a stairstep diagonal line, and several elements near this line are often called metalloids (Si, Ge, As, Sb, Te, and At). Metalloids are elements that look like metals and in some ways behave like metals but also have some nonmetallic properties. The group to the farthest right of the table, shaded orange, is known as the noble gases. Noble gases are treated as a special group of nonmetals.

Alkali Metals/Alkali Earth Metals

The Alkali metals are comprised of group 1 of the periodic table and consist of Lithium, Sodium, Rubidium, Cesium, and Francium. These metals are highly reactive and form ionic compounds (when a nonmetal and a metal come together) as well as many other compounds. Alkali metals all have a charge of +1 and have the largest atom sizes than any of the other elements on each of their respective periods.

Alkali Earth Metals are located in group 2 and consist of Beryllium, Magnesium, Calcium, Strontium, Barium, and Radium. Unlike the Alkali metals, the earth metals have a smaller atom size and are not as reactive. These metals may also form ionic and other compounds and have a charge of +2.

Transition Metals

The transition metals range from groups IIIB to XIIB on the periodic table. These metals form positively charged ions, are very hard, and have very high melting and boiling points. Transition metals are also good conductors of electricity and are malleable.

Lanthanides and Actinides

Lanthanides (shown in row ** in chart above) and Actinides (shown in row * in chart above), form the block of two rows that are placed at the bottom of the periodic table for space issues. These are also considered to be transition metals. Lanthanides are form the top row of this block and are very soft metals with high boiling and melting points. Actinides form the bottom row and are radioactive. They also form compounds with most nonmetals. To find out why these elements have their own section, check out the electron configurations page.

Metalloids

Metalloids are located along the staircase separating the metals from the nonmetals on the periodic table. Boron, silicon, germanium, arsenic, antimony, and tellurium all have metal and nonmetal properties. For example, Silicon has a metallic luster but

is brittle and is an inefficient conductor of electricity like a nonmetal. As the metalloids have a combination of both metallic and nonmetal characteristics, they are intermediate conductors of electricity or "semiconductors".

Halogens

Halogens are comprised of the five nonmetal elements Flourine, Chlorine, Bromine, Iodine, and Astatine. They are located on group 17 of the periodic table and have a charge of -1. The term "halogen" means "salt-former" and compounds that contain one of the halogens are salts. The physical properties of halogens vary significantly as they can exist as solids, liquids, and gases at room temperature. However in general, halogens are very reactive, especially with the alkali metals and earth metals of groups 1 and 2 with which they form ionic compounds.

Noble Gases

The noble gases consist of group 18 (sometimes reffered to as group O) of the periodic table of elements. The noble gases have very low boiling and melting points and are all gases at room temperature. They are also very nonreactive as they already have a full valence shell with 8 electrons. Therefore, the noble gases have little tendency to lose or gain electrons.

A Summary of Periodic Properties

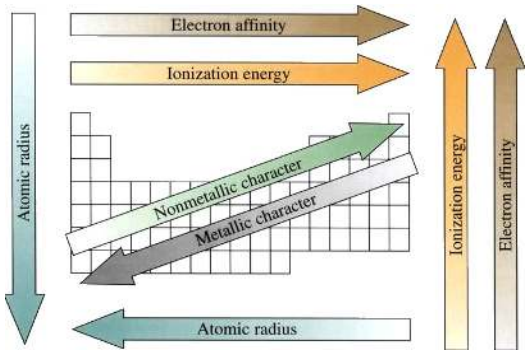


Figure 1.3.1: Courtesy of Wikipedia for releasing this image into the public domain

Problems

? Exercise 1.3.1

Which element is an example of a metalloid

a. S
b. Zn
c. Ge
d. Re
e. none of these

Answer

c. Ge

? Exercise 1.3.2

In the periodic table, the vertical (up and down) columns are called

a. periods
b. transitions
c. families/groups
d. metalloids
e. none of these

Answer

c. families/groups

Exercise 1.3.3

Why are noble gases inert (nonreactive)?

Answer

Noble gases are inert because they already have a full valence electron shell and have little tendency to gain or lose electrons.

Exercise 1.3.4

Lanthanides and Actinides are

a. alkali earth metals
b. transition metals
c. metalloids
d. alkali metals
e. none of these

Answer

b. transtion metals

1.3: Periodic Properties of the Periodic Table is shared under a CC BY-NC-SA 4.0 license and was authored, remixed, and/or curated by Kathryn A. Newton, Northern Michigan University.

- **Periodic Properties of the Elements** is licensed CC BY-NC-SA 4.0.

1.3.1: Atomic Radius

Estimated Time to Read: 6 min

Determining Atomic Radius

The atomic radius is one-half the distance between the nuclei of two atoms (just like a radius is half the diameter of a circle). However, this idea is complicated by the fact that not all atoms are normally bound together in the same way. Some are bound by covalent bonds in molecules, some are attracted to each other in ionic crystals, and others are held in metallic crystals. The SI units for measuring atomic radii are the nanometer (nm) and the picometer (pm). $1\,nm = 1 \times 10^{-9}\,m$ and $1\,pm = 1 \times 10^{-12}\,m$.

Atomic radii can be obtained from quantum mechanical calculations or can be determined experimentally. When calculated, the atomic radius is defined as the radius of the spherical volume in which the electron can be observed with 90% probability. Calculate atomic radii are shown in Figure **1.3.1.1**.

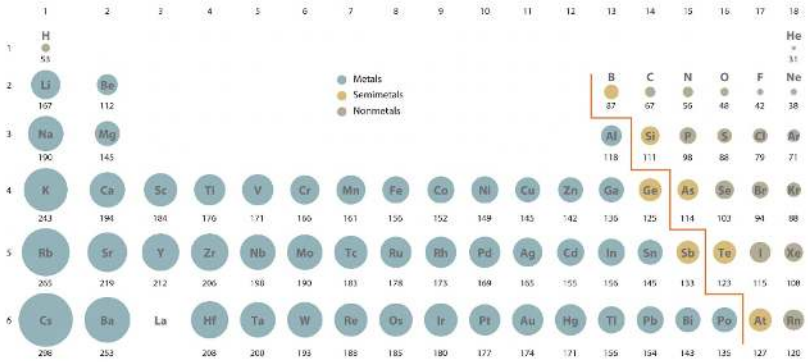


Figure 1.3.1.1: Calculated atomic radii of the elements in the periodic table (CC-BY-NC-SA; Kai Ladskron)

The measurement of atomic or ionic size will depend on a number of factors, including the covalent character of bonding in any particular molecule, coordination number, physical state (liquid, solid, gas), the identity of nearby atoms/ions, variation in crystal structure, and distortions within regular crystal structures. You should keep in mind that the size of an atom or ion is a "fuzzy" measure, and the radius under a different set of conditions will probably change slightly. Depending on how the atomic radius is measured, it will be classified as a (Figure **1.3.1.2**):

- **Covalent radius:** The radius of an atom is derived from the bond length within a nonpolar molecule; one-half the distance between the nuclei of two atoms within a covalent bond.
- **Metallic or Crystal radius**: The radius of an atom is determined using electron density maps from X-ray data; one-half the distance between the nuclei of two neighboring atoms in a crystal structure.
- **van der Waals radius:** The radius of an atom is determined by collision with other atoms; one-half the distance between two atoms that are not bonded but are brought together by intermolecular forces.

The relative atomic sizes shown in Figure **1.3.1.3** were derived from crystallographic data.

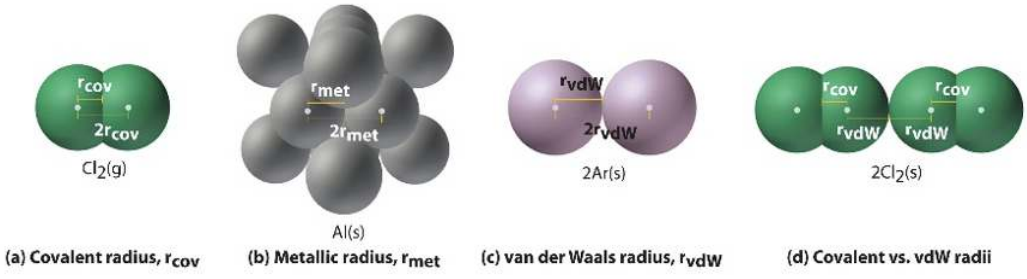


Figure 1.3.1.2: Definitions of Measured Atomic Radii: a) covalent radius, b) metallic radius, c) van der Waals radius, and d) a comparison of covalent and van der Waals radii (CC-BY-NC-SA; Kai Ladskron)

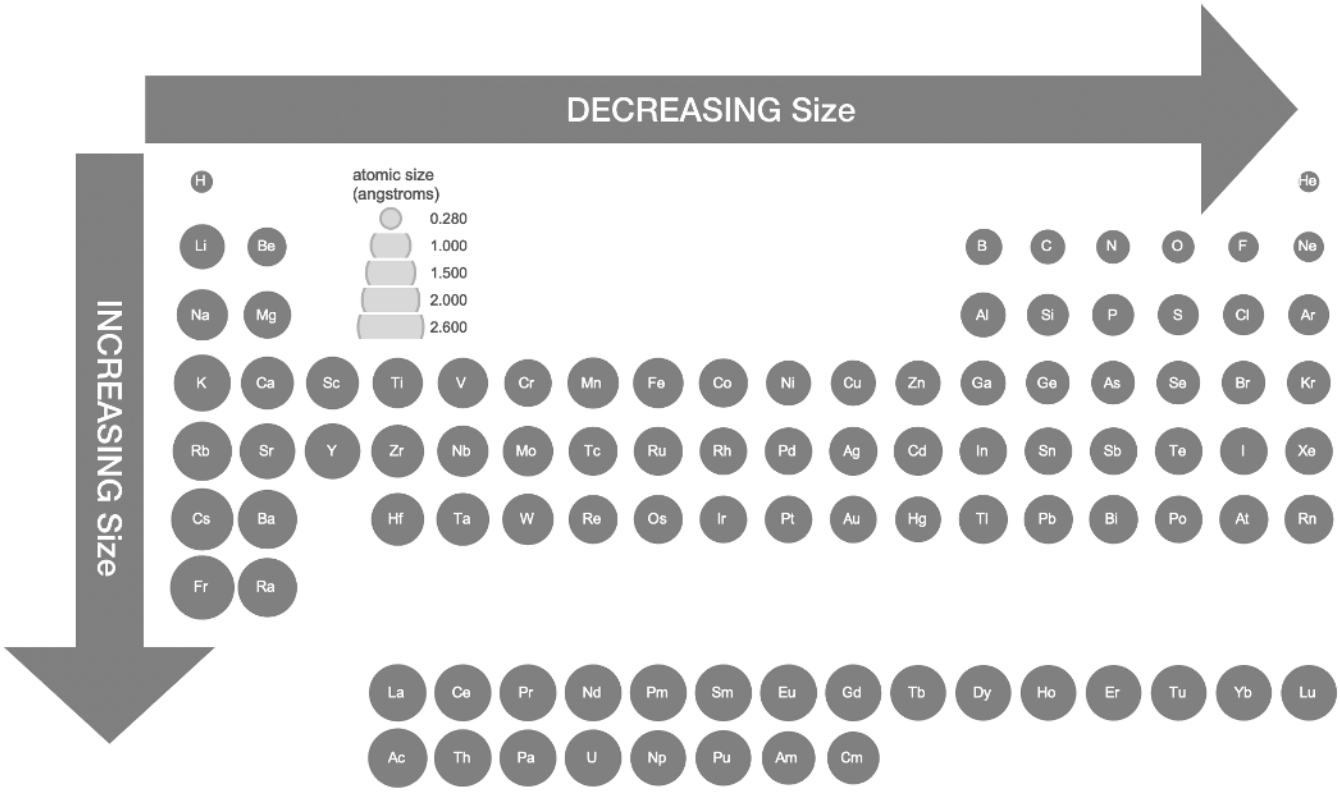


Figure 1.3.1.3. *Atomic Radii Calculated from Crystalographic Data. Data from Cordero, Beatriz, Veronica Gomez, Ana E. Platero-Prats, Marc Reves, Jorge Echeverria, Eduard Cremades, Flavia Barragan, and Santiago Alvarez. "Covalent Radii Revisited." Dalton Transactions, no. 21 (2008): 2832–38. doi:10.1039/b801115j.*[1] (CC-BY-NC-SA; LibreText)

Trends in Atomic Radius

Moving from left to right across a period, a proton is added to the nucleus for each element, making the nucleus more positively charged. At the same time, an electron is added the the electron energy shell, adding negative charge. The effect of increasing the number of protons is greater than that of increasing the number of electrons; therefore, there nuclear attraction for the electrons increases with the addition of each proton and electron. This means that the nucleus attracts the electrons more strongly, pulling the atom's shell closer to the nucleus. As a result, the atomic radius decreases as you move left to right across a period (Figure **1.3.1.4**).

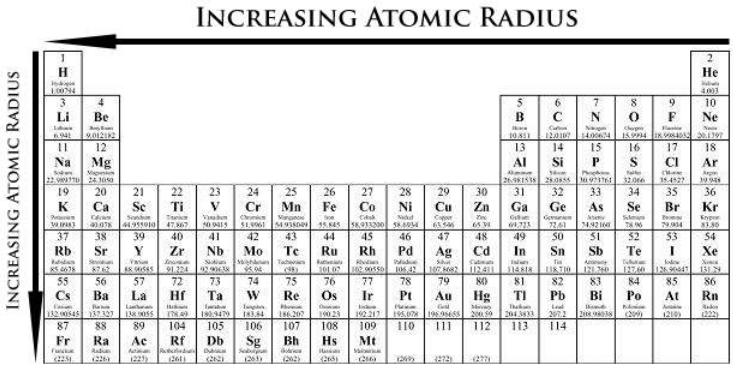


Figure 1.3.1.4: Periodic Table showing Atomic Radius Trend (LibreText)

Down a group, atomic radius increases. The valence electrons occupy higher energy shells due to the increasing quantum number (*n*). As a result, the valence electrons are further away from the nucleus as *n* increases.

https://chem.libretexts.org/@go/page/551188

- Atomic radius **decreases** from left to right within a period. This is caused by the increase in the number of protons and electrons across a period. One proton has a greater effect than one electron; thus, electrons are pulled towards the nucleus, resulting in a smaller radius.
- Atomic radius **increases from top to bottom** within a group. This is caused by electrons being add to higher energy levels that are futher from the nucleus.

Trends in Ionic Radius

An ionic radius is one-half the distance between the nuclei of two ions in an ionic bond. The distance must be apportioned for the smaller cation and larger anion. Trends in ionic radius follow the general trends in atomic radius for ions of the same charge. Ionic radius varies with the charge of the ion (and number of electrons) and the electron configuration.

Cations

Compared to their atoms, cations have the same number of protons but fewer electrons. Removal of electrons from an atom to form a cation results in a significant increase in effective nuclear charge, resulting in all other electrons being more strongly attracted to the nucleus. The result is a contraction in size from the atom to cation. Figure **1.3.1.5** visually illustrates the relative size of atoms and some cations of the first four periods; the data is available in tabular format in Figure **1.3.1.6**.

Anions

Compared to their atoms, anions have the same number of protons but more electrons. Addition of electrons to an atom to form an anion results in a decrease in effective nuclear charge, which corresponds to a decrease in attractive force between the nucleus and electrons. Lower attractive force leads to expansion, where the size of the atom becomes larger in the formation of an anion. Figure **1.3.1.5** visually illustrates the relative size of atoms and some anions of the first four periods, while the data is available in tabular format in Figure **1.3.1.6**.

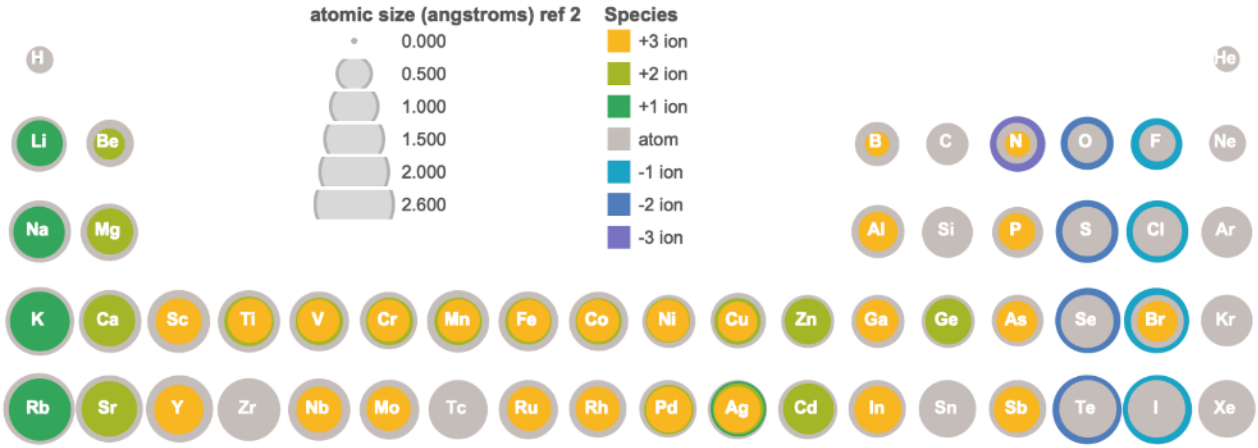


Figure 1.3.1.5. The relative size of atoms and ions of the first four periods of the periodic table. Atomic radii are indicated by grey circles. Cationic radii are shown in green (+1), yellow-green(+2), and yellow (+3) circles. Anionic radii are shown as aqua (-1), blue (-2), and purple (-3) circles.[1-3] (ChemLibre)

H 0.31 (atom) 0 (+1)																	He 0.28 (atom)
Li 1.28 (atom) 0.9 (+1) - -	Be 0.96 (atom) 0.41 (+2) -												B 0.84 (atom) 0.25 (+1)	C 0.76 (atom) 0.29 (+4)	N 1.32 (-3) 0.71 (atom) 0.3 (+3) 0.27 (+5)	O 1.21 (-2) 0.66 (atom)	F 1.145 (-1) 0.57 (atom)	Ne 0.58 (atom)
Na 1.66 (atom) 1.16 (+1)	Mg 1.41 (atom) 0.86 (+2)												Al 1.21 (atom) 0.675 (+3)	Si 1.11 (atom) 0.4 (+4)	P 1.07 (atom) 0.58 (+3) 0.31 (+5)	S 1.7 (-2) 1.05 (atom) 0.51 (+4) 0.26 (+6)	Cl 1.67 (-1) 1.02 (atom)	Ar 1.06 (atom)
K 2.03 (atom) 1.52 (+1)	Ca 1.76 (atom) 1.14 (+2)	Sc 1.7 (atom) 0.885 (+3)	Ti 1.6 (atom) 1 (+2) 0.81 (+3) 0.745 (+4)	V 1.53 (atom) 0.93 (+2) 0.78 (+3) 0.72 (+4)	Cr 1.39 (atom) 0.94 (+2 hs) 0.87 (+2 ls) 0.7555 (+3) 0.69 (+4) 0.63 (+5) 0.58 (+6)	Mn 1.61 (atom) 0.97 (+2 hs) 0.81 (+2 ls) 0.785 (+3 hs) 0.72 (+3 ls) 0.67 (+4) 0.47 (+5) 0.395 (+6) 0.39 (+7)	Fe 1.52 (atom) 0.92 (+2 hs) 0.785 (+3 hs) 0.75 (+2 ls) 0.725 (+4) 0.69 (+3 ls) 0.39 (+6)	Co 1.5 (atom) 0.885 (+2 hs) 0.79 (+2 ls) 0.75 (+3 hs) 0.685 (+3 ls) 0.67 (+4 hs)	Ni 1.24 (atom) 0.83 (+2) 0.74 (+3 hs) 0.7 (+3 ls) 0.62 (+4)	Cu 1.32 (atom) 0.91 (+1, cn6) 0.87 (+2, cn6) 0.68 (+3, cn6)	Zn 1.22 (atom) 0.88 (+2)	Ga 1.22 (atom) 0.76 (+3)	Ge 1.2 (atom) 0.87 (+2) 0.67 (+4)	As 1.19 (atom) 0.72 (+3) 0.6 (+5)	Se 1.84 (-2) 1.2 (atom) 0.64 (+4) 0.56 (+6)	Br 1.82 (-1) 1.2 (atom) 0.73 (+3) 0.53 (+7) 0.45 (+5)	Kr 1.16 (atom)
Rb 2.2 (atom) 1.66 (+1)	Sr 1.95 (atom) 1.32 (+2)	Y 1.9 (atom) 1.04 (+3)	Zr 1.75 (atom) 0.86 (+4)	Nb 1.64 (atom) 0.86 (+3) 0.82 (+4) 0.78 (+5)	Mo 1.54 (atom) 0.83 (+3) 0.79 (+4) 0.75 (+5) 0.73 (+6)	Tc 1.47 (atom) 0.785 (+4) 0.74 (+5) 0.7 (+7)	Ru 1.46 (atom) 0.82 (+3) 0.76 (+4) 0.705 (+5) 0.52 (+7) 0.5 (+8)	Rh 1.42 (atom) 0.805 (+3) 0.74 (+4) 0.69 (+5)	Pd 1.39 (atom) 0.73 (+1) 1 (+2) 0.9 (+3) 0.755 (+4)	Ag 1.45 (atom) 1.29 (+1) 1.08 (+2) 0.89 (+3)	Cd 1.44 (atom) 1.09 (+2)	In 1.42 (atom) 0.94 (+3)	Sn 1.39 (atom) 0.83 (+4)	Sb 1.39 (atom) 0.9 (+3) 0.74 (+5)	Te 2.07 (-2) 1.38 (atom) 1.1 (+4) 0.7 (+6)	I 2.06 (-1) 1.39 (atom) 1.09 (+5) 0.67 (+7)	Xe 1.4 (atom) 0.62 (+8)

Figure 1.3.1.6. Atomic and ionic radii in Angstroms of elements in the first four periods of the periodic table. Radii from each element are listed from largest to smallest. Ionic charge is indicated in parentheses. (hs = high spin, ls = low spin, cn6 = coordination number is 6).[1-3] (ChemLibre)

Problems

? Exercise 1.3.1.1

True or False? Nitrogen has a larger atomic radius than oxygen.

Answer

True

Atomic radius increases from right to left on the periodic table. Therefore, nitrogen is larger than oxygen.

? Exercise 1.3.1.2

Which atom has a smaller atomic radius smaller than that of sulfur (S)?

a. Oxygen (O)
b. Chlorine (Cl)
c. Calcium (Ca)
d. Lithium (Li)
e. None of the above

Answer

a. Oxygen (O)

Periodic trends indicate that atomic radius increases up a group and from left to right across a period. Therefore, oxygen has a smaller atomic radius sulfur

? Exercise 1.3.1.3

True or False? A nonmetal has a smaller ionic radius compared with a metal of the same period.

Answer

False

The reasoning behind this lies in the fact that a metal usually loses an electron in becoming an ion while a non-metal gains an electron. This results in a smaller ionic radius for the metal ion and a larger ionic radius for the non-metal ion.

? Exercise 1.3.1.4

Arrange these elements according to decreasing atomic size: Na, C, Sr, Cu, Fr

Answer

Fr, Sr, Cu, Na, C

? Exercise 1.3.1.5

Which has a larger atomic radius: nitrogen or oxygen?

Answer

Atomic radius increases from right to left on the periodic table. Therefore, nitrogen is larger than oxygen

? Exercise 1.3.1.6

Which of these elements has a smaller atomic radius than sulfur (S): O, Cl, Ca, Li

Answer

Oxygen (O) is the only element in the list with a smaller atomic radius than S. Periodic trends indicate that atomic radius increases down a group (from top to bottom) and from left to right across a period.

References

1. Cordero, Beatriz, Veronica Gomez, Ana E. Platero-Prats, Marc Reves, Jorge Echeverria, Eduard Cremades, Flavia Barragan, and Santiago Alvarez. *"Covalent Radii Revisited." Dalton Transactions, no. 21 (2008): 2832–38. doi:10.1039/b801115j.*
2. R. D. Shannon (1976). "Revised effective ionic radii and systematic studies of interatomic distances in halides and chalcogenides". *Acta Crystallogr A.* **32** (5): 751–767. Bibcode:1976AcCrA..32..751S. doi:10.1107/S0567739476001551.
3. Wikipedia articles on Atomic Radius and Ionic Radius.

1.3.1: Atomic Radius is shared under a CC BY-NC-SA 4.0 license and was authored, remixed, and/or curated by Kathryn A. Newton, Northern Michigan University.

- **Periodic Trends** by Bingyao Zheng, Emily Nguyen, Swetha Ramireddy is licensed CC BY-NC-SA 4.0.
- **1.3: Periodic Properties of Atoms** by Kai Landskron is licensed CC BY 4.0.
- **2.3.3: Covalent and Ionic Radii** by Bingyao Zheng, Emily Nguyen, Kathryn Haas, Swetha Ramireddy is licensed CC BY-NC 4.0.
- **2.4: Problems** by Kathryn Haas has no license indicated.

1.3.2: Ionization Energy

Estimated Time to Read: 4 min

Definition of Ionization Energy

Ionization energy is the energy required to remove an electron from a neutral atom in its gaseous phase. Ionization energy is always positive. Some elements can lose more than one electron and thus have several ionization energies. The first ionization energy is the energy required to remove the outermost, or highest energy, valence electron. The second ionization energy is the energy required to remove the next highest energy valence electron from a gaseous cation, etc. Below are the chemical equations describing the first and second ionization energies:

Equation 1.3.2.1: First Ionization Energy

$$X_{(g)} \rightarrow X^{+}_{(g)} + e^{-}$$

Equation 1.3.2.2: Second Ionization Energy

$$X^{+}_{(g)} \rightarrow X^{2+}_{(g)} + e^{-}$$

Table **1.3.2.1** gives the ionization energies for the period three elements. Notice how the second ionization energy for sodium, third ionization energy for magnesium, fourth ionization energy for aluminum, etc. are all much greater than the preceding ionization energy. This occurs because the preceding configuration was in a stable octet formation; therefore a much larger amount of energy is required to ionize the valence electron and break the octet formation.

Table 1.3.2.1: Ionization Energies of certain elements (1st IE, 2nd IE, etc.)

Element	1st	2nd	3rd	4th	5th	6th	7th
Na	496	4562					
Mg	738	1451	7733				
Al	577	1817	2745	11580			
Si	786	1577	3232	4356	16090		
P	1060	1903	2912	4957	6274	21270	
S	999.6	2251	3361	4564	7013	8496	27110
Cl	1256	2297	3822	5158	6542	9362	11020
Ar	1520	2666	3931	5771	7238	8781	12000

Trends in Ionization Energy

The lower the ionization energy is, the more readily the atom becomes a cation. Therefore, the higher the ionization energy is, the less readily the atom becomes a cation (Figure **1.3.2.1**). Generally, elements on the right side of the periodic table have a higher ionization energy because their valence shell is nearly filled. The highest ionization energies are the noble gases because they all have high effective charge due to their octet formation. Elements on the left side of the periodic table have low ionization energies because losing an electron allows them to have the noble gas configuration. Therefore, it requires less energy to remove one of their valence electrons, and ionization energy increases from left to right on the periodic table.

This trend can also be explained by the fact that the effective nuclear charge increases from the left to the right within a period as the number of protons increases. With each addition of a proton, the pull of the nucleus on the outmost electron increases, and it becomes more difficult to overcome the attractive forces of the nucleus and remove this electron from the atom.

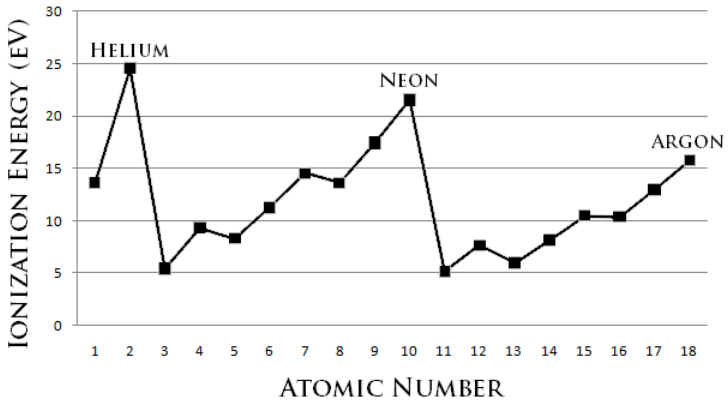


Figure 1.3.2.1: Graph showing the Ionization Energy of the Elements from Hydrogen to Argon (LibreText)

Within the main group elements, the trend is broken two times (Figure **1.3.2.2**). First, the group 13 elements have a lower ionization energy than the group 2 elements. Second, the group 16 elements have a lower ionization energy than the group 15 elements. This is explained by the fact that the filled and half-filled subshells in group 2 and group 15, respectively, are particularly stable electron configurations; thus, the electrons within these subshells have unusually low energy and require greater energy to be removed from the atom.

The increase in ionization energy across the period is less pronounced within the d-block, and even less pronounced within the f-block. This is because the effective nuclear charge on the outmost electrons does not increase as much because inner d and f orbitals are getting filled. Following the d-block, group 13 elements have a lower ionization energy than the group 12 elements. This is because in group 13 electrons are added to a new p subshell.

Ionization energy becomes smaller down a group as electrons are added to higher energy shells and the distance from the nucleus increases (*n* increases). The attractive forces of the nucleus are diminished as the electrons are further from the nucleus.

Generally, any subsequent ionization energies (2nd, 3rd, etc.) follow the same periodic trend as the first ionization energy.

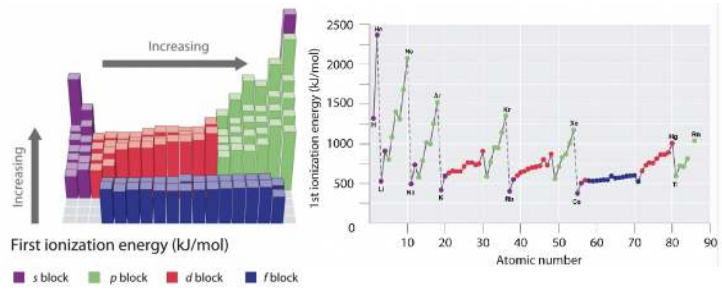


Figure 1.3.2.2: First ionization energies as a third dimension in the periodic table (left) and as function of atomic number (right) (CC-BY-NC-SA, LibreText)

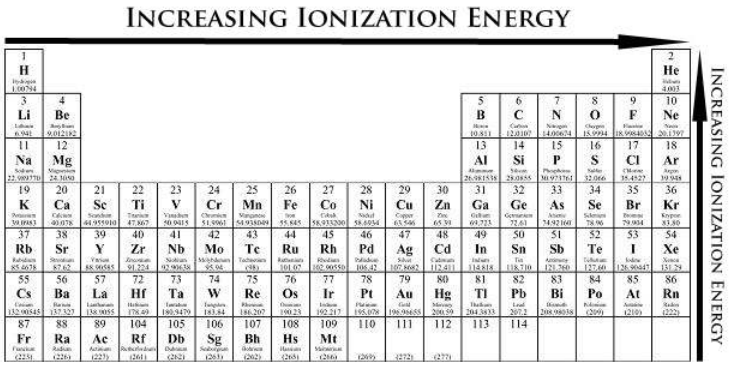


Figure 1.3.2.3: Periodic Table Showing Ionization Energy Trend (LibreText)

- The ionization energy of the elements within a period generally increases from left to right. This is due to valence shell stability.
- The ionization energy of the elements within a group generally decreases from top to bottom. This is due to increasing electron energy shell.
- The noble gases possess very high ionization energies because of their full valence shells.

Problems

? Exercise 1.3.2.1

Based on the periodic trends for ionization energy, which element has the highest ionization energy?

a. Fluorine (F)
b. Nitrogen (N)
c. Helium (He)

Answer

c. Helium (He)

? Exercise 1.3.2.2

Which reaction do you expect to occur?

a. $\mathrm{I_2(g) + 2\,Br(aq) \longrightarrow Br_2(s) + 2\,I(aq)}$
b. $\mathrm{Cl_2(g) + 2\,I(aq) \longrightarrow I_2(s) + 2\,Cl(aq)}$

Answer

a.

? Exercise 1.3.2.3

Based on the periodic trends for ionization energy, which element has the highest ionization energy?

Answer

Helium,He

References

- Cotton, F.A.; Wilkinson, G. (1988). *Advanced Inorganic Chemistry* (5th Edn). New York: Wiley. ISBN 0-471-84997p. 1385.
- Hutchinson, John. "Journal of Chemical Education." Concept Development Studies in Chemistry (2007). Print. Outside Links
- Jolly, William L. (1991). *Modern Inorganic Chemistry* (2nd Edn.). New York: McGraw-Hill. ISBN 0-07-112651-1.
- Petrucci, Ralph H. General Chemistry. 9th ed. New Jersey: Pearson Prentice Hall, 2005.

1.3.2: Ionization Energy is shared under a CC BY-NC-SA 4.0 license and was authored, remixed, and/or curated by Kathryn A. Newton, Northern Michigan University.

- **Periodic Trends** by Bingyao Zheng, Emily Nguyen, Swetha Ramireddy is licensed CC BY-NC-SA 4.0.
- **Periodic Properties of the Elements** is licensed CC BY-NC-SA 4.0.
- **2.4: Problems** by Kathryn Haas has no license indicated.

1.3.3: Electron Affinity

Estimated Time to Read: 4 min

Definition of Electron Affinity

Electron affinity is a quantitative measurement of the energy change that occurs when an electron is added to a neutral gaseous atom. The more negative the electron affinity value, the higher the electron affinity and the more easily an electron is added to an atom. Electron affinity can be either positive or negative. The greater the negative value, the more stable the anion is.

Equation 1.3.3.1: Exothermic, positive electron affinity

$$\mathbf{X(g) + e^- \longrightarrow X^- + Energy}$$

Equation 1.3.3.2: Endothermic, negative electron affinity

$$\mathbf{X(g) + e^- + Energy \longrightarrow X^-}$$

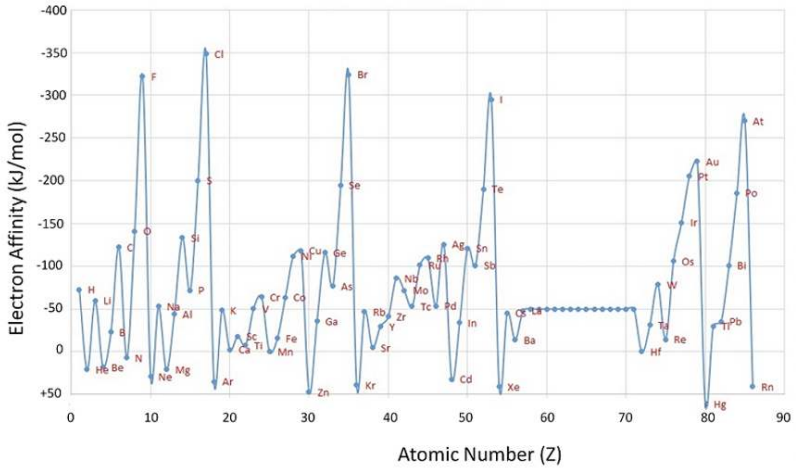


Figure 1.3.3.1: Electron affinity values (CC-BY-NC-SA, LibreText)

Figure **1.3.3.1** shows that most elements have negative electron affinities, meaning that the addition of a free electron to a neutral atom is exothermic. However, this is not always the case. Some elements (the noble gases, Be, N, Mg, Zn, Cd, and Hg) have positive electron affinities. Zn, Cd, and Hg are group 12 elements with a full d subshell, which is particularly stable, and an additional electron would need to be added to a p orbital of a higher shell which is energetically unfavorable. Similarly, Be and Mg have filled s subshells, which are also stable, and adding an additional electron would require a new subshell, which is energetically unfavorable. Ca and Sr have electron affinities of about 0, and that of Ba is only slightly negative. This shows that higher periods make the addition of an electron to a new p subshell slightly more favorable. Nitrogen has a half-filled p subshell, which is also a quite stable electron configuration, and therefore, adding an electron is not favorable. The addition of an electron is slightly more favorable for the other group 15 elements, however.

Trends in Electron Affinity

Moving from left to right across a period, atoms become smaller as the nuclear charge and the attractive forces of the nucleus become stronger. Electrons added to the valence shell are stabilized by the attractive force of the nucleus, thus the electron affinity increases (becomes more negative) more from left to right across a period. Electron affinity generally decreases (becomes less negative) down a group of elements as the distance from the nucleus of valence electrons increases as electrons are added to higher energy shells (*n* increases). The attractive forces of the nucleus decrease with a larger distance between the negatively-charged electron and the positively-charged nucleus, and therefore, electron affinity decreases.

Generally, the elements on the right side of the periodic table will have large negative electron affinity. However, Nitrogen, Oxygen, and Fluorine do not follow this trend. The noble gas electron configuration will be close to zero because they will not easily gain electrons. The general trend is also broken for group 2 and group 15 elements because these elements have full and half-

filled subshells, respectively. In addition, group 1 elements have higher electron affinities than group 3 elements. This is because adding an electron to a group 1 element produces a full s subshell, which is fairly stable. For the d-block elements, the electron affinity tends to increase from group 3 to group 11, but the trend is broken multiple times and each element would need to be investigated individually. There is a large drop in electron affinity from group 17 to group 18 which is explained by the fact that the addition of an electron to a group 17 element produces a filled shell, while a group 18 element already has a full shell and the addition of an electron would require a new shell. Similarly, there is a sharp drop in electron affinity from group 11 to group 12, as an addition of an electron to a group 11 atom produces a full subshell, while the addition of an electron to a group 12 element would require the start of new subshell.

In general, electron affinity decreases down a group. For the s-block there is a steady decrease down a group.For the p block elements the electron affinity tends to first increase from period 2 to 3, and then decreases. For d block elements there is no clear trend for the electron affinity.

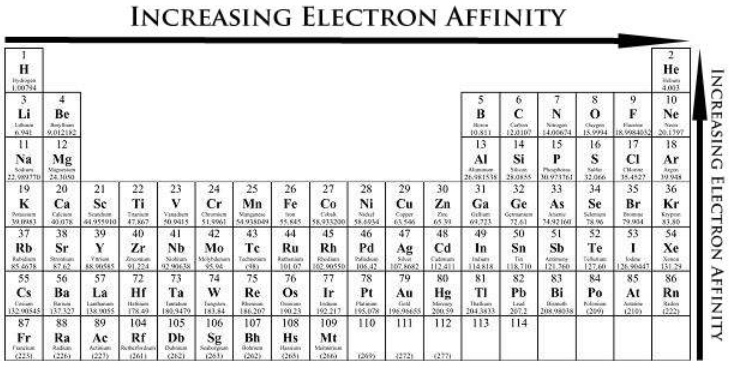


Figure 1.3.3.2: Periodic Table showing Electron Affinity Trend

- Electron affinity increases (becomes more negative) from left to right within a period. This is caused by the decrease in atomic radius.
- Electron affinity decreases (becomes less negative) from top to bottom within a group. This is caused by the increase in atomic radius.

Problems

? Exercise 1.3.3.1

Arrange the following elements in order of decreasing electron affinity: fluorine (F), phosphorous (P), sulfur (S), boron (B).

Answer

F > S > P > B

? Exercise 1.3.3.2

Arrange these elements according to increasingly negative electron affinity: Ba, F, Si, Ca, O .

Answer

Ba, Ca, Si, O, F

The following series of problems reviews general understanding of the aforementioned material.

Exercise 1.3.3.3

Rewrite the following list in order of decreasing electron affinity: fluorine (F), phosphorous (P), sulfur (S), boron (B).

Answer

Fluorine (F)>Sulfur (S)>Phosphorous (P)>Boron (B). Explanation: Electron affinity generally increases from left to right and from bottom to top.

1.3.3: Electron Affinity is shared under a CC BY-NC-SA 4.0 license and was authored, remixed, and/or curated by Swetha Ramireddy, Bingyao Zheng, Emily Nguyen, & Emily Nguyen.

- **Periodic Trends** by Bingyao Zheng, Emily Nguyen, Swetha Ramireddy is licensed CC BY-NC-SA 4.0.
- **Periodic Properties of the Elements** is licensed CC BY-NC-SA 4.0.
- **1.3: Periodic Properties of Atoms** by Kai Landskron is licensed CC BY 4.0.
- **2.4: Problems** by Kathryn Haas has no license indicated.

1.3.4: Electronegativity --- a molecular property

Electronegativity is the measurement of an atom to compete for electrons in a bond. The higher the electronegativity, the greater its ability to gain electrons in a bond. Electronegativity will be important when we later determine polar and nonpolar molecules. Electronegativity is related with ionization energy and electron affinity. Electrons with low ionization energies have low electronegativities because their nuclei do not exert a strong attractive force on electrons. Elements with high ionization energies have high electronegativities due to the strong pull exerted by the positive nucleus on the negative electrons. Therefore the electronegativity increases from bottom to top and from left to right.

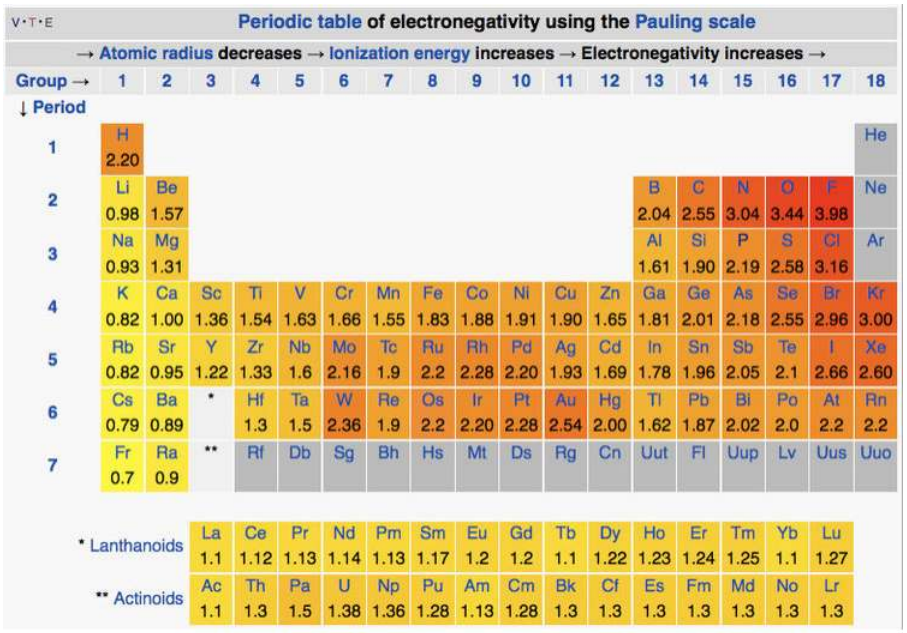
Definitions of Electronegativity

Linus Pauling introduced the first electronegativity scale in 1932 in order to explain the extra stability of molecules with polar bonds.[1] The electronegativity of an atom, represented by the Greek letter χ (chi), can be defined as the tendency of an atom to draw electrons to itself *in a chemical bond*. On the Pauling scale, the electronegativity difference between two atoms A and B was defined in terms of the dissociation energies E_d of the A-A, B-B, and A-B bonds:

Equation **1.3.4.1**:

$$\chi_A - \chi_B = \sqrt{E_d(AB) - [E_d(AA) + E_d(BB)]/2}$$

where the energies are expressed in electron volts. Pauling's scale of electronegativity ranges from Fluorine (most electronegative = 4.0) to Francium (least electronegative = 0.7). [2,3] The polarity of bonds and assignment of formal charges is predicted by electronegativity differences.



V·T·E **Periodic table of electronegativity using the Pauling scale**

→ Atomic radius decreases → Ionization energy increases → Electronegativity increases →

Group →	1	2	3	4	5	6	7	8	9	10	11	12	13	14	15	16	17	18
↓ Period																		
1	H 2.20																	He
2	Li 0.98	Be 1.57											B 2.04	C 2.55	N 3.04	O 3.44	F 3.98	Ne
3	Na 0.93	Mg 1.31											Al 1.61	Si 1.90	P 2.19	S 2.58	Cl 3.16	Ar
4	K 0.82	Ca 1.00	Sc 1.36	Ti 1.54	V 1.63	Cr 1.66	Mn 1.55	Fe 1.83	Co 1.88	Ni 1.91	Cu 1.90	Zn 1.65	Ga 1.81	Ge 2.01	As 2.18	Se 2.55	Br 2.96	Kr 3.00
5	Rb 0.82	Sr 0.95	Y 1.22	Zr 1.33	Nb 1.6	Mo 2.16	Tc 1.9	Ru 2.2	Rh 2.28	Pd 2.20	Ag 1.93	Cd 1.69	In 1.78	Sn 1.96	Sb 2.05	Te 2.1	I 2.66	Xe 2.60
6	Cs 0.79	Ba 0.89	*	Hf 1.3	Ta 1.5	W 2.36	Re 1.9	Os 2.2	Ir 2.20	Pt 2.28	Au 2.54	Hg 2.00	Tl 1.62	Pb 1.87	Bi 2.02	Po 2.0	At 2.2	Rn 2.2
7	Fr 0.7	Ra 0.9	**	Rf	Db	Sg	Bh	Hs	Mt	Ds	Rg	Cn	Uut	Fl	Uup	Lv	Uus	Uuo

* Lanthanoids	La 1.1	Ce 1.12	Pr 1.13	Nd 1.14	Pm 1.13	Sm 1.17	Eu 1.2	Gd 1.2	Tb 1.1	Dy 1.22	Ho 1.23	Er 1.24	Tm 1.25	Yb 1.1	Lu 1.27
** Actinoids	Ac 1.1	Th 1.3	Pa 1.5	U 1.38	Np 1.36	Pu 1.28	Am 1.13	Cm 1.28	Bk 1.3	Cf 1.3	Es 1.3	Fm 1.3	Md 1.3	No 1.3	Lr 1.3

Figure **1.3.4.1**: Table of Pauling electronegativities from [Wikipedia]

While directly relevant to the strength of chemical bonds, the Pauling definition of electronegativity has a significant limitation: calculating each value requires data from several compounds in which specific atoms are bonded. This means that the scale cannot be successfully applied to all situations. To overcome this limitation, alternative electronegativity scales were developed based on different thermochemical measurements or calculations. These other scales are listed in Table \PageIndes1 below. More thorough descriptions of how values in each scale are calculated are described on Wikipedia's Electronegativity page and a concise history of electronegativity scales is summarized in ref 4.

Table **1.3.4.1**: Electronegativity Scales and Their Defining Characterisitics

Scale Developer	Year first described	Characteristics
Linus Pauling[1]	1932	Based on bond energies
Robert S. Mulliken[5,6]	1934	Based on valence electron properties of atoms (electron affinity and ionization energy)
Louis Allred & Eugene G. Rochow[7]	1958	Based on electrostatic force (effective nuclear charge)
Robert T. Sanderson[8]	1983	Based on atomic electron density
Ralph G. Pearson[9]	1985	Related to Hard-Soft Acid-Based theory
Leland C. Allen, Joseph Mann, Terry L. Meek[10,11,12]	1989, 2000	Average ionization energies of valence shell electrons, configuration energies (CE) $$\mathrm{CE} = \frac{n\varepsilon_s + m\varepsilon_p}{n+m}$$ n = number of s electrons m = number of p electrons $\varepsilon_s, \varepsilon_p$ = experimental 1-electron s and p energies

The primary advantage to the scale developed by Mann, Meek, and Allen[12] is that it is based on configuration energy (CE), the average ionization energies of valence electrons in ground state free atoms. A scale based on ionization energies can be calculated more directly for any element. However, a critique of all electronegativity scales, including this one, is that they are all based on assumptions that fail in some cases.

There is a relationship between electronegativity and atomic size because both are related to ionization energy. Like ionization energy, there is a general trend across the periodic table for both electronegativity and atomic size; in general, smaller atoms toward the top right-hand side of the periodic table have greater electronegativity values and smaller atomic size.

Electronegativity Trends

Electronegativity is a qualitative property, and although there is no standardized method for calculating electronegativity the most common scale for quantifying electronegativity is the Pauling scale (Table A2), named after the chemist Linus Pauling. The numbers assigned by the Pauling scale are dimensionless due to the qualitative nature of electronegativity. Electronegativity values for each element can be found on certain periodic tables (Figure **1.3.4.2**.

Periodic Table of Elements

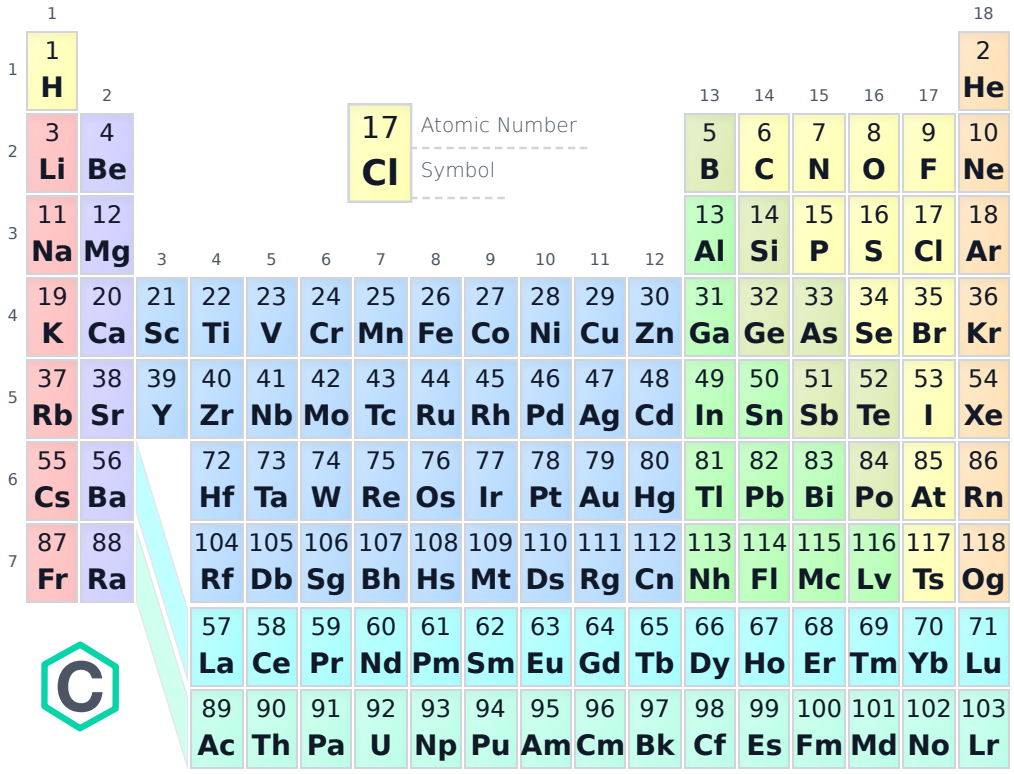


Figure 1.3.4.2: Periodic Table with Electronegativity Values

Electronegativity measures an atom's tendency to attract and form bonds with electrons. This property exists due to the electronic configuration of atoms. Most atoms follow the octet rule (having the valence, or outer, shell comprise of 8 electrons). Because elements on the left side of the periodic table have less than a half-full valence shell, the energy required to gain electrons is significantly higher compared with the energy required to lose electrons. As a result, the elements on the left side of the periodic table generally lose electrons when forming bonds. Conversely, elements on the right side of the periodic table are more energy-efficient in gaining electrons to create a complete valence shell of 8 electrons. The nature of electronegativity is effectively described thus: the more inclined an atom is to gain electrons, the more likely that atom will pull electrons toward itself.

- **From left to right across a period of elements, electronegativity increases.** If the valence shell of an atom is less than half full, it requires less energy to lose an electron than to gain one. Conversely, if the valence shell is more than half full, it is easier to pull an electron into the valence shell than to donate one.
- **From top to bottom down a group, electronegativity decreases.** This is because atomic number increases down a group, and thus there is an increased distance between the valence electrons and nucleus, or a greater atomic radius.
- **Important exceptions of the above rules include the noble gases, lanthanides, and actinides.** The noble gases possess a complete valence shell and do not usually attract electrons. The lanthanides and actinides possess more complicated chemistry that does not generally follow any trends. Therefore, noble gases, lanthanides, and actinides do not have electronegativity values.
- **As for the transition metals, although they have electronegativity values, there is little variance among them across the period and up and down a group.** This is because their metallic properties affect their ability to attract electrons as easily as the other elements.

According to these two general trends, the *most electronegative element is* ***fluorine***, with 3.98 Pauling units.

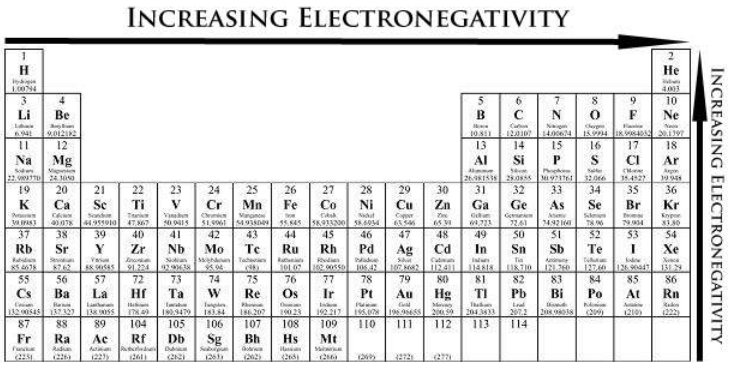


Figure 1.3.4.3: Periodic Table showing Electronegativity Trend (LibreText)

Acknowledgment

- Matthew Salem (UC Davis) (Pauling Electronegativity)
- Introduction to Inorganic Chemistry Wikibook (https://chem.libretexts.org/Bookshel..._Bond_Strength)
- Kathryn Haas (Duke) (https://chem.libretexts.org/@go/page/219071)

1.3.4: Electronegativity --- a molecular property is shared under a CC BY-NC-SA 4.0 license and was authored, remixed, and/or curated by Kathryn A. Newton, Northern Michigan University.

- **Periodic Properties of the Elements** is licensed CC BY-NC-SA 4.0.
- **3.2.3: Electronegativity and Atomic Size Effects** by Kathryn Haas has no license indicated.
- **Periodic Trends** by Bingyao Zheng, Emily Nguyen, Swetha Ramireddy is licensed CC BY-NC-SA 4.0.

1.4: Effective Nuclear Charge (Zeff) and Shielding (S); the Reason for Periodicity

Estimated Time to Read: 4 min

Definition of Electron Affinity

Electron affinity is a quantitative measurement of the energy change that occurs when an electron is added to a neutral gaseous atom. The more negative the electron affinity value, the higher the electron affinity and the more easily an electron is added to an atom. Electron affinity can be either positive or negative. The greater the negative value, the more stable the anion is.

Equation 1.4.1: Exothermic, positive electron affinity

$$\mathbf{X(g) + e^- \longrightarrow X^- + Energy}$$

Equation 1.4.2: Endothermic, negative electron affinity

$$\mathbf{X(g) + e^- + Energy \longrightarrow X^-}$$

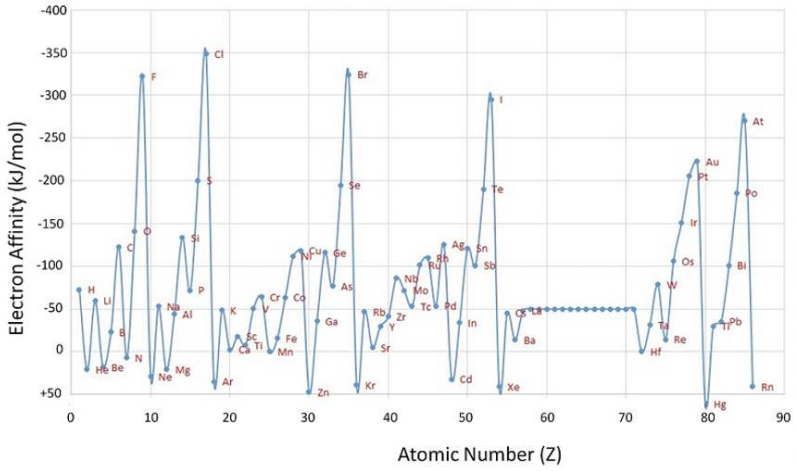


Figure 1.4.1: Electron affinity values (CC-BY-NC-SA, LibreText)

Figure **1.4.1** shows that most elements have negative electron affinities, meaning that the addition of a free electron to a neutral atom is exothermic. However, this is not always the case. Some elements (the noble gases, Be, N, Mg, Zn, Cd, and Hg) have positive electron affinities. Zn, Cd, and Hg are group 12 elements with a full d subshell, which is particularly stable, and an additional electron would need to be added to a p orbital of a higher shell which is energetically unfavorable. Similarly, Be and Mg have filled s subshells, which are also stable, and adding an additional electron would require a new subshell, which is energetically unfavorable. Ca and Sr have electron affinities of about 0, and that of Ba is only slightly negative. This shows that higher periods make the addition of an electron to a new p subshell slightly more favorable. Nitrogen has a half-filled p subshell, which is also a quite stable electron configuration, and therefore, adding an electron is not favorable. The addition of an electron is slightly more favorable for the other group 15 elements, however.

Trends in Electron Affinity

Moving from left to right across a period, atoms become smaller as the nuclear charge and the attractive forces of the nucleus become stronger. Electrons added to the valence shell are stabilized by the attractive force of the nucleus, thus the electron affinity increases (becomes more negative) more from left to right across a period. Electron affinity generally decreases (becomes less negative) down a group of elements as the distance from the nucleus of valence electrons increases as electrons are added to higher energy shells (*n* increases). The attractive forces of the nucleus decrease with a larger distance between the negatively-charged electron and the positively-charged nucleus, and therefore, electron affinity decreases.

Generally, the elements on the right side of the periodic table will have large negative electron affinity. However, Nitrogen, Oxygen, and Fluorine do not follow this trend. The noble gas electron configuration will be close to zero because they will not easily gain electrons. The general trend is also broken for group 2 and group 15 elements because these elements have full and half-

filled subshells, respectively. In addition, group 1 elements have higher electron affinities than group 3 elements. This is because adding an electron to a group 1 element produces a full s subshell, which is fairly stable. For the d-block elements, the electron affinity tends to increase from group 3 to group 11, but the trend is broken multiple times and each element would need to be investigated individually. There is a large drop in electron affinity from group 17 to group 18 which is explained by the fact that the addition of an electron to a group 17 element produces a filled shell, while a group 18 element already has a full shell and the addition of an electron would require a new shell. Similarly, there is a sharp drop in electron affinity from group 11 to group 12, as an addition of an electron to a group 11 atom produces a full subshell, while the addition of an electron to a group 12 element would require the start of new subshell.

In general, electron affinity decreases down a group. For the s-block there is a steady decrease down a group.For the p block elements the electron affinity tends to first increase from period 2 to 3, and then decreases. For d block elements there is no clear trend for the electron affinity.

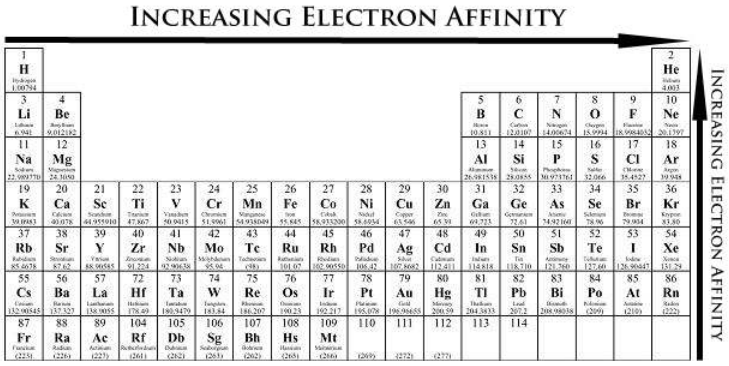


Figure 1.4.2: Periodic Table showing Electron Affinity Trend

- Electron affinity increases (becomes more negative) from left to right within a period. This is caused by the decrease in atomic radius.
- Electron affinity decreases (becomes less negative) from top to bottom within a group. This is caused by the increase in atomic radius.

Problems

? Exercise 1.4.1

Arrange the following elements in order of decreasing electron affinity: fluorine (F), phosphorous (P), sulfur (S), boron (B).

Answer

F > S > P > B

? Exercise 1.4.2

Arrange these elements according to increasingly negative electron affinity: Ba, F, Si, Ca, O .

Answer

Ba, Ca, Si, O, F

The following series of problems reviews general understanding of the aforementioned material.

Exercise 1.4.3

Rewrite the following list in order of decreasing electron affinity: fluorine (F), phosphorous (P), sulfur (S), boron (B).

Answer

Fluorine (F)>Sulfur (S)>Phosphorous (P)>Boron (B). Explanation: Electron affinity generally increases from left to right and from bottom to top.

1.4: Effective Nuclear Charge (Zeff) and Shielding (S); the Reason for Periodicity is shared under a CC BY-NC-SA 4.0 license and was authored, remixed, and/or curated by Swetha Ramireddy, Bingyao Zheng, Emily Nguyen, & Emily Nguyen.

- **Periodic Trends** by Bingyao Zheng, Emily Nguyen, Swetha Ramireddy is licensed CC BY-NC-SA 4.0.
- **Periodic Properties of the Elements** is licensed CC BY-NC-SA 4.0.
- **1.3: Periodic Properties of Atoms** by Kai Landskron is licensed CC BY 4.0.
- **2.4: Problems** by Kathryn Haas has no license indicated.

1.4.1: Slater's Rules

Estimated Time to Read: 7 min

We have previously described the concepts of electron shielding, orbital penetration and effective nuclear charge, but we did so in a qualitative manner. In this section, we explore one model for quantitatively estimating electron shielding and calculating the effective nuclear charge experienced by an electron in an atom. The model we will use is known as Slater's Rules (J.C. Slater, *Phys Rev* **1930**, *36*, 57).

Effective Nuclear Charge

The effective nuclear charge Z_{eff} is less than the actual nuclear charge (Z) because of the repulsive interaction between core and valence electrons. We can quantitatively represent this difference between Z and Z_{eff} as follows:

Equation **1.4.1.1**

$$S = Z - Z_{eff} \tag{1.4.1.1}$$

Rearranging this formula to solve for Z_{eff} we obtain Equation **1.4.1.1**

$$Z_{eff} = Z - S \tag{1.4.1.2}$$

The shielding constant S is estimated using Slater's Rules. Then the shielding constant is substituted into Equation **1.4.1.2** to calculate an estimate of Z_{eff} for the corresponding atomic electron.

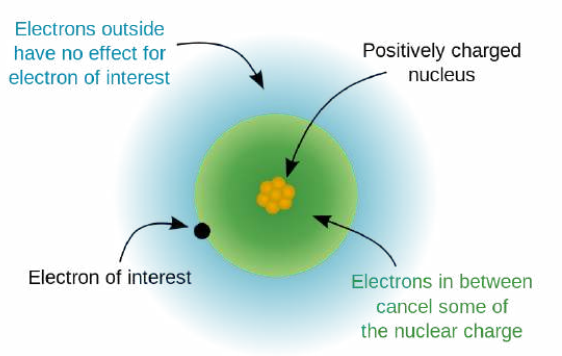


Figure 1.4.1.1: Shielding by electrons closer to the nucleus results in a lower effective nuclear charge. (Copyright; author via source)

Slater's Rules

Shielding is calculated for an electron-of-interest. Shielding occurs when "other" electrons in lower energy shells (or the same energy shell) provide a repulsive force to an electron-of-interest in a higher energy shell. The repulsive force negates some of the attractive force from the positive nucleus on the electron-of-interest. The "other" electrons in the same shell as the electron-of-interest shield least effectively, while those closest to the nucleus shield the most effectively. Slater's rules specify the degree of shielding for each inner shell electron and are used to calculate the overall shielding experienced by an electron in an s-, p-, d-, or f-orbital.

The shielding numbers in Table **1.4.1.1** were derived semi-empirically (i.e., derived from experiments) as opposed to theoretical calculations. This is because quantum mechanics makes calculating shielding effects quite difficult and outside the scope of this text.

Slater's Rules estimate effective nuclear charge for an electron-of-interest based on how many other electrons exist in the atom and on the location of the electron-of-interest. In the calculation of the shielding constant S, it is assumed that electrons closer to the nucleus than the electron-of-interest cancel some of the nuclear charge; those farther from the nucleus have no effect. For an electron-of-interest in an s or p orbital, electrons in the same shell (with the same principle quantum number *n*)will shield the electron-of-interest 0.35 units. *Conceptually, this means electrons in the same shell shield each other 35%.* Electrons in the lower energy shell *n-1* contribute 0.85 to S. All the electrons in even lower shells contribute 1.00 to S. *Conceptually, this means that s and*

p electrons are shielded 85% by the electrons one shell lower, and 100% by all electrons in shells n - 2 or lower. For an electron-of-interest in a d or f orbital, all electrons in the same shell (with the same principle quantum number *n*) and subshell (with the same angular momentum quantum number *l*) will shield the electron-of-interest 0.35 units. All other electrons contribute 1.00 to S. *Conceptually, this means that electrons in the same subshell shield each other 35%, and all other electrons shield 100%.* Note: The shielding constant S of a 1s electron is just S=0.3, no matter the element.

Table 1.4.1.1: Shielding values for electrons in inner orbitals based on their principle and angular moment quantum numbers relative to the orbital-of-interest.

Orbital of Electron-of-Interest	*n* and *l*	*n* and *l-1*	*n* and *l-2*	*n-1*	*n-2, n-3, etc.*
1s	0.30	-	-	-	-
ns, np	0.35	0.35	-	0.85	1.0
nd, nf	0.35	1.0	1.0	1.0	1.0

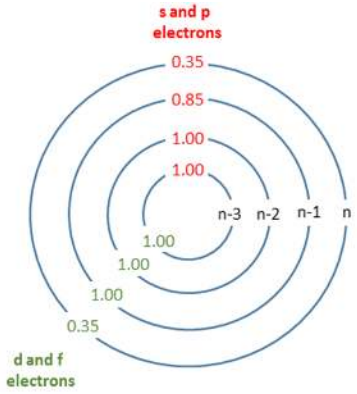


Figure 1.4.1.2: Graphical depiction of Slater's rules with shielding constants indicated. (CC-BY-NC-SA, Brett McCollum)

Calculating Shielding and Effective Nuclear Charge

Steps to Calculate Shielding and Effective Nuclear Charge

1. Write the electron configuration of the atom with orbitals arranged by increasing principle quantum number *n*, as shown here:

   (1s) (2s, 2p) (3s, 3p) (3d) (4s, 4p) (4d) (4f) (5s, 5p) . . .

2. Identify the electron of interest, and ignore all electrons that are higher in energy (to the right in the list). Higher energy electrons do not shield lower energy electrons.
3. Identify the principle quantum number *n* and angular momentum quantum number *l* of the electron-of-interest.
4. Assign shielding values to all other electrons that are lower in energy (to the right in the list).
   a. When the electron-of-interest is in a 1s orbital, the other electrons shield **0.30**.
   b. When the electron of interest is in a *ns* or *np* orbital
      - electrons in the same orbital shield **0.35**
      - electrons with *n* and *l-1* shield **0.35**
      - electrons with *n-1* shield **0.85**
      - all other electrons shield **1.00**
   c. When the electron-of-interest is in a *nd* or *nf* orbital
      - electrons in the same orbital shield **0.35**
      - all other electrons shield **1.00**

5. Sum the contributions of all electrons (except the electron-of-interest) to obtain the shielding constant S from the shielding values assigned to each electron, S_i.

Equation **1.4.1.3**

$$S = \sum n_i S_i \tag{1.4.1.3}$$

6. Subtract the shielding constant S from the nuclear charge Z to obtain the effective nuclear charge, as shown in Equation **1.4.1.2**



Example 1.4.1.1: Shielding of a 2*p* Electron on Nitrogen

What is the shielding constant experienced by a 2*p* electron in the nitrogen atom? What is the effective nuclear charge experienced by this electron?

Strategy:

1. Determine the electron configuration of nitrogen, then write it in the appropriate form.
2. Use the appropriate Slater Rules to calculate the shielding constant for the electron.
3. Subtract the shielding contant from the nuclear charge to find the effective nuclear charge.

Solution:

N: $1s^2\ 2s^2\ 2p^3$

N: $(1s^2)(2s^2,2p^3)$

From Table **1.4.1.1**:

- There are four 2s and 2p electrons that shield the 2p electron-of-interest equally at 0.35 units. The electron of interest does not shield itself!
- There are two 1s electrons that shield the 2p electron-of-interest at 0.85 units.

$$S[2p] = \underbrace{0.35(4)}_{\text{the 2s and 2p electrons}} + \underbrace{0.85(2)}_{\text{the 1s electrons}} = 3.10$$

For N, Z = 7

$$Z_{eff} = 7 - 3.1 = 3.9 \tag{1.4.1.4}$$

Example 1.4.1.2: Shielding of a 3d Electron on Bromine

What is the shielding constant experienced by a 3*d* electron in the bromine atom? What is the effective nuclear charge experienced by this electron?

Strategy:

1. Determine the electron configuration of nitrogen, then write it in the appropriate form.
2. Use the appropriate Slater Rules to calculate the shielding constant for the electron.
3. Subtract the shielding contant from the nuclear charge to find the effective nuclear charge.

Solution:

Br: $1s^2\ 2s^2\ 2p^6\ 3s^2\ 3p^6\ 4s^2\ 3d^{10}\ 4p^5$

Br: $(1s^2)(2s^2,2p^6)(3s^2,3p^6)(3d^{10})(4s^2,4p^5)$

Ignore the group to the right of the 3d electrons. These are in higher energy orbtials and do not contribute to the shielding constant.

From Table **1.4.1.1**:

- There are nine 3d electrons that shield the 3d electron-of-interest equally at 0.35 units.
- There are eight 3s and 3p electrons that shield the 4d electron-of-interest equally at 1.00 units.
- There are eight 2s and 2p electrons that shield the 4d electron-of-interest at 1.00 units.
- There are two 1s electrons that shield the 4p electron-of-interest at 1.00 units.

$$S[3d] = \underbrace{0.35(9)}_{\text{the 3d electrons}} + \underbrace{1.00(8)}_{\text{the 3s and 3p electrons}} + \underbrace{1.00(8)}_{\text{the 2s and 2p electrons}} + \underbrace{1.00(2)}_{\text{the 1s electrons}} = 21.15$$

For Br, Z = 35

$$Z_{eff} = 35 - 21.15 = 13.85 \tag{1.4.1.5}$$

Problems

Exercise 1.4.1.1: Shielding of a Valence Electron on Boron

What is the shielding constant experienced by a valence *p*-electron in the boron atom? What is the effective nuclear charge experienced by this electron?

Answer

B: $1s^2\ 2s^2\ 2p^1$

B: $(1s^2)(2s^1)$

From Table **1.4.1.1**:

- There are two 2s electrons that shield the 2p electron-of-interest equally at 0.35 units. The electron of interest does not shield itself!
- There are two 1s electrons that shield the 2p electron-of-interest at 0.85 units.

$$S[2p] = \underbrace{0.35(2)}_{\text{the 2s electrons}} + \underbrace{0.85(2)}_{\text{the 1s electrons}} = 2.40$$

For B, Z = 5

$$Z_{eff} = 5 - 2.4 = 2.6 \tag{1.4.1.6}$$

Exercise 1.4.1.2: Shielding of a Valence Electron on Bromine

What is the shielding constant experienced by a valence *p*-electron in the bromine atom? What is the effective nuclear charge experienced by this electron?

Answer

Br: $(1s^2)(2s^2,2p^6)(3s^2,3p^6,3d^{10})(4s^2,4p^5)$

From Table **1.4.1.1**:

- There are six 4s and 4p electrons that shield the 4p electron-of-interest equally at 0.35 units.
- There are 18 3s, 3p, and 3d electrons that shield the 4p electron-of-interest equally at 0.85 units.
- There are eight 2s and 2p electrons that shield the 4p electron-of-interest at 1.00 units.
- There are two 1s electrons that shield the 4p electron-of-interest at 1.00 units.

$$S[4p] = \underbrace{0.35(6)}_{\text{the 4s and 4p electrons}} + \underbrace{0.85(18)}_{\text{the 3s, 3p, and 3d electrons}} + \underbrace{1.00(8)}_{\text{the 2s and 2p electrons}} + \underbrace{1.00(2)}_{\text{the 1s electrons}} = 27.4$$

For Br, Z = 35

$$Z_{eff} = 35 - 27.4 = 7.6 \tag{1.4.1.7}$$

Exercise 1.4.1.3: Shielding of a Valence Electron on Isoelectronic Species

What is the shielding constant experienced by the valence *p*-electrons in the three isoelectronic species: fluoride (F^-), neon (Ne), and sodium cation (Na^+)? What is the effective nuclear charge experienced by these electrons?

Answer

F^-, Ne, Na^+: $1s^2\ 2s^2\ 2p^6$

F^-, Ne, Na^+:: $(1s^2)(2s^2,2p^6)$

From Table **1.4.1.1**:

- There are five 2s and 2p electrons that shield the 2p electron-of-interest equally at 0.35 units.
- The electron of interest does not shield itself! There are two 1s electrons that shield the 2p electron-of-interest at 0.85 units.

$$S[2p] = \underbrace{0.35(6)}_{\text{the 2s and 2p electrons}} + \underbrace{0.85(2)}_{\text{the 1s electrons}} = 3.80$$

For F, Z = 9

$$Z_{eff} = 9 - 3.8 = 5.2 \tag{1.4.1.8}$$

For Ne, Z = 10

$$Z_{eff} = 10 - 3.8 = 6.2 \tag{1.4.1.9}$$

For Na, Z = 11

$$Z_{eff} = 11 - 3.8 = 7.2 \tag{1.4.1.10}$$

Exercise 1.4.1.4: Shielding of a 3d Electron on Copper

What is the shielding constant experienced by a valence *d*-electron in the copper atom?What is the effective nuclear charge experienced by this electron?

Answer

Cu: $1s^2\ 2s^2\ 2p^6\ 3s^2\ 3p^6\ 4s^1\ 3d^{10}$

Cu: $(1s^2)(2s^2,2p^6)(3s^2,3p^6)(3d^{10})(4s^1)$

Ignore the group to the right of the 3d electrons. These are in higher energy orbtials and do not contribute to the shielding constant.

From Table **1.4.1.1**

- There are nine 3d electrons that shield the 3d electron-of-interest equally at 0.35 units.
- There are eight 3s and 3p electrons that shield the 4d electron-of-interest equally at 1.00 units.
- There are eight 2s and 2p electrons that shield the 4d electron-of-interest at 1.00 units.
- There are two 1s electrons that shield the 4p electron-of-interest at 1.00 units.

$$S[3d] = \underbrace{0.35(9)}_{\text{the 3d electrons}} + \underbrace{1.00(8)}_{\text{the 3s and 3p electrons}} + \underbrace{1.00(8)}_{\text{the 2s and 2p electrons}} + \underbrace{1.00(2)}_{\text{the 1s electrons}} = 21.15$$

For Cu, Z = 29

$$Z_{eff} = 29 - 21.15 = 7.85 \tag{1.4.1.11}$$

Exercise 1.4.1.5: Shielding of a 3*d* Electron on Zinc

What is the shielding constant experienced by a valence *d*-electron in the zinc atom? What is the effective nuclear charge experienced by this electron?

Answer

Zn: $1s^2\ 2s^2\ 2p^6\ 3s^2\ 3p^6\ 4s^2\ 3d^{10}$

Zn: $(1s^2)(2s^2,2p^6)(3s^2,3p^6)(3d^{10})(4s^2)$

Ignore the group to the right of the 3d electrons. These are in higher energy orbtials and do not contribute to the shielding constant.

From Table **1.4.1.1**

- There are nine 3d electrons that shield the 3d electron-of-interest equally at 0.35 units.
- There are eight 3s and 3p electrons that shield the 4d electron-of-interest equally at 1.00 units.
- There are eight 2s and 2p electrons that shield the 4d electron-of-interest at 1.00 units.
- There are two 1s electrons that shield the 4p electron-of-interest at 1.00 units.

$$S[3d] = \underbrace{0.35(9)}_{\text{the 3d electrons}} + \underbrace{1.00(8)}_{\text{the 3s and 3p electrons}} + \underbrace{1.00(8)}_{\text{the 2s and 2p electrons}} + \underbrace{1.00(2)}_{\text{the 1s electrons}} = 21.15$$

For Cu, Z = 30

$$Z_{eff} = 30 - 21.15 = 8.85 \tag{1.4.1.12}$$

References

- James L. Reed, "The Genius of Slater's Rules" , J. Chem. Educ., 1999, 76 (6), p 802
- David Tudela, "Slater's rules and electron configurations", J. Chem. Educ., 1993, 70 (11), p 956
- Kimberley A. Waldron, Erin M. Fehringer, Amy E. Streeb, Jennifer E. Trosky and Joshua J. Pearson, "Screening Percentages Based on Slater Effective Nuclear Charge as a Versatile Tool for Teaching Periodic Trends", J. Chem. Educ., 2001, 78 (5), p 635

1.4.1: Slater's Rules is shared under a CC BY-NC-SA 4.0 license and was authored, remixed, and/or curated by Kathryn A. Newton, Northern Michigan University.

- **2.6: Slater's Rules** by Brett McCollum is licensed CC BY-NC-SA 4.0.
- **2.2.4: Shielding** by Kathryn Haas is licensed CC BY-NC-SA 4.0.

1.4.2: Periodic Trends of Zeff

Estimated Time to Read: 3 min

Idealized Values for Z_{eff}

Slater's rules are a set of simple rules for predicting S and Z_{eff} based on empirical evidence from quantum mechanical calculations. In other words, the Z_{eff} calculated from Slater's rules are approximate values. The values considered to be the most accurate are derived from quantum mechanical calculations directly. You can find these values in Figure **1.4.2.1** for convenience:

Z or Z_{eff}	H																	He
Z	1.00																	2.00
1s	1.00																	1.69
	Li	Be											B	C	N	O	F	Ne
Z	3.00	4.00											5.00	6.00	7.00	8.00	9.00	10.00
1s	2.69	3.69											4.68	5.67	6.67	7.66	8.65	9.64
2s	1.28	1.91											2.58	3.22	3.85	4.49	5.13	5.76
2p													2.42	3.14	3.83	4.45	5.10	5.76
	Na	Mg											Al	Si	P	S	Cl	Ar
Z	11.00	12.00											13.00	14.00	15.00	16.00	17.00	18.00
1s	10.63	11.61											12.59	13.58	14.56	15.54	16.52	17.51
2s	6.57	7.39											8.21	9.02	9.83	10.63	11.43	12.23
2p	6.80	7.83											8.96	9.95	10.96	11.98	12.99	14.01
3s	2.51	3.31											4.12	4.90	5.64	6.37	7.07	7.76
3p													4.07	4.29	4.89	5.48	6.12	6.76
	K	Ca	Sc	Ti	V	Cr	Mn	Fe	Co	Ni	Cu	Zn	Ga	Ge	As	Se	Br	Kr
Z	19.00	20.00	21.00	22.00	23.00	24.00	25.00	26.00	27.00	28.00	29.00	30.00	31.00	32.00	33.00	34.00	35.00	36.00
1s	18.49	19.47	20.46	21.44	22.43	23.41	24.40	25.38	26.37	27.35	28.34	29.33	30.31	31.29	32.28	33.26	34.25	35.23
2s	13.01	13.78	14.57	15.38	16.18	16.98	17.79	18.60	19.41	20.21	21.02	21.83	22.60	23.37	24.13	24.89	25.64	26.40
2p	15.03	16.04	17.06	18.07	19.07	20.08	21.08	22.09	23.09	24.10	25.10	26.10	27.09	28.08	29.07	30.07	31.06	32.05
3s	8.68	9.60	10.34	11.03	11.71	12.37	13.02	13.68	14.32	14.96	15.59	16.22	17.00	17.79	18.60	19.40	20.22	21.03
3p	7.73	8.66	9.41	10.10	10.79	11.47	12.11	12.78	13.44	14.09	14.73	15.37	16.20	17.01	17.85	18.71	19.57	20.43
4s	3.50	4.40	4.63	4.82	4.98	5.13	5.28	5.43	5.58	5.71	5.84	5.97	7.07	8.04	8.94	9.76	10.55	11.32
3d			7.12	8.14	8.98	9.76	10.53	11.18	11.86	12.53	13.20	13.88	15.09	16.25	17.38	18.48	19.56	20.63
4p													6.22	6.78	7.45	8.29	9.03	9.34
	Rb	Sr	Y	Zr	Nb	Mo	Tc	Ru	Rh	Pd	Ag	Cd	In	Sn	Sb	Te	I	Xe
Z	37.00	38.00	39.00	40.00	41.00	42.00	43.00	44.00	45.00	46.00	47.00	48.00	49.00	50.00	51.00	52.00	53.00	54.00
1s	36.21	37.19	38.18	39.16	40.14	41.13	42.11	43.09	44.08	45.06	46.04	47.03	48.01	48.99	49.97	50.96	51.94	52.92
2s	27.16	27.90	28.62	29.37	30.13	30.88	31.63	32.38	33.16	33.88	34.63	35.39	36.12	36.86	37.60	38.33	39.07	39.80
2p	33.04	34.03	35.00	35.99	36.98	37.97	38.94	39.95	40.94	41.93	42.92	43.91	44.90	45.89	46.87	47.86	48.85	49.84
3s	21.84	22.66	23.55	24.36	25.17	25.98	26.79	27.60	28.44	29.22	30.03	30.84	31.63	32.42	33.21	34.00	34.79	35.58
3p	21.30	22.17	23.09	23.85	24.62	25.47	26.38	27.22	28.15	29.02	29.81	30.69	31.52	32.35	33.18	34.01	34.84	35.67
4s	12.39	13.44	14.26	14.90	15.28	16.10	17.20	17.66	18.58	18.99	19.87	20.87	21.76	22.66	23.54	24.41	25.30	26.17
3d	21.68	22.73	25.40	25.57	26.25	27.23	28.35	29.36	30.41	31.45	32.54	33.61	34.68	35.74	36.80	37.84	38.90	39.95
4p	10.88	11.93	12.75	13.46	14.08	14.98	15.81	16.44	17.14	17.72	18.56	19.41	20.37	21.27	22.18	23.12	24.03	24.96
5s	4.99	6.07	6.26	6.45	5.92	6.11	7.23	6.49	6.64	(empty)	6.76	8.19	9.51	10.63	11.62	12.54	13.40	14.22
4d			15.96	13.07	11.24	11.39	12.88	12.81	13.44	13.62	14.76	15.88	16.94	17.97	18.97	19.96	20.93	21.89
5p													8.47	9.10	10.00	10.81	11.61	12.43

Figure 1.4.2.1: Z_{eff} values calculated by Clementi et al. in 1963 and 1967 that are consistent with SCF Calculations. [Wikipedia: Effective Nuclear Charge]

General Periodic Trends in Ze_{ff}

The data from Figure **1.4.2.1** is plotted below in Figure **1.4.2.2**. Close inspection of Figure **1.4.2.2** shows that there are some predictable trends in Z_{eff}. The Z_{eff} for electrons in a given shell and subshell generally increase as atomic number increases; this trend holds true going across the periodic table and down the periodic table. You can see this trend as the positive slope in each series in Figure **1.4.2.2**. There is one obvious exception in Period 5 in elements 39 (Y) to 41. For Nb, the Z_{eff} of the 4s electrons actually decreases as atomic number increases. There is also an exception between Y and Zr in the 3d subshell, and between Tc and Ru in the 5s subshell.

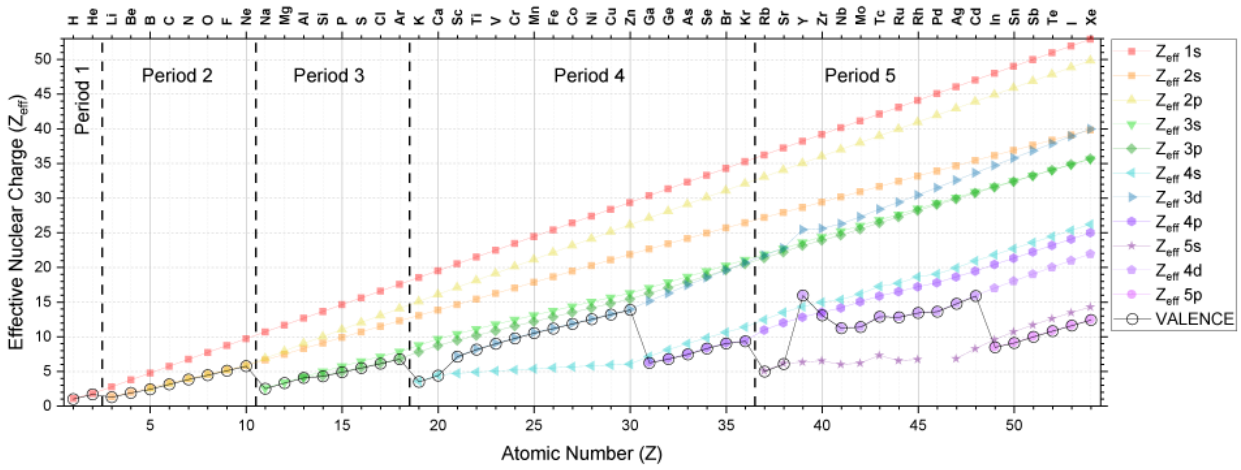


Figure 1.4.2.2: The Z_{eff} values for electrons in each subshell of the first 54 elements (H to Xe). Each subshell is plotted as a different series (see legend) and the valence shell is highlighted by a solid black line with open circles. (CC-BY-NC-SA, LibreText)

Trends in Z_{eff} of Valence Electrons

It is useful to understand trends Z_{eff} for the valence electrons specifically because the valence electrons determine atomic/ionic properties and chemical reactivity. The trends in the Z_{eff} of the valence electrons are not simple because as atomic number increases, the valence shell and/or subshell also change. The valence Z_{eff} is indicated in Figure **1.4.2.2** as a black line with open circles.

Down a column of the periodic table, the Z_{eff} of the valence electrons increases. This is a simple trend because type of subshell is consistent and there is an increase only in shell and in atomic number, Z. This trend is best illustrated by inspection of Figure **1.4.2.1**.

Across a row of the periodic table, generally Z_{eff} of the valence electrons increases across a period, but the trend does depend on shell and subshell.

- **Periods 1-3 (s and p subshells only):** The valence electron shell is constant as Z increases and the subshell changes from s to p. There is a gradual increase in valence Z_{eff}.
- **Periods 4 and 5 (s, p, and d subshells):** The valence shell and subshell change as atomic number increases. The Z_{eff} of the valence electrons generally increases going across a period as long as the subshell does not change. (There is an exception within the 4d subshell for elements 39-44, Y-Ru.) In general, going from an $(n)s$ subshell to an $(n-1)d$ subshell, there is a relatively large increase in valence Z_{eff}. Going from an $(n-1$d\) subshell to an $(n)p$ subshell, there is a relatively large decrease in Z_{eff}.
- **Crossing from one period to the next:** From Figure **1.4.2.2**, we can see that when Z increases by one proton and the period increases (for example, going from Ne to Na), there is a relatively large decrease in Z_{eff}. As Z increases by a small interval, the shell number increases, and so the electrons in the valence shell are much farther from the nucleus and are more shielded by the electrons in the lower energy shells.

References

1. Petrucci, Ralph H., William S. Harwood, F. Geoffrey Herring, and Jeffry D. Madura. General Chemistry: Principles and Modern Applications, Ninth Edition. Pearson Education Inc. Upper Saddle River, New Jersey: 2007.
2. Raymond Chang. Physical Chemistry for Biological Sciences. Sausalito, California: University Science Books, 2005
3. R. S. Mulliken, Electronic Structures of Molecules and Valence. II General Considerations, Physical Review, vol. 41, pp. 49-71 (1932)
4. Anastopoulos, Charis (2008). *Particle Or Wave: The Evolution of the Concept of Matter in Modern Physics*. Princeton University Press. pp. 236–237. ISBN 0691135126. http://books.google.com/?id=rDEvQZhpltEC&pg=PA236.

Contributors and Attributions

- Sidra Ayub (UCD), Alan Chu (UCD)
- Emily V Eames (City College of San Francisco)
- Kathryn Haas (Duke)

1.4.2: Periodic Trends of Zeff is shared under a CC BY-NC-SA 4.0 license and was authored, remixed, and/or curated by Kathryn A. Newton, Northern Michigan University.

- **2.2.4: Shielding** by Kathryn Haas is licensed CC BY-NC-SA 4.0.

1.4.3: Zeff Controls "Exceptions" to Periodic Trends

Estimated Time to Read: 8 min

Z_{eff} modulates attraction

A modified form of Coulomb's Law is given in Equation \(\PageIndex{1}\), where \(e\) is the charge of an electron, Z_{eff} is the effective nuclear charge experienced by that electron, and \(r\) is the radius (distance of the electron from the nucleus).

Equation \(\PageIndex{1}\):

$$\[F_{eff}=k \dfrac{ Z_{eff} e^2}{r^2} \nonumber \]$$

This formula suggests that if we can estimate Z_{eff}, then we can predict the attractive force experienced by and the energy of an electron in a multi-electron atom. The attraction of the nucleus to the valence electrons determines the atomic radius, ionization energy, and electron affinity. The stronger the attraction, and the stronger Z_{eff}, the closer the electrons are pulled toward the nucleus. This in turn results in a smaller size, higher ionization energy, and higher electron affinity.

The Lanthanide Contraction describes the atomic radius trend that the Lanthanide series exhibits. Another important feature of the The Lanthanide Contraction is the 5s and 5p orbitals penetrate the 4f sub-shell so the 4f orbital is not shielded from the increasing nuclear change, which causes the atomic radius of the atom to decrease. This decrease in size continues throughout the series.

Atomic Radius

Atomic radius generally decreases from left to right across a period of elements. As the nuclear charge (Z) increases, the effective nuclear charge (Z*) of the valence electrons also increases. However, with each addition of a proton there is an addition of an electron. The electrons are added into the valence shell and weakly shielded by the other electrons in the valence shell. Therefore, as Z increases, Z_{eff} increases more gradually due to shielding. The observed change in atomic radius is a balance of a compression caused by increasing Z and an expansion in the number of electrons. As a result, the atomic radius decreases *gradually* across a period.

Atomic size generally increases going down a group. As valence electrons occupy higher level shells due to the increasing quantum number (n), size increases despite the fact that Z and Z* are increasing going down the group.

Scandide Contraction

The Scandide Contraction is an atomic radius trend experienced by the d-block elements. Normally atomic radius decreases significantly as nuclear charge increases across a period of the periodic table. In the transition metal elements, the atomic radii only decreases slightly as compared to decreases across the s or p block. D-block elements have the same number of s orbital electrons and only differing in the number of d orbital electrons. The d orbital electrons are inner shell electrons and each additional electron is added to the same shell and subshell. The d orbital electrons are poorly shielding compared to the s and p orbital electrons so effective nuclear charge increases more rapidly across the d-block, resulting in a smaller change in the atomic radius across the period.

Lanthanide Contraction

The Lanthanide series is in the f-block of the periodic table and includes elements 57-70 (La-Yb). As expected based on the periodic trend, the atomic radius of these elements decreases as the atomic number increases (Figure \(\PageIndex{1}\)).

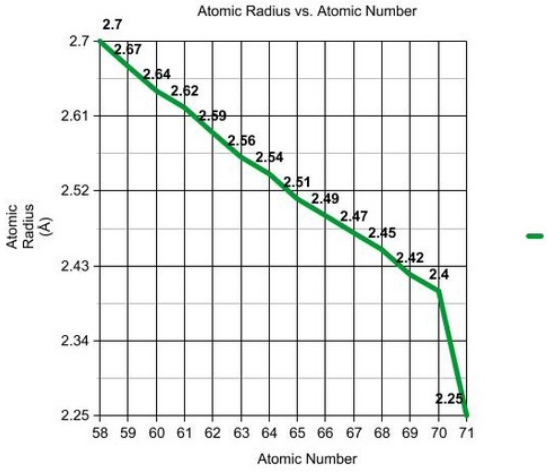
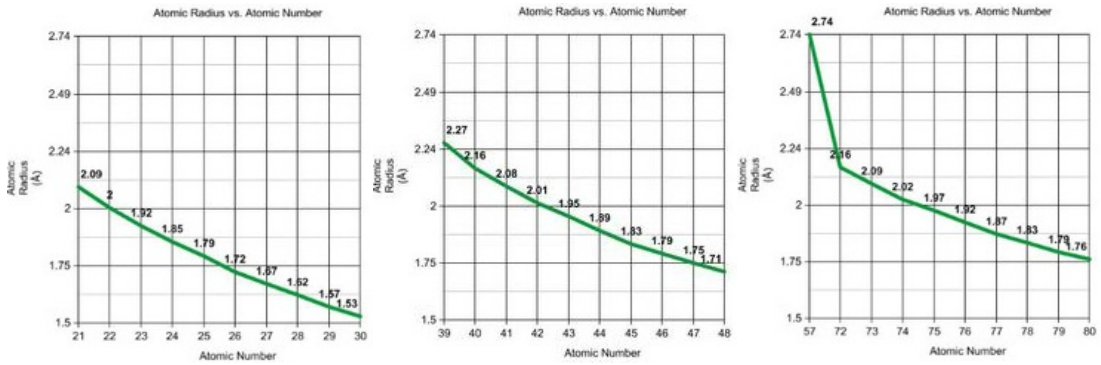


Figure \(\PageIndex{1}\): Atomic radius decreases as the atomic number increases across the Lanthanide Series. [LibreText]

Figure \(\PageIndex{2}\) shows the atomic radii of the first three rows of transition metal elements. Consider the elements with atomic numbers 23, 41, and 73, which are in the same column of the periodic table. The elements 23 and 41 they have a large difference in atomic radii, but the elements 41 and 73 have only a small difference in atomic radii. In general for d-block elements, the atomic radii differ greatly between the Row 1 and Row 2 elements, but the atomic radii differ little between Row 2 and Row 3 elements. This is deviation in the trend is caused by the introduction of 4f electrons in Row 3 and is known as *Lanthanide Contraction*. As a reminder, s orbitals are the most effective at shielding, followed by the p and d orbitals with the f orbitals being the least effective. The Lanthanide Contraction is the result of the poor shielding effect of the 4f electrons. Because the 4f electrons are poorly shielding, the 5d valence electrons experience a greater effective nuclear charge than would otherwise be expected. When shielding is poor, the positively charged nucleus has a greater attraction to the electrons, and atomic radius decreases more rapidly as the atomic number increases.



Row 1 3d Elements | Row 2, 4d Elements | Row 3, 5d Elements

Figure \(\PageIndex{2}\): Atomic radii of transition metals elements in Period 4 (left), Period 5 (center), and Period 6 (right) [LibreText]

The Lanthanide Contraction can be seen by further comparing the elements with f electrons and those without f electrons in the d block. Pd and Pt are such elements. Pd has 4d electrons while Pt has 5d and 4f electrons. These 2 elements have roughly the same atomic radius. This is due to Lanthanide Contraction and shielding. While we would expect Pt to have a significantly larger radius because more electrons and protons are added, it does not because the 4f electrons are poor at shielding. When the shielding is not good there will be a greater nuclear charge, thus pulling the electrons in closer, resulting in a smaller than expected radius.

Ionization Energy

Ionization energy is the energy required to remove an electron from a neutral gaseous atom. Across a period, the number of protons and the effective nuclear charge increase. As a result, the atomic radius decreases. If we consider Equation 1, increasing effective charge and decreasing radii results in greater attractive forces by the nucleus for electrons. Thus, greater energy is required for an electron to overcome the attractive force of the nucleus and the ionization energy increases.

In general, ionization energies increase from left to right and decrease down a group; however, there are variations in these trends that would be expected from the effects of penetration and shielding.

- **Across a period:** As Z_{eff} increases across a period, the ionization energy of the elements generally increases from left to right. However there are breaks or variation in the trends in the following cases:
  - IE is especially low when removal of an electron creates a newly empty p subshell (examples include B, Al, Sc)
  - IE energy is especially low where removal of an electron results in a half-filled p or d subshell (examples include O, S)
  - IE increases more gradually across the d- and f-subshells compared to s- and p- subshells. This is because d- and f-electrons are weakly penetrating and experience especially low Z_{eff}.
- **From one period to the next:** There is an especially large decrease in IE with the start of every new period (from He to Li or from Ne to Na for example). This is consistent with the idea that IE is especially low when removal of an electron creates a newly empty s-subshell.
- **Noble gases:** The noble gases posses very high ionization energies. Note that helium has the highest ionization energy of all the elements.
- **Down a group:** Although Z_{eff} increases going down a group, there is no reliable trend in IE going down any group; in some cases IE increases going down a group, while in other cases IE decreases going down a group.

Trends in Electron Affinity

Electron affinity is the change in energy when an electron is added to a neutral gaseous atom. The trends in electron affinity mimic the trends in ionization energy.

- **Across a period**: Similar to ionization energy, EA generally increases (more negative, more exothermic)across a row of the periodic table; this observation is consistent with the increase in effective nuclear charge (Z_{eff}) from left to right across a period. However, there are variations across a period that are similar to variations in ionization energy and that can be explained by shielding, penetration, and electron configuration.
- **Down a group**: Like the case of ionization energy trends, EA does not consistently decrease going down a column of the periodic table despite the fact that Z_{eff} increases down a group.

The trend in EA follows a zig-zag pattern similar to the one seen with ionization energies, except that it is displaced by one unit from the trend in IE_1, two units from IE_2, and so on. For example, EA peaks at F, while IE_1 peaks at Ne, IE_2 peaks at Na, and IE_3 peaks at Mg. A plot of EA for the first 13 elements is shown overlaid on plots of IE_1, IE_2, and IE_3 in Figure \(\PageIndex{3}\), where the shifts in the peaks and valleys within each zig-zag trend are indicated.

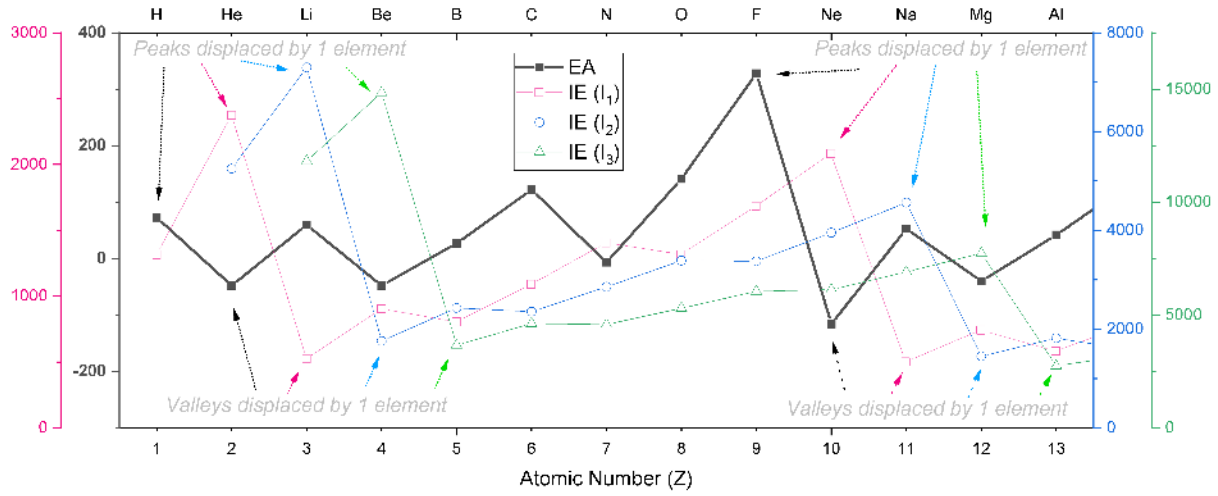


Figure \(\PageIndex{3}\): A plot of electron affinity (the zeroth ionization energy) is overlaid on plots of the first (IE_1), second (IE_2), and third (IE_3) ionization energies. Each plot is shown using separate y-axes. Trends in EA are similar to those in ionization energies, except that the peaks and valleys of the trends are shifted by one unit, as indicated. These plots are shown in units of kJ/mole. (CC-BY-NC-SA; Kathryn Haas)

Problems

Exercise \(\PageIndex{1}\)

Compare trends in Z* and atomic size. Explain how and why atomic size depends on Z_{eff}.

Answer

On the periodic table, atomic radius generally decreases across the periods (left to right) and increases down the groups. As atomic number increases across the periodic table, nuclear charge (Z) increases and Z* increases. In turn, the atomic radius decreases because the higher nuclear charge (and thus higher Z*) pulls electrons closer to the nucleus. Atomic radius increases down the periodic table because the shell number increases. Despite an increase in Z* going down the periodic table, larger atomic radii result from electrons occupying higher shells.

Exercise \(\PageIndex{2}\)

Compare trends in Z_{eff} and ionization energy. Explain how and why ionization energy depends on Z_{eff}.

Answer

Ionization energies (IE) are inversely related to atomic radius; IE increases across the periods and decreases down the groups. Since the nucleus holds valence electrons more strongly (due to higher Z*) across the periods, IE increases because valence electrons are harder to remove. Down the periodic table, larger atomic radii cause electrons in valence orbitals to be shielded by core electrons. Recall that shielding reduces the nuclear charge available to electrons in higher orbital levels, resulting in a lower Z*. With more shielding and lower Z*, the valence electrons are held less tightly by the nucleus such that ionization energy decreases (i.e., valence electrons are easier to remove).

Exercise \(\PageIndex{3}\)

What is the cause of Lanthanide Contraction?

Answer

The Lanthanide Contraction is caused by a poor shielding effect of the 4f electrons

Exercise \(\PageIndex{4}\)

Which element has a greater atomic radius Gd or Tb and why?

Answer

Gd because as atomic number increases, the atomic radius decreases..

Exercise \(\PageIndex{5}\)

Which element has a smaller atomic radius Dy or Yb and why?

Answer

Yb because it has a larger atomic number.

Exercise \(\PageIndex{6}\)

Why do elements in Rows 2 and 3 that are in the same column have similar atomic radii?

Answer

Because the elements in Row 3 have 4f electrons. These electrons are do not shield good, causing a greater nuclear charge. This greater nuclear charge has a greater pull on the electrons.

Exercise \(\PageIndex{7}\)

Place the following elements in order of increasing atomic radius: Eu, Ce, Pr, Ho.

Answer

Ho, Eu, Pr, Ce

References

1. Petrucci, Harwood, Herring, and Madura. *General Chemistry Principles & Modern Applications*. 9th ed. Prentice Hall. Print.
2. Cotton, Simon. *Lanthanide and Actinide Chemistry*. Wiley. Print.
3. Electron Affinity (data page), Wikipedia. en.Wikipedia.org/wiki/Electron_affinity_(data_page) Accessed 12/3/19.

1.4.3: Zeff Controls "Exceptions" to Periodic Trends is shared under a CC BY-NC-SA 4.0 license and was authored, remixed, and/or curated by Kathryn A. Newton, Northern Michigan University.

- **2.2.4: Shielding** by Kathryn Haas is licensed CC BY-NC-SA 4.0.
- **Lanthanide Contraction** is licensed CC BY-NC-SA 4.0.
- **2.3.3: Covalent and Ionic Radii** by Bingyao Zheng, Emily Nguyen, Kathryn Haas, Swetha Ramireddy is licensed CC BY-NC 4.0.
- **2.3.1: Ionization energy** by Bingyao Zheng, Emily Nguyen, Kathryn Haas, Swetha Ramireddy is licensed CC BY-NC-SA 3.0.

CHAPTER OVERVIEW

2: Bonding Theory Overview

2.1: Covalent- Lewis Octet

2.1.1: Lewis- Formal Charge

2.1.2: Lewis- Expanded Octet

2.1.3: Lewis- Resonance

2.1.4: Lewis- Electron-Deficient "Octets" of B and Be

2.1.5: Molecule Shape from Valence Shell Electron Repulsion Theory (VSEPR)

2.1.6: Shape Change from Lone Pairs

2.1.7: Shape Change from Double and Triple Bonds

2.2: Covalent- Molecular Orbital Theory

2.2.1: MO- s orbital MOs

2.2.2: MO- p orbital MOs

2.2.3: MO- d orbital MOs

2.2.4: MO- Nonbonding MOs

2.2.5: MO- MO Diagram Features

2.2.6: MO- MO Diagrams of 1st and 2nd row diatomic molecules

2.2.7: MO- MO Diagrams of Heteronuclear Diatomics

2.3: Metallic- Sea of Electrons and the van Arkel-Ketelaar Triangle

2.4: Structures of Metals and Ionic Compounds

2.5: Ionic- Charge and Size Determine Ionic Bonding

2.5.1: Ionic- Measurement of Ionic Bond Strength

2.5.2: Ionic- Examples of Ionic Structures

2.5.2.1: Ionic- Rock Salt

2.5.2.2: Ionic- Caesium Chloride (CsCl)

2.5.2.3: Ionic- Fluorite and Anti-Fluorite

2.5.2.4: Ionic- Zinc Blende (ZnS)

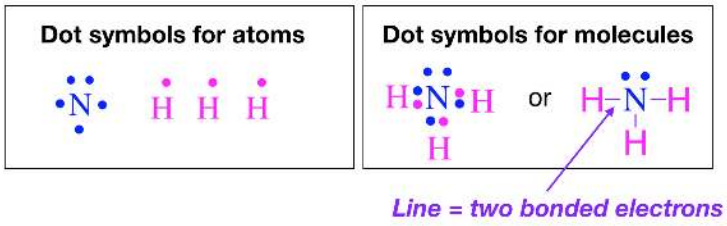
2.5.3: Predicting Ionic Structure Type

2: Bonding Theory Overview is shared under a not declared license and was authored, remixed, and/or curated by LibreTexts.

2.1: Covalent- Lewis Octet

In 1916, Gilbert Lewis Newton introduced a simple way to show the bonding between atoms in a molecule though Lewis electron dot diagrams. Creating Lewis diagrams is rather simple and requires only a few steps and some accounting of the valence electrons on each atom. Valence electrons are represented as dots. When two electrons are paired (lone pairs), they are represented by two adjacent dots located on an atom, and when two paired electrons are shared between atoms (bonds), they are shown as lines. For example, below are the electron dot structures of atoms and the Lewis electron dot structures of the molecules.

These diagrams are helpful because they allow us to show how atoms are connected, and when coupled with Valence Shell Electron Repulsion Theory (VSEPR), we can use Lewis structures to predict the shape of the molecule.



The drawing of Lewis electron-dot structures is guided largely by the **octet rule**: that atoms form bonds to achieve eight electrons in their valence shell. For many elements, a full valence shell has an electron configuration of s^2p^6, or eight electrons. A common exception to this rule is the first row elements, H and He. These two elements have $n = 1$ as their valence shell, and so they have only two electrons in a full valence shell ($1s^2$ electron configuration). Although H and He are exceptions to the "octet rule", they still form bonds to achieve a full valence shell. It may be better to think of this as the "full valence" rule of bonding. We will see many more violations to the "octet" rule as we progress through this course. In the case of metals and metalloids, breaking of the rules is particularly common. (CC-BY-NC-SA; Kathryn Haas)

Common violations of the octet rule

- **Less than eight electrons (hypovalency)**: H and He are examples of elements that cannot have more than two electrons in their full valence shell. Additionally, there are cases where a valid Lewis structure contains atoms with ***hypovalency:*** *partially-filled valence shells*. An example of this is a *carbocation, a positively charged carbon with only six electrons in its valence shell.* Carbocations are important intermediates in organic chemistry, and they are highly reactive (unstable) Lewis acids (electrophiles). Another example of hypovalency is the Lewis structure for BH_3, which shows boron with three bonds, and only six electrons in its valence shell. Boron hydride is a strong Lewis Acid. (Side note: the actual chemical form of BH_3 is not well-predicted by the Lewis structure and we'll see more about this in Section 3.1.4.)
- **More than eight electrons (hypervalency)**: This is a case where an element has more than eight electrons in its valence shell. It is common for larger atoms ($n \geq 3$), and it is discussed further in Section 3.1.2.

Pitfall alert! There are different rules for counting electrons depending on the purpose of the counting. These are the rules for counting for "octets". The rules for counting for calculation of an atom's formal charge are different and are described in Section 3.1.3. When an atom is part of a molecule, all electrons that are associated with the atom are counted as contributing to the atom's valence. This includes electrons that are lone pairs on the atoms, and *all* electrons that are shared in bonds. If four electrons are shared between two atoms, it is a double bond. If six electrons are shared between atoms, it is a triple bond.

Electrons in valence (octet) = total unbonded electrons on the atom + total bonded electrons (2 electrons per bond)

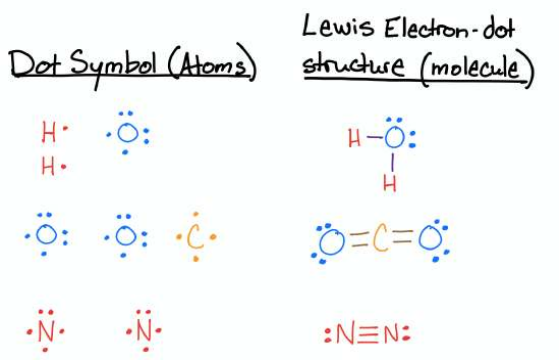
Even if you're an old pro at drawing Lewis structures, it's a good idea to polish up. Please complete the practice exercises below.

Problems

Exercise 2.1.1

Draw the Lewis structures for H_2O, CO_2, and N_2.

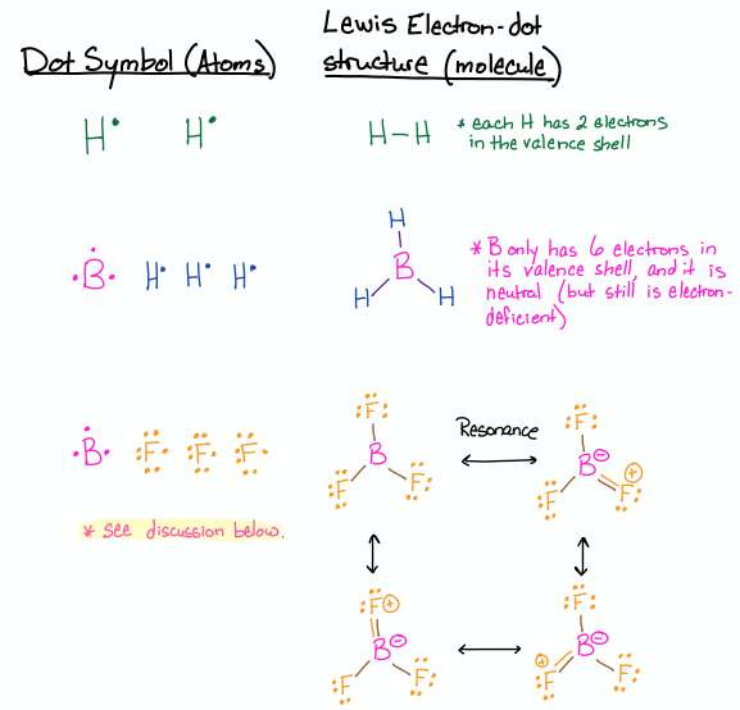
Answer



Exercise 2.1.2

Draw the Lewis structures for H_2, BH_3 and BF_3.

Answer



These three examples include atoms that have less than eight electrons in their valence shell. In the case of H, it is satisfied with only two electrons in its valence, as was discussed earlier in this section. The case of BH_3 was also discussed above. In the Lewis structure of BH_3, the boron can only have six electrons in its octet and it is neutral in charge. The boron is electron deficient even though it has neutral charge.

The case of BF_3 deserves a discussion: If you are unfamiliar with resonance and formal charge, see Sections 3.1.1 (Resonance) and 3.1.3 (Formal Charge) first and come back to this afterward. You might have drawn the BF_3 structure similar to the one that is drawn for BH_3, where boron has three bonds and only six electrons in its valence shell. If you did that, then you are correct; but if you only gave this structure, then your answer is not complete. There are three other correct

ways to draw the structure. Since F has lone pairs of electrons, other valid Lewis structures would each have a double bond to one of the fluorines (three total). All of these structures are called resonance structures, and based on the four of them, we could predict that BF_3 would have B-F bonds that have some double-bond character. If fact, this is the case for BF_3; it has bond lengths that are shorter than single bonds, but longer than double bonds. Read more about it on its Wikipedia page here (click).

Outside Links

- en.Wikipedia.org/wiki/Lewis_structures
- http://www.ausetute.com.au/lewisstr.html
- cost.georgiasouthern.edu/chem...cule/lewis.htm

2.1: Covalent- Lewis Octet is shared under a CC BY-NC-SA 4.0 license and was authored, remixed, and/or curated by Kathryn A. Newton, Northern Michigan University.

- **3.1: Lewis Electron-Dot Diagrams** by Kathryn Haas is licensed CC BY-NC 4.0.
- **2.1B: Lewis Structures** by Andrew Iskandar is licensed CC BY 4.0.

2.1.1: Lewis- Formal Charge

The formal charge of an atom in a molecule is the *hypothetical* charge the atom would have if we could redistribute the electrons in the bonds evenly between the atoms. Another way of saying this is that formal charge results when we take the number of valence electrons of a neutral atom, subtract the nonbonding electrons, and then subtract the number of bonds connected to that atom in the Lewis structure.

Calculating Formal Charges

We calculate the formal charge of an atom in a molecule or polyatomic ions as follows:

Formal Charge = (valence electrons of the "free" element) - (unshared electrons) - 1/2 (bonding electrons).

Alternatively:

Formal Charge = (valence electrons of the "free" element) - (unshared electrons) - (bonds).

We can double-check formal charge calculations by determining the sum of the formal charges for the whole structure. The sum of the formal charges of all atoms in a molecule must be zero; the sum of the formal charges in an ion should equal the charge of the ion.

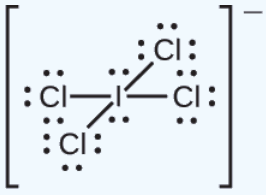
We must remember that the formal charge calculated for an atom is not the *actual* charge of the atom in the molecule. Formal charge is only a useful bookkeeping procedure; it does not indicate the presence of actual charges.

Example 2.1.1.1: ICl_4^-

Assign formal charges to each atom in the interhalogen ion $\mathbf{ICl_4^-}$.

Solution

We divide the bonding electron pairs equally for all **I–Cl** bonds:



We assign lone pairs of electrons to their atoms. Each **Cl** atom now has seven electrons assigned to it, and the I atom has eight.

Subtract this number from the number of valence electrons for the neutral atom:

- I: 7 – 8 = –1
- Cl: 7 – 7 = 0

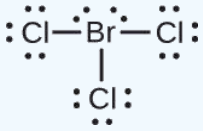
The sum of the formal charges of all the atoms equals –1, which is identical to the charge of the ion (–1).

Example 2.1.1.2: $BrCl_3$

Assign formal charges to each atom in the interhalogen molecule $\mathbf{BrCl_3}$.

Solution

Assign one of the electrons in each Br–Cl bond to the Br atom and one to the Cl atom in that bond:



Assign the lone pairs to their atom. Now each Cl atom has seven electrons and the Br atom has seven electrons.

Subtract this number from the number of valence electrons for the neutral atom. This gives the formal charge:

- Br: 7 – 7 = 0
- Cl: 7 – 7 = 0

All atoms in $BrCl_3$ have a formal charge of zero, and the sum of the formal charges totals zero, as it must in a neutral molecule.

Problems

Exercise 2.1.1.1

Calculate the formal charge for each atom in the carbon monoxide molecule:



Answer

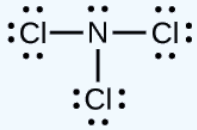
C −1, O +1

Exercise 2.1.1.2

Determine the formal charge for each atom in NCl_3.

Answer

N: 0; all three Cl atoms: 0



2.1.1: Lewis- Formal Charge is shared under a CC BY-NC-SA 4.0 license and was authored, remixed, and/or curated by Kathryn A. Newton, Northern Michigan University.

- **7.5: Formal Charges and Resonance** by OpenStax is licensed CC BY 4.0. Original source: https://openstax.org/details/books/chemistry-2e.

2.1.2: Lewis- Expanded Octet

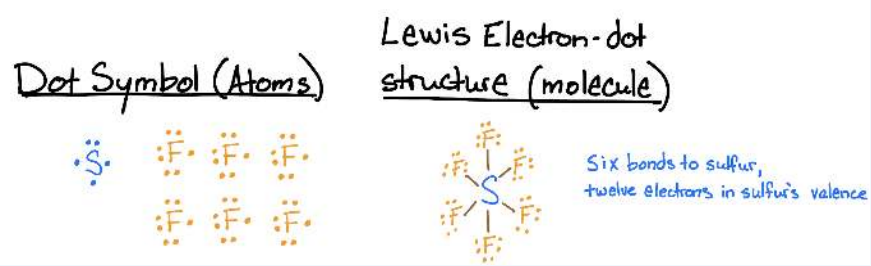
The octet rule applies well to atoms in the second row of the periodic table, where a full valence shell includes eight electrons with an electron configuration of s^2p^6. Even elements in the third and fourth row are known to follow this rule *sometimes*, but not always. In larger atoms, where $n \geq 3$ the valence shell contains additional subshells: the $d, f, g...$ subshells. Therefore, atoms with $n \geq 3$ can have higher valence shell counts by "expanding" into these additional subshells. When atoms contain more than eight electrons in their valence shell, they are said to be **hypervalent**. Hypervalency allows atoms with $n \geq 3$ to break the octet rule by having more than eight electrons. This also means they can have five or more bonds; something that is nearly unheard of for atoms with $n \leq 2$. Complete the exercises below to see examples of molecules containing hypervalent atoms.

? Exercise 2.1.2.1

Draw the Lewis structures for sulfur hexafluoride (SF_6).

Answer

Each fluorine atom has one valence electron and will make one bond each. The sulfur has six valence electrons, and must make six bonds to form a molecule with the six fluorine atoms. The molecular structure has six bonds to sulfur, with twelve valence electrons. The sulfur is hypervalent.

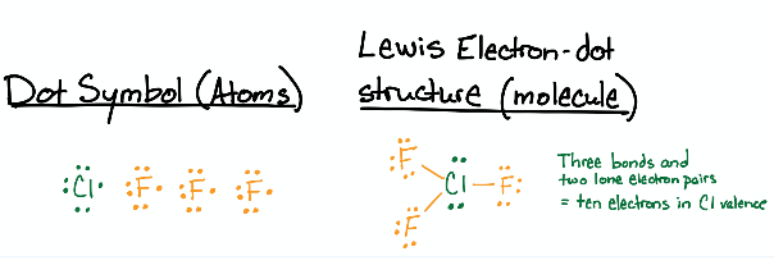


? Exercise 2.1.2.2

Draw the Lewis structure for chlorine trifluoride (ClF_3.

Answer

All atoms are halogens and each has seven valence electrons. Chlorine is capable of hypervalency because it is in the third row of the periodic table; however fluorine cannot have more than eight valence electrons in its valence because it is in the second row. The structure has the three fluorine atoms bonded to a central chlorine atom. The chlorine has a valence of ten electrons due to its three bonds and two lone pairs.



Is hypervalency real? Not exactly. Hypervalency is a concept associated with hybrid orbital theory and Lewis theory. It's useful for some simple things, like predicting how atoms are connected and predicting molecular shape. But the idea that the d-orbitals are involved in bonding isn't accurate according to wave mechanics.

For main group molecules, chemists (like Pauling) thought a long time ago that hypervalence is due to expanded s^2p^6 octets. The consensus is now clear that d orbitals are NOT involved in bonding in molecules like SF_6 any more than they are in SF_4 and SF_2. In all three cases, there is a small and roughly identical participation of d-orbitals in the wavefunctions. This has been established in both MO and VB theory. However, using hybrid orbitals with d-orbital contributions equips us with a language which can pragmatically describe the geometries of highly coordinated substances.

While hybrid orbitals are a powerful tool to describe the geometries and shape of molecules and metal complexes, in "real" molecules their significance may be debated. Often a more realistic molecular orbitals approach is needed. However, from an epistemologically simple point of view, bonding theories can only be judged by their predictions. To the extent that hybridization can explain the shapes of PF_5 and SF_6, valence bond theory is a perfectly good theory. To the extent that if you write out the valence bond wavefunction using hybridized orbitals and calculate energies and other properties à la Pauling (i.e., ionization energy and electron affinities) and find them to be off from experimental results (by tens of kcals/mol), then valence bond theory is not accurate.

> *Bonding theories can only be judged by their predictions.*

A simple explanation that can be given is that molecular wavefunctions constructed out of hybridized atomic orbitals are accurate enough to predict some things, but not others. Predictions of any theory must be compared with empirical evidence to assess when they work and when they fail. When a theory gives the wrong answer, at least one assumption must not hold. In this case, the valence bond wavefunction is not accurate enough to capture some important features of a system's electronic structure. It may not be the most intellectually satisfying answer, but to say more would result in a much more complicated answer and certainly far beyond the level reasonably expected from general chemistry discussions.

2.1.2: Lewis- Expanded Octet is shared under a CC BY-NC-SA 4.0 license and was authored, remixed, and/or curated by Kathryn A. Newton, Northern Michigan University.

- **3.1.2: Breaking the octet rule with higher electron counts (hypervalent atoms)** by Kathryn Haas is licensed CC BY-NC 4.0.

2.1.3: Lewis- Resonance

Resonance structures are a set of two or more Lewis Structures that collectively describe the electronic bonding of a single polyatomic species including fractional bonds and fractional charges. Resonance structures are capable of describing delocalized electrons that cannot be expressed by a single Lewis formula with an integral number of covalent bonds.

Sometimes one Lewis Structure is not Enough

Sometimes, even when formal charges are considered, the bonding in some molecules or ions cannot be described by a single Lewis structure. Resonance is a way of describing delocalized electrons within certain molecules or polyatomic ions where the bonding cannot be expressed by a single Lewis formula. A molecule or ion with such delocalized electrons is represented by several contributing structures (also called resonance structures or canonical forms). Such is the case for ozone ($\mathbf{O_3}$), an allotrope of oxygen with a V-shaped structure and an O–O–O angle of 117.5°.

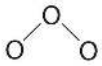
Ozone (O_3)

1. We know that ozone has a V-shaped structure, so one O atom is central:



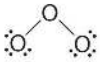
2. Each O atom has 6 valence electrons, for a total of 18 valence electrons.

3. Assigning one bonding pair of electrons to each oxygen–oxygen bond gives



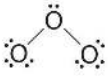
with 14 electrons left over.

4. If we place three lone pairs of electrons on each terminal oxygen, we obtain

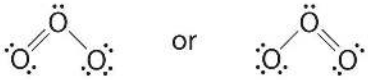


and have 2 electrons left over.

5. At this point, both terminal oxygen atoms have octets of electrons. We therefore place the last 2 electrons on the central atom:

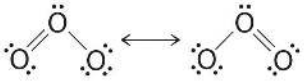


6. The central oxygen has only 6 electrons. We must convert one lone pair on a terminal oxygen atom to a bonding pair of electrons —but which one? Depending on which one we choose, we obtain either



Which is correct? In fact, neither is correct. Both predict one O–O single bond and one O=O double bond. As you will learn, if the bonds were of different types (one single and one double, for example), they would have different lengths. It turns out, however, that both O–O bond distances are identical, 127.2 pm, which is shorter than a typical O–O single bond (148 pm) and longer than the O=O double bond in O_2 (120.7 pm).

Equivalent Lewis dot structures, such as those of ozone, are called **resonance structures**. The position of the *atoms* is the same in the various resonance structures of a compound, but the position of the *electrons* is different. Double-headed arrows link the different resonance structures of a compound:



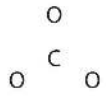
The double-headed arrow indicates that the actual electronic structure is an *average* of those shown, not that the molecule oscillates between the two structures.

> *When it is possible to write more than one equivalent resonance structure for a molecule or ion, the actual structure is the average of the resonance structures.*

The Carbonate (CO_3^{2-}) Ion

Like ozone, the electronic structure of the carbonate ion cannot be described by a single Lewis electron structure. Unlike O_3, though, the actual structure of CO_3^{2-} is an average of *three* resonance structures.

1. Because carbon is the least electronegative element, we place it in the central position:



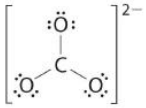
The three oxygens are drawn in the shape of a triangle with the carbon at the center of the triangle.

2. Carbon has 4 valence electrons, each oxygen has 6 valence electrons, and there are 2 more for the −2 charge. This gives 4 + (3 × 6) + 2 = 24 valence electrons.

3. Six electrons are used to form three bonding pairs between the oxygen atoms and the carbon:



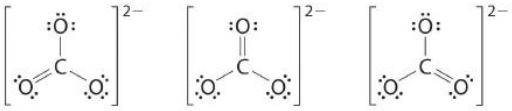
4. We divide the remaining 18 electrons equally among the three oxygen atoms by placing three lone pairs on each and indicating the −2 charge:



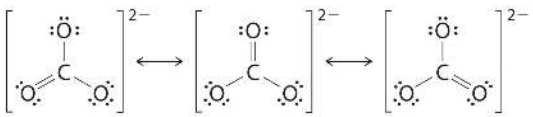
The Lewis dot structure has a central carbon that is bonded to 3 oxygens. Each oxygen has 3 lone pairs. The molecule is inside square brackets and has a charge of minus 2.

5. No electrons are left for the central atom.

6. At this point, the carbon atom has only 6 valence electrons, so we must take one lone pair from an oxygen and use it to form a carbon–oxygen double bond. In this case, however, there are *three* possible choices:



As with ozone, none of these structures describes the bonding exactly. Each predicts one carbon–oxygen double bond and two carbon–oxygen single bonds, but experimentally all C–O bond lengths are identical. We can write resonance structures (in this case, three of them) for the carbonate ion:



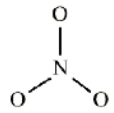
The resonance structure includes all three Lewis dot structures with double headed arrows between them.

The actual structure is an average of these three resonance structures.

The Nitrate (NO_3^-) ion

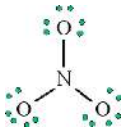
1. Count up the valence electrons: (1*5) + (3*6) + 1(ion) = **24** electrons

2. Draw the bond connectivities:

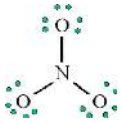


The three oxygens are drawn in the shape of a triangle with the nitrogen at the center of the triangle.

3. Add octet electrons to the atoms bonded to the center atom:

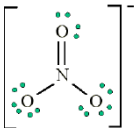


4. Place any leftover electrons (24-24 = **0**) on the center atom:



5. Does the central atom have an octet?

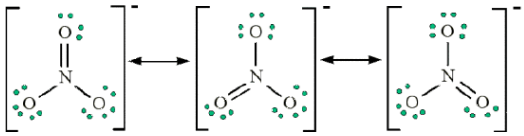
- **NO**, it has 6 electrons
- Add a multiple bond (first try a double bond) to see if the central atom can achieve an octet:



A double bond is added between one oxygen and the central nitrogen. The molecule has a negative charge.

6. Does the central atom have an octet?

- YES
- Are there possible resonance structures? YES



Note: We would expect that the bond lengths in the NO_3^- ion to be somewhat shorter than a single bond.



Example 2.1.3.1: Benzene

Benzene is a common organic solvent that was previously used in gasoline; it is no longer used for this purpose, however, because it is now known to be a carcinogen. The benzene molecule (C_6H_6) consists of a regular hexagon of carbon atoms, each of which is also bonded to a hydrogen atom. Use resonance structures to describe the bonding in benzene.

Given: molecular formula and molecular geometry

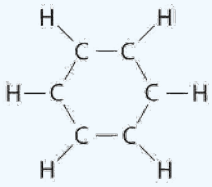
Asked for: resonance structures

Strategy:

A. Draw a structure for benzene illustrating the bonded atoms. Then calculate the number of valence electrons used in this drawing.
B. Subtract this number from the total number of valence electrons in benzene and then locate the remaining electrons such that each atom in the structure reaches an octet.
C. Draw the resonance structures for benzene.

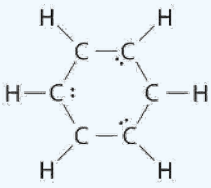
Solution:

A Each hydrogen atom contributes 1 valence electron, and each carbon atom contributes 4 valence electrons, for a total of (6 × 1) + (6 × 4) = 30 valence electrons. If we place a single bonding electron pair between each pair of carbon atoms and between each carbon and a hydrogen atom, we obtain the following:



Each carbon atom in this structure has only 6 electrons and has a formal charge of +1, but we have used only 24 of the 30 valence electrons.

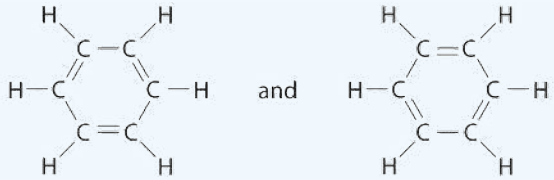
B If the 6 remaining electrons are uniformly distributed pairwise on alternate carbon atoms, we obtain the following:



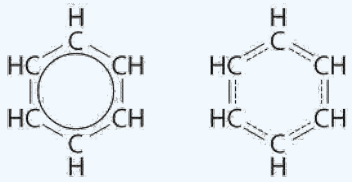
Three carbon atoms now have an octet configuration and a formal charge of −1, while three carbon atoms have only 6 electrons and a formal charge of +1. We can convert each lone pair to a bonding electron pair, which gives each atom an octet of

electrons and a formal charge of 0, by making three C=C double bonds.

C There are, however, two ways to do this:



Each structure has alternating double and single bonds, but experimentation shows that each carbon–carbon bond in benzene is identical, with bond lengths (139.9 pm) intermediate between those typically found for a C–C single bond (154 pm) and a C=C double bond (134 pm). We can describe the bonding in benzene using the two resonance structures, but the actual electronic structure is an average of the two. The existence of multiple resonance structures for aromatic hydrocarbons like benzene is often indicated by drawing either a circle or dashed lines inside the hexagon:



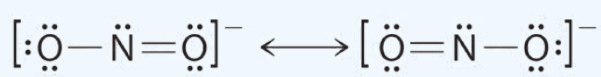
Benzene

Problems

? Exercise 2.1.3.1: Nitrite Ion

The sodium salt of nitrite is used to relieve muscle spasms. Draw two resonance structures for the nitrite ion (NO_2^-).

Answer



There is a double bond between one oxygen and the nitrogen, It can be found on the left oxygen or the right oxygen.

Resonance structures are particularly common in oxoanions of the *p*-block elements, such as sulfate and phosphate, and in aromatic hydrocarbons, such as benzene and naphthalene.

Warning

If several reasonable resonance forms for a molecule exists, the "actual electronic structure" of the molecule will probably be intermediate between all the forms that you can draw. The classic example is benzene in Example **2.1.3.1**. One would expect the double bonds to be shorter than the single bonds, but if one overlays the two structures, you see that one structure has a single bond where the other structure has a double bond. The best measurements that we can make of benzene do not show two bond lengths - instead, they show that the bond length is intermediate between the two resonance structures.

Resonance structures is a mechanism that allows us to use all of the possible resonance structures to try to predict what the actual form of the molecule would be. Single bonds, double bonds, triple bonds, +1 charges, -1 charges, these are our limitations in explaining the structures, and the true forms can be in between - a carbon-carbon bond could be mostly single bond with a little bit of double bond character and a partial negative charge, for example.

Summary

Some molecules have two or more chemically equivalent Lewis electron structures, called resonance structures. Resonance is a mental exercise and method within the Valence Bond Theory of bonding that describes the delocalization of electrons within

molecules. These structures are written with a **double-headed arrow** between them, indicating that none of the Lewis structures accurately describes the bonding but that the actual structure is an average of the individual resonance structures. Resonance structures are used when one Lewis structure for a single molecule cannot fully describe the bonding that takes place between neighboring atoms relative to the empirical data for the actual bond lengths between those atoms. The net sum of valid resonance structures is defined as a resonance hybrid, which represents the overall delocalization of electrons within the molecule. A molecule that has several resonance structures is more stable than one with fewer. Some resonance structures are more favorable than others.

2.1.3: Lewis- Resonance is shared under a CC BY-NC-SA 4.0 license and was authored, remixed, and/or curated by Kathryn A. Newton, Northern Michigan University.

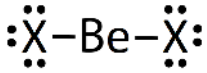
- **8.6: Resonance Structures** is licensed CC BY-NC-SA 3.0.

2.1.4: Lewis- Electron-Deficient "Octets" of B and Be

Two notable cases where Lewis theory fails to predict structure are the cases of beryllium (\(\ce{Be}\)) and boron (\(\ce{B}\)). These two atoms are in period 2 (\(n=2\)) of the periodic table and their atoms have the valence electron configurations of \(2s^2\) and \(2s^22p^1\), respectively.

Beryllium

The Lewis electron dot structures are shown below for \(\ce{BeX2}\), where \(\ce{X}\) is one of the halogens, \(\ce{F}\) or \(\ce{Cl}\).



Each of the structures above would predict a linear geometry for the \(\ce{BeX2}\) molecule. Together the three resonance structures suggest partial double-bond character in the Be-X bond, which results in an intermediate bond length between a single and double bond.

There are issues with each of these resonance structures. The structure on the left would predict only four electrons around \(\ce{Be}\); thus, the atom does not fulfill the octet rule. The structure on the left suggests multiple bonds for the halogen (\(\ce{X}\)) and high separation of charge with formal charge on each atom. The structure in the middle is a mix of these problems. None of these situations is ideal according to Lewis theory. Further, experimental data is not consistent with any of these structures or their resonance hybrid (except in the case of \(\ce{BeCl2}\) at very high temperatures).

It turns out that the monomer of \(\ce{BeX2}\) does exist, but only at very high temperatures and low pressures. Even under extreme conditions, the monomer is not particularly stable due to the electron deficiency around \(\ce{Be}\).

BeF_2

At ambient temperature and pressure, BeF_2 is a solid that looks similar to quartz (Figure \(\PageIndex{1}\)) The Be is four-coordinate with tetrahedral geometry; each F is two-coordinate and the Be-F bond length is 1.54 Å. This structure is possible due to an extended 3-dimensional network in the solid where adjacent BeF_2 units are bonded to one another, as shown in Figure \(\PageIndex{1}\).

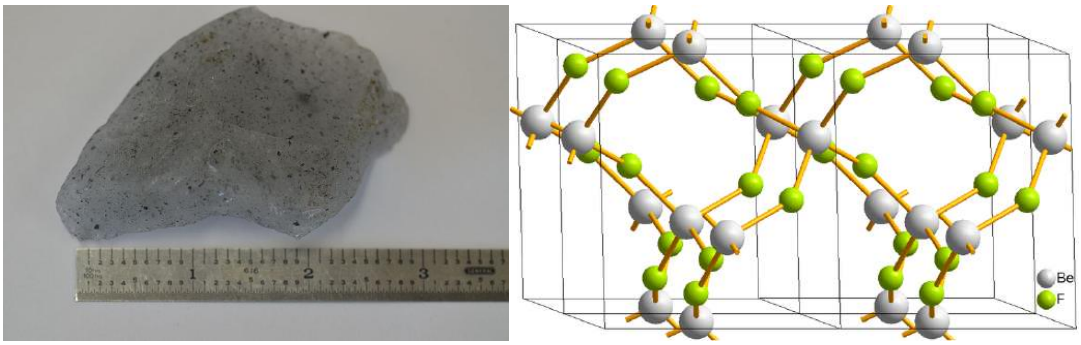


Figure \(\PageIndex{1}\): (left) A nugget of beryllium fluoride obtained from Materion. Black spots are carbon (CC BY-SA 3.0; Bckelleher via Wikipedia). (right) BeF2 structure (CC BY-SA 3.0 Unported; Materialscientist via Wikipedia)

In the liquid phase, \(\ce{BeF2}\) has a fluctuating tetrahedral structure where Be and F ions exchange. The vapor phase is reached at temperatures higher than 1000 °C (at ~ 1 atm). In the vapor phase, \(\ce{BeF2}\) exists as a monomer with linear geometry and a bond length of 1.43 Å, consistent with a double bond between \(\ce{Be}\) and \(\ce{F}\).

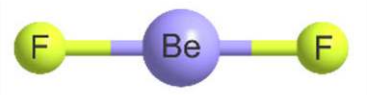


Figure \(\PageIndex{2}\): Geometries of \(\ce{BeF2}\). (CC BY; Ibon Alkorta and Anthony C. Legoe via Inorganics)

$BeCl_2$

At ambient temperature and pressure, \(\ce{BeCl2}\) is a solid. As in \(\ce{BeF2}\) described above, \(\ce{BeCl2}\) has four-coordinate, tetrahedral Be and two-coordinate Cl. In contrast to BeF_2, solid $BeCl_2$ is a 1-dimensional polymer consisting of edge-shared tetrahedral.

In the gas phase, $BeCl_2$ exists as a dimer with two chlorine atoms bridging two Be atoms. In the dimer, the Be atoms are 3-coordinate. Bridging Cl atoms are two-coordinate, while terminal Cl atoms are one-coordinate. At higher temperatures in the vapor phase, the linear monomer also exists.

Boron (\(2s^22p^1\))

Prediction based on Lewis structures:

Lewis structures of \(\ce{BH3}\) and \(\ce{BF3}\) were described in Exercise 3.1.2, and are drawn again below for convenience.

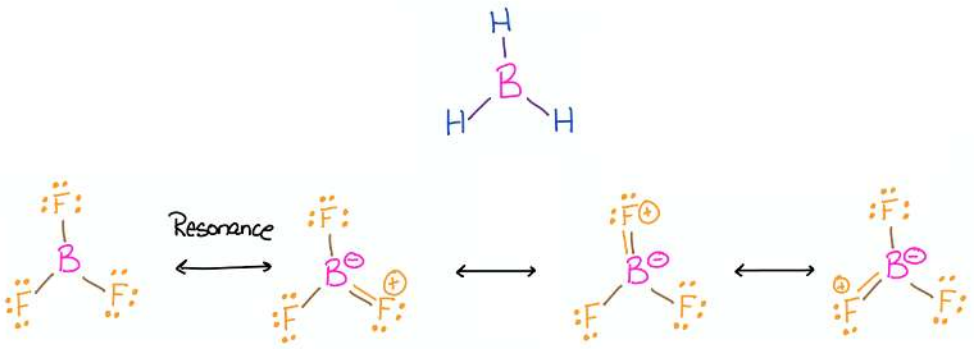


Figure \(\PageIndex{2}\): Lewis structures of \(\ce{BH3}\) and \(\ce{BF3}\). (Kathryn Haas; CC-NC-BY-SA)

Boron trihalides

Boron trihalides, like \(\ce{BF3}\), have properties that are largely predicted by Lewis structures and VSEPR theory. The Lewis structure for \(\ce{BF3}\) includes several resonance structures. The structure with only single bonds is the most common representation for this molecule because the charge separation shown in the other structures is considered to be unfavorable. The highly polarized B-F bond has a dipole moment that lies opposite to the indicated formal charges shown in the resonance structures with double bonds between boron and fluorine.

The resonance hybrid of \(\ce{BF3}\) predicts partial double bond character between boron and fluorine, thus a bond length shorter than a single bond. Using the Lewis structures and VSEPR theory, we would predict a trigonal planar geometry around boron. In fact, the actual structure of \(\ce{BF3}\) is a monomer with trigonal planar geometry and with bond length that is shorter than a single bond. The case is similar to structures of other boron trihalides as well.

Boron trihalides are electron deficient at the boron center and react readily with Lewis bases. In other words they are strong Lewis acids (electrophiles).

Boron trihydride (BH_3 is really B_2H_6)

The properties of boron trihydride (\(\ce{BH3}\)) are not predicted by the simple predictions made through Lewis structures and VSEPR. The monomer, BH_3, is not stable, but when dissolved in the presence of a Lewis base, BH_3 can form a stable acid-base adduct. In its pure form, the compound actually exists as a dimeric gas with a molecular unit of B_2H_6 (try drawing a valid Lewis structure for that!). Its unexpected structure includes two H's that bridge the two boron atoms in 3-center-2-electron bonds. You can read more about B_2H_6 on the Wikipedia page for Diborane(6). The unique bonding observed for boron is described more in Chapter 8 and Chapter 15.

2.1.4: Lewis- Electron-Deficient "Octets" of B and Be is shared under a CC BY-NC-SA 4.0 license and was authored, remixed, and/or curated by Kathryn A. Newton, Northern Michigan University.

- **3.1.4: Lewis Fails to Predict Unusual Cases - Boron and Beryllium** by Kathryn Haas is licensed CC BY-NC 4.0.

2.1.5: Molecule Shape from Valence Shell Electron Repulsion Theory (VSEPR)

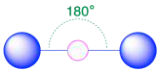
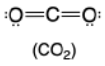
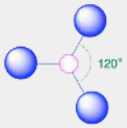
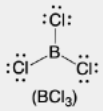
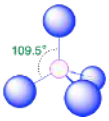
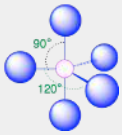
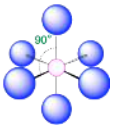
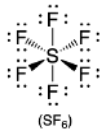
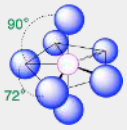
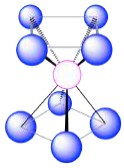
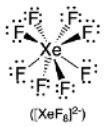
Introduction to VSEPR

The **Valence Shell Electron Repulsion (VSEPR)** model can predict the structure of most molecules and polyatomic ions in which the central atom is a nonmetal; it also works for some structures in which the central atom is a metal. VSEPR builds on Lewis electron dot structures (discussed in Section 3.1); Lewis structures alone predict only connectivity while the Lewis structure and VSEPR together can predict the geometry of each atom in a molecule. The main idea of VSEPR theory is that pairs of electrons (in bonds and in lone pairs) repel each other. The pairs of electrons (in bonds and in lone pairs) are called "groups". Because electrons repel each other electrostatically, the most stable arrangement of electron groups (i.e., the one with the lowest energy) is the one that minimizes repulsion. Groups are positioned around the central atom in a way that produces the molecular structure with the lowest energy. In other words, the repulsion between groups around an atom favors a geometry in which the groups are as far apart from each other as possible. Although VSEPR is simplistic because it does not account for the subtleties of orbital interactions that influence molecular shapes, it accurately predicts the three-dimensional structures of a large number of compounds.

We can use the VSEPR model to predict the geometry around the atoms in a polyatomic molecule or ion by focusing on the number of electron pairs (groups) around a *central atom* of interest. Groups include bonded and unbonded electrons; a single bond, a double bond, a triple bond, a lone pair of electrons, or even a single unpaired electron each count as one group. The molecule or polyatomic ion is given an AX_mE_n designation, where **A is the central atom**, **X is a bonded atom**, **E is a nonbonding** valence electron group (usually a lone pair of electrons), and m and n are integers. The number of groups is equal to the sum of m and n. Using this information, we can describe the molecular geometry around a central atom, that is, the arrangement of the *bonded atoms* in a molecule or polyatomic ion. The geometries that are predicted from VSEPR when a central atom has only bonded groups ($n = 0$) are listed below in Table **2.1.5.1**. The cases where lone pairs contribute to the total groups ($n \geq 1$) are discussed in the next section about lone pair repulsion.

Table 2.1.5.1. Geometries predicted using VSEPR theory (bonded groups only).

https://chem.libretexts.org/@go/page/551686

Groups around central atom (m + n)	Geometry Name	Geometry Sketch	Predicted bond Angle	Example
2	linear		180°	
3	trigonal plane		120°	
4	tetrahedron		109.5°	
5	trigonal bipyramid		90° and 120°	
6	octahedron		90°	
7	pentagonal bipyramid		90° and 72°	
8	square antiprism		70.5°, 99.6° and 109.5°	

Practice

VSEPR to predict Molecular Geometry

You can follow these four steps to predict the geometry around an atom using VSEPR:

1. Draw the Lewis electron structure of the molecule or polyatomic ion.
2. For the central atom of interest, assign the AX_mE_n designation and the total number of groups (m+n).
3. Determine the electron group arrangement around the central atom that minimizes repulsions.
4. Describe the molecular geometry.

Use the procedure above to complete the exercises below

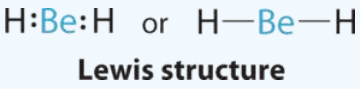
Problems

? Exercise 2.1.5.1

Predict the geometry around the central atom in BeH_2.

Answer

1. The central atom, beryllium, contributes two valence electrons, and each hydrogen atom contributes one. The Lewis electron structure is



Lewis structure

2. There are two groups around the central atom, and both groups are single bonds. Thus BeH_2 is designated as AX_2.

3. We see from Table **2.1.5.1** that the arrangement that minimizes repulsions places the groups 180° apart.

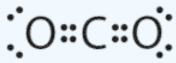
4. From Table **2.1.5.1** we see that with two bonding pairs, the molecular geometry that minimizes repulsions in BeH_2 is *linear.*

? Exercise 2.1.5.2

Predict the geometry around the central atom in CO_2.

Answer

1. The central atom, carbon, contributes four valence electrons, and each oxygen atom contributes six. The Lewis electron structure is



2. There are two groups around the central atom, and both groups are double bonds. Thus CO_2 is designated as AX_2.

3. Wee see from the Table **2.1.5.1** that the arrangement that minimizes repulsions places the groups 180° apart.

4. From Table **2.1.5.1** we see that with two bonding pairs, the molecular geometry that minimizes repulsions in CO_2 is *linear.*

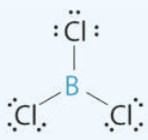
Note: VSEPR only recognizes groups around the *central* atom (the carbon). Thus the lone pairs on the oxygen atoms do not influence the molecular geometry.

? Exercise 2.1.5.3

Predict the geometry around the central atom in BCl_3 .

Answer

1. The central atom, boron, contributes three valence electrons, and each chlorine atom contributes seven valence electrons. The Lewis electron structure is



Lewis structure

2. There are three groups around the central atom and all are single bonds. The structure is designated as AX_3.

3. To minimize repulsions, the groups are placed 120° apart (Table **2.1.5.1**).

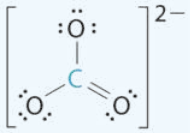
4. From Table **2.1.5.1** we see that with three bonding pairs around the central atom, the molecular geometry of BCl_3 is *trigonal planar*.

Exercise 2.1.5.4

Predict the geometry around the central atom in CO_3^{2-}.

Answer

1. The central atom, carbon, has four valence electrons, and each oxygen atom has six valence electrons. The Lewis electron structure of one of three resonance forms is represented as

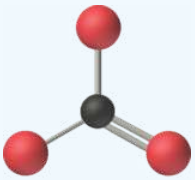


Lewis structure

2. The structure of CO_3^{2-} is a resonance hybrid. It has three identical bonds, each with a bond order of $1\frac{1}{3}$. All electron groups are bonds. With three bonding groups around the central atom, the structure is designated as AX_3.

3. We minimize repulsions by placing the three groups 120° apart (Table **2.1.5.1**).

4. We see from Table **2.1.5.1** that the molecular geometry of CO_3^{2-} is trigonal planar with bond angles of 120°.



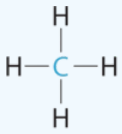
Molecular geometry
(trigonal planar)

Exercise 2.1.5.5

Predict the geometry around the central atom in CH_4.

Answer

1. The central atom, carbon, contributes four valence electrons, and each hydrogen atom has one valence electron, so the full Lewis electron structure is

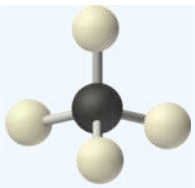


Lewis structure

2. There are four electron groups around the central atom. All electron groups are bonding pairs, so the structure is designated as AX_4.

3. As shown in Table **2.1.5.1**, repulsions are minimized by placing the groups in the corners of a tetrahedron with bond angles of 109.5°.

4. With four bonding pairs, the molecular geometry of methane is *tetrahedral* (Table **2.1.5.1**).



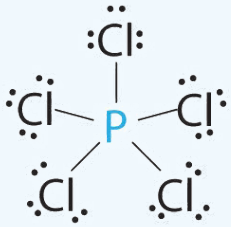
Molecular geometry (tetrahedral)

? Exercise Extra close brace or missing open brace

Predict the geometry around the central atom in PCl_5.

Answer

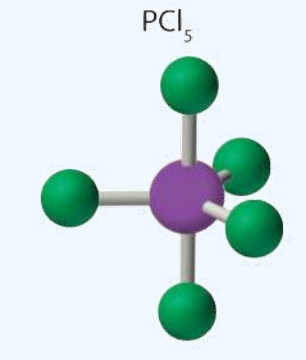
1. Phosphorus has five valence electrons and each chlorine has seven valence electrons, so the Lewis electron structure of PCl_5 is



2. There are five bonding groups around phosphorus, the central atom. All electron groups are bonds, so the structure is designated as AX_5.

3. The structure that minimizes repulsions is a *trigonal bipyramid*, which consists of two trigonal pyramids that share a base (Table **2.1.5.1**).

4. The molecular geometry of PCl_5 is *trigonal bipyramidal*, as shown below. The molecule has three atoms in a plane in *equatorial* positions and two atoms above and below the plane in *axial* positions. The three equatorial positions are separated by 120° from one another, and the two axial positions are at 90° to the equatorial plane. The axial and equatorial positions are not chemically equivalent.

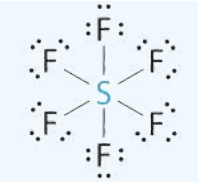


? Exercise 2.1.5.7

Predict the geometry around the central atom in SF_6.

Answer

1. The central atom, sulfur, contributes six valence electrons, and each fluorine atom has seven valence electrons, so the Lewis electron structure is



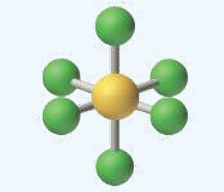
Lewis structure

With an expanded valence, this species is an exception to the octet rule.

2. There are six electron groups around the central atom, each a bonding pair. We see from Figure **2.1.5.2** that the geometry that minimizes repulsions is *octahedral*.

3. With only bonding pairs, SF_6 is designated as AX_6. All positions are chemically equivalent, so all electronic interactions are equivalent.

4. There are six nuclei, so the molecular geometry of SF_6 is octahedral.



Molecular geometry
(octahedral)

2.1.5: Molecule Shape from Valence Shell Electron Repulsion Theory (VSEPR) is shared under a CC BY-NC-SA 4.0 license and was authored, remixed, and/or curated by Kathryn A. Newton, Northern Michigan University.

- **3.2: Valence Shell Electron-Pair Repulsion** by Kathryn Haas is licensed CC BY-NC-SA 4.0.

2.1.6: Shape Change from Lone Pairs

In the previous section, we saw how to use VSEPR to predict the geometry around a central atom based on the number of groups attached to a central atom. However, our previous discussion was limited to the simple cases where all of the groups were bonded groups (i.e., in the designation AX_mE_n , n=0). When all of the groups are bonds, the geometries can be predicted using information in Table 3.2.1 in the previous section. Now we will consider cases where one or more of these groups are lone pairs.

Lone pairs have stronger repulsive forces than bonded groups.

When one or more of the groups is a lone pair of electrons (non-bonded electrons), the experimentally-observed geometry around an atom is slightly different than in the case where all groups are bonds. The actual bond angles are similar, but not exactly the same, as those predicted based on the *total number of groups* (the "parent" geometry). When there is a mixture of group types (**lone pairs (E)** ***and*** **bonded groups (X)**) there are three different types of angles to consider: bond angles between two bonded atoms (**X-X** angles), angles between a bonded atom and a lone pair (**X-E** angles), and angles between two lone pairs (**E-E** angles). Empirical evidence shows the following trend in the degree of bond angles around atoms with a mixture of group types:

Trend in bond angles:

E-E >**X-E** >**X-X**

Using empirical evidence as a guide, we can predict that lone pairs repel other electron groups more strongly than bonded pairs. The molecular geometry of molecules with lone pairs of electrons is better predicted when we consider that electronic repulsion created by lone pairs is stronger than the repulsion from bonded groups. It is difficult to predict the exact bond angle based on this principle, but we can predict approximate angles, as described and summarized below in Table **2.1.6.1**.

Table **2.1.6.1**: Predictions of molecular geometry and bond angles around atoms with a mixture of bonded (X) and unbonded (E) electron groups.

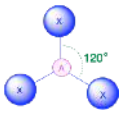
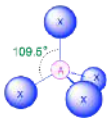
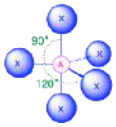
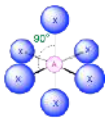
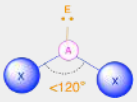
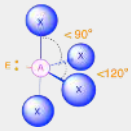
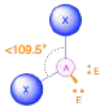
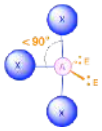
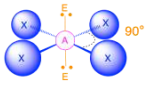
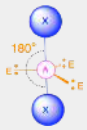
Electron Groups (m + n)					
	2 (steric number = 2)	**3** (steric number = 3)	**4** (steric number = 4)	**5** (steric number = 5)	**6** (steric number = 6)
Parent Geometry (0 lone pairs) AX_m	 AX_2, linear 180°	 AX_3, trig. plane 120°	 $AX4$, tetrahedron 109.5°	 AX_5, trig. bipyramid 90°, 120°	 AX_6, octahedron 90°
1 lone pair AX_mE_1		 $AX2E_1$, bent <120°	 AX_3E_1, trig. pyramid <109.5°	 AX_4E_1, see-saw <90°, <120°	 AX_5E_1, square pyramid 90°, <90°
2 lone pairs AX_mE_2			 AX_2E_2, bent <109.5°	 AX_3E_2, T-shape <90°	 AX_4E_2, square plane 90°
3 lone pairs AX_mE_3				 AX_2E_3, linear 180°	

Table **2.1.6.1** summarizes the geometries and bond angles predicted for nearest-neighbor bonded groups on central atoms with a mixture of lone pairs and bonded groups. The table does not cover all possible situations; it only includes cases where there are two bonded groups in which an X-X angle is measurable between nearest-neighbors. A more detailed description of some selected cases is given below.

Two Electron Groups (m + n = 2)

(Steric number = 2) In the case that there are only two electron groups around a central atom, those groups will lie 180° from one another. This results in a linear molecular geometry with 180° bond angles.

Three Electron Groups (m + n = 3)

(Steric number = 3) In the case that there are three electron groups around a central atom, those groups will lie approximately 120° from one another in space. This results in an electronic geometry that is approximately **trigonal planar**. There are two different molecular geometries that are possible in this category:

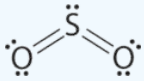
- When all of the electron groups are bonds (m = 3 or AX_3), the molecular geometry is a ***trigonal plane*** with **120°** bond angles.
- When there is one lone pair (m=2, n=1 or AX_2E_1), the molecular geometry is ***bent*** with a bond angle that is slightly **less than 120°**.

Example 2.1.6.1: AX_2E

Predict the geometry and bond angles in SO_2.

Solution

1. The central atom, sulfur, has 6 valence electrons, as does each oxygen atom. With 18 valence electrons, the Lewis electron structure is shown below.



2. There are three electron groups around the central atom: two double bonds and one lone pair. We initially place the groups in a trigonal planar arrangement to minimize repulsions (Table **2.1.6.1**).

3. With two bonding pairs and one lone pair, the structure is designated as AX_2E. This designation has a total of three electron pairs, two X and one E. The lone pair occupies more space around the central atom than a bonding pair (even double bonds!). Bonding pairs and lone pairs repel each other electrostatically in the order BP–BP < LP–BP < LP–LP. In SO_2, we have one BP–BP interaction and two LP–BP interactions.

4. The molecular geometry is described only by the positions of the nuclei, *not* by the positions of the lone pairs. Thus, with two nuclei and one lone pair the shape is *bent*, or *V shaped*, which can be viewed as a trigonal planar arrangement with a missing vertex. The O-S-O bond angle is expected to be *less than* 120° because of the extra space taken up by the lone pair.

Four Electron Groups (m + n = 4)

(Steric number = 4) In the case that there are four electron groups around a central atom, those groups will lie approximately 109.5° from one another in space. This results in an electronic geometry that is approximately **tetrahedral**. There are three different molecular geometries that are possible in this category:

- When all electron groups are bonds (m=4 or AX_4), the molecular geometry is a ***tetrahedron*** with bond angles of **109.5°**.
- When there is one lone pair (m=3, n=1 or AX_3E_1), the molecular geometry is a ***trigonal pyramid*** with bond angles of **slightly less than 109.5°**.
- When there are two lone pairs (m=2, n=2 or AX_2E_2), the molecular geometry is ***bent*** with bond angles of **slightly less than 109.5°**.

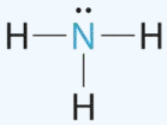
Example 2.1.6.2: AX_3E

Predict the geometry and bond angles in NH_3.

Solution

One of the limitations of Lewis structures is that they depict molecules and ions in only two dimensions. With four electron groups, we must learn to show molecules and ions in three dimensions.

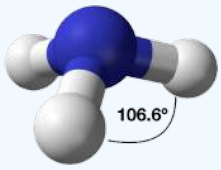
1. In ammonia, the central atom, nitrogen, has five valence electrons and each hydrogen donates one valence electron, producing the Lewis electron structure



Lewis structure

2. There are four electron groups around nitrogen, three bonding pairs and one lone pair. Repulsions are minimized by directing each hydrogen atom and the lone pair to the corners of a tetrahedron.

3. With three bonding pairs and one lone pair, the structure is designated as AX_3E. This designation has a total of four electron pairs, three X and one E. We expect the LP–BP interactions to cause the bonding pair angles to deviate significantly from the angles of a perfect tetrahedron.



The Difference in the Space Occupied by a Lone Pair of Electrons and by a Bonding Pair

As with SO_2, this composite model of electron distribution and negative electrostatic potential in ammonia shows that a lone pair of electrons occupies a larger region of space around the nitrogen atom than does a bonding pair of electrons that is shared with a hydrogen atom.

4. There are three nuclei and one lone pair, so the molecular geometry is *trigonal pyramidal*. In essence, this is a tetrahedron with a vertex missing. However, the H–N–H bond angles are less than the ideal angle of 109.5° because of LP–BP repulsion. The bond angles in ammonia are 106.6°.

Example 2.1.6.3: AX_2E_2

Predict the geometry and in H_2O.

Solution

1. Oxygen has six valence electrons and each hydrogen has one valence electron, producing the Lewis electron structure



2. There are four groups around the central oxygen atom, two bonding pairs and two lone pairs. Repulsions are minimized by directing the bonding pairs and the lone pairs to the corners of a tetrahedron.

3. With two bonding pairs and two lone pairs, the structure is designated as AX_2E_2 with a total of four electron pairs. Due to LP–LP, LP–BP, and BP–BP interactions, we expect a significant deviation from idealized tetrahedral angles.

4. With two hydrogen atoms and two lone pairs of electrons, the structure has significant lone pair interactions. There are two nuclei about the central atom, so the molecular shape is *bent*, or *V shaped*, with an H–O–H angle that is even less than the H–N–H angles in NH_3, as we would expect because of the presence of two lone pairs of electrons on the central atom rather than one. This molecular shape is essentially a tetrahedron with two missing vertices.

Five Electron Groups (m + n = 5)

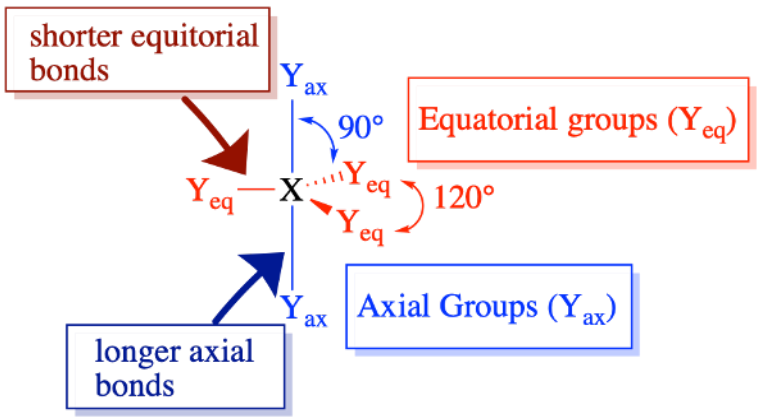


Figure: Trigonal pyramidal molecules (steric number 5) possess different bond angles and lengths for axial (ax) and equatorial (eq) pendant atoms. (CC-BY-NC-SA; Kathryn Haas).

(Steric number = 5) In the case that there are five electron groups around a central atom, there are two different types of positions around the central atom: equatorial positions and axial positions. The three equatorial ligands are 120° from one another and are

90° from each of the two axial ligands. The axial positions have three adjacent groups oriented 90° away in space. Axial groups are thus more crowded than the equatorial positions with only two adjacent groups at 90°. The crowding of axial positions results in slight differences in bond distances; crowded axial groups have longer bonds than the less crowded equatorial groups. Lone pairs of electrons generally prefer to occupy equatorial positions rather than axial positions. The justification for this preference, according to VSEPR theory, is that the lone electron pairs are more repulsive than bonding electron pairs, and thus the lone pairs prefer the less crowded equatorial positions.

The arrangement of five groups around a central atom results in a **trigonal bipyramidal** electronic geometry. There are four different molecular geometries that are possible in this category, depending upon the number of bonded groups and lone pairs of electrons:

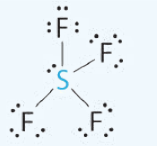
- When all electron groups are bonds (m=5 or AX_5), the molecular geometry is a ***trigonal bipyramid*** with bond angles of **120°** and **90°** between adjacent ligands.
- When there is one lone pair (m=4, n=1 or AX_4E_1), the lone pair occupies one of the equatorial positions. The molecular geometry is called a ***see saw*** with bond angles of **slightly less than 120°** and **slightly less than 90°**.
- When there are two lone pairs (m=3, n=2 or AX_3E_2), each lone pair occupies one of the three equatorial positions. The molecular geometry is ***T-shaped*** with bond angles of **slightly less than 120°** and **slightly less than 90°**.
- When there are three lone pairs (m=1, n=3 or AX_3E_2), the lone pairs occupy the three equatorial positions. The molecular geometry is ***linear*** with bond angles of **180°**.

Example 2.1.6.4: AX_4E

Predict the geometry and bond angles in SF_4.

Solution

1. The sulfur atom has six valence electrons and each fluorine has seven valence electrons, so the Lewis electron structure is



Lewis structure

With an expanded valence, this species is an exception to the octet rule.

2. There are five groups around sulfur, four bonding pairs and one lone pair. With five electron groups, the lowest energy arrangement is a trigonal bipyramid.

3. We designate SF_4 as AX_4E; it has a total of five electron pairs. However, because the axial and equatorial positions are not chemically equivalent, where do we place the lone pair? If we place the lone pair in the axial position, we have three LP–BP repulsions at 90°. If we place it in the equatorial position, we have two 90° LP–BP repulsions at 90°. With fewer 90° LP–BP repulsions, we can predict that the structure with the lone pair of electrons in the *equatorial position is more stable than the one with the lone pair in the axial position*. We also expect a deviation from ideal geometry because a lone pair of electrons occupies more space than a bonding pair.

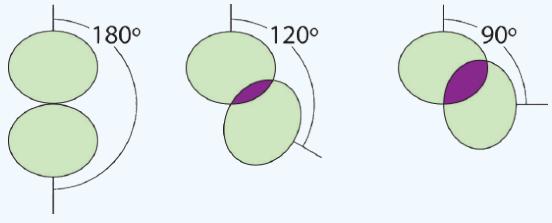
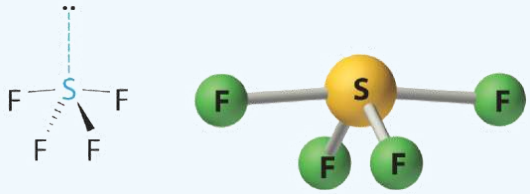


Illustration of the Area Shared by Two Electron Pairs versus the Angle between Them

At 90°, the two electron pairs share a relatively large region of space, which leads to strong repulsive electron–electron interactions.

4. With four nuclei and one lone pair of electrons, the molecular structure is based on a trigonal bipyramid with a missing equatorial vertex; it is described as a *seesaw*. The F_{axial}–S–F_{axial} angle is 173° rather than 180° because of the lone pair of electrons in the equatorial plane.



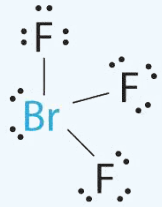
Molecular geometry (seesaw)

Example 2.1.6.5: AX_3E_2

Predict the geometry and bond angles in BrF_3.

Solution

1. The bromine atom has seven valence electrons, and each fluorine has seven valence electrons, so the Lewis electron structure is

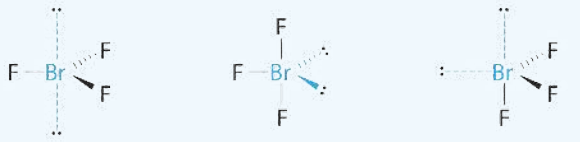


Lewis structure

Once again, we have a compound that is an exception to the octet rule.

2. There are five groups around the central atom, three bonding pairs and two lone pairs. We again direct the groups toward the vertices of a trigonal bipyramid.

3. With three bonding pairs and two lone pairs, the structural designation is AX_3E_2 with a total of five electron pairs. Because the axial and equatorial positions are not equivalent, we must decide how to arrange the groups to minimize repulsions. If we place both lone pairs in the axial positions, we have six LP–BP repulsions at 90°. If both are in the equatorial positions, we have four LP–BP repulsions at 90°. If one lone pair is axial and the other equatorial, we have one LP–LP repulsion at 90° and three LP–BP repulsions at 90°:



	Lone pairs axial (a)	Lone pairs equatorial (b)	Lone pairs axial and equatorial (c)
Interactions			
90° LP–LP	0	0	1
90° LP–BP	6	4	3

Structure (c) can be eliminated because it has a LP–LP interaction at 90°. Structure (b), with fewer LP–BP repulsions at 90° than (a), is lower in energy. However, we predict a deviation in bond angles because of the presence of the two lone pairs of electrons.

4. The three nuclei in BrF_3 determine its molecular structure, which is described as *T shaped*. This is essentially a trigonal bipyramid that is missing two equatorial vertices. The F_{axial}–Br–F_{axial} angle is 172°, less than 180° because of LP–BP repulsions.

Because lone pairs occupy more space around the central atom than bonding pairs, electrostatic repulsions are more important for lone pairs than for bonding pairs.

Example 2.1.6.6: AX_2E_3

Predict the geometry and bond angles in I_3^-.

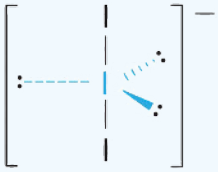
Solution

1. Each iodine atom contributes seven electrons and the negative charge one, so the Lewis electron structure is



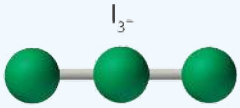
2. There are five electron groups about the central atom in I_3^-, two bonding pairs and three lone pairs. To minimize repulsions, the groups are directed to the corners of a trigonal bipyramid.

3. With two bonding pairs and three lone pairs, I_3^- has a total of five electron pairs and is designated as AX_2E_3. We must now decide how to arrange the lone pairs of electrons in a trigonal bipyramid in a way that minimizes repulsions. Placing them in the equatorial positions eliminates 90° LP–LP repulsions and minimizes the number of 90° LP–BP repulsions.



The three lone pairs of electrons have equivalent interactions with the three iodine atoms, so we do not expect any deviations in bonding angles.

4. With three nuclei and three lone pairs of electrons, the molecular geometry of I_3^- is linear. This can be described as a trigonal bipyramid with three equatorial vertices missing. The ion has an I–I–I angle of 180°, as expected.



Six Electron Groups (m + n = 6)

(Steric number = 6) In the case that there are six electron groups around a central atom, the nearest groups will lie approximately 90° from one another in space. This results in an electronic geometry that is approximately **octahedral**. There are three relevant molecular geometries in this category:

- When all electron groups are bonds (m=6 or AX_6), the molecular geometry is an ***octahedron*** with bond angles of **90°** between adjacent bonds.
- When there is one lone pair (m=5, n=1 or AX_5E_1) we now distinguish between the axial and equitorial positions; the lone pair is considered to be in one of the axial positions, while the bond directly opposite of the lone pair is the axial bond. The molecular geometry is a ***square pyramid*** with bond angles of **90°** between adjacent equatorial bonds and **slightly less than 90°** between the axial bond and equatorial groups.
- When there are two lone pairs (m=4, n=2 or AX_4E_2), the lone pairs are opposite of one another and each occupy an axial position. The molecular geometry is ***square planar*** with bond angles of **90°**.

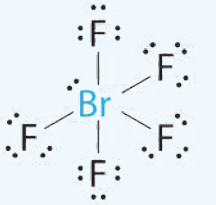
Example 2.1.6.7: AX_5E

Predict the geometry and bond angles in BrF_5.

Solution

AX_5E Molecules: BrF_5

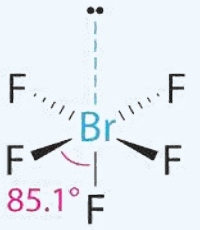
1. The central atom, bromine, has seven valence electrons, as does each fluorine, so the Lewis electron structure is



Lewis structure

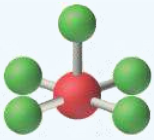
With its expanded valence, this species is an exception to the octet rule.

2. There are six electron groups around the Br, five bonding pairs and one lone pair. Placing five F atoms around Br while minimizing BP–BP and LP–BP repulsions gives the following structure:



3. With five bonding pairs and one lone pair, BrF_5 is designated as AX_5E; it has a total of six electron pairs. The BrF_5 structure has four fluorine atoms in a plane in an equatorial position and one fluorine atom and the lone pair of electrons in the axial positions. We expect all F_{axial}–Br–$F_{equatorial}$ angles to be less than 90° because of the lone pair of electrons, which occupies more space than the bonding electron pairs.

4. With five nuclei surrounding the central atom, the molecular structure is based on an octahedron with a vertex missing. This molecular structure is *square pyramidal*. The F_{axial}–B–$F_{equatorial}$ angles are 85.1°, less than 90° because of LP–BP repulsions.



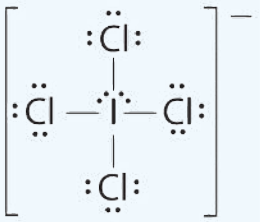
Molecular geometry
(square pyramidal)

Example 2.1.6.8: AX_4E_2

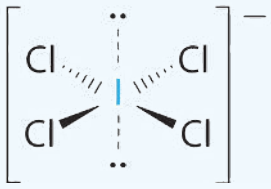
Predict the bond angles in ICl_5^-.

Solution

1. The central atom, iodine, contributes seven electrons. Each chlorine contributes seven, and there is a single negative charge. The Lewis electron structure is

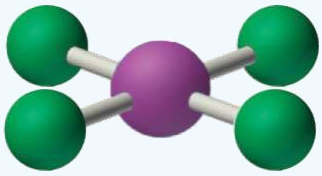


2. There are six electron groups around the central atom, four bonding pairs and two lone pairs. The structure that minimizes LP–LP, LP–BP, and BP–BP repulsions is



3. ICl_4^- is designated as AX_4E_2 and has a total of six electron pairs. Although there are lone pairs of electrons, with four bonding electron pairs in the equatorial plane and the lone pairs of electrons in the axial positions, all LP–BP repulsions are the same. Therefore, we do not expect any deviation in the Cl–I–Cl bond angles.

4. With five nuclei, the ICl4− ion forms a molecular structure that is *square planar*, an octahedron with two opposite vertices missing.



Summary

The arrangement of bonded atoms in a molecule or polyatomic ion is crucial to understanding the chemistry of a molecule, but Lewis electron structures give no information about **molecular geometry**. The **valence-shell electron-pair repulsion (VSEPR) model** allows us to predict which of the possible structures is actually observed in most cases. VSEPR is based on the assumption that pairs of electrons occupy space, and the lowest-energy structure is the one that minimizes repulsions between electron pairs. In the VSEPR model, the molecule or polyatomic ion is given an AX_mE_n designation, where A is the central atom, X is a bonded atom, E is a nonbonding valence electron group (usually a lone pair of electrons), and *m* and *n* are integers. Each group around the central atom is designated as a bonding pair (BP) or lone (nonbonding) pair (LP). From the BP and LP interactions we can predict both the relative positions of the atoms and the angles between the bonds, called the **bond angles**. From this we can describe the **molecular geometry**. The VSEPR model can be used to predict the shapes of many molecules and polyatomic ions, but it gives no information about bond lengths and the presence of multiple bonds. A combination of VSEPR and a bonding model, such as Lewis electron structures, is necessary to understand the presence of multiple bonds.

The relationship between the number of electron groups around a central atom, the number of lone pairs of electrons, and the molecular geometry is summarized in Table **2.1.6.1**.

Problems

? Exercise 2.1.6.1

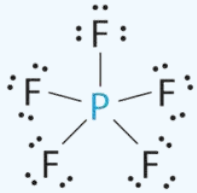
Using the VSEPR model, predict the molecular geometry of PF_5 (a catalyst used in certain organic reactions).

Answer

Strategy:

1. Draw the Lewis electron structure of the molecule or polyatomic ion.
2. Determine the electron group arrangement around the central atom that minimizes repulsions.
3. Assign an AX_mE_n designation; then identify the LP–LP, LP–BP, or BP–BP interactions and predict deviations in bond angles.
4. Describe the molecular geometry.

The central atom, P, has five valence electrons and each fluorine has seven valence electrons, so the Lewis structure of PF_5 is



There are five bonding groups about phosphorus. The structure that minimizes repulsions is a trigonal bipyramid.

All electron groups are bonding pairs, so PF_5 is designated as AX_5. Notice that this gives a total of five electron pairs. With no lone pair repulsions, we do not expect any bond angles to deviate from the ideal.

The PF_5 molecule has five nuclei and no lone pairs of electrons, so its molecular geometry is trigonal bipyramidal.



? Exercise 2.1.6.2

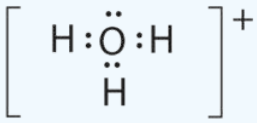
Using the VSEPR model, predict the molecular geometry of H_3O^+ (hydronium ion).

Answer

Strategy:

1. Draw the Lewis electron structure of the molecule or polyatomic ion.
2. Determine the electron group arrangement around the central atom that minimizes repulsions.
3. Assign an AX_mE_n designation; then identify the LP–LP, LP–BP, or BP–BP interactions and predict deviations in bond angles.
4. Describe the molecular geometry.

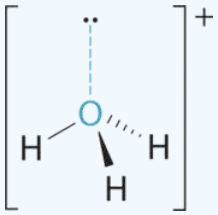
The central atom, O, has six valence electrons, and each H atom contributes one valence electron. Subtracting one electron for the positive charge gives a total of eight valence electrons, so the Lewis electron structure is



There are four electron groups around oxygen, three bonding pairs and one lone pair. Like NH_3, repulsions are minimized by directing each hydrogen atom and the lone pair to the corners of a tetrahedron.

With three bonding pairs and one lone pair, the structure is designated as AX_3E and has a total of four electron pairs (three X and one E). We expect the LP–BP interactions to cause the bonding pair angles to deviate significantly from the angles of a perfect tetrahedron.

There are three nuclei and one lone pair, so the molecular geometry is *trigonal pyramidal*, in essence a tetrahedron missing a vertex. However, the H–O–H bond angles are less than the ideal angle of 109.5° because of LP–BP repulsions:



? Exercise 2.1.6.3

Using the VSEPR model, predict the molecular geometry of XeO_3.

Answer a

trigonal pyramidal

? Exercise 2.1.6.4

Using the VSEPR model, predict the molecular geometry of PF_6^-.

Answer

octahedral

? Exercise 2.1.6.5

Using the VSEPR model, predict the molecular geometry of NO_2^+.

Answer

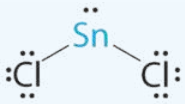
linear

? Exercise 2.1.6.6

Predict the molecular geometry of $SnCl_2$.

Answer

The tin atom donates 4 valence electrons and each chlorine atom donates 7 valence electrons. With 18 valence electrons, the Lewis electron structure is



There are three electron groups around the central atom, two bonding groups and one lone pair of electrons. To minimize repulsions the three groups are initially placed at 120° angles from each other.

From B we designate $SnCl_2$ as AX_2E. It has a total of three electron pairs, two X and one E. Because the lone pair of electrons occupies more space than the bonding pairs, we expect a decrease in the Cl–Sn–Cl bond angle due to increased LP–BP repulsions.

With two nuclei around the central atom and one lone pair of electrons, the molecular geometry of $SnCl_2$ is bent, like SO_2, but with a Cl–Sn–Cl bond angle of 95°. The molecular geometry can be described as a trigonal planar arrangement with one vertex missing.

Exercise 2.1.6.7

Predict the molecular geometry of XeF_2.

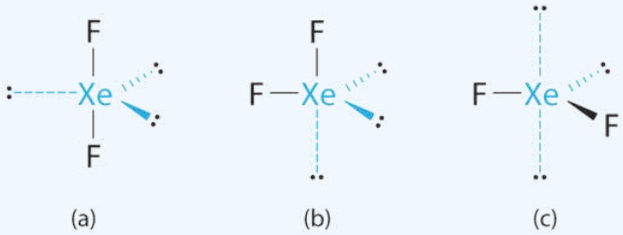
Answer

Xenon contributes eight electrons and each fluorine seven valence electrons, so the Lewis electron structure is



There are five electron groups around the central atom, two bonding pairs and three lone pairs. Repulsions are minimized by placing the groups in the corners of a trigonal bipyramid.

From B, XeF_2 is designated as AX_2E_3 and has a total of five electron pairs (two X and three E). With three lone pairs about the central atom, we can arrange the two F atoms in three possible ways: both F atoms can be axial, one can be axial and one equatorial, or both can be equatorial:



Interactions			
90 LP–LP	0	2	2

The structure with the lowest energy is the one that minimizes LP–LP repulsions. Both (b) and (c) have two 90° LP–LP interactions, whereas structure (a) has none. Thus both F atoms are in the axial positions, like the two iodine atoms around the central iodine in I_3^-. All LP–BP interactions are equivalent, so we do not expect a deviation from an ideal 180° in the F–Xe–F bond angle.

With two nuclei about the central atom, the molecular geometry of XeF_2 is linear. It is a trigonal bipyramid with three missing equatorial vertices.

Exercise 2.1.6.8

Predict the molecular geometry of SO_3.

Answer

trigonal planar

Exercise 2.1.6.9

Predict the molecular geometry of XeF_4.

Answer

square planar

2.1.6: Shape Change from Lone Pairs is shared under a CC BY-NC-SA 4.0 license and was authored, remixed, and/or curated by Kathryn A. Newton, Northern Michigan University.

- **3.2.1: Lone Pair Repulsion** by Kathryn Haas has no license indicated.

2.1.7: Shape Change from Double and Triple Bonds

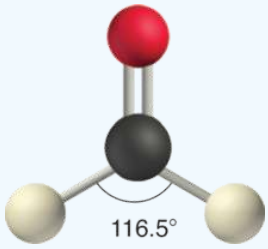
In the previous sections, we saw how to predict the approximate geometry around an atom using VSEPR theory, and we learned that lone pairs of electrons slightly distort bond angles from the "parent" geometry. This page discusses the effect of multiple (double and triple) bonds between bonded atoms.

Double and triple bonds are more repulsive than single bonds

VSEPR theory predicts that double and triple bonds have stronger repulsive forces than single bonds. Like lone pairs of electrons, multiple bonds occupy more space around the central atom than a single bond. The result is that bond angles are slightly distorted compared to the parent geometry. Since a multiple bond has a higher electron density than a single bond, its electrons occupy more space than those of a single bond. Double and triple bonds distort bond angles in a way similar to what lone pairs do. Due to the stronger repulsion, double and triple bonds occupy positions similar to those of lone pairs in groups with 5 and 6 electron groups.

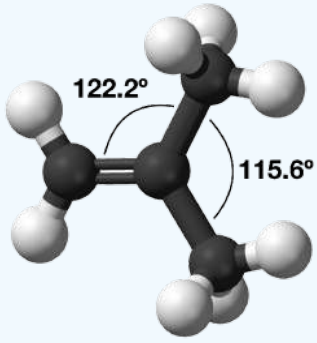
Example 2.1.7.1: CH_2O

In a molecule such as CH_2O (AX_3), whose structure is shown below, the double bond repels the single bonds more strongly than the single bonds repel each other. This causes a deviation from ideal geometry (an H–C–H bond angle of 116.5° rather than 120°).



Example 2.1.7.2: 2-Methylbutene

In the molecule, $CH_2C(CH_3)_2$, the methyl—C—methyl bond angle is 115.6°, which is less than the 120° bond angle that would be expected of the parent geometry. On the other hand, the acetyl—C—methyl bond angle is greater than 120°, with an actual bond angle of 122.2°.



Atoms with both lone pairs and multiple bonds

In general, we expect that a lone pair has slightly greater repulsive force than a multiple bond, and that a multiple bond has slightly greater repulsive force than a single bond. The **order of expected repulsive force** is:

$$\text{lone pair} > \text{double or triple bond} > \text{single bond}$$

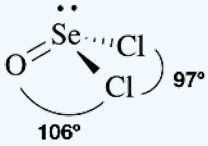
Example 2.1.7.3: $IO_2F_2^-$

With five electron groups, the IO_2F_2 molecule has an approximately trigonal bipyramidal electronic (parent) geometry. The central iodine atom has a single bond to each of the fluorine atoms, a double bond to each oxygen, and a lone pair. The lone pair and the double bonds will occupy more space around iodine than each of the single bonds. Thus, we expect the lone pair and double bonds to occupy equatorial positions around the central iodine. The O=I=O bond angle is 102° (*much* smaller than the 120° angle expected from the parent geometry). This dramatically smaller angle is a result of the increased repulsion between the lone pair and the double bond.



Example 2.1.7.4: $SeOCl_2$

With four electron groups, the $SeOCl_2$ molecule has four electron groups and approximately tetrahedral electronic (parent) geometry. It has both a lone pair and a double bond on the central selenium atom. The two chlorine atoms are singly bonded to selenium, while the oxygen is double bonded. The lone pair is most repulsive, followed by the double bonded oxygen, and then the chlorine bonds. This gives a Cl—Se—Cl bond angle of 97° and a Cl—Se—O bond angle of 106°; both angles are less than the 109.5° angles expected for the ideal tetrahedral geometry.



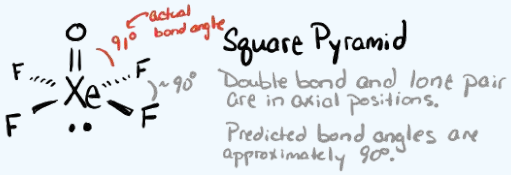
Problems

Exercise 2.1.7.1

Use VSEPR theory to predict the geometries and draw the structures of $XeOF_4$.

Answer

This molecule has six electron groups around the central Xe atom (steric number 6), and thus has an approximately octahdral electronic (parent) geometry. There is a double bond to O and a lone pair, both of which are more strongly repulsive than the single bonds to F. The double bond and lone pair will be directly opposite to each other, designated as axial positions. The result is a square pyramidal molecular geometry. VSEPR theory predicts F—Xe—F bond angles of 90°. As a general rule, lone pairs are slightly more repulsive than multiple bonds, and so we might expect the O—Xe—F bond angles to be <90°; *however in this case the actual O—Xe—F bond angle is observed to be 91°* (you could not have predicted the latter).



Exercise 2.1.7.2

Use VSEPR theory to predict the geometries and draw the structures of NO_2^-.

Answer

This molecule has three electron groups around the central atom: one lone pair and two double bonds to oxygen atoms. This results in an approximately trigonal planar electronic (parent geometry). We expect the lone pair to be slightly more repulsive than double bonds, and so we expect the O—N—O bond angle to be slightly less than 120°. *The actual O—N—O angle is 115°.*

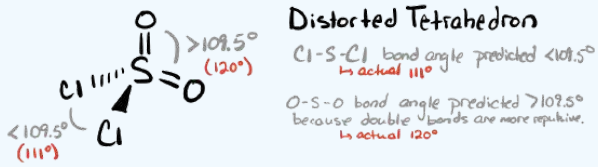


Exercise 2.1.7.3

Use VSEPR theory to predict the geometries and draw the structures of $SOCl_2$.

Answer

This molecule has four electron groups (steric number 4) with an approximately tetrahedral electronic (parent) geometry. Each double bonded oxygen will take up more space around the central S than the single bonded Cl atoms. We should expect the double bonds to repel each other more strongly than they repel each single bond, with the least repulsive interaction being between the two single bonds. The bond angle for Cl—S—Cl is expected to be <109.5° according to VSEPR theory (however, it is actually 111°). We would expect the bond angle for O—S—O to be larger than the angle for Cl—S—Cl and for Cl—S—O. The O—S—O bond angle is predicted to be >109.5° (and the actual bond angle is 120°). The molecular geometry is a distorted tetrahedron.

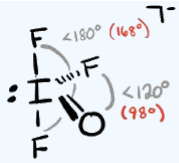


Exercise 2.1.7.4

Use VSEPR theory to predict the geometries and draw the structures of IOF_3^-.

Answer

This molecule has five electron groups (steric number 5) with an approximately trigonal bipyramidal electronic (parent) geometry. There is one lone pair, a double bond to O, and three single bonds to F atoms around the central I atom. The lone pair and double bond are most repulsive, and should occupy the less crowded equatorial positions rather than the more crowded axial positions. This results in a seesaw molecular geometry. With the more repulsive lone pair and the strongest equatorial repulsive force being between the double bond and lone pair, we should expect the $F_{equatorial}$—I—O bond angle to be less than the 120° angle expected for the parent geometry (*it is actually much less, at 98°*). Due to repulsion between the axial F atoms and both the lone pair and double bond, we should expect the F—S—F bond angles to be compressed. The F_{axial}—I—F_{axial} is actually 168°.



Distorted see saw

Lone pair and double bond in equitorial positions.

Predicted bond angles:

F-I-O <120° /actual 98°

F_{axial}-I-F_{axial} <180° /actual 168°

References

- Miessler, G.; Fischer, P.J.; Tarr, D. (2014). Inorganic Chemistry. New Jersey: Prentice-Hall. pp. 55

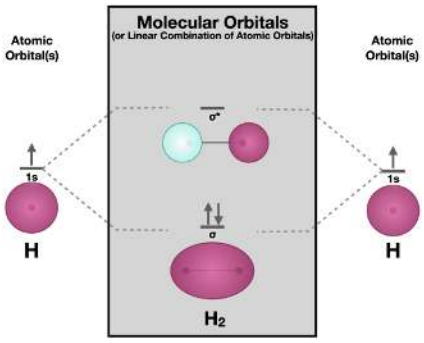
2.1.7: Shape Change from Double and Triple Bonds is shared under a CC BY-NC-SA 4.0 license and was authored, remixed, and/or curated by Kathryn A. Newton, Northern Michigan University.

- **3.2.2: Multiple Bonds** by Kathryn Haas has no license indicated.

SECTION OVERVIEW

2.2: Covalent- Molecular Orbital Theory

Molecular Orbital Theory



Molecular Orbital (MO) Theory is a sophisticated bonding model. It is generally considered to be more powerful than *Lewis* and *Valence Bond Theories* for predicting molecular properties; however, this power comes at the price of complexity. In its full development, MO Theory requires complex mathematics, though the ideas behind it are simple. Atomic orbitals (AOs) that are localized on individual atoms combine to make molecular orbitals (MOs) that are distributed over the molecule. The simplest example is the molecule dihydrogen (H_2), in which two independent hydrogen 1s orbitals combine to form the σ bonding MO and the σ antibonding MO of the dihydrogen molecule (see figure). The MO's are also called Linear Combinations of Atomic Orbitals (LCAO).

Types of Bonds

Inorganic compounds use s, p, and d orbitals (and more rarely f orbitals) to make bonding and antibonding combinations. These combinations result in **σ, π,** and **δ** bonds (and antibonds).

In inorganic chemistry, π bonds can be made from p- and/or d-orbitals. δ bonds are more rare and occur by face-to-face overlap of d-orbitals, as in the ion $Re_2Cl_8^{2-}$. The fact that the Cl atoms are eclipsed in this anion is evidence of δ bonding.

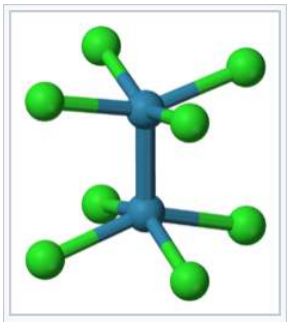
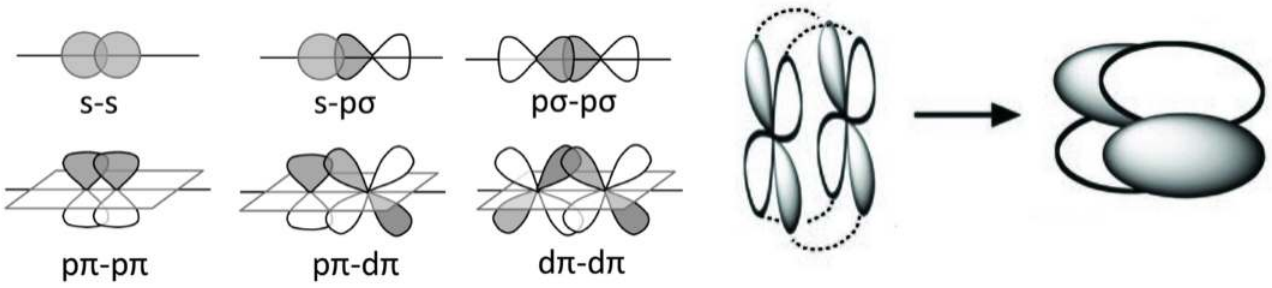


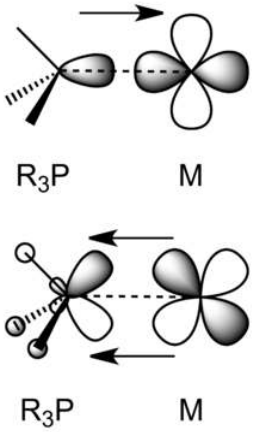
Figure **2.2.1**: The octachlorodirhenate(III) anion, $[Re_2Cl_8]^{2-}$, which has a quadruple Re-Re bond.[3]

Some possible σ (top row), π (bottom row), and δ bonding combinations (right) of s, p, and d orbitals are sketched below. In each case, we can make bonding or antibonding combinations, depending on the signs of the AO wavefunctions. Because pπ-pπ bonding involves sideways overlap of p-orbitals, it is most commonly observed with second-row elements (C, N, O). π-bonded compounds of heavier elements are rare because the larger cores of the atoms prevent good π-overlap. For this reason, compounds containing C=C double bonds are very common, but those with Si=Si bonds are rare. δ bonds are generally quite weak compared to σ and π bonds. Compounds with metal-metal δ bonds occur in the middle of the transition series.

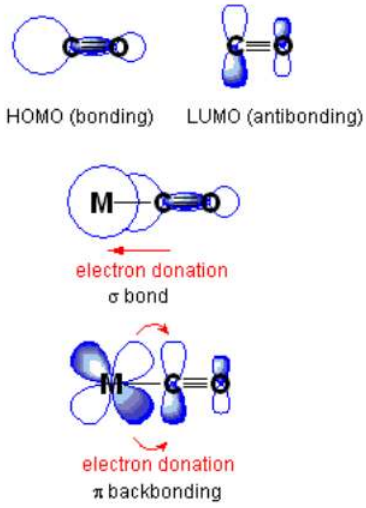


https://chem.libretexts.org/@go/page/551689

Transition metal d-orbitals can also form σ bonds, typically with s-p hybrid orbitals of appropriate symmetry on ligands. For example, phosphines (R_3P:) are good σ donors in complexes with transition metals, as shown below.



pπ-dπ bonding is also important in transition metal complexes. In metal carbonyl complexes such as $Ni(CO)_4$ and $Mo(CO)_6$, there is sideways overlap between filled metal d-orbitals and the empty π-antibonding orbitals (the LUMO) of the CO molecule, as shown in the figure below. This interaction strengthens the metal-carbon bond but weakens the carbon-oxygen bond. The C-O infrared stretching frequency is diagnostic of the strength of the bond and can be used to estimate the degree to which electrons are transferred from the metal d-orbital to the CO π-antibonding orbital.



The same kind of backbonding occurs with phosphine complexes, which have empty π orbitals, as shown at the right. Transition metal complexes containing halide ligands can also have significant pπ-dπ bonding, in which a filled pπ orbital on the ligand donates electron density to an unfilled metal dπ orbital. We will encounter these bonding situations in Chapter 5.

Attributions

- 2.4: σ, π, and δ orbitals, Chemistry 310, Penn State University, CC-BY-SA 4.0
- 5: Molecular Orbitals, Kathryn Haas, Duke University, CC-BY-SA 4.0

2.2.1: MO- s orbital MOs

2.2.2: MO- p orbital MOs

2.2.3: MO- d orbital MOs

2.2.4: MO- Nonbonding MOs

2.2.5: MO- MO Diagram Features

2.2.6: MO- MO Diagrams of 1st and 2nd row diatomic molecules

2.2.7: MO- MO Diagrams of Heteronuclear Diatomics

2.2: Covalent- Molecular Orbital Theory is shared under a CC BY-NC-SA 4.0 license and was authored, remixed, and/or curated by Kathryn A. Newton, Northern Michigan University.

2.2.1: MO- s orbital MOs

Sigma Bonding with s-orbitals (ex: Dihydrogen)

In the case of the hydrogen molecule, two atomic orbitals are combined to form two molecular orbitals. These new molecular orbitals have different wavelengths than the two atomic orbitals: one has a longer wavelength and is a little lower in energy, while the other has a shorter wavelength and is a little higher in energy. If we take into account the energy of the two original atomic wavefunctions, and compare them to the total energy of the two new molecular wavefunctions, there is no change overall.

We started with two atomic orbitals, and by combining them we produced two molecular orbitals. The average energy of the orbitals has remained almost constant, and the number of wavefunctions has remained constant.

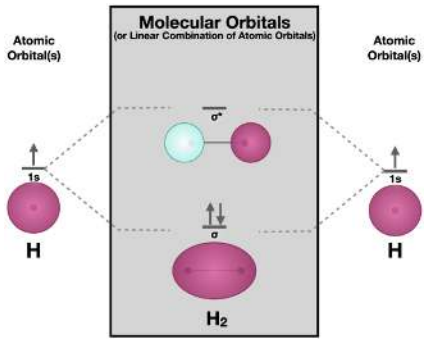


Figure 2.2.1.1: Molecular Orbital Diagram for H_2 [LibreText]

Of course, from the point of view of the two real electrons, some remarkable changes have occurred. Both of these electrons have adopted a longer wavelength and a lower energy and that has made all the difference. There is an occupied molecular orbital and an unoccupied molecular orbital; only the occupied orbital makes a real energetic contribution to the overall stability of the molecule. The unoccupied orbital is completely imaginary. The electrons have a lower kinetic energy in the bond than they had before bonding; lectronic energy has decreased. A stable bond has formed.

A bonding picture of He_2 would look exactly the same because it would also involve the overlap of 1s electrons on one atom with 1s electrons on the other atom. However, there would be a difference in the electronic energy because each He has two valence electrons: both the bonding and antibonding orbitals would be occupied. Having both orbitals fully occupied results in no net gain in stability, which makes the helium-helium bond unlikely to form.

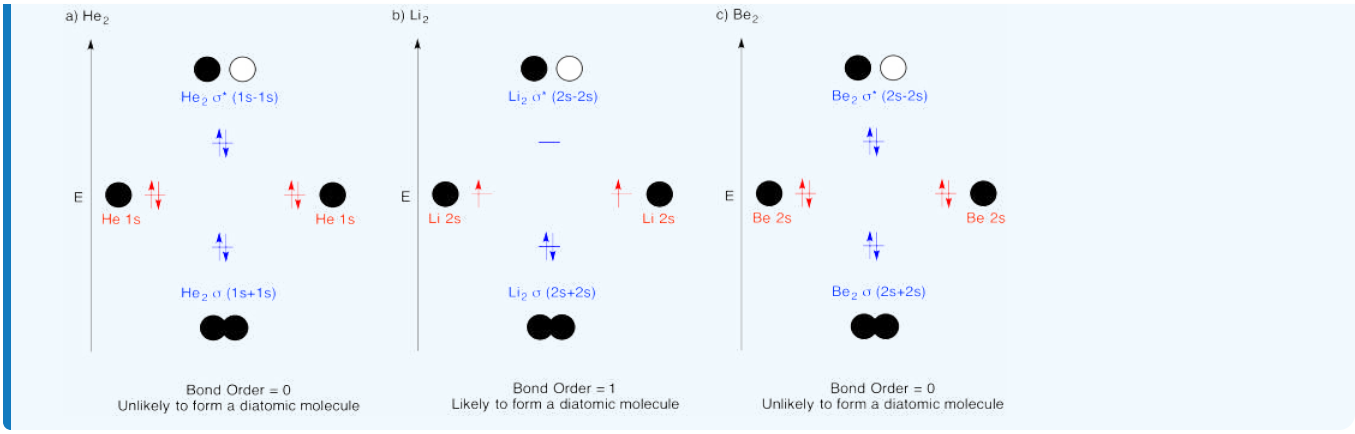
Problems

? Exercise 2.2.1.1

Construct molecular orbital diagrams for the following diatomic species and discuss the likelihood of bond formation in each case.

a. He_2.
b. Li_2.
c. Be_2.

Answer



2.2.1: MO- s orbital MOs is shared under a CC BY-NC-SA 4.0 license and was authored, remixed, and/or curated by Chris Schaller, Kathryn Haas, Kathryn A. Newton, Northern Michigan University, & Kathryn A. Newton, Northern Michigan University.

2.2.2: MO- p orbital MOs

Some Assumptions

Other diatomic molecules can be constructed in a similar way to that of H_2. Consider dinitrogen, N_2.

Nitrogen has five valence electrons, and these electrons are found in the 2s and 2p levels. There are three possible atomic orbitals in the 2p level where some of these electrons could be found: p_x, p_y and p_z. We need to look at the interaction between the s and p_x, p_y and p_z orbitals on one nitrogen atom with the s and p_x, p_y and p_z orbitals on the other nitrogen. That process could be extremely complicated, but is simplified because orbital interactions are governed by symmetry. Orbitals interact most easily with other orbitals that have the same element of symmetry. For now, we can simplify this idea and say that orbitals on one atom only interact with the same type of orbitals on the other atom.

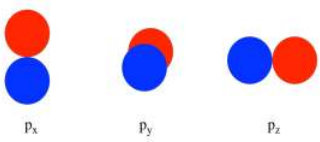
- s orbitals interact with s orbitals. We can already see how that will work out in dinitrogen, because that is what happened in dihydrogen.
- p_x orbitals interact with p_x orbitals.
- p_y orbitals interact with p_y orbitals.
- p_z orbitals interact with p_z orbitals.

Another complication here is that the s and p orbitals do not start out at the same energy level. When the orbitals mix, one combination goes up in energy and one goes down. Does the s antibonding combination go higher in energy than the combinations from p orbitals? Do the p bonding combinations go lower in energy than the combinations from s orbitals? We will **simplify** and **assume** that the s and p levels remain completely separate from each other. This is not always true, but the situation varies depending on what atoms we are dealing with.

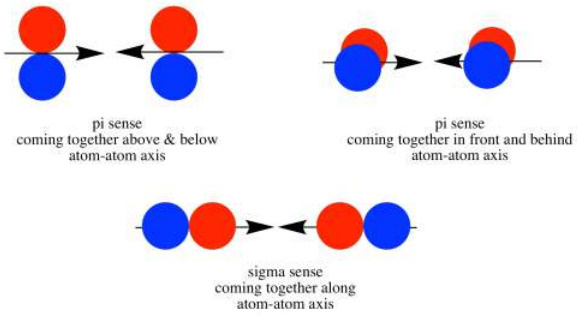
- The combination of one s orbital with another is just like in hydrogen. Two original orbitals will combine and rearrange to produce two new orbitals.
- There is a bonding combination in which the orbitals are in phase. The new orbital produced has a longer wavelength than the original orbital. It is lower in energy.
- There is an antibonding combination in which the orbitals are out of phase. The new orbital produced has a shorter wavelength than the original orbital. It is higher in energy.

Sigma bonding with p-orbitals

In considering the interaction of two p orbitals, we have to keep in mind that p orbitals are directional. A p orbital lies along a particular axis: x, y or z. The three p orbitals on nitrogen are all mutually perpendicular (or orthogonal) to each other. That situation is in contrast to s orbitals, which are spherical and thus look the same from any direction.

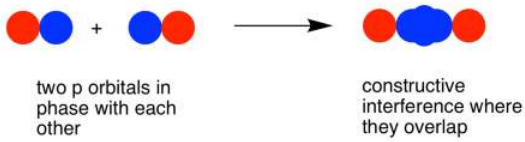


We first need to define one axis as lying along the N-N bond. It does not really matter which one. However, by convention we say the N-N bond lies along the z axis. The p_z orbitals have a different spatial relationship to each other compared to the p_y and p_x. The p_z orbitals lie along the bond axis, whereas the p_y and p_x are orthogonal (perpendicular) to it.

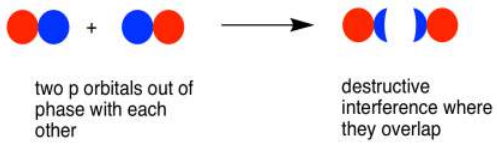


As the nitrogen atoms are brought together, one lobe on one p_z orbital overlaps strongly with one lobe on the other p_z orbital. The other lobes point away from each other and do not interact in any obvious way.

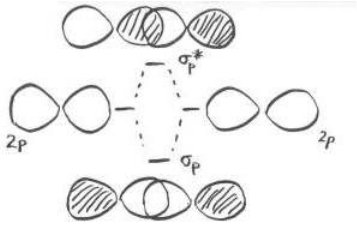
As with the s orbital, the p_z orbitals can be in-phase or out-of-phase. The in-phase combination results in constructive interference. (Here, "in-phase" means the lobes that overlap are in-phase; for that to happen the two p orbitals are actually completely out-of-phase with each other mathematically, so that one orbital is the mirror image of the other.) This combination is at a longer wavelength than the original orbital. It is a lower energy combination.



The out-of-phase combination (meaning in this case that the overlapping lobes are out-of-phase) results in destructive interference. This combination is at shorter wavelength than the original orbital. It is a higher energy combination.



As a result, we have two different combinations stemming from two different p orbitals coming together in two different ways. We get a low-energy, in-phase, bonding combination and a high-energy, out-of-phase, antibonding combination.



Pi-bonding with p-orbitals

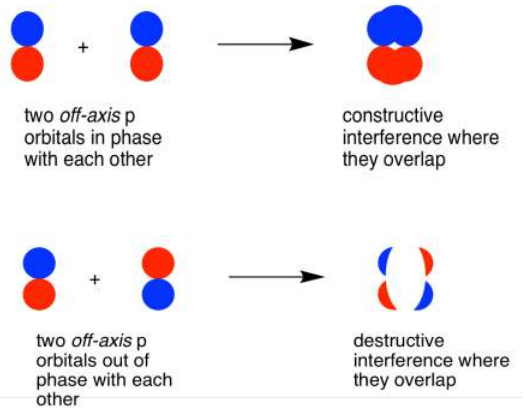
As the nitrogen atoms are brought together, one lobe on one p_z orbital overlaps strongly with one lobe on the other p_z orbital. The other lobes point away from each other and do not interact in any obvious way.

As with the s orbital, the p_z orbitals can be in-phase or out-of-phase. The in-phase combination results in constructive interference. (Here, "in-phase" means the lobes that overlap are in-phase; for that to happen the two p orbitals are actually completely out-of-phase with each other mathematically, so that one orbital is the mirror image of the other.) This combination is at a longer wavelength than the original orbital. It is a lower energy combination.

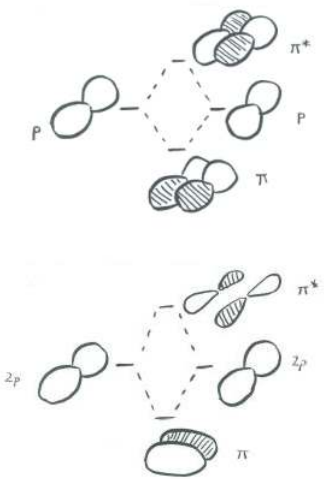
As the nitrogen atoms are brought together, the parallel (but not collinear), p orbitals can also interact with each other. The p_x orbital on one atom will interact with the p_x orbital on the other atom. The p_y orbital on one atom will interact with the p_y orbital

on the other atom. As the two atoms approach along the internuclear axis (z axis), the orbitals would approach each other side by side, with their lobe interacting above and below the bond axis between the two atoms. Although the p_x and p_y orbitals can be close enough to each other to overlap, they do not overlap as strongly as p_z orbitals lying along the bond axis.

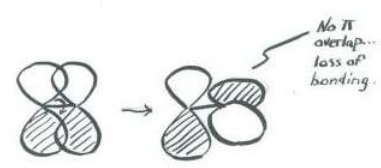
The interaction of a pair of p_x (or p_y) orbitals produces a bonding and an antibonding combination. The in-phase combination (bonding) is shown below, followed by the out-of-phase combination. The resulting orbitals contain nodes along the bond axis, and the electron density is found above and below the bond axis. This bond is called a p (pi) bond.



The illustration above is for one set of p orbitals that are orthogonal to the bond axis. The second picture shows the result of the constructive (or destructive) interference. A similar picture could be shown for the other set of p orbitals.



An important consequence of the spatial distribution or "shape" of a p orbital is that it is not symmetric with respect to the bond axis. An s orbital is not affected when the atom at one end of the bond is rotated with respect to the other. A p orbital is affected by such a rotation. If one atom turns with respect to the other, the p orbital would have to stretch to maintain the connection. The orbitals would not be able to overlap, so the connection between the atoms would be lost.

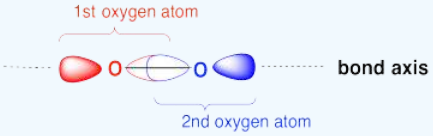


Problems

Exercise 2.2.2.1

Draw an MO cartoon of a sigma bonding orbital formed by the overlap of two p orbitals between two oxygen atoms. Label the positions of the oxygen nuclei with the symbol "O". Label the O-O bond axis.

Answer



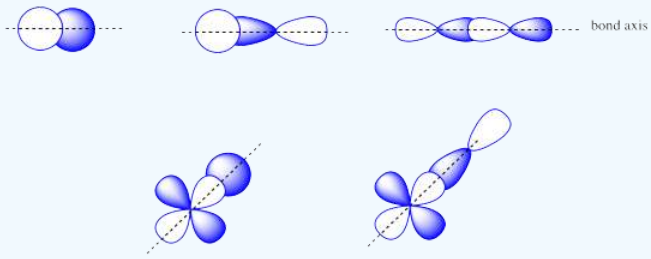
Exercise 2.2.2.2

The combinations of _____ atomic orbitals leads to σ orbitals.

Draw pictures.

Answer

The combinations of s + s; s + p; p + p; s + d; p + d atomic orbitals can lead to σ orbitals.



Exercise 2.2.2.3

The combinations of _____ atomic orbitals leads to π orbitals.

Draw pictures.

Answer

The combinations of side by side p + p or p + d atomic orbitals leads to π orbitals.



Exercise 2.2.2.4

Which molecular orbital is typically the highest in energy?

a. p
b. σ
c. π*
d. π
e. σ*

Answer

e. σ*

Exercise 2.2.2.5

Why would a *core* 1s orbital not interact with a *valence* 2s orbital?

Hint: Why is a Li_2O bond stronger than a K_2O bond?

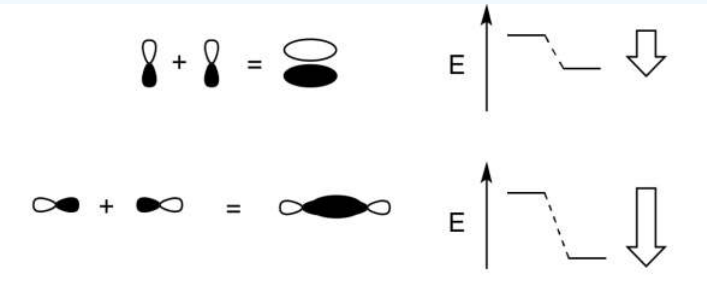
Answer

Li^+ and O^{2-} are more similar in size than K^+ and O^{2-}, so the bond between Li^+ and O^{2-} is stronger.

The energy difference between any core orbitals and valence orbitals is too large, so they cannot interact. In order for orbitals to interact, the orbitals need to have the same symmetry, be in the same plane, and be similar in energy.

Exercise 2.2.2.6

Add a few words to explain the ideas conveyed in these drawings.



Answer

When two parallel p orbitals combine out-of-phase, destructive interference occurs.

There is a node between the atoms.

The energy of the electrons increases.

When two parallel p orbitals combine in-phase, constructive interference occurs.

There is no node between the atoms; the electrons are found above and below the axis connecting the atoms.

The energy of the electrons decreases.

Attribution

Chris P Schaller, Ph.D., (College of Saint Benedict / Saint John's University)

Curated or created by Kathryn Haas

2.2.2: MO- p orbital MOs is shared under a CC BY-NC-SA 4.0 license and was authored, remixed, and/or curated by Kathryn A. Newton, Northern Michigan University.

- **5.1.2: Molecular Orbitals from p Orbitals** by Chris Schaller is licensed CC BY-NC 3.0.

2.2.3: MO- d orbital MOs

In transition metals and other heavier elements, the d orbitals may combine with other orbitals of compatible symmetry (and energy) to form molecular orbitals. Generally, there are three types of bonding and antibonding interactions that may occur with d orbitals: sigma (σ), pi (π), and delta (δ) bonds.

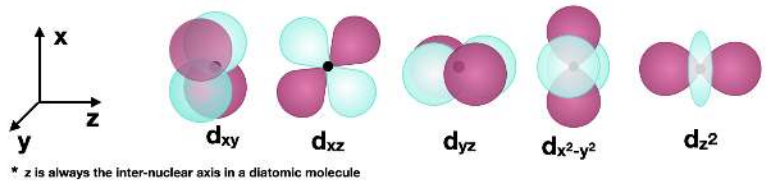


Figure 2.2.3.1: The five $3d$ orbitals are shown. The orientation of the axes is consistent and the z axis is horizontal for convenience in drawing bonding along the z axis (see examples below). (CC-BY-SA; Kathryn Haas)

Sigma (σ) bonding with d orbitals

σ bonds are symmetric with respect to the inter-nuclear axis (in a diatomic molecule, this is the z axis). An example of a σ bond formed by d orbitals is that of two d_{z^2} orbitals (see Figure 2.2.3.2). If a bonded atom is in a position other than on the z axis (in an octahedral geometry, for example), σ bonds can also form. For example, two $d_{x^2-y^2}$ orbitals on atoms bonded along the x or y axes could also form a σ bond.

d orbitals can also form σ bonds with other types of orbitals with the appropriate symmetry. Examples of orbitals with appropriate symmetry are the s orbital and certain p orbitals on another atom, as shown below in Figure 2.2.3.2.

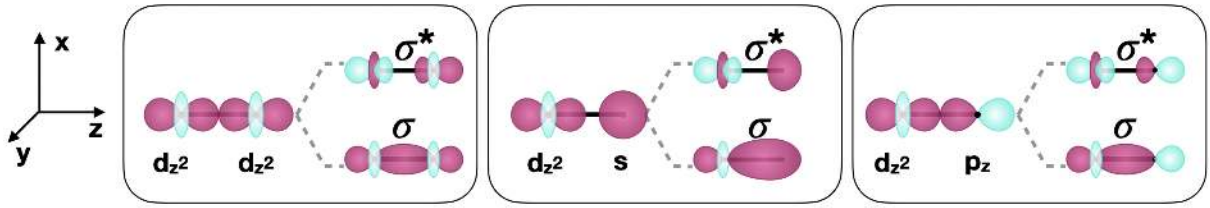


Figure 2.2.3.2: Selected examples of σ bonds involving d orbitals along the z internuclear axis (shown as a bold horizontal line) between two atoms. (CC-BY-SA; Kathryn Haas)

Pi (π) bonding with d orbitals

π bonds are those with one node that is in-plane with the internuclear axis. A π bond can form between two d orbitals or between d orbitals and other types of orbitals with comparable symmetry. An example of a π bond between two d orbitals is that formed by two d_{xz} orbitals along the z axis (shown in Figure 2.2.3.3). d orbitals can also form π bonds using p orbitals with compatible symmetry, as shown in Figure 2.2.3.3.

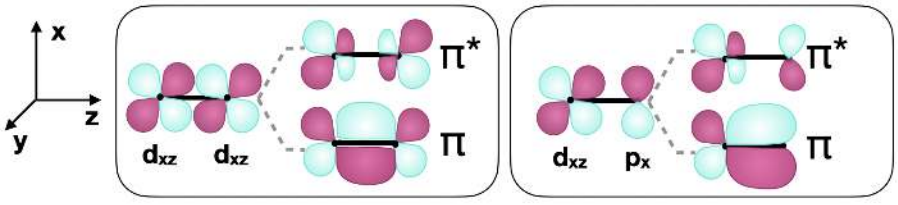


Figure 2.2.3.3: Selected examples of π bonds involving d orbitals along the z internuclear axis (shown as a bold horizontal line) between two atoms. (CC-BY-SA; Kathryn Haas)

Delta (δ) bonding with d orbitals

δ bonds are those with two nodes that are in-plane with the internuclear axis. δ bonds can form between two d orbitals with appropriate symmetry. For example, when two atoms bond along the z axis, the d_{xy} orbitals and the two $d_{x^2-y^2}$ orbitals can form δ bonds (Figure 2.2.3.4).

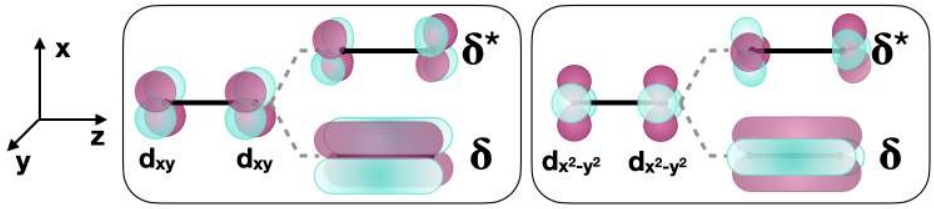


Figure 2.2.3.4: Selected examples of δ bonds involving d orbitals along the z internuclear axis (shown in bold horizontal line) between two atoms. (CC-BY-SA; Kathryn Haas)

Incompatible orbitals

In the descriptions above, we focused on how bonds (and antibonds) can be formed with d orbitals. All bonding and non-bonding interactions require that orbitals have compatible symmetry to form productive interactions. It is worth mentioning that orbitals with symmetry that is incompatible with the d orbitals will not have bonding or antibonding interactions with d orbitals. The figure below shows several sets of orbitals that are incompatible for bonding.

Curated or created by Kathryn Haas

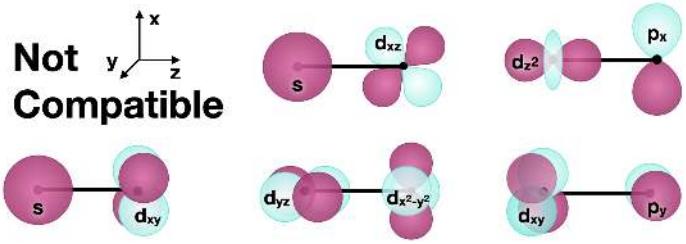


Figure 2.2.3.5: Several incompatible pairs of orbitals. (CC-BY-SA; Kathryn Haas)

2.2.3: MO- d orbital MOs is shared under a CC BY-NC-SA 4.0 license and was authored, remixed, and/or curated by Kathryn A. Newton, Northern Michigan University.

- **5.1.3: Molecular orbitals from d orbitals** by Kathryn Haas is licensed CC BY-SA 4.0.

2.2.4: MO- Nonbonding MOs

The simplest case is when there is an even number of atomic orbitals that all combine to form strong bonding and antibonding orbitals. But what if there is an uneven number of atomic orbitals? Or what if there are some orbitals that don't meet the criteria for bonding? Or what if the bonding interactions are weak? In these cases, there will be molecular orbitals on the molecule that have non-bonding character.

It is important to note that the bonding, non-bonding, and antibonding nature of orbitals exist on a spectrum. Some bonding and anti-bonding orbitals may have some non-bonding character depending on where their energies lie with respect to the original atomic orbital energies. When molecular orbitals have energies similar to their original atomic orbitals, they will have some non-bonding character. The closer the energies of atomic and molecular orbitals, the more non-bonding the molecular orbitals.

Differences in symmetry

The MO picture for a molecule gets complicated when many valence AOs are involved. We can simplify the problem enormously by noting (without proof here) that orbitals of different symmetry do not interact. Here we will take a simple approach understanding the symmetry of orbitals based on their **nodal symmetry**. Note, a more rigorous approach to the symmetry classes of bonds aand orbitals is defined by **group theory** and is the topic of advanced inorganic courses.

To form a molecular orbital, atomic orbitals must have the same **nodal symmetry** or their overlap is zero. This means that two orbitals must have the same symmetry with respect to the bonding axis in order to form a molecular orbital. Figure \PageIndes1 shows a hydrogen 1s orbital and a chlorine $3p_y$ orbital. The H 1s orbital is symmetric about the bonding axis; the sign of the orbital is unchanged by a 180° rotation about the bond axis. However, the Cl $3p_y$ orbital is antisymmetric about the bonding axis; the same rotation inverts the sign of the Cl $3p_y$ wavefunction. Because these two orbitals have different symmetries, the Cl $3p_y$ orbital is **nonbonding** and doesn't interact with the H 1s. The same is true of the Cl $3p_x$ orbital. The p_x and p_y orbitals have π symmetry (nodal plane containing the bonding axis) and are labeled π_{nb} in the MO energy level diagram shown in Figure **2.2.4.2**. In contrast, the H 1s and Cl $3p_z$ orbitals both have σ symmetry so they can make the bonding and antibonding combinations.

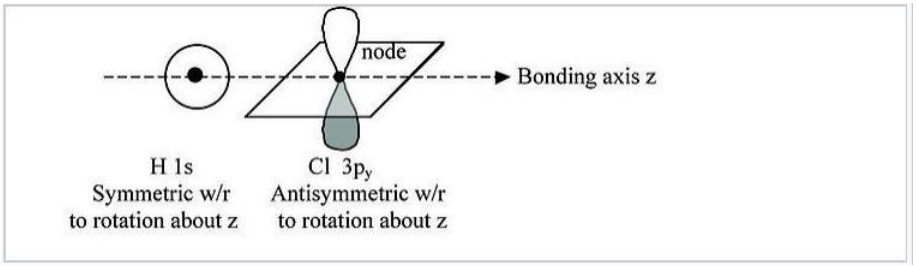


Figure **2.2.4.1**: Orbitals of σ and π symmetry do not interact.

The MO diagram of HCl that includes all the valence orbitals of the Cl atom is shown in Figure **2.2.4.2**. Two of the Cl valence orbitals ($3p_x$ and $3p_y$) have the wrong symmetry to interact with the H 1s orbital. The Cl 3s orbital has the same σ symmetry as H 1s, but it is much lower in energy so there is little orbital interaction. The energy of the Cl 3s orbital is thus affected only slightly by forming the molecule. The pairs of electrons in the π_{nb} and σ_{nb} orbitals are therefore **nonbonding**.

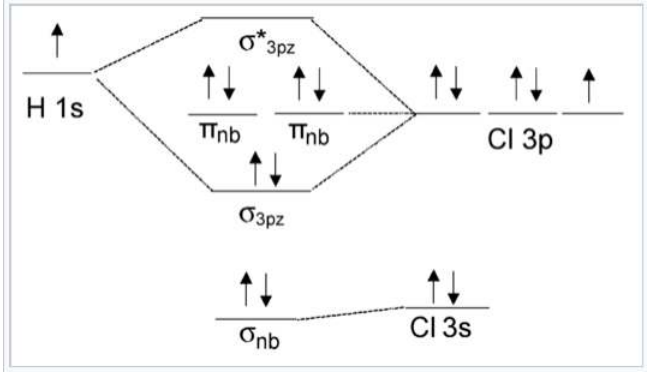


Figure **2.2.4.2**: Energy level diagram of the HCl molecule showing MOs derived from the valence AOs.

Note that the MO result in Figure 2.2.4.2 (1 bond and three pairs of nonbonding electrons) is the same as we would get from valence bond theory for HCl. The nonbonding orbitals are localized on the Cl atom, just as we would surmise from the valence bond picture. In order to differentiate it from the σ bonding orbital, the σ antibonding orbital, which is empty in this case, is designated with an asterisk.

Differences in energy

Combination of orbitals with different energies may lead to orbitals with non-bonding character. Atomic orbitals that have similar energies will have the strongest interactions, and result in bonding molecular orbitals with much lower energies than the component atomic orbitals. On the other hand, atomic orbitals with very unequal energies have a weaker interaction because the molecular orbitals are closer in energy to the atomic orbital energies, thus there is less energy benefit to putting electrons in the bonding molecular orbitals (Figure 2.2.4.3). When bonding or antibonding orbitals are close to the energies of the contributing atomic orbitals, those molecular orbitals may have some non-bonding character.

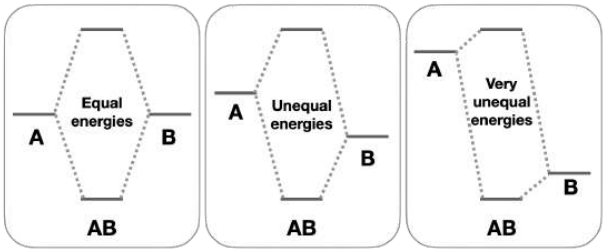


Figure 2.2.4.3. This figure illustrates how relative energies of atomic orbitals result in molecular orbitals that are more or less favorable. The greater the energy difference between atomic orbitals and the bonding molecular orbital, the more eneretically favorable it is for bonding to occur. (CC-BY-NC-SA, Kathryn Haas)

Uneven number of atomic orbitals

In the case that there is an uneven number of atomic orbitals with compatible symmetry, orbitals with non-bonding character will form. For example, in the case where three atomic orbitals combine, the most common result is formation of a low-energy bonding orbital, a high energy antibonding orbital, and a non-bonding orbital of intermediate energy (Figure 2.2.4.4).

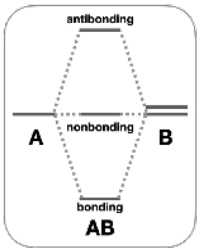


Figure 2.2.4.4. This figure illustrates the most common case for three atomic orbitals that combine to form three molecular orbitals; formation of one low-energy bonding, one high-energy antibonding, and one intermediate energy non-bonding molecular orbital. (CC-BY-NC-SA, Kathryn Haas)

Problems

Exercise 1

What will most likely lead to the smallest covalent interaction?

a) Overlap of a small and a large orbital.

b) Overlap of two small orbitals.

c) Overlap of two large orbitals.

Answer

a) Overlap of a small and a large orbital.

Exercise 2

What will most likely lead to the largest covalent interaction?

a) orbital overlap in sigma-fashion

b) orbital overlap in pi-fashion

c) orbital overlap in delta-fashion

Answer

a) orbital overlap in sigma-fashion

Exercise 4

Decide by "inspection" which of the following combinations of orbitals have the "right" symmetries to form molecular orbitals.

a) The $2p_x$ orbital of the first N atom and the $2p_y$ orbital of the second N atom in the molecule N_2. The z axis is defined as the bond axis in N_2.

b) The F $2p_x$ and the H 1s orbital in the HF molecule. The z axis is defined as the bond axis.

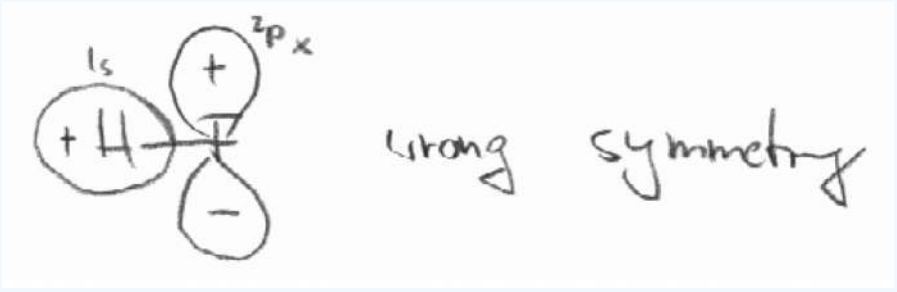
c) The $2p_z$ orbital of F and the 1s orbital in the HF molecule. The z axis is defined as the bond axis.

Answer

a)



b)



c)



2.2.4: MO- Nonbonding MOs is shared under a CC BY-NC-SA 4.0 license and was authored, remixed, and/or curated by Kathryn A. Newton, Northern Michigan University.

- **5.1.4: Nonbonding Orbitals and Other Factors** by Kathryn Haas is licensed CC BY-SA 4.0.
- **2.3: Orbital Symmetry** by Chemistry 310 is licensed CC BY-SA 4.0. Original source: https://en.wikibooks.org/wiki/Introduction_to_Inorganic_Chemistry.
- **Homework Problems Chapter 3** by Kai Landskron is licensed CC BY 4.0.

2.2.5: MO- MO Diagram Features

There are several cases where our more elementary models of bonding (like Lewis Theory and Valence Bond Theory) fail to predict the actual molecular properties and reactivity. A classic example is the case of O_2 and its magnetic properties. At very cold temperatures, O_2 is attracted to a magnetic field, and thus it must be paramagnetic (unpaired electrons give rise to magnetism). Watch the video below!



The magnetic properties of O_2 are easily rationalized by its **molecular orbital diagram**, which shows the relative energies and identities of each molecular orbital in a molecule. Figure 2.2.5.1 shows a simplified and generic molecular orbital diagram for a second-row homonuclear diatomic molecule. The diagram is simplified in that it assumes that interactions are limited to degenerate orbitals from two atoms.

There are some things you should note as you inspect Figure 2.2.5.1 (and keep these in mind as you draw your own diagrams!). First, notice that there are the **same number of molecular orbitals as there are atomic orbitals**. Second, the diagram in Figure 2.2.5.1 lacks electrons (because it is generic for any second-row diatomic molecule). If this were a *complete* molecular orbital diagram it would **include the electrons for each atom and for the molecule**. Electrons in molecular orbitals are filled in the same way an atomic orbital diagram would be filled, following Hund's Rule and the Aufbau principle, where electrons occupy lower energy orbitals before higher energy orbitals, and electrons occupy empty degenerate orbitals before pairing.

A complete molecular orbital diagram would show whether the molecule is diamagnetic or paramagnetic. It can also be used to calculate the bond order of the molecule (the number of bonds between atoms) using the formula below:

$$\text{Bond order } = \frac{1}{2}\left[\left(\begin{array}{c}\text{number of electrons}\\ \text{in bonding orbitals}\end{array}\right) - \left(\begin{array}{c}\text{number of electrons}\\ \text{in antibonding orbitals}\end{array}\right)\right]$$

In general, non-valence (core) electrons can be ignored because they contribute nothing to the bond order. In fact, many molecular orbital diagrams will ignore the core orbitals, as they are insignificant for bonding interactions and reactivity.

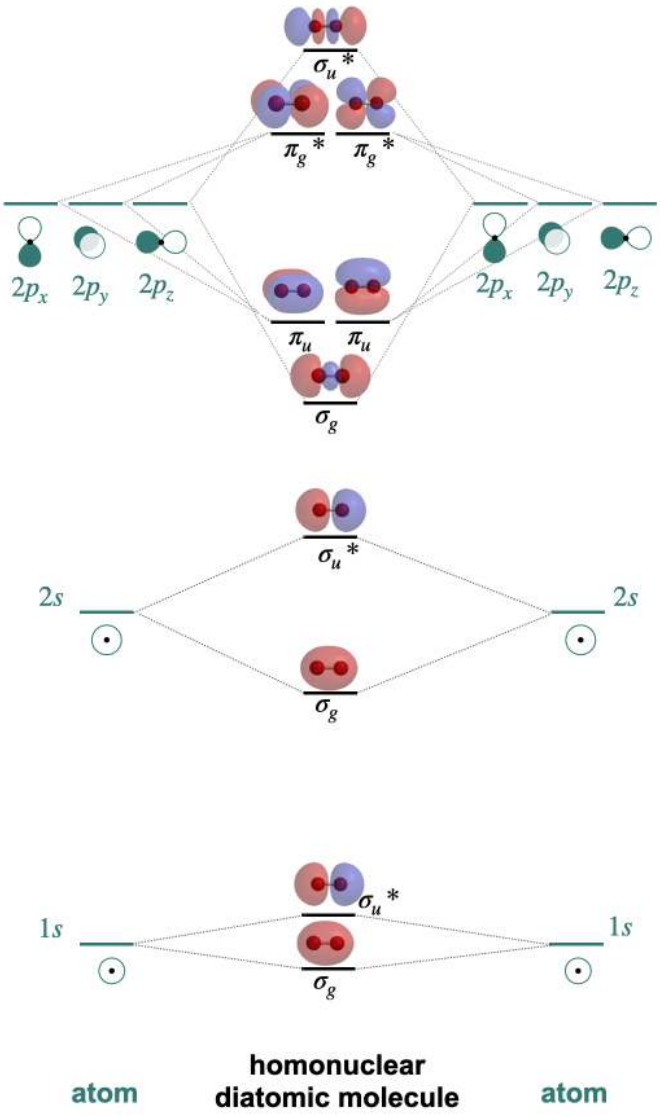


Figure 2.2.5.1: A generic molecular orbital diagram for a homonuclear diatomic molecule of second-row elements assuming no orbital mixing (interactions are formed by orbitals of the same energy from each atom). (CC-BY-NC-SA, Kathryn Haas)

Now, to see how this molecular orbital diagram can explain the magnetic behaviour of O_2, complete the example below.

Example 2.2.5.1

Let's change Figure 2.2.5.1 to make it specific for O_2. Re-draw the MO diagram (no need to draw the shapes of orbitals). Fill in the correct number of electrons for each oxygen atom on either side of the diagram. Then, fill in the total molecular electrons in the center. Calculate the bond order and determine whether it is diamagnetic or paramagnetic.

Solution

The diagram in Figure 2.2.5.1 includes core orbitals (the 1s) and valence electrons (2s, 2p). Therefore, we will consider all the electrons in an oxygen atom and a dioxygen molecule. An oxygen atom has eight total electrons. So we fill eight electrons into the atomic orbitals for the oxygen atom on the right, and eight electrons into the atomic orbitals for oxygen on the left. The total number of electrons for the molecule is sixteen, so fill in 16 electrons into the molecular orbitals, being sure to apply Hund's rule and the Aufbau principle. The result is a diagram that looks like the one drawn below in Figure 2.2.5.2.

The bond order is calculated using the molecular orbitals (we can ignore atomic orbitals). There are 10 electrons in binding orbitals and 6 electrons in antibonding orbitals). This gives a bond order of $\frac{1}{2}(10-6)=2$. This bond order is consistent with valence bond theory!

This diagram indicates that dioxygen is paramagnetic; it has two unpaired electrons in the π^* orbitals. This paramagnetic electron configuration explains why dioxygen is attacted to magnetic fields!

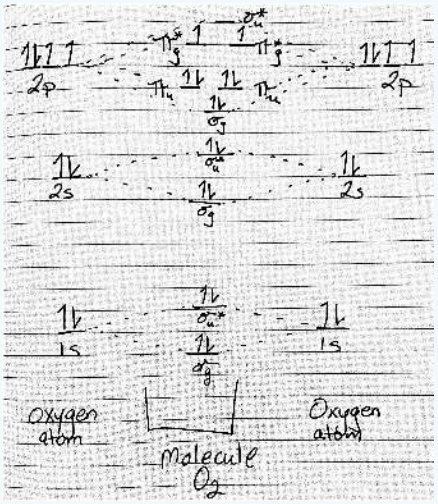


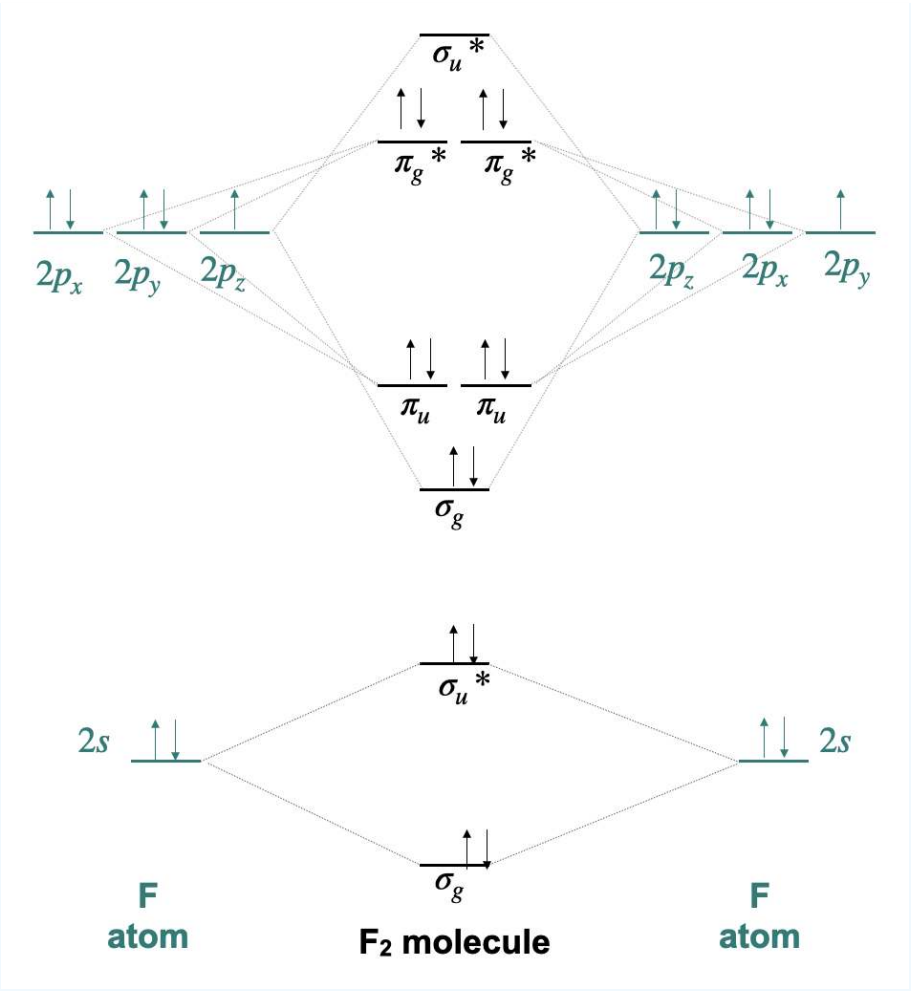
Figure 2.2.5.2: Hand-drawn molecular orbital diagram for dioxygen. (CC-BY-SA; Kathryn Haas)

? Exercise 2.2.5.2

Draw the molecular orbital diagram for $\mathbf{F_2}$; be sure to label your orbitals with the appropriate symmetry and count your orbitals to make sure that the total number of atomic orbitals and molecular orbitals is the same. As a shortcut, include only the valence orbitals and electrons. What is the bond order? Is the molecule diamagnetic or paramagnetic?

Answer

The valence orbitals on an F atom are 2s and 2p. And, there are seven valence electrons in F. This gives fourteen total valence electrons. The MO diagram of the valence molecular orbitals can be constructed by combining the valence 2s and valence 2p orbitals from each F atom. The bond order is 1 and the molecule is diamagnetic.



Exercise 2.2.5.3

A Molecular Orbital Diagram for a diatomic molecule (two atoms) always has the same basic pattern.

- Draw a picture of the levels.
- Label each level with σ, σ*, π, π*

Answer

—— σ*

—— —— π*

—— —— π

—— σ

—— σ*

—— σ

Exercise 2.2.5.4

A Molecular Orbital Diagram for a diatomic molecule (two atoms) varies in the number of electrons. How do you populate the electrons?

Answer

- Count the valence electrons on the molecule. That's the number of valence electrons on each atom, adjusted for any charge on the molecule. (eg C_2^{2-} has 10 valence electrons: 4 from each carbon -- that's 8 -- and two more for the 2- charge).
- Fill electrons into the lowest energy orbitals first.
- Pair electrons after all orbitals at the same energy level have one electron.

2.2.5: MO- MO Diagram Features is shared under a CC BY-NC-SA 4.0 license and was authored, remixed, and/or curated by Kathryn A. Newton, Northern Michigan University.

- **5.2.1: Molecular Orbitals** by Kathryn Haas is licensed CC BY-SA 4.0.
- **13.6: Assembling the Complete Diagram and Electron Population** by Chris Schaller is licensed CC BY-NC 3.0. Original source: https://employees.csbsju.edu/cschaller/structure.htm.

2.2.6: MO- MO Diagrams of 1st and 2nd row diatomic molecules

First Period Homonuclear Diatomic Molecules

In the first row of the periodic table, the valence atomic orbitals are **1*s***. There are two possible homonuclear diatomic molecules of the first period:

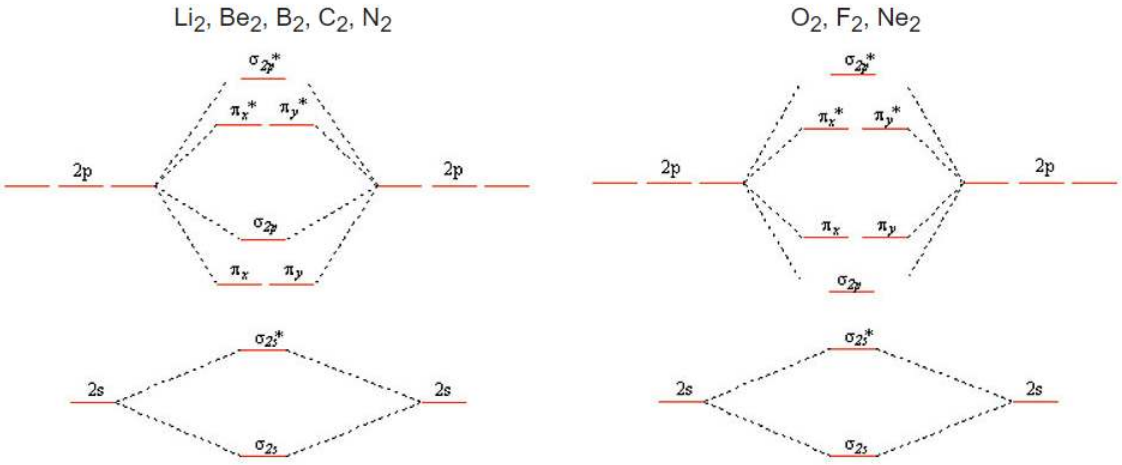
Dihydrogen, H_2 [$\sigma_g^2(1s)$]: This is the simplest diatomic molecule. It has only two molecular orbitals (σ_g and σ_u^*), two electrons, a bond order of 1, and is diamagnetic. Its bond length is 74 pm. MO theory would lead us to expect bond order to decrease and bond length to increase if we either add or subtract one electron. The calculated bond length for the H_2^+ ion is approximately 105 pm.[1]

Dihelium, He_2 [$\sigma_g^2\sigma_u^{*2}(1s)$]: This molecule has a bond order of zero due to equal number of electrons in bonding and antibonding orbitals. Like other noble gases, He exists in the atomic form and does not form bonds at ordinary temperatures and pressures.

Second Period Homonuclear Diatomic Molecules

The second period elements span from Li to Ne. The valence orbitals are 2s and 2p. In their molecular orbital diagrams, non-valence orbitals (1s in this case) are often disregarded in molecular orbital diagrams.

Valence bond theory fails for a number of the second row diatomics, most famously for O_2, where it predicts a diamagnetic, doubly bonded molecule with four lone pairs. O_2 does have a double bond, but it has two unpaired electrons in the ground state, a property that can be explained by the MO picture. We can construct the MO energy level diagrams for these molecules as follows

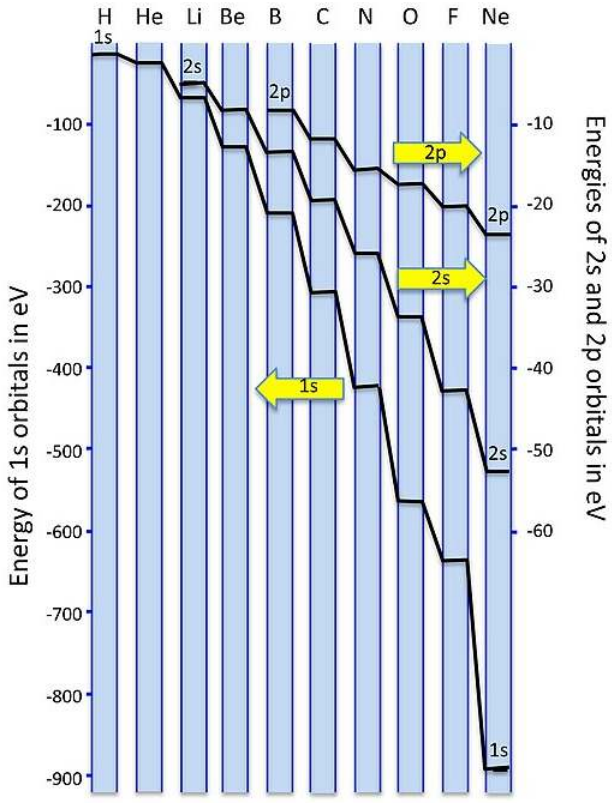


We get the simpler diatomic MO picture on the right when the 2s and 2p atomic orbitals are well separated in energy, as they are for O, F, and Ne. The picture on the left results from **mixing** of the σ_{2s} and σ_{2p} molecular orbitals, which are close in energy for Li_2, Be_2, B_2, C_2, and N_2. Mixing has two effects: 1 - to push the σ_{2s}* down in energy; and 2 - to push the σ_{2p} up in energy to the point where the pπ orbitals are below the σ_{2p}.

Mixing does not occur for O_2 and F_2 because of the energies of the σ_{2s} and σ_{2p} molecular orbitals, which are not drawn to scale in the simple picture above. As we move across the second row of the periodic table from Li to F, we are progressively adding protons to the nucleus. The 2s orbital, which has finite amplitude at the nucleus, "feels" the increased nuclear charge more than the 2p orbital. This means that as we progress across the periodic table (and also when we move down the periodic table), the **energy difference between the s and p orbitals increases**. As the 2s and 2p energies become farther apart in energy, there is less interaction between the orbitals (i.e., less mixing).

A plot of orbital energies is shown below. Because of the very large energy difference between the 1s and 2s/2p orbitals, we plot them on different energy scales, with the 1s to the left and the 2s/2p to the right. For elements at the left side of the 2nd period (Li, Be, B) the 2s and 2p energies are only a few eV apart. The energy difference becomes very large - more than 20 electron volts - for O and F. Since single bond energies are typically about 3-4 eV, this energy difference would be very large on the scale of our MO

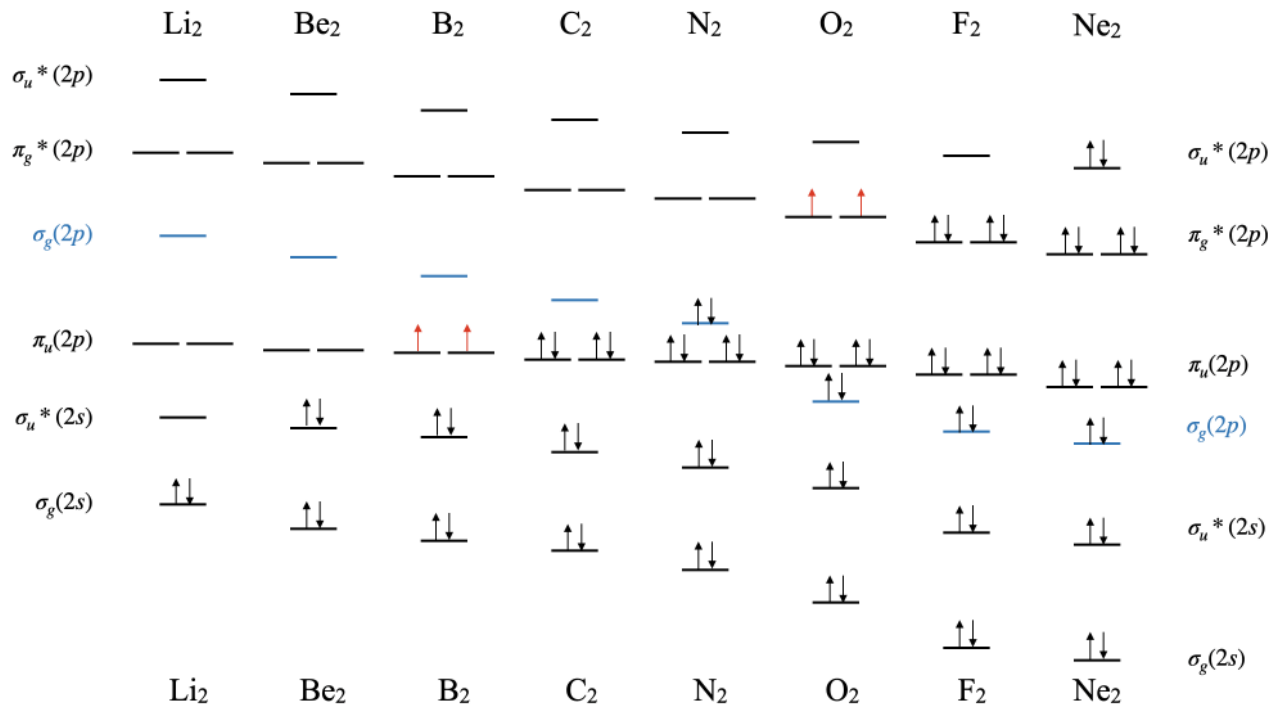
diagrams. For all the elements in the 2nd row of the periodic table, the 1s (core) orbitals are very low in energy compared to the 2s/2p (valence) orbitals, so we don't need to consider them in drawing our MO diagrams.



Period 1 and 2 Elements (CC-BY-SA 4.0, Chemistry 310)

Figure **2.2.6.1**: Energies of 1s, 2s, and 2p atomic orbitals for

Orbital mixing has significant consequences for the magnetic and spectroscopic properties of second period homonuclear diatomic molecules because it affects the order of filling of the $\sigma_g(2p)$ and $\pi_u(2p)$ orbitals. Early in period 2 (up to and including nitrogen), the $\pi_u(2p)$ orbitals are lower in energy than the $\sigma_g(2p)$ (see Figure **2.2.6.1**). However, later in period 2, the $\sigma_g(2p)$ orbitals are pulled to a lower energy. This lowering in energy of $\sigma_g(2p)$ is not unique; all of the σ orbitals in the molecule are pulled to lower energy due to the increasing positive charge of the nucleus. The π orbitals in the molecule are also affected, but to a much lesser extent than σ orbitals. The reason has to do with the high penetration of s atomic orbitals compared to p atomic orbitals. The σ molecular orbitals have more s character and thus their energy is more influenced by increasing nuclear charge. As nuclear charge increases, the energy of the $\sigma_g(2p)$ orbital is lowered significantly more than the energy of the $\pi_u(2p)$ orbitals (Figure **2.2.6.1**).



	Li_2	Be_2	B_2	C_2	N_2	O_2	F_2	Ne_2
Unpaired e⁻	0	0	2	0	0	2	0	0
Bond Order	1	0	1	2	3	2	1	0
Experimental* Bond Length (pm)	267.3	246.0	159.0	124.3	109.8	120.8	141.2	310.0

*Experimental bond lengths from "List of Experimental Diatomic Bond Lengths", NIST, https://cccbdb.nist.gov/diatomicexpbondx.asp

Figure 2.2.6.1: Molecular orbital energy-level diagrams for the diatomic molecules of the period 2 elements. Unlike earlier diagrams, *only the valence molecular orbital energy levels for the **molecules** are shown here (atomic orbitals not shown for simplicity).* For Li_2 through N_2, the $\sigma_g(2p)$ orbital is higher in energy than the $\pi_u(2p)$ orbitals. In contrast, from O_2 onward, the $\sigma_g(2p)$ orbital is *lower* in energy than the $\pi_u(2p)$ orbitals because the nuclear charge increases across the row. The experimental bond lengths correlate with the calculated bond order. (CC-BY-NC-SA, Kathryn Haas)

Dilithium, Li_2 $[\sigma_g^2(2s)]$: This molecule has a bond order of one and is observed experimentally in the gas phase to have one Li-Li bond.

Diberylium, Be_2 $[\sigma_g^2\sigma_u^{*2}(2s)]$: This molecule has a bond order of zero due to the equal number of electrons in bonding and antibonding orbitals. Although Be_2 does not exist under ordinary conditions, it can be produced in a laboratory and its bond length measured (Figure 2.2.6.2). Although the bond is very weak, its bond length is surprisingly ordinary for a covalent bond of the second period elements.[2]

Diboron, B_2 $[\sigma_g^2\sigma_u^{*2}(2s)\pi_u^1\pi_u^1(2p)]$: The case of diboron is one that is much better described by molecular orbital theory than by Lewis structures or valence bond theory. This molecule has a bond order of one. The molecular orbital description of diboron also predicts, accurately, that diboron is paramagnetic. The paramagnetism is a consequence of orbital mixing, resulting in the σ_g orbital's being at a higher energy than the two degenerate π_u^* orbitals.

Dicarbon, C_2 $[\sigma_g^2\sigma_u^{*2}(2s)\pi_u^2\pi_u^2(2p)]$: This molecule has a bond order of two. Molecular orbital theory predicts two bonds with π symmetry, and no σ bonding. C_2 is rare in nature because its allotrope, diamond, is much more stable.

Dinitrogen, N_2 $[\sigma_g^2\sigma_u^{*2}(2s)\pi_u^2\pi_u^2\sigma_g^2(2p)]$: This molecule is predicted to have a triple bond. This prediction is consistent with its short bond length and bond dissociation energy. The energies of the $\sigma_g(2p)$ and $\pi_u(2p)$ orbitals are very close, and their relative energy levels have been a subject of some debate (see next section for discussion).

Dioxygen, O_2 $[\sigma_g^2\sigma_u^{*2}(2s)\sigma_g^2\pi_u^2\pi_u^2\pi_g^{*1}\pi_g^{*1}(2p)]$: This is another case where valence bond theory fails to predict actual properties. Molecular orbital theory correctly predicts that dioxygen is paramagnetic, with a bond order of two. Here, the molecular orbital diagram returns to its "normal" order of orbitals where orbital mixing could be somewhat ignored, and where $\sigma_g(2p)$ is lower in energy than $\pi_u(2p)$.

Difluorine, F_2 $[\sigma_g^2\sigma_u^{*2}(2s)\sigma_g^2\pi_u^2\pi_u^2\pi_g^{*2}\pi_g^{*2}(2p)]$: This molecule has a bond order of one and like oxygen, the $\sigma_g(2p)$ is lower in energy than $\pi_u(2p)$.

Dineon, Ne_2 $[\sigma_g^2\sigma_u^{*2}(2s)\sigma_g^2\pi_u^2\pi_u^2\pi_g^{*2}\pi_g^{*2}\sigma_u^{*2}(2p)]$: Like other noble gases, Ne exists in the atomic form and does not form bonds at ordinary temperatures and pressures. Like Be_2, Ne_2 is an unstable species that has been created in extreme laboratory conditions and its bond length has been measured (Figure **2.2.6.2**).

Bond Lengths in Homonuclear Diatomic Molecules

The trends in experimental bond lengths are predicted by molecular orbital theory, specifically by the calculated bond order. The values of bond order and experimental bond lengths for the second period diatomic molecules are given in Figure **2.2.6.1**, and shown in graphical format on the plot in Figure **2.2.6.2**. From the plot, we can see that bond length correlates well with bond order, with a minimum bond length occurring where the bond order is greatest ($\mathbf{N_2}$). The shortest bond distance is at $\mathbf{N_2}$ due to its high bond order of 3. From $\mathbf{N_2}$ to $\mathbf{F_2}$ the bond distance increases despite the fact that atomic radius decreases.

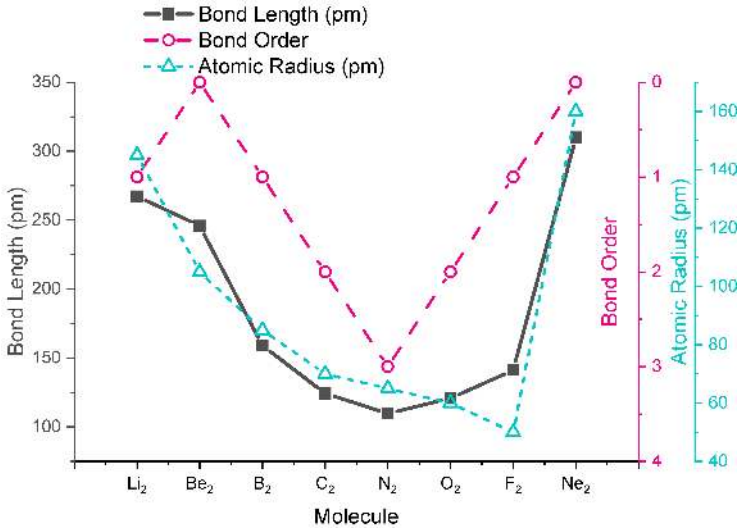


Figure **2.2.6.2**: Overlayed plots of bond length (black squares), bond order (pink circles), and atomic radius (teal triangles) versus atomic number for second period homonuclear diatomic molecules. (CC-BY-NC-SA; Kathryn Haas)

Problems

? Exercise 2.2.6.2

Draw the complete molecular orbital diagrams for $\mathbf{H_2}$ and for $\mathbf{He_2}$. Include sketches of the atomic and molecular orbitals.

Answer

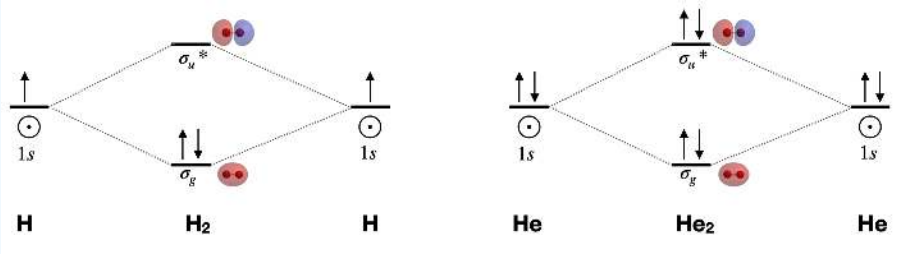


Figure for Exercise **2.2.6.1**: Molecular orbital diagrams for dihydrogen and dihelium. Molecular orbital surfaces calculated using Spartan software. (CC-BY-NC-SA; Kathryn Haas)

A complete molecular orbital diagram includes all atomic orbitals and molecular orbitals, their symmetry labels, and electron filling.

Exercise 2.2.6.2

Draw the complete molecular orbital diagram for O_2. Show calculation of its bond order and tell whether it is diamagnetic or paramagnetic.

Answer

O_2 is paramagnetic with a bond order of 2. Its $\sigma_g(2p)$ molecular orbital is lower in energy that the set of $\pi_u(2p)$ orbitals.

$$\text{Bond order} = \frac{1}{2}\left[\left(\begin{array}{c}\textbf{8 electrons in}\\ \textbf{valence bonding orbitals}\end{array}\right) - \left(\begin{array}{c}\textbf{4 electrons in}\\ \textbf{valence antibonding orbitals}\end{array}\right)\right]$$

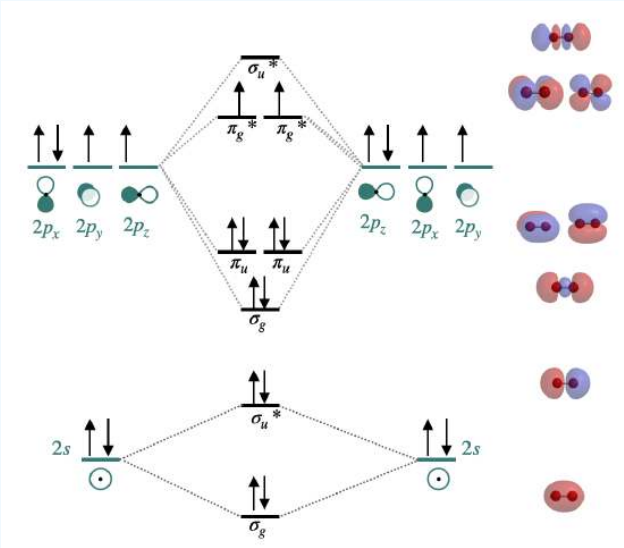


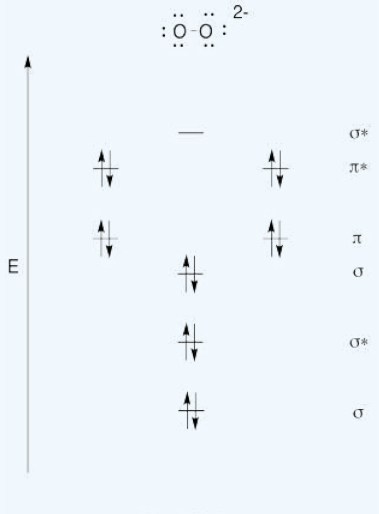
Figure for Exercise **2.2.6.2**. Molecular orbital diagram of O_2. (CC-BY-NC-SA, Kathryn Haas)

Exercise 2.2.6.3: The Peroxide Ion

Use a qualitative molecular orbital energy-level diagram to predict the electron configuration, the bond order, and the number of unpaired electrons in the peroxide ion (O_2^{2-}).

Answer

This diagram looks similar to that of $\mathbf{O_2}$, except that there are two additional electrons.
$(\sigma_g(2s))^2\,(\sigma_u^*(2s))^2\,(\sigma_g(2p))^2\,(\pi_u(2p))^4\,(\pi_g(2p))^4$; bond order of 1; no unpaired electrons.

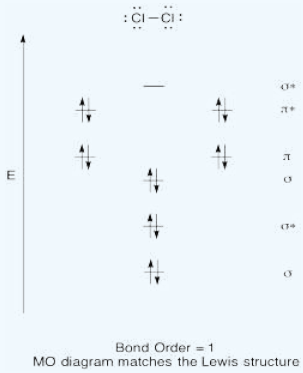


Bond Order = 1
MO diagram matches the Lewis structure. Both predict a Bond Order of 1 and 6 lone pairs of electrons. The addition of two electrons to O_2 to O_2^{2-} would be possible.

Exercise 2.2.6.4

Construct a qualitative molecular orbital diagram for chlorine, Cl_2. Compare the bond order to that seen in the Lewis structure (remember that an electron in an antibonding orbital cancels the stabilization due to bonding of an electron in a bonding orbital).

Answer

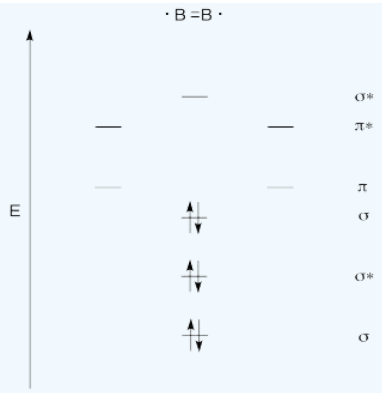


Bond Order = 1
MO diagram matches the Lewis structure

Exercise 2.2.6.5

Construct a qualitative molecular orbital diagram for diboron, B_2. Do you think boron-boron bonds could form easily, based on this picture?

Answer

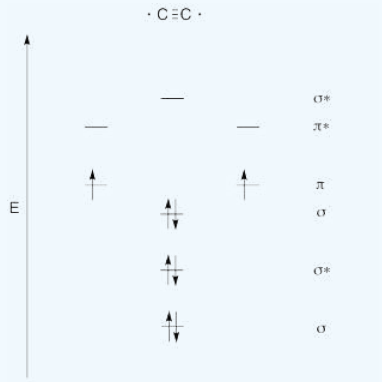


Bond Order = 1
Boron-Boron bonding should be possible

Exercise 2.2.6.6

a. Construct a qualitative molecular orbital diagram for dicarbon, C_2.
b. Compare the bond order to that seen in the Lewis structure.
c. How else does this MO picture of oxygen compare to the Lewis structure? What do the two structures tell you about electron pairing?

Answer

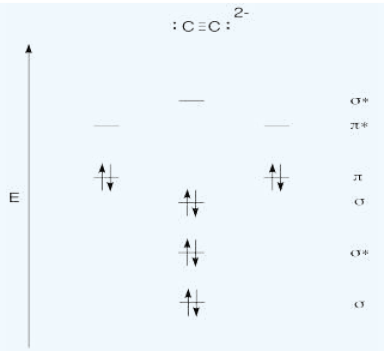


Bond Order = 2
MO diagram does not match the Lewis structure.
However, the MO diagram does concur about the
2 unpaired electrons.

Exercise 2.2.6.7

a. Construct a qualitative molecular orbital diagram for acetylide anion, C_2^{2-}.
b. Compare the bond order to that seen in the Lewis structure.
c. How else does this MO picture of oxygen compare to the Lewis structure? What do the two structures tell you about electron pairing?
d. Based on molecular orbital pictures, how easily do you think dicarbon could be reduced to acetylide (through the addition of two electrons)?

Answer

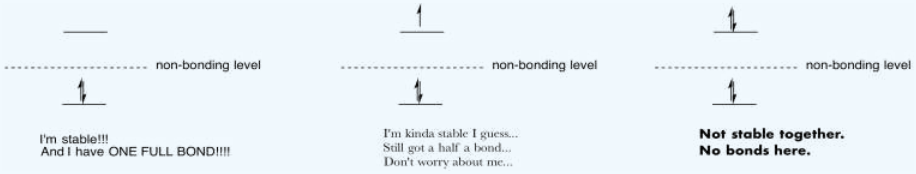


Bond Order = 3
MO diagram matches the Lewis structure. Both predict a Bond Order of 3 and 2 lone pairs of electrons. The addition of two electrons to C_2 to C_2^{2-} would be possible.

Exercise 2.2.6.8

Make drawings and notes to summarize the effect of populating antibonding orbitals.

Answer

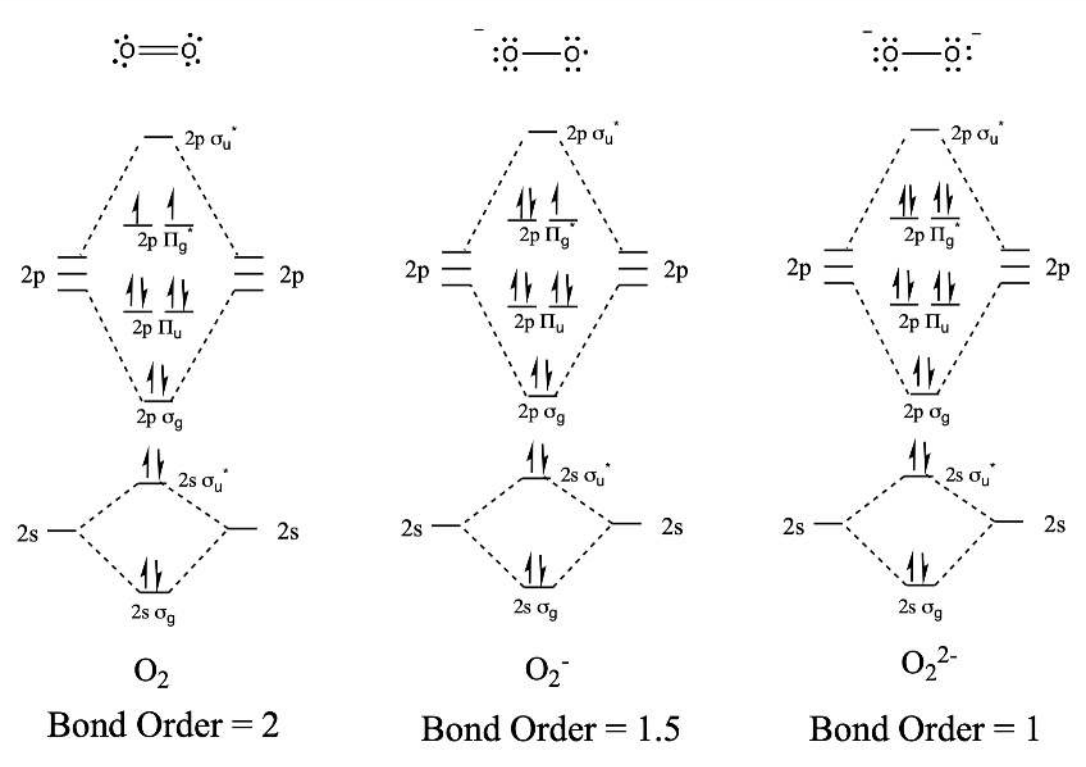


Exercise 2.2.6.9

Draw and compare the molecular orbital diagrams to the Lewis structure diagrams for O_2, O_2^-, and O_2^{2-}.

Answer

The Lewis structures and MO diagrams are shown below. In general, the bond order derived from the MO diagram agrees with the Lewis structure for each species. In the case of the two ions, the number of unpaired electrons from MO theory and the Lewis structure also agrees. In the case of dioxygen, however, there is an inconsistency between the Lewis representation and the MO diagram. While the Lewis structure would lead us to believe that all electrons are paired, the MO diagram indicates paramagnetism, with two unpaired electrons. The MO diagram explains the magnetic behaviour of dioxygen.



References

1. NIST, Calculated Geometries available for H_2^+ (Hydrogen cation) 2Σg+ D∞h, available at https://cccbdb.nist.gov/diatomicexpbondx.asp
2. Merritt, J. M.; Bondybey, V. E.; Heaven, M. C., Beryllium Dimer-Caught in the Act of Bonding. *Science* **2009,** *324* (5934), 1548-1551.

2.2.6: MO- MO Diagrams of 1st and 2nd row diatomic molecules is shared under a CC BY-NC-SA 4.0 license and was authored, remixed, and/or curated by Kathryn A. Newton, Northern Michigan University.

- **5.2.3: Diatomic Molecules of the First and Second Periods** by Kathryn Haas is licensed CC BY-SA 4.0.
- **2.5: Diatomic Molecules** by Chemistry 310 is licensed CC BY-SA 4.0. Original source: https://en.wikibooks.org/wiki/Introduction_to_Inorganic_Chemistry.
- **5.P: Problems** is licensed CC BY-SA 4.0.
- **13.6: Assembling the Complete Diagram and Electron Population** by Chris Schaller is licensed CC BY-NC 3.0. Original source: https://employees.csbsju.edu/cschaller/structure.htm.

2.2.7: MO- MO Diagrams of Heteronuclear Diatomics

Diatomic molecules with two non-identical atoms are called **heteronuclear** diatomic molecules. When atoms are not identical, the molecule forms by combining atomic orbitals of unequal energies. *The result is a bond in which atomic orbitals contribute unevenly to each molecular orbital*. The application of molecular orbital theory to heteronuclear diatomic molecules is similar to the case of homonuclear diatomics, except that the atomic orbitals from each atom have different energies and contribute unequally to molecular orbitals. As a result both the symmetry of the atomic orbitals and their energies must be considered to determine if they will combine into molecular orbitals.

Energies of Atomic Orbitals

In the case where atomic orbitals of like symmetry have different energies, they combine less favorably than orbitals that are closer to one another in energy. As a general rule, orbitals that have energy differences of greater than 10-14 eV do not combine favorably. In the molecular orbital diagram, the closer a molecular orbital is to an atomic orbital, the more that atomic orbital contributes to the molecular orbital. This last point is helpful for back-of-the napkin estimations of what the molecular orbitals "look" like. Although an estimation of the differences in energy is usually sufficient, the energy difference between atomic orbitals can be calculated from orbital ionization energies

Orbital Ionization Energies

There are two approaches you can use to "know" or estimate the atomic orbital energy levels.

1. Use a table of atomic orbital ionization energies, like those found in Table **2.2.7.1**.
2. When you do not have access to a table of values like the one below, use periodic trends in electronegativity and/or ionization energies as your guide to approximate relative values for different atoms.

Table **2.2.7.1**: These are one-electron ionization energies of the valence orbitals calculated by average energies of both the ground-state and ionized-state configurations. (From Harry Gray, “Electrons and Chemical Bonding,” Benjamin, 1964, Appendix)

Atom	1s	2s	2p	3s	3p	4s	4p	Atom	3d	4s	4p
H	−13.64							Sc	−4.71	−5.70	−3.22
He	−24.55							Ti	−5.58	−6.08	−3.35
Li		−5.46						V	−6.32	−6.32	−3.47
Be		−9.30						Cr	−7.19	−6.57	−3.47
B		−14.01	−8.31					Mn	−7.93	−6.82	−3.60
C		−19.47	−10.66					Fe	−8.68	−7.07	−3.72
N		−25.54	−13.14					Ni	−10.04	−7.56	−3.84
O		−32.36	−15.87					Cu	−10.66	−7.69	−3.97
F		−46.37	−18.72								
Ne		−48.48	−21.57								
Na				−5.21							
Mg				−7.69							
Al				−11.28	−5.95						
Si				−15.00	−7.81						
P				−18.72	−10.17						
S				−20.71	−11.65						
Cl				−25.29	−13.76						
Ar				−29.26	−15.87						
K						−4.34					
Ca						−6.08					
Zn						−9.42					
Ga						−12.65	−5.95				
Ge						−15.62	−7.56				
As						−17.61	−9.05				
Se						−20.83	−10.79				
Br						−24.05	−12.52				
Kr						−27.52	−14.26				

Molecular Orbital Diagrams for Heteronuclear Diatomic Molecules

The molecular orbital diagram of a heteronuclear diatomic molecule is approached in a way similar to that of a homonuclear diatomic molecule. The heteronuclear diatomic molecular orbital diagrams look similar to those of homonuclear diatomics, but with the difference that the more electronegative atom will have orbitals at a lower energy level. The more electronegative atom will be placed on the right side of the diagram with its atomic orbitals shown lower in energy than those of the less electronegative atom on the left. As with homonuclear diatomics, orbital mixing can affect the arrangement of the molecular orbitals. Molecular orbital diagrams describing the bonding of two elements that are both oxygen, fluorine, or a later element do not show sp mixing, and will have an arrangement like that for O_2 or F_2. Diagrams describing bonding of an atom that shows sp mixing (such as CO, NO, NO^+) will have the ordering of energy levels shown by N_2. A good animation of the molecular orbitals in the CO molecule can be found on the University of Liverpool **Structure and Bonding** website. Two examples of heteronuclear diatomic molecules will be explored below as illustrative examples.

Carbon monoxide MO diagram

Carbon monoxide is an example of a heteronuclear diatomic molecule where both atoms are second-row elements. The valence molecular orbitals in both atoms are the $2s$ and $2p$ orbitals. The molecular orbital diagram for carbon monoxide (Figure **2.2.7.1**) is constructed in a way similar to how you would construct dicarbon or dioxygen, except that the oxygen orbitals have a lower potential energy than analogous carbon orbitals. The labeling of molecular orbitals in this diagram follows a convention by which orbitals are given serial labels according to type of orbital (σ, π, etc.). The lowest energy orbitals of any type are assigned a value of 1 and higher energy orbitals of the same type are assigned by increasing intervals (..2, 3, 4...).

A consequence of unequal atomic orbital energy levels is that orbital mixing is significant. Notice the order of the molecular orbitals labeled 1π and 3σ in Figure **2.2.7.1**. This is a similar order of π and σ orbitals to the one we saw in the case of the σ_g and π_u orbitals of N_2 and lighter diatomics of the second period. Because the oxygen $2p_z$ orbital is close in energy to both the carbon $2p_z$

and carbon $2s$, these three orbitals will have significant interaction (mixing). The result is an increase in the energy of the 3σ orbital and a decrease in energy of the $2\sigma^*$ orbital, resulting in the diagram shown in Figure 2.2.7.1.

In the case of carbon monoxide (Figure 2.2.7.1), atomic orbitals contribute unequally to each molecular orbital. For example, because the $2s$ orbital of oxygen is very close in energy to the 2σ moelcular orbital, it contributes to that molecular orbital more than the $2s$ orbital from carbon. Notice the shape of this 2σ orbital and how it is unevenly distributed over the two atoms; it is more heavily distributed on the oxygen because it is most like the oxygen $2s$. This is in line with the assumption that electron density is distributed more on oxygen because it is more electronegative than carbon. Likewise, the 1π orbitals are unevenly distributed, with more distribution close to the oxygen.

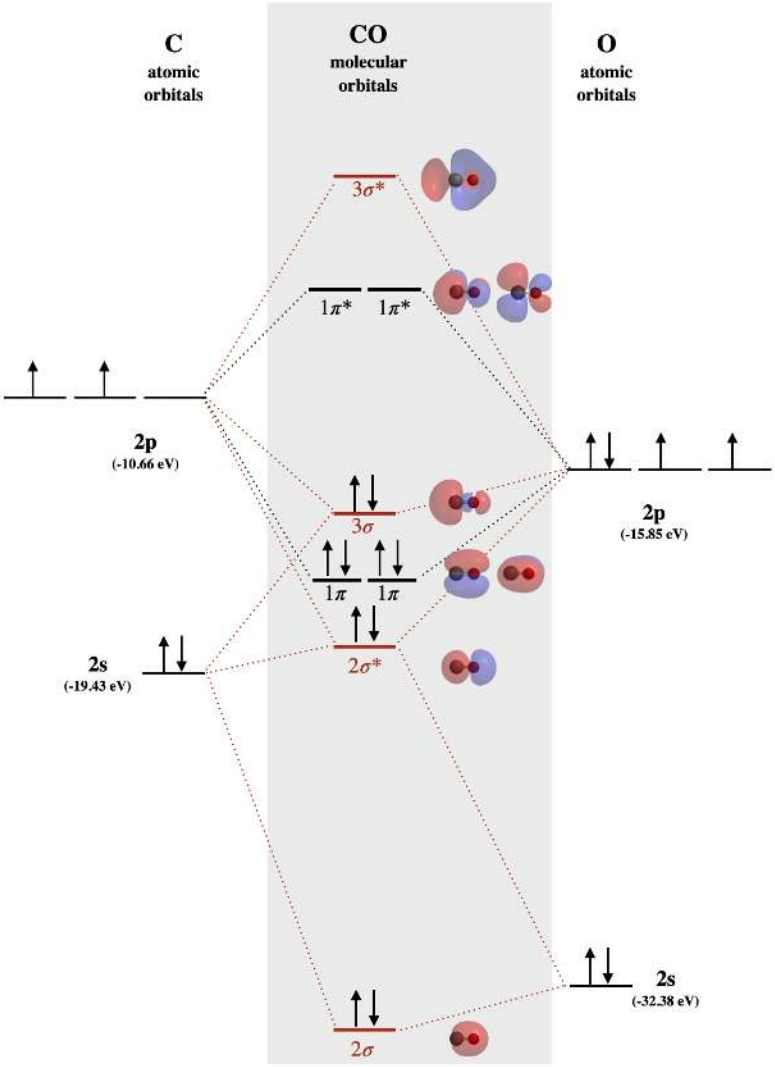


Figure 2.2.7.1: Molecular orbital diagram of carbon monoxide. The labeling of molecular orbitals in this diagram follows a convention by which orbitals are given serial names according to the type of orbital (σ, π, etc.). The lowest energy orbitals of any type are assigned a value of 1 and higher energy orbitals of the same type are assigned by increasing intervals (..2, 3, 4...). The orbital labeling system described previously is inappropriate for heteronuclear diatomic molecules that cannot be assigned g and u subscripts. Molecular orbital surfaces were calculated using Spartan software. (Kathryn Haas, CC-BY-NC-SA)

Hydrogen fluoride MO diagram

Hydrogen fluoride is an example of a heteronuclear diatomic molecule in which the two atoms are from different periods. In this case, the valence orbital of H is $1s$ while those of F are $2s$ and $2p$. The molecular orbital diagram for HF is shown in Figure 2.2.7.2.

Three of these orbitals have compatible symmetry for mixing; these are the hydrogen $1s$, fluorine $2s$, and fluorine $2p$. However, the extent to which they will interact depends on their relative energies. Fluorine is more electronegative than H, and the fluorine atom has a higher first ionization energy than does hydrogen. From these trends, we can expect that the fluorine valence orbitals are

lower in energy than that of hydrogen. From Table **2.2.7.1** we find that the 1s orbital of H (-13.6 eV) is higher in energy than both fluorine orbitals (-18.7 and -40.2 eV, respectively for $2p$ and $2s$). The energies of hydrogen $1s$ and fluorine $2p$ are a good match for combination; however, the fluorine $2s$ orbital is much too different to create a productive interaction. Therefore, we expect that the fluorine $2s$ will create a non-bonding molecular orbital, while the $1s$ and $2p_z$ orbitals combine to make σ bonding and σ^* antibonding molecular orbitals. The remaining $2p_x$ and $2p_y$ orbitals do not have compatible symmetry for bonding with hydrogen, and they will form non-bonding π molecular orbitals. The non-bonding orbitals will have similar energy and character as their component atomic orbitals.

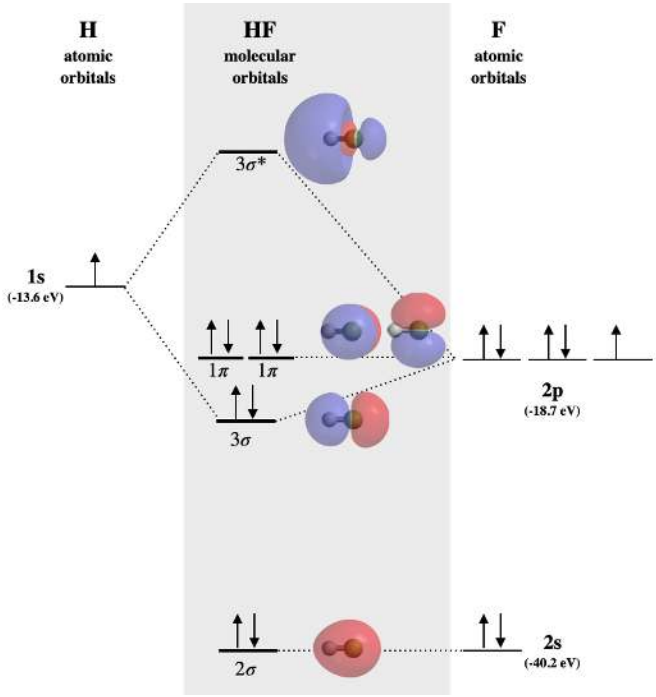


Figure **2.2.7.2**: Molecular Orbital diagram of hydrogen fluoride. Molecular orbitals calculated using Spartan software. (Kathryn Haas, CC-BY-NC-SA)

Chemical reactions take place at the HOMO and LUMO orbitals

Knowledge of molecular orbital diagrams, and the shapes of molecular orbitals, can be used to accurately explain and predict chemical reactivity. Chemical reactions take place using the highest occupied molecular orbitals (HOMO) of a nucleophile or Lewis base, and the lowest unoccupied molecular orbital (LUMO) of an electrophile or Lewis acid.

> *Lewis bases react using electrons in the HOMO, while Lewis acids react using the empty LUMO.*

Example: Reactivity of CO with metal ions

CO is an excellent ligand for many metal ions. In fact, the strong affinity between CO and the heme iron (Fe) ions in hemoglobin can explain the mechanism of carbon monoxide poisoning. When CO binds in place of O_2 to hemoglobin, that hemoglobin can no longer carry O_2 to tissue cells. CO binding to hemoglobin is strong and practically irreversible. When CO binds to metal ions, it does so through the carbon atom. This is contrary to expectations based on the Lewis structure and the known bond polarity, where electron density is polarized toward oxygen. The distribution of the electron density of the HOMO of CO can explain this observation!

Problems

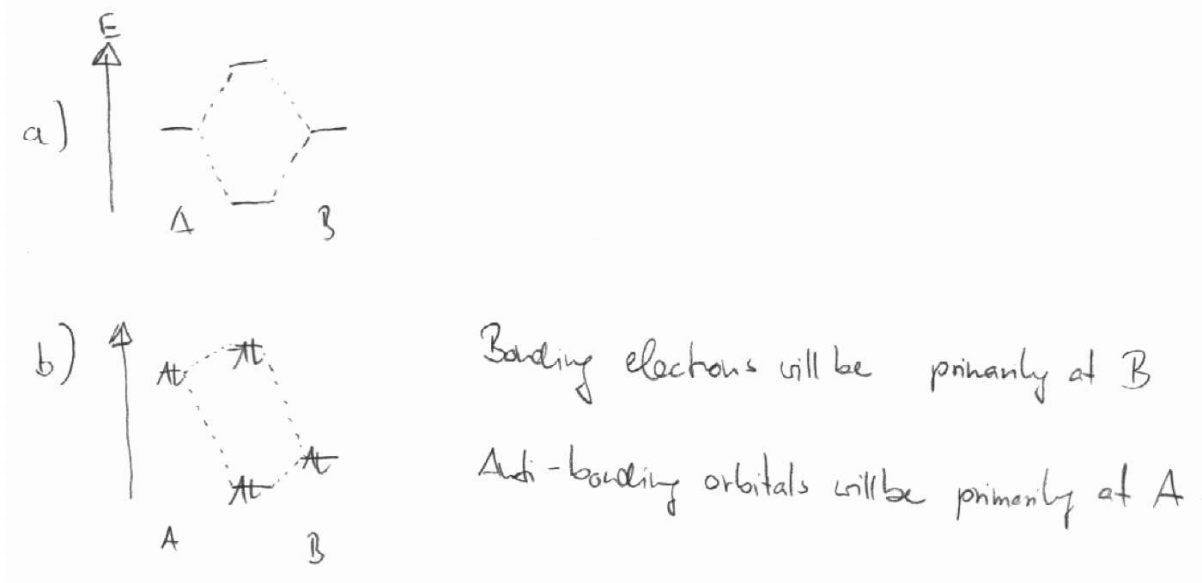
Exercise 2.2.7.1

Qualitatively construct the MO diagrams composed of

a) two 2s atom orbitals A and B of equal energy.

b) two 2s atom orbitals where the orbital energy of atom A is significantly higher than that of B. If both the bonding and the antibonding MO are filled with electrons, where will bonding and antibonding electrons primarily be located? Briefly explain your decision.

Answer



? Exercise 2.2.7.2

Examine the shape of the 3σ orbital of carbon monoxide in Figure 2.2.7.1. Describe what ways this shape is different from the shape of the σ_g orbitals from second period homonuclear diatomic molecules (see Fig. 5.2.1.1). Rationalize these differences. Both orbitals are re-created below for convenience.



σ_g of homonuclear diatomic

3σ of CO

Answer

The 3σ orbital is like the σ_g in that it has three lobes and two nodes distributed along the internuclear bond. They are different in their distribution. The two external lobes of σ_g are evenly distributed because they are an equal combination of two p_z orbitals (one from each atom). The 3σ orbital is more heavily distributed toward the carbon atom, the less electronegative atom, than toward the oxygen. The unequal distribution of 3σ is apparent in the unequal sizes of its exterior lobes and the uneven shape of the interior lobe. The heavier distribution within the exterior lobe on carbon is caused by the mixing of the carbon $2s$ orbital with carbon and oxygen $2p_z$ orbitals. The uneven shape of the interior lobe, where it leans toward oxygen, is best explained by the fact that the 3σ orbital is closer in energy to the oxygen $2p_z$ than the carbon $2p_z$.

? Exercise \(\PageIndex{3}\)

Refer to the MO diagram for CO. Identify the HOMO and explain why CO bonds to metal ions through the carbon atom rather than through the oxygen atom.

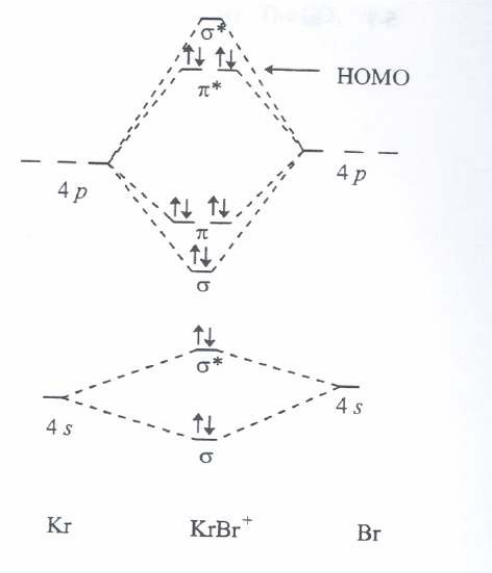
Answer

In the interaction between CO and a metal ion, CO would act as a Lewis base; thus it will react using electrons in its HOMO. The MO diagram for CO is shown in Figure **2.2.7.1**: the HOMO is the **3σ** orbital (also discussed in ? Exercise **2.2.7.1**). The electron density of that MO is centered around the carbon atom, thus the carbon atom will be a better Lewis base than the O atom.

Exercise 2.2.7.4

For the hypothetical $BrKr^+$ molecule: Toward which atom is the HOMO polarized? Explain briefly why.

Answer



Sources:

- Gray, Harry. *Electrons and Chemical Bonding*, Benjamin, 1964.
- Miessler, Gary L, and Donald A. Tarr. *Inorganic Chemistry*. Upper Saddle River, N.J: Pearson Education, 2014. Print.

2.2.7: MO- MO Diagrams of Heteronuclear Diatomics is shared under a CC BY-NC-SA 4.0 license and was authored, remixed, and/or curated by Kathryn A. Newton, Northern Michigan University.

- **5.3: Heteronuclear Diatomic Molecules** by Kathryn Haas is licensed CC BY-SA 4.0.
- **5.3.2: Polar bonds** by Kathryn Haas is licensed CC BY-SA 4.0.
- **Homework Problems Chapter 3** by Kai Landskron is licensed CC BY 4.0.

2.3: Metallic- Sea of Electrons and the van Arkel-Ketelaar Triangle

In the early 1900's, Paul Drüde came up with the "sea of electrons" metallic bonding theory by modeling metals as a mixture of atomic cores (atomic cores = positive nuclei + inner shell of electrons) and valence electrons. Metallic bonds occur among metal atoms. Whereas ionic bonds join metals to non-metals, *metallic bonding joins a bulk of metal atoms*. A sheet of aluminum foil and a copper wire are both places where you can see metallic bonding in action.

Metals tend to have high melting points and boiling points suggesting strong bonds between the atoms. Even a soft metal like sodium (melting point 97.8°C) melts at a considerably higher temperature than the element (neon) which precedes it in the Periodic Table. Sodium has the electronic structure $1s^2 2s^2 2p^6 3s^1$. When sodium atoms come together, the electron in the 3s atomic orbital of one sodium atom shares space with the corresponding electron on a neighboring atom to form a molecular orbital - in much the same sort of way that a covalent bond is formed.

The difference, however, is that each sodium atom is being touched by eight other sodium atoms - and the sharing occurs between the central atom and the 3s orbitals on all of the eight other atoms. Each of these eight is in turn being touched by eight sodium atoms, which in turn are touched by eight atoms - and so on and so on, until you have taken in all the atoms in that lump of sodium. *All* of the 3s orbitals on all of the atoms overlap to give a vast number of molecular orbitals that extend over the whole piece of metal. There have to be huge numbers of molecular orbitals, of course, because any orbital can only hold two electrons.

The electrons can move freely within these molecular orbitals, and so each electron becomes detached from its parent atom. The electrons are said to be delocalized. The metal is held together by the strong forces of attraction between the positive nuclei and the delocalized electrons (Figure **2.3.1**).

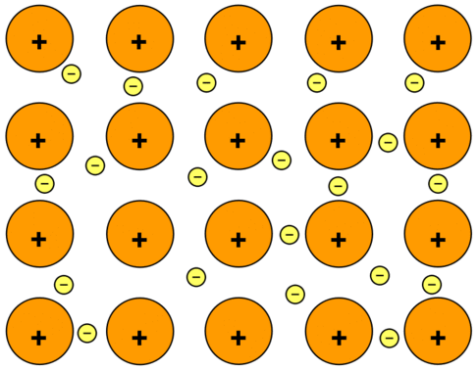


Figure **2.3.1**: Metallic Bonding: The Electron Sea Model: Positive atomic nuclei (orange circles) surrounded by a sea of delocalized electrons (yellow circles).

This is sometimes described as "an array of positive ions in a sea of electrons". If you are going to use this view, beware! Is a metal made up of atoms or ions? It is made of atoms**.** Each positive center in the diagram represents all the rest of the atom apart from the outer electron, but that electron has not been lost - it may no longer have an attachment to a particular atom, but it's still there in the structure. Sodium metal is therefore written as **Na**, not $\mathbf{Na^+}$.

✔ Example **2.3.1**: Metallic bonding in magnesium

Use the sea of electrons model to explain why Magnesium has a higher melting point (650 °C) than sodium (97.79 °C).

Solution

If you work through the same argument above for sodium with magnesium, you end up with stronger bonds and hence a higher melting point.

Magnesium has the outer electronic structure $3s^2$. Both of these electrons become delocalized, so the "sea" has twice the electron density as it does in sodium. The remaining "ions" also have twice the charge (if you are going to use this particular view of the metal bond) and so there will be more attraction between "ions" and "sea".

More realistically, each magnesium atom has 12 protons in the nucleus compared with sodium's 11. In both cases, the nucleus is screened from the delocalized electrons by the same number of inner electrons - the 10 electrons in the $1s^2$ $2s^2$ $2p^6$ orbitals.

That means that there will be a net pull from the magnesium nucleus of 2+, but only 1+ from the sodium nucleus.

So not only will there be a greater number of delocalized electrons in magnesium, but there will also be a greater attraction for them from the magnesium nuclei. Magnesium atoms also have a slightly smaller radius than sodium atoms, and so the delocalized electrons are closer to the nuclei. Each magnesium atom also has twelve near neighbors rather than sodium's eight. Both of these factors increase the strength of the bond still further.

Note: Transition metals tend to have particularly high melting points and boiling points. The reason is that they can involve the 3d electrons in the delocalization as well as the 4s. The more electrons you can involve, the stronger the attractions tend to be.

Bulk properties of metals

Metals have several qualities that are unique, such as the ability to conduct electricity and heat, a low ionization energy, and a low electronegativity (so they will give up electrons easily to form cations). Their physical properties include a lustrous (shiny) appearance, and they are malleable and ductile. Metals have a crystal structure but can be easily deformed. In this model, the valence electrons are free, delocalized, mobile, and not associated with any particular atom. This model may account for:

- **Conductivity**: Since the electrons are free, if electrons from an outside source were pushed into a metal wire at one end (Figure **2.3.2**), the electrons would move through the wire and come out at the other end at the same rate (conductivity is the movement of charge).

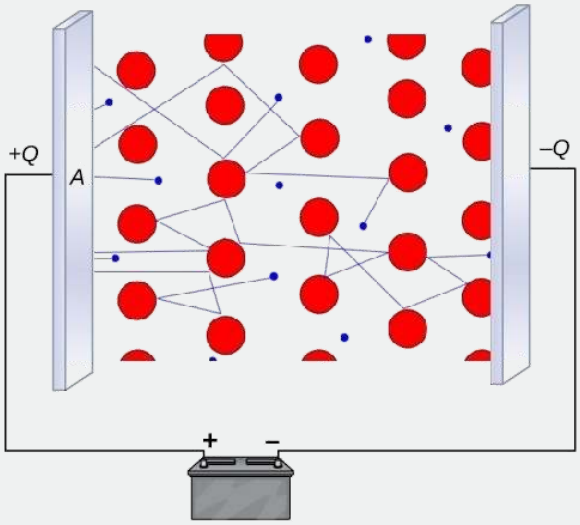


Figure **2.3.2**: The "sea of electrons" is free to flow about the crystal of positive metal ions. These flowing electron can conduct electrical change when an electric field is applied (e.g., a battery). (CC-BY-SA; OpenStax and Rafaelgarcia).

- **Malleability** and **Ductility**: The electron-sea model of metals not only explains their electrical properties but their malleability and ductility as well. The sea of electrons surrounding the protons acts like a cushion, and so when the metal is hammered on, for instance, the overall composition of the structure of the metal is not harmed or changed. The protons may be rearranged but the sea of electrons with adjust to the new formation of protons and keep the metal intact. When one layer of ions in an electron sea moves along one space with respect to the layer below it, the crystal structure does not fracture but is only deformed (Figure **2.3.3**).



Figure **2.3.3**: Malleability of metals originate from each of moving layer of atoms with respect to each other. The final situation is much the same as the initial. Thus if we hit a metal with a hammer, the crystals do not shatter, but merely change their shape, This is very different from the behavior of ionic crystals.

- **Heat capacity**: This is explained by the ability of free electrons to move about the solid.
- **Luster**: The free electrons can absorb photons in the "sea," so metals are opaque-looking. Electrons on the surface can bounce back light at the same frequency that the light hits the surface, therefore the metal appears to be shiny.

> However, these observations are only qualitative, and not quantitative, so they cannot be tested. The "Sea of Electrons" theory stands today only as an oversimplified model of how metallic bonding works.

In a molten metal, the metallic bond is still present, although the ordered structure has been broken down. The metallic bond is not fully broken until the metal boils. That means that boiling point is actually a better guide to the strength of the metallic bond than melting point is. On melting, the bond is loosened, not broken. The strength of a metallic bond depends on three things:

1. The number of electrons that become delocalized from the metal
2. The charge of the cation (metal).
3. The size of the cation.

A **strong** metallic bond will be the result of more delocalized electrons, which causes the effective nuclear charge on electrons on the cation to increase, in effect making the size of the cation smaller. Metallic bonds are strong and require a great deal of energy to break, and therefore **metals have high melting and boiling points.** A metallic bonding theory must explain how so much bonding can occur with such few electrons (since metals are located on the left side of the periodic table and do not have many electrons in their valence shells). The theory must also account for all of a metal's unique chemical and physical properties.

Expanding the Range of Bonding Possible

Previously, we argued that bonding between atoms can classified as range of possible bonding between **ionic bonds** (fully charge transfer) and **covalent bonds** (fully shared electrons). When two atoms of slightly differing electronegativities come together to form a covalent bond, one atom attracts the electrons more than the other; this is called a polar covalent bond. However, simple “ionic” and “covalent” bonding are idealized concepts and most bonds exist on a two-dimensional continuum described by the van Arkel-Ketelaar Triangle (Figure **2.3.4**).

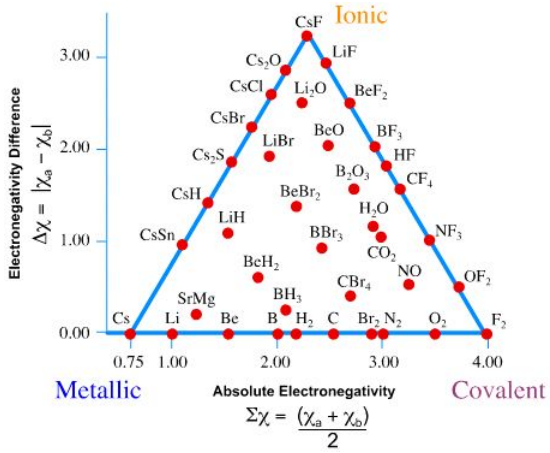


Figure **2.3.4**: van Arkel-Ketelaar Triangle plots the difference in electronegativity ($\Delta\chi$) and the average electronegativity in a bond ($\sum\chi$). the top region is where bonds are mostly ionic, the lower left region is where bonding is metallic, and the lower right region is where the bonding is covalent.

Bond triangles or **van Arkel–Ketelaar** triangles (named after Anton Eduard van Arkel and J. A. A. Ketelaar) are triangles used for showing different compounds in varying degrees of ionic, metallic and covalent bonding. In 1941 van Arkel recognized three extreme materials and associated bonding types. Using 36 main group elements, such as metals, metalloids and non-metals, he placed ionic, metallic and covalent bonds on the corners of an equilateral triangle, as well as suggested intermediate species. The bond triangle shows that chemical bonds are not just particular bonds of a specific type. Rather, bond types are interconnected and different compounds have varying degrees of different bonding character (for example, polar covalent bonds).



Video 2.3.1: What is the van Arkel-Ketelaar Triangle of Bonding?

Using electronegativity - two compound average electronegativity on x-axis of Figure 2.3.4.

$$\sum\chi = \frac{\chi_A + \chi_B}{2} \tag{2.3.1}$$

and electronegativity difference on y-axis,

$$\Delta\chi = |\chi_A - \chi_B| \tag{2.3.2}$$

we can rate the dominant bond between the compounds. On the right side of Figure 2.3.4 (from ionic to covalent) should be compounds with varying difference in electronegativity. The compounds with equal electronegativity, such as Cl_2 (chlorine) are placed in the covalent corner, while the ionic corner has compounds with large electronegativity difference, such as NaCl (table salt). The bottom side (from metallic to covalent) contains compounds with varying degree of directionality in the bond. At one extreme is metallic bonds with delocalized bonding and at the other are covalent bonds in which the orbitals overlap in a particular direction. The left side (from ionic to metallic) is meant for delocalized bonds with varying electronegativity difference.

The Three Extremes in bonding

In general:

- Metallic bonds have low $\Delta\chi$ **and** low average $\sum\chi$.
- Ionic bonds have moderate-to-high $\Delta\chi$ and moderate values of average $\sum\chi$.
- Covalent bonds have moderate to high average $\sum\chi$ and can exist with moderately low $\Delta\chi$.

Example 2.3.2

Use the tables of electronegativities (Table A2) and Figure 2.3.4 to estimate the following values

- difference in electronegativity ($\Delta\chi$)
- average electronegativity in a bond ($\sum\chi$)
- percent ionic character
- likely bond type

for the selected compounds:

a. AsH (e.g., in arsine AsH)
b. SrLi
c. KF.

Solution

a: AsH

- The electronegativity of As is 2.18

- The electronegativity of **H** is 2.22

Using Equations 2.3.1 and 2.3.2:

$$\begin{aligned}\sum\chi &= \frac{\chi_A + \chi_B}{2} \\ &= \frac{2.18 + 2.22}{2} \\ &= 2.2\end{aligned}$$

$$\begin{aligned}\Delta\chi &= \chi_A - \chi_B \\ &= 2.18 - 2.22 \\ &= 0.04\end{aligned}$$

- From Figure **2.3.4**, the bond is fairly nonpolar and has a low ionic character (10% or less)
- The bonding is in the middle of a covalent bond and a metallic bond

b: **SrLi**

- The electronegativity of **Sr** is 0.95
- The electronegativity of **Li** is 0.98

Using Equations 2.3.1 and 2.3.2:

$$\begin{aligned}\sum\chi &= \frac{\chi_A + \chi_B}{2} \\ &= \frac{0.95 + 0.98}{2} \\ &= 0.965\end{aligned}$$

$$\begin{aligned}\Delta\chi &= \chi_A - \chi_B \\ &= 0.98 - 0.95 \\ &= 0.025\end{aligned}$$

- From Figure **2.3.4**, the bond is fairly nonpolar and has a low ionic character (~3% or less)
- The bonding is likely metallic.

c: **KF**

- The electronegativity of **K** is 0.82
- The electronegativity of **F** is 3.98

Using Equations 2.3.1 and 2.3.2:

$$\begin{aligned}\sum\chi &= \frac{\chi_A + \chi_B}{2} \\ &= \frac{0.82 + 3.98}{2} \\ &= 2.4\end{aligned}$$

$$\begin{aligned}\Delta\chi &= \chi_A - \chi_B \\ &= |0.82 - 3.98| \\ &= 3.16\end{aligned}$$

- From Figure **2.3.4**, the bond is fairly polar and has a high ionic character (~75%)
- The bonding is likely ionic.

? Exercise 2.3.2

Contrast the bonding of **NaCl** and silicon tetrafluoride.

Answer

NaCl is an ionic crystal structure, and an electrolyte when dissolved in water; $\Delta\chi = 1.58$, average $\sum\chi = 1.79$, while silicon tetrafluoride is covalent (molecular, non-polar gas; $\Delta\chi = 2.08$, average $\sum\chi = 2.94$.

Contributors and Attributions

- Jim Clark (Chemguide.co.uk)
- Daniel James Berger
- Wikipedia
- Ed Vitz (Kutztown University), John W. Moore (UW-Madison), Justin Shorb (Hope College), Xavier Prat-Resina (University of Minnesota Rochester), Tim Wendorff, and Adam Hahn.

2.3: Metallic- Sea of Electrons and the van Arkel-Ketelaar Triangle is shared under a CC BY-NC-SA 4.0 license and was authored, remixed, and/or curated by LibreTexts.

- **Metallic Bonding** by Jim Clark is licensed CC BY-NC 4.0.

2.4: Structures of Metals and Ionic Compounds

Introduction

The term "closest packed structures" refers to the most tightly packed or space-efficient composition of crystal structures (lattices). Imagine an atom in a crystal lattice as a sphere. While cubes may easily be stacked to fill up all empty space, unfilled space will always exist in the packing of spheres. To maximize the efficiency of packing and minimize the volume of unfilled space, the spheres must be arranged as close as possible to each other. These arrangements are called **closest packed structures**. The packing of spheres can describe the solid structures of crystals. In a crystal structure, the centers of atoms, ions, or molecules lie on the lattice points. Atoms are assumed to be spherical to explain the bonding and structures of metallic crystals. These spherical particles can be packed into different arrangements. In closest packed structures, the arrangement of the spheres are densely packed in order to take up the greatest amount of space possible.

Close-Packing of Identical Spheres

Crystals are of course three-dimensional objects, but we will begin by exploring the properties of arrays in two-dimensional space. This will make it easier to develop some of the basic ideas without the added complication of getting you to visualize in 3-D — something that often requires a bit of practice. Suppose you have a dozen or so marbles. How can you arrange them in a single compact layer on a table top? Obviously, they must be in contact with each other in order to minimize the area they cover. It turns out that there are two efficient ways of achieving this:



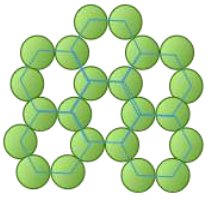
The essential difference here is that any marble within the interior of the square-packed array is in contact with four other marbles, while this number rises to six in the hexagonal-packed arrangement. It should also be apparent that the latter scheme covers a smaller area (contains less empty space) and is therefore a more efficient packing arrangement. If you are good at geometry, you can show that square packing covers 78 percent of the area, while hexagonal packing yields 91 percent coverage.

If we go from the world of marbles to that of atoms, which kind of packing would the atoms of a given element prefer?



If the atoms are identical and are bound together mainly by dispersion forces which are completely non-directional, they will favor a structure in which as many atoms can be in direct contact as possible. This will, of course, be the hexagonal arrangement.

Directed chemical bonds between atoms have a major effect on the packing. The version of hexagonal packing shown at the right occurs in the form of carbon known as *graphite* which forms 2-dimensional sheets. Each carbon atom within a sheet is bonded to three other carbon atoms. The result is just the basic hexagonal structure with some atoms missing.



The coordination number of 3 reflects the sp^2-hybridization of carbon in graphite, resulting in plane-trigonal bonding and thus the sheet structure. Adjacent sheets are bound by weak dispersion forces, allowing the sheets to slip over one another and giving rise to the lubricating and flaking properties of graphite.

Types of Holes From Close-Packing of Spheres

When a single layer of spheres is arranged into the shape of a hexagon, gaps are left uncovered. The hole formed between three spheres is called a **trigonal hole** because it resembles a triangle. In Figure **2.4.1**, two out of the the six trigonal holes have been highlighted green.

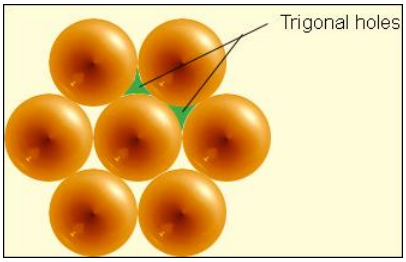


Figure **2.4.1**: Trigonal holes (green) between close packed spheres in a single layer

Once the first layer of spheres is laid down, a second layer may be placed on top of it. The second layer of spheres may be placed to cover the trigonal holes from the first layer. Holes now exist between the first layer (the orange spheres) and the second (the lime spheres), but this time the holes are different (Figure **2.4.2**). The triangular-shaped hole created over a orange sphere from the first layer is known as a **tetrahedral hole** because the surrounding spheres are in a tetrahedral arrangement. A hole from the second layer that also falls directly over a hole in the first layer is called an **octahedral hole** because the surrounding spheres are in an octahedral arrangement.

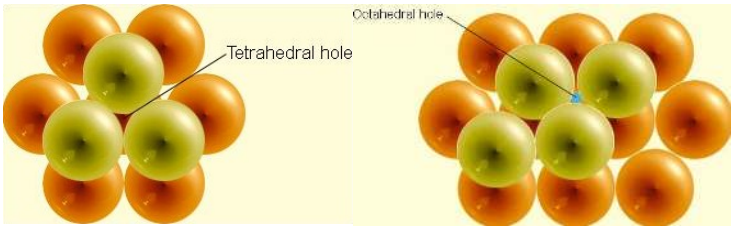


Figure **2.4.2**: Illustrations of tetrahedral (left) and octahedral (right) holes formed between two close packed layers

Close Packed Crystal Structures

Hexagonal Close-Packed (hcp)

In a hexagonal close-packed structure, the third layer has the same arrangement of spheres as the first layer and covers all the tetrahedral holes. Since the structure repeats itself after every two layers, the stacking for hcp may be described as "a-b-a-b-a-b." The atoms in a hexagonal close-packed structure efficiently occupy 74% of space while 26% is empty space.

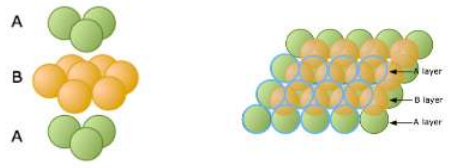


Figure **2.4.3**: Side and top views of the layers in the hexagonal close-packed (hpc) structure.

Cubic Close-Packed (ccp)

The arrangement in a cubic closest packing also efficiently fills up 74% of space. Similar to hexagonal closest packing, the second layer of spheres is placed on to of half of the depressions of the first layer. The third layer is completely different than that first two layers and is stacked in the depressions of the second layer, thus covering all of the octahedral holes. The spheres in the third layer are not in line with those in layer A, and the structure does not repeat until a fourth layer is added. The fourth layer is the same as the first layer, so the arrangement of layers is "a-b-c-a-b-c."

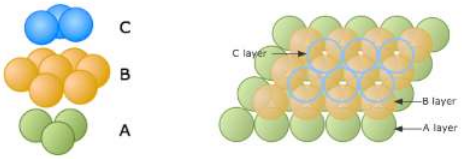


Figure 2.4.4: Side and top views of the layers in cubic close-packed (ccp) structure.

Coordination Number and Number of Atoms Per Unit Cell

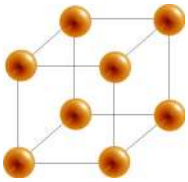
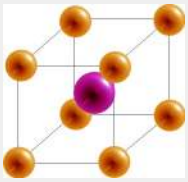
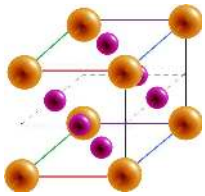
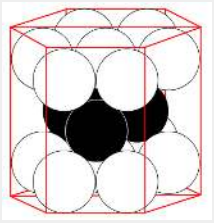
A unit cell is the smallest representation of an entire crystal. All crystal lattices are built of repeating unit cells. In a unit cell, an atom's coordination number is the number of atoms it is touching.

- The simple cubic has a sphere at each corner of a cube. Each sphere has a coordination number of 6 and there is 1 atom per unit cell.
- The body-centered cubic (bcc) has a sphere at each corner of a cube and one in the center. Each sphere has a coordination number 8 and there are 2 atoms per unit cell.
- The cubic closest packed, also called face-centered cubic (fcc) has has a sphere at each corner and each face of a cube. Each sphere has a coordination number of 12 and there are 4 atoms per unit cell.
- The hexagonal closest packed has spheres arranged in hexagons with one in the center. each sphere has a coordination number of 12 and there are 6 atoms per unit cell.

Atoms Per Unit Cell

The amount that an atom contributes to a unit cell depends on its position in the unit cell

- Each corner atom contributes $\frac{1}{8}$ to the unit cell in the cubic cells and $\frac{1}{6}$ to the unit cell in hcp
- Each edge atom contributes $\frac{1}{4}$ to the unit cell
- Each face atom contributes $\frac{1}{2}$ to the unit cell
- Each center atom contributes 1 to the unit cell

Unit Cell	Coordination Number	# of Atoms Per Unit Cell	% space
Simple Cubic 	**6**	**1**	**52%**
Body-Centered Cubic 	**8**	**2**	**68%**
Face-centered Cubic 	**12**	**4**	**74.04%**
Hexagonal Closest Packed 	**12**	**6**	**74.04%**

Inorganic Crystals

Many common inorganic crystals have structures that are related to cubic close packed (face-centered cubic) or hexagonal close packed sphere packings. One component of the material will pack in one of the arrangements above. The remaining component(s) will fill some or all of the holes between the layers. An interstitial atom filling a tetrahedral hole is coordinated to four packing atoms, and an atom filling an octahedral hole is coordinated to six packing atoms. In both the hexagonal close packed and cubic close packed lattices, there is one octahedral hole and two tetrahedral holes per packing atom.

Are Anions or Cations Better Packing Atoms?

We might expect that anions, which are often larger than cations, would be better suited to the positions of packing atoms. While this is often true, there are many examples of structures in which cations are the packing atoms, and others in which the distinction is arbitrary. The NaCl structure is a good example of the latter.

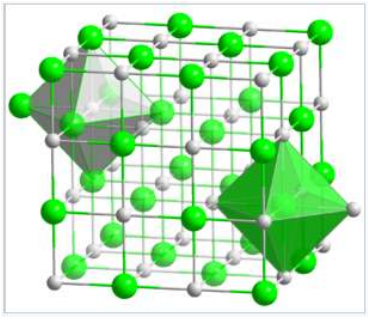


Figure 2.4.5: Crystal structure of NaCl. Both the Na^+ (grey) and Cl^- (green) ions are octahedrally coordinated.

In the rock salt or NaCl structure, shown in Figure 2.4.5, the green spheres are the Cl^- ions and the gray spheres are the Na^+ ions. The packing atoms (Na^+) are in a face centered cubic arrangement. The octahedral holes in a face-centered cubic lattice can be found at the edges and in the center of the unit cell, and they are filled by the chloride ions. Alternatively the structure can be described as the Cl^- ions in a fcc arrangement with the Na^+ ions occupying the octrahedral holes. Another way of stating this is that the structure consists of **two interpenetrating fcc lattices**, which are related to each other by a translation of half the unit cell along any of the three Cartesian axes. Thus the distinction between packing and interstitial atoms in this case is arbitrary.

NaCl is interesting in that it is a three-dimensional checkerboard, and thus there are no NaCl "molecules" that exist in the structure. When this structure was originally solved (in 1913 by using X-ray diffraction) by W. L. Bragg, his interpretation met resistance by chemists who thought that precise integer stoichiometries were a consequence of the valency of atoms in molecules. The German chemist Pfeiffer noted in 1915 that ‘the ordinary notion of valency didn’t seem to apply’, and fourteen years later, the influential chemist Armstrong still found Bragg’s proposed structure of sodium chloride ‘more than repugnant to the common sense, not chemical cricket’! Nevertheless, Bragg and his father, W. H. Bragg, persevered and used the then-new technique of X-ray diffraction to determine the structures of a number of other compounds, including diamond, zincblende, calcium fluoride, and other alkali halides. These experiments gave chemists their first real look at the atomic structure of solids, and laid the groundwork for X-ray diffraction experiments that later elucidated the structures of DNA, proteins, and many other compounds. For their work on X-ray diffraction the Braggs received the Nobel prize in Physics in 1915.

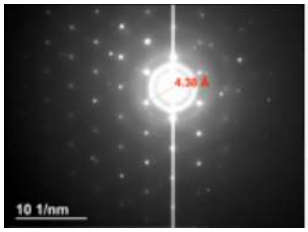


Figure 2.4.6: X-ray difffraction pattern for a NaCl crystal. The lattice dimensions and positions of atoms in crystals such as NaCl are inferred from diffraction patterns.

Since each type of atom in the NaCl structure forms a face-centered cubic lattice, there are four Na and four Cl atoms per NaCl unit cell. It is because of this ratio that NaCl has a 1:1 stoichiometry. The shaded green and gray octahedra in the NaCl lattice (Figure 2.4.5) show that the Na^+ ions are coordinated to six Cl^- ions, and vice versa.

Other materials with the NaCl structure

- Alkali Halides (except CsCl, CsBr, and CsI)
- Transition Metal Monoxides (TiO, VO,..., NiO)
- Alkali Earth Oxides and Sulfides (MgO, CaO, BaS... except BeO and MgTe)
- Carbides and Nitrides (TiC, TiN, ZrC, NbC) -these are very stable refractory, interstitial alloys (metallic)

Other Unit Cell Types

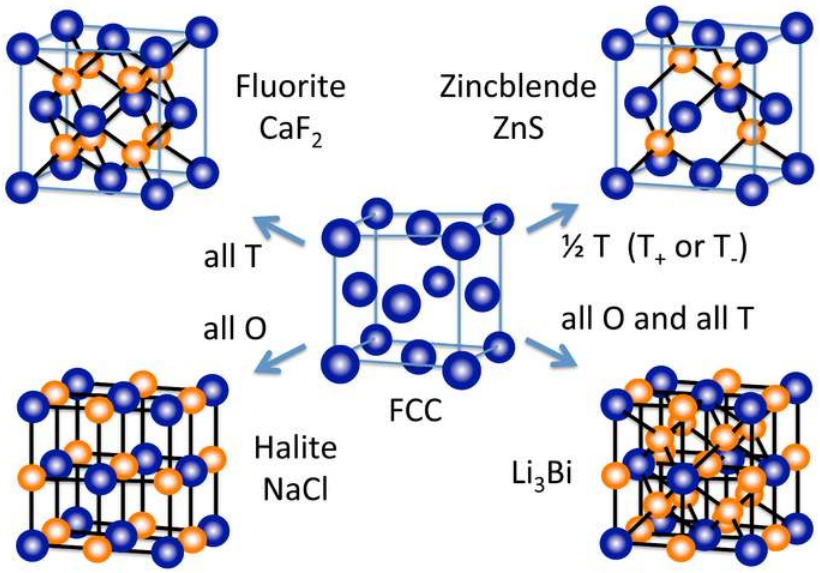


Figure **2.4.7**: Illustration of how different unit cell types are formed by filling holes in the fcc lattice

A number of other inorganic crystal structures are formed (at least conceptually) by filling octahedral and/or tetrahedral holes in close-packed lattices. Figure **2.4.7** shows some of the most common structures (fluorite, NaCl, and zincblende) as well as a rather rare one (Li_3Bi) that derive from the fcc lattice. From the hcp lattice, we can make the NiAs and wurzite structures, which are the hexagonal relatives of NaCl and zincblende, respectively.

An alternative and very convenient way to represent inorganic crystal structures (especially complex structures such as Li_3Bi) is to draw the unit cell in slices along one of the unit cell axes. This kind of representation is shown at the left for the fcc lattice and the NaCl structure. Since all atoms in these structures have z-coordinates of either 0 or 1/2, only those sections need to be drawn in order to describe the contents of the unit cell. It is a useful exercise to draw some of the fcc compound structures (above) in sections.

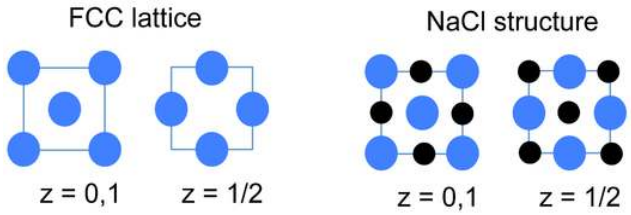


Figure **2.4.8**: Alternative representation of the fcc lattice (left) and the NaCl structure (right). The z = 0,1 represent the bottom and top faces of the unit cell. The z = $\frac{1}{2}$ represents a slice through the center of the unit cell

Fluorite

In ccp and hcp lattices, there are two tetrahedral holes per packing atom. A stoichiometry of either M_2X or MX_2 gives a structure that fills all tetrahedral sites, while an MX structure fills only half of the sites. An example of an MX_2 structure is fluorite, CaF_2, whose structure is shown in the figure at the left. The packing atom in fluorite is Ca^{2+} and the structure is composed of three interpenetrating fcc lattices. It should be noted that the Ca^{2+} ion (gray spheres) as a packing atom defies our "rule" that anions are larger than cations and therefore must be the packing atoms. The fluorite structure is common for ionic MX_2 (MgF_2, ZrO_2, etc.) and M_2X compounds (Li_2O). In contrast, the hcp relative of the fluorite structure is quite rare because of unfavorable close contacts between like-charged ions.

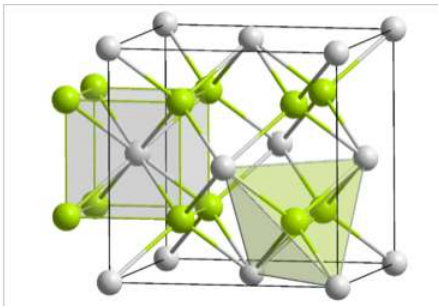


Figure **2.4.9**: The fluorite (CaF_2) crystal structure showing the coordination environments of the Ca (grey) and F (green) atoms

In terms of geometry, Ca^{2+} is in cubic coordination with eight F^- neighbors, and the fluoride ions are tetrahedrally coordinated by four Ca^{2+} ions. The 8:4 coordination geometry is consistent with the 1:2 Ca:F stoichiometry; in all crystal structures the ratio of the coordination numbers is the inverse of the stoichiometric ratio. Looking more closely at the tetrahedral sites in fluorite, we see that they fall into two distinct groups: T_+ and T_-. If a tetrahedron is oriented with a vertex pointing upwards along the stacking axis, the site is T_+. Likewise, a tetrahedron with a vertex oriented downward is T_-. The alternation of T_+ and T_- sites allows for efficient packing of ions in the structure.

Zincblende and wurtzite

Tetrahedrally bonded compounds with a 1:1 stoichiometry (MX compounds) have only half of the tetrahedral sites (either the T_+ or T_- sites) filled. In this case, both the M and the X atoms are tetrahedrally coordinated. The zincblende and wurtzite structures of ZnS are 1:1 tetrahedral structures based on fcc and hcp lattices, respectively. Both structures are favored by p-block compounds that follow the octet rule, and these compounds are usually semiconductors or insulators. The zincblende structure, Figure **2.4.10**, can be thought of as two interpenetrating fcc lattices, one of anions and one of cations, offset from each other by a translation of 1/4 along the body diagonal of the unit cell. Examples of compounds with the zincblende structure include CuCl, CuI, ZnSe, HgS, BeS, CdTe, AlP, GaP, SnSb, CSi, and diamond. Using ZnS as a representative of zincblende, the coordination of both Zn and S atoms is tetrahedral.

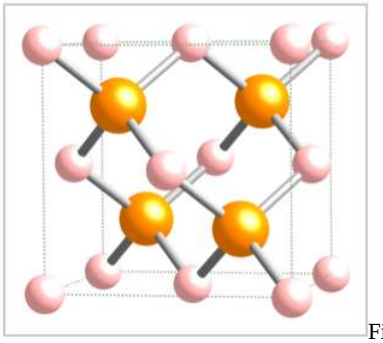


Figure **2.4.10**: The zincblende structure of ZnS. The Zn^{2+} ions are in pink and the S^{2-} ions are in orange.

The wurtzite structure is a close relative of zincblende, based on filling half the tetrahedral holes in the hcp lattice. Like zincblende, wurtzite contains planes of fused six-membered rings in the chair conformation. Unlike zincblende, however, the rings joining these planes contain non-planar, six-membered rings. The structure aligns the anions so that they are directly above the cations in the structure, a less favorable situation sterically but a more favorable one in terms of electrostatics. As a result, the wurtzite structure tends to favor more polar or ionic compounds (e.g., ZnO, $NH_4^+F^-$) than the zincblende structure. As with zincblende, both ions are in tetrahedral (4:4) coordination and there are typically eight valence electrons in the MX compound. Examples of compounds with this structure include: BeO, ZnO, MnS, CdSe, MgTe, AlN, and NH_4F.

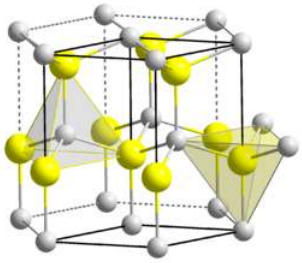


Figure 2.4.11: The wurtzite structure of ZnS with the tetrahedral coordination of anion and cation highlighted. The Zn^{2+} ions are in grey and the S^{2-} ions are in yellow. (Public domain; Solid State via Wikimedia Commons)

An interesting consequence of the layer stacking in the wurtzite structure is that the crystals are polar. When cleaved along the c-axis (the stacking axis), crystals of ZnO, ZnS, and GaN have one negatively charged face and an opposite positively charged face. An applied electric field interacts with the crystal dipole, resulting in compression or elongation of the lattice along this direction. For this reason crystals of compounds in the wurtzite structure are typically piezoelectric (increasing the pressure on the material generates a voltage in the material).

Some compounds are diamorphic and can have either the zincblende or wurtzite structure. Examples of these compounds that have intermediate polarities include CdS and ZnS. SiO_2 exists in polymorphs (crystobalite and tridymite) that resemble zincblende and wurtzite with O atoms midway between each of the Si atoms. The zincblende and wurtzite structures have efficient packing arrangements for tetrahedrally bonded networks and are commonly found in compounds that have tetrahedral bonding. Water, for example, has a tetrahedral hydrogen bonding network and is wurtzite-type. The undistorted wurtzite and zincblende structures are typically found for AX compounds with eight valence electrons, which follow the octet rule. AX compounds with nine or ten electrons such as GaSe and GaAs crystallize in distorted variants of the wurtzite structure. In GaSe, the extra electrons form lone pairs and this creates layers in the structure, as can be seen in the figure below. To the right of GaSe, the structures of As, Sb, and SbAs show an ever further breakdown of the structure into layers as more valence electrons are added.

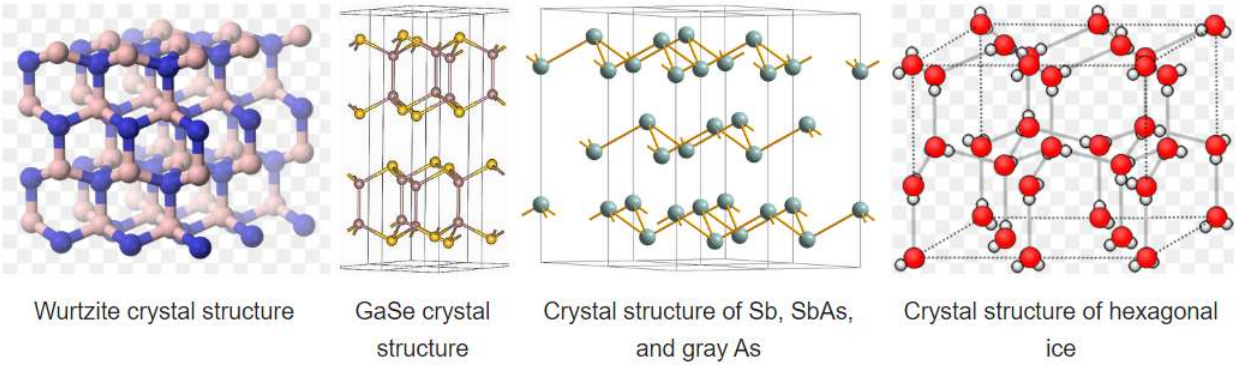


Figure 2.4.12: Different variations of the wurtzite crystal structure (Copyright; author via source)

Hexagonal ice is the most stable polymorph of ice, which is obtained upon freezing at 1 atmosphere pressure. This polymorph (ice-I) has a hcp wurtzite-type structure. Looking at the structure shown at the right, we see that there are irregular arrangements of the O-H---O bonds. In the structure, hydrogen bonding enforces the tetrahedral coordination of each water molecule, resulting in a relatively open structure that is less dense than liquid water. For this reason, ice floats in water.

References

1. Conway, J. H. and Sloane, N. J. A. *Sphere Packings, Lattices, and Groups, 2nd ed.* New York: Springer-Verlag, 1993.
2. Krishna, P. and Verma, A. R. Closed Packed Structures, Chester, UK: International Union of Crystallography, 1981.
3. Petrucci, Ralph H., William S. Harwood, F. Geoffrey Herring, and Jeffry D. Madura. "Crystal Structures" General Chemistry: Principles & Modern Applications, ninth Edition. New Jersey: Pearson Education, Inc., 2007. 501-508.

Contributors and Attributions

- Stephen Lower, Professor Emeritus (Simon Fraser U.) Chem1 Virtual Textbook
- Brittanie Harbick, Laura Suh, Jenny Fong

2.4: Structures of Metals and Ionic Compounds is shared under a CC BY-NC-SA 4.0 license and was authored, remixed, and/or curated by LibreTexts.

- **5.1: Crystal Structures and Unit Cells** is licensed CC BY-NC-SA 4.0.
- **7.8: Cubic Lattices and Close Packing** by Stephen Lower is licensed CC BY 3.0. Original source: http://www.chem1.com/acad/webtext/virtualtextbook.html.
- **8.2: Close-packing and Interstitial Sites** by Chemistry 310 is licensed CC BY-SA 4.0. Original source: https://en.wikibooks.org/wiki/Introduction_to_Inorganic_Chemistry.
- **8.4: Tetrahedral Structures** by Chemistry 310 is licensed CC BY-SA 4.0. Original source: https://en.wikibooks.org/wiki/Introduction_to_Inorganic_Chemistry.

2.5: Ionic- Charge and Size Determine Ionic Bonding

Lattice Energy

Many ionic compounds have simple structures. Because the forces holding the atoms together are primarily electrostatic, we can calculate the cohesive energy of the crystal lattice with good accuracy. Interesting questions to ask about these lattice energy calculations are:

- How accurate are lattice energy calculations?
- What do they teach us about the chemical bonds in ionic crystals?
- Can we use lattice energies to predict properties such as solubility, stability, and reactivity?
- Can we use lattice energies to predict the crystal structures of ionic compounds?

Let's start by looking at the forces that hold ionic lattices together. There are mainly two kinds of force that determine the energy of an ionic bond.

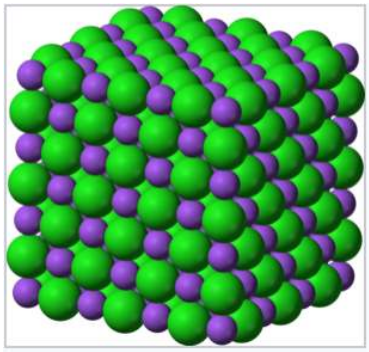


Figure **2.5.1**: The NaCl crystal structure is the archetype for calculating lattice energies and computing enthalpies of formation from Born-Haber cycles.

Electrostatic force

Electrostatic force is the attraction and repulsion between ions described by Coulomb's Law. Two ions with charges z_+ and z_-, separated by a distance r, experience a force F:

$$\mathbf{F} = -\frac{e^2}{4\pi\varepsilon_0}\frac{z_+z_-}{r^2} \tag{2.5.1}$$

where

e = 1.6022×10^{-19} C

$4\,\pi\,\varepsilon_0$ = 1.112×10^{-10} $C^2/(J\ m)$

This force is attractive for ions of opposite charge and repulsive for ions of the same charge.

Closed-shell repulsion

When electrons in the core shells of one ion overlap with those of another ion, there is a repulsive force due to the Pauli exclusion principle. A third electron cannot enter an orbital that already contains two electrons. This force is short range, and is typically modeled as falling off exponentially or with a high power of the distance r between atoms. For example, in the Born approximation, B is a constant and ρ is a number with units of length, which is usually empirically determined from compressibility data. A typical value of ρ is 0.345 Å.

$$\mathbf{E}_{repulsion} = Bexp(\frac{-r}{\rho}) \tag{2.5.2}$$

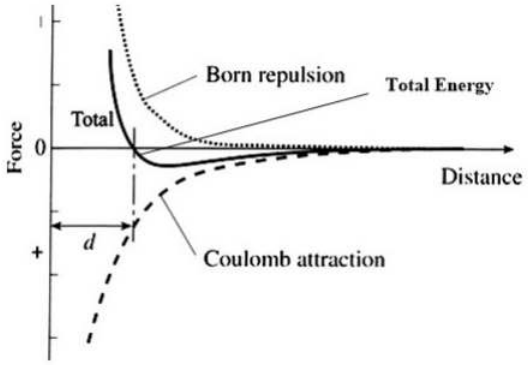


Figure **2.5.2**: Total energy of an ionic bond (solid) determined by the combination of Coulombic attraction (dashed) and Born (closed-shell) repulsion (dotted).

The energy of the ionic bond between two atoms is then calculated as the combination of net electrostatic and the closed-shell repulsion energies, as shown in Figure **2.5.2**. Note that for the moment we are ignoring the attractive van der Waals forces between ions. For a pair of ions, the equilibrium distance between ions is determined by the minimum in the total energy curve.

Madelung Constant

We can use the above equations to calculate the lattice energy of a crystal by summing up the interactions between all pairs of ions. Because the closed-shell repulsion force is short range, this term is typically calculated only for interactions between neighboring ions. However, the Coulomb force is long range, and must be calculated over the entire crystal. This problem was first solved in 1918 by Erwin Madelung, a German physicist.

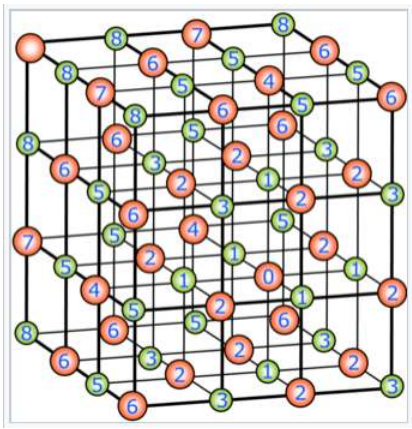


Figure **2.5.3**: The Madelung constant is calculated by summing up electrostatic interactions with ion labeled 0 in the expanding spheres method. Each number designates the order in which it is summed. For example, ions labeled 1 represent the six nearest neighbors (attractive interaction), ions labeled 2 are the 12 next nearest neighbors (repulsive interaction) and so on.

Consider an ion in the NaCl structure labeled "0" in Figure **2.5.3**. We can see that the nearest neighbor interactions (+ -) with ions labeled "1" are attractive, the next nearest neighbor interactions (- - and + +) are repulsive, and so on. In the NaCl structure, counting from the ion in the center of the unit cell, there are 6 nearest neighbors (on the faces of the cube), 12 next nearest neighbors (on the edges of the cube), 8 in the next shell (at the vertices of the cube), and so on. Their distances from ion "0" increase progressively: r_o, $\sqrt{2}\ r_o$, $\sqrt{3}\ r_o$, and so on, where r_o is the nearest neighbor distance.

We can now write the electrostatic energy at ion "0" as:

$$\mathbf{E}_{elec} = -6\frac{e^2}{4\pi\varepsilon_0}\frac{z_+z_-}{r_o} + 12\frac{e^2}{4\pi\varepsilon_0}\frac{z_+z_-}{\sqrt{2}r_o} - 8\frac{e^2}{4\pi\varepsilon_0}\frac{z_+z_-}{\sqrt{3}r_o} + \ldots \tag{2.5.3}$$

Factoring out constants and the nearest-neighbor bond distance r_o we obtain:

$$\mathbf{E}_{elec} = \frac{e^2}{4\pi\varepsilon_0}\frac{z_+z_-}{r_o}\left(6 - \frac{12}{\sqrt{2}} + \frac{8}{\sqrt{3}} - \frac{6}{\sqrt{4}} + \ldots\right) \tag{2.5.4}$$

Where the sum in parentheses, which is unitless, slowly converges to a value of A = 1.74756. Generalizing this formula for any three-dimensional ionic crystal we get a function:

$$\mathbf{E}_{elec} = \frac{e^2}{4\pi\varepsilon_0}\frac{z_+ z_-}{r_o}NA \tag{2.5.5}$$

where N is Avogadro's number (because we are calculating energy per mole of ions) and A is called the *Madelung constant*. The **Madelung constant** depends only on the geometrical arrangement of the ions and so it varies between different types of crystal structures, but within a given structure type it does not change. Thus MgO and NaCl have the same Madelung constant because they both have the NaCl structure.

Table **2.5.1**: Madelung Constants

Compound	*Crystal Lattice*	*M*	*A : C*	*Type*
NaCl	NaCl	1.74756	6 : 6	Rock salt
CsCl	CsCl	1.76267	6 : 6	CsCl type
CaF_2	Cubic	2.51939	8 : 4	Fluorite
$CdCl_2$	Hexagonal	2.244	6 : 3	
MgF_2	Tetragonal	2.381		
ZnS (wurtzite)	Hexagonal	1.64132	4 : 4	Wurtzite
TiO_2 (rutile)	Tetragonal	2.408	6 : 3	Rutile
$bSiO_2$	Hexagonal	2.2197		
Al_2O_3	Rhombohedral	4.1719	6 : 4	Corundum

A is the number of anions coordinated to cation and *C* is the numbers of cations coordinated to anion.

Born–Landé Equation

There are other factors to consider for the evaluation of lattice energy and the treatment by Max Born and Alfred Lande led to the formula for the evaluation of lattice energy for a mole of **crystalline solid**. The Born–Landé equation (Equation 2.5.6) is a means of calculating the lattice energy of a crystalline ionic compound and derived from the electrostatic potential of the ionic lattice and a repulsive potential energy term

$$U = \frac{N_A M Z^2 e^2}{4\pi\epsilon_o r}\left(1 - \frac{1}{n}\right) \tag{2.5.6}$$

where

- N_A is Avogadro constant;
- M is the Madelung constant for the lattice
- z^+ is the charge number of cation
- z^- is the charge number of anion
- e is elementary charge, 1.6022×10^{-19} C
- ε_0 is the permittivity of free space
- r_0 is the distance to closest ion
- n is the **Born exponent** that is typically between 5 and 12 and is determined experimentally. n is a number related to the electronic configurations of the ions involved (Table **2.5.3**).

Table **2.5.2**: n values for select solids

Atom/Molecule	*n*
He	5
Ne	7
Ar	9
Kr	10
Xe	12
LiF	5.9
LiCl	8.0
LiBr	8.7
NaCl	9.1
NaBr	9.5

Example 2.5.1: NaCl

Estimate the lattice energy for **NaCl**.

Solution

Using the values giving in the discussion above, the estimation is given by

$$U_{NaCl} = \frac{(6.022 \times 10^{23}/mol)(1.74756)(1.6022 \times 10^{-19})^2(1.747558)}{4\pi\,(8.854 \times 10^{-12} C^2/m)(282 \times 10^{-12}\ m)} \left(1 - \frac{1}{9.1}\right)$$
$$= -756\ kJ/mol$$

Much more should be considered in order to evaluate the lattice energy accurately, but the above calculation leads you to a good start. When methods to evaluate the energy of crystallization or lattice energy lead to reliable values, these values can be used in the Born-Hable cycle to evaluate other chemical properties, for example the electron affinity, which is really difficult to determine directly by experiment.



Figure 2.5.4: Lithium fluoride (shown here as a large single crystal in a beaker of water) is the only alkali halide that is not freely soluble in water. The lattice energy of LiF is the most negative of the alkali fluorides because Li^+ and F^- are both small ions and lattice energy is proportional to $1/r_0$.

2.5: Ionic- Charge and Size Determine Ionic Bonding is shared under a CC BY-NC-SA 4.0 license and was authored, remixed, and/or curated by LibreTexts.

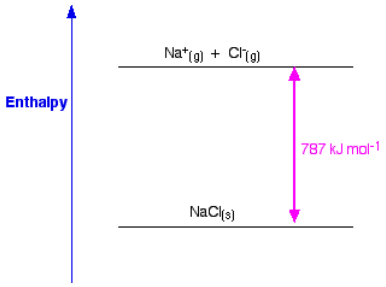
- **5.2: Energetics of Ionic Solids- Lattice Energy** is licensed CC BY-NC-SA 4.0.
- **9.3: Energetics of Crystalline Solids- The Ionic Model** by Chemistry 310 is licensed CC BY-SA 4.0. Original source: https://en.wikibooks.org/wiki/Introduction_to_Inorganic_Chemistry.
- **6.13E: Madelung Constants** is licensed CC BY-NC-SA 4.0.

2.5.1: Ionic- Measurement of Ionic Bond Strength

Lattice enthalpy is a measure of the strength of the forces between the ions in an ionic solid. The greater the **lattice enthalpy**, the stronger the forces. This page introduces lattice enthalpies (lattice energies) and Born-Haber cycles.

Defining Lattice Enthalpy

There are two different ways of defining lattice enthalpy which directly contradict each other, and you will find both in common use. In fact, there is a simple way of sorting this out, but many sources do not use it. Lattice enthalpy is a measure of the strength of the forces between the ions in an ionic solid. The greater the lattice enthalpy, the stronger the forces. Those forces are only completely broken when the ions are present as gaseous ions, scattered so far apart that there is negligible attraction between them. You can show this on a simple enthalpy diagram.



For sodium chloride, the solid is more stable than the gaseous ions by 787 kJ mol^{-1}, and that is a measure of the strength of the attractions between the ions in the solid. Remember that energy (in this case heat energy) is released when bonds are made, and is required to break bonds.

So lattice enthalpy could be described in either of two ways.

- It could be described as the enthalpy change when 1 mole of sodium chloride (or whatever) was formed from its scattered gaseous ions. In other words, you are looking at a downward arrow on the diagram.
- Or, it could be described as the enthalpy change when 1 mole of sodium chloride (or whatever) is broken up to form its scattered gaseous ions. In other words, you are looking at an upward arrow on the diagram.

Both refer to the same enthalpy diagram, but one looks at it from the point of view of making the lattice, and the other from the point of view of breaking it up. Unfortunately, both of these are often described as "lattice enthalpy".

Definitions

- The *lattice dissociation enthalpy* is the enthalpy change needed to convert 1 mole of solid crystal into its scattered gaseous ions. Lattice dissociation enthalpies are **always positive**.
- The *lattice formation enthalpy* is the enthalpy change when 1 mole of solid crystal is formed from its separated gaseous ions. Lattice formation enthalpies are **always negative**.

This is an absurdly confusing situation which is easily resolved by never using the term "lattice enthalpy" without qualifying it.

- You should talk about "lattice dissociation enthalpy" if you want to talk about the amount of energy needed to split up a lattice into its scattered gaseous ions. For NaCl, the lattice dissociation enthalpy is +787 kJ mol^{-1}.
- You should talk about "lattice formation enthalpy" if you want to talk about the amount of energy released when a lattice is formed from its scattered gaseous ions. For NaCl, the lattice formation enthalpy is -787 kJ mol^{-1}.

That immediately removes any possibility of confusion.

Factors affecting Lattice Enthalpy

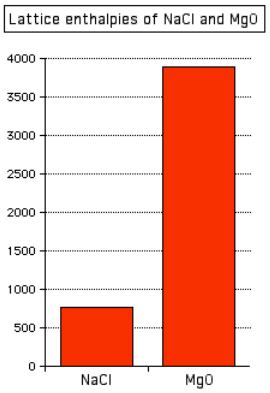
The two main factors affecting lattice enthalpy are

- The charges on the ions and

- The ionic radii (which affects the distance between the ions).

The charges on the ions

Sodium chloride and magnesium oxide have exactly the same arrangements of ions in the crystal lattice, but the lattice enthalpies are very different.

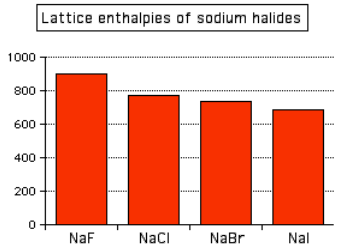


You can see that the lattice enthalpy of magnesium oxide is much greater than that of sodium chloride. That's because in magnesium oxide, 2+ ions are attracting 2- ions; in sodium chloride, the attraction is only between 1+ and 1- ions.

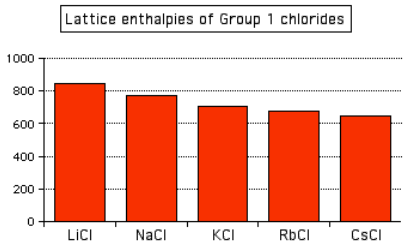
The Radius of the Ions

The lattice enthalpy of magnesium oxide is also increased relative to sodium chloride because magnesium ions are smaller than sodium ions, and oxide ions are smaller than chloride ions. That means that the ions are closer together in the lattice, and that increases the strength of the attractions.

This effect of ion size on lattice enthalpy is clearly observed as you go down a Group in the Periodic Table. For example, as you go down Group 7 of the Periodic Table from fluorine to iodine, you would expect the lattice enthalpies of their sodium salts to fall as the negative ions get bigger - and that is the case:



Attractions are governed by the distances between the centers of the oppositely charged ions, and that distance is obviously greater as the negative ion gets bigger. And you can see exactly the same effect if as you go down Group 1. The next bar chart shows the lattice enthalpies of the Group 1 chlorides.



Calculating Lattice Enthalpy

It is impossible to measure the enthalpy change starting from a solid crystal and converting it into its scattered gaseous ions. It is even more difficult to imagine how you could do the reverse - start with scattered gaseous ions and measure the enthalpy change when these convert to a solid crystal. Instead, lattice enthalpies always have to be calculated, and there are two entirely different ways in which this can be done.

1. You can can use a Hess's Law cycle (in this case called a Born-Haber cycle) involving enthalpy changes which can be measured. Lattice enthalpies calculated in this way are described as experimental values.
2. Or you can do physics-style calculations working out how much energy would be released, for example, when ions considered as point charges come together to make a lattice. These are described as theoretical values. In fact, in this case, what you are actually calculating are properly described as lattice energies.

Born-Haber Cycles

Standard Atomization Enthalpies

Before we start talking about Born-Haber cycles, we need to define the **atomization enthalpy**, ΔH_a^o. The standard atomization enthalpy is the enthalpy change when 1 mole of gaseous atoms is formed from the element in its standard state. Enthalpy change of atomization is always positive. You are always going to have to supply energy to break an element into its separate gaseous atoms. All of the following equations represent changes involving atomization enthalpy:

$$\frac{1}{2}Cl_2(g) \rightarrow Cl(g) \quad \Delta H_a^o = +122\,kJ\,mol^{-1}$$

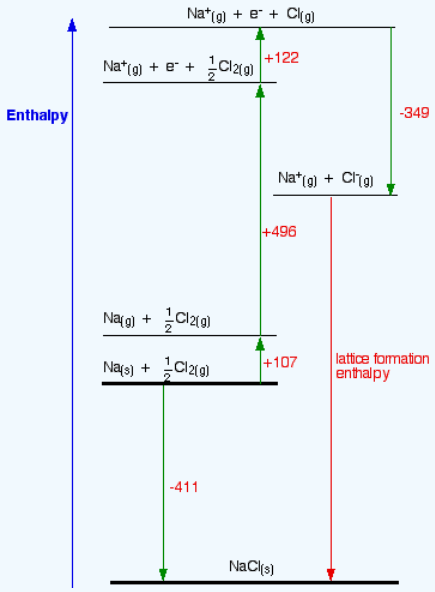
$$\frac{1}{2}Br_2(l) \rightarrow Br(g) \quad \Delta H_a^o = +122\,kJ\,mol^{-1}$$

$$Na(s) \rightarrow Na(g) \quad \Delta H_a^o = +107\,kJ\,mol^{-1}$$

Notice particularly that the "mol^{-1}" is per mole of atoms **formed** - NOT per mole of element that you start with. You will quite commonly have to write fractions into the left-hand side of the equation. Getting this wrong is a common mistake.

Example 2.5.1.1: Born-Haber Cycle for NaCl

Consider a Born-Haber cycle for sodium chloride, and then talk it through carefully afterwards. You will see that I have arbitrarily decided to draw this for lattice formation enthalpy. If you wanted to draw it for lattice dissociation enthalpy, the red arrow would be reversed - pointing upwards.



Focus to start with on the higher of the two thicker horizontal lines. We are starting here with the elements sodium and chlorine in their standard states. Notice that we only need half a mole of chlorine gas in order to end up with 1 mole of NaCl. The arrow pointing down from this to the lower thick line represents the enthalpy change of formation of sodium chloride.

The Born-Haber cycle now imagines this formation of sodium chloride as happening in a whole set of small changes, most of which we know the enthalpy changes for - except, of course, for the lattice enthalpy that we want to calculate.

- The +107 is the atomization enthalpy of sodium. We have to produce gaseous atoms so that we can use the next stage in the cycle.
- The +496 is the first ionization energy of sodium. Remember that first ionization energies go from gaseous atoms to gaseous singly charged positive ions.
- The +122 is the atomization enthalpy of chlorine. Again, we have to produce gaseous atoms so that we can use the next stage in the cycle.
- The -349 is the first electron affinity of chlorine. Remember that first electron affinities go from gaseous atoms to gaseous singly charged negative ions.
- And finally, we have the positive and negative gaseous ions that we can convert into the solid sodium chloride using the lattice formation enthalpy.

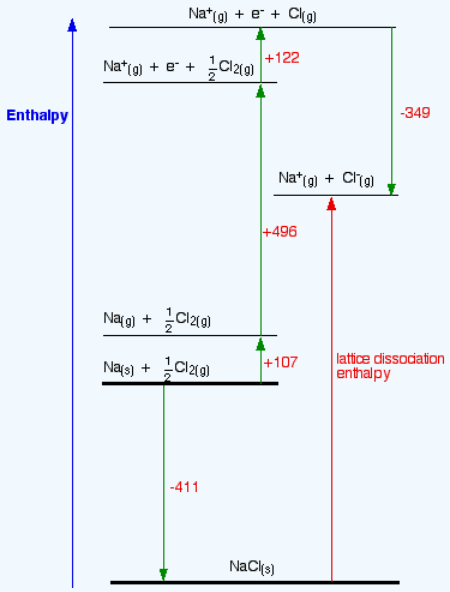
Now we can use Hess' Law and find two different routes around the diagram which we can equate. As drawn, the two routes are obvious. The diagram is set up to provide two different routes between the thick lines. So, from the cycle we get the calculations directly underneath it . . .

$$-411 = +107 + 496 + 122 - 349 + LE$$

$$LE = -411 - 107 - 496 - 122 + 349$$

$$LE = -787 \text{ kJ mol}^{-1}$$

How would this be different if you had drawn a lattice dissociation enthalpy in your diagram? Your diagram would now look like this:



The only difference in the diagram is the direction the lattice enthalpy arrow is pointing. It does, of course, mean that you have to find two new routes. You cannot use the original one, because that would go against the flow of the lattice enthalpy arrow. This time both routes would start from the elements in their standard states, and finish at the gaseous ions.

$$-411 + LE = +107 + 496 + 122 - 349$$

$$LE = +107 + 496 + 122 - 349 + 411$$

$$LE = +787 \text{ kJ mol}^{-1}$$

Once again, the cycle sorts out the sign of the lattice enthalpy.

Theoretical Estimates of Lattice Energies

Let's assume that a compound is fully ionic. Let's also assume that the ions are point charges - in other words that the charge is concentrated at the center of the ion. By doing physics-style calculations, it is possible to calculate a theoretical value for what you would expect the lattice energy to be. Calculations of this sort end up with values of *lattice energy*, and not *lattice enthalpy*. If you know how to do it, you can then fairly easily convert between the two.

There are several different equations, of various degrees of complication, for calculating lattice energy in this way. There are two possibilities:

- There is reasonable agreement between the experimental value (calculated from a Born-Haber cycle) and the theoretical value. Sodium chloride is a case like this - the theoretical and experimental values agree to within a few percent. That means that for sodium chloride, the assumptions about the solid being ionic are fairly good.
- The experimental and theoretical values do not agree. A commonly quoted example of this is silver chloride, AgCl. Depending on where you get your data from, the theoretical value for lattice enthalpy for AgCl is anywhere from about 50 to 150 kJ mol^{-1} less than the value that comes from a Born-Haber cycle. In other words, treating the AgCl as 100% ionic underestimates its lattice enthalpy by quite a lot.

The explanation is that silver chloride actually has a significant amount of covalent bonding between the silver and the chlorine, because there is not enough electronegativity difference between the two to allow for complete transfer of an electron from the silver to the chlorine. Comparing experimental (Born-Haber cycle) and theoretical values for lattice enthalpy is a good way of judging how purely ionic a crystal is.

Example 2.5.1.2: Born-Haber Cycle for $MgCl_2$

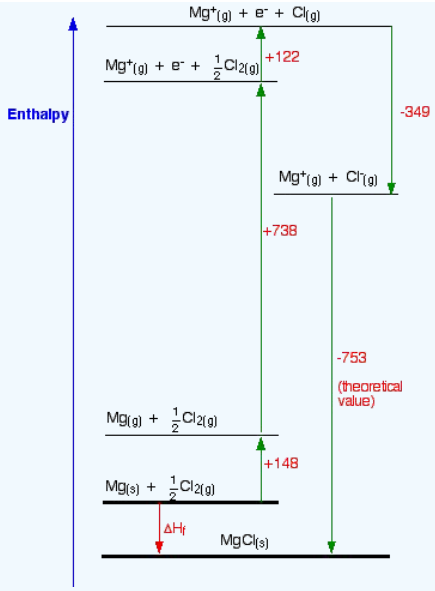
The question arises as to why, from an energetics point of view, magnesium chloride is $MgCl_2$ rather than MgCl or $MgCl_3$ (or any other formula you might like to choose). It turns out that $MgCl_2$ is the formula of the compound which has the most negative enthalpy change of formation - in other words, it is the most stable one relative to the elements magnesium and chlorine.

Let's look at this in terms of Born-Haber cycles of and contrast the enthalpy change of formation for the imaginary compounds MgCl and $MgCl_3$. That means that we will have to use theoretical values of their lattice enthalpies. We ca not use experimental ones, because these compounds obviously do not exist! I'm taking theoretical values for lattice enthalpies for these compounds that I found on the web. I can't confirm these, but all the other values used by that source were accurate. The exact values do not matter too much anyway, because the results are so dramatically clear-cut.

1. The Born-Haber cycle for MgCl

We will start with the compound MgCl, because that cycle is just like the NaCl one we have already looked at.

$$Mg(s) + \frac{1}{2} Cl_2(g) \rightarrow MgCl(s)$$



Find two routes around this without going against the flow of any arrows. That's easy:

$$\Delta H_f = +148 + 738 + 122 - 349 - 753$$

$$\Delta H_f = -94 \text{ kJ mol}^{-1}$$

So the compound MgCl is definitely energetically **more stable** than its elements. I have drawn this cycle very roughly to scale, but that is going to become more and more difficult as we look at the other two possible formulae. So I am going to rewrite it as a table. You can see from the diagram that the enthalpy change of formation can be found just by adding up all the other numbers in the cycle, and we can do this just as well in a table.

	kJ
atomization enthalpy of Mg	+148
1st IE of Mg	+738
atomization enthalpy of Cl	+122
electron affinity of Cl	-349
lattice enthalpy	-753
calculated ΔH_f	-94

2. The Born-Haber cycle for $MgCl_2$

The equation for the enthalpy change of formation this time is

$$\mathrm{Mg\,(s) + Cl_2\,(g) \ \rightarrow MgCl_2\,(s)}$$

So how does that change the numbers in the Born-Haber cycle?

- You need to add in the second ionization energy of magnesium, because you are making a 2+ ion.
- You need to multiply the atomization enthalpy of chlorine by 2, because you need 2 moles of gaseous chlorine atoms.
- You need to multiply the electron affinity of chlorine by 2, because you are making 2 moles of chloride ions.
- You obviously need a different value for lattice enthalpy.

	kJ
atomization enthalpy of Mg	+148
1st IE of Mg	+738
2nd IE of Mg	+1451
atomization enthalpy of Cl (x 2)	+244
electron affinity of Cl (x 2)	-698
lattice enthalpy	-2526
calculated ΔH_f	-643

You can see that much more energy is released when you make $MgCl_2$ than when you make MgCl. Why is that? You need to put in more energy to ionize the magnesium to give a 2+ ion, but a lot more energy is released as lattice enthalpy. That is because there are stronger ionic attractions between 1- ions and 2+ ions than between the 1- and 1+ ions in MgCl. So what about $MgCl_3$? The lattice energy here would be even greater.

3. The Born-Haber cycle for $MgCl_3$

The equation for the enthalpy change of formation this time is

$$\mathrm{Mg\,(s) + \tfrac{3}{2}\,Cl_2\,(g) \rightarrow MgCl_3\,(s)}$$

So how does that change the numbers in the Born-Haber cycle this time?

- You need to add in the third ionization energy of magnesium, because you are making a 3+ ion.
- You need to multiply the atomization enthalpy of chlorine by 3, because you need 3 moles of gaseous chlorine atoms.
- You need to multiply the electron affinity of chlorine by 3, because you are making 3 moles of chloride ions.
- You again need a different value for lattice enthalpy.

	kJ
atomization enthalpy of Mg	+148
1st IE of Mg	+738
2nd IE of Mg	+1451
3rd IE of Mg	+7733
atomization enthalpy of Cl (x 3)	+366
electron affinity of Cl (x 3)	-1047
lattice enthalpy	-5440
calculated ΔH_f	+3949

This time, the compound is hugely energetically unstable, both with respect to its elements, and also to other compounds that could be formed. You would need to supply nearly 4000 kJ to get 1 mole of $MgCl_3$ to form!

Look carefully at the reason for this. The lattice enthalpy is the **highest** for all these possible compounds, but it is not high enough to make up for the very large third ionization energy of magnesium.

Why is the third ionization energy so big? The first two electrons to be removed from magnesium come from the 3s level. The third one comes from the 2p. That is closer to the nucleus, and lacks a layer of screening as well - and so

much more energy is needed to remove it. The 3s electrons are screened from the nucleus by the 1 level and 2 level electrons. The 2p electrons are only screened by the 1 level (plus a bit of help from the 2s electrons).

Conclusion

Magnesium chloride is $MgCl_2$ because this is the combination of magnesium and chlorine which produces the most energetically stable compound - the one with the most negative enthalpy change of formation.

Contributors and Attributions

- Jim Clark (Chemguide.co.uk)

This page titled 2.5.1: Ionic- Measurement of Ionic Bond Strength is shared under a CC BY-NC-SA 4.0 license and was authored, remixed, and/or curated by Jim Clark.

- **Lattice Enthalpies and Born Haber Cycles** by Jim Clark is licensed CC BY-NC 4.0.

SECTION OVERVIEW

2.5.2: Ionic- Examples of Ionic Structures

Topic hierarchy

2.5.2.1: Ionic- Rock Salt

2.5.2.2: Ionic- Caesium Chloride (CsCl)

2.5.2.3: Ionic- Fluorite and Anti-Fluorite

2.5.2.4: Ionic- Zinc Blende (ZnS)

2.5.2: Ionic- Examples of Ionic Structures is shared under a CC BY-NC-SA 4.0 license and was authored, remixed, and/or curated by LibreTexts.

2.5.2.1: Ionic- Rock Salt

Rock salt also known as NaCl is an ionic compound. It occurs naturally as white cubic crystals. The structure of NaCl is formed by repeating the unit cell. It has an organized structure and has a 1:1 ratio of Na:Cl.

Introduction

Rock salt ($\mathbf{NaCl}$) is an ionic compound that occurs naturally as white crystals. It is extracted from the mineral form halite or evaporation of seawater. The structure of NaCl is formed by repeating the face centered cubic unit cell. It has 1:1 stoichiometry ratio of Na:Cl with a molar mass of 58.4 g/mol. Compounds with the sodium chloride structure include alikali halides and metal oxides and transition-metal compounds. An important role to many important applications is structure and dynamics of water. Some applications include crystallization of proteins and conformational behavior of peptides and nucleic acids.

Structure

Figure **2.5.2.1.1** shows how the Na^+ and Cl^- ions occupy the space. The smaller ions are the Na^+ with has an atomic radius of 102 pm, and the larger ions are the Cl^- with an atomic radium of 181 pm. Since NaCl are one to one ratio as a compound, the coordination numbers of Na and Cl are equal. The larger green ions represent Cl^- and the smaller purple ions represent Na^+. However, the structure of this molecule allows their positions to be switched since the coordination numbers are equivalent.

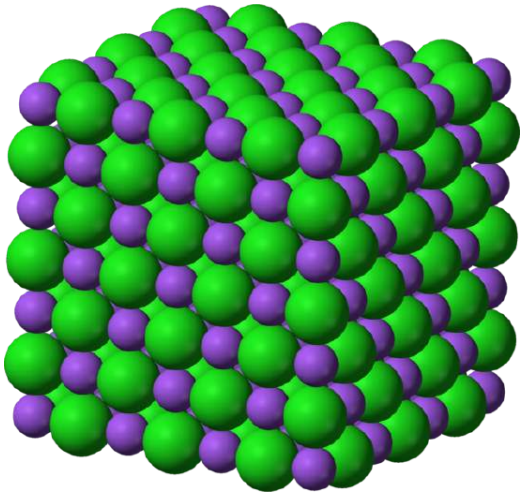


Figure **2.5.2.1.1**: The crystal structure of sodium chloride, $\mathbf{NaCl}$, a typical ionic compound. The smaller purple spheres represent sodium cations, $\mathbf{Na^+}$, and the larger green spheres represent chloride anions, $\mathbf{Cl^-}$. (Public Domain; Benjah-bmm27 via Wikipedia)

A Unit Cell

The unit cell of $\mathbf{NaCl}$ consists of $\mathbf{Na^+}$ ions and $\mathbf{Cl^-}$ ions. There are four types of site: unique central position, face site, edge sites and corner site, which are used to determine the number of Na^+ ions and Cl^- ions in the unit cell of NaCl. When counting the number of ions, a corner site would be shared by 7 other unit cells. Therefore, 1 corner would be 1/8 of an ion. A similar occurrence happens with the face site and the edge sites. For a face site, it is shared by 1 other unit cell and for an edge site, the ion is shared by 3 other unit cells. $\mathbf{NaCl}$ is a face centered cubic unit cell which has four cations and four anions. This can be shown by counting the number of ions and multiplying them in relation to their position.

- $\mathbf{Na^+}$:

$$1_{center} + 12_{edge} \times \frac{1}{4} = 4\,\text{sodium ions total per cell}$$

- $\mathbf{Cl^-}$:

$$4_{face} \times \frac{1}{2} + 8_{corner} \times \frac{1}{8} = 4\,\text{chloride ions total per cell}$$

Each ion in this lattice has six of the other kind of ion as its nearest neighbors, and twelve of the same kind of ions as its second nearest neighbors. There are many ionic compounds that assume this structure including all other halides of Na, Li, K and Rb. CsF, AgF, AgCl, BaO, CoO, and SrS are also among many that will form similar structures to NaCl.

Outside Links

- Video about structure of NaCl: http://www.youtube.com/watch?v=csfOBynrF8E
- Unit Cell. http://www.case.edu/artsci/chem/chim...ids/xtal1.html

References

1. Gao, H.X., L.-M. Peng, and J.M Zuo. "Lattice dynamics and Debye-Waller factors of some compounds with the sodium chloride structure." *Acta Crystallographica: Section A (Wiley-Blackwell)* 55.6 (1999): 1014. *Academic Search Complete*. EBSCO. Web.
2. Housecroft, Catherine E., and Alan G. Sharpe. *Inorganic Chemistry*. 3rd ed. Harlow: Pearson Education, 2008. Print.
3. Jun Soo, Kim, and Yethiraj Arun. "A Diffusive Anomaly of Water in Aqueous Sodium Chloride Solutions at Low Temperatures." *Journal of Physical Chemistry B* 112.6 (2008): 1729-1735. *Academic Search Complete*. EBSCO. Web.

Contributors and Attributions

- Michael Ford

2.5.2.1: Ionic- Rock Salt is shared under a CC BY-NC-SA 4.0 license and was authored, remixed, and/or curated by LibreTexts.

- **6.11A: Structure - Rock Salt (NaCl)** is licensed CC BY-NC-SA 4.0.

2.5.2.2: Ionic- Caesium Chloride (CsCl)

This page is going to discuss the structure of the molecule cesium chloride (**CsCl**), which is a white hydroscopic solid with a mass of 168.36 g/mol. Cesium Chloride is a type of unit cell that is commonly mistaken as Body-Centered Cubic. This misconception is easy to make, since there is a center atom in the unit cell, but CsCl is really a **non-closed packed structure** type.

Introduction

CsCl has a boiling point of 1303 degrees Celsius, a melting point of 646 degrees Celsius, and is very soluble in water. For the most part this molecule is stable, but is not compatible with strong oxidizing agents and strong acids. Although it is not hazardous, one should not prolong their exposure to CsCl. CsCl is an ionic compound that can be prepared by the reaction:

$$\mathrm{Cs_2CO_3 + 2\,HCl \longrightarrow 2\,CsCl + H_2O + CO_2} \qquad (2.5.2.2.1)$$

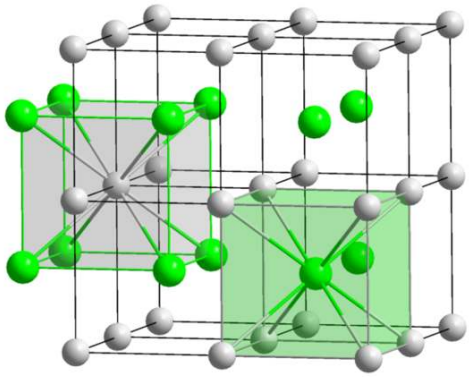


Figure **2.5.2.2.1**: **CsCl** Coordination Cubes. (Public Domain; Solid State via Wikipedia)

CsCl crystallize in a primitive cubic lattice which means the cubic unit cell has nodes only at its corners. The structure of CsCl can be seen as two interpenetrating cubes, one of Cs^+ and one of Cl^-. The ions are not touching one another. Touching would cause repulsion between the anion and cation. Some may mistake the structure type of CsCl with NaCl, but really the two are different. CsCl is more stable than NaCl, for it produces a more stable crystal and more energy is released.

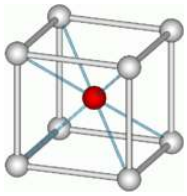


Figure **2.5.2.2.2**: Unit Cell of CsCl (en.Wikipedia.org/wiki/Caesium_chloride

Anions and cations have similar sizes. Each Cs^+ is surrounded by 8 Cl^- at the corners of its cube and each Cl^- is also surrounded by 8 Cs^+ at the corners of its cube. The cations are located at the center of the anions cube and the anions are located at the center of the cations cube. There is one atom in CsCl. To determine this, the following equation is given:

8 Corners of a given atom x 1/8 of the given atom's unit cell = 1 atom

Applications

Cesium chloride is used in centrifugation, a process that uses the centrifugal force to separate mixtures based on their molecular density. It is also used in the preparation of electrically conducting glasses. Radioactive CsCl is used in some types of radiation therapy for cancer patients, although it is blamed for some deaths.

References

1. Carter, C. Barry., and M. Grant. Norton. "Binary Compounds." *Ceramic Materials Science and Engineering*. New York, NY: Springer, 2007. pg87-88
2. Quéré, Yves. "Stable Structure of Halides." *Physics of Materials*. Amsterdam: Gordon and Breach Science, 1998.

Contributors and Attributions

- Ana Popovich

2.5.2.2: Ionic- Caesium Chloride (CsCl) is shared under a not declared license and was authored, remixed, and/or curated by LibreTexts.

- **6.11B: Structure - Caesium Chloride (CsCl)** is licensed CC BY-NC-SA 4.0.

2.5.2.3: Ionic- Fluorite and Anti-Fluorite

Fluorite

Calcium Fluoride is a solid and forms a cube like structure that is centralized around the calcium molecules. The crystal lattice structure that Calcium Fluoride is also known as the fluorite structure (Figure **2.5.2.3.1**) where the Ca^{2+} ions are eight-coordinate, being centered in a cube of eight F^- ions. Each F^- is coordinated to four Ca^{2+} in the shape of a tetrahedron.

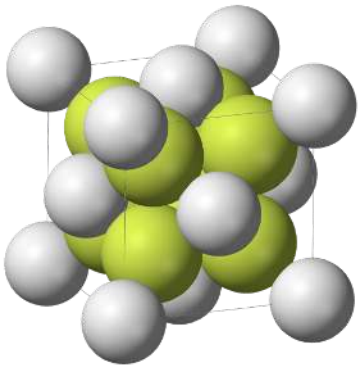


Figure **2.5.2.3.1**: Fluorite unit cell. (Public Domain; Benjah-bmm27 via Wikipedia)

When Calcium Fluoride is in a single molecule it forms a Quasilinear structure. Quasilinear means the molecule resonates between a linear shape and a bent shape.Calcium Fluoride is a polyatomic molecule that contains one calcium molecule and two fluoride molecules. Calcium Fluoride is a quasilinear molecule the bonds are created from the single electrons of calcium and the single electron from fluoride. $\mathbf{CaF_2}$ has its electrons contained with in the 3d orbitals and are able to move between d_{yz} and d_z^2 squared. The molecule in linear when they are in the d_z^2 orbitals the molecule is also the most stable in this shape. When the electrons are in the d_{yz} orbitals the molecule becomes bent. The molecule resonates between these two shapes making it quasilinear.

Antifluorite

Antifluorite is a mineral with a crystal structure identical with that of fluorite but with the positions of the cations and anions reversed (Figure **2.5.2.3.2**).

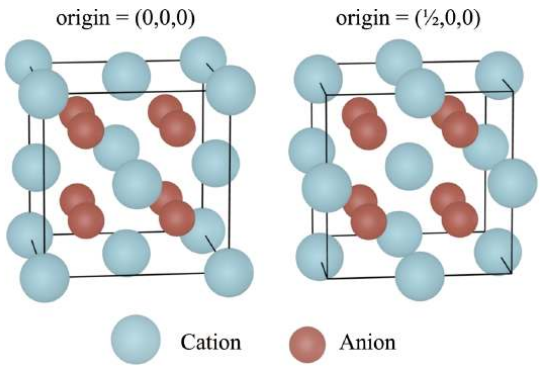


Figure **2.5.2.3.2**: Unit cell of the fluorite structure, from two equivalent perspectives. In the antifluorite structure, the blue positions are taken by the anion, the red positions by the cation. (CC BY-SA 4.0; Paburr via source)

The same crystal structure is found in numerous ionic compounds with formula AB2, such as ceria (CeO2), zirconia (cubic ZrO2), uranium dioxide (UO2). In the corresponding anti-structure, called the antifluorite structure, anions and cations are swapped, such as beryllium carbide (Be2C) or lithium oxide (Li2O), potassium sulfate (K2SO4).

Contributors and Attributions

- en.Wikipedia.org/wiki/Anti-structure

2.5.2.3: Ionic- Fluorite and Anti-Fluorite is shared under a CC BY-NC-SA 4.0 license and was authored, remixed, and/or curated by LibreTexts.

- 6.11C: Structure - Fluorite (CaF2) is licensed CC BY-NC-SA 4.0.
- 6.11D: Structure - Antifluorite is licensed CC BY-NC-SA 4.0.

2.5.2.4: Ionic- Zinc Blende (ZnS)

ZnS has a unique structure type compared to other molecules, having different types of unique structures. ZnS can have a zinc blende structure which is a "diamond-type network" and at a different temperature, ZnS can become the wurtzite structure type which has a hexagonal type symmetry. Structure-wise, the zinc blende structure is more thermodynamically favored, however, because of the wurtzite structures slow construction, both forms of ZnS can be found.

Summary: Zinc blend is a compound that comes in two forms: sphalerite and wurtzite. These are characterized by a 1:1 stoichiometric ratio of Zinc to Sulfur. It maintains a tetrahedral arrangement in both forms.

Introduction

Zinc sulfide (ZnS) is a unique compound that forms two types of crystalline structures. These two polymorphs are wurtzite and zincblende (also known as sphalerite). Wurtzite has a hexagonal structure, while zincblende is cubic. It is characterized by single bonds between each atom and maintenance of a 1:1 zinc to sulfur ratio.

sphalerite:

Site	Zn	S
Central	4	0
Face	0	6(1/2) = 3
Corner	0	8(1/8) = 1
Total	4	4

Since the number of atoms in a single unit cell of Zn and S is the same, it is consistent with the formula ZnS.

The ionic radius for Zn^{2+} is 74pm and for S^{2-} is 190pm. Therefore the ratio between cationic and anionic radii in zinc blend is 0.39 (74pm/190 pm) .This suggests a tetrahedral ion arrangement and four nearest neighbors from standard crystal structure prediction tables. Therefore, four sulfur atoms surround each zinc atom and four zinc atoms surround each sulfur atom.$_2$ The coordination number, the number of of electron pairs donated to a metal by its ligands, for both zinc an sulfur is four.[1,2] The difference between wurtzite and zincblende lies in the different arrangements of layers of ions.[2]

Zincblende (Sphalerite)

Zincblende is characterized as a **cubic closet packing** (ccp), also known as face-centered cubic, structure.[1,4] This crystal lattice structure is shown in Figures 1 & 2 below.

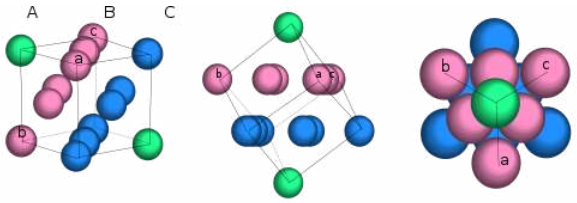


Fig. 1. A break down of cubic closest packing. (Author: Maghémite Date: May 5, 2008. Licensed under the Creative Commons Attribution-Share Alike 3.0 Unported, 2.5 Generic, 2.0 Generic and 1.0 Generic license.)

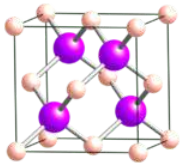


Fig. 2. A representation of ccp structure. (from Public Domain)

Notice how only half of the tetrahedral sites are occupied.

Thermal stability

Density tends to decrease as temperature increases. In this case, since ccp structures are more dense than hcp structures, so a conversion from sphalerite to wurtzite occurs naturally over time at a rate similar to that of diamond to graphite. The sphalerite structure is favored at 298k by 13kJ/mol, but at 1296K the transition to wurtzite occurs.[3]

Wurtzite

Wurtzite has a hexagonal closest packing structure (hcp), which is characterized by 12 ions in the corners of each unit that create a hexagonal prism (seen in Fig. 3).[2] As discussed previously, zincblende slowly transforms to wurtzite due to thermodynamic stability.

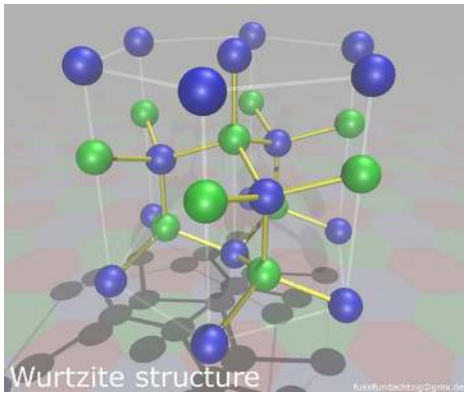


Fig 3. HCP structure of wurtzite. (Creator: Alexander Mann Date: 01/14/2006 Licensed under the Creative Commons Attribution-Share Alike 2.0 Germany license)

Calculating density of a crystal structure

Density = Mass of unit cell / volume of unit cell.

where:

Mass of unit cell = Number of atoms in a unit cell x the mass of each atom

volume of unit cell = $a^3 \times 10^{-30}$

Contributors and Attributions

- Emma Mele, UC Davis Animal Biology

2.5.2.4: Ionic- Zinc Blende (ZnS) is shared under a CC BY-NC-SA 4.0 license and was authored, remixed, and/or curated by LibreTexts.

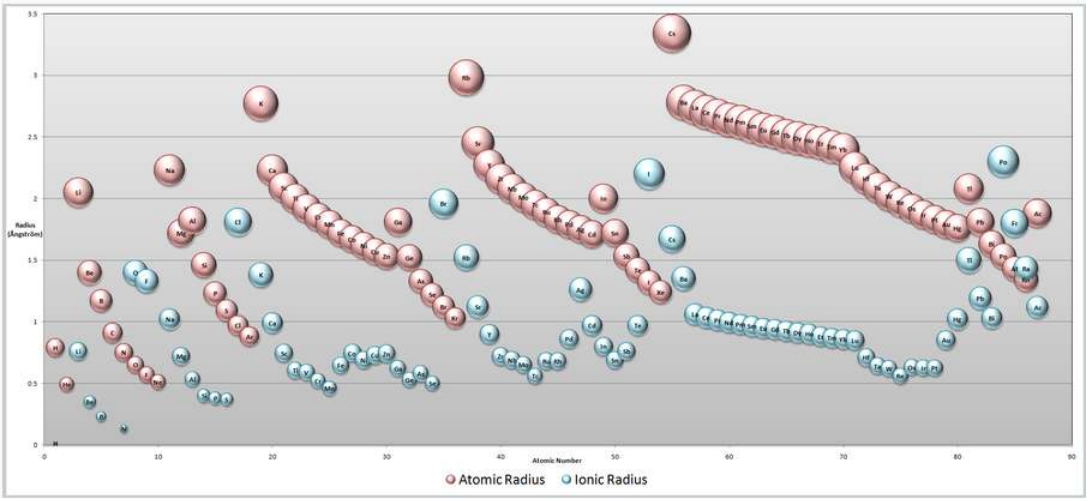
- **6.11E: Structure - Zinc Blende (ZnS)** is licensed CC BY-NC-SA 4.0.

2.5.3: Predicting Ionic Structure Type

Atoms in crystals are held together by electrostatic forces, van der Waals interactions, and covalent bonding. It follows that arrangements of atoms that can maximize the strength of these attractive interactions should be most favorable and lead to the most commonly observed crystal structures.

Radius ratio rules

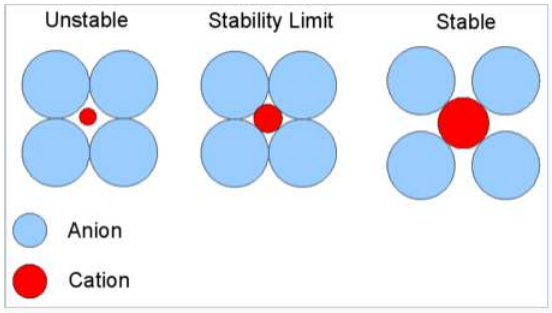
Early crystallographers had trouble solving the structures of inorganic solids using X-ray diffraction because some of the mathematical tools for analyzing the data had not yet been developed. Once a trial structure was proposed, it was relatively easy to calculate the diffraction pattern, but it was difficult to go the other way (from the diffraction pattern to the structure) if nothing was known *a priori* about the arrangement of atoms in the unit cell. It was (and still is!) important to develop some guidelines for guessing the coordination numbers and bonding geometries of atoms in crystals. The first such rules were proposed by Linus Pauling, who considered how one might pack together oppositely charged spheres of different radii. Pauling proposed from geometric considerations that the quality of the "fit" depended on the **radius ratio** of the anion and the cation.



Atomic and Ionic Radii. Note that cations are always smaller than the neutral atom (pink) of the same element, whereas anions are larger. Going from left to right across any row of the periodic table, neutral atoms and cations contract in size because of increasing nuclear charge. (click for larger image)

The basic idea of radius ratio rules is illustrated at the right. We consider that the anion is the packing atom in the crystal and the smaller cation fills interstitial sites ("holes"). Cations will find arrangements in which they can contact the largest number of anions. If the cation can touch all of its nearest neighbor anions, as shown at the right for a small cation in contact with larger anions, then the fit is good. If the cation is too small for a given site, that coordination number will be unstable and it will prefer a

lower coordination structure. The table below gives the ranges of cation/anion radius ratios that give the best fit for a given coordination geometry.



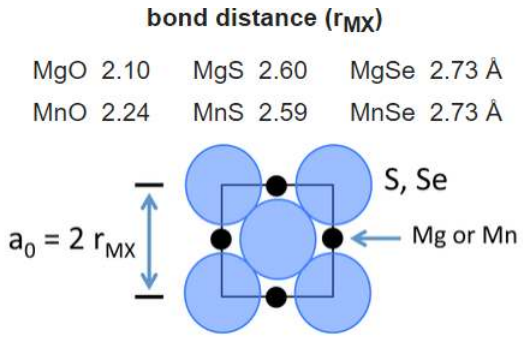
Critical Radius Ratio. This diagram is for coordination number six: 4 anions in the plane are shown, 1 is above the plane and 1 is below. The stability limit is at $r_C/r_A = 0.414$

Coordination number	Geometry	$\rho = r_{cation}/r_{anion}$
2	linear	0 - 0.155
3	triangular	0.155 - 0.225
4	tetrahedral	0.225 - 0.414
4	square planar	0.414 - 0.732
6	octahedral	0.414 - 0.732
8	cubic	0.732 - 1.0
12	cuboctahedral	1.0

There are unfortunately several challenges with using this idea to predict crystal structures:

- We don't know the radii of individual ions
- Atoms in crystals are not really ions - there is a varying degree of covalency depending electronegativity differences
- Bond distances (and therefore ionic radii) depend on bond strength and coordination number (remember Pauling's rule D(n) = D(1) - 0.6 log n)
- Ionic radii depend on oxidation state (higher charge => smaller cation size, larger anion size)

We can build up a table of ionic radii by assuming that the bond length is the sum of the radii ($r_+ + r_-$) if the ions are in contact in the crystal. Consider for example the compounds MgX and MnX, where X = O, S, Se. All of these compounds crystallize in the NaCl structure:



For the two larger anions (S^{2-} and Se^{2-}), the unit cell dimensions are the same for both cations. This suggests that the anions are in contact in these structures. From geometric considerations, the anion radius in this case is given by:

Extra close brace or missing open brace

and thus the radii of the S^{2-} and Se^{2-} ions are 1.84 and 1.93 Å, respectively. Once the sizes of these anions are fixed, we can obtain a self-consistent set of cation and anion radii from the lattice constants of many MX compounds.

How well does this model work? Let's consider the structures of tetravalent metal oxides (MO_2), using Pauling radii and the predictions of the radius ratio model:

Oxide MO_2	Radius ratio	Predicted coord. no.	Observed coord no. (structure)
CO_2	~0.1	2	2 (linear molecule)
SiO_2	0.32	4	4 (various tetrahedral structures)
GeO_2	0.43	4	4 (silica-like structures)
"	0.54	6	6 (rutile)
TiO_2	0.59	6	6 (rutile)
ZrO_2	0.68	6	7 (baddleyite)
"	0.77	8	8 (fluorite)
ThO_2	0.95	8	8 (fluorite)

Note that cations have different radii depending on their coordination numbers, and thus different radius ratios are calculated for Ge^{4+} with coordination numbers 4 and 6, and for Zr^{4+} with coordination numbers 6 and 8.

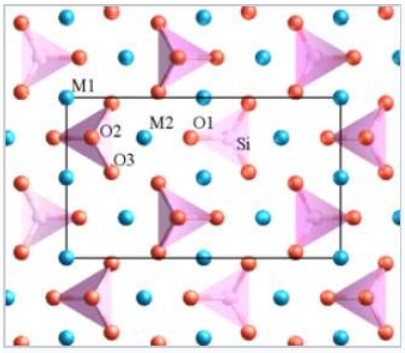
For this series of oxides, the model appears to work quite well. The correct coordination number is predicted in all cases, and borderline cases such as GeO_2 and ZrO_2 are found in structures with different coordination numbers. The model also correctly predicts the structures of BeF_2 (SiO_2 type), MgF_2 (rutile), and CaF_2 (fluorite).

What about the alkali halides NaCl, KBr, LiI, CsF, etc.? All of them have the NaCl structure except for CsCl, CsBr, and CsI, which have the CsCl (8-8) structure. In this case the radius ratio model fails rather badly. The Li^+ salts LiBr and LiI are predicted to have tetrahedral structures, and KF is predicted to have an 8-8 structure like CsCl. We can try adjusting the radii (e.g., making the cations larger and anions smaller), but the best we can do with the alkali halides is predict about half of their structures correctly. Since the alkali halides are clearly ionic compounds, this failure suggests that there is something very wrong with the radius ratio model, and its success with MO_2 compounds was coincidental.

In addition to the radius ratio rule, Linus Pauling developed other useful rules that are helpful in rationalizing and also predicting the structures of inorganic compounds. Pauling's rules[1] state that:

- Stable structures are **locally electroneutral**. For example, in the structure of the double perovskite Sr_2FeMoO_6, MO_6 (M = Fe^{2+}, Mo^{6+}) octahedra share all their vertices, and Sr^{2+} ions fill the cubooctahedral cavities that are flanked by eight MO_6 octahedra.[2] Each O^{2-} ion is coordinated to one Fe^{2+} and one Mo^{6+} ion in order to achieve local electroneutrality, and thus the FeO_6 and MoO_6 octahedra alternate in the structure.
- **Cation-cation repulsion** should be minimized. Anion polyhedra can share vertices (as in the perovskite structure) without any energetic penalty. Shared polyhedral edges, and especially shared faces, cause cation-cation repulsion and should be avoided. For example, in rutile, the most stable polymorph of TiO_2, the TiO_6 octahedra share vertices and two opposite edges, forming ribbons in the structure. In anatase TiO_2, each octahedron shares four edges so the anatase polymorph is less thermodynamically stable.

- **Highly charged cations** in anion polyhedra tend not to share edges or even vertices, especially when the coordination number is low. For example, in orthosilicates such as olivine (M_2SiO_4), there are isolated SiO_4^{4-} tetrahedra.



Structure of olivine. M (Mg or Fe) = blue spheres, Si = pink tetrahedra, O = red spheres.

As we will soon see, all of Pauling's rules are justified on the basis of lattice energy considerations. In ionic compounds, the arrangement of atoms that maximizes anion-cation interactions while minimizing cation-cation and anion-anion contacts is energetically the best.

This page titled 2.5.3: Predicting Ionic Structure Type is shared under a CC BY-NC-SA 4.0 license and was authored, remixed, and/or curated by Chemistry 310 (Wikibook) via source content that was edited to the style and standards of the LibreTexts platform.

- **9.1: Ionic Radii and Radius Ratios** by Chemistry 310 is licensed CC BY-SA 4.0. Original source: https://en.wikibooks.org/wiki/Introduction_to_Inorganic_Chemistry.

CHAPTER OVERVIEW

3: Oxidation and Reduction of Elements

3.1: Redox Reactions
3.2: Balancing Redox Reactions
3.3: Electrochemical Cells
3.4: Standard Reduction Potentials
3.5: Thermodynamic Considerations
3.6: General Trends in Reactivity
3.7: Latimer Diagrams
3.8: Frost Diagrams
3.9: Pourbaix Diagrams
3.10: Corrosion

3: Oxidation and Reduction of Elements is shared under a not declared license and was authored, remixed, and/or curated by LibreTexts.

3.1: Redox Reactions

Skills to Develop

- To identify a chemical reaction as an oxidation-reduction reaction.

When zinc metal is submerged into a quantity of aqueous HCl, the following reaction occurs (Figure 3.1.1):

$$\mathrm{Zn\,(s) + 2\,HCl\,(aq) \longrightarrow H_2\,(g) + ZnCl\ 2\,(aq)} \tag{3.1.1}$$

This is one example of what is sometimes called a *single replacement reaction* because Zn replaces H in combination with Cl.



Figure* 3.1.1*: *Zinc Metal plus Hydrochloric Acid. It is fairly obvious that zinc metal reacts with aqueous hydrochloric acid! The bubbles are hydrogen gas.*

Because some of the substances in this reaction are aqueous, we can separate them into ions:

$$\mathrm{Zn\,(s) + 2\,H^+\,(aq) + 2\,Cl^-\,(aq) \longrightarrow H_2\,(g) + Zn^{2+}\,(aq) + 2\,Cl^-\,(aq)} \tag{3.1.2}$$

Viewed this way, the net reaction seems to be a charge transfer between zinc and hydrogen atoms. (There is no net change experienced by the chloride ion.) In fact, electrons are being transferred from the zinc atoms to the hydrogen atoms (which ultimately make a molecule of diatomic hydrogen), changing the charges on both elements.

To understand electron-transfer reactions like the one between zinc metal and hydrogen ions, chemists separate them into two parts: one part focuses on the loss of electrons, and one part focuses on the gain of electrons. The loss of electrons is called oxidation. The gain of electrons is called reduction. Because any loss of electrons by one substance must be accompanied by a gain in electrons by something else, oxidation and reduction always occur together. As such, electron-transfer reactions are also called oxidation-reduction reactions, or simply **redox reactions**. The atom that loses electrons is **oxidized**, and the atom that gains electrons is **reduced**. Also, because we can think of the species being oxidized as causing the reduction, the species being oxidized is called the reducing agent, and the species being reduced is called the oxidizing agent.

> *Because batteries are used as sources of electricity (that is, of electrons), all batteries are based on redox reactions.*

Although the two reactions occur together, it can be helpful to write the oxidation and reduction reactions separately as half reactions. In half reactions, we include only the reactant being oxidized or reduced, the corresponding product species, any other species needed to balance the half reaction, and the electrons being transferred. Electrons that are lost are written as products; electrons that are gained are written as reactants. For example, in our earlier equation, now written without the chloride ions,

$$\mathrm{Zn\,(s) + 2\,H^+\,(aq) \longrightarrow Zn^{2+}\,(aq) + H_2\,(g)} \tag{3.1.3}$$

zinc atoms are oxidized to Zn^{2+}. The half reaction for the oxidation reaction, omitting phase labels, is as follows:

$$\mathrm{Zn \longrightarrow Zn^{2+} + 2\,e^-} \tag{3.1.4}$$

This half reaction is balanced in terms of the number of zinc atoms, and it also shows the two electrons that are needed as products to account for the zinc atom losing two negative charges to become a 2+ ion. With half reactions, there is one more item to balance:

the overall charge on each side of the reaction. If you check each side of this reaction, you will note that both sides have a zero net charge.

Hydrogen is reduced in the reaction. The balanced reduction half reaction is as follows:

$$2\,H^+ + 2\,e^- \longrightarrow H_2 \tag{3.1.5}$$

There are two hydrogen atoms on each side, and the two electrons written as reactants serve to neutralize the 2+ charge on the reactant hydrogen ions. Again, the overall charge on both sides is zero.

The overall reaction is simply the combination of the two half reactions and is shown by adding them together.

$$\begin{aligned} &Zn \rightarrow Zn^{2+} + \cancel{2e^-} \\ &\cancel{2H^+ + 2e^-} \rightarrow H_2 \\ \hline &Zn + 2H^+ \rightarrow Zn^{2+} + H_2 \end{aligned}$$

Because we have two electrons on each side of the equation, they can be canceled. This is the key criterion for a balanced redox reaction: the electrons have to cancel exactly. If we check the charge on both sides of the equation, we see they are the same—2+. (In reality, this positive charge is balanced by the negative charges of the chloride ions, which are not included in this reaction because chlorine does not participate in the charge transfer.)

Redox reactions are often balanced by balancing each individual half reaction and then combining the two balanced half reactions. Sometimes a half reaction must have all of its coefficients multiplied by some integer for all the electrons to cancel. The following example demonstrates this process.

Example 3.1.1: Reducing Silver Ions

Write and balance the redox reaction that has silver ions and aluminum metal as reactants and silver metal and aluminum ions as products.

SOLUTION

We start by using symbols of the elements and ions to represent the reaction:

$$Ag^+ + Al \longrightarrow Ag + Al^{3+} \tag{3.1.6}$$

The equation looks balanced as it is written. However, when we compare the overall charges on each side of the equation, we find a charge of +1 on the left but a charge of +3 on the right. This equation is not properly balanced. To balance it, let us write the two half reactions. Silver ions are reduced, and it takes one electron to change Ag^+ to Ag:

$$Ag^+ + e^- \longrightarrow Ag \tag{3.1.7}$$

Aluminum is oxidized, losing three electrons to change from Al to Al^{3+}:

$$Al \longrightarrow Al^{3+} + 3\,e^- \tag{3.1.8}$$

To combine these two half reactions and cancel out all the electrons, we need to multiply the silver reduction reaction by 3:

$$\begin{aligned} &3\left(Ag^+ + e^- \rightarrow Ag\right) \\ &Al \rightarrow Al^{3+} + 3e^- \\ \hline &3Ag^+ + Al \rightarrow 3Ag + Al^{3+} \end{aligned}$$

Now the equation is balanced, not only in terms of elements but also in terms of charge.

Exercise 3.1.1

Write and balance the redox reaction that has calcium ions and potassium metal as reactants and calcium metal and potassium ions as products.

> *Potassium has been used as a reducing agent to obtain various metals in their elemental form.*

To Your Health: Redox Reactions and Pacemaker Batteries

All batteries use redox reactions to supply electricity because electricity is basically a stream of electrons being transferred from one substance to another. Pacemakers—surgically implanted devices for regulating a person's heartbeat—are powered by tiny batteries, so the proper operation of a pacemaker depends on a redox reaction.

Pacemakers used to be powered by NiCad batteries, in which nickel and cadmium (hence the name of the battery) react with water according to this redox reaction:

$$\mathrm{Cd\,(s) + 2\,NiOOH\,(s) + 2\,H_2O(\ell) \longrightarrow Cd(OH)_2\,(s) + 2\,Ni(OH)\ 2\,(s)} \tag{3.1.9}$$

The cadmium is oxidized, while the nickel atoms in NiOOH are reduced. Except for the water, all the substances in this reaction are solids, allowing NiCad batteries to be recharged hundreds of times before they stop operating. Unfortunately, NiCad batteries are fairly heavy batteries to be carrying around in a pacemaker. Today, the lighter lithium/iodine battery is used instead. The iodine is dissolved in a solid polymer support, and the overall redox reaction is as follows:

$$\mathrm{2\,Li\,(s) + I_2\,(s) \longrightarrow 2\,LiI\,(s)} \tag{3.1.10}$$

Lithium is oxidized, and iodine is reduced. Although the lithium/iodine battery cannot be recharged, one of its advantages is that it lasts up to 10 years. Thus, a person with a pacemaker does not have to worry about periodic recharging; about once per decade a person requires minor surgery to replace the pacemaker/battery unit. Lithium/iodine batteries are also used to power calculators and watches.



***Figure* 3.1.1**: *A small button battery like this is used to power a watch, pacemaker, or calculator. Image used with permission from Gerhard H Wrodnigg (via Wikipedia)*

Oxidation and reduction can also be defined in terms of changes in composition. The original meaning of oxidation was "adding oxygen," so when oxygen is added to a molecule, the molecule is being oxidized. The reverse is true for reduction: if a molecule loses oxygen atoms, the molecule is being reduced. For example, the acetaldehyde ($CH3CHO$) molecule takes on an oxygen atom to become acetic acid ($\mathrm{CH_3COOH}$).

$$\mathrm{2\,CH_3CHO + O_2 \longrightarrow 2\,CH_3COOH} \tag{3.1.11}$$

Thus, acetaldehyde is being oxidized.

Similarly, oxidation and reduction can be defined in terms of the gain or loss of hydrogen atoms. If a molecule adds hydrogen atoms, it is being reduced. If a molecule loses hydrogen atoms, the molecule is being oxidized. For example, in the conversion of acetaldehyde into ethanol ($\mathbf{CH_3CH_2OH}$), hydrogen atoms are added to acetaldehyde, so the acetaldehyde is being reduced:

$$\mathbf{CH_3CHO + H_2 \longrightarrow CH_3CH_2OH} \tag{3.1.12}$$

Example 3.1.2

In each conversion, indicate whether oxidation or reduction is occurring.

a. $N_2 \rightarrow NH_3$
b. $CH_3CH_2OHCH_3 \rightarrow CH_3COCH_3$
c. $HCHO \rightarrow HCOOH$

SOLUTION

a. Hydrogen is being added to the original reactant molecule, so reduction is occurring.
b. Hydrogen is being removed from the original reactant molecule, so oxidation is occurring.
c. Oxygen is being added to the original reactant molecule, so oxidation is occurring.

Exercise 3.1.2

In each conversion, indicate whether oxidation or reduction is occurring.

a. $CH_4 \rightarrow CO_2 + H_2O$
b. $NO_2 \rightarrow N_2$
c. $CH_2{=}CH_2 \rightarrow CH_3CH_3$

Summary

Chemical reactions in which electrons are transferred are called oxidation-reduction, or redox, reactions. Oxidation is the loss of electrons. Reduction is the gain of electrons. Oxidation and reduction always occur together, even though they can be written as separate chemical equations.

Concept Review Exercises

1. Give two different definitions for oxidation and reduction.
2. Give an example of each definition of oxidation and reduction.

Answers

1. Oxidation is the loss of electrons or the addition of oxygen; reduction is the gain of electrons or the addition of hydrogen.
2. $Zn \rightarrow Zn^{2+} + 2e^-$ (oxidation); $C_2H_4 + H_2 \rightarrow C_2H_6$ (reduction) (answers will vary)

Exercises

1. Which reactions are redox reactions? For those that are redox reactions, identify the oxidizing and reducing agents.
   a. $NaOH + HCl \rightarrow H_2O + NaCl$
   b. $3Mg + 2AlCl_3 \rightarrow 2Al + 3MgCl_2$
   c. $H_2O_2 + H_2 \rightarrow 2H_2O$
   d. $KCl + AgNO_3 \rightarrow AgCl + KNO_3$
2. Which reactions are redox reactions? For those that are redox reactions, identify the oxidizing and reducing agents.
   a. $3Cu + 8HNO_3 \rightarrow 3Cu(NO_3)_2 + 2NO + 4H_2O$
   b. $2C_2H_6 + 7O_2 \rightarrow 4CO_2 + 6H_2O$
   c. $2NaHCO_3 \rightarrow Na_2CO_3 + CO_2 + H_2O$
   d. $2K + 2H_2O \rightarrow 2KOH + H_2$

3. Balance each redox reaction by writing appropriate half reactions and combining them to cancel the electrons.

   a. $Ca(s) + H^+(aq) \rightarrow Ca^{2+}(aq) + H_2(g)$
   b. $I^-(aq) + Br_2(\ell) \rightarrow Br^-(aq) + I_2(s)$

4. Balance each redox reaction by writing appropriate half reactions and combining them to cancel the electrons.

   a. $Fe(s) + Sn^{4+}(aq) \rightarrow Fe^{3+}(aq) + Sn^{2+}(aq)$
   b. $Pb(s) + Pb^{4+}(aq) \rightarrow Pb^{2+}(aq)$ (Hint: both half reactions will start with the same reactant.)

Answers

1. a. no
   b. yes; oxidizing agent: $AlCl_3$; reducing agent: Mg
   c. yes; oxidizing agent: H_2O_2; reducing agent: H_2
   d. no

3. a. $Ca \rightarrow Ca^{2+} + 2e^-$

   $2H^+ + 2e^- \rightarrow H_2$

   Combined: $Ca + 2H^+ \rightarrow Ca^{2+} + H_2$

   b. $Br_2 + 2e^- \rightarrow 2Br^-$

   $2I^- \rightarrow I_2 + 2e^-$

   Combined: $Br_2 + 2I^- \rightarrow 2Br^- + I_2$

3.1: Redox Reactions is shared under a CC BY-NC-SA 4.0 license and was authored, remixed, and/or curated by LibreTexts.

3.2: Balancing Redox Reactions

In studying redox chemistry, it is important to begin by learning to balance electrochemical reactions. Simple redox reactions (for example, $H_2 + I_2 \rightarrow 2\ HI$) can be balanced by inspection, but for more complex reactions it is helpful to have a foolproof, systematic method. The **ion-electron method** allows one to balance redox reactions regardless of their complexity. We illustrate this method with two examples.

Example 1:
I^- is oxidized to **IO_3^-** by **MnO_4^-**, which is reduced to **Mn^{2+}**.

How can this reaction be balanced? In the ion-electron method we follow a series of four steps:

Step 1A: Write out the (unbalanced) reaction and identify the elements that are undergoing redox.

$\mathbf{Mn}O_4^- + \mathbf{I}^- \rightarrow \mathbf{I}O_3^- + \mathbf{Mn}^{2+}$ (The elements undergoing redox are **Mn** and **I**)

Step 1B: Separate the reaction into two **half reactions**, balancing the element undergoing redox in each.

$\mathbf{Mn}O_4^- \rightarrow \mathbf{Mn}^{2+}$
$\mathbf{I}^- \rightarrow \mathbf{I}O_3^-$

Step 2A: Balance the **oxygen** atoms by adding water to one side of each half reaction.

$Mn\mathbf{O_4}^- \rightarrow Mn^{2+} + \mathbf{4}H_2\mathbf{O}$
$\mathbf{3}H_2\mathbf{O} + I^- \rightarrow I\mathbf{O_3}^-$

Step 2B: Balance the **hydrogen** atoms by adding H^+ ions.

$\mathbf{8H^+} + MnO_4^- \rightarrow Mn^{2+} + \mathbf{4H_2}O$

The left side has a net charge of **+7** and the right side has a net charge of **+2**

$\mathbf{3H_2}O + I^- \rightarrow IO_3^- + \mathbf{6H^+}$

The left side has a net charge of **-1** and the right side has a net charge of **+5**

Step 2C: Balance the overall charge by adding **electrons**

$8H^+ + \mathbf{5e}^- + MnO_4^- \rightarrow Mn^{2+} + 4H_2O$

The left side has a charge of **+2** while the right side has a charge of **+2**. They are balanced.

$3H_2O + I^- \rightarrow IO_3^- + 6H^+ + \mathbf{6e}^-$

The left side has a charge of **-1** while the right side has a charge of **-1**. They are balanced.
Note: We did not need to explicitly determine the oxidation states of Mn or I to arrive at the correct number of electrons in each half reaction.

Step 3: Combine the half reactions so that there are equal numbers of electrons on the left and right sides

6 $(8H^+ + \mathbf{5e}^- + MnO_4^- \rightarrow Mn^{2+} + 4H_2O)$
5 $(3H_2O + I^- \rightarrow IO_3^- + 6H^+ + \mathbf{6e}^-)$

$48H^+ + \mathbf{30e}^- + 15H_2O + 6MnO_4^- + 5I^- \rightarrow 5IO_3^- + 6Mn^{2+} + 24H_2O + \mathbf{30e}^- + 30H^+$
Cancel the **H^+**, **electrons**, and **water**:
~~$48H^+$~~ + ~~$30e^-$~~ + ~~$15H_2O$~~ + $6MnO_4^- + 5I^- \rightarrow 5IO_3^- + 6Mn^{2+}$ + ~~$24H_2O$~~ + ~~$30e^-$~~ + ~~$30H^+$~~

The overall balanced reaction is therefore:
$\mathbf{18H^+ + 6MnO_4^- + 5I^- \rightarrow 5IO_3^- + 6Mn^{2+} + 9H_2O}$

Check your work by making sure that all **elements** and **charges** are balanced.

Step 4: If the reaction occurs under basic conditions, we add OH^- to each side to cancel H^+
$\mathbf{18H^+} + \mathbf{18OH^-} + 6MnO_4^- + 5I^- \rightarrow 5IO_3^- + 6Mn^{2+} + \mathbf{9H_2O} + \mathbf{18OH^-}$

The $\mathbf{18H^+} + \mathbf{18OH^-}$ will become $\mathbf{18H_2O}$ so the overall balanced reaction is:

$\mathbf{9H_2O + 6MnO_4^- + 5I^- \rightarrow 5IO_3^- + 6Mn^{2+} + 18OH^-}$

Again, it is a good idea to check and make sure that all of the elements are balanced, and that the charge is the same on both sides. If this is not the case, you need to find the error in one of the earlier steps.

Example 2:
Redox reaction of $S_2O_3^{2-}$ and H_2O_2
$\mathbf{S_2O_3^{2-}} + \mathbf{H_2O_2} \rightarrow \mathbf{S_4O_6^{2-}} + \mathbf{H_2O}$

Which elements are undergoing redox? **S** and **O**

Step 1: Write out half reactions, balancing the element undergoing redox

$\mathbf{2S_2O_3^{2-} \rightarrow S_4O_6^{2-}}$
$\mathbf{H_2O_2 \rightarrow 2H_2O}$

Step 2A: Balance oxygen (already balanced)

Step 2B: Balance hydrogen:

$\mathbf{2S_2O_3^{2-} \rightarrow S_4O_6^{2-}}$
$\mathbf{H_2O_2 + 2H^+ \rightarrow 2H_2O}$

Step 2C: Balance charge by adding electrons:

$\mathbf{2S_2O_3^{2-} \rightarrow S_4O_6^{2-} + 2e^-}$
$\mathbf{H_2O_2 + 2H^+ + 2e^- \rightarrow 2H_2O}$

Step 3: Combine the half reactions so that there are equal numbers of electrons on the left and right sides (already equal)
Overall balanced reaction:

$\mathbf{2S_2O_3^{2-} + H_2O_2 + 2H^+ \rightarrow S_4O_6^{2-} + 2H_2O}$

Note that again, we did not need to know the formal oxidation states of S or O in the reactants and products in order to balance the reaction. In this case, assigning the oxidation states would be rather complex, because $S_2O_3^{2-}$ and $S_4O_6^{2-}$ both contain sulfur in more than one oxidation state.

This page titled 3.2: Balancing Redox Reactions is shared under a CC BY-NC-SA 4.0 license and was authored, remixed, and/or curated by Chemistry 310 (Wikibook) via source content that was edited to the style and standards of the LibreTexts platform.

- **4.2: Balancing Redox Reactions** by Chemistry 310 is licensed CC BY-SA 4.0. Original source: https://en.wikibooks.org/wiki/Introduction_to_Inorganic_Chemistry.

3.3: Electrochemical Cells

Consider what happens when a clean piece of copper metal is placed in a solution of silver nitrate (Figure **3.3.1**). As soon as the copper metal is added, silver metal begins to form and copper ions pass into the solution. The blue color of the solution on the far right indicates the presence of copper ions. The reaction may be split into its two half-reactions. Half-reactions separate the oxidation from the reduction, so each can be considered individually.

$$\text{oxidation: } \mathrm{Cu}(s) \longrightarrow \mathrm{Cu}^{2+}(aq) + 2\,\mathrm{e}^- \tag{3.3.1}$$

$$\text{reduction: } 2 \times (\mathrm{Ag}^+(aq) + \mathrm{e}^- \longrightarrow \mathrm{Ag}(s)) \quad \text{or} \quad 2\,\mathrm{Ag}^+(aq) + 2\,\mathrm{e}^- \longrightarrow 2\,\mathrm{Ag}(s) \tag{3.3.2}$$

$$\text{overall: } 2\,\mathrm{Ag}^+(aq) + \mathrm{Cu}(s) \longrightarrow 2\,\mathrm{Ag}(s) + \mathrm{Cu}^{2+}(aq) \tag{3.3.3}$$

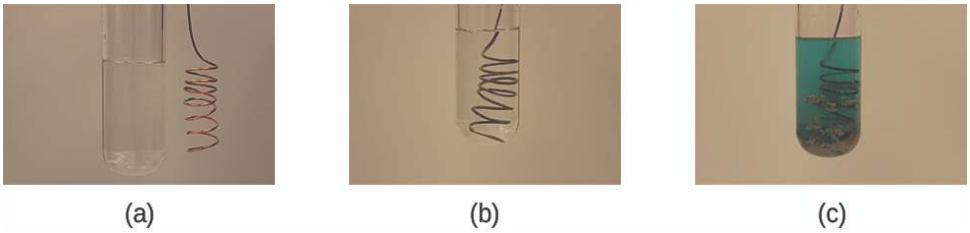


Figure **3.3.1**: When a clean piece of copper metal is placed into a clear solution of silver nitrate (a), an oxidation-reduction reaction occurs that results in the exchange of Cu^{2+} for Ag^+ ions in solution. As the reaction proceeds (b), the solution turns blue (c) because of the copper ions present, and silver metal is deposited on the copper strip as the silver ions are removed from solution. (credit: modification of work by Mark Ott)

Parts of an Electrochemical Cell

The redox reaction between Cu(s) and Ag^+ (aq) involves the movement of electrons. The two half-reactions can be physically separated to make an electrochemical cell as shown in Figure **3.3.2**. The beaker on the left side of the figure is called a half-cell, and contains a 1 *M* solution of copper(II) nitrate [$Cu(NO_3)_2$] with a piece of copper metal partially submerged in the solution. The copper metal is an electrode. The copper is undergoing oxidation; therefore, the copper electrode is the anode. The anode is connected to a voltmeter with a wire and the other terminal of the voltmeter is connected to a silver electrode by a wire. Electrons flow from the anode to the cathode. The silver is undergoing reduction; therefore, the silver electrode is the cathode. The half-cell on the right side of the figure consists of the silver electrode in a 1 *M* solution of silver nitrate ($AgNO_3$).

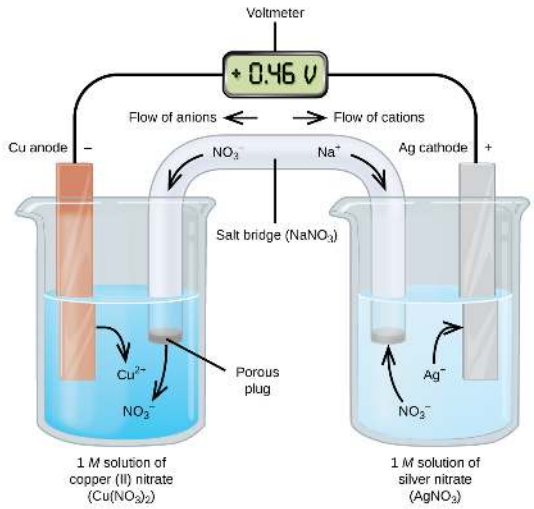


Figure **3.3.2**: In this standard galvanic cell, the half-cells are separated; electrons can flow through an external wire and become available to do electrical work.

The circuit is closed using a salt bridge, which transmits the current with moving ions. The salt bridge consists of a concentrated, nonreactive, electrolyte solution such as the sodium nitrate ($NaNO_3$) solution used in this example. As electrons flow from left to right through the electrode and wire, nitrate ions (anions) pass through the porous plug on the left into the copper(II) nitrate solution. This keeps the beaker on the left electrically neutral by neutralizing the charge on the copper(II) ions that are produced in

the solution as the copper metal is oxidized. At the same time, the nitrate ions are moving to the left, sodium ions (cations) move to the right, through the porous plug, and into the silver nitrate solution on the right. These added cations “replace” the silver ions that are removed from the solution as they were reduced to silver metal, keeping the beaker on the right electrically neutral. Without the salt bridge, the compartments would not remain electrically neutral and no significant current would flow. However, if the two compartments are in direct contact, a salt bridge is not necessary.

The voltmeter connected in the electrochemical circuit reads +0.46 V; this is called the ***cell potential***. The cell potential is created when the two dissimilar metals are connected, and is a measure of the energy per unit charge available from the oxidation-reduction reaction. The volt is the derived SI unit for electrical potential

$$\text{volt} = V = \frac{\text{J}}{\text{C}}$$

In this equation, A is the current in amperes and C the charge in coulombs. Note that volts must be multiplied by the charge in coulombs (C) to obtain the energy in joules (J).

Some oxidation-reduction reactions involve species that are poor conductors of electricity, and so an electrode is used that does not participate in the reactions. Frequently, the electrode is platinum, gold, or graphite, all of which are inert to many chemical reactions. One such system is shown in Figure **3.3.3**. Magnesium undergoes oxidation at the anode on the left in the figure and hydrogen ions undergo reduction at the cathode on the right. The reaction may be summarized as

$$\text{oxidation: } \text{Mg}(s) \longrightarrow \text{Mg}^{2+}(aq) + 2\,\text{e}^- \tag{3.3.4}$$
$$\text{reduction: } 2\,\text{H}^+(aq) + 2\,\text{e}^- \longrightarrow \text{H}_2(g) \tag{3.3.5}$$
$$\text{overall: } \text{Mg}(s) + 2\,\text{H}^+(aq) \longrightarrow \text{Mg}^{2+}(aq) + \text{H}_2(g) \tag{3.3.6}$$

The magnesium electrode is an active electrode because it participates in the oxidation-reduction reaction. Inert electrodes, like the platinum electrode in Figure **3.3.3**, do not participate in the oxidation-reduction reaction and are present so that current can flow through the cell. Platinum or gold generally make good inert electrodes because they are chemically unreactive.

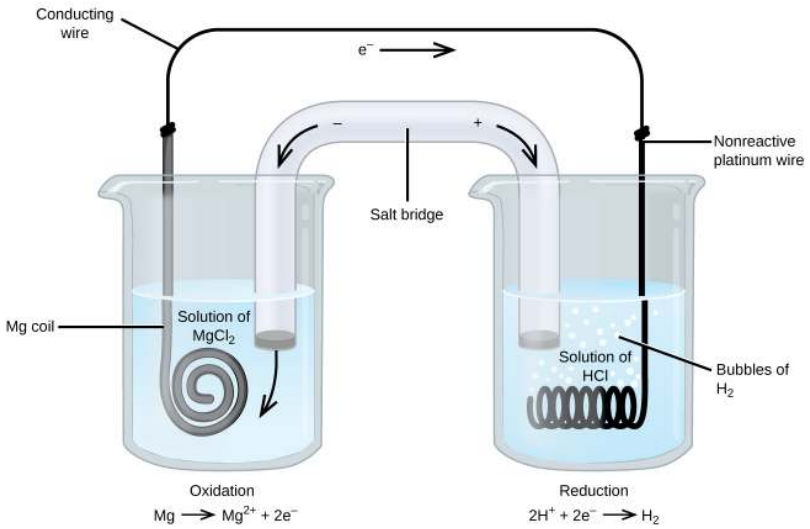


Figure **3.3.3**: The oxidation of magnesium to magnesium ion occurs in the beaker on the left side in this apparatus; the reduction of hydrogen ions to hydrogen occurs in the beaker on the right. A nonreactive, or inert, platinum wire allows electrons from the left beaker to move into the right beaker. The overall reaction is: $\text{Mg} + 2\,\text{H}^+ \longrightarrow \text{Mg}^{2+} + \text{H}_2$, *which is represented in cell notation as:* $\text{Mg}(s)\,|\,\text{Mg}^{2+}(aq)\,\|\,\text{H}^+(aq)\,|\,\text{H}_2(g)\,|\,\text{Pt}(s)$.

Two Types of Electrochemical Cells

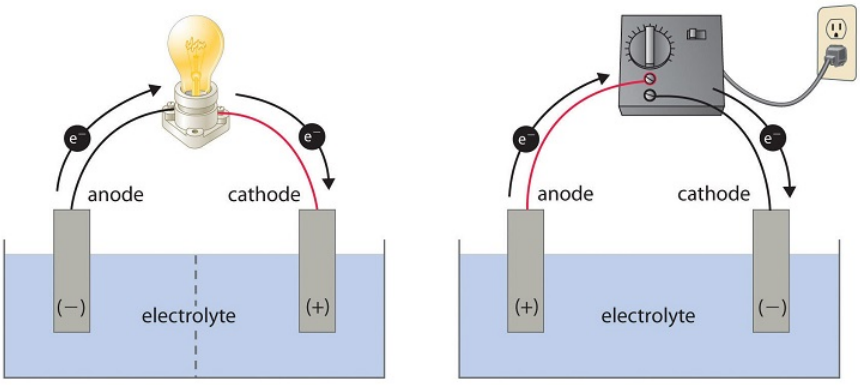
Galvanic/Voltaic Cells

Galvanic cells, also known as voltaic cells, are electrochemical cells in which the oxidation-reduction reactions occur spontaneously and produce electrical energy. The examples shown in Figures **3.3.1** and **3.3.2** are galvanic cells. Galvanic cells have a positive cell potential. These cells are important because they are the basis for the batteries that fuel modern society.

Electrolytic Cells

It is possible to construct a cell that does work on a chemical system by driving an electric current through the system. These cells are called **electrolytic cells.** Electrolytic cells, like galvanic cells, are composed of two half-cells--one is a reduction half-cell, the other is an oxidation half-cell. The direction of electron flow in electrolytic cells, however, may be reversed from the direction of spontaneous electron flow in galvanic cells, but the definition of both cathode and anode remain the same, where reduction takes place at the cathode and oxidation occurs at the anode. Because the directions of both half-reactions have been reversed, the sign, but not the magnitude, of the cell potential has been reversed.

Electrolytic cells are very similar to voltaic (galvanic) cells in the sense that both require a salt bridge, both have a cathode and anode side, and both have a consistent flow of electrons from the anode to the cathode. However, there are also striking differences between the two cells. The main differences are outlined below:



GALVANIC CELL

Energy released by spontaneous redox reaction is converted to electrical energy.

Oxidation half-reaction:
$Y \rightarrow Y^+ + e^-$

Reduction half-reaction:
$Z^+ + e^- \rightarrow Z$

Overall cell reaction:
$Y + Z \rightarrow Y^+ + Z^-$ $(G < 0)$

ELECTROLYTIC CELL

Electrical energy is used to drive nonspontaneous redox reaction.

Oxidation half-reaction:
$Z^- \rightarrow Z + e^-$

Reduction half-reaction:
$Y^+ + e^- \rightarrow Y$

Overall cell reaction:
$Y^+ + Z^- \rightarrow Y + Z$ $(G > 0)$

Figure 3.3.1: Electrochemical Cells. A galvanic cell (left) transforms the energy released by a spontaneous redox reaction into electrical energy that can be used to perform work. The oxidative and reductive half-reactions usually occur in separate compartments that are connected by an external electrical circuit; in addition, a second connection that allows ions to flow between the compartments (shown here as a vertical dashed line to represent a porous barrier) is necessary to maintain electrical neutrality. The potential difference between the electrodes (voltage) causes electrons to flow from the reductant to the oxidant through the external circuit, generating an electric current. In an electrolytic cell (right), an external source of electrical energy is used to generate a potential difference between the electrodes that forces electrons to flow, driving a nonspontaneous redox reaction; only a single compartment is employed in most applications. In both kinds of electrochemical cells, the anode is the electrode at which the oxidation half-reaction occurs, and the cathode is the electrode at which the reduction half-reaction occurs.

Table **3.3.1**: Properties of Galvanic and Electrochemical Cells

Electrochemical cell (Galvanic Cell)	Electrolytic cell
A Galvanic cell converts chemical energy into electrical energy.	An electrolytic cell converts electrical energy into chemical energy.
Here, the redox reaction is spontaneous and is responsible for the production of electrical energy.	The redox reaction is not spontaneous and electrical energy has to be supplied to initiate the reaction.
The two half-cells are set up in different containers, being connected through the salt bridge or porous partition.	Both the electrodes are placed in a same container in the solution of molten electrolyte.
Here the anode is negative and cathode is the positive electrode. The reaction at the anode is oxidation and that at the cathode is reduction.	Here, the anode is positive and cathode is the negative electrode. The reaction at the anode is oxidation and that at the cathode is reduction.
The electrons are supplied by the species getting oxidized. They move from anode to the cathode in the external circuit.	The external battery supplies the electrons. They enter through the cathode and come out through the anode.

3.3: Electrochemical Cells is shared under a CC BY-NC-SA 4.0 license and was authored, remixed, and/or curated by Kathryn A. Newton, Northern Michigan University.

- **17.2: Galvanic Cells** by OpenStax is licensed CC BY 4.0. Original source: https://openstax.org/details/books/chemistry-2e.
- **Electrolytic Cells** is licensed CC BY-NC-SA 4.0.

3.4: Standard Reduction Potentials

In redox reactions the thermodynamic driving force can be measured as the **cell potential**. The cell potential results from the difference in the electrical potentials for each electrode. Standard cell potential determined using the *standard reduction cell potential* and the *standard oxidation cell potential*. The standard reduction potential is a measure of the likelihood that a species will be reduced. Likewise, the standard oxidation potential is a measure of the likelihood that a species will be oxidized. The equations that relate these three potentials are shown below:

$$E^o_{cell} = E^o_{reduction} \text{ of reaction at cathode} + E^o_{oxidation} \text{ of reaction at anode} \tag{3.4.1}$$

or alternatively

$$E^o_{cell} = E^o_{reduction} \text{ of reaction at cathode} - E^o_{reduction} \text{ of reaction at anode} \tag{3.4.2}$$

The standard oxidation potential and the standard reduction potential are opposite in sign to each other for the same chemical species.

- Relation Between Standard Reduction Potential (SRP) and the Standard Oxidation Potential (SOP)

$$E^o_0(SRP) = -E^o_0(SOP) \tag{3.4.3}$$

How the Standard Reduction Cell Potential is Experimentally Determined

It is impossible to determine the electrical potential of a single electrode; therefore, we use a reference electrode. This means, we assign an electrode an electrical potential value of zero and then compare the electrical potential of other electrodes to it. The standard hydrogen electrode (SHE) is commonly used for assessing the potential of half-cells. The SHE consists of 1 atm of hydrogen gas bubbled through a 1 M HCl solution at 298 K. Platinum, which is chemically inert, is used as the electrode. The reduction half-reaction chosen as the reference is

$$2\,H^+(aq,\ 1\ M) + 2\,e^- \rightleftharpoons H_2(g,\ 1\ \text{atm}) \quad E^\circ = 0\ V$$

$E°$ is the standard reduction potential. The superscript "°" on the E denotes standard conditions (1 bar or 1 atm for gases, 1 M for solutes). The voltage is defined as zero for all temperatures.

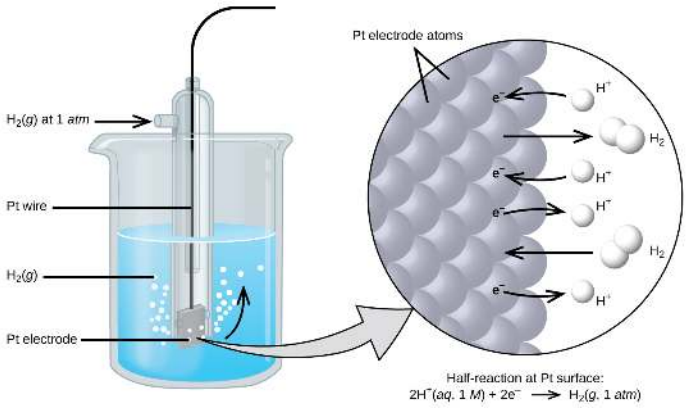


Figure **3.4.1**: Hydrogen gas at 1 atm is bubbled through 1 M HCl solution. Platinum, which is inert to the action of the 1 M HCl, is used as the electrode. Electrons on the surface of the electrode combine with H^+ in solution to produce hydrogen gas.

A galvanic cell consisting of a SHE and Cu^{2+}/Cu half-cell can be used to determine the standard reduction potential for Cu^{2+} (Figure **3.4.2**). Electrons flow from the anode to the cathode. The reactions, which are reversible, are

$$\begin{aligned}
&\text{Anode (oxidation): } H_2(g) \longrightarrow 2\,H^+(aq) + 2\,e^- \\
&\text{Cathode (reduction): } Cu^{2+}(aq) + 2\,e^- \longrightarrow Cu(s) \\
&\overline{\text{Overall: } Cu^{2+}(aq) + H_2(g) \longrightarrow 2\,H^+(aq) + Cu(s)}
\end{aligned}$$

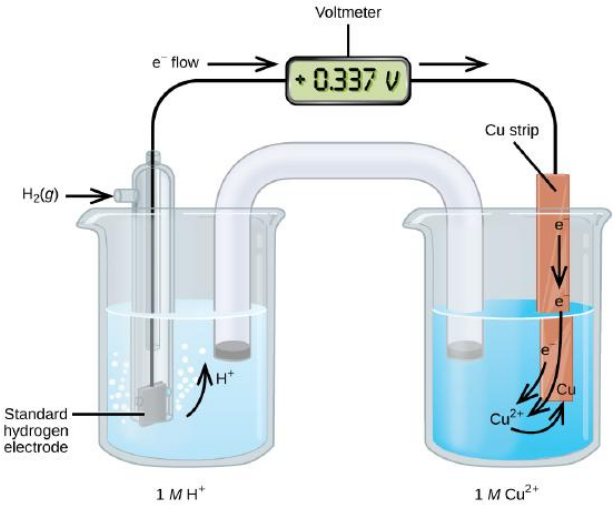


Figure **3.4.2**: A galvanic cell can be used to determine the standard reduction potential of Cu^{2+}.

The standard reduction potential can be determined by subtracting the standard reduction potential for the reaction occurring at the anode from the standard reduction potential for the reaction occurring at the cathode. The minus sign is necessary because oxidation is the reverse of reduction.

$$E^\circ_{\text{cell}} = E^\circ_{\text{cathode}} - E^\circ_{\text{anode}}$$

$$+0.34\,\text{V} = E^\circ_{\text{Cu}^{2+}/\text{Cu}} - E^\circ_{\text{H}^+/\text{H}_2} = E^\circ_{\text{Cu}^{2+}/\text{Cu}} - 0 = E^\circ_{\text{Cu}^{2+}/\text{Cu}}$$

Using the SHE as a reference, other standard reduction potentials can be determined. Consider the cell shown in Figure **3.4.3**, where the electrons flow from left to right, and the reactions are

$$\begin{aligned}&\textbf{anode (oxidation):}\ \text{H}_2(g) \longrightarrow 2\,\text{H}^+(aq) + 2\,\text{e}^-\\ &\textbf{cathode (reduction):}\ 2\,\text{Ag}^+(aq) + 2\,\text{e}^- \longrightarrow 2\,\text{Ag}(s)\\ &\textbf{overall:}\ 2\,\text{Ag}^+(aq) + \text{H}_2(g) \longrightarrow 2\,\text{H}^+(aq) + 2\,\text{Ag}(s)\end{aligned}$$

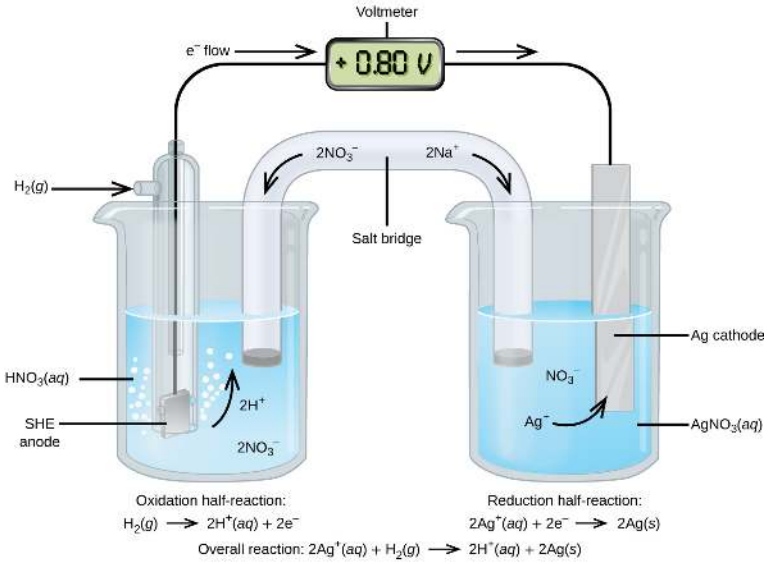


Figure **3.4.3**: A galvanic cell can be used to determine the standard reduction potential of Ag^+. The SHE on the left is the anode and assigned a standard reduction potential of zero.

The standard reduction potential can be determined by subtracting the standard reduction potential for the reaction occurring at the anode from the standard reduction potential for the reaction occurring at the cathode. The minus sign is needed because oxidation is the reverse of reduction.

$$E^\circ_{\text{cell}} = E^\circ_{\text{cathode}} - E^\circ_{\text{anode}}$$

$$+0.80\ \text{V} = E^\circ_{\text{Ag}^+/\text{Ag}} - E^\circ_{\text{H}^+/\text{H}_2} = E^\circ_{\text{Ag}^+/\text{Ag}} - 0 = E^\circ_{\text{Ag}^+/\text{Ag}}$$

It is important to note that the potential is *not* doubled for the cathode reaction. The reason we don't need to multiply the Ag potential by 2 is that E^o is a measure of the free energy change **per electron**. Dividing the free energy change by the number of electrons makes E^o an **intensive property** (like pressure, temperature, etc.).

The SHE is rather dangerous and rarely used in the laboratory. Its main significance is that it established the zero for standard reduction potentials. Once determined, standard reduction potentials can be used to determine the standard cell potential, E°_{cell}, for any cell. For example, for the following cell:

$$\begin{aligned}&\text{anode (oxidation): } \text{Cu}(s) \longrightarrow \text{Cu}^{2+}(aq) + 2\,\text{e}^-\\ &\text{cathode (reduction): } 2\,\text{Ag}^+(aq) + 2\,\text{e}^- \longrightarrow 2\,\text{Ag}(s)\\ &\text{overall: } \text{Cu}(s) + 2\,\text{Ag}^+(aq) \longrightarrow \text{Cu}^{2+}(aq) + 2\,\text{Ag}(s)\end{aligned}$$

$$E^\circ_{\text{cell}} = E^\circ_{\text{cathode}} - E^\circ_{\text{anode}} = E^\circ_{\text{Ag}^+/\text{Ag}} - E^\circ_{\text{Cu}^{2+}/\text{Cu}} = 0.80\ \text{V} - 0.34\ \text{V} = 0.46\ \text{V}$$

Again, note that when calculating E°_{cell}, standard reduction potentials always remain the same even when a half-reaction is multiplied by a factor.

The Activity Series

When solving for the standard cell potential, the species oxidized and the species reduced must be identified. This can be done using an activity series. The Table **3.4.1** shown below is an activity series; which is simply a table of standard reduction potentials in decreasing order. The species at the top have a greater likelihood of being reduced while the ones at the bottom have a greater likelihood of being oxidized. Therefore, when a species at the top is coupled with a species at the bottom, the one at the top will become reduced while the one at the bottom will become oxidized. A more complete list of standard reduction potentials is is provided in Tables P1 or P2.

Table **3.4.1**: Activity Series - Standard Reduction Potential for Selected Species

Reduction Half-Reaction	Standard Reduction Potential (V)
$F_2(g)+2e^- \rightarrow 2F^-(aq)$	+2.87
$S_2O_8^{2-}(aq)+2e^- \rightarrow 2SO_4^{2-}(aq)$	+2.01
$O_2(g)+4H^+(aq)+4e^- \rightarrow 2H_2O(l)$	+1.23
$Br_2(l)+2e^- \rightarrow 2Br^-(aq)$	+1.09
$Ag^+(aq)+e^- \rightarrow Ag(s)$	+0.80
$Fe^{3+}(aq)+e^- \rightarrow Fe^{2+}(aq)$	+0.77
$I_2(l) + 2e^- \rightarrow 2I^-(aq)$	+0.54
$Cu^{2+}(aq)+2e^- \rightarrow Cu(s)$	+0.34
$Sn^{4+}(aq)+2e^- \rightarrow Sn^{2+}(aq)$	+0.15
$S(s)+2H^+(aq)+2e^- \rightarrow H_2S(g)$	+0.14
$2H^+(aq)+2e^- \rightarrow H_2(g)$	**0.00**
$Sn^{2+}(aq)+2e^- \rightarrow Sn(g)$	-0.14
$V^{3+}(aq)+e^- \rightarrow V^{2+}(aq)$	-0.26
$Fe^{2+}(aq)+2e^- \rightarrow Fe(s)$	-0.44
$Cr^{3+}(aq)+3e^- \rightarrow Cr(s)$	-0.74
$Zn^{2+}(aq)+2e^- \rightarrow Zn(s)$	-0.76
$Mn^{2+}(aq)+2e^- \rightarrow Mn(s)$	-1.18
$Na^+(aq)+e^- \rightarrow Na(s)$	-2.71
$Li^+(aq)+e^- \rightarrow Li(s)$	-3.04

Problems

Exercise 3.4.1: Cell Potentials from Standard Reduction Potentials

What is the standard cell potential for a galvanic cell that consists of Au^{3+}/Au and Ni^{2+}/Ni half-cells? Identify the oxidizing and reducing agents.

Answer

Using Table **3.4.1**, the reactions involved in the galvanic cell, both written as reductions, are

$$\mathrm{Au^{3+}}(aq) + 3\,\mathrm{e^-} \longrightarrow \mathrm{Au}(s) \quad E^\circ_{\mathrm{Au^{3+}/Au}} = +1.498\ \mathrm{V}$$

$$\mathrm{Ni^{2+}}(aq) + 2\,\mathrm{e^-} \longrightarrow \mathrm{Ni}(s) \quad E^\circ_{\mathrm{Ni^{2+}/Ni}} = -0.257\ \mathrm{V}$$

Galvanic cells have positive cell potentials, and all the reduction reactions are reversible. The reaction at the anode will be the half-reaction with the smaller or more negative standard reduction potential. Reversing the reaction at the anode (to show the oxidation) but *not* its standard reduction potential gives:

$$\text{Anode (oxidation): } \mathrm{Ni}(s) \longrightarrow \mathrm{Ni^{2+}}(aq) + 2\,\mathrm{e^-} \quad E^\circ_{\text{anode}} = E^\circ_{\mathrm{Ni^{2+}/Ni}} = -0.257\ \mathrm{V}$$
$$\text{Cathode (reduction): } \mathrm{Au^{3+}}(aq) + 3\,\mathrm{e^-} \longrightarrow \mathrm{Au}(s) \quad E^\circ_{\text{cathode}} = E^\circ_{\mathrm{Au^{3+}/Au}} = +1.498\ \mathrm{V}$$

The least common factor is six, so the overall reaction is

$$3\,\mathrm{Ni}(s) + 2\,\mathrm{Au^{3+}}(aq) \longrightarrow 3\,\mathrm{Ni^{2+}}(aq) + 2\,\mathrm{Au}(s)$$

The reduction potentials are *not* scaled by the stoichiometric coefficients when calculating the cell potential, and the unmodified standard reduction potentials must be used.

$$E^\circ_{\text{cell}} = E^\circ_{\text{cathode}} - E^\circ_{\text{anode}} = 1.498\ \mathrm{V} - (-0.257\ \mathrm{V}) = 1.755\ \mathrm{V}$$

From the half-reactions, Ni is oxidized, so it is the reducing agent, and Au^{3+} is reduced, so it is the oxidizing agent.

Exercise 3.4.1

A galvanic cell consists of a Mg electrode in 1 *M* $Mg(NO_3)_2$ solution and a Ag electrode in 1 *M* $AgNO_3$ solution. Calculate the standard cell potential at 25 °C.

Answer

$$\mathrm{Mg}(s) + 2\,\mathrm{Ag^+}(aq) \longrightarrow \mathrm{Mg^{2+}}(aq) + 2\,\mathrm{Ag}(s) \quad E^\circ_{\text{cell}} = 0.7996\ \mathrm{V} - (-2.372\ \mathrm{V}) = 3.172\ \mathrm{V}$$

Exercise 3.4.3

True or False?

1. Hydrogen has oxidation potentials of 0.
2. The standard oxidation potential is not much like the standard reduction potential.
3. The standard reduction cell potential and the standard oxidation cell potential can never be combined.

Answer

1. True
2. False: the standard oxidation potential is much like the standard reduction potential
3. False: The standard reduction cell potential and the standard oxidation cell potential can be combined to determine the overall cell potential

Exercise 3.4.4

1. What does the standard reduction potential measure?
2. What are the differences between the standard reduction potential and standard oxidation potential, and how are the two related?
3. What conditions must be met for a potential to be standard?
4. When standard reduction potentials are measured, what are the potentials relative to?
5. How is a standard reduction potential measured?
6. Explain how the activity series is used.
7. Explain how standard reduction potentials or standard oxidation potentials are applied.
8. Draw and label a SHE.

Answer

1. Standard reduction potential measures the tendency for a given chemical species to be reduced.
2. The standard oxidation potential measures the tendency for a given chemical species to be oxidized as opposed to be reduced. For the same chemical species the standard reduction potential and standard oxidation potential are opposite in sign.
3. The cell must be at 298K, 1atm, and all solutions must be at 1M. Standard reduction potentials are measured with relativity to hydrogen which has be universally set to have a potential of zero.
4. A standard reduction potential is measured using a galvanic cell which contains a SHE on one side and an unknown chemical half cell on the other side.
5. The amount of charge that passes between the cells is measured using a voltmeter.
6. The activity series is a list of standard reduction potentials in descending order of the tendency for chemical species to be reduced. Species at the top are more likely to be reduced while species at the bottom are more likely to be oxidized.
7. Standard reduction and oxidation potentials can be applied to solve for the standard cell potential of two different non hydrogen species. Examples can be seen in Cell Potentials.
8. See Figure (2).

Exercise 3.4.5

Based on the activity series, which species will be oxidized and reduced: Zn^{2+} or H^{+}.

Answer

H^{+} is farther up on the activity series then Zn^{2+} so H^{+} is reduced while Zn^{2+} is oxidized.

Exercise 3.4.6

The standard reduction potential of Fe^{3+} is +0.77V. What is its standard oxidation potential.

Answer

The standard oxidation potential and standard reduction potential are always opposite in sign for the same species. The oxidation potential is -0.77V.

3.4: Standard Reduction Potentials is shared under a CC BY-NC-SA 4.0 license and was authored, remixed, and/or curated by Kathryn A. Newton, Northern Michigan University.

- **17.3: Standard Reduction Potentials** by OpenStax is licensed CC BY 4.0. Original source: https://openstax.org/details/books/chemistry-2e.
- **Standard Reduction Potential** is licensed CC BY-NC-SA 4.0.

3.5: Thermodynamic Considerations

Electrochemical Potential and Free Energy

We will now extend electrochemistry by determining the relationship between E°_{cell} and the thermodynamics quantities such as ΔG° (Gibbs free energy) and K (the equilibrium constant). In spontaneous redox reactions, chemical energy is converted into electrical energy, which can do work. The electrical work is the product of the charge transferred multiplied by the potential difference (voltage):

$$\textbf{electrical work} = \textbf{volts} \times (\textbf{charge in coulombs}) = \textbf{J}$$

The charge on 1 mole of electrons is given by Faraday's constant (F)

$$\begin{aligned} F &= \frac{6.022 \times 10^{23}\ e^-}{mol} \times \frac{1.602 \times 10^{-19}\ C}{e^-} \\ &= 9.648 \times 10^4\ \frac{C}{mol} \\ &= 9.648 \times 10^4\ \frac{J}{V \cdot mol} \end{aligned}$$

Therefore

$$\textbf{total charge} = (\textbf{number of moles of e}^-) \times F = nF$$

In this equation, n is the number of moles of electrons for the *balanced* oxidation-reduction reaction. The measured cell potential is the maximum potential the cell can produce and is related to the electrical work (w_{ele}) by

$$E_{\text{cell}} = \frac{-w_{\text{ele}}}{nF} \qquad \text{or} \qquad w_{\text{ele}} = -nFE_{\text{cell}}$$

The negative sign for the work indicates that the electrical work is done by the system (the galvanic cell) on the surroundings. Free energy is defined as the energy that is available to do work. In particular, the change in free energy is defined in terms of the maximum work (w_{max}), which is w_{ele} for electrochemical systems.

$$\begin{aligned} \Delta G &= w_{\text{max}} = w_{\text{ele}} \\ &= -nFE_{\text{cell}} \end{aligned}$$

We can verify the signs are correct when we realize that n and F are positive constants and that galvanic cells, which have positive cell potentials, involve spontaneous reactions. Thus, spontaneous reactions, which have $\Delta G < 0$, must have $E_{cell} > 0$. If all the reactants and products are in their standard states, this becomes

$$\Delta G^\circ = -nFE^\circ_{\text{cell}}$$

Although the sign of E°_{cell} tells us whether a particular redox reaction will occur spontaneously under standard conditions, it does not tell us to what extent the reaction proceeds, and it does not tell us what will happen under nonstandard conditions. To answer these questions requires a more quantitative understanding of the relationship between electrochemical cell potential and equilibrium constants. Since

$$\Delta G^\circ = -RT \ln K$$

$$-nFE^\circ_{\text{cell}} = -RT \ln K$$

or

$$E^\circ_{\text{cell}} = \frac{RT}{nF} \ln K$$

Most of the time, the electrochemical reactions are run at standard temperature (298.15 K). Collecting terms at this temperature yields

$$E^\circ_{\text{cell}} = \frac{RT}{nF} \ln K$$
$$= \frac{\left(8.314 \frac{\text{J}}{\text{K·mol}}\right)(298.15\ K)}{n \times 96,485\ \text{C/V·mol}} \ln K$$
$$= \frac{0.0257\ \text{V}}{n} \ln K$$

where n is the number of moles of electrons. The logarithm in equations involving cell potentials is often expressed using base 10 logarithms (i.e., $\log_{10}$ or just log), which changes the constant by a factor of 2.303:

$$E^\circ_{\text{cell}} = \frac{0.0592\ \text{V}}{n} \log K$$

Thus, if $\Delta G°$, K, or E°_{cell} is known or can be calculated, the other two quantities can be readily determined. The relationships are shown graphically in Figure 3.5.1. Given any one of the quantities, the other two can be calculated.

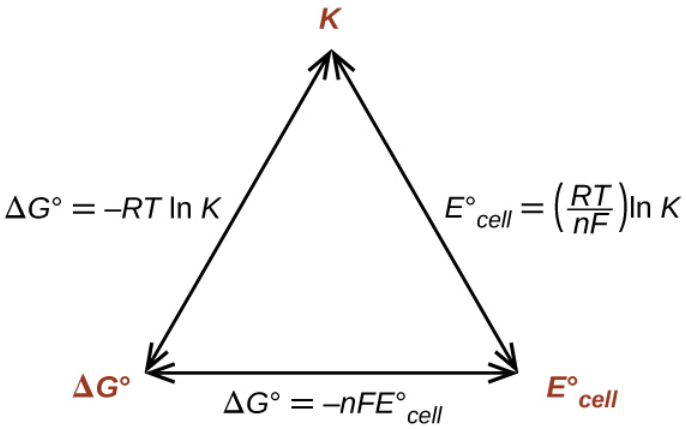


Figure 3.5.1: The relationships between ΔG°, K, and E°_{cell}. *Given any one of the three quantities, the other two can be calculated, so any of the quantities could be used to determine whether a process was spontaneous.*

Example 3.5.1: Equilibrium Constants, Potentials, & Free Energy Changes

What is the standard Gibbs free energy change and equilibrium constant for the following reaction at 25 °C?

$$2\,\text{Ag}^+(aq) + \text{Fe}(s) \rightleftharpoons 2\,\text{Ag}(s) + \text{Fe}^{2+}(aq)$$

Solution

The reaction involves an oxidation-reduction reaction, so the standard cell potential can be calculated using the data in Table P1.

$$\text{anode (oxidation): } \text{Fe}(s) \longrightarrow \text{Fe}^{2+}(aq) + 2\,\text{e}^- \qquad E^\circ_{\text{Fe}^{2+}/\text{Fe}} = -0.447\ \text{V}$$
$$\text{cathode (reduction): } 2 \times (\text{Ag}^+(aq) + \text{e}^- \longrightarrow \text{Ag}(s)) \qquad E^\circ_{\text{Ag}^+/\text{Ag}} = 0.7996\ \text{V}$$
$$E^\circ_{\text{cell}} = E^\circ_{\text{cathode}} - E^\circ_{\text{anode}} = E^\circ_{\text{Ag}^+/\text{Ag}} - E^\circ_{\text{Fe}^{2+}/\text{Fe}} = +1.247\ \text{V}$$

Remember that the cell potential for the cathode is not multiplied by two when determining the standard cell potential. With n = 2, the equilibrium constant is then

$$E^\circ_{\text{cell}} = \frac{0.0592\ \text{V}}{n} \log K$$
$$K = 10^{n \times E^\circ_{\text{cell}}/0.0592\ \text{V}}$$
$$= 10^{2 \times 1.247\ \text{V}/0.0592\ \text{V}}$$
$$= 10^{42.128}$$
$$= 1.3 \times 10^{42}$$

The standard free energy is then

$$\Delta G^\circ = -nFE^\circ_{\text{cell}}$$

$$\Delta G^\circ = -2 \times 96,485 \ \frac{\text{J}}{\text{V·mol}} \times 1.247 \ \text{V} = -240.6 \ \frac{\text{kJ}}{\text{mol}}$$

Check your answer: A positive standard cell potential means a spontaneous reaction, so the standard free energy change should be negative, and an equilibrium constant should be >1.

The Nernst Equation

Thus far, we have addressed electrochemical reactions that occur under standard conditions. The Nernst Equation will be introduced to address reactions that occur under nonstandard Conditions. Recall that

$$\Delta G = \Delta G^\circ + RT \ln Q$$

where Q is the reaction quotient (see the chapter on equilibrium fundamentals). Converting to cell potentials:

$$-nFE_{\text{cell}} = -nFE^\circ_{\text{cell}} + RT \ln Q \tag{3.5.1}$$

or

$$E_{\text{cell}} = E^\circ_{\text{cell}} - \frac{RT}{nF} \ln Q \tag{3.5.2}$$

Equation 3.5.2 is the generalized Nernst equation that is applicable at any temperature. However, is can be simplified for reactions occuring at 25 °C (298.15 K) by rewriting it as

$$E_{\text{cell}} = E^\circ_{\text{cell}} - \frac{0.0257 \ \text{V}}{n} \ln Q \tag{3.5.3}$$

or

$$E_{\text{cell}} = E^\circ_{\text{cell}} - \frac{0.0592 \ \text{V}}{n} \log_{10} Q \tag{3.5.4}$$

If the temperature is not 298.15 K, it is necessary to recalculate the potential with Equation3.5.2. With the Nernst equation, it is possible to calculate the cell potential at nonstandard conditions. This adjustment is necessary because potentials determined under different conditions will have different values.

✔ Example 3.5.2: Cell Potentials at Nonstandard Conditions

Consider the following reaction at room temperature:

$$\text{Co}(s) + \text{Fe}^{2+}(aq, \ 1.94 \ M) \longrightarrow \text{Co}^{2+}(aq, \ 0.15 \ M) + \text{Fe}(s)$$

Is the process spontaneous?

Solution

There are two ways to solve the problem. If the thermodynamic information in Table T1 were available, you could calculate the free energy change. If the free energy change is negative, the process is spontaneous. The other approach, which we will use, requires information like that given in Table P1. Using those data, the cell potential can be determined. If the cell potential is positive, the process is spontaneous. Collecting information from Table P1 and the problem,

$$\text{Anode (oxidation): } \text{Co}(s) \longrightarrow \text{Co}^{2+}(aq) + 2\,\text{e}^- \qquad E^\circ_{\text{Co}^{2+}/\text{Co}} = -0.28 \ \text{V}$$
$$\text{Cathode (reduction): } \text{Fe}^{2+}(aq) + 2\,\text{e}^- \longrightarrow \text{Fe}(s) \qquad E^\circ_{\text{Fe}^{2+}/\text{Fe}} = -0.447 \ \text{V}$$
$$E^\circ_{\text{cell}} = E^\circ_{\text{cathode}} - E^\circ_{\text{anode}} = -0.447 \ \text{V} - (-0.28 \ \text{V}) = -0.17 \ \text{V}$$

The process is not spontaneous under standard conditions. Using the Nernst equation and the concentrations stated in the problem and $n = 2$,

$$Q = \frac{[Co^2+]}{[Fe^2+]} = \frac{0.15\ M}{1.94\ M} = 0.077$$

Now we can insert these into the Nernst Equation at room temperature (Equation 3.5.4)

$$\begin{aligned} E_{\text{cell}} &= E^\circ_{\text{cell}} - \frac{0.0592\ \text{V}}{n} \log Q \\ &= -0.17\ \text{V} - \frac{0.0592\ \text{V}}{2} \log 0.077 \\ &= -0.17\ \text{V} + 0.033\ \text{V} = -0.14\ \text{V} \end{aligned}$$

The process is (still) nonspontaneous.

Finally, we will take a brief look at a special type of cell called a concentration cell. In a concentration cell, the electrodes are the same material and the half-cells differ only in concentration. Since one or both compartments is not standard, the cell potentials will be unequal; therefore, there will be a potential difference, which can be determined with the aid of the Nernst equation.

✔ Example 3.5.3: Concentration Cells

What is the cell potential of the concentration cell described by

$$\text{Zn}(s)\,|\,\text{Zn}^{2+}(aq,\ 0.10\ M)\,\|\,\text{Zn}^{2+}(aq,\ 0.50\ M)\,|\,\text{Zn}(s)$$

Solution

From the information given:

$$\begin{aligned} &\text{Anode: } \text{Zn}(s) \longrightarrow \text{Zn}^{2+}(aq,\ 0.10\ M) + 2\,\text{e}^- \qquad E^\circ_{\text{anode}} = -0.7618\ \text{V} \\ &\text{Cathode: } \text{Zn}^{2+}(aq,\ 0.50\ M) + 2\,\text{e}^- \longrightarrow \text{Zn}(s) \qquad E^\circ_{\text{cathode}} = -0.7618\ \text{V} \\ &\text{Overall: } \text{Zn}^{2+}(aq,\ 0.50\ M) \longrightarrow \text{Zn}^{2+}(aq,\ 0.10\ M) \qquad E^\circ_{\text{cell}} = 0.000\ \text{V} \end{aligned}$$

The standard cell potential is zero because the anode and cathode involve the same reaction; only the concentration of Zn^{2+} changes. Substituting into the Nernst equation,

$$E_{\text{cell}} = 0.000\ \text{V} - \frac{0.0592\ \text{V}}{2} \log \frac{0.10}{0.50} = +0.021\ \text{V}$$

and the process is spontaneous at these conditions.

Check your answer: In a concentration cell, the standard cell potential will always be zero. To get a positive cell potential (spontaneous process) the reaction quotient Q must be <1. $Q < 1$ in this case, so the process is spontaneous.

Problems

? Exercise 3.5.1

What is the standard Gibbs free energy change and the equilibrium constant for the following reaction at room temperature? Is the reaction spontaneous?

$$\text{Sn}(s) + 2\,\text{Cu}^{2+}(aq) \rightleftharpoons \text{Sn}^{2+}(aq) + 2\,\text{Cu}^{+}(aq)$$

Answer

Spontaneous; $n = 2$; $E^\circ_{\text{cell}} = +0.291\ \text{V}$; $\Delta G^\circ = -56.2\ \frac{\text{kJ}}{\text{mol}}$; $K = 6.8 \times 10^9$.

? Exercise 3.5.2

What is the cell potential for the following reaction at room temperature?

$$\text{Al}(s)\,|\,\text{Al}^{3+}(aq,\ 0.15\ M)\,\|\,\text{Cu}^{2+}(aq,\ 0.025\ M)\,|\,\text{Cu}(s)$$

What are the values of *n* and Q for the overall reaction? Is the reaction spontaneous under these conditions?

Answer

n = 6; *Q* = 1440; E_{cell} = +1.97 V, spontaneous.

Exercise 3.5.3

What value of *Q* for the previous concentration cell would result in a voltage of 0.10 V? If the concentration of zinc ion at the cathode was 0.50 *M*, what was the concentration at the anode?

Answer

Q = 0.00042; $[Zn^{2+}]_{cat}$ = 2.1 \times 10^{-4} *M*.

Exercise 3.5.4: Silver Sulfide

The black tarnish that forms on silver objects is primarily Ag_2S. The half-reaction for reversing the tarnishing process is as follows:

$$Ag_2S(s) + 2e^- \longrightarrow 2Ag(s) + S^{2-}(aq) \qquad E° = -0.69\,V$$

a. Referring to Table 3.5.1, predict which species—H_2O_2(aq), Zn(s), I^-(aq), Sn^{2+}(aq)—can reduce Ag_2S to Ag under standard conditions.
b. Of these species—H_2O_2(aq), Zn(s), I^-(aq), Sn^{2+}(aq), identify which is the strongest reducing agent in aqueous solution and thus the best candidate for a commercial product.
c. From the data in Table 3.5.1, suggest an alternative reducing agent that is readily available, inexpensive, and possibly more effective at removing tarnish.



Answer

We can solve the problem in one of two ways: (1) compare the relative positions of the four possible reductants with that of the Ag_2S/Ag couple in Table 3.5.1 or (2) compare E° for each species with E° for the Ag_2S/Ag couple (−0.69 V).

a. The species in Table 3.5.1 are arranged from top to bottom in order of increasing reducing strength. Of the four species given in the problem, I^-(aq), Sn^{2+}(aq), and H_2O_2(aq) lie above Ag_2S, and one [Zn(s)] lies below it. We can therefore conclude that Zn(s) can reduce Ag_2S(s) under standard conditions, whereas I^-(aq), Sn^{2+}(aq), and H_2O_2(aq) cannot. Sn^{2+}(aq) and H_2O_2(aq) appear twice in the table: on the left side (oxidant) in one half-reaction and on the right side (reductant) in another.
b. The strongest reductant is Zn(s), the species on the right side of the half-reaction that lies closer to the bottom of Table 3.5.1 than the half-reactions involving I^-(aq), Sn^{2+}(aq), and H_2O_2(aq). (Commercial products that use a piece of zinc are often marketed as a “miracle product” for removing tarnish from silver. All that is required is to add warm water and

salt for electrical conductivity.)

c. Of the reductants that lie below Zn(s) in Table **3.5.1**, and therefore are stronger reductants, only one is commonly available in household products: Al(s), which is sold as aluminum foil for wrapping foods.

? Exercise 3.5.5

Use the data in Table **3.5.1** to determine whether each reaction is likely to occur spontaneously under standard conditions:

$$\mathrm{Sn(s) + Be^{2+}(aq) \longrightarrow Sn^{2+}(aq) + Be(s)}$$

Answer

Metallic tin is oxidized to $\mathrm{Sn^{2+}(aq)}$, and $\mathrm{Be^{2+}(aq)}$ is reduced to elemental beryllium. We can find the standard electrode potentials for the latter (reduction) half-reaction (−1.99 V) and for the former (oxidation) half-reaction (−0.14 V) directly from Table **3.5.1**.

Adding the two half-reactions gives the overall reaction:

$$\begin{aligned} \mathrm{cathode: Be^{2+}(aq) + 2e^- \rightarrow Be(s)} \\ \mathrm{anode: Sn(s) \rightarrow Sn^{2+}(s) + 2e^-} \\ \hline \mathrm{overall: Sn(s) + Be^{2+}(aq) \rightarrow Sn^{2+}(aq) + Be(s)} \end{aligned}$$

with

$$\begin{aligned} E^\circ_{\text{cathode}} &= \text{-1.99 V} \\ E^\circ_{\text{anode}} &= \text{-0.14 V} \\ E^\circ_{\text{cell}} &= E^\circ_{\text{cathode}} - E^\circ_{\text{anode}} \\ &= -1.85 \text{ V} \end{aligned}$$

The standard cell potential is quite negative, so the reaction will not occur spontaneously as written. That is, metallic tin cannot reduce Be^{2+} to beryllium metal under standard conditions. Instead, the reverse process, the reduction of stannous ions (Sn^{2+}) by metallic beryllium, which has a positive value of $E°_{cell}$, will occur spontaneously.

? Exercise 3.5.6

Use the data in Table **3.5.1** to determine whether each reaction is likely to occur spontaneously under standard conditions:

$$\mathrm{MnO_2(s) + H_2O_2(aq) + 2H^+(aq) \longrightarrow O_2(g) + Mn^{2+}(aq) + 2H_2O(l)}$$

Answer

$\mathrm{MnO_2}$ is the oxidant ($\mathrm{Mn^{4+}}$ is reduced to $\mathrm{Mn^{2+}}$), while $\mathrm{H_2O_2}$ is the reductant ($\mathrm{O^{2-}}$ is oxidized to $\mathrm{O_2}$). We can obtain the standard electrode potentials for the reduction and oxidation half-reactions directly from Table **3.5.1**.

The two half-reactions and their corresponding potentials are as follows:

$$\begin{aligned} \mathrm{cathode: MnO_2(s) + 4H^+(aq) + 2e^- \rightarrow Mn^{2+}(aq) + 2H_2O(l)} \\ \mathrm{anode: H_2O_2(aq) \rightarrow O_2(g) + 2H^+(aq) + 2e^-} \\ \hline \mathrm{overall: MnO_2(s) + H_2O_2(aq) + 2H^+(aq) \rightarrow O_2(g) + Mn^{2+}(aq) + 2H_2O(l)} \end{aligned}$$

with

$$\begin{aligned} E^\circ_{\text{cathode}} &= 1.23 \text{ V} \\ E^\circ_{\text{anode}} &= 0.70 \text{ V} \\ E^\circ_{\text{cell}} &= E^\circ_{\text{cathode}} - E^\circ_{\text{anode}} \\ &= +0.52 \text{ V} \end{aligned}$$

The standard potential for the reaction is positive, indicating that under standard conditions, it will occur spontaneously as written. Hydrogen peroxide will reduce $\mathbf{MnO_2}$, and oxygen gas will evolve from the solution.

Exercise 3.5.7

Use the data in Table **3.5.1** to determine whether each reaction is likely to occur spontaneously under standard conditions:

a. $\mathbf{2\,Ce^{4+}\,(aq) + 2\,Cl^{-}\,(aq) \longrightarrow 2\,Ce^{3+}\,(aq) + Cl_2\,(g)}$

b. $\mathbf{4\,MnO_2\,(s) + 3\,O_2\,(g) + 4\,OH^{-}\,(aq) \longrightarrow 4\,MnO_4^{-}\,(aq) + 2\,H_2O}$

Answer a

spontaneous with $E^{o}_{cell} = 1.61\,V - 1.396\,V = 0.214\,V$

Answer b

nonspontaneous with $E^{\circ}_{cell} = -0.20\,V$

3.5: Thermodynamic Considerations is shared under a CC BY-NC-SA 4.0 license and was authored, remixed, and/or curated by Kathryn A. Newton, Northern Michigan University.

- **17.4: The Nernst Equation** by OpenStax is licensed CC BY 4.0. Original source: https://openstax.org/details/books/chemistry-2e.
- **Comparing Strengths of Oxidants and Reductants** is licensed CC BY-NC-SA 4.0.

3.6: General Trends in Reactivity

Trends in the Redox Properties of the Elements

The redox properties of the elements very roughly follow the following general trends:

1. Elements on the left of the periodic table tend to act as reductants; those on the right as oxidants
2. The noble gases are inert and as elements tend not to act as good oxidants or reductants
3. As one moves towards the left of the periodic table, elements tend to act as good reductants, while those towards the right tend to act as increasingly good oxidants.
4. As one moves down a group of the periodic table, elements tend to act as either weaker oxidants or better reductants.

These trends are summarized in Figure **3.6.2**.

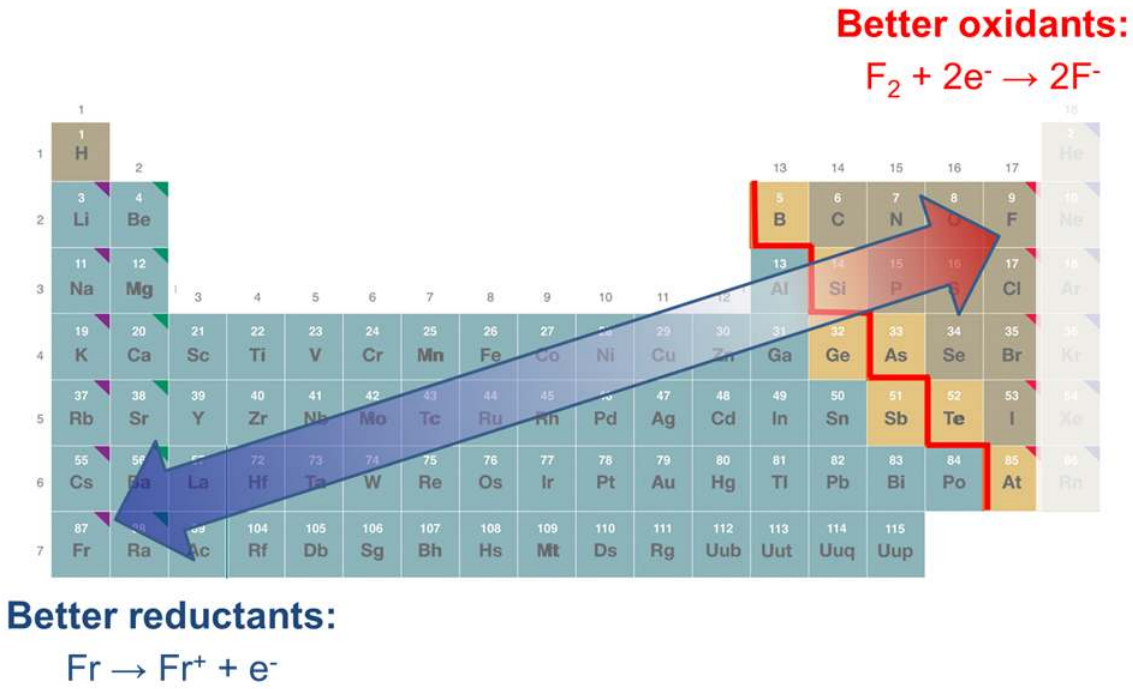


Figure **3.6.2**. Idealized scheme showing how elements' ability to act as reductants roughly increases towards the lower left of the periodic table while, noble gases excepted, their oxidizing power increases towards the upper left.

Since substances' ability to act as oxidants and reductants also depends on the stability of their oxidation and reduction products, these trends should be regarded as at best approximate. As can be seen from the data given in Table **3.6.1**, the alkali metals furnish an important exception to the general trend that substances become more reducing towards the lower left of the periodic table. Among the elements included,[2] lithium and not cesium is the most powerful reducing agent due to the high stability of the lithium cation in aqueous solution (anomalously high hydration energy). Further, from the potentials given in Table **3.6.1**, it can also be seen that on going from K^+ to Rb^+ and Cs^+ the reduction potentials do not decrease but instead remain approximately constant. In this case the decrease in ionization energy throughout this series is compensated for by a set of similar factors.[3]

Table 3.6.1 . Standard reduction potentials of aqueous alkali metal cations.

Reduction	$E°$
$Li^+(aq) + e^- \rightarrow Li(s)$	-3.040
$Na^+(aq) + e^- \rightarrow Na(s)$	-2.713
$K^+(aq) + e^- \rightarrow K(s)$	-2.924
$Rb^+(aq) + e^- \rightarrow Rb(s)$	-2.924
$Cs^+(aq) + e^- \rightarrow Cs(s)$	-2.923

3.6: General Trends in Reactivity is shared under a CC BY-NC-SA 4.0 license and was authored, remixed, and/or curated by Kathryn A. Newton, Northern Michigan University.

- **8.1.4: As may be seen from considering an element's redox diagrams, main group elements (aside from the noble gases) generally are more oxidizing towards the upper left of the periodic table and more reducing towards the lower right of the periodic table** has no license indicated.

3.7: Latimer Diagrams

A selection of the redox reactions nitrogen is known to undergo in 1.0 *M* aqueous acid is given in Figure **3.7.1**.

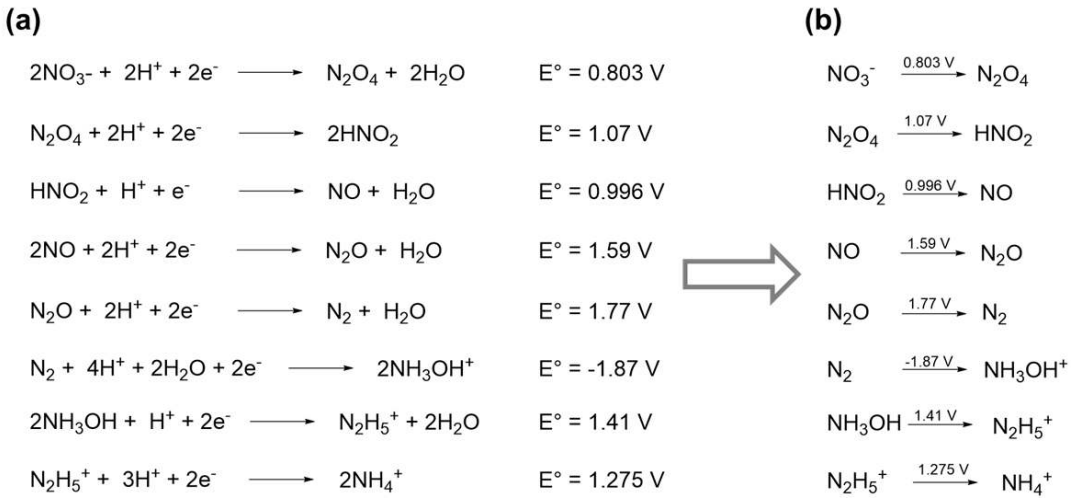


Figure **3.7.1**. (a) Full and (b) compact presentation of selected standard reduction half reactions for nitrogenous species in aqueous solution at pH 0.

The most important information in Figure **3.7.1** is the redox potentials and the identity of each nitrogen-containing species. In fact, if the latter are known, the number of electrons, water molecules, and any H^+ (in acid) or OH^- (in base) involved in the reduction may be deduced from the stoichiometry of the reaction. Consequently, the information in Figure **3.7.1** may be presented more compactly by only giving the nitrogen-containing species and the associated redox potential.

An Introduction to Latimer Diagrams

Latimer diagrams helpfully summarize elements' redox chemistry in a compact format, showing only the redox-active species and the associated redox potentials. A **Latimer diagram** is shown in Figure **3.7.2**. In a Latimer diagram, the product of each reduction half reaction is the reactant in the succeeding reduction half reaction, and the associated reduction potential is written above the reaction arrow. Because of this it is possible to represent the entire sequence of redox reactions even more compactly by writing out the reactions on a single line.

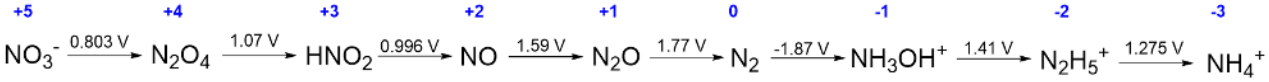


Figure **3.7.2**: Latimer diagram for nitrogen in acidic conditions.

Latimer diagrams include two additional pieces of information that are helpful for their interpretion.

1. The diagram should specify whether it represents reactivity in acidic (pH 0), basic (pH 14), or other solution conditions. In cases where it is not specified, it is customary to assume the diagram refers to behavior in pH 0 aqueous solution.
2. The oxidation state of the element is given at the top of the diagram, as shown in blue in Figure **3.7.2**. This helps to makes it easier to keep track of the number of electrons involved in each reduction reaction and to compare the redox behavior of related species.

More Complicated Latimer Diagrams

When it is possible to convert between two species by more than one pathway, the multiple pathways may be represented in the Latimer diagram. As shown in Figure **3.7.3**, additional reaction arrows can be added above or below the main pathway to represent the additional reactions that may occur. The diagram in Figure **3.7.2** presents a large number of possible interconversions. However, every possible interconversion is not represented. For example, the reduction potential for the reduction of N_2O_4 to NO is not presented. This type of selectivity is common in Latimer diagrams, but it does not necessarily mean that the missing conversions are not possible or that the potential has not been measured experimentally.

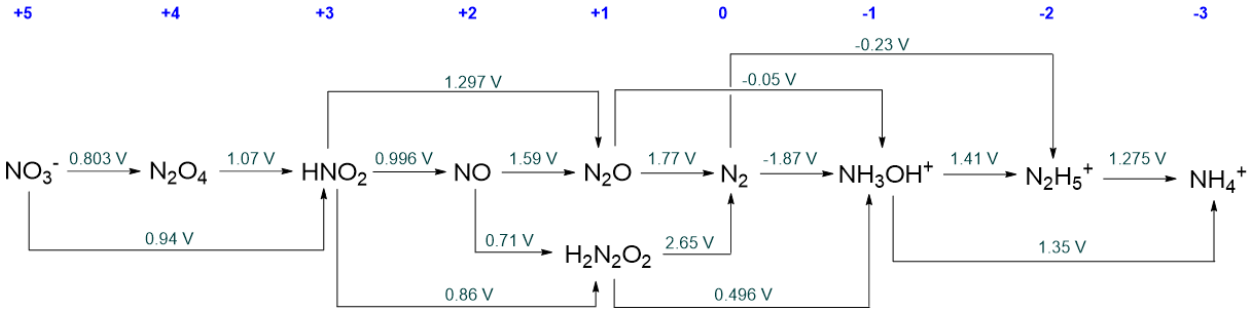


Figure **3.7.3**. Latimer Diagram for Nitrogen at pH 0. Redrawn from reference 1.

Since $\Delta G° = -nFE°$, the potentials in Latimer diagrams are thermodynamic quantities and may always be calculated from solution thermodynamic parameters. In fact, some redox potentials reported in Latimer diagrams have been only determined that way. An example is the reduction potential of fluorine,

$$F_2(g) \; + \; 2H^+ \; 2e^- \; \rightarrow \; 2HF \quad E° \; = \; 3.053 \text{ V} \;\; \text{in} \;\; \text{acid}$$

This potential has not been experimentally measured since F_2 is unstable in aqueous solution, reacting rapidly to give HF and O_2.

$$2\,F_2 \; + \; 2\,H_2O \xrightarrow{\text{fast}} 4\,HF \; + O_2$$

When a potential is missing from a Latimer diagram, it may always be calculated by constructing a thermodynamic cycle involving the known and unknown potentials, as explained in Note **3.7.1** at the bottom of this page.

Disproportionation

Latimer diagrams are useful for determining if a species is thermodynamically stable or will undergo disproportionation. **Disproportionation** occurs when a species undergoes a redox reaction with itself to produce two or more stable products. For instance, in basic solution ReO_3 can undergo disproportionation to ReO_4^- and $ReO_2{\cdot}2H_2O$.

$$2Re^{VI}O_3 + 2H_2O \rightarrow Re^{VII}O_4^- + Re^{V}O_2 \cdot 2H_2O$$

As with all redox reactions, disproportionation reactions are thermodynamically favored when they possess a positive reaction potential. To see when this will be the case it is helpful to separate the disproportionation reaction into its half reactions:

$$\underset{\text{Reduction}}{:} \; Re^{VI}O_3 + H_2O + 2H^+ + e^- \rightarrow Re^{V}O_2 \cdot 2H_2O \qquad E° = -0.446V$$

$$\underset{\text{Oxidation}}{:} \; Re^{VI}O_3 + H_2O \rightarrow Re^{VII}O_4^- + 2H^+ + e^- \qquad E° = +0.889V$$

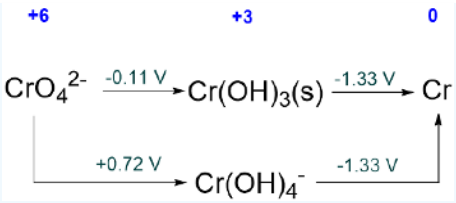
$$\text{Sum} : 2Re^{VI}O_3 + 2H_2O \rightarrow Re^{VII}O_4^- + Re^{V}O_2 \cdot 2H_2O \qquad E° = -0.446V + 0.889V = +0.443V$$

Notice that the disproportionation of ReO_3 in basic solution is favored because the favorable reaction potential for ReO_3 oxidation is larger in magnitude than the negative oxidation potential for ReO_3 reduction.

The ReO_3 disproportionation reaction is a specific instance of a general case. Any species possessing a standard reduction potential that is more positive than the standard reduction potential leading to their formation is thermodynamically unstable with respect to disproportionation. This situation is easy to recognize using a Latimer diagram; species are unstable to disproportionation (will disproportionate) if the potential on their right is more positive than that on their left.

✔ Example 3.7.1

The Latimer diagram that has been reported for Cr in pH 14 aqueous solution is given below. Which, if any, species are unstable with respect to disproportionation?



Solution

All of the species are stable with respect to disproportionation since all the potentials on the right of all the Cr^{3+} intermediates are less than those on their left.

Comparing Redox Chemistry with Latimer Diagrams

Acidic and Basic Conditions

Latimer diagrams are useful for comparing the redox chemistry of an element under different conditions (typically pH 0 and pH 14). This is well-illustrated by the Latimer diagrams of chromium explored in Examples **3.7.1** and **3.7.2** above. Another simple example involves the acidic and basic Latimer diagrams of mercury shown in Figure **3.7.4**.

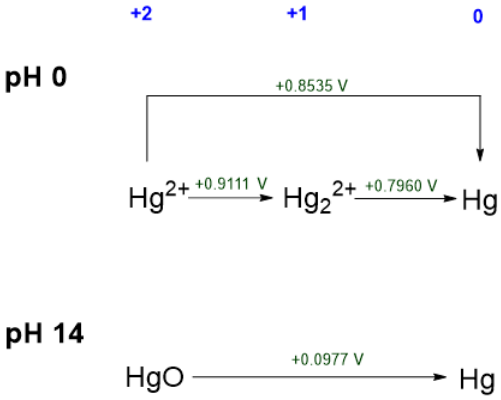


Figure**3.7.4**: Latimer diagrams for mercury in aqueous solution.

From Scheme **3.7.*IV***, several things are clear about mercury's redox chemistry under acidic and basic conditions:

- Mercury(I) ion, Hg_2^{2+}, is thermodynamically stable under acidic conditions, but it is not likely stable under basic conditions. This may be inferred from its absence in the pH 14 diagram, which suggests that it is not readily formed under basic conditions.
- Elemental mercury is the thermodynamically most stable form of the element under both acidic and basic conditions. This may be inferred because the standard reduction potential for all mercury +2 and +1 species is positive.
- In both its +1 and +2 oxidation states (Hg^{2+} and Hg_2^{2+} ions), mercury is a fairly powerful oxidant under acidic conditions (with **E°** 0.796 - 0.9111 V). In contrast, under basic conditions the +2 form of mercury (HgO) is only a weak oxidant **E°** = 0.0977 V.
- All of the mercury species represented are thermodynamically stable towards disproportionation.

Comparing Elements Under Similar Conditions

Latimer diagrams are useful for comparing the redox chemistry of different elements under similar conditions. For instance, the redox behavior of mercury and its congeners in acid solution may be easily compared using the Latimer diagrams. From Figure **3.7.5**, it is clear that Zn and Cd exhibit similar redox behavior. Both should dissolve at pH 0 to give dications. In contrast, elemental mercury should be stable towards acid. Mercury is also the only group 12 element for which the +1 oxidation state is stable.

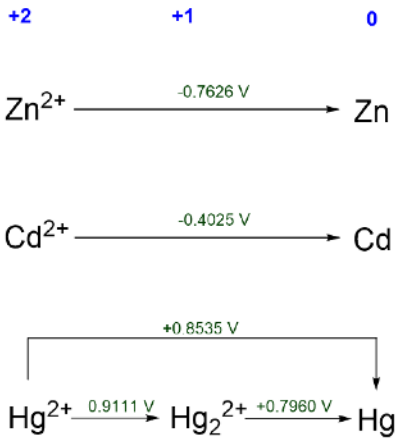


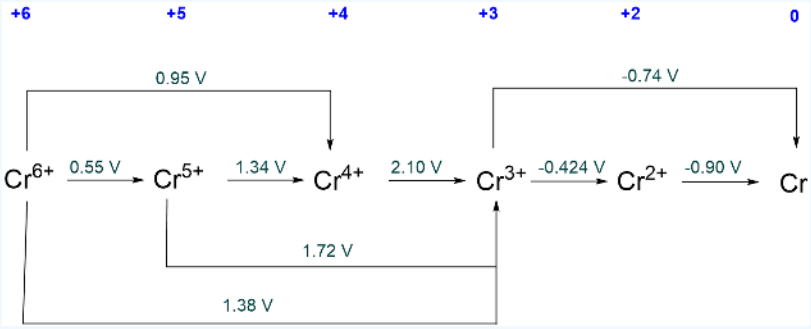
Figure **3.7.5**. Latimer diagrams for the group 12 elements in pH 0 aqueous solution.

As the examples above indicate, Latimer diagrams are helpful summaries of elements' redox chemistry, but it still requires a fair bit of careful reading to use them to make sense of trends in elements' redox chemistry or to trace out the disproportionation products of a given redox state. The published diagrams also tend to be limited to describing the redox chemistry of the elements under conditions of extreme pH. Fortunately, a variety of graphical representations of elements' redox chemistry have been developed that are particularly useful for estimating the dominant form of an element under a given set of conditions and for making sense of trends in elements' redox chemistry. These graphical methods will be described in the next two sections.

Problems

? Exercise 3.7.1

The Latimer diagram for Cr in pH 0 aqueous solution is given below. Which, if any, species are unstable with respect to disproportionation?

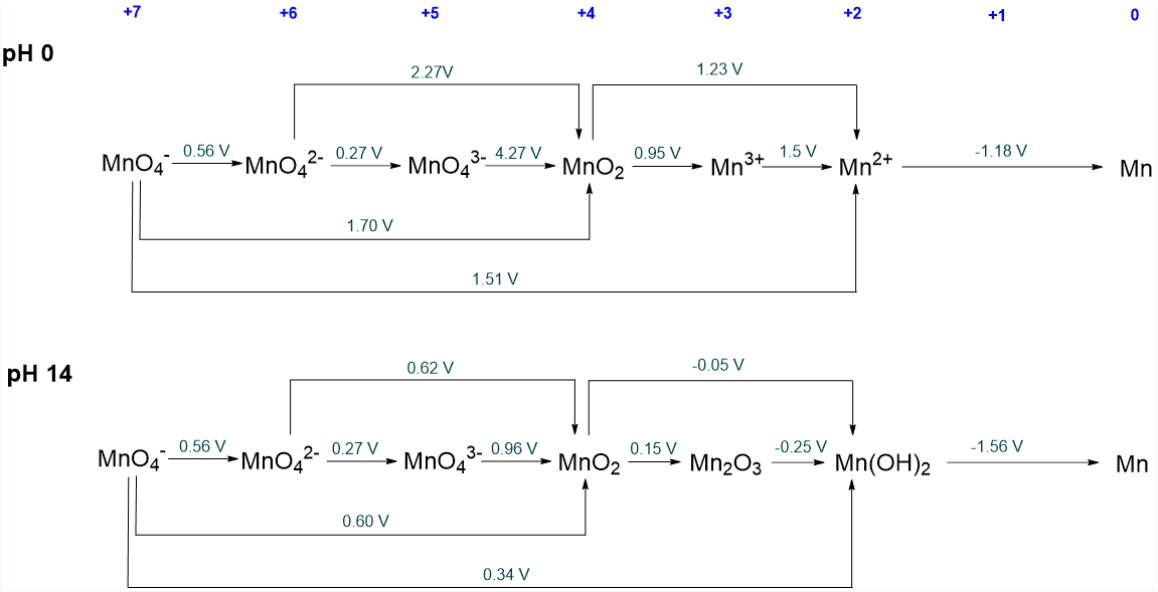


Answer

Both Cr^{5+} and Cr^{4+} are unstable towards disproportionation since the potentials on their right (for their reduction) are greater than the potentials on their left (for their formation by reduction).

? Exercise 3.7.2

Which manganese species are unstable with respect to disproportionation in aqueous solution under acidic and basic conditions? What will each of these metastable species give on disproportionation? The Latimer diagrams for manganese are given below.



Answer

Under acidic conditions the following species are unstable with respect to disproportionation:

MnO_4^{2-} is unstable with respect to disproportionation to MnO_4^- and MnO_2. MnO_4^{3-} is unstable with respect to MnO_4^{2-} and MnO_2. However, since MnO_4^{2-} is unstable with respect to disproportionation the ultimate products of the disproportionation will be MnO_4^- and MnO_2. Mn^{3+} is unstable towards disproportionation to MnO_2 and Mn^{2+}.

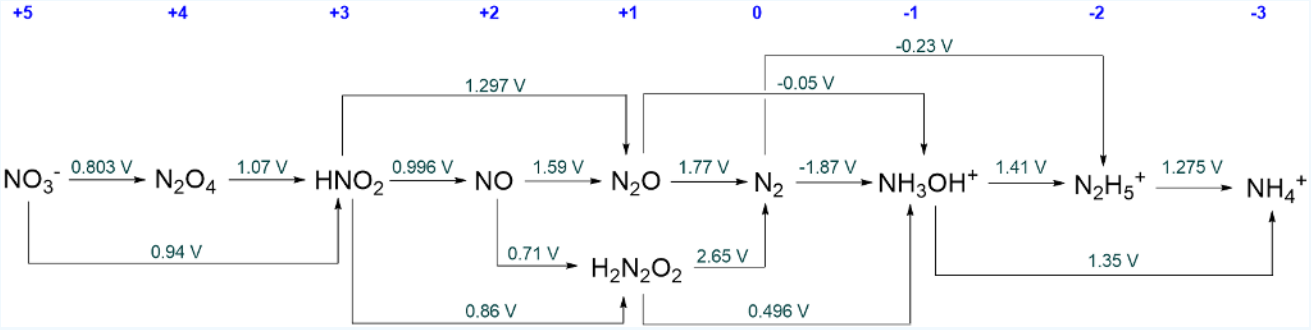
Notice that the +3 oxidation state of Mn is stable under basic conditions but not acidic ones.

MnO_4^{2-} is unstable with respect to disproportionation to MnO_4^- and MnO_2. MnO_4^{3-} is unstable with respect to MnO_4^{2-} and MnO_2. However, since MnO_4^{2-} is unstable with respect to disproportionation, the ultimate products of the disproportionation will be MnO_4^- and MnO_2.

Under basic conditions the following species are unstable with respect to disproprtionation:

Exercise 3.7.3

Which nitrogen species in the Figure **3.7.1**, (which for convenience is reproduced below) are unstable with respect to disproportionation?



Answer

They will be all the intermediate species for which the redox potential on their right is more positive than that on their left. These are N_2O_4, HNO_2, NO, N_2O, $H_2N_2O_2$, and NH_3OH^+.

? Exercise 3.7.4

As far as you are able, determine what each metastable nitrogen species will disproportionate to at pH 0.

Answer

Initially the metastable species will disproportionate to give their immediate neighbors in the Latimer diagram.

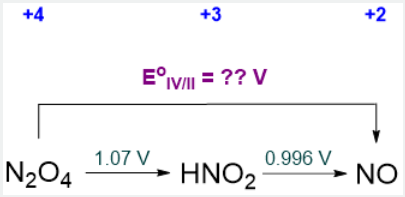
However, many of these neighbors are themselves metastable with respect to disproportionation, and so ultimately disproportionation will only stop when species that are stable towards disproportionation are reached.

In the case of N_2O_4, HNO_2, NO, N_2O, and $H_2N_2O_2$, disproportionation will ultimately give NO_3^- and N_2.

For NH_3OH^+, disproportionation will give N_2 and N_2H_5.

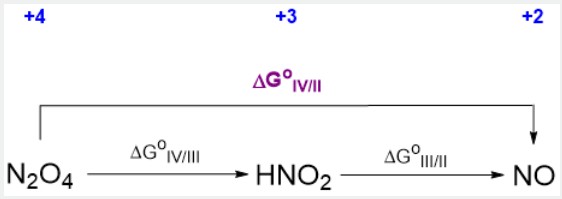
Note 3.7.1.

Potentials that are not shown in a Latimer diagram may always be calculated by constructing a **thermodynamic cycle**. Consider the interconversion of N_2O_4 to NO, $E^\circ_{IV/II}$, the value of which is not given in the standard nitrogen Latimer diagram presented in Scheme **3.7.*sfII***. Part of that diagram is reproduced as Scheme **3.7.VI** below.



Scheme **3.7.VI**. Partial Latimer diagram for nitrogen in acid.

The relevant thermodynamic cycle that may be used to calculate the unknown potential involves the free energies and is depicted in Scheme **3.7.VII**.

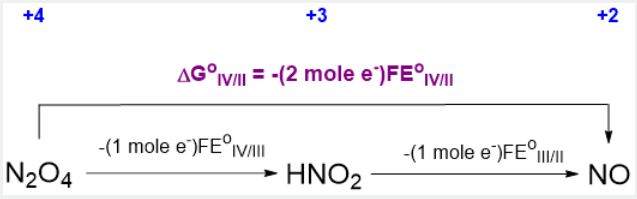


Scheme **3.7.VII**. Thermodynamic cycle that may be used to determine $E^\circ_{N_2O_4 \rightarrow NO}$.

The free energy for each conversion step in the cycle is related to the corresponding potential by the relationship

$$\Delta G^\circ = nFE^\circ$$

where n is the number of electrons involved in each step. With this substitution, the thermodynamic cycle above may be converted to the one shown in Scheme **3.7.VIII**.



Scheme **3.7.VIII**. Thermodynamic cycle expressed in terms of standard potentials.

From Scheme **3.7.VIII** it may be seen that

$$\Delta G^\circ_{IV/II} = -(2 \text{ mol } e^-)FE^\circ_{IV/II} = -(1 \text{ mol } e^-)FE^\circ_{IV/III} - (1 \text{ mol } e^-)FE^\circ_{III/II}$$

Cancelling the constant F and replacing the unknown potentials with the values in Scheme **3.7.VI** gives

$$-(2\ \text{mol}\ e^-)E^\circ_{IV/II} \quad = \quad -(1\ \text{mol}\ e^-)(1.07\ \text{V}) \quad - \quad (1\ \text{mol}\ e^-)(0.996\ \text{V})$$

from which $E^\circ_{IV/II}$ may be calculated, giving $E^\circ_{IV/II}$ = +1.033 V.

References

1. All standard reduction potentials are taken from Bard, A. J.; Parsons, R.; Jordan, J. Standard potentials in aqueous solution. M. Dekker: New York, 1985.

3.7: Latimer Diagrams is shared under a CC BY-NC-SA 4.0 license and was authored, remixed, and/or curated by Kathryn A. Newton, Northern Michigan University.

- **8.1.4.1: Latimer Diagrams summarize elements' redox properties on a single line** by Stephen M. Contakes is licensed CC BY 4.0.

3.8: Frost Diagrams

Frost diagrams show how stable an element's redox states are relative to the free element

Frost diagrams represent how stable an element's redox states are relative to the free element. In a Frost diagram, a proxy for the free energy relative to that of the free element (oxidation state zero) is plotted as a function of oxidation state. To avoid ambiguity, sometimes the points are labeled with the identity of the chemical species involved.

The proxy used in place of the free energy is $\boldsymbol{NE°}$, sometimes expressed as $\boldsymbol{nE°}$. On this page $\boldsymbol{N}$ will be used in place of $\boldsymbol{n}$ to avoid confusion with the common use of $\boldsymbol{n}$ in redox chemistry to denote the number of electrons involved in individual oxidation or reduction reaction steps.

In Frost diagrams the quantity $\boldsymbol{NE°}$ is used since it is proportional to the standard free energy change for conversion of the free element to that oxidation state.

In $\boldsymbol{NE°}$

- $\boldsymbol{N}$ is the oxidation state.
- $\boldsymbol{E°}$ is the standard *reduction potential* associated with *interconversion between the free element and that oxidation state*.

For a proof that $\boldsymbol{NE°}$ is proportional to the free energy of an element's oxidation state and more information on how $\boldsymbol{NE°}$ may be calculated, see Note **3.8.1** at the end of this page.

Frost diagrams allow for rapid estimation of the relative stability of elements' redox states.

Because Frost diagrams directly show oxidation states' relative stabilities, they enable the rapid assessment of the following:

1. *The relative stability of an element's oxidation states under a given set of conditions.* Since $\boldsymbol{NE°}$ is a measure of thermodynamic stability, the lower its value the more stable the state. Moreover, since $\boldsymbol{NE°}$ measures stability relative to the free element, negative values of $\boldsymbol{NE°}$ indicate that a state is more stable than the element, while positive values indicate that the state is less stable.

Consider the Frost diagram for copper at pH 0 shown in Figure **3.8.1**.

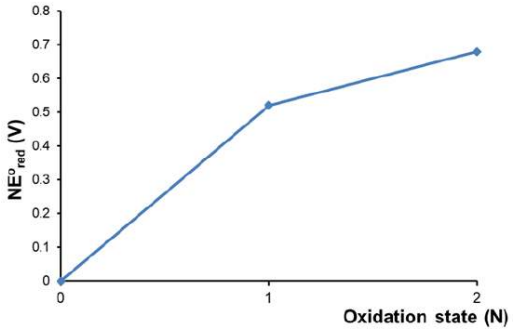


Figure **3.8.1**. Frost diagram for copper in aqueous acid. (CC BY-SA 4.0 International; Stephen Contakes)

As can be seen in Figure **3.8.1**, Cu^{+} and Cu^{2+} are both higher in free energy ($\propto \boldsymbol{NE°}$) than free Cu. This is consistent with copper's status as a noble metal that can only be dissolved in acid with the aid of oxidizing agents like O_2, H_2O_2, or NO_3^- (*e.g.*, as in HNO_3).

The acidic Frost diagram of Nickel shown in Figure **3.8.2** provides an example of a metal which dissolves in acid under otherwise nonoxidizing conditions (*i.e.*, without the aid of oxidants like O_2 or H_2O_2).

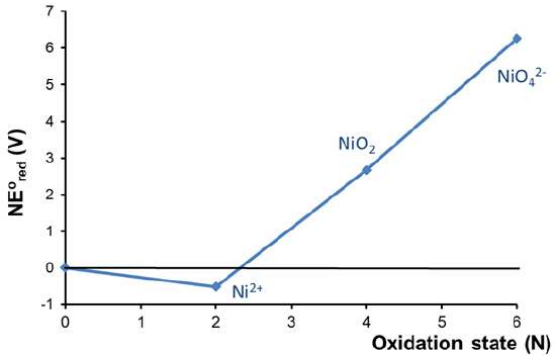


Figure **3.8.2**. Frost diagram for nickel in aqueous acid. (CC BY-SA 4.0 International; Stephen Contakes)

In this case the diagram shows that the Ni^{2+} oxidation state is lower in free energy than the free element, indicating that Ni spontaneously dissolves in acid to give Ni^{2+}. The diagram also reveals that higher nickel oxidation states (+4 and +6) are known but unstable with respect to both Ni^{2+} and free nickel.

Example 3.8.1. Interpreting a Frost Diagram

Consider the Frost diagram of Cr in acid shown in Figure **3.8.3**. What can be determined about the relative stability of chromium's oxidation states in acid?

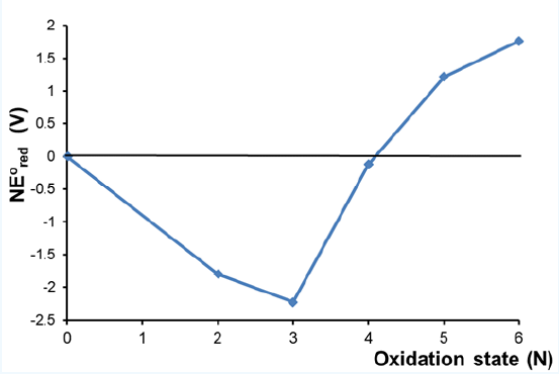


Figure **3.8.3**. Frost diagram for Cr in acidic solution. This work by Stephen Contakes is licensed under a Creative Commons Attribution 4.0 International License.

Solution

A cursory glance at the diagram reveals that

- The +3 oxidation state is the most stable since it has the lowest $\boldsymbol{NE°}$.
- The +2, +3, and +4 oxidation states are all more stable than the free element while the +5 and +6 oxidaton states are less stable.
- The diagram also reveals information about the susceptibility of the chromium species to undergo disproportionation and comproportionation reactions. For details see example 2.

2. *The redox behavior of an element under different conditions.* Consider the Frost diagrams of sulfur at pH 0 and 14 shown in Figure **3.8.4**.

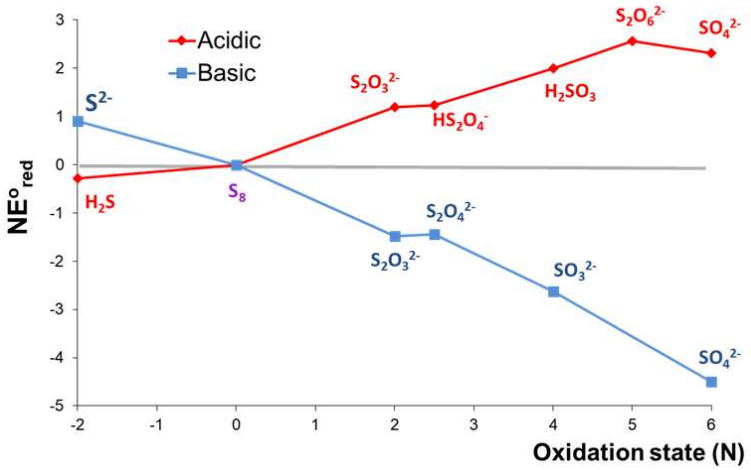


Figure **3.8.4**. Frost diagrams for sulfur at pH 0 and 14. This work by Stephen Contakes is licensed under a Creative Commons Attribution 4.0 International License.

As can be seen in Figure **3.8.4**, the relative stabilities of high and low sulfur oxidation states are roughly inverted between acidic and basic conditions. Under basic conditions, the oxidized forms of sulfur are all more stable than the free element, with sulfate most stable overall. In contrast, H_2S is the most stable form of sulfur under acidic conditions, while all the oxidized forms of sulfur are less stable than the free element.

3. *Comparison of the redox behavior of a series of elements.* Consider the pH 0 Frost diagrams of the group 6 elements shown in Figure **3.8.5**.

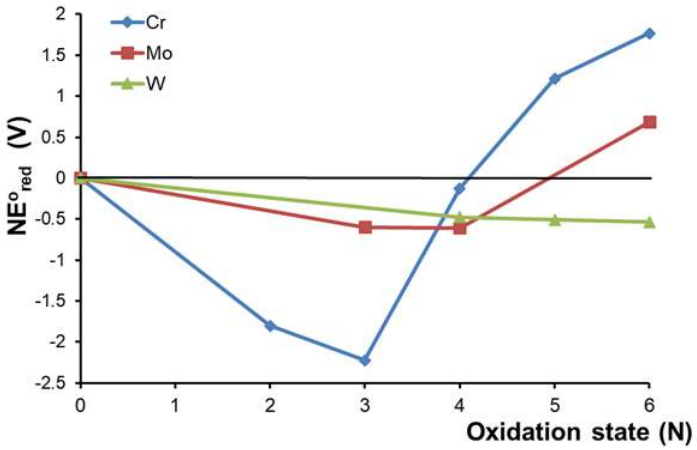


Figure **3.8.5**. Frost diagrams for the group 6 elements at pH 0. This work by Stephen Contakes is licensed under a Creative Commons Attribution 4.0 International License.

Several trends may be noted from the data in Figure **3.8.5**. First, on moving down the group from Cr to W, there is an increasing preference for higher oxidation states, with the most stable forms being Cr^{4+}, Mo^{4+}, and W^{6+}. Second, the coincidentally low stabilization of Cr^{4+} aside, the stabilization or destabilization of oxidation states relative to the free element decreases down a group - *i.e.*, Cr^{4+} is stabilized relative to Cr more so than Mo^{4+} is relative to Mo, and W^{6+} is stabilized relative to W even less so.

One of the most striking examples of the utility of Frost diagrams for comparing the empirical redox behavior of a series of elements involves the first row transition elements, the pH 0 Frost diagrams for which are shown in Figure **3.8.6**.[2,3] A number of trends may be noted. For example, as in the case of the group 6 elements, a shift in the most stable oxidation state may be observed, with Sc through Cr exhibiting a preference for the +3 oxidation state and Mn through Cu the +2 oxidation state. The diagram also shows that Sc through Mn lose all their valence electrons to form d^0 species, while similar species have not been observed for later members of the series (although an iron(VII) complex has been isolated[4] and iron's heavier cogeners, Ru and Os, do form d^0 species, RuO_4 and OsO_4).

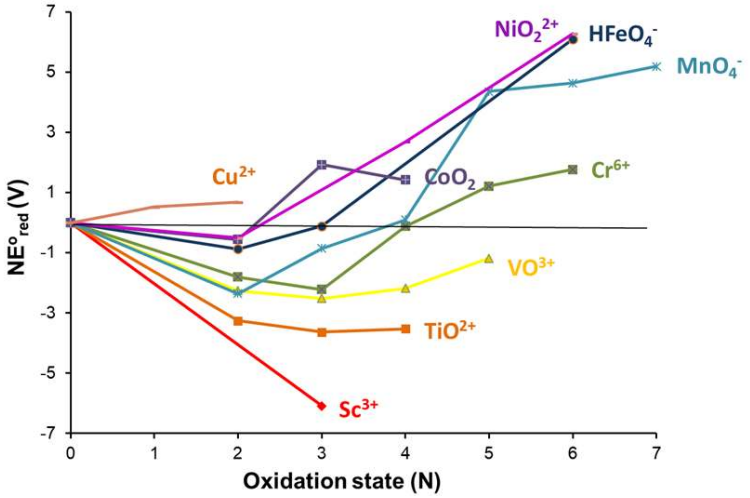


Figure **3.8.6**. Frost diagrams for the first transition series at pH 0. This work by Stephen Contakes is licensed under a Creative Commons Attribution 4.0 International License.

4. *Whether a redox state is unstable towards disproportionation* may be determined from the relative positions of that state and the states on either side of it on the diagram.[5] Remember that in **disproportionation** a species reacts with itself to produce two or more stable products. For example, NO can in principle undergo disproportionation in aqueous acid to give nitrate and N_2.

$$10\ NO\ +\ 2H_2O \rightarrow 3\ N_2 + 4\ NO_3^- + 4H^+$$

A Frost diagram can be used to determine when a redox state is unstable with respect to such disproportionation because the slope of a line between any two points is equal to the standard *reduction* potential interconverting the species involved. This means that *if a line is drawn between any two redox states then any states above the line will be unstable towards disproportionation to those states.* This is because in that case the potential for the reduction half reaction in the disproportionation will be more positive than the potential for the oxidation half reaction, rendering the overall reaction potential positive and so spontaneous. For proof of a specific example see Exercise 1.

To see how a disproportionation analysis may be performed using a Frost diagram, it can be helpful to examine the pH 0 Frost diagram for Cr more carefully. In this case the instability of Cr^{4+} and Cr^{5+} towards disproportionation may be revealed by placing a tie line drawn between the Cr^{3+} and Cr^{6+} states, as shown in Figure **3.8.7*a***.

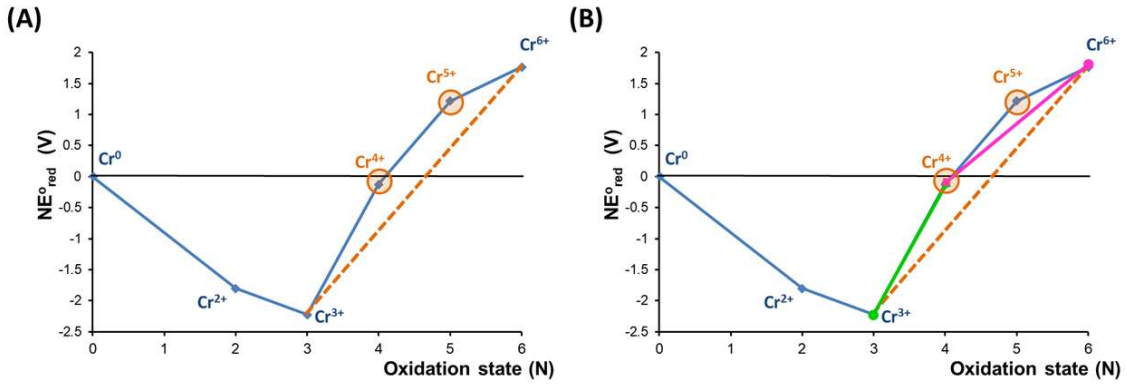


Figure **3.8.7**. (a) Frost diagram for Cr in acidic solution showing that the Cr^{4+} and Cr^{5+} states lie above a tie-line between the Cr^{3+} and Cr^{6+} states. (b) In the case of Cr^{4+}, disproportionation is favored because the $Cr^{4/3+}$ potential (slope of the green tie-line connecting the Cr^{4+} and Cr^{3+} states) is larger than the $Cr^{6/4+}$ potential (slope of the pink tie-line connecting Cr^{6+} and Cr^{4+}). This work by Stephen Contakes is licensed under a Creative Commons Attribution 4.0 International License.

As shown in Figure **3.8.7*a***, the Cr^{4+} and Cr^{5+} states are unstable towards disproportionation because they lie above a tie-line between the Cr^{3+} and Cr^{6+} states. This is because the potential for Cr^{4+} reduction to Cr^{3+}, represented by the tie-line connecting those species in Figure **3.8.7*b***, is larger than the potential for Cr^{6+} reduction to Cr^{4+}, as indicated by the lower slope of the tie-line connecting Cr^{6+} and Cr^{4+}.

Sometimes states which are unstable towards disproportionation correspond to concave down points on the Frost diagram. However, as this is not always the case, a systematic approach for finding metastable redox states is recommended. An example of such an approach is given in Example 3.8.2.

✔ Example 3.8.2. Systematic identification of Mn redox states that are unstable towards disproportionation in acid.

Consider the Frost diagram of Mn in acid shown in Figure 3.8.8. Which, if any, of manganese's oxidation states are unstable towards disproportionation at pH 0?

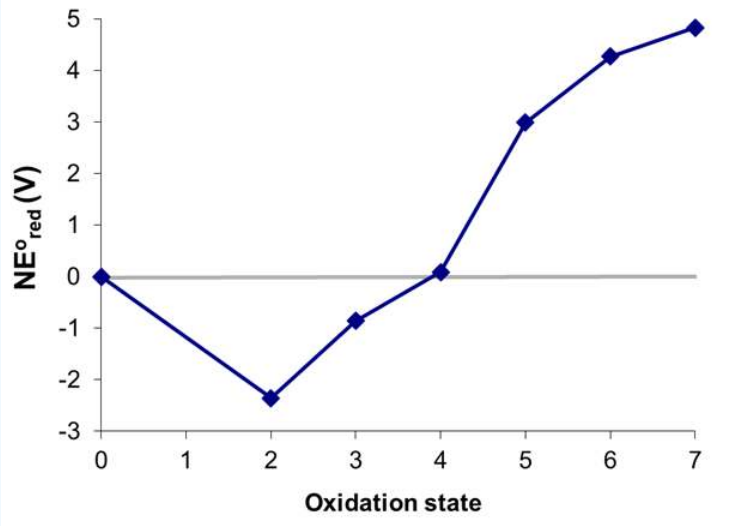
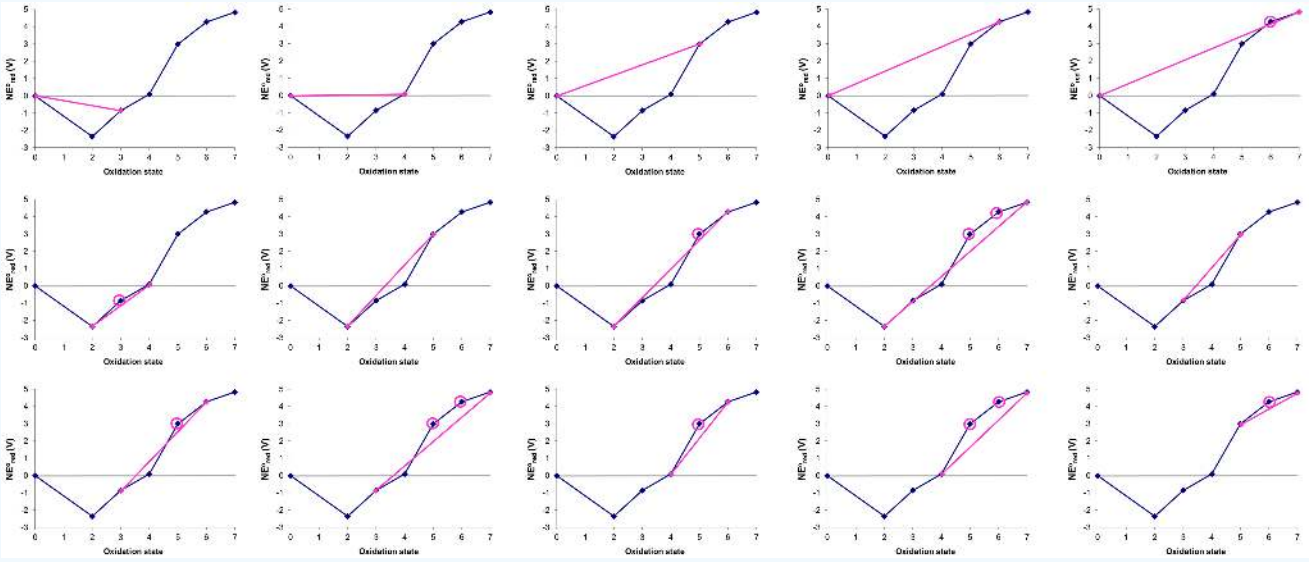


Figure 3.8.8. Frost diagram for Mn at pH 0. This work by Stephen Contakes is licensed under a Creative Commons Attribution 4.0 International License.

Solution

States that are unstable towards disproportionation may be identified by drawing all the possible tie-lines between nonadjacent states spanning the lowest and highest oxidation states in the diagram, which in this case are Mn^0 and Mn^7. The possible permutations beginning with Mn^0 are given below



In the figure above the states that are thermodynamically unstable towards disproportionation (circled) are +3, +5, and +6.

The figure above by Stephen Contakes is licensed under a Creative Commons Attribution 4.0 International License.

4. Whether *two species are unstable towards comproportionation* may be assessed from the relative positions of the two species and all intervening species on the diagram. In **comproportionation,** two related species react to give a more stable product. For example, NO and hydrazinium ion can in principle undergo comproportionation in aqueous acid to give N_2.

$$2\ NO\ +\ N_2H_5^+ \rightarrow 2\ N_2\ +\ 2\ H_2O\ +\ H^+$$

A Frost diagram may be used to determine when two species are thermodynamically favored to undergo comproportionation. *Draw a line between the two species on the diagram. If there are states below the line then the two species are unstable towards forming those states by comproportionation.* Again, it can be helpful to examine the acidic condition Frost diagram for Cr to see how this works. In this case consider a tie line drawn between the Cr^{4+} and Cr^{2+} states, as shown in Figure **3.8.9*a***.

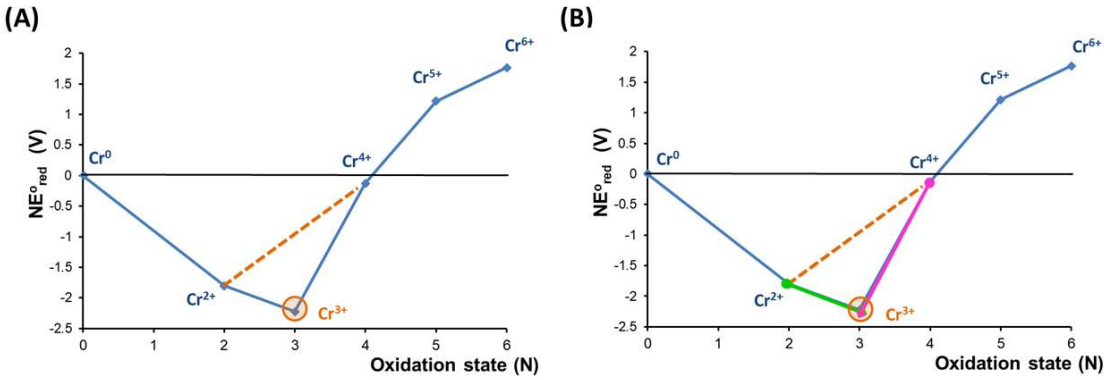


Figure **3.8.9**. (a) Frost diagram for Cr in acidic solution showing that the Cr^{3+} redox state lies below a tie-line between the Cr^{2+} and Cr^{4+} states. (b) The slope of the green line connecting the Cr^{2+} and Cr^{3+} states is less than that of the pink line connecting the Cr^{3+} and Cr^{4+} states. This work by Stephen Contakes is licensed under a Creative Commons Attribution 4.0 International License.

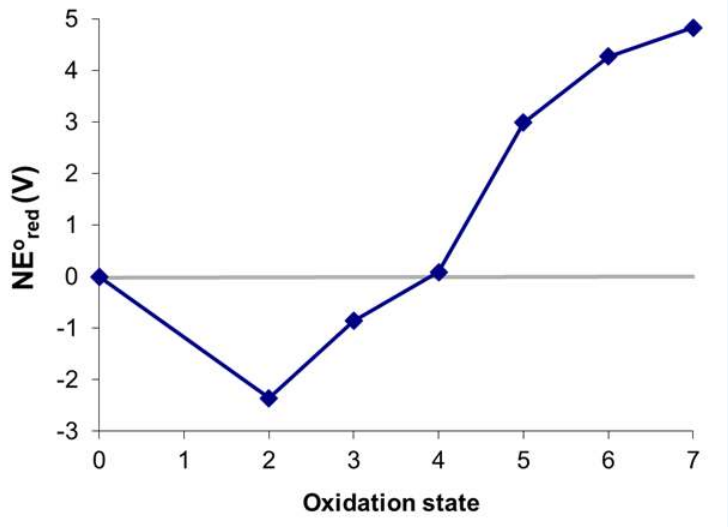
As shown in Figure **3.8.9*a***, a mixture of Cr^{2+} and Cr^{4+} is unstable towards comproportionation because on the Frost diagram Cr^{3+} lies below the tie-line between Cr^{2+} and Cr^{4+}. This shows that the standard potential for reduction of Cr^{3+} to Cr^{2+} (equal to the slope of the line connecting those states) is less than that for the reduction of Cr^{4+} to Cr^{3+} (again, equal to that of the line connecting the states), in consequence of which the potential for comproportionation will be positive.

The analysis of a Frost diagram for all favorable comproportionations is similar to the analysis used to detect species that are unstable towards disproportionation. The products of thermodynamically favored comproportionations are sometimes concave up points but since this is not always the case a systematic approach should be used. An example is given in Example **3.8.3**.

✔ Example **3.8.3**. Systematic identification of pairs of Mn redox states that are unstable towards comproportionation in acid.

Consider the Frost diagram of Mn at pH 0 in Figure **3.8.8** of Example **3.8.2**, which for convenience is reproduced below. Which, if any, pairs of manganese species are unstable towards comproportionation under these conditions and what products could they form?

https://chem.libretexts.org/@go/page/553796



Solution

The possible tie-lines were already identified in Exercise 3.8.2.

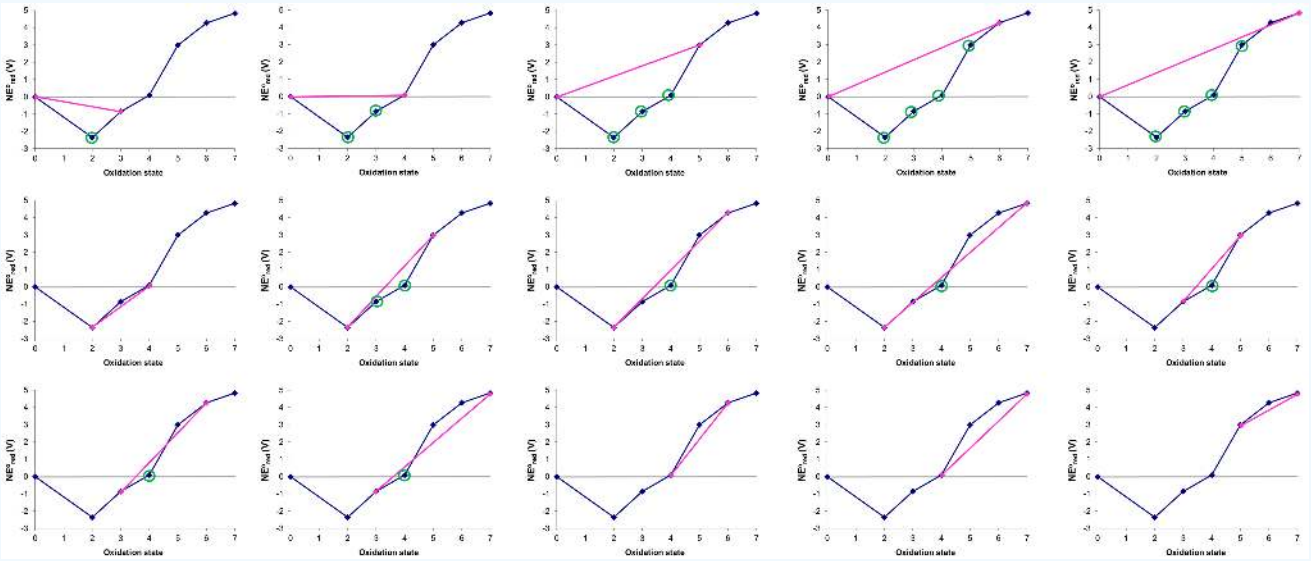


Figure above: the lower energy comproportionation products that species form are circled in green. The comproportionations identified involve the following pairs of oxidation states:

- 0 and +3 → +2
- 0 and +4 → +2 or +3
- 0 and +5 → +2 or +3 or +4
- 0 and +6 → +2 or +3 or +4 or +5
- 0 and +7 → +2 or +3 or +4 or +5
- +2 and +5 → +3 or +4
- +2 and +6 → +4
- +2 and +7 → +4
- +3 and +5 → +4
- +3 and +6 → +4
- +3 and +7 → +4

The figures in this problem are by Stephen Contakes and licensed under a Creative Commons Attribution 4.0 International License.

Additional analysis is needed to determined the thermodynamic product of many comproportionation reactions - but fortunately such an analysis is not necessary to understand the descriptive chemistry of the elements.

This list of possible comproportionation reactions identified in Example **3.8.3** raises several interesting questions:

1. When more than one comproportionation product is possible, which one(s) will be formed?

    In this case the answer is that all species can be formed in thermodynamically favored comproportionation reactions. However, the system still only possesses one state of lowest free energy. For example, depending on the stoichiometry of the reactants, the lowest energy products that can be formed from a mixture of Mn^0 and Mn^{VII} might be a mixture of Mn^{II} and Mn^{IV}. The identification of this state in a given case is complicated and involves minimizing the system energy subject to the constraints of a mass and charge balance. Fortunately, such an analysis is not needed to make sense of the chemistry of the elements.

    What should be noted is that if a comproportionation product can itself undergo a comproportionation reaction with one or more reactants, then that reaction can take place in solution. For instance, if the case of the comproportionation between Mn^0 and Mn^{IV} produces Mn^{III}, then that Mn^{III} can undergo an additional comproportionation reaction with Mn^0 to give Mn^{II}.

2. What happens if a species formed by comproportionation is susceptible to disproportionation?

    If the conditions allow, then that species will undergo disproportionation. Again, thermodynamic measures like those shown on Frost diagrams describe what can happen, not what will occur under a given set of conditions.

Exercises

? Exercise 3.8.1

Using the simplified Latimer diagram for Cr in aqueous acid, reproduced below, verify that the disproportionation of Cr^{4+} to Cr^{3+} and Cr^{6+} is thermodynamically spontaneous.



Answer

The disproportionation of Cr^{4+} to Cr^{3+} and Cr^{6+} is the sum of two processes:

$$Cr^{4+}\text{reduction}: \quad Cr^{4+} + e^- \rightarrow Cr^{3+} \qquad E^\circ_{Cr^{4/3+}} = 2.10\ V$$

$$Cr^{4+}\text{oxidation}: \quad Cr^{4+} \rightarrow Cr^{6+} + 2e^- \qquad E^\circ = -E^\circ_{Cr^{6/4+}}$$

$$\text{Sum}: \quad 3Cr^{4+} + \rightarrow Cr^{6+} + 2Cr^{3+} \qquad E^\circ_{disproportionation} = E^\circ_{Cr^{4/3+}} - E^\circ_{Cr^{6/4+}}$$

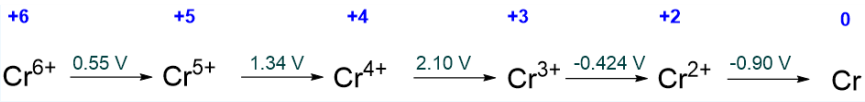
The value of $E^\circ_{Cr^{6/4+}}$ is just the sum of the $Cr^{6/5+}$ and $Cr^{5/4+}$ reduction potentials (+0.55 V + 1.34 V) or +1.89 V. Consequently,

$$E^\circ_{disproportionation} = E^\circ_{Cr^{4/3+}} \qquad E^\circ_{Cr^{6/4+}} = 2.10\ V - 1.89\ V = +0.21\ V$$

which is spontaneous.

? Exercise 3.8.2

Using the simplified Latimer diagram for Cr in aqueous acid, reproduced below, verify that the comproportionation of Cr^{2+} and Cr^{4+} to Cr^{3+} is thermodynamically spontaneous.



Answer

The comproportionation of Cr^{2+} and Cr^{4+} to Cr^{3+} is the sum of two processes:

$$Cr^{4+}\text{reduction}: \quad Cr^{4+} + e^- \rightarrow Cr^{3+} \qquad E^\circ_{Cr^{4+/3+}} = +2.10\ V$$

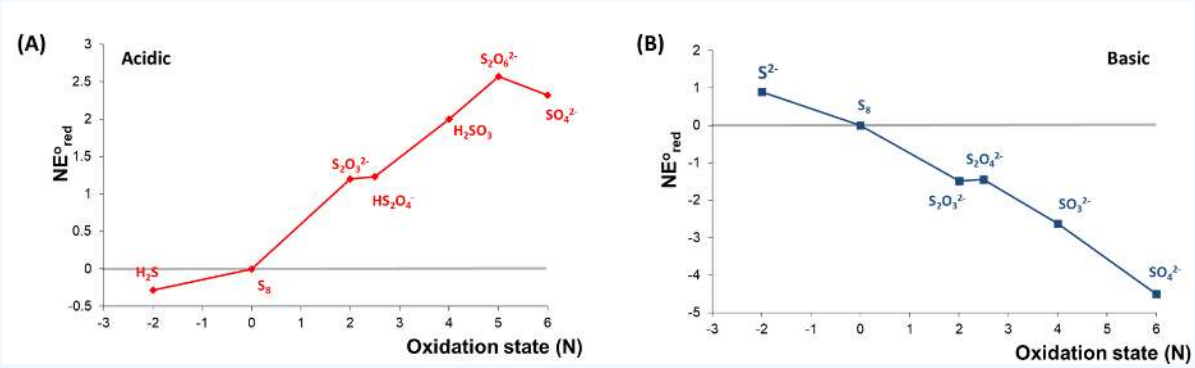
$$Cr^{2+}\text{oxidation}: \quad Cr^{2+} \rightarrow Cr^{3+} + e^- \qquad E^\circ = -E^\circ_{Cr^{3+/2+}} = -(-0.424\ V) = +0.424\ V$$

$$\text{Sum}: \quad Cr^{2+} + Cr^{4+} \rightarrow 2Cr^{3+} \qquad E^\circ_{\text{comproportionation}} = +2.10\ V + 0.424\ V = +2.524\ V$$

Since $E^\circ_{\text{comproportionation}}$ is positive, the comproportionation is spontaneous.

? Exercise 3.8.3. Identifying thermodynamically favored comproportionation and disproportionation reactions.

The Frost diagrams for acidic and basic solutions of sulfur are given below.



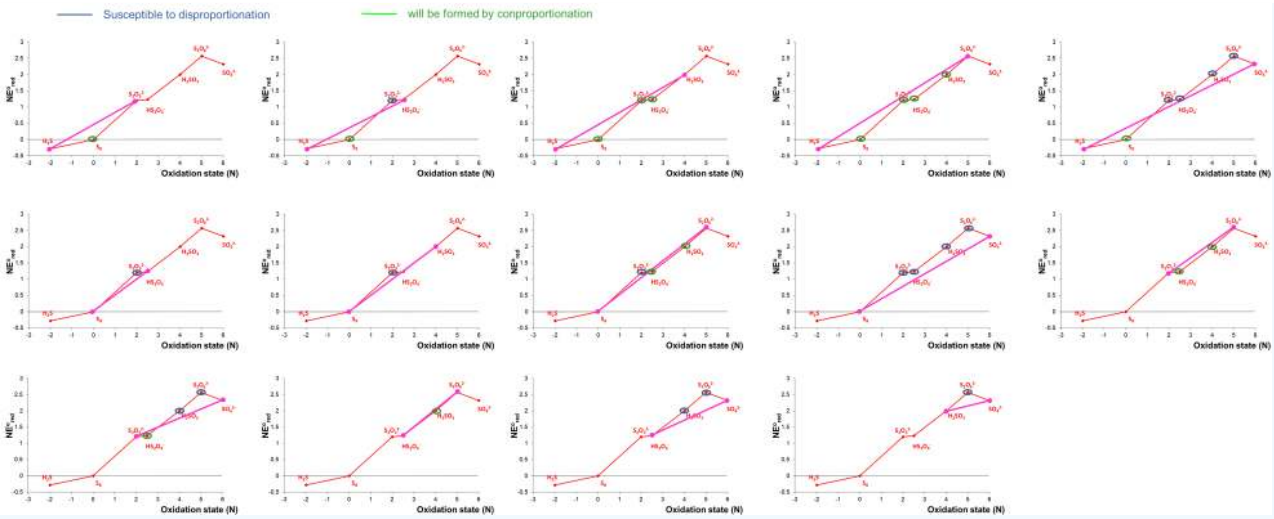
a. Identify any species that are unstable towards disproportionation under acidic or basic conditions.

b. Identify any species that can be formed by comproportionation under acidic or basic conditions.

Answer

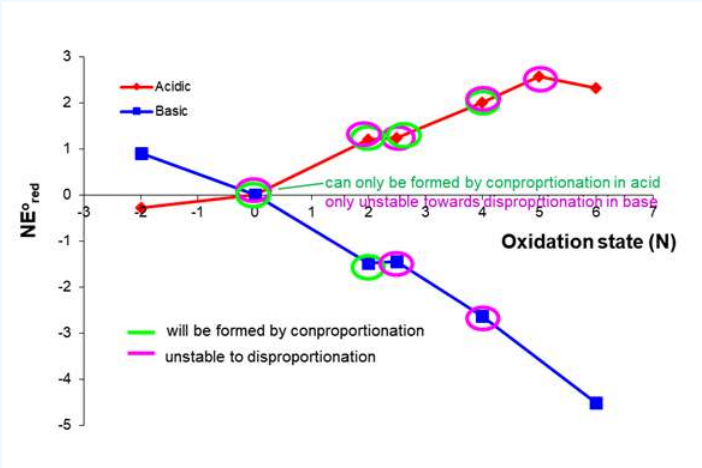
The species that are unstable towards *disproportionation* and *comproportionation* may be identified by constructing tie-lines between nonadjacent redox states and identifying any that fall above and below these lines. Species that are unstable to *disproportionation* will lie above a line; those that will be formed by *comproportionation* will lie below a line. Note that some species may be both capable of being formed by *comproportionation* and thermodynamically susceptible to *disproportionation.*

The possible tie-lines for acidic conditions are as follows:



Notice that in some cases it can be difficult to tell whether a point lies above or below a tie-line based on inspection alone. In these cases the relevant redox potential should be calculated to determine whether disproportionation or comproportionation is thermodynamically favored or even if the process is free energy neutral.

The possibilities for basic conditions are left as an exercise for the reader. To check your work the species that are susceptible to disproportionation and those which can be formed by comproportionation are summarized below.



The figures in this problem are by Stephen Contakes and licensed under a Creative Commons Attribution 4.0 International License.

Appendix

Note 3.8.1. Construction of a Frost Diagram.

Since Frost diagrams use $NE°$ as a proxy for oxidation free energy, the construction of a Frost diagram is a matter of calculating $NE°$ for each oxidation state, where $E°$ is the standard potential for the *formation of that oxidation state (O.S.)* from the free element. To see why this quantity is a useful proxy for oxidation state free energy, it is helpful to recognize that the oxidation state, N, is formally equal to the number of electrons that are *removed* from the free element when the oxidation state is formed. From this perspective the formation of negative oxidation states by adding electrons to the free element may be thought of as involving the removal of a negative number of electrons.

The free energy for formation of each oxidation state is determined as follows:

1. For free elements the free energy of formation, $E°$, and consequently $NE°$, are all by definition zero.

2. Negative oxidation states are formed by reduction of the free element

$$E + ne^- \rightarrow E^{O.S.} \qquad E^\circ = E^\circ_{red}$$

so that

$$\Delta G^\circ = -nFE^\circ_{red}$$

in which F is the Faraday constant.

In this case the oxidation state, N, is equal to $-n$ and the expression above becomes

$$\Delta G^\circ_{red} = F \times (NE^\circ)$$

from which it can also be seen why NE° is a useful proxy for free energy. It is proportional to ΔG°:

$$NE^\circ = \frac{1}{F}\Delta G^\circ_{red}$$

3. Positive oxidation states are formed by oxidation of the element:

$$E \rightarrow E^{O.S.} + ne^- \qquad E^\circ_{ox} = E^\circ = -E^\circ_{red}$$

in which the number of electrons, n, is equal to the oxidation state, N and

$$E^\circ_{ox} = E^\circ = -E^\circ_{red}$$

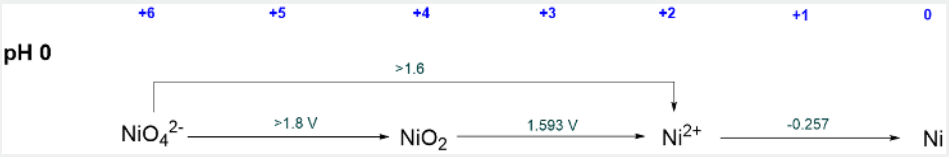
So that for positive oxidation states,

$$\Delta G^\circ_{ox} = -\Delta G^\circ_{red} = -(-nFE^\circ_{red}) = F(NE^\circ)$$

This is the same expression obtained for the negative oxidation states in which NE° is proportional to ΔG°.

From considering these cases, it is clear that as long as N is taken as the oxidation state and E° the associated standard reduction potential, the quantity NE° is proportional to the free energy.

In many cases the relevant standard reduction potentials are neither tabulated nor listed in the element's Latimer diagram. For example, in nickel's acidic Latimer diagram, the standard reduction potentials for formation of elemental Ni from NiO_4^{2-} or NiO_2 are not given.



In such cases the relevant reduction potential should be calculated by taking into account the fact that since free energy is a state function, the free energy for formation of that oxidation state is the sum of the free energies of the steps described in the Latimer diagram. For example, to calculate NE° for the formation of NiO_2, the following relationship may be used:

$$\Delta G^\circ_{NiO_2 \rightarrow Ni} = \Delta G^\circ_{NiO_2 \rightarrow Ni^{2+}} + \Delta G^\circ_{Ni^{2+} \rightarrow Ni}$$

But since $\Delta G = -nFE^\circ$, where n is the number of electrons involved in each reduction, then the above expression may be rewritten as

$$-n_{e^-,NiO_2 \rightarrow Ni} FE^\circ_{NiO_2 \rightarrow Ni} = -n_{e^-,NiO_2 \rightarrow Ni^{2+}} FE^\circ_{NiO_2 \rightarrow Ni^{2+}} + -n_{e^-,Ni^{2+} \rightarrow Ni} FE^\circ_{Ni^{2+} \rightarrow Ni}$$

which may be further simplified by cancelling the Faraday constant, F, from both sides, giving an expression for the desired value of NE°:

$$-n_{e^-,NiO_2 \rightarrow Ni} E^\circ_{NiO_2 \rightarrow Ni} = NE^\circ_{Ni \rightarrow NiO_2} = -n_{e^-,NiO_2 \rightarrow Ni^{2+}} E^\circ_{NiO_2 \rightarrow Ni^{2+}} + -n_{e^-,Ni^{2+} \rightarrow Ni} E^\circ_{Ni^{2+} \rightarrow Ni}$$

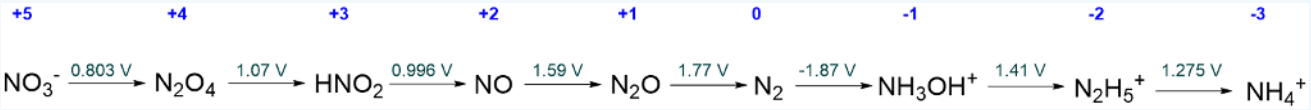
From this expression the value of $NE^\circ_{Ni \rightarrow NiO_2}$ may be calculated by inserting the relevant reduction potentials and number of electrons:

$$NE^{\circ}_{Ni \rightarrow NiO_2} = 2 \times (+1.593V) + 2 \times (-0.257V) = +2.672V$$

For complex cases it can be helpful to tabulate the calculations, as is done in the following example.

Example 3.8.1: Calculating the Frost Diagram for nitrogen in aqueous acid

Calculate the acidic Frost diagram of nitrogen from the information given in the simplified acidic Latimer diagram for nitrogen given below.



Solution

The value of NE° for each oxidation state is calculated as described in Table 3.8.1. The calculations follow the procedure:

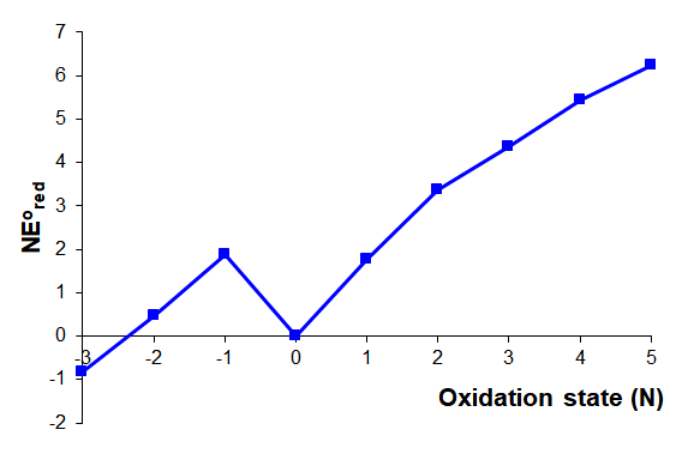
1. Set NE° = 0 for the free element.
2. Use NE° = O.S. × associated E° to calculate NE° for the lowest positive and negative oxidation states.
3. Iteratively use $NE^{\circ} = NE^{\circ}_{\text{last step}} + NE^{\circ}_{\text{one lower oxidation state}}$ to calculate NE° for all higher oxidation states.

Table 3.8.1: Calculation of NE° for each oxidation state of nitrogen.

Oxidation State	Step	$\mathbf{NE^\circ}$ =	Calculated as the sum of the steps	Notes
5	$N_2 \rightarrow NO_3^-$	$5 \times (E^\circ_{NO_3^- \rightarrow N_2})$	$\mathbf{N_2 \rightarrow N_2O_4 \rightarrow NO_3^-}$ $NE^\circ = 1 \times E^\circ_{NO_3^- \rightarrow N_2O_4} + 4 \times E^\circ_{N_2O_4 \rightarrow N_2}$ $NE^\circ = 1 \times E^\circ_{NO_3^- \rightarrow N_2O_4} + NE^\circ_{+4\ O.S.}$ $NE^\circ = 1 \times 0.803V + 5.426V = 6.229V$	Calculate NE° for the +4 oxidation state, NO, first. Then use it in this calculation.
4	$N_2 \rightarrow N_2O_4$	$4 \times (E^\circ_{N_2O_4 \rightarrow N_2})$	$\mathbf{N_2 \rightarrow HNO_2 \rightarrow N_2O_4}$ $NE^\circ = 1 \times E^\circ_{HNO_2 \rightarrow NO} + 3 \times E^\circ_{HNO_2 \rightarrow N_2}$ $NE^\circ = 1 \times E^\circ_{N_2O_4 \rightarrow HNO_2} + NE^\circ_{+3\ O.S.}$ $NE^\circ = 1 \times 1.07V + 4.356V = 5.426V$	Calculate NE° for the +3 oxidation state, NO, first. Then use it in this calculation.
3	$N_2 \rightarrow HNO_2$	$3 \times (E^\circ_{HNO_2 \rightarrow N_2})$	$\mathbf{N_2 \rightarrow NO \rightarrow HNO_2}$ $NE^\circ = 1 \times E^\circ_{HNO_2 \rightarrow NO} + 2 \times E^\circ_{NO \rightarrow N_2}$ $NE^\circ = 1 \times E^\circ_{NO \rightarrow N_2O} + NE^\circ_{+2\ O.S.}$ $NE^\circ = 1 \times 0.996V + 3.36V = 4.356V$	Calculate NE° for the +2 oxidation state, NO, first. Then use it in this calculation.
2	$N_2 \rightarrow NO$	$2 \times (E^\circ_{NO \rightarrow N_2})$	$\mathbf{N_2 \rightarrow N_2O \rightarrow NO}$ $NE^\circ = 1 \times E^\circ_{NO \rightarrow N_2O} + 1 \times E^\circ_{N_2O \rightarrow N_2}$ $NE^\circ = 1 \times E^\circ_{NO \rightarrow N_2O} + NE^\circ_{+1\ O.S.}$ $NE^\circ = 1 \times 1.59V + 1.77V = 3.36V$	Calculate NE° for the +1 oxidation state, NO, first. Then use it in this calculation.
1	$N_2 \rightarrow N_2O$	$1 \times E^\circ_{N_2O \rightarrow N_2}$	$\mathbf{N_2 \rightarrow N_2O}$ $NE^\circ = 1 \times E^\circ_{N_2O \rightarrow N_2}$ $NE^\circ = 1 \times +1.77V = +1.77V$	
0	None	0 V	$NE^\circ = 0V$ by definition.	Defined as 0 V
-1	$N_2 \rightarrow NH_3OH^+$	$(-1) \times E^\circ_{N_2 \rightarrow NH_3OH^+}$	$\mathbf{N_2 \rightarrow NH_3OH^+}$ $NE^\circ = (-1)E^\circ_{N_2 \rightarrow NH_3OH^+}$ $NE^\circ = (-1) \times (-1.87V) = +1.87V$	
-2	$N_2 \rightarrow N_2H_5^+$	$(-2) \times E^\circ_{N_2 \rightarrow N_2H_5^+}$	$\mathbf{N_2 \rightarrow NH_3OH^+ \rightarrow N_2H_5^+}$ $NE^\circ = (-1) \times E^\circ_{N_2 \rightarrow NH_3OH^+} + (-1)E^\circ_{NH_3OH^+ \rightarrow N_2H_5^+}$ $NE^\circ = NE^\circ_{-1\ O.S.} + (-1)E^\circ_{NH_3OH^+ \rightarrow N_2H_5^+}$ $NE^\circ = +1.87V + (-1) \times 1.41V = 0.46V$	Calculate NE° for the -1 oxidation state, NO, first. Then use it in this calculation.

Oxidation State	Step	$NE°$ =	Calculated as the sum of the steps	Notes
-3	$N_2 \rightarrow NH_4^+$	$(-3) \times E°_{N_2 \rightarrow NH_4^+}$	$N_2 \rightarrow N_2H_5^+ \rightarrow NH_4^+$ $NE° = (-1)E°_{N_2 \rightarrow N_2H_5^+} + (-1)E°_{N_2H_5^+ \rightarrow NH_4^+}$ $NE° = NE°_{-2\ O.S.} + (-1)E°_{N_2H_5^+ \rightarrow NH_4^+}$ $NE° = +0.46V + (-1) \times 1.275V = -0.815V$	Calculate $NE°$ for the -2 oxidation state, NO, first. Then use it in this calculation.

The resulting Frost diagram for acidic aqueous nitrogen is given below.



The figure above by Stephen Contakes is licensed under a Creative Commons Attribution 4.0 International License.

References

1. Unless otherwise noted all potentials are for strongly acidic solutions and taken from Bard, A. J.; Parsons, R.; Jordan, J. Standard potentials in aqueous solution. M. Dekker: New York, 1985.
2. This diagram is inspired by the similar diagram given in M. Gerken Chemistry 2810 Lecture Notes. Posted on classes.uleth.ca/200501/chem2...lecture_20.pdf
3. The estimated $Fe^{6/3+}$ reduction potential of +2.07 V used to construct the Frost diagram for the first row transition metals is taken from Huheey, J. E.; Keiter, E. A.; Keiter, R. L., Inorganic chemistry : principles of structure and reactivity. 4th ed.; HarperCollins College Publishers: New York, NY, 1993; pg. 596.
4. Lu, J.-B.; Jian, J.; Huang, W.; Lin, H.; Li, J.; Zhou, M., Experimental and theoretical identification of the Fe(vii) oxidation state in FeO4−. Physical Chemistry Chemical Physics 2016, 18 (45), 31125-31131.
5. In some pedagogical applications only the adjoining states are considered.

Contributors and Attributions

- Stephen Contakes, Westmont College

3.8: Frost Diagrams is shared under a CC BY-NC-SA 4.0 license and was authored, remixed, and/or curated by LibreTexts.

- **8.1.4.2: Frost Diagrams show how stable element's redox states are relative to the free element** has no license indicated.

3.9: Pourbaix Diagrams

Pourbaix diagrams depict the most stable species or phase of an element as a function of potential and pH. Pourbaix or potential-pH/E-pH diagrams were developed and popularized by Marcel Pourbaix, who used them to study corrosion. Pourbaix diagrams depict the most stable species or phase of an element in aqueous solution as a function of potential (on the y-axis) and pH (on the x-axis). Pourbaix's *Atlas of Electrochemical Equilibria in Aqueous Solution* contains diagrams for many elements along with extensive notes on their construction.[1]

Introduction to Pourbaix Diagrams

Pourbaix diagrams are similar to phase diagrams in that they show species as a function of potential and pH. Unlike a conventional phase diagram, the regions depict the dominant species instead of the only species present under a given set of conditions (for more detail see Note 1).[1] For solution phase species, the dominant chemical species will not only depend on potential and pH as depicted in the diagram; the formal concentration of the species is important too. For the sort of corrosion applications Pourbaix envisioned, these concentrations are typically quite low, so for this reason the regions depicted in most Pourbaix diagrams correspond to 1 mM total concentration.

The lines in Pourbaix diagrams represent redox reactions that occur in neutral solutions (horizontal lines), acid-base reactions (vertical lines), and redox reactions that occur in acid or basic conditions (diagonal lines). Each lines indicate a equilibrium between two species. For example, in the Pourbaix diagram for Fe below, the horizontal line between the Fe^{3+} and Fe^{2+} regions represents the reaction $\mathbf{Fe^{3+}_{(aq)} + e^- = Fe^{2+}_{(aq)}}$, which has a standard potential of +0.77 V (Figure **3.9.1**. While we could use standard potentials for all these lines, in practice Pourbaix diagrams are usually plotted for lower ion concentrations (often 1 mM) that are more relevant to corrosion and electrochemical experiments. The areas contained by the lines represent potential and pH conditions in which a given species is stable.

Example: Iron Pourbaix diagram

Areas in the Pourbaix diagram mark regions where a single species (Fe^{2+}(aq), Fe_3O_4(s), etc.) is stable. More stable species tend to occupy larger areas.

Lines mark places where two species exist in equilibrium.

- **Pure redox** reactions are **horizontal** lines - these reactions are not pH-dependent
- **Pure acid-base** reactions are **vertical** lines - these do not depend on potential
- Reactions that are **both** acid-base and redox have a slope of -0.0592 V/pH x # H^+/# e^-)

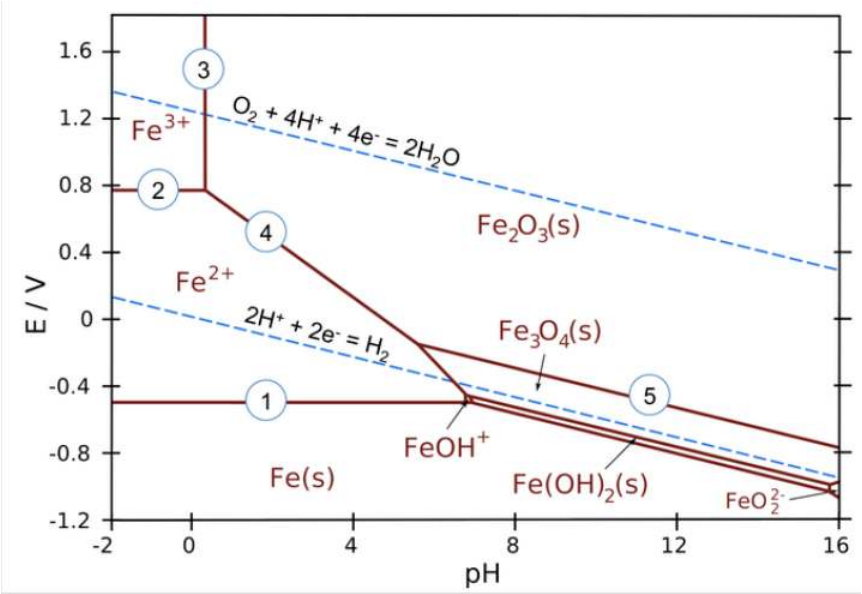


Figure **3.9.1**: Pourbaix diagram for iron at ionic concentrations of 1.0 mM. (CC BY-SA 3.0 Unported; Metallos via Wikipedia)

Examples of equilibria in the iron Pourbaix diagram (numbered in Figure 3.9.1):

1. $Fe^{2+} + 2e^- \longrightarrow Fe_{(s)}$ (pure redox reaction - no pH dependence)
2. $Fe^{3+} + e^- \longrightarrow Fe^{2+}$ (pure redox reaction - no pH dependence)
3. $2Fe^{3+} + 3H_2O \longrightarrow Fe_2O_{3(s)} + 6H^+$ (pure acid-base, no redox)
4. $2Fe^{2+} + 3H_2O \longrightarrow Fe_2O_{3(s)} + 6H^+ + 2e^-$ (slope = -59.2 x 6/2 = -178 mV/pH)
5. $2Fe_3O_{4(s)} + H_2O \longrightarrow 2H^+ + 2e^-$ (slope = -59.2 x 2/2 = -59.2 mV/pH)

Water in Pourbaix Diagrams

The water redox reactions typically are plotted as dotted lines on these more complicated Pourbaix diagrams for other elements. In Figure 3.9.1, water redox reactions are shown as the blue dotted diagonal lines. Liquid water is stable *only* in the region between the dotted lines. Above the O_2 line, water is unstable and will be oxidized:

$$O_2 + 4H^+ + 4e^- \rightarrow 2H_2O.$$

Below the H_2 line, water is unstable and H^+ will be reduced:

$$2H^+ \quad + \quad 2e^- \rightarrow H_2$$

These lines are useful for several reasons.

- First, in cases where water oxidation and reduction are fast relative to the electrochemical phenomenon of interest, the water oxidation and reduction potentials limit the potential that the element can experience - *i.e.*, if a solution is exposed to a more extreme potential in the form of an electrode or a strong chemical or photochemical oxidant or reductant, then that substance will oxidize or reduce water instead of the element depicted in the diagram.
- Second, the oxygen reduction equilibrium is important for corrosion applications taking place in an oxygen-containing environment. In these environments, the pH-dependent standard potential of oxygen reduction depicted by the upper blue line in Figure 3.9.1 determines the potential of the system. As can be seen in Figure 3.9.1, the potential of this equilibrium is above that of the region of stability of metallic iron. This indicates that metallic iron is not thermodynamically stable at the oxygen partial pressures of the diagram; Fe^{3+} species are instead. Moreover, the precise species that metallic iron will form when it is exposed to a higher potential varies with pH. At higher pH values, an oxide will be produced - either $Fe(OH)_2$(s), Fe_3O_4(s), or Fe_2O_3(s). If these solid phases coat the surface of the iron so as to insulate it from reaction with oxygen, they will effectively prevent iron's oxidation. Such layers are said to be **passivating**, and the resulting **anodic passivation** is a form of kinetic, not thermodynamic, stabilization of the metal.

For active metals such as Fe, the region where the pure element is stable is typically below the H_2 line. This means that iron metal is unstable in contact with water, undergoing reactions:

$Fe_{(s)} + 2H^+ \longrightarrow Fe^{2+}{}_{(aq)} + H_2$ (in acid)

$fe_{(s)} + 2H_2O \longrightarrow Fe(OH)_{2\,(s)} + H_2$ (in base)

Iron (and most other metals) are also thermodynamically unstable in air-saturated water, where the potential of the solution is close to the O_2 line in the Pourbaix diagram. Here the spontaneous reactions are:

$4Fe_{(s)} + 3O_2 + 12H^+ \longrightarrow 4Fe^{3+} + 6H_2O$ (in acid)

\(\ce{4Fe_{(s)} + 3O2 -> 2Fe2O3_{(s)} (in base)

Straightforward applications of Pourbaix diagrams involve estimating how the potential of a system at equilibrium changes with conditions, as illustrated in Example 3.9.1.

Example 3.9.1

Metal indicator electrodes are used to measure the potential of solutions. The potential is determined by the redox equilibria taking place therein. This potential may be measured by immersing the metal indicator electrode and a reference electrode in the solution to be tested.

Use the information in Figure **3.9.2** (Do not use the information in Figure **3.9.1** since it corresponds to a different Fe concentration) to:

1. Explain how you might construct a pH-sensitive electrode from a Pt wire metal indicator electrode, $FeSO_4$ (which is water soluble) and rust, which for the purposes of this problem you may take as equivalent to $Fe_2O_3(s)$ and its hydrates.
2. What would be the pH range limits of the sensor?
3. What voltages would it read (vs. NHE) over this range?
4. Are there any limitations that should be observed when using this electrode to measure pH?

Solution

1. The electrode may be made by dissolving the $FeSO_4$ in the solution to be tested to give a solution that is ~1mM Fe^{2+}. Then enough rust would be added to give a cloudy solution, indicating that solid is present and the equilibrium between Fe^{2+} and $FeSO_4$ established. Finally, the Pt wire and a suitable reference electrode would be inserted into the solution and the potential measured.
2. The electrode would only work between pH values of ~0.5 and 7. Below pH 0.5 the Fe_2O_3 would dissolve, while above pH 7 the Fe^{2+} will precipitate.
3. The voltages should range from ~0.77 V (vs. SHE) at pH ~0.5 to ~-0.44V (vs. SHE) at pH~7.
4. There are several limitations and much would need to be done to validate this as a suitable method for the determination of pH. First, the potentials listed above assume that the iron concentration in the test solution is the same as that used to construct the diagram in Figure **3.9.1**. Thus they are at best rough estimates, and the electrode would need to be calibrated using solutions of known pH before use. Second, if the electrode is used in air, over time the Fe^{2+} will oxidize to Fe^{3+} species, shifting the response of the electrode. Because of this the electrode should either be used in an anoxic environment or prepared just before use.

What do the lines in a Pourbaix diagram mean?

The phase lines in Pourbaix diagrams correspond to switchpoints between the dominant species in solution for solution phase species or the points at which precipitation or phase change occurs for equilibria involving solid and/or pure liquid phases. To see how this works it helps to consider the three common cases:

- *Equilibria that involve electron transfer only* give rise to horizontal lines because the potential does not depend on pH. An example is the line between the Fe^{3+} and Fe^{2+} regions, marked 2 in Figure **3.9.2**. In this case the reaction potential when $\frac{Fe^{2+}}{Fe^{3+}}$=1 is $E^\circ_{Fe^{3/2+}}$:

$$Fe^{3+} + e^- \rightarrow Fe^{2+} \quad E = E^\circ_{Fe^{3/2+}} - \frac{0.05916\ V}{1}\log\frac{[Fe^{2+}]}{[Fe^{3+}]}$$
$$= E^\circ_{Fe^{3/2+}} - (0.05916\ V)\log 1 = E^\circ_{Fe^{3/2+}}$$

- *Acid-base equilibria that do not involve changes in the redox state of the elements involved* give rise to vertical lines, the position of which depend on the stated concentration of the diagram. An example is the line between the Fe^{3+}(aq) and Fe_2O_3(s) regions, marked 3 in Figure **3.9.2**. This corresponds to the equilibrium:

$$2\ Fe^{3+} + 3\ H_2O \rightarrow Fe_2O_3(s) + 6\ H^+$$

  The equilibrium line in this case is determined by the reaction's equilibrium constant

$$K = \frac{[H^+]^6}{[Fe^{3+}]^2}$$

  From this it can be seen that the pH ($[H^+]$) is a function only of the value of $[Fe^{3+}]$ used to construct the diagram (since $[H^+] = (K[Fe^{3+}]^2)^{1/6} = constant$), so the line is vertical.

- *Equilibria that involve a combination of electron transfer and acid-base chemistry* give rise to slanted lines. An example is the equilibrium between Fe^{2+} and Fe_2O_3(s), marked 4 in Figure **3.9.2**. This corresponds to the equilibrium:

$$Fe_2O_3(s) + 6\ H^+ + 2\ e^- \rightarrow 2\ Fe^{2+} + 3\ H_2O$$

for which

$$E = E^{\circ}_{Fe_2O_3/Fe^{2+}} - \frac{0.05916\ V}{2} \log \frac{[Fe^{2+}]^2}{[H^+]^6}$$

from which it can be seen that the potential will be pH dependent.

Corrosion and Passivation

Corrosion and passivation. It certainly sounds bad for our friend Fe: unstable in water, no matter what the pH or potential. Given enough time, it will all turn into rust. But iron (and other active metals) can corrode, or can be stabilized against corrosion, depending on the conditions. Because our civilization is dependent on the use of active metals such as Fe, Al, Zn, Ti, Cr... for practically everything, it is important to understand this, and we can do so by referring to the Pourbaix diagram.

The **corrosion** of iron (and other active metals such as Al) is indeed rapid in parts of the Pourbaix diagram where the element is oxidized to a soluble, ionic product such as Fe^{3+}(aq) or Al^{3+}(aq). However, solids such as Fe_2O_3, and especially Al_2O_3, form a protective coating on the metal that greatly impedes the corrosion reaction. This phenomenon is called **passivation.**

Draw a vertical line through the iron Pourbaix diagram at the pH of tap water (about 6) and you will discover something interesting: at slightly acidic pH, iron is quite unstable with respect to corrosion by the reaction:

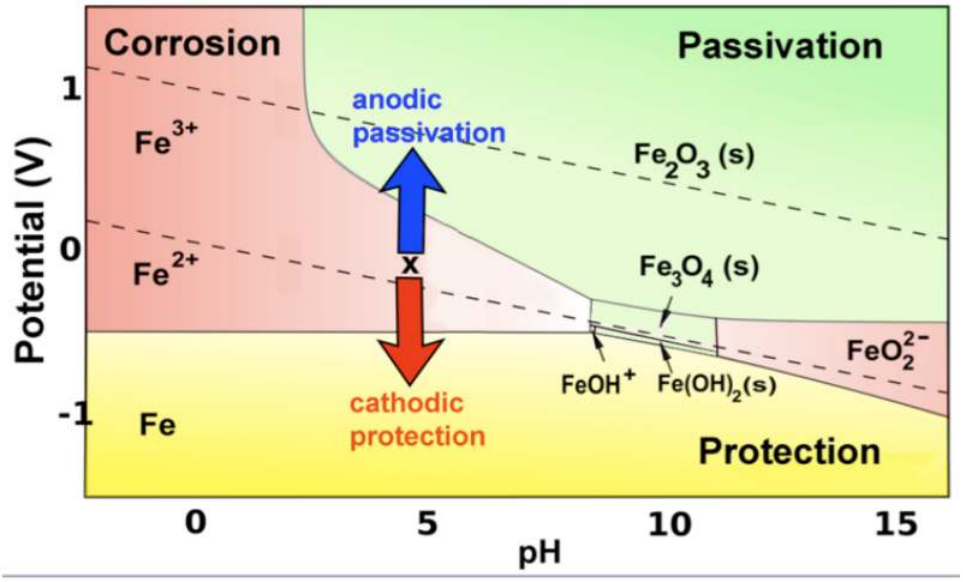
$$Fe_{(s)} + 2H^+ \longrightarrow Fe^{2+}{}_{(aq)} + H_2 \tag{3.9.1}$$

but *only in water that contains relatively little oxygen*, i.e., in solutions where the potential is near the H_2 line. Saturating the water with air or oxygen moves the system closer to the O_2 line, where the most stable species is Fe_2O_3 and the corrosion reaction is:

$$4Fe_{(s)} + 3O_2 \longrightarrow 2Fe_2O_{3\,(s)} \tag{3.9.2}$$

This oxidation reaction is orders of magnitude slower because the oxide that is formed *passivates* the surface. Therefore iron corrodes much more slowly in oxygenated solutions.

More generally, iron (and other active metals) are passivated whenever they oxidize to produce a solid product, and corrode whenever the product is ionic and soluble. This behavior can be summed up on the color-coded Pourbaix diagram below. The red and green regions represent conditions under which oxidation of iron produces soluble and insoluble products, respectively.



In the yellow part of the diagram, an active metal such as iron can be **protected** by a second mechanism, which is to bias it so that its potential is below the oxidation potential of the metal. This **cathodic protection** strategy is most frequently carried out by

connecting a more active metal such as Mg or Zn to the iron or steel object (e.g., the hull of a ship, or an underground gas pipeline) that is being protected. The active metal (which must be higher than Fe in the activity series) is also in contact with the solution and slowly corrodes, so it must eventually be replaced. In some cases a battery or DC power supply - the anode of which oxidizes water to oxygen in the solution - is used instead to apply a negative bias.



The white patches visible on the ship's hull are zinc block sacrificial anodes.

Another common mode of corrosion of iron and carbon steel is **differential aeration.** In this case, part of the iron object - e.g., the base of a bridge, or the drill in an oil rig - is under water or in an anoxic environment such as mud or soil. The potential of the solution is close to the H_2 line in the Pourbaix diagram, where Fe can corrode to Fe^{2+} (aq). Another part of the iron object is in the air, or near the surface where water is well oxygenated. At that surface oxygen can be reduced to water, $O_2 + 4H^+ + 4e^- = 2\ H_2O$. The conductive iron object completes the circuit, carrying electrons from the anode (where Fe is oxidized) to the cathode (where O_2 is reduced). Corrosion by differential aeration can be rapid because soluble ions are produced, and the reaction has a driving force of over 1 V. Iron or carbon steel that is subjected to frequent weathering, such as the cast iron bridge and lamppost shown below, is corroded on the surface by differential aeration.



Rusty cast iron bridge and lamppost, North Ayrshire, Scotland

Differential aeration is involved in the formation of a rust ring around wet areas of cast iron, e.g., an iron frying pan left partially submerged in water for a day or more. (You may have seen this mechanism of corrosion in action when you did not get to the dirty dishes right away). Under the water, Fe is oxidized to soluble Fe^{2+}, and at the water line O_2 is reduced to H_2O. As Fe^{2+} ions diffuse towards the water surface, they encounter oxygen molecules and are oxidized to Fe^{3+}. However Fe^{3+} is insoluble at neutral pH and deposits as rust, typically just below the water line, forming the rust ring.

References

1. Pourbaix, M., Atlas of electrochemical equilibria in aqueous solutions. 2nd ed. Houston: National Association of Corrosion Engineers, 1974.

3.9: Pourbaix Diagrams is shared under a CC BY-NC-SA 4.0 license and was authored, remixed, and/or curated by Kathryn A. Newton, Northern Michigan University.

- **4.6: Pourbaix Diagrams** by Chemistry 310 is licensed CC BY-SA 4.0. Original source: https://en.wikibooks.org/wiki/Introduction_to_Inorganic_Chemistry.
- **8.1.4.3: Pourbaix Diagrams are Redox Phase Diagrams that Summarize the most stable form of an element at a given pH and solution potential** has no license indicated.

3.10: Corrosion

Learning Objectives

- Define corrosion
- List some of the methods used to prevent or slow corrosion

Corrosion is usually defined as the degradation of metals due to an electrochemical process. The formation of rust on iron, tarnish on silver, and the blue-green patina that develops on copper are all examples of corrosion. The total cost of corrosion in the United States is significant, with estimates in excess of half a trillion dollars a year.

Changing Colors

The Statue of Liberty is a landmark every American recognizes. The Statue of Liberty is easily identified by its height, stance, and unique blue-green color. When this statue was first delivered from France, its appearance was not green. It was brown, the color of its copper "skin." So how did the Statue of Liberty change colors? The change in appearance was a direct result of corrosion. The copper that is the primary component of the statue slowly underwent oxidation from the air. The oxidation-reduction reactions of copper metal in the environment occur in several steps. Copper metal is oxidized to copper(I) oxide ($\mathbf{Cu_2O}$), which is red, and then to copper(II) oxide, which is black.

$$2\,\mathrm{Cu\,(s)} + \tfrac{1}{2}\,\mathrm{O_2\,(g)} \rightarrow \underset{\text{red}}{\mathrm{Cu_2O\,(s)}}$$

$$\mathrm{Cu_2O\,(s)} + \tfrac{1}{2}\,\mathrm{O_2\,(g)} \rightarrow 2\,\underset{\text{black}}{\mathrm{CuO\,(s)}}$$

Coal, which was often high in sulfur, was burned extensively in the early part of the last century. As a result, sulfur trioxide, carbon dioxide, and water all reacted with the $\mathbf{CuO}$.

$$2\,\mathrm{CuO\,(s)} + \mathrm{CO_2\,(g)} + \mathrm{H_2O\,(l)} \rightarrow \underset{\text{green}}{\mathrm{Cu_2CO_3(OH)_2\,(s)}}$$

$$3\,\mathrm{CuO\,(s)} + 2\,\mathrm{CO_2\,(g)} + \mathrm{H_2O\,(l)} \rightarrow \underset{\text{blue}}{\mathrm{Cu_2(CO_3)_2(OH)_2\,(s)}}$$

$$4\,\mathrm{CuO\,(s)} + \mathrm{SO_3\,(g)} + 3\,\mathrm{H_2O\,(l)} \rightarrow \underset{\text{green}}{\mathrm{Cu_4SO_4(OH)_6\,(s)}}$$

These three compounds are responsible for the characteristic blue-green patina seen today. Fortunately, formation of the patina created a protective layer on the surface, preventing further corrosion of the copper skin. The formation of the protective layer is a form of passivation, which is discussed further in a later chapter.

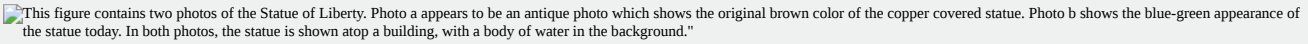

This figure contains two photos of the Statue of Liberty. Photo a appears to be an antique photo which shows the original brown color of the copper covered statue. Photo b shows the blue-green appearance of the statue today. In both photos, the statue is shown atop a building, with a body of water in the background."

Figure **3.10.1**: (a) The Statue of Liberty is covered with a copper skin, and was originally brown, as shown in this painting. (b) Exposure to the elements has resulted in the formation of the blue-green patina seen today.

Perhaps the most familiar example of corrosion is the formation of rust on iron. Iron will rust when it is exposed to oxygen and water. The main steps in the rusting of iron appear to involve the following. Once exposed to the atmosphere, iron rapidly oxidizes.

$$\text{anode: } \mathrm{Fe_{(s)}} \rightarrow \mathrm{Fe^{2+}{}_{(aq)}} + 2\,\mathrm{e^-} \quad E^\circ_{\mathrm{Fe^{2+}/Fe}} = -0.44\ \mathrm{V}$$

The electrons reduce oxygen in the air in acidic solutions.

$$\text{cathode: } \mathrm{O_{2(g)}} + 4\,\mathrm{H^+{}_{(aq)}} + 4\,\mathrm{e^-} \rightarrow 2\,\mathrm{H_2O_{(l)}} \quad E^\circ_{\mathrm{O_2/O_2}} = +1.23\ \mathrm{V}$$

$$\text{overall: } 2\,\mathrm{Fe_{(s)}} + \mathrm{O_{2(g)}} + 4\,\mathrm{H^+{}_{(aq)}} \rightarrow 2\,\mathrm{Fe^{2+}{}_{(aq)}} + 2\,\mathrm{H_2O_{(l)}} \quad E^\circ_{\text{cell}} = +1.67\ \mathrm{V}$$

What we call rust is hydrated iron(III) oxide, which forms when iron(II) ions react further with oxygen.

$$4\,\mathrm{Fe^{2+}{}_{(aq)}} + \mathrm{O_{2(g)}} + (4+2x)\mathrm{H_2O_{(l)}} \rightarrow 2\,\mathrm{Fe_2O_3 \cdot}\,x\mathrm{H_2O_{(s)}} + 8\,\mathrm{H^+{}_{(aq)}}$$

The number of water molecules is variable, so it is represented by *x*. Unlike the patina on copper, the formation of rust does not create a protective layer and so corrosion of the iron continues as the rust flakes off and exposes fresh iron to the atmosphere.

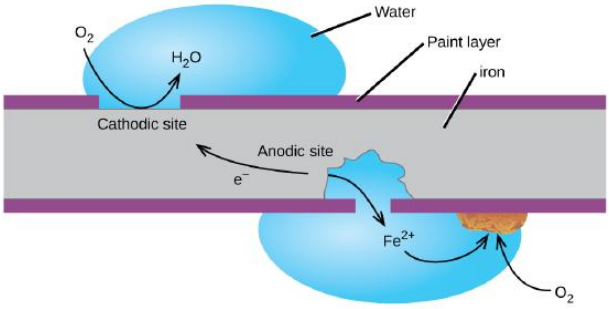


Figure **3.10.2**: Once the paint is scratched on a painted iron surface, corrosion occurs and rust begins to form. The speed of the spontaneous reaction is increased in the presence of electrolytes, such as the sodium chloride used on roads to melt ice and snow or in salt water.

A grey rectangle, labeled “iron,” is shown with thin purple layers, labeled “Paint layer,” at its upper and lower surfaces. A gap in the upper purple layer at the upper left of the diagram is labeled “Cathodic site.” A blue droplet labeled “water” is positioned on top of the gap. A curved arrow extends from a space above the droplet to the surface of the grey region and into the water droplet. The base of the arrow is labeled “O subscript 2” and the tip of the arrow is labeled “H subscript 2 O.” A gap to the right and on the bottom side of the grey region shows that some of the grey region is gone from the region beneath the purple layer. A water droplet covers this gap and extends into the open space in the grey rectangle. The label “F e superscript 2 positive” is at the center of the droplet. A curved arrow points from the edge of the grey area below to the label. A second curved arrow extends from the F e superscript 2 positive arrow to a rust brown chunk on the lower surface of the purple layer at the edge of the water droplet. A curved arrow extends from O subscript 2 outside the droplet into the droplet to the rust brown chunk. The grey region at the lower right portion of the diagram is labeled “Anodic site.” An arrow extends from the anodic site toward the cathodic site, which is labeled “e superscript negative.”

One way to keep iron from corroding is to keep it painted. The layer of paint prevents the water and oxygen necessary for rust formation from coming into contact with the iron. As long as the paint remains intact, the iron is protected from corrosion.

Other strategies include alloying the iron with other metals. For example, stainless steel is mostly iron with a bit of chromium. The chromium tends to collect near the surface, where it forms an oxide layer that protects the iron.

Zinc-plated or galvanized iron uses a different strategy. Zinc is more easily oxidized than iron because zinc has a lower reduction potential. Since zinc has a lower reduction potential, it is a more active metal. Thus, even if the zinc coating is scratched, the zinc will still oxidize before the iron. This suggests that this approach should work with other active metals.



Figure **3.10.3**: One way to protect an underground iron storage tank is through cathodic protection. Using an active metal like zinc or magnesium for the anode effectively makes the storage tank the cathode, preventing it from corroding (oxidizing).

A diagram is shown of an underground storage tank system. Underground, to the left end of the diagram is a horizontal grey tank which is labeled “Object to be protected.” A black line extends upward from the center of the tank above ground. An arrow points upward at the left side of the line segment. A horizontal black line segment continues right above ground, which is labeled “No power source is needed.” A line segment extends up and to the right, which is labeled “ Lead wire.” A line segment with a downward pointing arrow to its right extends downward below the ground to a second metal tank-like structure, labeled “Sacrificial anode” which is vertically oriented. Five black arrows point left underground toward the first tank. These arrows are collectively labeled “Protective current.”

Another important way to protect metal is to make it the cathode in a galvanic cell. This is cathodic protection and can be used for metals other than just iron. For example, the rusting of underground iron storage tanks and pipes can be prevented or greatly reduced by connecting them to a more active metal such as zinc or magnesium. This is also used to protect the metal parts in water heaters. The more active metals (lower reduction potential) are called sacrificial anodes because as they get used up as they corrode (oxidize) at the anode. The metal being protected serves as the cathode, and so does not oxidize (corrode). When the anodes are properly monitored and periodically replaced, the useful lifetime of the iron storage tank can be greatly extended.

Summary

Corrosion is the degradation of a metal caused by an electrochemical process. Large sums of money are spent each year repairing the effects of, or preventing, corrosion. Some metals, such as aluminum and copper, produce a protective layer when they corrode

in air. The thin layer that forms on the surface of the metal prevents oxygen from coming into contact with more of the metal atoms and thus “protects” the remaining metal from further corrosion. Iron corrodes (forms rust) when exposed to water and oxygen. The rust that forms on iron metal flakes off, exposing fresh metal, which also corrodes. One way to prevent, or slow, corrosion is by coating the metal. Coating prevents water and oxygen from contacting the metal. Paint or other coatings will slow corrosion, but they are not effective once scratched. Zinc-plated or galvanized iron exploits the fact that zinc is more likely to oxidize than iron. As long as the coating remains, even if scratched, the zinc will oxidize before the iron. Another method for protecting metals is cathodic protection. In this method, an easily oxidized and inexpensive metal, often zinc or magnesium (the sacrificial anode), is electrically connected to the metal that must be protected. The more active metal is the sacrificial anode, and is the anode in a galvanic cell. The “protected” metal is the cathode, and remains unoxidized. One advantage of cathodic protection is that the sacrificial anode can be monitored and replaced if needed.

Glossary

cathodic protection
: method of protecting metal by using a sacrificial anode and effectively making the metal that needs protecting the cathode, thus preventing its oxidation

corrosion
: degradation of metal through an electrochemical process

galvanized iron
: method for protecting iron by covering it with zinc, which will oxidize before the iron; zinc-plated iron

sacrificial anode
: more active, inexpensive metal used as the anode in cathodic protection; frequently made from magnesium or zinc

---

This page titled 3.10: Corrosion is shared under a CC BY license and was authored, remixed, and/or curated by OpenStax.

- **17.6: Corrosion** by OpenStax is licensed CC BY 4.0. Original source: https://openstax.org/details/books/chemistry-2e.

CHAPTER OVERVIEW

4: Inorganic Acids and Bases

4.1: Overview

4.2: Arrhenius/Bronsted and Lowry

4.2.1: Trends of Binary Acids

4.2.2: Trends of Oxyacids

4.2.3: Trends in Metal Hydroxide Basicity/Solubility

4.3: Lewis Acids and Bases

4.3.1: Conjugate Acids of Lewis Bases are Bronsted Acids

4.3.2: Acidity of Metal Ions in Water

4.3.3: Hard-Soft Designation of Lewis Acids and Bases

4: Inorganic Acids and Bases is shared under a not declared license and was authored, remixed, and/or curated by LibreTexts.

4.1: Overview

There are three primary theories of acid-base chemistry that are often taught together: Arrhenius theory, Brønsted-Lowry theory, and Lewis acid-base theory. Each theory is introduced below.

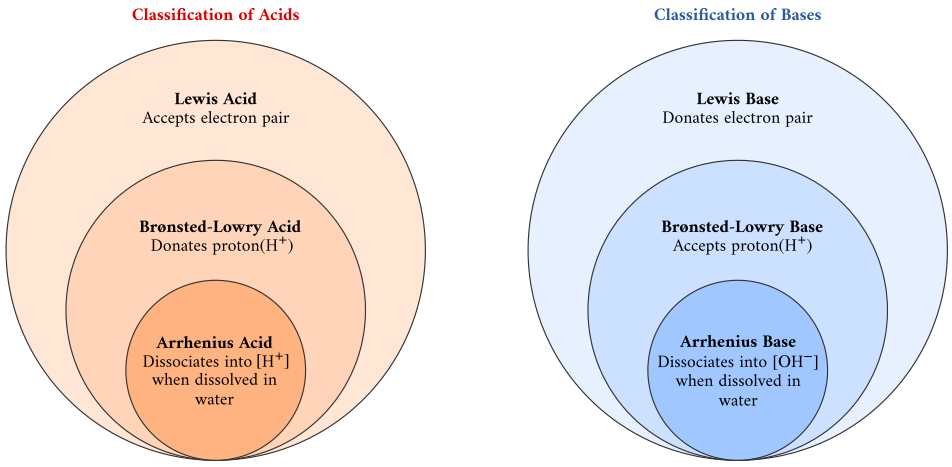


Figure **4.1.1**: Hierarchal definitions of acids and bases via the three primary theories. These theories are designed to be "superset" of the previous classification. (CC BY-NC 4.0; Ümit Kaya via LibreTexts)

Arrhenius Definition of Acids and Bases

The Swedish chemist Svante Arrhenius attributed the properties of acidity to hydrogen ions ($\mathbf{H^+}$) in 1884. An Arrhenius acid is a substance that, when added to water, increases the concentration of $\mathbf{H^+}$ ions in the water. Note that chemists often write $\mathbf{H^+(aq)}$ and refer to the hydrogen ion when describing acid-base reactions, but the free hydrogen nucleus does not exist alone in water. It exists in a hydrated form which for simplicity is often written as the hydronium (hydroxonium) ion, $\mathbf{H_3O^+}$. Thus, an Arrhenius acid can also be described as a substance that increases the concentration of hydronium ions when added to water. This definition stems from the equilibrium dissociation (self-ionization) of water into hydronium and hydroxide ($\mathbf{OH^-}$) ions:

$$\mathbf{H_2O(l) + H_2O(l) \rightleftharpoons H_3O^+(aq) + OH^-(aq)}$$

with K_w defined as $[H^+][OH^-]$.

The value of K_w varies with temperature, as shown in the table below where at 25 °C K_w is approximately 1.0×10^{-14}, i.e. $pK_w = 14$.

Water temperature	$K_w / 10^{-14}$	pK_w
0 °C	0.112	14.95
25 °C	1.023	13.99
50 °C	5.495	13.26
75 °C	19.95	12.70
100 °C	56.23	12.25

In pure water the majority of molecules are $\mathbf{H_2O}$, but the molecules are constantly dissociating and re-associating, and at any time a small number of the molecules (about 1 in 10^7) are hydronium and an equal number are hydroxide. Because the numbers are equal, pure water is neutral (not acidic or basic) and has an electrical conductivity of 5.5 microSiemen, μS/m. For comparison, sea water's conductivity is about one million times higher, 5 S/m (due to the dissolved salt).

Proton vs. Hydron

Although the term proton is often used for H^+, this should really be reserved for H (protium) not D (deuterium) or T (tritium). The more general term, hydron covers all isotopes of hydrogen.

An Arrhenius base, on the other hand, is a substance which increases the concentration of hydroxide ions when dissolved in water, hence decreasing the concentration of hydronium ions.

Upshot

To qualify as an Arrhenius acid, upon the introduction to water, the chemical must either cause, directly or otherwise:

- an increase in the aqueous hydronium concentration, or
- a decrease in the aqueous hydroxide concentration.

Conversely, to qualify as an Arrhenius base, upon the introduction to water, the chemical must either cause, directly or otherwise:

- a decrease in the aqueous hydronium concentration, or
- an increase in the aqueous hydroxide concentration.

The definition is expressed in terms of an equilibrium expression:

$$\text{acid} + \text{base} \rightleftharpoons \text{conjugate base} + \text{conjugate acid}.$$

With an acid, HA, the equation can be written symbolically as:

$$HA + B \rightleftharpoons A^- + HB^+$$

The double harpoons sign, $\rightleftharpoons$, is used because the reaction can occur in both forward and backward directions. The acid, HA, can lose a hydron to become its conjugate base, A^-. The base, B, can accept a hydron to become its conjugate acid, HB^+. Most acid-base reactions are fast so that the components of the reaction are usually in dynamic equilibrium with each other.

Brønsted-Lowry Definition of Acids and Bases

While the Arrhenius concept is useful for describing many reactions, it has limitations. In 1923, chemists Johannes Nicolaus Brønsted and Thomas Martin Lowry independently recognized that acid-base reactions involve the transfer of a hydron. A Brønsted-Lowry acid (or simply Brønsted acid) is a species that donates a hydron to a Brønsted-Lowry base. The Brønsted-Lowry acid-base theory has several advantages over the Arrhenius theory. Consider the following reactions of acetic acid (CH_3COOH):

$$CH_3COOH + H_2O \rightleftharpoons CH_3COO^- + H_3O^+$$

$$CH_3COOH + NH_3 \rightleftharpoons CH_3COO^- + NH_4^+$$

Both theories easily describe the first reaction: CH_3COOH acts as an Arrhenius acid because it acts as a source of H_3O^+ when dissolved in water, and it acts as a Brønsted acid by donating a hydron to water. In the second example CH_3COOH undergoes the same transformation, in this case donating a hydron to ammonia (NH_3), but it cannot be described using the Arrhenius definition of an acid because the reaction does not produce hydronium ions.

Upshot

To qualify as an Brønsted-Lowry acid, the chemical must either cause, directly or otherwise:

- donate a proton.

Conversely, to qualify as an Brønsted-Lowry base, the chemical must either cause, directly or otherwise:

- accept a proton.

Lewis Definition of Acids and Bases

A third concept was proposed in 1923 by Gilbert N. Lewis which includes reactions with acid-base characteristics that do not involve a hydron transfer. A Lewis acid is a species that reacts with a Lewis base to form a Lewis adduct. The Lewis acid accepts a pair of electrons from another species; in other words, it is an electron pair acceptor. Brønsted acid-base reactions involve hydron

transfer reactions while Lewis acid-base reactions involve electron pair transfers. All Brønsted acids are Lewis acids, but not all Lewis acids are Brønsted acids.

$$BF_3 + F^- \rightleftharpoons BF_4^-$$

$$NH_3 + H^+ \rightleftharpoons NH_4^+$$

In the first example BF_3 is a Lewis acid since it accepts an electron pair from the fluoride ion. This reaction cannot be described in terms of the Brønsted theory because there is no hydron transfer. The second reaction can be described using either theory. A hydron is transferred from an unspecified Brønsted acid to ammonia, a Brønsted base; alternatively, ammonia acts as a Lewis base and transfers a lone pair of electrons to form a bond with a hydrogen ion.

Upshot

To qualify as an Lewis acid, the chemical must

- accept an electron pair

Conversely, to qualify as an Lewis base, the chemical must:

- donate an electron pair

Other Acid-Base Definitions

Lux-Flood acid-base definition

This acid-base theory was a revival of the oxygen theory of acids and bases, proposed by German chemist Hermann Lux in 1939 and further improved by Håkon Flood circa 1947. It is still used in modern geochemistry and for the electrochemistry of molten salts. This definition describes an acid as an oxide ion (O^{2-}) acceptor and a base as an oxide ion donor. For example:

$$MgO\ (base) + CO_2\ (acid) \rightleftharpoons MgCO_3$$

$$CaO\ (base) + SiO_2\ (acid) \rightleftharpoons CaSiO_3$$

$$NO_3^-\ (base) + S_2O_7^{2-}\ (acid) \rightleftharpoons NO_2^+ + 2\,SO_4^{2-}$$

Usanovich acid-base definition

Mikhail Usanovich developed a general theory that does not restrict acidity to hydrogen-containing compounds, and his approach, published in 1938, was even more general than the Lewis theory. Usanovich's theory can be summarized as defining an acid as anything that *accepts negative species, anions or electrons* or *donates positive ones, cations*, and a base as the reverse. This definition could even be applied to the concept of redox reactions (oxidation-reduction) as a special case of acid-base reactions. Some examples of Usanovich acid-base reactions include:

- species exchanged: anion O^{2-}

$$Na_2O\ (base) + SO_3\ (acid) \longrightarrow 2\,Na^+ + SO_4^{2-}$$

- species exchanged: anion S^{2-}

$$3\,(NH_4)_2S\ (base) + Sb_2S_5\ (acid) \longrightarrow 6\,NH_4^+ + 2\,SbS_4^{3-}$$

- species exchanged: electron

$$2\,Na\ (base) + Cl_2\ (acid) \longrightarrow 2\,Na^+ + 2\,Cl^-$$

A comparison of the above definitions of Acids and Bases shows that the Usanovich concept encompasses all of the others but some feel that because of this it is too general to be useful.

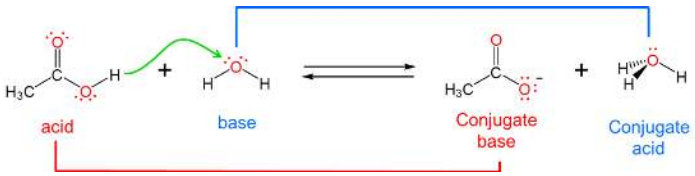
4.1: Overview is shared under a CC BY-NC-SA 4.0 license and was authored, remixed, and/or curated by Stephen M. Contakes.

- **7.1A: Acid-Base Theories and Concepts** by Stephen M. Contakes is licensed CC BY-NC 4.0.

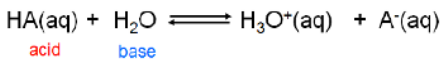
4.2: Arrhenius/Bronsted and Lowry

The Brønsted-Lowry acid-base concept

The Brønsted-Lowry acid-base concept overcomes the Arrhenius system's inability to describe reactions that take place outside of aqueous solution by moving the focus away from the solution and onto the acid and base themselves. It does this by redefining acid-base reactivity as involving the transfer of a hydrogen ion, H^+, between an acid and a base. Specifically, a Brønsted acid is a substance that loses an H^+ ion by donating it to a base. This means that a Brønsted base is defined as a substance which accepts H^+ from an acid when it reacts.

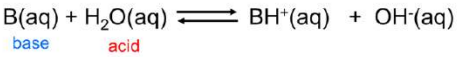


Because the Brønsted-Lowry concept is concerned with H^+ ion transfer rather than the creation of a particular chemical species, it is able to handle a diverse array of acid-base concepts. In fact, from the viewpoint of the Brønsted-Lowry concept, Arrhenius acids and bases are just a special case involving hydrogen ion donation and acceptance involving water. Arrhenius acids donate H^+ ion to water, which acts as a Brønsted base in accepting it to give H_3O^+:



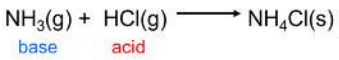
(4.2.1)

Similarly, Arrhenius bases act as Brønsted bases in accepting a hydrogen ion from the Brønsted acid water:



In this way it can be seen that Arrhenius acids and bases are defined in terms of their causing hydrogen ions to be donated to and abstracted from water, respectively, while Brønsted acids and bases are defined in terms of their ability to donate and accept hydrogen ions to and from anything.

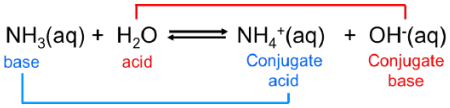
Becasue the Brønsted-Lowry concept can handle any sort of hydrogen ion transfer it readily accommodates many reactions that Arrhenius theory cannot, including those that take place outside of water, such as the reaction between gaseous hydrochloric acid and ammonia:



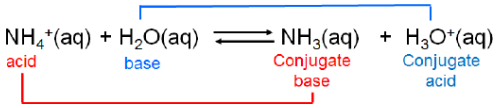
The classification of acids as strong or weak usually refers to their ability to donate or abstract hydrogen ions to or from water to give H_3O^+ and OH^-, respectively, *i.e.*, their Arrhenius acidity and basicity. However, acids and bases may be classified as strong and weak under the Brønsted-Lowry definition based on whether they completely transfer or accept hydrogen ions; it is just that in this case it is important to specify the conditions under which a given acid or base acts strong or weak. For example, acetic acid acts as a weak acid in water but is a strong acid in triethylamine, since in the latter case it completely transfers a hydrogen ion to triethylamine to give triethylammonium acetate. Alternatively, the acidity or basicity of a compound may be specified using a thermodynamic scale like the Hammett acidity.

Conjugate Acids and Bases

By redefining acids and bases in terms of hydrogen ion donation and acceptance, the Brønsted-Lowry system makes it easy to recognize that when an acid loses its hydrogen ion it becomes a substance that is capable of receiving it back again, namely, a base. Consider, for example, the base dissociation of ammonia in water. When ammonia acts as a Brønsted base and receives a hydrogen ion from water, ammonium ion and hydroxide are formed:

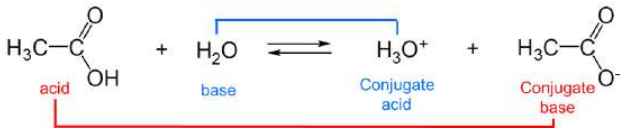


The ammonium ion is itself a weak acid that can undergo dissociation:

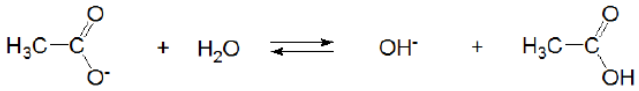


In this case ammonia and ammonium ion are acid-base conjugates. In general acids and bases that differ by a *single ionizable hydrogen ion* are said to be conjugates of one another.

The strengths of conjugates vary reciprocally with one another, so the stronger the acid the weaker the base and vice versa. For example, in water, acetic acid acts as a weak Brønsted acid:



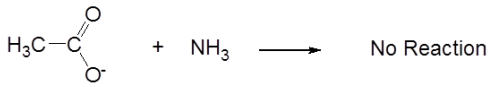
and acetic acid's conjugate base, acetate, acts as a weak Brønsted base.



However, in liquid ammonia acetic acid acts as a strong Brønsted acid:



while its conjugate base, acetate, is neutral.



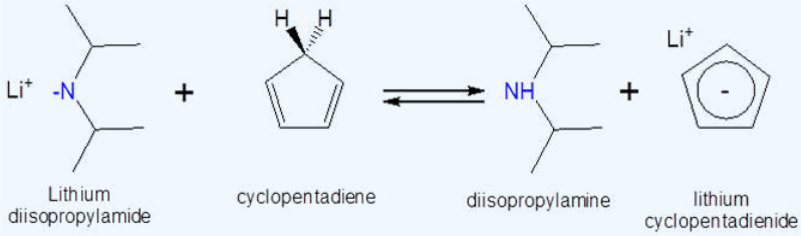
The reciprocal relationship between the strengths of acids and their conjugate bases has several consequences:

1. Under conditions when an acid or base acts as a weak acid or base its conjugate acts as weak as well. Conversely, when an acid or base acts as a strong acid or base its conjugate acts as a neutral species.

2. When a Brønsted acid and base react with one another, the equilibrium favors formation of the weakest acid-base pair. That is why the acid-base reaction between acetic acid and ammonia in liquid ammonia proceeded to give the weak acid ammonium ion and neutral acetate. This consequence is particularly important for understanding the behavior of acids and bases in nonaqueous solvents, as illustrated by the following example.

Example 4.2.1

Can a solution of lithium diisopropylamide in heptane be used to form lithium cyclopentadienide? The pK_a of cyclopentadiene and diisopropylamine are ~15 and 40, respectively, and the proposed reaction is as follows:



Solution:

Since cyclopentadiene is a stronger acid than diisopropylamine (the stronger the acid the lower the pK_a) the equilibrium will favor protonation of the diisopropylamine by cyclopentadiene. Consequently addition of a heptane solution of lithium diisopropylamide to monomeric cyclopentadiene should give lithium cyclopentadienide.

4.2: Arrhenius/Bronsted and Lowry is shared under a CC BY-NC-SA 4.0 license and was authored, remixed, and/or curated by Stephen M. Contakes.

- **6.3.1: Brønsted-Lowry Concept** by Stephen M. Contakes is licensed CC BY 4.0.

4.2.1: Trends of Binary Acids

The compounds formed between the elements and hydrogen are called binary hydrides. All such compounds can in principle act as Brønsted acids in reactions with a suitably strong base. However, as the electronegativity decreases down a group and increases from left to right across the periodic table, the acidity of binary hydrides increases. In fact, on the left side of the periodic table the hydrides of extremely electropositive alkali and alkaline earth metals are not acidic but basic. They are perhaps best considered to be ionic salts of the hydride ion (H^-). Consequently substances such as **NaH** and CaH_2 tend to act as Brønsted bases in their reactions.

$$NaH\,(s) + H_2O\,(l) \longrightarrow Na^+\,(aq) + OH^-\,(aq) + H_2\,(g)$$

$$CaH_2\,(s) + 2\,H_2O\,(l) \longrightarrow Ca^{2+}\,(aq) + 2\,OH^-\,(aq) + 2\,H_2\,(g)$$

On the right side of the periodic table the binary hydrides of the nonmetals exhibit appreciable acidity.

$$HBr\,(aq) + H_2O\,(l) \longrightarrow H^+\,(aq) + Br^-\,(aq)$$

For this reason the binary nonmetal hydrides are termed acidic hydrides. Nevertheless not all are equally acidic. The dilute aqueous acid ionization constants for these hydrides are given in Figure **4.2.1.1**. As can be seen from the constants in Figure **4.2.1.2**, the ability of the hydrides to transfer a hydrogen to water increases across a period and down a group.

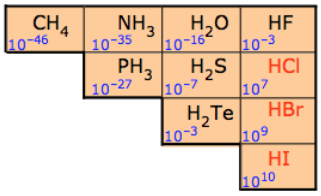


Figure **4.2.1.1**: The acid ionization constants of nonmetal hydrides increase across a period and down a group. (CC BY-NC 3.0; Stephen Lower via Chem1)

These trends are largely due to changes in the electronegativity and size of the nonmetal atom:

1. Foing across a period, the acid strength increases as there is an increase in electronegativity and the molecule gets more polar, with the hydrogen getting a larger partial positive charge. This makes it easier to heterolytically cleave the E-H bond to produce a stable anion.

$$E - H \rightarrow E:^- + H^+$$

2. Going down a group, the acid strength increases because the bond strength decreases as a function of increasing size of the nonmetal, and this has a larger effect than the electronegativity. In fact **HF** is a weak acid because it is so small that the hydrogen-fluorine bond is so strong that it is difficult to break. Remember, the weaker the bond, the stronger the acid strength. This is further illustrated in Table **4.2.1.1**, where the weakest bond has produced the strongest acid.

Table **4.2.1.1** Acid strength as function of bond energy

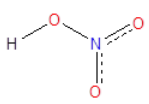
Relative Acid Strength	HF	<<	HCl	<	HBr	<	HI
H–X Bond Energy (kJ/mol)	570		432		366		298
K_a	10^{-3}		10^{7}		10^{9}		10^{10}

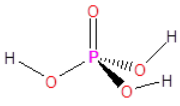
4.2.1: Trends of Binary Acids is shared under a CC BY-NC-SA 4.0 license and was authored, remixed, and/or curated by Stephen M. Contakes.

- **6.3.3: The acid-base behavior of binary element hydrides is determined primarily by the element's electronegativity and secondarily by the element-hydrogen bond strength** by Stephen M. Contakes is licensed CC BY-SA 4.0.

4.2.2: Trends of Oxyacids

Oxyacids (also known as **oxoacids**) are compounds of the general formula H_nEO_m, where **E** is a nonmetal or early transition metal and the acidic hydrogens are attached directly to oxygen (not **E**). This class of compounds includes such well-know acids as nitric acid (HNO_3) and phosphoric acid, (H_3PO_4).





The acidity of oxyacids follows three trends:

Trend 1: In a homologous series the acidity increases with the electronegativity of the central atom

Elements in the same group frequently form oxyacids of the same general formula. For example, chlorine, bromine, and iodine all form oxyacids of formula **HOE**: hypochlorous, hypobromous and hypoiodous acids. In the case of these homologous oxyacids, the acidity is largely determined by the electronegativity of the central element. Central atoms that are better able to inductively pull electron density towards themselves make the oxygen-hydrogen bond that is to be ionized more polar and stabilize the conjugate base, OE^-. Thus the acid strength in such homologous series increases with the electronegativity of the central atom. This may be seen from the data for the hypohalous acids in Table **4.2.2.1**, in which the acid strength increases with the electronegativity of the halogen so that the order of acidity is:

$$HClO > HBrO > HIO$$

and the order of basicity is:

$$ClO^- < BrO^- < IO^-$$

Table **4.2.2.1**: Relationship of central atom's electronegativity to acid ionization constant in the hypohalous acids.

HOX	Electronegativity of X	K_a
HOCl	3.0	4.0×10^{-8}
HOBr	2.8	2.8×10^{-9}
HOI	2.5	3.2×10^{-11}

Note that the influence of central atom electronegativity on the strength of oxyacids is exactly the opposite to that observed for the binary hydrides in Table **4.2.2.5**, for which the acidity increased down a group, giving the order of acidity:

$$HI > HBr > HCl \gg HF$$

The reason for this is that in the hydrogen halides, the bond to be broken (H-E bond) decreased in strength down the group, while in oxyacids the bond to be broken is always an O-H bond and so varies much less in strength with the electronegativity of the central atom.

Trend 2: For oxoacids of a given central atom the acidity increases with the central element's oxidation state or, in other words, the number of oxygens bound to the central atom.

Here we are looking at the trend for acids in which there are variable numbers of oxygen bound to a given central atom. An examples is the perchloric (ClO_4^-), chloric (ClO_3^-), chlorous (ClO_2^-), and hypochlous (ClO^-) acid series. In such a series, the greater the number of oxygens, the stronger the acid. This can be explained in several ways. From the viewpoint of the acid itself the key factor is again the inductive effect, in this case involving the ability of the oxygens attached to the central atom to pull on electron density across the OH bond. This is seen from the charge density diagram for the chlorine oxoacids shown in Figure **4.2.2.1**, in which the partial positive charge on the acidic hydrogen increases with the number of oxygens present.

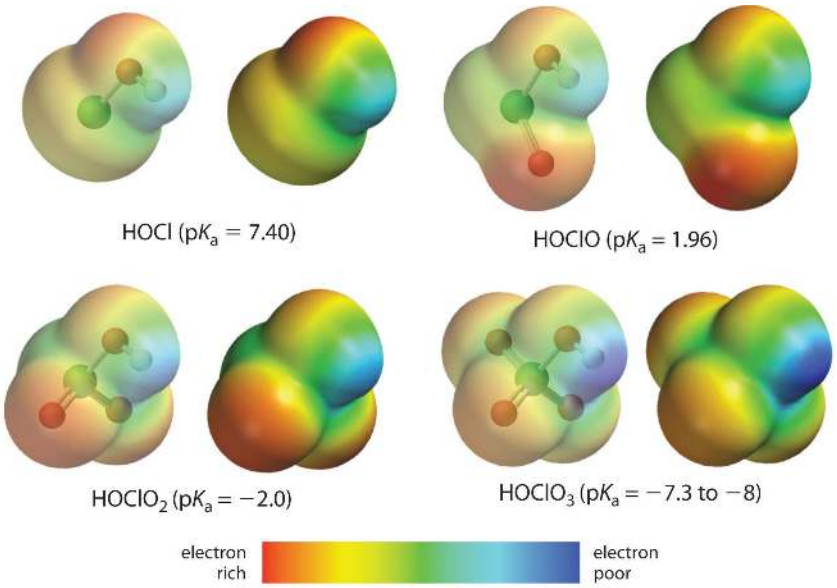


Figure **4.2.2.1**: Increasing the number of oxygens increases K_a, as evidenced by the decreased electron density on the acidic hydrogen (which is most blue in $HClO_4$). Note, $K_a = 10^{-pK_a}$, and so the larger the pK_a, the smaller the K_a. (CC BY-SA-NC; anonymous)

The increase in oxoacid acidity with the number of oxygens bound to the central atom may also be seen by considering the stability of the conjugate oxyanion. That the stability of the conjugate base increases with the number of oxygens may be seen from the charge distribution diagrams and Lewis bonding models for the chlorine oxyanions shown in figure **4.2.2.2**. As the negative charge is spread over more oxygen atoms it becomes increasingly diffuse.

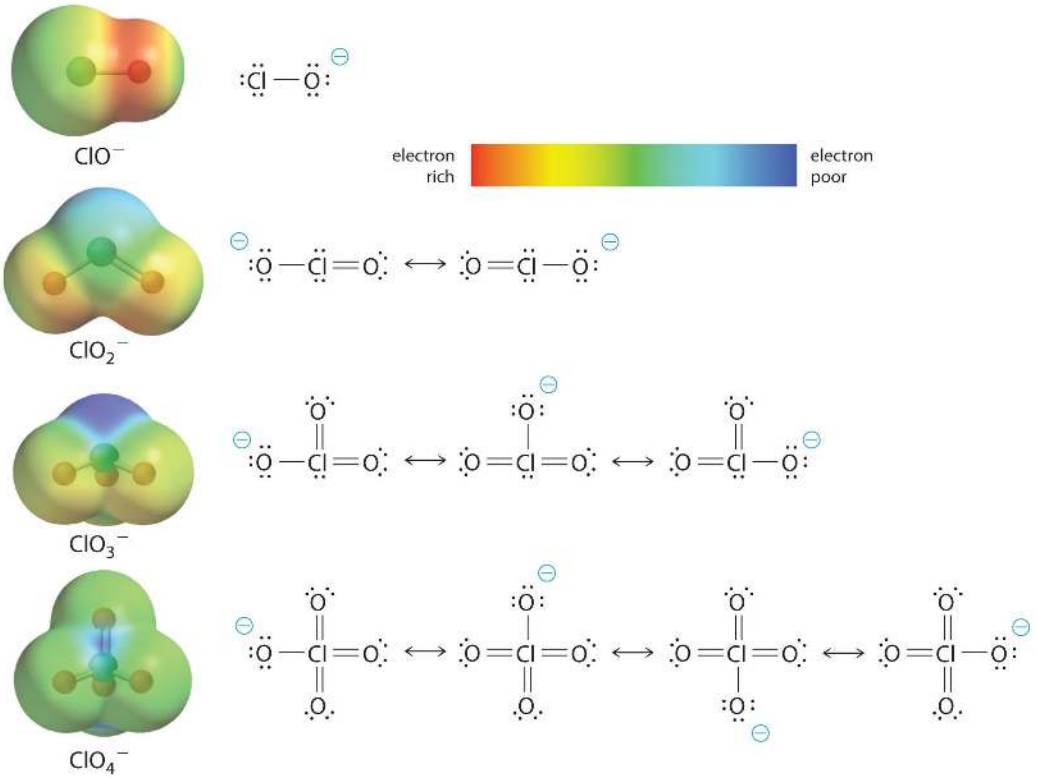


Figure **4.2.2.2**: Increased diffusion of charge in chlorine oxyanions with increasing number of oxygens. The larger the ion the more dispersed the charge and thus the less the charge density, making the perchlorate the most stable anion in the series. Even the simplistic treatment of bonding depicted in the resonance structures correctly shows an increased dispersion of the charge density. (CC BY-SA-NC 3.0; anonymous)

Exercise 4.2.2.1

Sulfur and selenium both forms oxoacids of formula $\mathbf{H_2EO_3}$, where **E** is either **S** or **Se**. These are called sulfurous and selenous acid, respectively. Which oxoacid would you expect to be more acidic: selenous acid or sulfurous acid?

Answer

Sulfurous acid should be more acidic. Since sulfur is more electronegative than selenium sulfur will polarize **OH** bonds to a greater extent, making them more acidic. This prediction is borne out by a comparison of the pK_a values for the acids:

Acid	pK_{a1}	pK_{a2}
sulfurous acid, $\mathbf{H_2SO_3}$	1.85	7.2
selenous acid, $\mathbf{H_2SeO_3}$	2.62	8.32

Trend 3: For polyprotic oxoacids the acidity decreases as each successive proton is removed

Oxoacids with multiple O-H bonds are called **polyprotic** since they can donate more than one hydrogen ion. In this case hydrogen ions are removed in successive ionization reactions. Examples include phosphoric and carbonic acid:

$$\mathbf{H_3PO_4} \rightleftharpoons \mathbf{H^+ + H_2PO_4^-} \qquad pK_{a1} = 2.2$$
$$\mathbf{H_2PO_4^-} \rightleftharpoons \mathbf{H^+ + HPO_4^{2-}} \qquad pK_{a2} = 7.2$$
$$\mathbf{HPO_4} \rightleftharpoons \mathbf{H^+ + PO_4^{3-}} \qquad pK_{a3} = 12.4$$
$$\mathbf{H_2CO_3} \rightleftharpoons \mathbf{H^+ + HCO_3^-} \qquad pK_{a1} = 3.6$$
$$\mathbf{HCO_3^-} \rightleftharpoons \mathbf{H^+ + CO_3^{2-}} \qquad pK_{a1} = 10.3$$

The dissociation constants for successive ionization constants decrease by about five orders of magnitude between successive hydrogen ions. This is reflected in Linus Pauling's rules for oxoacids and their oxyanions:

Pauling's Rules

1. The pK_a for an oxyacid of general formula $\mathbf{E(OH)_q(O)_p}$ is given by

$$pK_a = 8 - 5 \times p \tag{4.2.2.1}$$

2. As an oxoaxid undergoes successive ionizations the pK_a increases by five each time (i.e., K_a decreases 10,000-fold).

The central theme of Pauling's Rules is that the more oxygens there are on the central atom, the more resonance structures that can be constructed for the conjugate base, which increases its stability and increases the acidity of the acid. However, as the acids successively ionize, they have fewer resonance structures. Pauling's Rules are phenomenological (i.e., not based on a theoretical framework). However, as empirical rules, they often work quite well, but it should be borne in mind that they are approximate.

Exercise 4.2.2.2: How well do Pauling's rules for oxoacids work?

Calculate the theoretical pK_a values for phosphoric and carbonic acid and their dissociation produces and compare the results with the experimental pK_a values.

Answer

For phosphoric acid, Pauling's rules (Equation 4.2.2.1) predict the pK_a values quite well:

- $\mathbf{H_3PO_4}$: $p = 3$ and $q = 1$ and

$$pK_{a1,\text{predicted}} = 8 - 5 \times 1 = 3$$

  This is slightly greater than the observed value of 2.2.
- $\mathbf{H_2PO_4^-}$:

$$pK_{a2,\text{predicted}} = pK_{a1,\text{experimental}} + 5 = 7.2$$

This is spot on with experiment.

- HPO_4^{2-}:

$$pK_{a3,\text{predicted}} = pK_{a2,\text{experimental}} + 5 = 12.2$$

This is slightly less than the experimental value of 12.4.

For carbonic acid Pauling's rules predict pK_{a1} reasonably well, but pK_{a2} less so:

- H_2CO_3: $p = 2$, $q = 1$ and

$$pK_{a1,\text{predicted}} = 8 - 5 \times 1 = 3$$

This is slightly lower than the observed value of 3.6.

- HCO_3^-:

$$pK_{a2,\text{predicted}} = pK_{a1,\text{experimental}} + 5 = 8.6$$

This is 1.7 units less than the experimental value of 10.3.

In some cases discrepancies between experimental pK_a values and those predicted by Pauling's rules suggest that structural rearrangements may be taking place upon ionization or else that the reported pK_a values do not really represent the ionization in question because they do not fully account for all the equilibria taking place in solution. In the case of carbonic acid, however, the reason for the discrepancy between the predicted and experimental pK_{a2} values is not entirely clear.

This page titled 4.2.2: Trends of Oxyacids is shared under a CC BY-NC-SA 3.0 license and was authored, remixed, and/or curated by Stephen M. Contakes.

- **6.3.7: The Acidity of an Oxoacid is Determined by the Electronegativity and Oxidation State of the Oxoacid's Central Atom*** is licensed CC BY-NC-SA 3.0.

4.2.3: Trends in Metal Hydroxide Basicity/Solubility

Learning Objectives

- Estimate the pH of the solution due to precipitate of a metal hydroxide.
- Calculate the maximum metal ion concentration when the pH is known.
- Explain behavior of amphoteric metal hydroxides.

Most metal hydroxides are insoluble; some such as $Ca(OH)_2$, $Mg(OH)_2$, $Fe(OH)_2$, $Al(OH)_3$ etc. are sparingly soluble. However, alkali metal hydroxides **CsOH**, **KOH**, and **NaOH** are very soluble, making them strong bases. When dissolved, these hydroxides are completely ionized. Since the hydroxide concentration, $[OH^-]$, is an integrated property of the solution, the solubility of metal hydroxide depends on pH, pOH or $[OH^-]$.

Alkali metal hydroxides **LiOH**, **NaOH**, **KOH**, **CsOH** are soluble, and their solutions are basic. Hydroxides of alkali earth metals are much less soluble. For example, quicklime (**CaO**) reacts with water to give slaked lime, which is slightly soluble.

$$\underset{\text{quicklime}}{CaO} + H_2O \rightleftharpoons \underset{\text{slaked lime (slightly soluble)}}{Ca(OH)_2} \tag{4.2.3.1}$$

Milk of magnesia is $Mg(OH)_2$ (K_{sp} = 7e-12) suspension. In an acidic solution such as stomach juice, the following reaction takes place,

$$Mg(OH)_2 + H^+ \rightleftharpoons Mg^{2+} + 2\,H_2O \tag{4.2.3.2}$$

Thus, it can neutralize excess acid in the stomach.

Example 1

Calculate the maximum concentration of Mg^{2+} in a solution which contains a buffer so that pH = 3 at 298 K.

Solution

As usual, we write the equilibrium equation so that we can write the concentration below the formula. If we do not know the concentration, we assume it to be a variable x.

$$\underset{}{Mg(OH)_2} \rightleftharpoons \underset{x}{Mg^{2+}} + \underset{1\times10^{-11}}{2\,OH^-} \tag{4.2.3.3}$$

$$K_{sp} = x(1\times10^{-11})^2 = 7\times10^{-12} \tag{4.2.3.4}$$

Solving for x results in $x = 7\times^{10}$

DISCUSSION

This value certainly is too large, unrealistic.

Example 2

Calculate the pH of a saturated $Mg(OH)_2$ solution.

Solution

We assume the concentration to be x M of **Mg(OH)**, and note that $[OH^-] = 2x$,

$$\underset{}{Mg(OH)_2} \rightleftharpoons \underset{x}{Mg^{2+}} + \underset{2x}{2\,OH^-} \tag{4.2.3.5}$$

$$K_{sp} = x(2x)^2 = 7\text{e-}12 \tag{4.2.3.6}$$

Solving for x; x = 1.2e-4

$$[OH] = 2.4e\text{-}4 \quad (4.2.3.7)$$
$$pOH = 3.62 \quad (4.2.3.8)$$
$$pH = 14 - 3.62 = 10.38 \quad (4.2.3.9)$$

DISCUSSION

The pH of a saturated lime ($Ca(OH)_2$) solution is about 10.0.

Amphoteric Hydroxides

Not all metal hydroxides behave the same way - that is precipitate as hydroxide solids. Metal hydroxides such as $Fe(OH)_3$ and $Al(OH)_3$ react with acids and bases, and they are called **amphoteric hydroxide**. In reality, $Al(OH)_3$ should be formulated as $Al(H_2O)_3(OH)_3$, and this neutral substance has a very low solubility. It reacts in the following way as $[H^+]$ increases.

$$Al(H_2O)_3(OH)_3 + H_3O^+ \rightleftharpoons Al(H_2O)_4(OH)_2{}^+ + HOH \quad (4.2.3.10)$$
$$Al(H_2O)_4(OH)_2{}^+ + H_3O^+ \rightleftharpoons Al(H_2O)_5(OH)^{2+} + H_2O \quad (4.2.3.11)$$
$$Al(H_2O)_5(OH)^{2+} + H_3O^+ \rightleftharpoons Al(H_2O)_6{}^{3+} + H_2O \quad (4.2.3.12)$$

When the pH increases, the following reactions take place:

$$Al(H_2O)_3(OH)_3 + OH^- \rightleftharpoons Al(H_2O)_2(OH)_4{}^- + H_2O \quad (4.2.3.13)$$
$$Al(H_2O)_2(OH)_4{}^- + OH^- \rightleftharpoons Al(H_2O)(OH)_5{}^{2-} + H_2O \quad (4.2.3.14)$$
$$Al(H_2O)(OH)_5{}^{2-} + OH^- \rightleftharpoons Al(OH)_6{}^{3-} + H_2O \quad (4.2.3.15)$$

The charged species are soluble in water. As a result, amphoteric hydroxides dissolve in acidic and basic solutions.

Questions

1. Assume the pH of gastric juice to be 2. Calculate the maximum $[Mg^{2+}]$.
2. Calculate the pH of a 0.10 M NH_3 solution.
3. Calculate the maximum $[Fe^{2+}]$ in a 0.10 M NH_3 solution. Give the value in M .
4. What are amphoteric metal hydroxides? (enter no more than one line)

Solutions

1. *Answer* $[Mg^{2+}] = 7e12\ M$

   Consider...

   We assume the temperature to be 298 K, which is too low.

   $$[Mg^{2+}] = \frac{7e\text{-}12}{(1e\text{-}12)^2} = ?$$

   This value is unrealistically large. The result is correct, but meaningless.

2. *Answer* pH = 11.12

   Consider...

   $[OH^-] = (0.10 \times 1.8e\text{-}5)^{1/2} = 1.34e\text{-}3$

   $[H^+] = \frac{1e\text{-}14}{1.34e\text{-}3} = 7.5e\text{-}12,\ pH = ?$

   This value is required for the calculation in next question. Better yet, remember that $[OH^-] = 1.34e\text{-}4$.

3. *Answer* 4.4e-10 M

   Consider...

   $[Fe^{2+}] = \frac{7.9e\text{-}16}{(1.34e\text{-}3)^2} = ?\ M$

   What is the value in g/L? Molar mass of Fe is 55.8 g/mol.

4. *Answer* Metal hydroxides such as $Fe(OH)_3$ and $Al(OH)_3$ that react with acids and bases are called amphoteric hydroxide.

Contributors and Attributions

- Chung (Peter) Chieh (Professor Emeritus, Chemistry @ University of Waterloo)

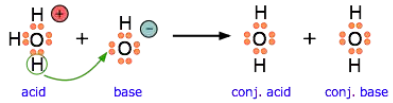
This page titled 4.2.3: Trends in Metal Hydroxide Basicity/Solubility is shared under a CC BY-NC-SA 3.0 license and was authored, remixed, and/or curated by Stephen M. Contakes.

- **Solubility of Metal Hydroxides** is licensed CC BY-NC-SA 4.0.

4.3: Lewis Acids and Bases

Lewis Acid-Base Neutralization Involving Electron-Pair Transfer

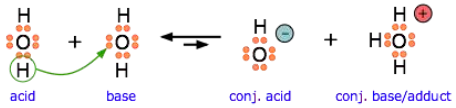
Just as any Arrhenius acid is also a Brønsted acid, any Brønsted acid is also a Lewis acid, so the various acid-base concepts are all "upward compatible". Although we do not really need to think about electron-pair transfers when we deal with ordinary aqueous-solution acid-base reactions, it is important to understand that it is the opportunity for electron-pair sharing that enables proton transfer to take place.



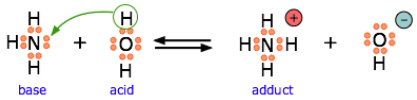
This equation for a simple acid-base neutralization shows how the Brønsted and Lewis definitions are really just different views of the same process. Take special note of the following points:

- The arrow shows the movement of a proton from the hydronium ion to the hydroxide ion.
- Note that the electron-pairs themselves do not move; they remain attached to their central atoms. The electron pair on the base is "donated" to the acceptor (the proton) only in the sense that it ends up being *shared* with the acceptor, rather than being the exclusive property of the oxygen atom in the hydroxide ion.
- Although the hydronium ion is the nominal Lewis acid here, it does not itself accept an electron pair, but acts merely as the source of the proton that coordinates with the Lewis base.

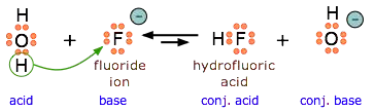
The point about the electron-pair remaining on the donor species is especially important to bear in mind. For one thing, it distinguishes a *Lewis acid-base reaction* from an *oxidation-reduction reaction*, in which a physical transfer of one or more electrons from donor to acceptor does occur. The product of a Lewis acid-base reaction is known formally as an "adduct" or "complex", although we do not ordinarily use these terms for simple proton-transfer reactions such as the one in the above example. Here, the proton combines with the hydroxide ion to form the "adduct" H_2O. The following examples illustrate these points for some other proton-transfer reactions that you should already be familiar with.



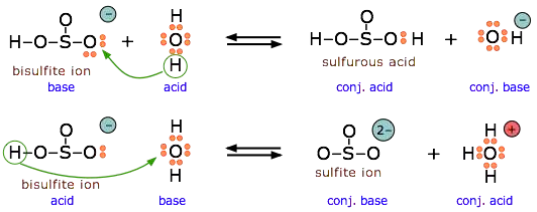
Another example, showing the autoprotolysis of water. Note that the conjugate base is also the adduct.



Ammonia is both a Brønsted and a Lewis base, owing to the unshared electron pair on the nitrogen. The reverse of this reaction represents the *hydrolysis* of the ammonium ion.



Because HF is a weak acid, fluoride salts behave as bases in aqueous solution. As a Lewis base, F^- accepts a proton from water, which is transformed into a hydroxide ion.

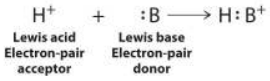


The bisulfite ion is *amphiprotic* and can act as an electron donor or acceptor.

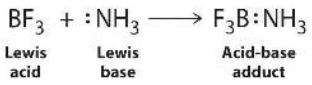
> **Note**
>
> All Brønsted–Lowry bases (proton acceptors), such as OH^-, H_2O, and NH_3, are also electron-pair donors. Thus the Lewis definition of acids and bases does not contradict the Brønsted–Lowry definition. Rather, it expands the definition of acids to include substances other than the H^+ ion.

Lewis Acid-Base Neutralization without Transferring Protons

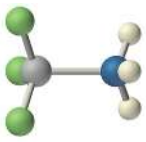
Electron-deficient molecules, such as BCl_3, contain less than an octet of electrons around one atom and have a strong tendency to gain an additional pair of electrons by reacting with substances that possess a lone pair of electrons. Lewis's definition, which is less restrictive than either the Brønsted–Lowry or the Arrhenius definition, grew out of his observation of this tendency. A general Brønsted–Lowry acid–base reaction can be depicted in Lewis electron symbols as follows:



The proton (H^+), which has no valence electrons, is a Lewis acid because it accepts a lone pair of electrons on the base to form a bond. The proton, however, is just one of many electron-deficient species that are known to react with bases. For example, neutral compounds of boron, aluminum, and the other Group 13 elements, which possess only six valence electrons, have a very strong tendency to gain an additional electron pair. Such compounds are therefore potent Lewis acids that react with an electron-pair donor such as ammonia to form an acid–base adduct, a new covalent bond, as shown here for boron trifluoride (BF_3):



The bond formed between a Lewis acid and a Lewis base is a *coordinate covalent bond* because both electrons are provided by only one of the atoms (N, in the case of $F_3B{:}NH_3$). After it is formed, however, a coordinate covalent bond behaves like any other covalent single bond.



Boron trifluoride-ammonia adduct

Species that are very weak Brønsted–Lowry bases can be relatively strong Lewis bases. For example, many of the group 13 trihalides are highly soluble in ethers (R–O–R′) because the oxygen atom in the ether contains two lone pairs of electrons, just as in H_2O. Hence the predominant species in solutions of electron-deficient trihalides in ether solvents is a Lewis acid–base adduct. A reaction of this type is shown in Figure **4.3.1** for boron trichloride and diethyl ether:

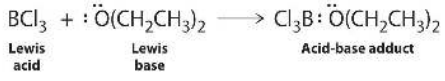
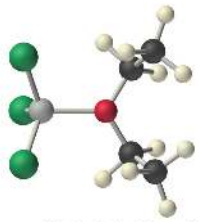


Figure 4.3.1: *Lewis Acid/Base reaction of boron trichloride and diethyl ether reaction*

Note

- Electron-deficient molecules (those with less than an octet of electrons) are Lewis acids.
- The acid-base behavior of many compounds can be explained by their Lewis electron structures.

Many molecules with multiple bonds can act as Lewis acids. In these cases, the Lewis base typically donates a pair of electrons to form a bond to the central atom of the molecule, while a pair of electrons displaced from the multiple bond becomes a lone pair on a terminal atom.



Boron trichloride-diethyl ether adduct

Figure 4.3.2. The highly electronegative oxygen atoms pull electron density away from carbon, so the carbon atom acts as a Lewis acid. Arrows indicate the direction of electron flow.

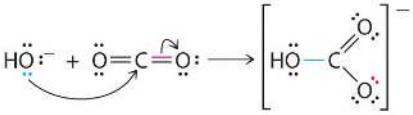


Figure 4.3.2: *Lewis Acid/Base reaction of the hydroxide ion with carbon dioxide*

Example 4.3.1

Identify the acid and the base in the Lewis acid–base reaction.

$BH_3 + (CH_3)_2S \rightarrow H_3B{:}S(CH_3)_2$

Solution

In each equation, identify the reactant that is electron deficient and the reactant that is an electron-pair donor. The electron-deficient compound is the Lewis acid, whereas the other is the Lewis base.

In BH_3, boron has only six valence electrons. It is therefore electron deficient and can accept a lone pair. Like oxygen, the sulfur atom in $(CH_3)_2S$ has two lone pairs. Thus $(CH_3)_2S$ donates an electron pair on sulfur to the boron atom of BH_3. The Lewis base is $(CH_3)_2S$, and the Lewis acid is BH_3

Example 4.3.2

Identify the acid and the base in the Lewis acid–base reaction.

$CaO + CO_2 \rightarrow CaCO_3$

Solution

In each equation, identify the reactant that is electron deficient and the reactant that is an electron-pair donor. The electron-deficient compound is the Lewis acid, whereas the other is the Lewis base.

CO_2 accepts a pair of electrons from the O^{2-} ion in CaO to form the carbonate ion. The oxygen in CaO is an electron-pair donor, so CaO is the Lewis base. Carbon accepts a pair of electrons, so CO_2 is the Lewis acid.

Problems

Exercise 4.3.1

Identify the acid and the base in the Lewis acid–base reaction.

$(CH_3)_2O + BF_3 \rightarrow (CH_3)_2O{:}BF_3$

Answer

Lewis base: $(CH_3)_2O$; Lewis acid: BF_3

Exercise 4.3.2

Identify the acid and the base in the Lewis acid–base reaction.

$H_2O + SO_3 \rightarrow H_2SO_4$

Answer

Lewis base: H_2O; Lewis acid: SO_3

Exercise 4.3.3

Identify the acid and the base in the Lewis acid–base reaction.

$BeCl_2 + 2\ Cl^- \rightarrow BeCl_4^{2-}$

Answer

The chloride ion contains four lone pairs. In this reaction, each chloride ion donates one lone pair to $BeCl_2$, which has only four electrons around Be. Thus the chloride ions are Lewis bases, and $BeCl_2$ is the Lewis acid

Exercise 4.3.4

Here are several more examples of Lewis acid-base reactions that **cannot** be accommodated within the Brønsted or Arrhenius models. Identify the Lewis acid and Lewis base in each reaction.

a. $Al(OH)_3 + OH^- \rightarrow Al(OH)_4^-$
b. $SnS_2 + S^{2-} \rightarrow SnS_3^{2-}$
c. $Cd(CN)_2 + 2CN^- \rightarrow Cd(CN)_4^{2+}$
d. $AgCl + 2NH_3 \rightarrow Ag(NH_3)_2^+ + Cl^-$
e. $Fe^{2+} + NO \rightarrow Fe(NO)^{2+}$
f. $[Ni^{2+} + 6NH_3 \rightarrow Ni(NH_3)_5^{2+}$

Answer a

Lewis base: OH^-; Lewis acid: $Al(OH)_3$

Answer b

Lewis base: S^{2-}; Lewis acid: SnS_2

Answer c

Lewis base: CN^-; Lewis acid: $Cd(CN)_2$

Answer d

Lewis base: NH_3; Lewis acid: AgCl

Answer e

Lewis base: NO; Lewis acid: Fe^{2+}

Answer f

Lewis base: NH_3; Lewis acid: Ni^{2+}

Contributors and Attributions

- Stephen Lower, Professor Emeritus (Simon Fraser U.) Chem1 Virtual Textbook
- Wikipedia

4.3: Lewis Acids and Bases is shared under a CC BY-NC-SA 4.0 license and was authored, remixed, and/or curated by Kathryn A. Newton, Northern Michigan University.

- **16.9: Lewis Acids and Bases** is licensed CC BY-NC-SA 4.0.

4.3.1: Conjugate Acids of Lewis Bases are Bronsted Acids

Learning Objectives

- Estimate the pH of the solution due to precipitate of a metal hydroxide.
- Calculate the maximum metal ion concentration when the pH is known.
- Explain behavior of amphoteric metal hydroxides.

Most metal hydroxides are insoluble; some such as $\mathbf{Ca(OH)_2}$, $\mathbf{Mg(OH)_2}$, $\mathbf{Fe(OH)_2}$, $\mathbf{Al(OH)_3}$ etc. are sparingly soluble. However, alkali metal hydroxides **CsOH**, **KOH**, and **NaOH** are very soluble, making them strong bases. When dissolved, these hydroxides are completely ionized. Since the hydroxide concentration, $[\mathbf{OH^-}]$, is an integrated property of the solution, the solubility of metal hydroxide depends on pH, pOH or $[\mathbf{OH^-}]$.

Alkali metal hydroxides **LiOH**, **NaOH**, **KOH**, **CsOH** are soluble, and their solutions are basic. Hydroxides of alkali earth metals are much less soluble. For example, quicklime (**CaO**) reacts with water to give slaked lime, which is slightly soluble.

$$\underset{\text{quicklime}}{\mathbf{CaO}} + \mathbf{H_2O} \rightleftharpoons \underset{\text{slaked lime (slightly soluble)}}{\mathbf{Ca(OH)_2}} \tag{4.3.1.1}$$

Milk of magnesia is $\mathbf{Mg(OH)_2}$ (K_{sp} = 7e-12) suspension. In an acidic solution such as stomach juice, the following reaction takes place,

$$\mathbf{Mg(OH)_2 + H^+ \rightleftharpoons Mg^{2+} + 2\,H_2O} \tag{4.3.1.2}$$

Thus, it can neutralize excess acid in the stomach.

Example 1

Calculate the maximum concentration of $\mathbf{Mg^{2+}}$ in a solution which contains a buffer so that pH = 3 at 298 K.

Solution

As usual, we write the equilibrium equation so that we can write the concentration below the formula. If we do not know the concentration, we assume it to be a variable x.

$$\underset{}{\mathbf{Mg(OH)_2}} \rightleftharpoons \underset{x}{\mathbf{Mg^{2+}}} + \underset{1\times10^{-11}}{\mathbf{2\,OH^-}} \tag{4.3.1.3}$$

$$K_{sp} = x(1\times10^{-11})^2 = 7\times10^{-12} \tag{4.3.1.4}$$

Solving for x results in $x = 7\times^{10}$

DISCUSSION

This value certainly is too large, unrealistic.

Example 2

Calculate the pH of a saturated $\mathbf{Mg(OH)_2}$ solution.

Solution

We assume the concentration to be x M of **Mg(OH)**, and note that $[\mathbf{OH^-}] = 2x$,

$$\underset{}{\mathbf{Mg(OH)_2}} \rightleftharpoons \underset{x}{\mathbf{Mg^{2+}}} + \underset{2x}{\mathbf{2\,OH^-}} \tag{4.3.1.5}$$

$$K_{sp} = x(2x)^2 = \text{7e-12} \tag{4.3.1.6}$$

Solving for x; x = 1.2e-4

$$[OH] = 2.4e\text{-}4 \quad (4.3.1.7)$$
$$pOH = 3.62 \quad (4.3.1.8)$$
$$pH = 14 - 3.62 = 10.38 \quad (4.3.1.9)$$

DISCUSSION

The pH of a saturated lime ($Ca(OH)_2$) solution is about 10.0.

Amphoteric Hydroxides

Not all metal hydroxides behave the same way - that is precipitate as hydroxide solids. Metal hydroxides such as $Fe(OH)_3$ and $Al(OH)_3$ react with acids and bases, and they are called **amphoteric hydroxide**. In reality, $Al(OH)_3$ should be formulated as $Al(H_2O)_3(OH)_3$, and this neutral substance has a very low solubility. It reacts in the following way as $[H^+]$ increases.

$$Al(H_2O)_3(OH)_3 + H_3O^+ \rightleftharpoons Al(H_2O)_4(OH)_2{}^+ + HOH \quad (4.3.1.10)$$
$$Al(H_2O)_4(OH)_2{}^+ + H_3O^+ \rightleftharpoons Al(H_2O)_5(OH)^{2+} + H_2O \quad (4.3.1.11)$$
$$Al(H_2O)_5(OH)^{2+} + H_3O^+ \rightleftharpoons Al(H_2O)_6{}^{3+} + H_2O \quad (4.3.1.12)$$

When the pH increases, the following reactions take place:

$$Al(H_2O)_3(OH)_3 + OH^- \rightleftharpoons Al(H_2O)_2(OH)_4{}^- + H_2O \quad (4.3.1.13)$$
$$Al(H_2O)_2(OH)_4{}^- + OH^- \rightleftharpoons Al(H_2O)(OH)_5{}^{2-} + H_2O \quad (4.3.1.14)$$
$$Al(H_2O)(OH)_5{}^{2-} + OH^- \rightleftharpoons Al(OH)_6{}^{3-} + H_2O \quad (4.3.1.15)$$

The charged species are soluble in water. As a result, amphoteric hydroxides dissolve in acidic and basic solutions.

Questions

1. Assume the pH of gastric juice to be 2. Calculate the maximum $[Mg^{2+}]$.
2. Calculate the pH of a 0.10 M NH_3 solution.
3. Calculate the maximum $[Fe^{2+}]$ in a 0.10 M NH_3 solution. Give the value in M .
4. What are amphoteric metal hydroxides? (enter no more than one line)

Solutions

1. *Answer* $[Mg^{2+}] = 7e12\ M$

   Consider...

   We assume the temperature to be 298 K, which is too low.

   $$[Mg^{2+}] = \frac{7e\text{-}12}{(1e\text{-}12)^2} = ?$$

   This value is unrealistically large. The result is correct, but meaningless.

2. *Answer* pH = 11.12

   Consider...

   $[OH^-] = (0.10 \times 1.8e\text{-}5)^{1/2} = 1.34e\text{-}3$

   $[H^+] = \frac{1e\text{-}14}{1.34e\text{-}3} = 7.5e\text{-}12,\ pH = ?$

   This value is required for the calculation in next question. Better yet, remember that $[OH^-] = 1.34e\text{-}4$.

3. *Answer* 4.4e-10 M

   Consider...

   $[Fe^{2+}] = \frac{7.9e\text{-}16}{(1.34e\text{-}3)^2} = ?\ M$

   What is the value in g/L? Molar mass of Fe is 55.8 g/mol.

4. *Answer* Metal hydroxides such as $Fe(OH)_3$ and $Al(OH)_3$ that react with acids and bases are called amphoteric hydroxide.

Contributors and Attributions

- Chung (Peter) Chieh (Professor Emeritus, Chemistry @ University of Waterloo)

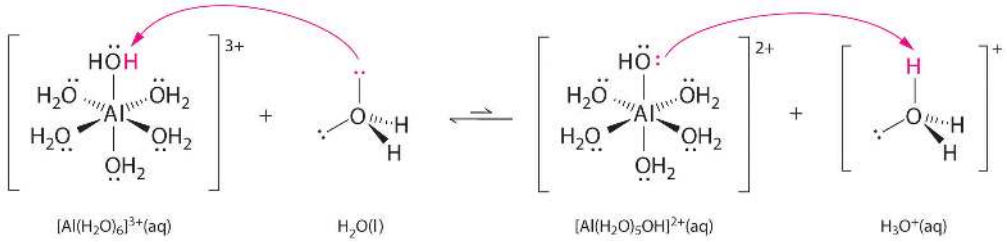
4.3.1: Conjugate Acids of Lewis Bases are Bronsted Acids is shared under a CC BY-NC-SA 4.0 license and was authored, remixed, and/or curated by LibreTexts.

- **Solubility of Metal Hydroxides** is licensed CC BY-NC-SA 4.0.

4.3.2: Acidity of Metal Ions in Water

Metal Ions Act as Acids by Polarizing Bound Water Molecules Called Aqua Ligands

Aqueous solutions of simple salts of metal ions can also be acidic, even though a metal ion cannot donate a proton directly to water to produce H_3O^+. Instead, a metal ion can act as a Lewis acid and interact with water, a Lewis base, by coordinating to a lone pair of electrons on the oxygen atom to form a hydrated metal ion.



A water molecule coordinated to a metal ion is more acidic than a free water molecule for two reasons. First, repulsive electrostatic interactions between the positively charged metal ion and the partially positively charged hydrogen atoms of the coordinated water molecule make it easier for the coordinated water to lose a proton.

Second, the positive charge on the Al^{3+} ion attracts electron density from the oxygen atoms of the water molecules, which decreases the electron density in the **O–H** bonds, as shown in Figure **4.3.2.5*b***. With less electron density between the *O* atoms and the H atoms, the **O–H** bonds are weaker than in a free H_2O molecule, making it easier to lose an H^+ ion. This is shown schematically in Figure **4.3.2.1**.

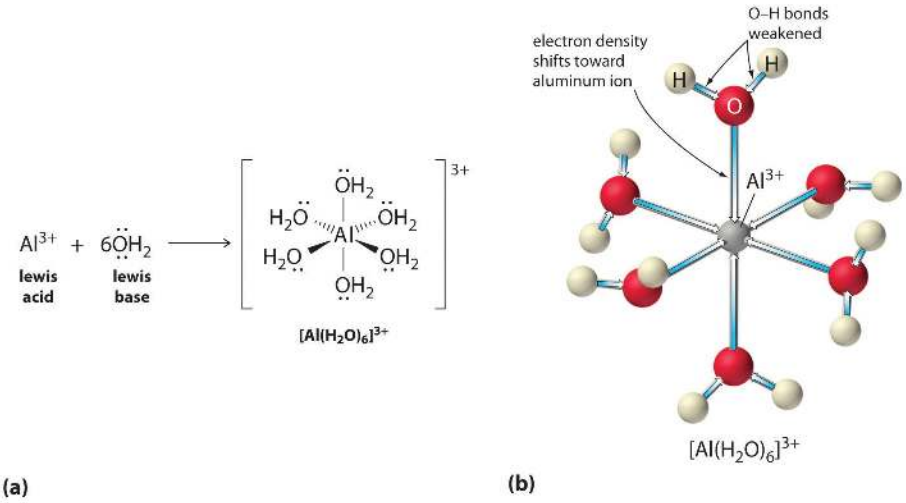


Figure **4.3.2.1**: Effect of a Metal Ion on the Acidity of Water (a) Reaction of the metal ion Al^{3+} with water to form the hydrated metal ion is an example of a Lewis acid–base reaction. (b) The positive charge on the aluminum ion attracts electron density from the oxygen atoms, which shifts electron density away from the O–H bonds. The decrease in electron density weakens the O–H bonds in the water molecules and makes it easier for them to lose a proton. (CC BY-NC-SA 3.0; anonymous)

The acidity of a given metal ion largely depends on its charge to size ratio and electronegativity, although in some cases hardness and ligand field effects also play a role.

The magnitude of this effect depends on the following factors, of which the first two are generally considered the most important (Figure **4.3.2.2**):

The charge on the metal ion

A divalent ion (M^{2+}) has approximately twice as strong an effect on the electron density in a coordinated water molecule as a monovalent ion (M^+) of the same radius.

The radius of the metal ion

For metal ions with the same charge, the smaller the ion, the shorter the internuclear distance to the oxygen atom of the water molecule and the greater the effect of the metal on the electron density distribution in the water molecule.

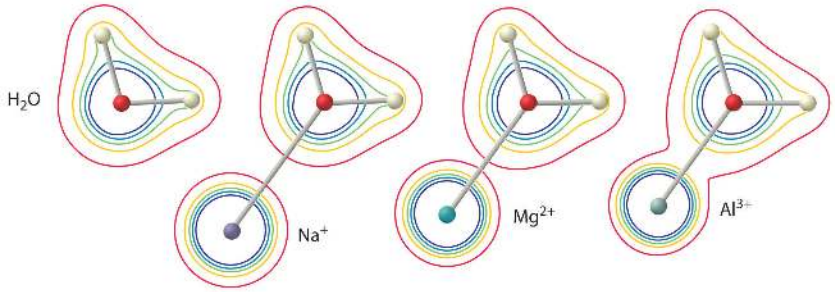


Figure **4.3.2.2**: The effect of the charge and radius of a metal ion on the acidity of a coordinated water molecule. The contours show the electron density on the O atoms and the H atoms in both a free water molecule (left) and water molecules coordinated to Na^{+}, Mg^{2+}, and Al^{3+} ions. These contour maps demonstrate that the smallest, most highly charged metal ion (Al^{3+}) causes the greatest decrease in electron density of the O–H bonds of the water molecule. Due to this effect, the acidity of hydrated metal ions increases as the charge on the metal ion increases and its radius decreases. (CC BY-NC-SA 3.0; anonymous)

The first two of these factors explain why most alkali metal cations exhibit little acidity while aqueous solutions of small, highly charged metal ions, such as Al^{3+} and Fe^{3+}, are acidic:

$$[Al(H_2O)_6]^{3+}(aq) \rightleftharpoons [Al(H_2O)_5(OH)]^{2+}(aq) + H^{+}(aq) \tag{4.3.2.1}$$

The $[Al(H_2O)_6]^{3+}$ ion has a pK_a of 5.0, making it almost as strong an acid as acetic acid. Because of the two factors described previously, the most important parameters for predicting the effect of a metal ion on the acidity of coordinated water molecules are the charge and ionic radius of the metal ion.

A simple empirical equation for predicting the pK_a of metal ions in water has been proposed by Wulfsberg:[1]

$$pK_a = 15.14 - 88.16\ pm\left(\frac{Z^2}{r}\right)$$

where Z is the charge on the metal ion and r its radius. As can be seen from figure **4.3.2.3**, in general the acidity of metal ions increases with $\frac{Z^2}{r}$). Nevertheless a number of ions have considerably lower pK_a values than predicted from this correlation, suggesting that the acidity of metal cations cannot be predicted using a simple electrostatic model alone.

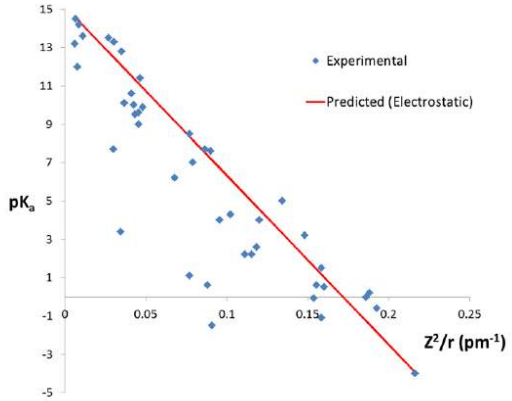


Figure **4.3.2.3**: The pK_a of metal ions (♦) as a function of $\frac{Z^2}{r}$ for 43 metal ions. Drawn using radii listed in reference 1.

Although the charge-to-size ratio is the simplest and most powerful predictor of metal ion acidity in water, three additional factors also can play a role:

Electronegativity

All other things being equal, more electronegative elements are better able to withdraw electron density from a bound water ligand and consequently better at enhancing the ability of that water molecule to lose a hydrogen ion. The electrostatic model of ion

acidity can be extended to account for electronegativity effects but only needs to be done so for metals with Pauling electronegativities greater than 1.5. The empirical relationship that has been proposed to account for the effect of electronegativity is:

$$pK_a = 15.14 - 88.16\left(\frac{Z^2}{r} + 0.096(\chi - 1.50)\right)$$

where r is the ion radius in pm and χ is its Pauling electronegativity. As can be seen from figure **4.3.2.4**, the electronegativity term accounts for some of the deviations in metal ion acidity predicted from charge and size effects alone.

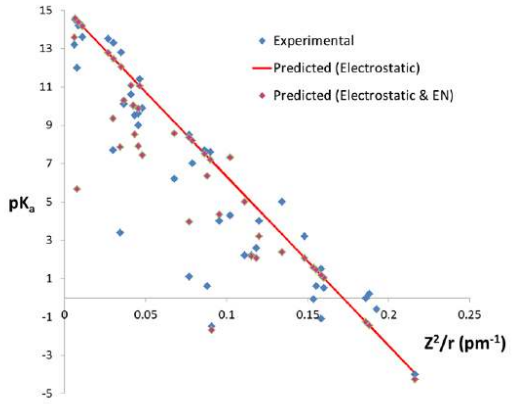


Figure **4.3.2.4**: Comparison between the experimental pK_a values (♦) for 43 metal ions and those predicted empirically accounting for size and charge effects (-) and accounting for size, charge, and electronegativity effects (♦). Drawn using radii listed in reference 1.

However, there are still large deviations between the predicted and observed pK_a for a number of ions. In particular, the modified electrostatic model overestimates the pK_a of Al^{3+} and Sn^{4+} and underestimates the pK_a of Hg^{2+}, Sn^{2+}, and Tl^{3+}. While the exact reasons for these discrepancies is not entirely clear, at least some are thought to arise from the impact of the fourth factor that determines metal ion acidity.

Hardness and Softness

Cation hardness or softness is assessed according to Pearson's Hard-Soft Acid Base Principle (HSABP). In general, soft cations are more acidic than hard cations of the same charge and radius, as may be seen from the examples in Table **4.3.2.1**. The greater than expected acidity of softer cations is thought to reflect the importance of covalent contributions to the metal-water bond.

Table **4.3.2.1**: Comparison of the pK_a values at 25°C of hard and soft cations with approximately the same radius and charge. Based on Gutmann[2] as reported by Burgess.[3]

Cation	Classification	Radius (pm)	pK_a1
K^+	hard	1.33	14
Ag^+	soft	1.26	10
Mg^{2+}	hard	0.65	12.2
Cu^{2+}	soft	0.69	7.3
Ca^{2+}	hard	0.99	12.6
Cd^{2+}	soft	0.97	9.0
Sr^{2+}	hard	1.13	13.1
Hg^{2+}	soft	1.10	3.6

Ligand field effects

Ligand field effects involve bonding and antibonding interactions between the *d* orbitals on a transition metal and ligand orbitals. The importance of ligand field interactions on cation acidity is not well established, but ligand field interactions might influence the acidity of a hydrated metal in two cases: (a) when the ligand field stabilization of the aqua complex (metal with H_2O or OH^- bound) is greater or less than that in its conjugate base and (b) in complexes which undergo Jahn-Teller distortions that alter the metal's ability to polarize the OH bond.

References

1. Wulfsberg, G. *Principles of Descriptive Inorganic Chemistry* University Science Books, 1991, pp. 28-30.
2. (a) Gutmann, V. *Allg. Prakt. Chem.* 1970, *21*, 116. (b) Gutmann, V. *Fortschr. Chem. Forsch.* 1972, *27*, 59.
3. Burgess, J. *Metal Ions in Solution* Ellis Horwood, 1978, pg. 268.

4.3.2: Acidity of Metal Ions in Water is shared under a CC BY-NC-SA 4.0 license and was authored, remixed, and/or curated by Stephen M. Contakes.

- **6.3.8: High Charge-to-Size Ratio Metal Ions Act as Brønsted Acids in Water** by Stephen M. Contakes is licensed CC BY-NC-SA 4.0.

4.3.3: Hard-Soft Designation of Lewis Acids and Bases

The Hard-Soft Acid-Base concept is a tool for thinking about patterns of Lewis acid-base reactivity. Arland, Chatt, and Davies' observed that *Lewis acids and bases could be classified into two groups based on their propensity to form stable compounds with one another* (*e.g.* acids in a class tend to form more stable adducts with bases in the same class than they did with bases in the other class).[1] Arland, Chatt, and Davies somewhat boringly termed these groups class a and class b but today they are known by Ralph Pearson's name for them. Pearson called the class a acids and bases *hard* and called the class b acids and bases *soft*. These terms reflect the polarizability of the electron cloud, or how "soft" these substance's electron clouds are towards distortion (Figure **4.3.3.1**). **Soft** acids and bases are relatively polarizable, and **hard** acids and bases are difficult to polarize.

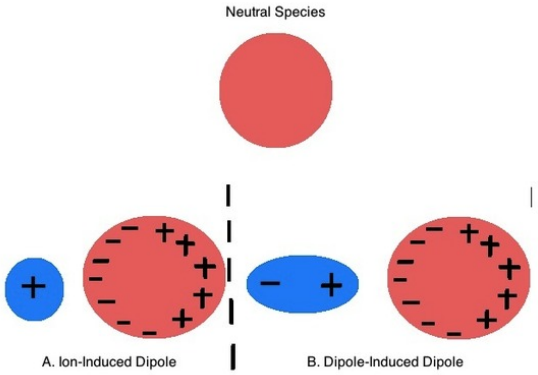


Figure **4.3.3.1**: Polarizability refers to the ease with which a substance's electron cloud may be distorted under the action of an electric field. Polarizability determines the degree to which a neutral species' electron cloud can be distorted to an induced dipole moment by an ion (as shown on the left) or by a polar molecule (as shown on the right). [CC-BY 4.0, LibreText]

Hard and Soft Classification

Hard Species

Hard acids and bases have a high charge density (highly charged relative to size), and polarization is difficult. Low polarizability is attributed to hard acids being relatively electron-poor and hard bases being relatively electron-rich. Low polarizability is also attributed to the localization of charge on an atom with electron-withdrawing substituents (in the case of a hard acid) or electron-donating substituents (in the case of a hard base). It is also observed that hard acids have high oxidation states or large positive formal charges, while hard bases have low oxidation states or negative formal charges.

For hard acids, which possess few valence electrons, polarization involves distorting core (inner shell) electrons, which are difficult to distort because they are close to the nucleus and experience a high nuclear charge. Hard acids tend to be found towards the left side of the periodic table and involve higher oxidation states and/or electron donating substituents

Soft Species

Soft acids and bases posses many valence electrons and are more readily polarized. Soft acids and bases are more likely to be found towards the middle or right of the periodic table. Soft acids and bases also have little charge density and/or are relatively electron rich. Soft acids are more common to the right of the periodic table and involve lower oxidation states and/or electron donating substituents.

Borderline Species

All hard acids and bases are not equally hard, and all soft acids and bases are not equally soft. There is a graduation in hardness and softness, and there are a number of intermediate acids and bases that do not fit neatly in either category. Figure **4.3.3.1** classifies each element as a hard, soft, or **borderline** (intermediate) acid or base. Some borderline acids can be considered hard or soft depending on their oxidation state. The higher oxidation state species can be considered hard acids, and the lower oxidation state species can be considered soft acids. Additional representative examples of hard, soft, and borderline bases are shown in Figure Extra close brace or missing open brace and Figure **4.3.3.3**.

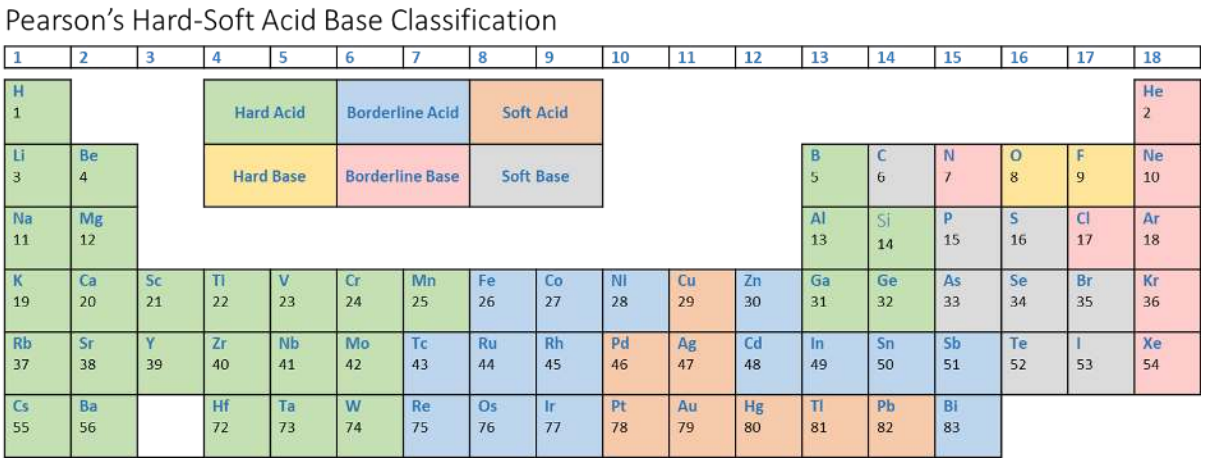


Figure 4.3.3.1: Pearson's Hard-Soft Acid Base Classification of the Elements (CC-BY-NC-SA; Kathryn A. Newton)

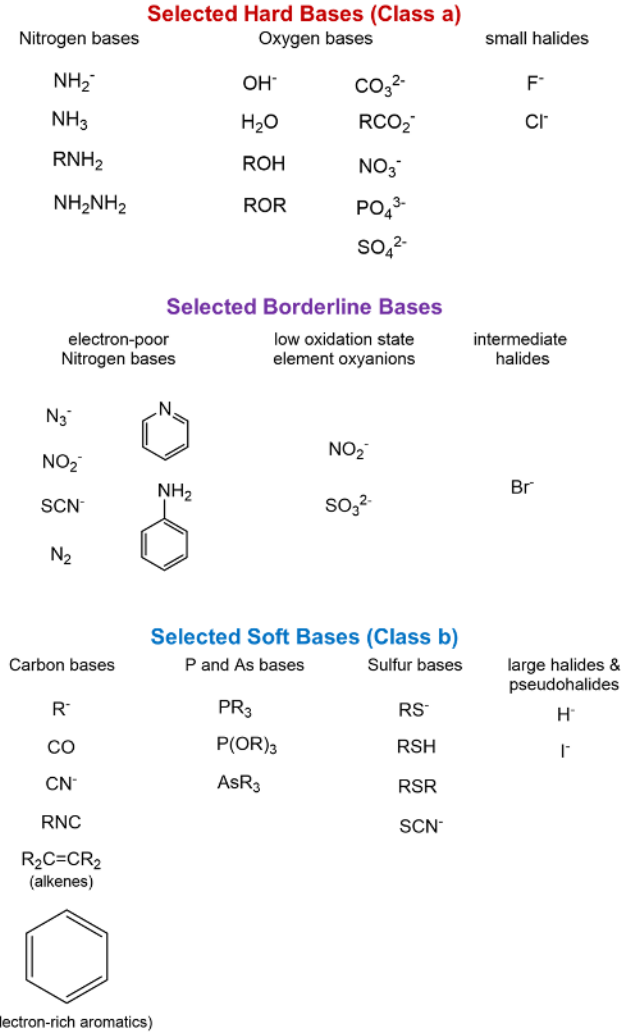


Figure 4.3.3.2: Representative examples of hard, soft, and borderline bases. (LibreText)

Hard Base	Soft Base	Borderline Base	Hard Acid	Soft Acid	Borderline Acid
NR_3 (R = alkyl group) O^{2-} F^- Cl^-	CO CN^- P S As Se Te I NCS^-	Br^- ^-NCS	Ti^{4+} V^{4+} Cr^{3+}, Cr^{6+} $Mn^{2+}, Mn^{4+}, Mn^{7+}$ Fe^{3+} Co^{3+} Ni^{3+}	Cu^+ M^{n-} (−oxidation state)	Fe^{2+} Co^{2+} Ni^{2+} Cu^{2+}

Figure **4.3.3.3**: HSAB classifcation of selected species. (CC-BY-NC-SA; Kathryn A. Newton)

The Hard-Soft Acid-Base Principle (HSAB Principle)

The **Hard-Soft Acid-Base Concept (HSAB Concept)** explains patterns in Lewis acid-base reactivity as a *like reacts with like* preference. Both thermodynamically and kinetically, hard acids prefer hard bases and soft acids soft bases. Specifically,

- Thermodynamically, hard acids form more stable acid-base complexes with hard bases while soft acids form more stable complexes with soft bases.
- Kinetically, hard acids/electrophiles react more quickly with hard bases/nucleophiles while soft acids/electrophiles react more quickly with soft bases/nucleophiles.

The HSAB principle can predict the equilibrium of Lewis acid-base metathesis and displacement reactions. In a Lewis acid-base **metathesis reaction** the acids and bases swap partners:

$$\mathbf{A_1 : B_1 + A_2 : B_2 \overset{k_1,\, K_{eq}}{\rightleftharpoons} A_1 : B_2 + A_2 : B_1}$$

For example, the equilibrium position of the metathesis reaction between $\mathbf{TlF}$ and $\mathbf{K_2S}$ favors the products:

$$\mathbf{2\,TlF + H_2S \rightleftharpoons Tl_2S + 2\,KF}$$

This is consistent with the HSAB's hard-hard and soft-soft preference.



The HSAB principle also allows for prediction of displacement reactions, in which a Lewis acid or base forms an adduct using a base or acid from an existing Lewis acid-base complex. In these reactions, the displacement of acid or base from the reactant complex may be thought of as a sort of metathesis reaction, one in which in the unbound acid or base switches places with one in the complex. For example, the reaction between $\mathbf{HI}$ and methylmercury cation involves displacement of an iodide from $\mathbf{HI}$ to give $\mathbf{CH_3HgI}$. The position of the equilibrium favors $\mathbf{CH_3HgI}$ since both $\mathbf{CH_3Hg^+}$ and $\mathbf{I^-}$ are soft, while $\mathbf{H^+}$ is a hard acid.

$$\mathbf{HI + HgSCH_3^+ \rightleftharpoons CH_3SHgI + H^+}$$



The hard-hard and soft-soft preferences in Lewis acid-base interactions reflect that:

- The lone pair of a hard base is strongly stabilized electrostatically by a hard acid.
- The lone pair of a soft base is strongly stabilized by forming a covalent bond with a soft acid.

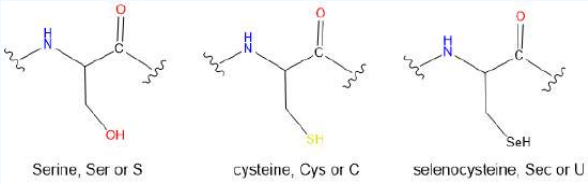
- The lone pair of a hard or soft base is comparatively weakly stabilized by an acid opposite to it in hardness or softness since the overall electrostatic and covalent stabilization of the adduct is comparatively weak.

Problems

Exercise 4.3.3.1

Rank the acids or bases in each set in increasing order of expected hardness.

a. Cr^{2+} and Cr^{3+}
b. H^+, Cs^+, and Tl^+
c. SCN^- (acting as a base at N) and SCN^- (acting as a base at S)
d. AlF_3, AlH_3, $AlMe_3$
e. The side chains of the following proteinogenic amino acids

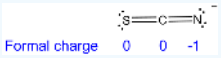


Answer

(a) $Cr^{2+} < Cr^{3+}$ All other things being equal, hardness increases with oxidation state.

(b) $Tl^+ < Cs^+ < H^+$ The order reflects Cs^+ and Tl^+'s larger size relative to H^+ (which doesn't possess any electrons that can be polarized anyway) and that Tl^+ still possesses two valence electrons while Cs^+ possesses none.

(c) SCN^- (acting as a base at S) < SCN^- (acting as a base at N). The order reflects the greater electronegativity of N than S and N's possession of a more negative formal charge of -1.



(d) $AlH_3 < AlMe_3 < AlF_3$. The hardness increases as the substituents on the Lewis acid Al center become less electron donating and more electron withdrawing (and, incidentally, harder bases) as their electronegativity increases in the order H^- < CH_3^- < F^-. Note that the order of electron donating ability for H^- and CH_3^- is the opposite observed for carbocations, for which hyperconjugation plays a larger role.

(e) Sec < Cys < Ser. The hardness increases as the electronegativity of the Lewis base chalcogen increases on going from a selenol to a thiol to an alcohol.

Exercise 4.3.3.2

Predict the position of equilibrium for the following reaction.

$$Fe_2O_3 + 3\,Ag_2S \rightleftharpoons Fe_2S_3 + 3\,Ag_2O$$

Answer

The equilibrium will favor the reactants (K<1) since the hard-hard and soft-soft interactions in the reactants are more stable than the hard-soft interactions in the products.



Exercise 4.3.3.3

Predict whether K for the following equilibria will be <<1, ~1, or >>1.

a. $2\,HF + (CH_3Hg)_2S \rightleftharpoons 2\,CH_3HgF + H_2S$
b. $Ag(NH_3)_2^+ + 2\,PH_3 \rightleftharpoons Ag(PH_3)_2^+ + 2\,NH_3$
c. $Ag(PH_3)_2^+ + 2\,H_3B{-}SH_2 \rightleftharpoons 2\,H_3B{-}PH_3 + Ag(SH_2)_2^+$
d. $H_3B{-}NH_3 + F_3B{-}SH_2 \rightleftharpoons H_3B{-}SH_2 + F_3B{-}NH_3$

Answer

a. K< < 1 since the reactant adducts are hard-hard and soft-soft while the products involve hard-soft interactions.

b. K>>1 since the reactant complex, diamine silver(I), is a complex of a hard base, NH_3, with the soft acid, Ag^+, while the product is a complex of the same soft acid with the soft base phosphine.

c. K~1 since all the adducts amongst the reactants and products involve soft acids and bases.

d. K>>1 since BH_3 is a softer acid than BF_3, so it will form a stronger complex with the softer base H_2S while the harder BF_3 forms a stronger complex with the harder base NH_3.

Exercise 4.3.3.4

Which acid will form the most stable complex with **CO**: BH_3, BF_3, or BMe_3?

Answer

BH_3. Since **CO** forms complexes primarily through its carbon lone pair, it is a soft base and so will form the strongest complex with the softest Lewis acid.

References

1. Ahrland, S.; Chatt, J.; Davies, N. R., The relative affinities of ligand atoms for acceptor molecules and ions. Quarterly Reviews, Chemical Society 1958, 12 (3), 265-276.

2. Pearson, R. G., Hard and Soft Acids and Bases. Journal of the American Chemical Society 1963, 85 (22), 3533-3539.

3. Fleming, I., Molecular orbitals and organic chemical reactions. Reference ed.; Wiley: Hoboken, N.J., 2010.

Notes

* Despite the fruitfulness of this observation, in general it is important to reduce the potential for observer bias by checking observations like these against compounds reported in the chemical literature and databases like the Inorganic Crystal Structure and Cambridge Crystallographic Databases.

** These are very soluble in water, to the point where some solutions are perhaps better described as solutions of water in the halide.

4.3.3: Hard-Soft Designation of Lewis Acids and Bases is shared under a CC BY-NC-SA 4.0 license and was authored, remixed, and/or curated by Kathryn A. Newton, Northern Michigan University.

- **6.6.2: Hard-Hard and Soft-Soft preferences may be explained and quantified in terms of electrostatic and covalent and electronic stabilization on the stability of Lewis acid-base adducts** by Stephen M. Contakes is licensed CC BY-NC 4.0.

CHAPTER OVERVIEW

5: Coordination Chemistry Introduction

5.1: Ligands
5.2: Electron Configuration of Gas-Phase Metal Ions
5.3: Crystal Field Theory, d orbital splitting in presence of ligands
5.4: Crystal Field Electron Configuration
5.5: Crystal Field Stabilization Energy
5.6: Thermodynamic and Structure Consequences of d orbital splitting
5.7: Ligand Exchange Reactions and Affinity Determination
5.8: Ligand Binding Thermodynamics and the Chelate Effect
5.9: Hard and Soft Ligands and Metal Ions
5.10: Potential Isomers of Complex Ions

5: Coordination Chemistry Introduction is shared under a not declared license and was authored, remixed, and/or curated by LibreTexts.

5.1: Ligands

Denticity

Ligands are classified based on whether they bind to the metal center through a single site on the ligand or whether they bind at multiple sites. Ligands that bind through only a single site are called ***monodentate*** from the Latin word for tooth; in contrast, those which bind through multiple sites are called ***chelating*** after the Greek **χαλε** for "claw". These relationships are summarized in Figure **5.1.1**.

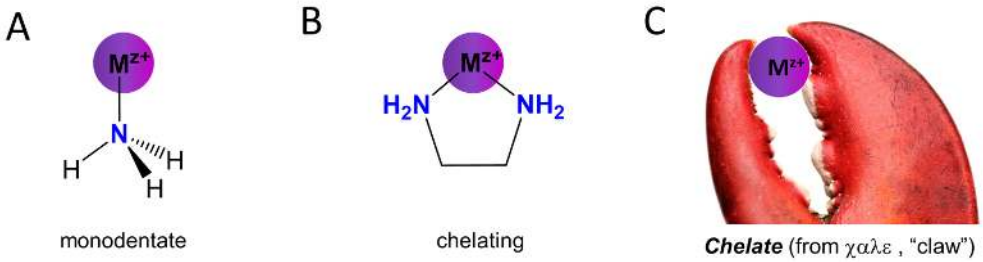


Figure **5.1.1**. (A) Ammonia is a monodentate ligand while (B) ethylene diamine is a chelating ligand owing to its capacity to bind metals via its two amine functional groups. (C) Chelating ligands act like a lobster claw in attaching to the metal via multiple sites. The lobster claw image is adapted from https://www.clipart.email/download/1127636.html. Otherwise this work by Stephen Contakes is licensed under a Creative Commons Attribution 4.0 International License.

Following naturally from the classification of non-chelating ligands as monodentate, chelating ligands are further classified according to the number of sites which they can use to bind a metal center. This number of binding sites is called the *denticity* and ligands are referred to as monodentate (non- chelating), bidentate, tridentate, etc., based on the number of sites available. Ligands with two binding sites have a denticity of two and are said to be bidentate; those with three are tridentate, four tetradentate, and so on. To illustrate this classification system examples of chelating ligands classified according to denticity are given in Figure **5.1.2**.

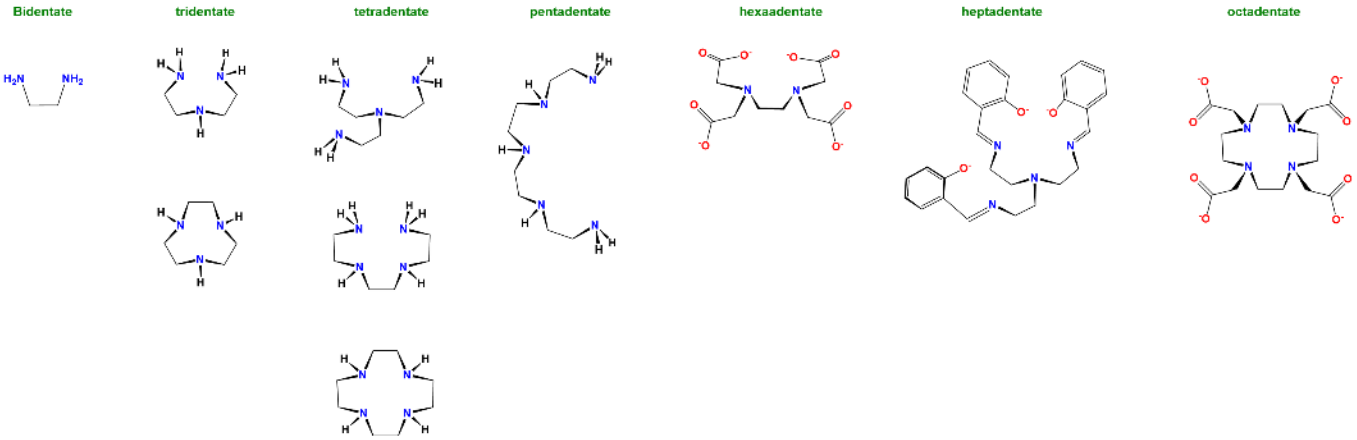


Figure **5.1.2**. Because only one oxygen per carboxylate *typically* binds, only one is counted when assigning a ligand's denticity. This work by Stephen Contakes is licensed under a Creative Commons Attribution 4.0 International License.

Ambidentate Ligands

A perusal of the ligands in Table **5.1.1** reveals that several can bind to a metal in multiple ways. For example, thiocyanate, SCN^- can bind metals through its S or N atoms. Such ligands are called ***ambidentate ligands***. In naming an ambidentate ligand, the atom through which it attaches to the metal is commonly specified after the ligand name using the italicized element symbol or, more formally, a **κ** followed by the italicized element symbol. An example is given in Figure **5.1.3**.[2]

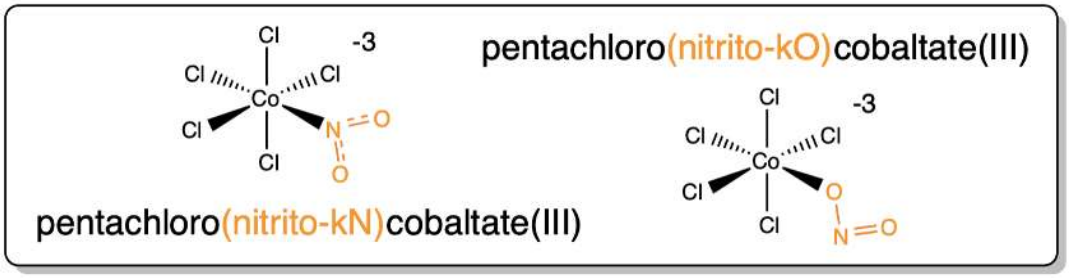
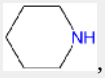
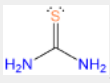


Figure **5.1.1**: Two possible binding modes of nitrite acting as a ligand.[3] This work by Stephen Contakes is licensed under a Creative Commons Attribution 4.0 International License.

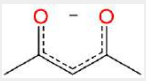
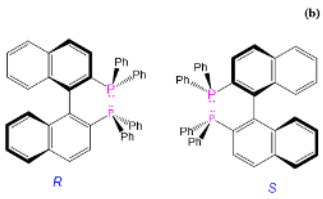
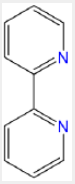
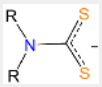
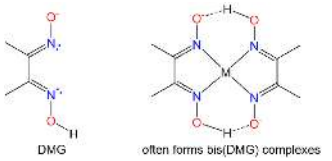
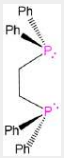
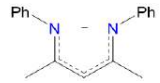
Examples of Ligands

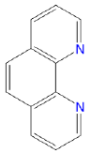
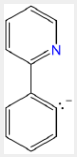
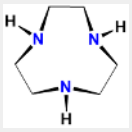
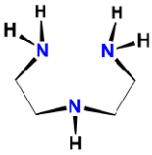
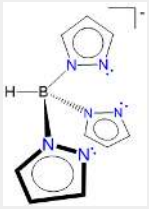
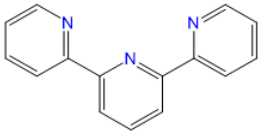
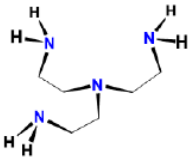
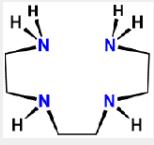
Table **5.1.1**. Common monodentate ligands. Most chemists still prefer common names over the IUPAC ones.

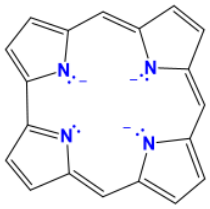
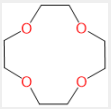
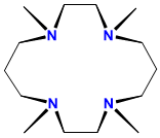
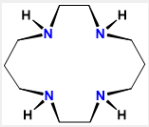
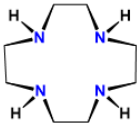
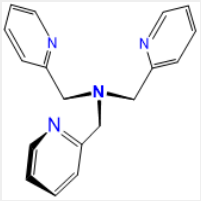
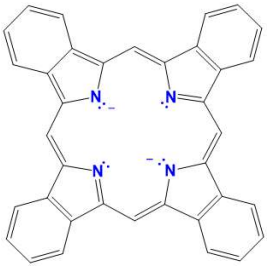
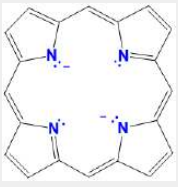
Ligand	Common name	IUPAC name
H^- (H ligands are always considered anions for naming purposes)	hydrido	hydrido
F^-	fluoro	fluorido
Cl^-	chloro	chlorido
Br^-	bromo	bromido
I^-	iodo	iodido
CN^-, as M-CN	cyano	cyanido or cyanido-κC or cyanido-*C*
CN^-, as M-NC	isocyano	isocyanido or cyanido-κN or cyanido-*N*
CH_3NC	methylisocyanide	methylisocyanide
N_3^-	azido	azido
SCN^-, *e.g.* thiocyanate as M-SCN	thiocyanato	thiocyanato-κS or thiocyanato-*S*
NCS^-, *e.g.* thiocyanate as M-NCS	isothiocyanato	thiocyanato-κN or thiocyanato-*N*
$CH_3CO_2^-$	acetato	ethanoato
N^{3-}	nitrido	nitrido
NH^{2-}	imido	azanediido
NH_2^-	amido	azanido
NH_3	ammine	ammine
RNH_2, R_2NH, R_3N	alkylamine, dialkylamine, trialkalyamine (*e.g.* methylamine for CH_3NH_2)	alkylamine, dialkylamine, trialkalyamine (*e.g.* methylamine for CH_3NH_2)
 , piperidine, abbreviated pip	piperidine	piperidine
 , pyridine, abbreviated py	pyridine	pyridine
CH_3CN, acetonitrile, abbreviated MeCN	acetonitrile	acetonitrile
P^{3-}	phosphido	phosphido
PH_3	phosphine	phosphane
PR_3	trialkylphosphine (*e.g.* trimethylphosphine for Me_3P)	trialkylphosphane (*e.g.* trimethylphosphane for Me_3P)
PAr_3	triarylphosphine (*e.g.* triphenylphosphine for Ph_3P)	triarylphosphine (*e.g.* triphenylphosphane for Ph_3P)
 , dimethylsulfoxide or DMSO or dmso	dimethylsulfoxide (sometimes called dimethylsulfoxo but this usage is rare and violates the nomenclature rules for neutral ligands)	(methanesulfinyl)methane or dimethyl(oxido)sulfur
 , thiourea or tu	thiourea	thiourea

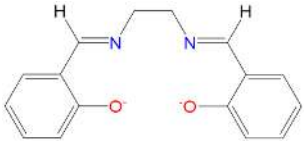
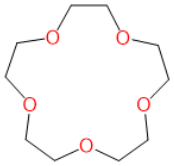
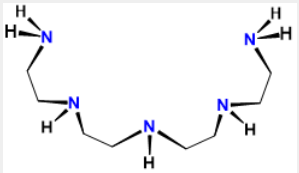
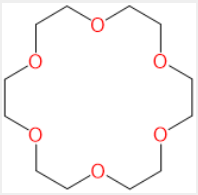
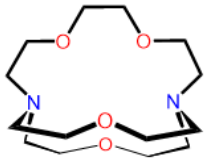
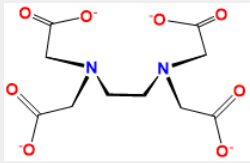
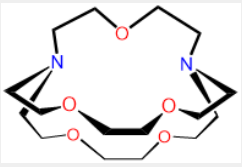
Ligand	Common name	IUPAC name
O^{2-}	oxo	oxido
OH^-	hydroxo	hydroxido
H_2O	aqua	aqua
S^{2-}	sulfo	sulfo
HS^-	hydrosulfido	hydrosulfido
RS^-	alkanethiolate (*e.g.* ethanthiolate for EtS^-)	thioalkanoate
H_2S	hydrogen sulfide	hydrogen sulfide
R_2S	alkylsulfanylalkane (*e.g.* ethylsulfanylethane for Et_2S)	dialkyl sulfide
O_2	dioxygen	dioxygen
O_2^-, superoxide	superoxido	dioxido(1-) or superoxido
O_2^{2-}, peroxide	peroxido	dioxido(2-) or peroxido
N_2	dinitrogen	dinitrogen
NO (are always considered neutral for naming purposes)	nitrosyl	nitrosyl
CO	carbonyl	carbonyl
CS	thiocarbonyl	thiocarbonyl
SO, as M-SO	sulfino	sulfur monoxide-κS or sulfur monoxide-*S*
NO_2, as M-NO_2	nitryl	nitrogen dioxide-κN or nitrogen dioxide-*N*
CO_3^{2-}	carbonato	carbonato
NO_2^-, as M-NO_2	nitro or nitrito-*N*	nitrito-κN or nitrito-*N*
NO_2^-, as M-ONO	nitrito or nitrito-*O*	nitrito-κO or nitrito-*O*
NO_3^-	nitrato	nitrato
SO_3^{2-}	sulfito	sulfito
SO_4^{2-}	sulfato	sulfato
$S_2O_3^{2-}$, as M-S-SO_2-O^-	thiosulfato-*S*	thiosulfato-κS or thiosulfato-*S*
$S_2O_3^{2-}$, as M-O-SO_2-S^-	thiosulfato-*O*	thiosulfato-κO or thiosulfato-*O*

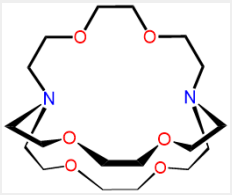
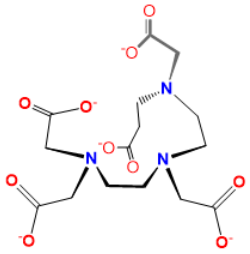
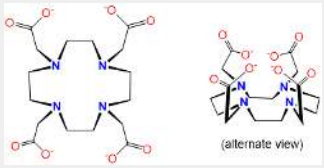
Table **5.1.2**. Common chelating ligands organized by denticity. Most chemists use the common names and abbreviations to describe these ligands.

Common Ligand name	IUPAC ligand name	abbreviation (if applicable)	structure or representative/parent structure (shown in the ionization state in which they bind to a metal)
	Bidentate Ligands		
acetylacetonato	2,4-pentanediono	acac	
R-BINAP and *S*-BINAP	*R*- or *S*-2,2'-bis(diphenylphosphino)-1,1'-binapthyl	BINAP	
2,2'-bipyridine	2,2'-bipyridine	bpy or bipy	
cyclooctadiene	1,5-cyclooctadiene	COD	 (binding to the metal occurs through the alkene π cloud)
dialkyldithiocarbamato	dialkylcarbamodithiolato	$R_2NCS_2^-$ or dtc	
dimethylgloximato	butanedienedioxime	Hdmg or DMG	
diphenylphosphinoethane or 1,2-(diphenylphosphino)ethane	Ethane-1,2-diylbis(diphenylphosphane)	dppe	
ethylenediamine	Ethane-1,2-diamine	en	
ethylenedithiolato	Ethane-1,2-dithiolato	$C_2H_2S_2^{2-}$	
nacnac	*N*,*N*'-diphenyl-2,4-pentanediiminato	nacnac	
oxalato	oxalato	ox	

Common Ligand name	IUPAC ligand name	abbreviation (if applicable)	structure or representative/parent structure (shown in the ionization state in which they bind to a metal)
1,10-phenanthroline or *o*-phenanthroline	1,10-phenanthroline	phen or *o*-phen	
phenylpyridinato	2-phenylpyridinato-C^2,*N* or 2-phenylpyridinato-κC^2,*N*	ppy	
Tridentate Ligands			
triazacyclononane	1,4,7-triazacyclononane	tacn	
diethylenetriamine	1,4,7-triazaheptane	dien	
pyrazoylborato (scorpionate)	hydrotris(pyrazo-1-yl)borato	Tp	
terpyridine or 2,2';6',2"-terpyridine	1^2,2^2:2^6,3^2-terpyridine or 2,6-bis(2-pyridyl)pyridine, tripyridyl, 2,2′:6′,2″-terpyridine	tpy or terpy	
Tetradentate Ligands			
β, *β*', *β*"-triaminotriethylamine	*β*, *β*', *β*"-tris(2-aminoethyl)amine	tren	
triethylenetetramine	1,4,7,10-tetraazadecane	trien	

Common Ligand name	IUPAC ligand name	abbreviation (if applicable)	structure or representative/parent structure (shown in the ionization state in which they bind to a metal)
corroles	variable and generally not used	cor or Cor	
12-crown-4	1,4,7,10-tetraoxacyclododecane	12-crown-4	
tetramethylcyclam	1,4,8,11-tetramethyl-1,4,8,11-tetraazacyclotetradecane	TMC or cyclam	
cyclam	1,4,8,11-tetraazacyclotetradecane	cyclam	
cyclen	1,4,7,10-tetraazacyclododecane	cyclen	
tris(2-pyridylmethyl)amine	1-pyridin-2-yl-*N*,*N*-bis(pyridin-2-ylmethyl)methanamine	tpa or TPA	
phthalocyanines	variable and generally not used	variable, usually a modified Pc	
porphyrins	variable and generally not used	variable, usually a modified por, Por, or P (e.g. TPP = tetraphenylporphyrin)	

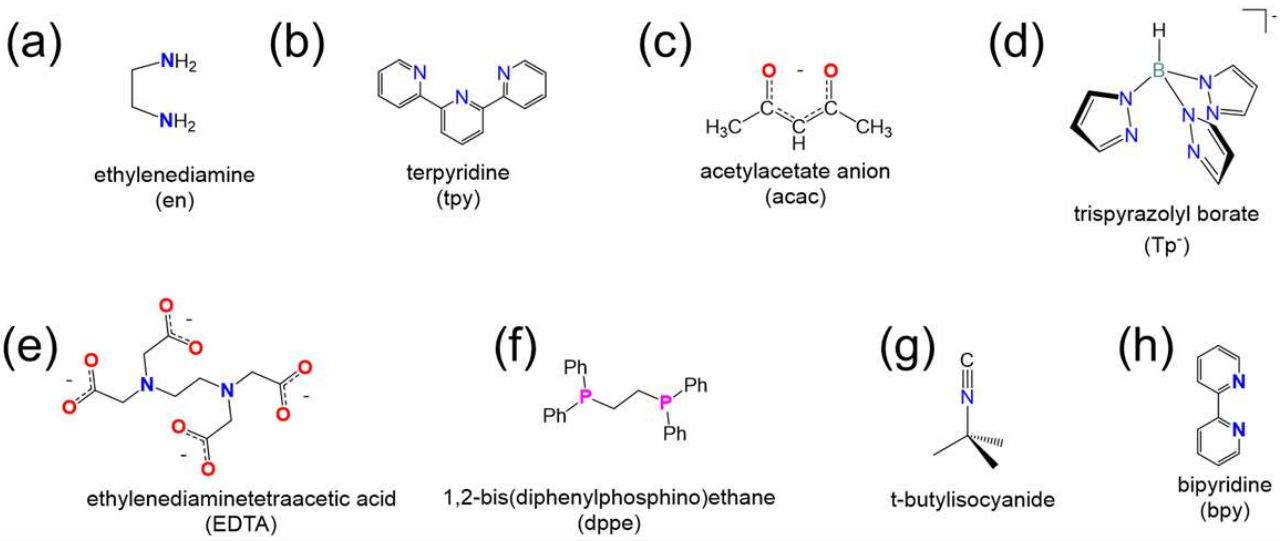
Common Ligand name	IUPAC ligand name	abbreviation (if applicable)	structure or representative/parent structure (shown in the ionization state in which they bind to a metal)
salen	2,2'-ethylenebis(nitrilomethylidene) diphenoxido	salen	
Pentadentate Ligands			
15-crown-5	1,4,7,10,13-Pentaoxacyclopentadecane	15-crown-5	
tetraethylenepentamine	1,4,7,10,13-pentaazatridecane	tepa or TEPA	
Hexadentate Ligands			
18-crown-6	1,4,7,10,13,16-hexaoxacyclooctadecane	18-crown-6	
2,1,1-cryptand	4,7,13,18-Tetraoxa-1,10-diazabicyclo[8.5.5]icosane	2,1,1-crypt or [2.1.1]-cryptand kryptofix 211 and variations thereof	
ethylenediaminetetraaceto	2,2′,2″,2‴-(Ethane-1,2-diyldinitrilo)tetraaceto	EDTA, edta, Y^{4-}	
Heptadentate Ligands			
2,2,1-cryptand	4,7,13,16,21-pentaoxa-1,10-diazabicyclo[8.8.5]icosane	2,2,1-crypt or [2.2.1]-cryptand kryptofix 221 and variations thereof	
Octadentate Ligands			

Common Ligand name	IUPAC ligand name	abbreviation (if applicable)	structure or representative/parent structure (shown in the ionization state in which they bind to a metal)
2,2,2-cryptand	4,7,13,16,21,24-Hexaoxa-1,10-diazabicyclo[8.8.8]hexacosan	2,2,2-crypt or [2.2.2]-cryptand kryptofix 222 and variations thereof	
pentetato acid or diethylenetriaminepentaacetato or DTPA	2-[bis[2-[bis(carboxylatomethyl)amino]ethyl]amino]acetato	DTPA	
DOTA or tetraxetan	1,4,7,10-Tetraazacyclododecane-1,4,7,10-tetraacetic acid	Dota, DOTA	

Problems

? Exercise 5.1.1

Determine the denticity of each ligand in the list below and classify them as monodentate, tridentate, etc.



Answer

(a) bidentate

(b) tridentate

(c) bidentate

(d) tridentate (only the lower N on each ring has a lone pair that can be used to bind the metal)

(e) hexadentate (remember that each carboxylate only counts as one point of attachment)

(f) bidentate

(g) monodentate (through the lone pair on the isocyanide C)

(h) bidentate

References

1. International Union of Pure and Applied Chemistry *Nomenclature of Inorganic Chemistry* Cambridge, UK, 2005.

2. The structure and name is taken from Choudhury, S. B.; Allan, C. B.; Maroney, M.; Wodward, A. D.; Lucas, C. R. *Inorg. Synth.* **1998**, *32*, 98-107.

3. Haas, K. Naming Transition Metal Complexes. https://chem.libretexts.org/Courses/Saint_Mary's_College%2C_Notre_Dame%2C_IN/CHEM_342%3A_Bio-inorganic_Chemistry/Readings/Week_2%3A_Introduction_to_Metal-Ligand_Interactions_and_Biomolecules/2.1_Transition_metal_complexes/2.1.6%3A_Naming_Transition_Metal_Complexes

Contributors and Attributions

Stephen Contakes, Westmont College, to whom comments, corrections, and criticisms should be addressed.

with some examples taken from Naming Transition Metal Complexes by Kathryn Haas.

Consistent with the policy for original artwork made as part of this project, all unlabeled drawings of chemical structures are by Stephen Contakes and licensed under a Creative Commons Attribution 4.0 International License.

5.1: Ligands is shared under a CC BY-NC-SA 4.0 license and was authored, remixed, and/or curated by Kathryn A. Newton, Northern Michigan University.

- **9.3: Nomenclature and Ligands** by Stephen M. Contakes has no license indicated.

5.2: Electron Configuration of Gas-Phase Metal Ions



To be able to use Crystal Field Theory (CFT) successfully, it is essential that you can determine the **electronic configuration** of the central metal ion in any complex.

This requires being able to recognize all the entities making up the complex and knowing whether the ligands are neutral or anionic, so that you can determine the **oxidation number** of the metal ion. The oxidation number is then used to determine the electron configuration and the number of electrons in d-orbitals for a metal ion.

Example 5.2.1

What is the electronic configuration of Fe(III)?

Solution

Start with the electron configuration of the neutral atom. It is sufficient to use the noble gas configuration.

Fe: [Ar] $4s^2$ $3d^6$

Then, remove (or add) electrons to reflect the oxidation state of the metal. Remember to remove electrons from the orbital with the highest principal quantum number first!

Fe(III) has lost 3 electrons relative to Fe(0). Fe^{3+}: [Ar] $3d^5$

From the electron configuration, we see that Fe^{3+} has 5 electrons in its outermost d-orbitals.

Oxidation Numbers and their Relative Stabilities

The IUPAC definition of the oxidation number in a coordination compound is:

> *the charge a central atom in a coordination entity would bear if all the ligands were removed along with the electron pairs that were shared with the central atom. It is represented by a Roman numeral.*

The transition metals show a wide range of oxidation numbers. The Table **5.2.1** summarizes the known oxidation numbers of the first row transition elements.

Table **5.2.1**: Known Oxidation Numbers of First Row Transition Elements*. The most prevalent oxidation numbers are shown in **bold.**

Sc	Ti	V	Cr	Mn	Fe	Co	Ni	Cu	Zn
	I	I	I	I	I	I	I	**I**	
	II	**II**	**II**	**II**	**II**	**II**	**II**	**II**	**II**
III	**III**	**III**	**III**	**III**	**III**	**III**	III	III	
	IV	**IV**	IV	**IV**	IV	IV	IV		
		V	V	V	V	V			
			VI	**VI**	VI				
				VII					

* The oxidation number zero usually assigned to the elemental state has been omitted from the Table. The elements Cr to Co form several metal carbonyl compounds where the metals are considered to have an oxidation number of zero.

A number of important conclusions can be drawn from Table **5.2.1**.

1. There is an increase in the number of oxidation numbers from Sc to Mn. All seven oxidation numbers are exhibited by Mn. The oxidation number of VII represents the formal loss of all seven electrons from 3d and 4s orbitals. In fact all of the elements in the series can utilize all the electrons in their 3d and 4s orbitals.
2. There is a decrease in the number of oxidation states from Mn to Zn. This is because the pairing of d-electrons occurs after Mn (Hund's rule) which in turn decreases the number of available unpaired electrons and hence, the number of oxidation states.
3. The stability of higher oxidation states decreases in moving from Sc to Zn. Mn(VII) and Fe(VI) are powerful oxidizing agents and the higher oxidation states of Co, Ni and Zn are unknown.
4. The relative stability of the +2 state with respect to higher oxidation states, particularly the +3 state increases in moving from left to right. This is justifiable since it will be increasingly difficult to remove the third electron from the d orbitals.
5. There is a tendency of intermediate oxidation states to disproportionate. For example, Mn(VI) → Mn(IV) + Mn(VII) and Cu(I) → Cu(0) + Cu(II).
6. The lower oxidation numbers are usually found in ionic compounds and higher oxidation numbers tend to be involved in covalent compounds.

The relative stability of oxidation numbers is an extremely important topic in transition metal chemistry and is usually discussed in terms of the standard reduction potential (E°) values. Thermodynamically E° values are equated to ΔG° values by the relationship: $\Delta G^\circ = -nFE^\circ$ where n = number of electrons involved and F = Faraday of electricity. Hence, the E° values indicate the possibility of spontaneous change from one oxidation state to the other. This value however, does not give any information about the reaction rate. Predictions regarding the stability of a particular oxidation state of an element can be made from the Tables of Redox values found in any standard text book or online.

5.2: Electron Configuration of Gas-Phase Metal Ions is shared under a CC BY-NC-SA 4.0 license and was authored, remixed, and/or curated by Kathryn A. Newton, Northern Michigan University.

- **19.2B: Electronic Configurations** is licensed CC BY-NC-SA 4.0.

5.3: Crystal Field Theory, d orbital splitting in presence of ligands

Crystal field theory (CFT) is a bonding model that explains many important properties of transition-metal complexes, including their colors, magnetism, structures, stability, and reactivity. The central assumption of CFT is that metal–ligand interactions are purely electrostatic in nature. CFT qualitatively describes the strength of the metal-ligand interactions; based on the strength of the metal-ligand interactions, the energy of the system is altered and the degeneracy of the d-orbitals in transition metal complexes breaks. Even though the initial assumption is not strictly valid for many complexes, such as those that contain neutral ligands like CO, CFT enables chemists to explain many of the properties of transition-metal complexes with a reasonable degree of accuracy. T

Crystal Field Theory was developed by Hans Bethe and John Hasbrouck van Vleck. As the name implies, crystal field theory was developed as a way of explaining observed colors and magnetic properties of ionic crystalline solids. The colors of transition metel complexes results from the wavelength of light absorbed, which reveals something about differences in electronic energy levels in the ions of the crystalline solid. The magnetic properties depend on the presence of unpaired electrons and, thus, also depend on electronic energy levels.

Basic Concept

Consider a transition metal ion in an octahedral hole in a crystalline lattice (Figure **5.3.1**). In Crystal Field Theory, it is assumed that the ions are *simple point charges* (a simplification). The blue metal ion is a positive point charge that has six nearest neighbors, and the red ligands/counterions are negative point charges. The ions are held together by electrostatics: the negative charges of the (red) counterions are attracted to the positive charge of the (blue) metal ion. The attractive and repulsive interactions between the ions can be described by Coulomb's Law:

$$E \propto \frac{q_1 q_2}{r}$$

with

- E the bond energy between the charges and
- q_1 and q_2 are the charges of the interacting ions and
- r is the distance separating them.

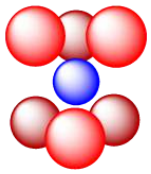


Figure **5.3.1**: A positively charged metal ion (blue) surrounded by six near neighbors with negative charges (red). (CC-BY-NC; Chris Schaller)

The attractive and repulsive forces between the positively charged metal ion and the surrounding ligands affect the energy of the electrons on the metal ion. To understand these interactions, we first consider a single transition metal ion; its five *d*-orbitals have the same energy (they are *degenerate*) (Figure **5.3.2**). When the metal ion is placed in a field of evenly distributed negative charge, there are repulsive forces between the metal ion's electrons and the surrounding negative charge. The result is the electrons on the metal increase in energy, and they all increase in energy by the same amount.

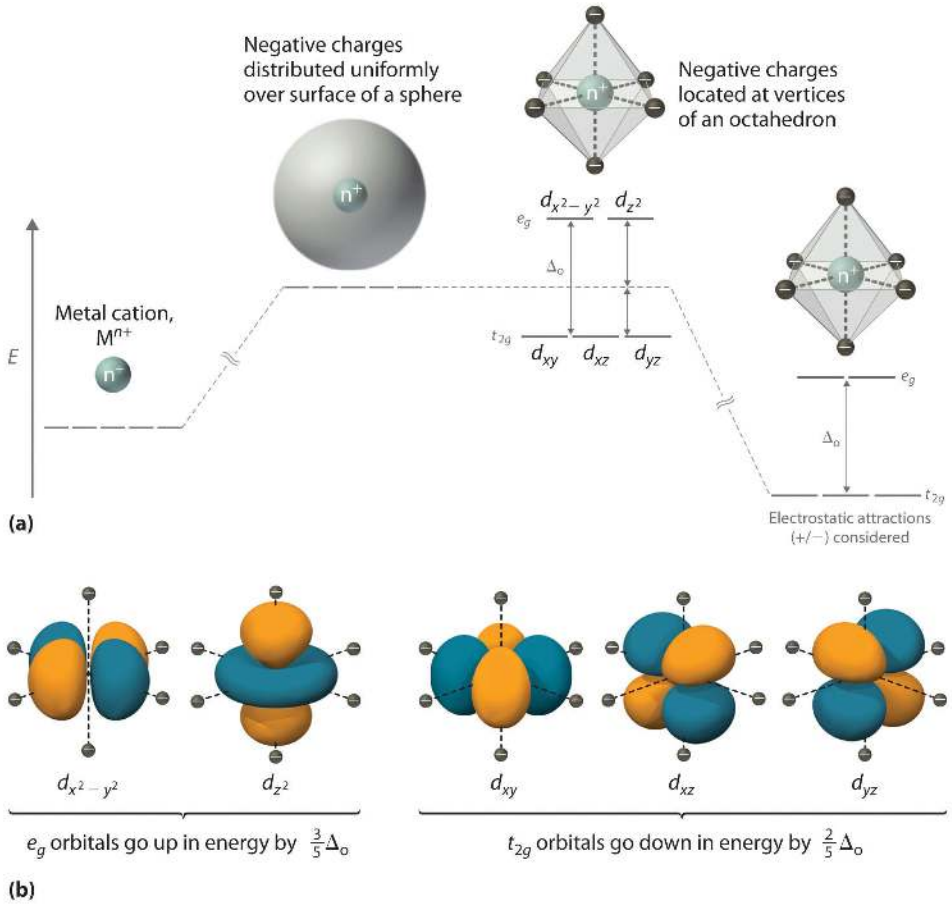


Figure **5.3.2**: An Octahedral Arrangement of Six Negative Charges around a Metal Ion Causes the Five d Orbitals to Split into Two Sets with Different Energies. (a) Distributing a charge of −6 uniformly over a spherical surface surrounding a metal ion causes the energy of all five d orbitals to increase due to electrostatic repulsions, but the five d orbitals remain degenerate. Placing a charge of −1 at each vertex of an octahedron causes the d orbitals to split into two groups with different energies: the $d_{x^2-y^2}$ and d_{z^2} orbitals increase in energy, while the d_{xy}, d_{xz}, and d_{yz} orbitals decrease in energy. The average energy of the five d orbitals is the same as for a spherical distribution of a −6 charge, however. Attractive electrostatic interactions between the negatively charged ligands and the positively charged metal ion (far right) cause all five d orbitals to decrease in energy but does not affect the splittings of the orbitals. (b) The two e_g orbitals (left) point directly at the six negatively charged ligands, which increases their energy compared with a spherical distribution of negative charge. In contrast, the three t_{2g} orbitals (right) point between the negatively charged ligands, which decreases their energy compared with a spherical distribution of charge. (CC BY-SA-NC; anonymous by request)

In reality, the negative charges in a transition metal complex are not uniformly distributed around the positive metal ion. When the ligand point charges approach the metal ion, some experience more repulsion from the d-orbital electrons than others based on the geometric structure of the molecule. Due to the variation in shape and orientation of the d-orbitals, some ligands will interact more directly with d-orbitals and others will have less direct interactions. For an octahedral complex, the ligands approach the metal ion along the x, y, and z axes. Therefore, the electrons in the d_{z^2} and $d_{x^2-y^2}$ orbitals, which lie along these axes, experience greater repulsion (Figure **5.3.2**). It requires more energy to have an electron in these orbitals than it would to put an electron in one of the other orbitals due to the electron-electron repulsions. The energies of the d_{z^2} and $d_{x^2-y^2}$ orbitals increase due to greater interactions with the ligands. By the same logic, the d_{xy}, d_{xz}, and d_{yz} orbitals have less-direct interactions and decrease in energy. This causes a splitting in the energy levels of the *d*-orbitals. This is known as **crystal field splitting**.

For an octahedral complex, the energy difference between the two sets of orbitals is called the *octahedral field splitting*, Δ_o. Because the total amount of repulsion is the same in the octahedral field and the spherical field (it is just distributed differently) the average energy level of the orbitals should be the same in the two fields. This average energy of the orbitals is called the **barycenter**, a term borrowed from astronomy. Because two of the orbitals are raised above the barycenter in the octahedral field and three are lowered below the barycenter, then the e_g set must be $\frac{3}{5}\Delta_o$ $(= 0.6\Delta_o)$ above the barycenter and the t_{2g} set must be $\frac{2}{5}\Delta_o$ $(= 0.4\Delta_o)$ below the barycenter. That means the average energy lies at the barycenter.

Thus far, we have considered only the effect of repulsive electrostatic interactions between electrons in the d orbitals and the six negatively charged ligands, which increases the total energy of the system and splits the d orbitals. Interactions between the positively charged metal ion and the ligands results in a net stabilization of the system, which decreases the energy of all five d orbitals without affecting their splitting (as shown at the far right in Figure **5.3.2**).

Three Complexes Explained

Description of *d*-Orbitals

To understand CFT, one must understand the description of the lobes:

- d_{xy}: lobes lie in-between the x and the y axes.
- d_{xz}: lobes lie in-between the x and the z axes.
- d_{yz}: lobes lie in-between the y and the z axes.
- $d_{x^2-y^2}$: lobes lie on the x and y axes.
- d_{z^2}: there are two lobes on the z axes and there is a donut shape ring that lies on the xy plane around the other two lobes.

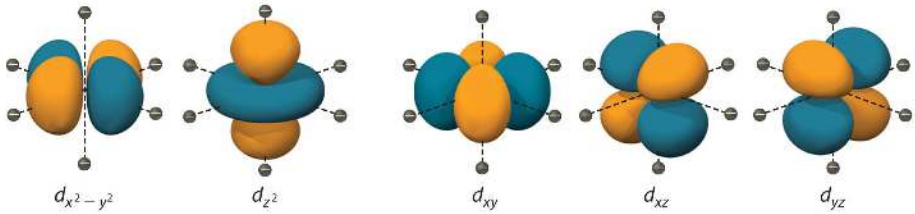


Figure **5.3.3**: Spatial arrangement of ligands in the an octahedral ligand field with respect to the five d-orbitals. (**LibreText**)

Octahedral Complexes

In an octahedral complex, there are six ligands attached to the central transition metal. The d-orbital splits into two different levels (Figure **5.3.4**). The bottom three energy levels are named d_{xy}, d_{xz}, and d_{yz} (collectively referred to as t_{2g}). The two upper energy levels are named $d_{x^2-y^2}$, and d_{z^2} (collectively referred to as e_g).

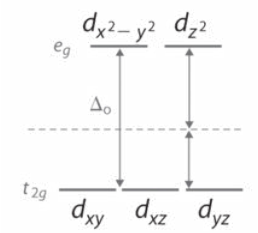


Figure **5.3.4**: Spllitting of degenerate d-orbitalsdue to an on octahedral ligand field. (**LibreText**)

The reason they split is because of the electrostatic interactions between the electrons of the ligand and the lobes of the d-orbital. In an octahedral, the electrons are attracted to the axes. Any orbital that has a lobe on the axes moves to a higher energy level. This means that in an octahedral, the energy levels of e_g are higher ($0.6\Delta_o$) while t_{2g} is lower ($0.4\Delta_o$). The distance that the electrons have to move from t_{2g} from e_g and it dictates the energy that the complex will absorb from white light, which will determine the color. Whether the complex is paramagnetic or diamagnetic will be determined by the spin state. If there are unpaired electrons, the complex is paramagnetic; if all electrons are paired, the complex is diamagnetic.

Tetrahedral Complexes

In a tetrahedral complex, there are four ligands attached to the central metal. The d orbitals also split into two different energy levels. The top three consist of the d_{xy}, d_{xz}, and d_{yz} orbitals. The bottom two consist of the $d_{x^2-y^2}$ and d_{z^2} orbitals. The reason for this is due to poor orbital overlap between the metal and the ligand orbitals. The orbitals are directed on the axes, while the ligands are not.

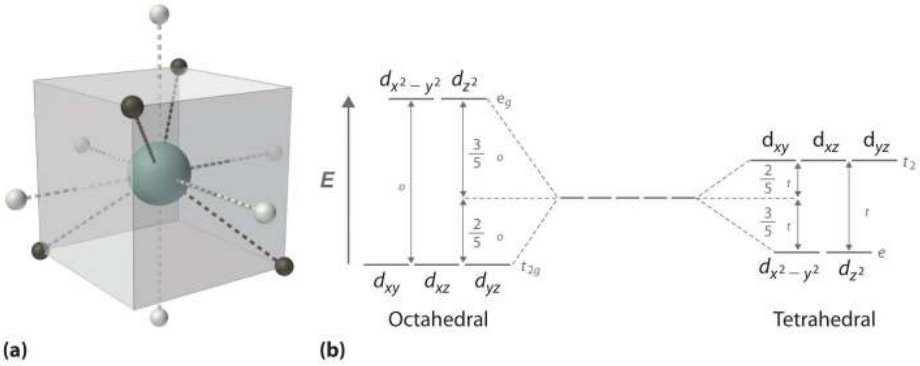


Figure 5.3.5: (a) Tetraheral ligand field surrounding a central transition metal (blue sphere). (b) Splitting of the degenerate d-orbitals (without a ligand field) due to an octahedral ligand field (left diagram) and the tetrahedral field (right diagram). (LibreText)

The difference in the splitting energy is tetrahedral splitting constant (Δ_t), which less than (Δ_o) for the same ligands:

$$\Delta_t = 0.44\,\Delta_o \tag{5.3.1}$$

Consequentially, Δ_t is typically smaller than the spin pairing energy, so tetrahedral complexes are usually **high spin**.

Square Planar Complexes

In a square planar, there are four ligands as well. However, the difference is that the electrons of the ligands are only attracted to the ***xy*** plane. Any orbital in the xy plane has a higher energy level (Figure 5.3.6). There are four different energy levels for the square planar (from the highest energy level to the lowest energy level): $d_{x^2-y^2}$, d_{xy}, d_{z^2}, and both d_{xz} and d_{yz}.

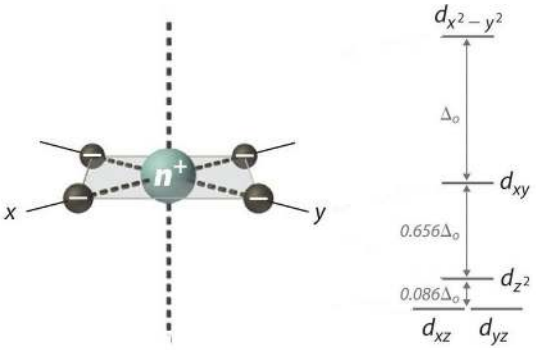


Figure 5.3.6: Splitting of the degenerate d-orbitals (without a ligand field) due to an square planar ligand field. (LibreText)

The splitting energy (from highest orbital to lowest orbital) is Δ_{sp} and tends to be larger then Δ_o

$$\Delta_{sp} = 1.74\,\Delta_o \tag{5.3.2}$$

Moreover, Δ_{sp} is also larger than the pairing energy, so the square planar complexes are usually **low spin** complexes.

5.3: Crystal Field Theory, d orbital splitting in presence of ligands is shared under a CC BY-NC-SA 4.0 license and was authored, remixed, and/or curated by Kathryn A. Newton, Northern Michigan University.

- **10.2.1: Crystal Field Theory** by Chris Schaller is licensed CC BY-NC 4.0.
- **Crystal Field Theory** is licensed CC BY-NC-SA 4.0.

5.4: Crystal Field Electron Configuration

Electronic Structures of Metal Complexes

According to the Aufbau principle, electrons are filled from lower to higher energy orbitals. For the octahedral case, this corresponds to filling the d_{xy}, d_{xz}, and d_{yz} orbitals first. Following Hund's rule, electrons are distributed into orbitals to give the highest number of unpaired electrons. For example, if one had a d^3 complex, there would be three unpaired electrons.

Consider several examples of electronic configurations for octahedral complexes shown in Figure **5.4.1**. The Ti^{3+} ion contains a single d electron, and additional configurations can be obtained as we proceed across the first row of the transition metals by adding a single electron at a time. Additional electrons are placed in the lowest-energy orbital available, while keeping their spins parallel as required by Hund's rule. As shown in Figure **5.4.1**, for d^1–d^3 systems—such as $[Ti(H_2O)_6]^{3+}$, $[V(H_2O)_6]^{3+}$, and $[Cr(H_2O)_6]^{3+}$, respectively—the electrons successively occupy the three degenerate t_{2g} orbitals with their spins parallel, giving one, two, and three unpaired electrons, respectively. We can summarize this for the complex $[Cr(H_2O)_6]^{3+}$, for example, by saying that the chromium ion has a d^3 electron configuration or, more succinctly, Cr^{3+} is a d^3 ion.

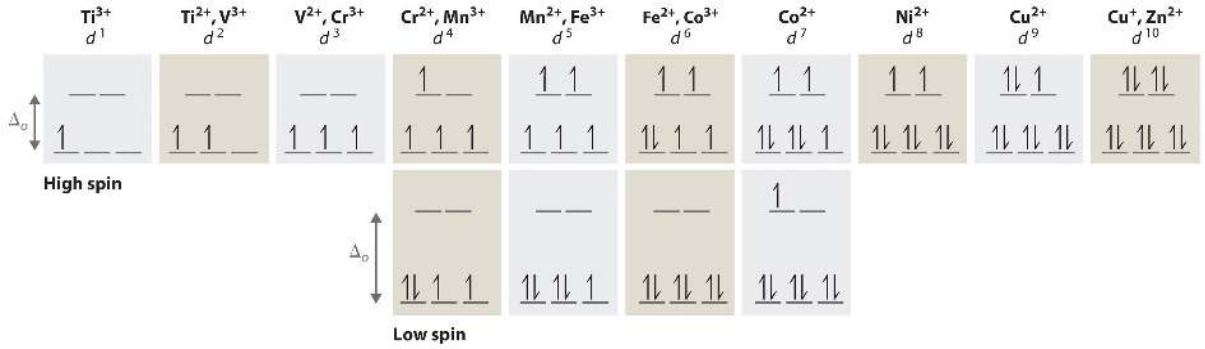


Figure **5.4.1**: The Possible Electron Configurations for Octahedral d^n Transition-Metal Complexes (n = 1–10). Two different configurations are possible for octahedral complexes of metals with d^4, d^5, d^6, and d^7 configurations; the magnitude of Δ_o determines which configuration is observed. (CC BY-SA-NC; anonymous by request)

When we reach the d^4 configuration, there are two possible choices for the fourth electron: it can occupy one of the empty, higher-energy e_g orbitals (d_{z^2} or $d_{x^2-y^2}$) or it can occupy one of the lower-energy, singly-occupied t_{2g} orbitals (d_{xy}, d_{xz}, or d_{yz}). Recall that placing an electron in an already occupied orbital results in electrostatic repulsions that increase the energy of the system; this increase in energy is called the spin-pairing energy (P). If Δ_o is less than P, then the lowest-energy arrangement places the fourth electron in one of the empty e_g orbitals. This configuration maximizes the spin multiplicity. Because this arrangement results in four unpaired electrons, it is called a **high-spin** configuration, and a complex with this electron configuration, such as the $[Cr(H_2O)_6]^{2+}$ ion, is called a high-spin complex. Conversely, if Δ_o is greater than P, then the lowest-energy arrangement places the fourth electron in one of the occupied t_{2g} orbitals. Because this arrangement results in only two unpaired electrons, it is called a **low-spin** configuration, and a complex with this electron configuration, such as the $[Mn(CN)_6]^{3-}$ ion, is called a low-spin complex. Similarly, metal ions with the d^5, d^6, or d^7 electron configurations can be either high spin or low spin, depending on the magnitude of Δ_o.

In contrast, only one arrangement of d electrons is possible for metal ions with d^8–d^{10} electron configurations. For example, the $[Ni(H_2O)_6]^{2+}$ ion is d^8 with two unpaired electrons, the $[Cu(H_2O)_6]^{2+}$ ion is d^9 with one unpaired electron, and the $[Zn(H_2O)_6]^{2+}$ ion is d^{10} with no unpaired electrons.

> *If Δ_o is less than the spin-pairing energy, a high-spin configuration results. Conversely, if Δ_o is greater, a low-spin configuration forms.*

A Note on units

The crystal field splitting energy, Δ_o, may be reported in units of J/mol or wave numbers (cm^{-1}). Typically, energies obtained by spectroscopic measurements are often given wave numbers; the wave number is the reciprocal of the wavelength of the corresponding electromagnetic radiation expressed in centimeters: 1 cm^{-1} = 11.96 J/mol.

Factors That Affect the Magnitude of Δ_o

The magnitude of the crystal field splitting energy, Δ_o, dictates whether a complex with four, five, six, or seven d electrons is high spin or low spin, which affects its magnetic properties, structure, and reactivity. Large values of Δ_o (i.e., Δ_o > P) yield a low-spin complex, whereas small values of Δ_o (i.e., Δ_o < P) produce a high-spin complex. As we noted, the magnitude of Δ_o depends on three factors: the charge on the metal ion, the principal quantum number of the metal (and thus its location in the periodic table), and the nature of the ligand. Values of Δ_o for some representative transition-metal complexes are given in Table **5.4.1**.

Table **5.4.1**: Crystal Field Splitting Energies for Some Octahedral (Δ_o) and Tetrahedral (Δ_t) Transition-Metal Complexes

Octahedral Complexes	Δ_o (cm^{-1})	Octahedral Complexes	Δ_o (cm^{-1})	Tetrahedral Complexes	Δ_t (cm^{-1})
$[Ti(H_2O)_6]^{3+}$	20,300	$[Fe(CN)_6]^{4-}$	32,800	VCl_4	9010
$[V(H_2O)_6]^{2+}$	12,600	$[Fe(CN)_6]^{3-}$	35,000	$[CoCl_4]^{2-}$	3300
$[V(H_2O)_6]^{3+}$	18,900	$[CoF_6]^{3-}$	13,000	$[CoBr_4]^{2-}$	2900
$[CrCl_6]^{3-}$	13,000	$[Co(H_2O)_6]^{2+}$	9300	$[CoI_4]^{2-}$	2700
$[Cr(H_2O)_6]^{2+}$	13,900	$[Co(H_2O)_6]^{3+}$	27,000		
$[Cr(H_2O)_6]^{3+}$	17,400	$[Co(NH_3)_6]^{3+}$	22,900		
$[Cr(NH_3)_6]^{3+}$	21,500	$[Co(CN)_6]^{3-}$	34,800		
$[Cr(CN)_6]^{3-}$	26,600	$[Ni(H_2O)_6]^{2+}$	8500		
$Cr(CO)_6$	34,150	$[Ni(NH_3)_6]^{2+}$	10,800		
$[MnCl_6]^{4-}$	7500	$[RhCl_6]^{3-}$	20,400		
$[Mn(H_2O)_6]^{2+}$	8500	$[Rh(H_2O)_6]^{3+}$	27,000		
$[MnCl_6]^{3-}$	20,000	$[Rh(NH_3)_6]^{3+}$	34,000		
$[Mn(H_2O)_6]^{3+}$	21,000	$[Rh(CN)_6]^{3-}$	45,500		
$[Fe(H_2O)_6]^{2+}$	10,400	$[IrCl_6]^{3-}$	25,000		
$[Fe(H_2O)_6]^{3+}$	14,300	$[Ir(NH_3)_6]^{3+}$	41,000		

Source of data: Duward F. Shriver, Peter W. Atkins, and Cooper H. Langford, Inorganic Chemistry, 2nd ed. (New York: W. H. Freeman and Company, 1994).

Factor 1: Charge on the Metal Ion

Increasing the charge on a metal ion has two effects: the radius of the metal ion decreases, and negatively charged ligands are more strongly attracted to it. Both effects decrease the metal–ligand distance, which in turn causes the negatively charged ligands to interact more strongly with the d-orbitals. Consequently, the magnitude of Δ_o increases as the charge on the metal ion increases. Typically, Δ_o for a +3 ion is about 50% greater than for the +2 ion of the same metal; for example, for $[V(H_2O)_6]^{2+}$, Δ_o = 11,800 cm^{-1}; for $[V(H_2O)_6]^{3+}$, Δ_o = 17,850 cm^{-1}.

Factor 2: Principal Quantum Number of the Metal

For a series of complexes of metals from the same group in the periodic table with the same charge and the same ligands, the magnitude of Δ_o increases with increasing principal quantum number: Δ_o (3d) < Δ_o (4d) < Δ_o (5d). The data for hexaammine complexes of the trivalent Group 9 metals illustrate this point:

$$[Co(NH_3)_6]^{3+}: \Delta_o = 22{,}900\ cm^{-1}$$

$$[Rh(NH_3)_6]^{3+}: \Delta_o = 34{,}100\ cm^{-1}$$

$$[Ir(NH_3)_6]^{3+}: \Delta_o = 40{,}000\ cm^{-1}$$

The increase in Δ_o with increasing principal quantum number is due to the larger radius of valence orbitals down a column. In addition, repulsive ligand–ligand interactions are most important for smaller metal ions. Relatively speaking, this results in shorter M–L distances and stronger d orbital–ligand interactions.

Factor 3: The Nature of the Ligands

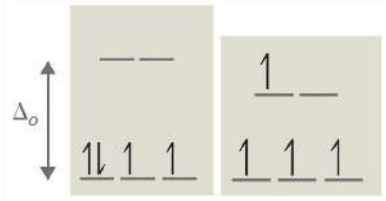


Figure 5.4.2: Low Spin, Strong Field (Δ_o > P) High Spin, Weak Field (Δ_o < P)Splitting for a d^4 complex under a strong field (left) and a weak field (right). The strong field is a low spin complex, while the weak field is a high spin complex.

Experimentally, it is found that the Δ_o observed for a series of complexes of the same metal ion depends strongly on the nature of the ligands. Ligands that cause a transition metal to have a small crystal field splitting, which leads to a high-spin configuration, are called **weak-field**

ligands. Ligands that produce a large crystal field splitting, which leads to a low-spin configuration, are called **strong field ligands** (Figure **5.4.2**).

For a series of chemically similar ligands, the magnitude of Δ_o decreases as the size of the donor atom increases. For example, Δ_o values for halide complexes generally decrease in the order $F^- > Cl^- > Br^- > I-$ because smaller, more localized charges, such as we see for F^-, interact more strongly with the d orbitals of the metal ion.

In addition, a small neutral ligand with a highly localized lone pair, such as NH_3, results in significantly larger Δ_o values than might be expected. Because the lone pair points directly at the metal ion, the electron density along the M–L axis is greater than for a spherical anion such as F^-.

The experimentally observed order of the crystal field splitting energies produced by different ligands is called the spectrochemical series. It is shown here in order of increasing Δ_o:

$$\underset{\text{weak-field ligands}}{I^- < Br^- < Cl^- < \underline{S}CN^- < CH_3COO^- < F^- < OH^- < ox^{2-}} < \underset{\text{intermediate-field ligands}}{ONO^- < H_2O < SC\underline{N}^-} < EDTA^{4-} < NH_3 < en < NO_2^- < \underset{\text{strong-field ligands}}{CN^- \approx CO}$$

Note that SCN^- and NO_2- ligands are represented twice in the above spectrochemical series since there are two different Lewis base sites (e.g., free electron pairs to share) on each ligand (e.g., for the SCN^- ligand, the electron pair on the sulfur or the nitrogen can form the coordinate covalent bond to a metal). The specific atom that binds in such ligands is underlined.

> *The largest Δ_o splittings are found in complexes of metal ions from the third row of the transition metals with charges of at least +3 and ligands with localized lone pairs of electrons.*

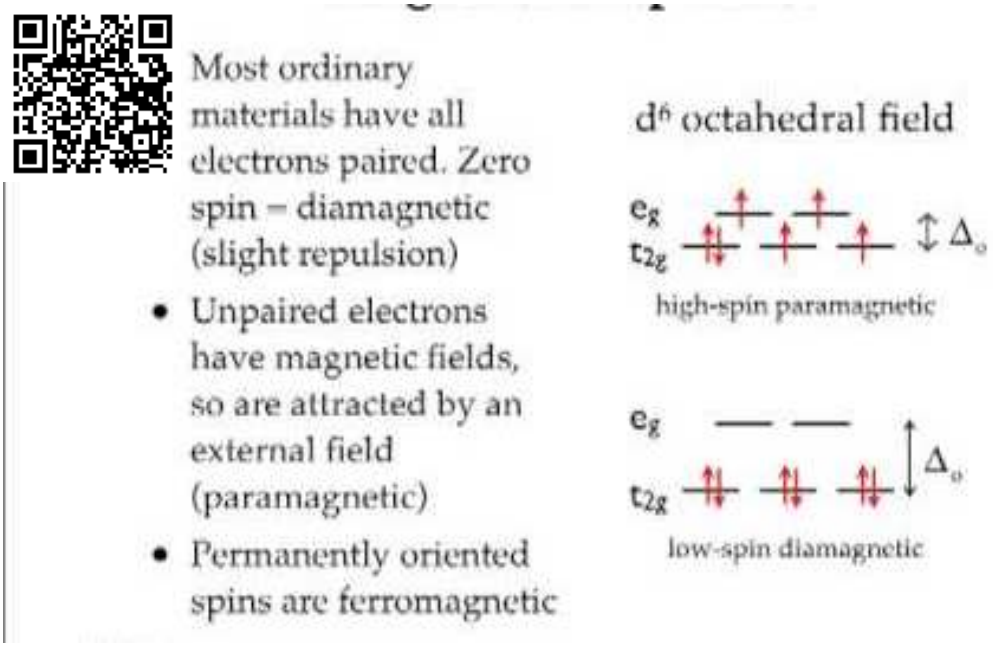
Factor 4: Molecular Geometry

In addition to octahedral complexes, two common geometries observed are that of tetrahedral and square planar. These complexes differ from the octahedral complexes in that the orbital levels are raised in energy due to the interference with electrons from ligands. For the tetrahedral complex, the d_{xy}, d_{xz}, and d_{yz} orbitals are raised in energy while the d_{z^2}, $d_{x^2-y^2}$ orbitals are lowered. For the square planar complexes, there is greatest interaction with the $d_{x^2-y^2}$ orbital and therefore it has higher energy. The next orbital with the greatest interaction is d_{xy}, followed below by d_{z^2}. The orbitals with the lowest energy are the d_{xz} and d_{yz} orbitals. There is a large energy separation between the d_{z^2} orbital and the d_{xz} and d_{yz} orbitals, meaning that the crystal field splitting energy is large. We find that the square planar complexes have the greatest crystal field splitting energy compared to all the other complexes. This means that most square planar complexes are low spin, strong field ligands.

The splitting energy (from highest orbital to lowest orbital) is Δ_{sp} and tends to be larger then Δ_o

$$\Delta_{sp} = 1.74\,\Delta_o \tag{5.4.1}$$

Moreover, Δ_{sp} is also larger than the pairing energy, so the square planar complexes are usually **low spin** complexes.



Example 5.4.1

For the complex, predict its structure, whether it is high spin or low spin, and the number of unpaired electrons present:

$[CoF_6]^{3-}$

Solution

With six ligands, we expect this complex to be octahedral.

The fluoride ion is a small anion with a concentrated negative charge, but compared with ligands with localized lone pairs of electrons, it is weak field. The charge on the metal ion is +3, giving a d^6 electron configuration.

Because of the weak-field ligands, we expect a relatively small Δ_o, making the compound high spin.

In a high-spin octahedral d^6 complex, the first five electrons are placed individually in each of the d orbitals with their spins parallel, and the sixth electron is paired in one of the t_{2g} orbitals, giving four unpaired electrons.

Example 5.4.2

For the complex, predict its structure, whether it is high spin or low spin, and the number of unpaired electrons present:

$[Rh(CO)_2Cl_2]^-$

Solution

This complex has four ligands, so it is either square planar or tetrahedral.

Because rhodium is a second-row transition metal ion with a d^8 electron configuration and CO is a strong-field ligand, the complex is likely to be square planar with a large Δ_o, making it low spin. Because the strongest d-orbital interactions are along the x and y axes, the orbital energies increase in the order $d_{z^2}d_{yz}$, and d_{xz} (these are degenerate); d_{xy}; and $d_{x^2-y^2}$.

The eight electrons occupy the first four of these orbitals, leaving the $d_{x^2-y^2}$. orbital empty. Thus there are no unpaired electrons.

Problems

Exercise 5.4.1

For the complex, predict its structure, whether it is high spin or low spin, and the number of unpaired electrons present.

$[Mn(H_2O)_6]^{2+}$

Answer

octahedral; high spin; five

Exercise 5.4.2

For the complex, predict its structure, whether it is high spin or low spin, and the number of unpaired electrons present.

$[PtCl_4]^{2-}$

Answer

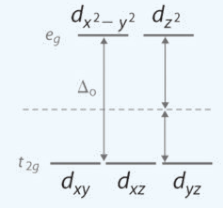
square planar; low spin; no unpaired electrons

Exercise 5.4.3

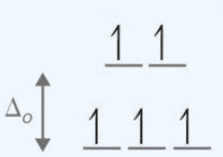
For the complex ion $[Fe(Cl)_6]^{3-}$ determine the number of d electrons for Fe, sketch the d-orbital energy levels and the distribution of d electrons among them, list the number of lone electrons, and label whether the complex is paramagnetic or diamagnetic.

Answer

Step 1: Determine the oxidation state of Fe. Here it is Fe^{3+}. Based on its electron configuration, Fe^{3+} has **5 d-electrons**. Step 2: Determine the geometry of the ion. Here it is an octahedral which means the energy splitting should look like:



Step 3: Determine whether the ligand induces is a strong or weak field spin by looking at the spectrochemical series. Cl^- is a weak field ligand (i.e., it induces high spin complexes). Therefore, electrons fill all orbitals before being paired.



Step four: Count the number of lone electrons. Here, there are **5 electrons**. Step five: The five unpaired electrons means this complex ion is **paramagnetic** (and strongly so).

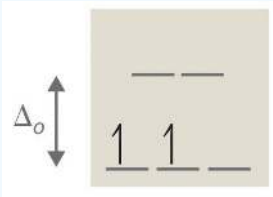
Exercise 5.4.4

For each of the following, sketch the d-orbital energy levels and the distribution of d electrons among them, state the geometry, list the number of d-electrons, list the number of lone electrons, and label whether they are paramagnetic or dimagnetic:

a. $[Ti(H_2O)_6]^{2+}$
b. $[NiCl_4]^{2-}$
c. $[CoF_6]^{3-}$ (also state whether this is low or high spin)
d. $[Co(NH_3)_6]^{3+}$ (also state whether this is low or high spin)
e. True or False: Square Planer complex compounds are usually low spin.

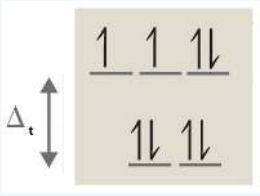
Answer a

octahedral, 2, 2, paramagnetic



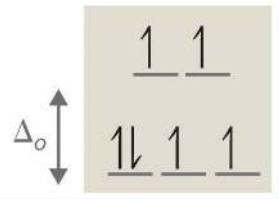
Answer b

tetrahedral, 8, 2, paramagnetic (see Octahedral vs. Tetrahedral Geometries)



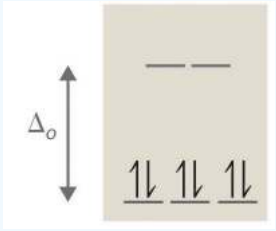
Answer c

octahedral, 6, 4, paramagnetic, high spin



Answer d

octahedral, 6, 0, diamagnetic, low spin



Answer e

True

Summary

Crystal field theory, which assumes that metal–ligand interactions are only electrostatic in nature, explains many important properties of transition-metal complexes, including their colors, magnetism, structures, stability, and reactivity. Crystal field theory (CFT) is a bonding model that explains many properties of transition metals that cannot be explained using valence bond theory. In CFT, complex formation is assumed to be due to electrostatic interactions between a central metal ion and a set of negatively charged ligands or ligand dipoles arranged around the metal ion. Depending on the arrangement of the ligands, the d orbitals split into sets of orbitals with different energies. The difference between the energy levels in an octahedral complex is called the crystal field splitting energy (Δ_o), whose magnitude depends on the charge on the metal ion, the position of the metal in the periodic table, and the nature of the ligands. The spin-pairing energy (P) is the increase in energy that occurs when an electron is added to an already occupied orbital. A high-spin configuration occurs when the Δ_o is less than P, which produces complexes with the maximum number of unpaired electrons possible. Conversely, a low-spin configuration occurs when the Δ_o is greater than P, which produces complexes with the minimum number of unpaired electrons possible. Strong-field ligands interact strongly with the d orbitals of the metal ions and give a large Δ_o, whereas weak-field ligands interact more weakly and give a smaller Δ_o. The colors of transition-metal complexes depend on the environment of the metal ion and can be explained by CFT.

Contributors and Attributions

- Asadullah Awan (UCD), Hong Truong (UCD)
- Prof. Robert J. Lancashire (The Department of Chemistry, University of the West Indies)

5.4: Crystal Field Electron Configuration is shared under a CC BY-NC-SA 4.0 license and was authored, remixed, and/or curated by Kathryn A. Newton, Northern Michigan University.

- **24.5: Bonding in Complex Ions: Crystal Field Theory** is licensed CC BY-NC-SA 4.0.
- **Crystal Field Theory** is licensed CC BY-NC-SA 4.0.

5.5: Crystal Field Stabilization Energy

The difference in energy between the two sets of d orbitals is called the crystal field splitting energy (Δ_o), where the subscript o stands for octahedral. The magnitude of the splitting depends on the charge on the metal ion, the position of the metal in the periodic table, and the nature of the ligands. Crystal field splitting energy also applies to tetrahedral complexes (Δ_t), where the subscript t standands for tetrahedral. It is important to note that the splitting of the d orbitals in a crystal field does not change the total energy of the five d orbitals. In an octahedral complex, the two e_g orbitals increase in energy by $0.6\Delta_o$, and the three t_{2g} orbitals decrease in energy by $0.4\Delta_o$ (Figure **5.5.1**). Thus the total change in energy is

Misplaced '#'

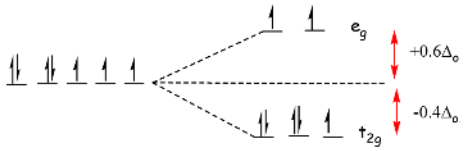


Figure **5.5.1**: Crystal field diagram of an octahedral complex showing the increased energy of the e_g and decreased energy of the t_{2g} orbitals. (LibreText)

> *Crystal field splitting does not change the total energy of the d orbitals.*

Quantifying Crystal Field Stabilization Energy

Recall that stable molecules contain more electrons in the lower-energy (bonding) molecular orbitals in a molecular orbital diagram than in the higher-energy (antibonding) molecular orbitals. If the lower-energy set of d orbitals (the t_{2g} orbitals) is selectively populated by electrons, then the stability of the complex increases relative to the d-orbitals on the free metal ion. For example, the single d electron in a d^1 complex such as $[Ti(H_2O)_6]^{3+}$ is located in one of the t_{2g} orbitals. Consequently, this complex will be more stable than expected on purely electrostatic grounds by $0.4\Delta_o$. The additional stabilization of a metal complex by selective population of the lower-energy d orbitals is called its **crystal field stabilization energy** (CFSE).

The CFSE of a complex can be calculated by multiplying the number of electrons in t_{2g} orbitals by the energy of those orbitals ($-0.4\Delta_o$), multiplying the number of electrons in e_g orbitals by the energy of those orbitals ($+0.6\Delta_o$), and summing the two. Using the high-spin d^7 configuration shown in Figure **5.5.1** as an example:

$$\mathbf{CFSE} = (5 \times -0.4\Delta_o) + (2 \times 0.6\Delta_o) = -0.8\Delta_o \tag{5.5.1}$$

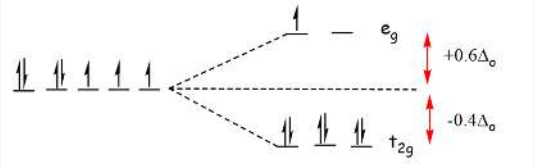
CFSEs are important for two reasons. First, the existence of CFSE nicely accounts for the difference between experimentally measured values for bond energies in metal complexes and values calculated based solely on electrostatic interactions. Second, CFSE represents relatively large amounts of energy (up to several hundred kilojoules per mole), which has important chemical consequences.

Example 5.5.1

What is the Crystal Field Stabilization Energy for a low spin d^7 octahedral complex?

Solution

The splitting pattern and electron configuration for both isotropic and octahedral ligand fields are compared below.



$$\mathbf{CFSE} = (6 \times -0.4\Delta_O) + (1 \times 0.6\Delta_O) = -1.8\Delta_O \tag{5.5.2}$$

Table 5.5.1 gives CFSE values for octahedral complexes with different d electron configurations. The CFSE is highest for low-spin d^6 complexes, which accounts in part for the extraordinarily large number of Co(III) complexes known. The other low-spin configurations also have high CFSEs, as does the d^3 configuration.

Table 5.5.1: CFSEs for Octahedral Complexes with Different Electron Configurations (in Units of Δo)

	High Spin		CFSE (Δ_o)	Low Spin		CFSE (Δ_o)
	t_{2g}	e_g		t_{2g}	e_g	
d^0			0			
d^1	↑		0.4			
d^2	↑ ↑		0.8			
d^3	↑ ↑ ↑		1.2			
d^4	↑ ↑ ↑	↑	0.6	↑↓ ↑ ↑		1.6
d^5	↑ ↑ ↑	↑ ↑	0.0	↑↓ ↑↓ ↑		2.0
d^6	↑↓ ↑ ↑	↑ ↑	0.4	↑↓ ↑↓ ↑↓		2.4
d^7	↑↓ ↑↓ ↑	↑ ↑	0.8	↑↓ ↑↓ ↑↓	↑	1.8
d^8	↑↓ ↑↓ ↑↓	↑ ↑	1.2			
d^9	↑↓ ↑↓ ↑↓	↑↓ ↑	0.6			
d^{10}	↑↓ ↑↓ ↑↓	↑↓ ↑↓	0.0			

> *Octahedral d^3 and d^8 complexes and low-spin d^6, d^5, d^7, and d^4 complexes exhibit large CFSEs.*

Octahedral Preference

Similar CFSE values can be constructed for non-octahedral ligand field geometries. In an octahedral complex, the two e_g orbitals decrease in energy by $0.6\Delta_t$, and the three t_{2g} orbitals increase in energy by $0.4\Delta_t$ (Figure 5.5.2). As for octahedral complexes, the total energy of the d-orbitals in a tetrahedral complex does not change; the total change in energy is

Misplaced '#'

Note: Δ_o and Δ_t represent different units of energy. The tetrahedral crystal field is smaller in energy than the octahedral crystal field, which contributes to the tetrahedral preference for high-spin complexes (Figure 5.5.2). The following conversion may be used for comparing octahedral and tetrahedral complexes that involve same ligands only:

$$\Delta_t \approx \frac{4}{9}\Delta_o \tag{5.5.3}$$

The CFSE for a tetrahedral complex is calculated in Table 5.5.2. These energies can then be compared to the octahedral CFSE to calculate a thermodynamic preference (Enthalpy-wise) for a metal-ligand combination to favor the octahedral geometry. This is quantified via a **Octahedral Site Preference Energy**:

$$OSPE = CFSE_{(oct)} - CFSE_{(tet)}$$

The OSPE quantifies the preference of a complex to exhibit an octahedral geometry vs. a tetrahedral geometry. Figure 5.5.3 compares the CFSE for tetrahedral and octahedral high-spin complexes for each d-electron configuration. From a simple inspection of Figure 5.5.3, the following observations can be made:

- The OSPE is *small* in d^1, d^2, d^5, d^6, d^7 complexes and other factors influence the stability of the complexes including steric factors.

- The OSPE is *large* in d^3 and d^8 complexes which strongly favor octahedral geometries.

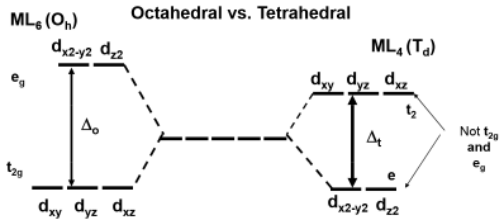


Figure **5.5.2**: A comparison of octahedral and tetrahedral crystal fields. (LibreText)

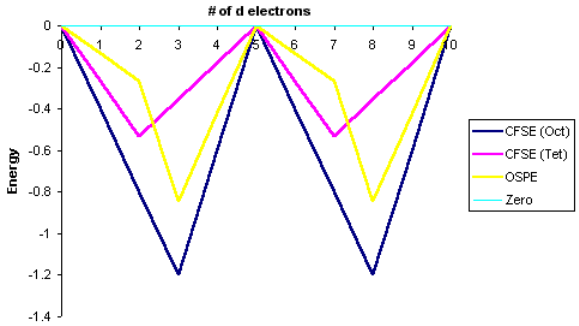


Figure **5.5.1**: Crystal Field Stabilization Energies for both octahedral fields ($CFSE_{oct}$) and tetrahedral fields ($CFSE_{tet}$). Octahedral Site Preference Energies (OSPE) are in yellow. This is for high spin complexes. (LibreText)

Table **5.5.2**: Octahedral Site Preference Energies (OSPE)

Total d-electrons	**CFSE(Octahedral)**		**CFSE(Tetrahedral)**		**OSPE (for high spin complexes)****
	High Spin	Low Spin	Configuration	**Always High Spin***	
d^0	0 Δ_o	0 Δ_o	e^0	0 Δ_t	0 Δ_o
d^1	-2/5 Δ_o	-2/5 Δ_o	e^1	-3/5 Δ_t	-6/45 Δ_o
d^2	-4/5 Δ_o	-4/5 Δ_o	e^2	-6/5 Δ_t	-12/45 Δ_o
d^3	-6/5 Δ_o	-6/5 Δ_o	$e^2t_2^1$	-4/5 Δ_t	-38/45 Δ_o
d^4	-3/5 Δ_o	-8/5 Δ_o + P	$e^2t_2^2$	-2/5 Δ_t	-19/45 Δ_o
d^5	0 Δ_o	-10/5 Δ_o + 2P	$e^2t_2^3$	0 Δ_t	0 Δ_o
d^6	-2/5 Δ_o	-12/5 Δ_o + P	$e^3t_2^3$	-3/5 Δ_t	-6/45 Δ_o
d^7	-4/5 Δ_o	-9/5 Δ_o + P	$e^4t_2^3$	-6/5 Δ_t	-12/45 Δ_o
d^8	-6/5 Δ_o	-6/5 Δ_o	$e^4t_2^4$	-4/5 Δ_t	-38/45 Δ_o
d^9	-3/5 Δ_o	-3/5 Δ_o	$e^4t_2^5$	-2/5 Δ_t	-19/45 Δ_o
d^{10}	0	0	$e^4t_2^6$	0 Δ_t	0 Δ_o

Example 5.5.2

For each complex, predict its structure, whether it is high spin or low spin, and the number of unpaired electrons present.

1. $[Cu(NH_3)_4]^{2+}$
2. $[Ni(CN)_4]^{2-}$

Solution

Because Δ_o is so large for the second- and third-row transition metals, all four-coordinate complexes of these metals are square planar due to the much higher crystal field stabilization energy (CFSE) for square planar versus tetrahedral structures. The only exception is for d^{10} metal ions such as Cd^{2+}, which have zero CFSE and are therefore tetrahedral as predicted by the VSEPR model. Four-coordinate complexes of the first-row transition metals can be either square planar or tetrahedral; the former is favored by strong-field ligands, whereas the latter is favored by weak-field ligands. For example, the $[Ni(CN)_4]^{2-}$ ion is square planar, while the $[NiCl_4]^{2-}$ ion is tetrahedral.

1.

The copper in this complex is a d^9 ion and it has a coordination number of 4. So it is probably either square planar or tetrahedral. To estimate which, we need to fill in the CFT splitting diagrams for each with 9 electrons and ask which has a lower energy. Comparing the square planer (Figure **5.5.1**) splitting diagram with tetrahedral (Figure **5.5.2**), suggests that 9 electrons will have a net lower total energy for square planar (since the $d_{x^2-y^2}$ orbital is high in energy, the others are lower).

For the square planar structure, neither high nor low spin states are possible (only one state) with a single unpaired electron.

2.

The nickle in this complex is a d^8 ion and it has a coordination number of 4. So it is probably either square planar or tetrahedral. To estimate which, we need to fill in the CFT splitting diagrams for each with 8 electrons and ask which has a lower energy. Comparing the square planer (Figure **5.5.1**) splitting diagram with tetrahedral (Figure **5.5.2**), suggests that 8 electrons will have a net lower total energy for square planar (since the $d_{x^2-y^2}$ orbital is high in energy, the others are lower).

For the square planar structure, it is a low spin complex since a high spin requires a lot of energy to promote to the $d_{x^2-y^2}$ orbital. Hence, there are no unpaired electrons.

Example 5.5.3

Which is the preferred configuration for a d^3 metal: tetrahedral or octahedral?

Solution

To answer this, the *Crystal Field Stabilization Energy* has to be calculated for a (d^3 metal in both configurations. The geometry with the greater stabilization will be the preferred geometry.

- For a d^3 *octahedral* configuration, the *Crystal Field Stabilization Energy* is

$$3 \times -0.4\Delta_o = -1.2\Delta_o$$

- For a d^3 *tetrahedral* configuration (assuming high spin), the *Crystal Field Stabilization Energy* is

$$-0.8\Delta_{tet}$$

Remember that because Δ_{tet} is less than half the size of Δ_o, tetrahedral complexes are often high spin. We can now put this in terms of Δ_o (we can make this comparison because we're considering the same metal ion and the same ligand: all that's changing is the geometry)

So for tetrahedral d^3, the Crystal Field Stabilization Energy is:

$$\text{CFSE} = -0.8 \times 4/9\ \Delta_o = -0.355\ \Delta_o.$$

And the difference in Crystal Field Stabilization Energy between the two geometries will be:

$$1.2 - 0.355 = 0.845\ \Delta_o.$$

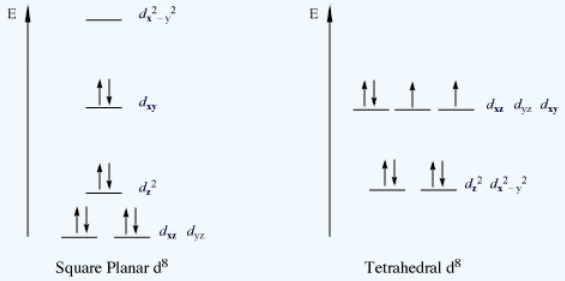
Example 5.5.4

The molecule $[PdCl_4]^{2-}$ is diamagnetic, which indicates a square planar geometry as all eight d-electrons are paired in the lower-energy orbitals. However, $[NiCl_4]^{2-}$ is also d^8 but has two unpaired electrons, indicating a tetrahedral geometry. Why is $[PdCl_4]^{2-}$ square planar if Cl^- is not a strong-field ligand?

Solution

The geometry of the complex changes going from $[NiCl_4]^{2-}$ to $[PdCl_4]^{2-}$. Clearly this cannot be due to any change in the ligand since it is the same in both cases. It is the other factor, the metal, that leads to the difference.

Consider the splitting of the d-orbitals in a generic d^8 complex. If it were to adopt a square planar geometry, the electrons will be stabilized (with respect to a tetrahedral complex) as they are placed in orbitals of lower energy. However, this comes at a cost: two of the electrons, which were originally unpaired in the tetrahedral structure, are now paired in the square-planer structure:



We can label these two factors as ΔE (stabilization derived from occupation of lower-energy orbitals) and P (spin pairing energy) respectively. One can see that:

- If $\Delta E > P$, then the complex will be square planar
- If $\Delta E < P$, then the complex will be tetrahedral.

This is analogous to deciding whether an octahedral complex adopts a high- or low-spin configuration; where the crystal field splitting parameter Δ_o ΔE does above. Unfortunately, unlike Δ_o in octahedral complexes, there is no simple graphical way to represent ΔE on the diagram above since multiple orbitals are changed in energy between the two geometries.

Interpreting the origin of metal-dependent stabilization energies can be tricky. However, we know experimentally that Pd^{2+} has a larger splitting of the d-orbitals and hence a larger ΔE than Ni^{2+} (moreover P is also smaller).

Practically all 4d and 5d d^8 ML_4 complexes adopt a square planar geometry, irrespective if the ligands are strong-field ligand or not. Other examples of such square planar complexes are $[PtCl_4]^{2-}$ and $[AuCl_4]^-$.

Problems

? Exercise 5.5.1

Determine the crystal field stabilization energy (CFSE) in the following octahedral ions:

a. V^{3+}
b. Ni^{2+}
c. Cr^{3+}
d. Zn^{2+}

Answer a

V^{3+} is d^2, with two electrons in the t_{2g} and zero electrons in e_g.

CFSE = $[2(-0.4) + 0(0.6)] \times \Delta_o = -0.8\Delta_o$

Answer b

Ni^{2+} is d^8, with six electrons in t_{2g} and two electrons in e_g.

CFSE = $[6(-0.4) + 2(0.6)] \times \Delta_o = -1.2\Delta_o$

Answer c

Cr^{3+} is d^3, with three electrons in t_{2g} and zero electrons in e_g.

CFSE = $[3(-0.4) + 0(0.6)] \times \Delta_o = -1.2\Delta_o$

Answer d

Zn^{2+} is d^{10}, with six electrons in t_{2g} and four electrons in e_g.

CFSE = $[6(-0.4) + 4(0.6)] \times \Delta_o = 0\Delta_o$.

? Exercise 5.5.2

What are the geometries of the following two complexes?

1. $[AlCl_4]^-$
2. $[Ag(NH_3)_2]^+$

Answer 1

tetrahedral

Answer 2

linear

Contributors and Attributions

- Asadullah Awan (UCD), Hong Truong (UCD)
- Prof. Robert J. Lancashire (The Department of Chemistry, University of the West Indies)

5.5: Crystal Field Stabilization Energy is shared under a CC BY-NC-SA 4.0 license and was authored, remixed, and/or curated by Kathryn A. Newton, Northern Michigan University.

- **24.5: Bonding in Complex Ions: Crystal Field Theory** is licensed CC BY-NC-SA 4.0.
- **Crystal Field Stabilization Energy** is licensed CC BY-NC-SA 4.0.
- **Non-octahedral Complexes** by Anonymous is licensed CC BY-NC-SA 4.0.
- **Octahedral vs. Tetrahedral Geometries** is licensed CC BY-NC-SA 4.0.
- **Tetrahedral vs. Square Planar Complexes** is licensed CC BY 4.0.
- **10.2.1: Crystal Field Theory** by Chris Schaller is licensed CC BY-NC 4.0.
- **Crystal Field Theory** is licensed CC BY-NC-SA 4.0.

5.6: Thermodynamic and Structure Consequences of d orbital splitting

The energy level splitting of the d-orbitals due to their interaction with the ligands in a complex has important structural and thermodynamic effects on the chemistry of transition-metal complexes. Although these two types of effects are interrelated, they are considered separately here.

Structural Effects

There are two major kinds of structural effects: effects on the ionic radii of metal ions with regular octahedral or tetrahedral geometries, and structural distortions observed for specific electron configurations.

Ionic Radii

Figure 5.6.1 is a plot of the ionic radii of the divalent fourth-period metal ions versus atomic number. The dashed line represents the behavior predicted based on the effects of screening and variation in effective nuclear charge (Z_{eff}), assuming a spherical distribution of the 3d electrons. Because these radii are based on the structures of octahedral complexes and Cr^{2+} and Cu^{2+} do not form truly octahedral complexes, the points for these ions are shown as open circles.

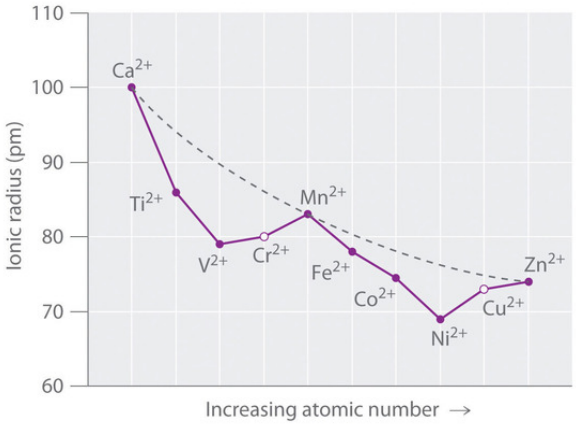


Figure 5.6.1: The Effect of d-Orbital Splittings on the Radii of the Divalent Ions of the Fourth-Period Metals. Only $Ca^{2+}(d^0)$, Mn^{2+} (high-spin d^5), and Zn^{2+} (d^{10}) lie on the smooth dashed curve. All other divalent ions fall below this curve because they have asymmetrical distributions of d electrons. To explain why an asymmetrical distribution of d electrons makes a metal ion smaller than expected, consider the Ti^{2+} ion, which has a d^2 configuration with both electrons in the t_{2g} orbitals. Because the t_{2g} orbitals are directed between the ligands, the two d-electrons are unable to shield the ligands from the nuclear charge. Consequently, the ligands experience a higher effective nuclear charge than predicted, the metal–ligand distance is unusually short, and the ionic radius is smaller than expected. If instead the two electrons were distributed uniformly over all five d orbitals, they would be much more effective at screening the ligands from the nuclear charge, making the metal–ligand distances longer and giving the metal a larger ionic radius.

A similar effect is observed for the V^{2+} ion, which has a d^3 configuration. Because the three electrons in the t_{2g} orbitals provide essentially no shielding of the ligands from the metal, the ligands experience the full increase of +1 in nuclear charge that occurs from Ti^{2+} to V^{2+}. Consequently, the observed ionic radius of the V^{2+} ion is significantly smaller than that of the Ti^{2+} ion.

Skipping the Cr^{2+} ion for the moment, consider the d^5 Mn^{2+} ion. Because the nuclear charge increases by +2 from V^{2+} to Mn^{2+}, Mn^{2+} might be expected to be smaller than V^{2+}. The two electrons added from V^{2+} to Mn^{2+} occupy the e_g orbitals, however, which are oriented directly toward the six ligands. Because these electrons are localized directly between the metal ion and the ligands, they are effective at screening the ligands from the increased nuclear charge. As a result, the ionic radius actually increases significantly from V^{2+} to Mn^{2+}, despite the higher nuclear charge of the latter.

The same effects are observed in the second half of the first-row transition metals. In the Fe^{2+}, Co^{2+}, and Ni^{2+} ions, the extra electrons are added successively to the t_{2g} orbitals, resulting in increasingly poor shielding of the ligands from the nuclei and in abnormally small ionic radii. Skipping over Cu^{2+}, adding the last two electrons causes a significant increase in the ionic radius of Zn^{2+}, despite its greater nuclear charge.

The Jahn–Teller Effect

Because simple octahedral complexes are not observed for the Cr^{2+} and Cu^{2+} ions, only estimated values for their radii are shown in Figure **5.6.1**. Since both Cr^{2+} and Cu^{2+} ions have electron configurations with an odd number of electrons in the e_g orbitals. Because the single electron (in the case of Cr^{2+}) or the third electron (in the case of Cu^{2+}) can occupy either one of two degenerate e_g orbitals, both systems have degenerate ground states. The Jahn–Teller theorem states that such non-linear systems are not stable; they undergo a distortion that makes the complex less symmetrical and splits the degenerate states, which decreases the energy of the system. The distortion and resulting decrease in energy are collectively referred to as the Jahn–Teller effect. Neither the nature of the distortion nor its magnitude is specified, and in fact, they are difficult to predict. In principle, Jahn–Teller distortions are possible for many transition-metal ions; in practice, however, they are observed only for systems with an odd number of electrons in the e_g orbitals, such as the Cr^{2+} and Cu^{2+} ions.

Consider an octahedral Cu^{2+} complex, $[Cu(H_2O)_6]^{2+}$, which is elongated along the z axis. As indicated in Figure **5.6.2**, this kind of distortion splits both the e_g and t_{2g} sets of orbitals. Because the axial ligands interact most strongly with the d_{z^2} orbital, the splitting of the e_g set (δ_1) is significantly larger than the splitting of the t_{2g} set (δ_2), but both δ_1 and δ_2 are much, much smaller than the Δ_o. This splitting does not change the centerpoint of the energy within each set, so a Jahn–Teller distortion results in no net change in energy for a filled or half-filled set of orbitals. If, however, the e_g set contains one electron (as in the d^4 ions, Cr^{2+} and Mn^{3+}) or three electrons (as in the d^9 ion, Cu^{2+}), the distortion decreases the energy of the system. For Cu^{2+}, for example, the change in energy after distortion is $2(-\delta_1/2) + 1(\delta_1/2) = -\delta_1/2$. For Cu^{2+} complexes, the observed distortion is always an elongation along the z axis by as much as 50 pm; in fact, many Cu^{2+} complexes are distorted to the extent that they are effectively square planar. In contrast, the distortion observed for most Cr^{2+} complexes is a compression along the z axis. In both cases, however, the net effect is the same: the distorted system is more stable than the undistorted system.

Jahn–Teller distortions are most important for d^9 and high-spin d^4 complexes; the distorted system is more stable than the undistorted one.

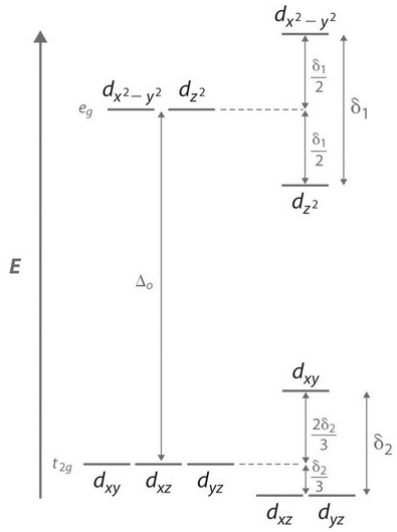


Figure **5.6.2**: The Jahn–Teller Effect

Increasing the axial metal–ligand distances in an octahedral d^9 complex is an example of a Jahn–Teller distortion, which causes the degenerate pair of e_g orbitals to split in energy by an amount δ_1; δ_1 and δ_2 are much smaller than Δ_o. As a result, the distorted system is more stable (lower in energy) than the undistorted complex by $\delta_1/2$.

Thermodynamic Effects

As previously noted, crystal field splitting energies (CFSEs) can be as large as several hundred kilojoules per mole, which is the same magnitude as the strength of many chemical bonds or the energy change in most chemical reactions. Consequently, CFSEs are important factors in determining the magnitude of hydration energies, lattice energies, and other thermodynamic properties of the transition metals.

Hydration Energies

The hydration energy of a metal ion is defined as the change in enthalpy for the following reaction:

$$M^{2+}_{(g)} + H_2O_{(l)} \rightarrow M^{2+}_{(aq)} \tag{5.6.1}$$

Although hydration energies cannot be measured directly, they can be calculated from experimentally measured quantities using thermochemical cycles. In Figure **5.6.3***a*, a plot of the hydration energies of the fourth-period metal dications versus atomic number forms a curve with two valleys. Note the relationship between the plot in Figure **5.6.3***a* and the plot of ionic radii in Figure **5.6.1** the overall shapes are essentially identical, and only the three cations with spherically symmetrical distributions of d electrons (Ca^{2+}, Mn^{2+}, and Zn^{2+}) lie on the dashed lines. In Figure **5.6.3***a*, the dashed line corresponds to hydration energies calculated based solely on electrostatic interactions. Subtracting the CFSE values for the $[M(H_2O)_6]^{2+}$ ions from the experimentally determined hydration energies gives the points shown as open circles, which lie very near the calculated curve. Therefore, CFSEs are primarily responsible for the differences between the measured and calculated values of hydration energies.

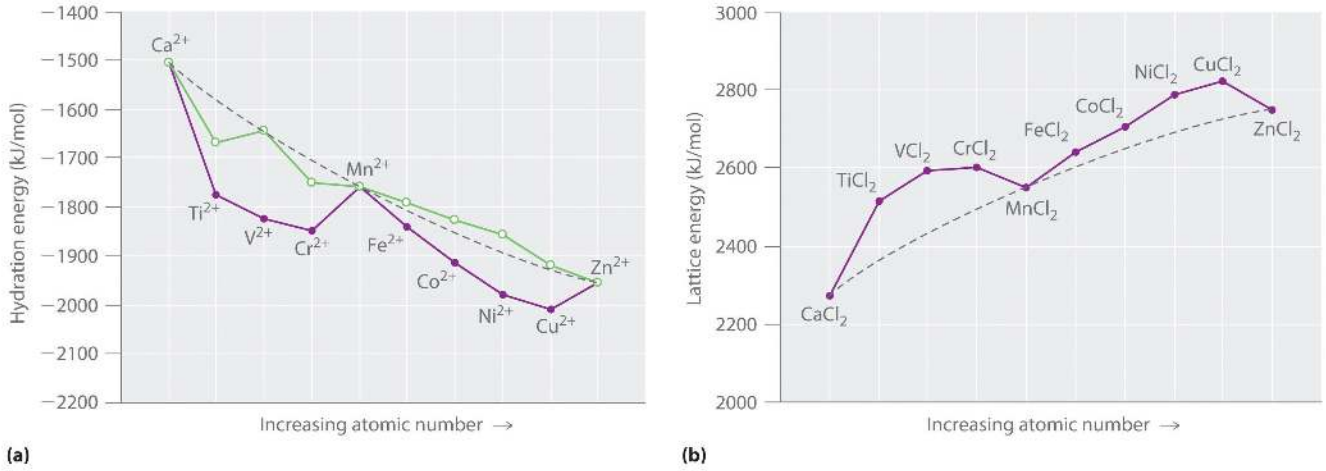


Figure **5.6.3**: Thermochemical Effects of d-Orbital Splittings. (a) A plot of the hydration energies of the divalent fourth-period metal ions versus atomic number (solid circles) shows large deviations from the smooth curve calculated, assuming a spherical distribution of d electrons (dashed line). Correcting for CFSE gives the points shown as open circles, which, except for Ti^{2+} and Cr^{2+}, are close to the calculated values. The apparent deviations for these ions are caused by the fact that solutions of the Ti^{2+} ion in water are not stable, and Cr^{2+} does not form truly octahedral complexes. (b) A plot of the lattice energies for the fourth-period metal dichlorides versus atomic number shows similar deviations from the smooth curve calculated, assuming a spherical distribution of d electrons (dashed lines), again illustrating the importance of CFSEs.

Lattice Energies

Values of the lattice energies for the fourth-period metal dichlorides are plotted against atomic number in part (b) of Figure **5.6.3**. Recall that the lattice energy is defined as the negative of the enthalpy change for the reaction below. Like hydration energies, lattice energies are determined indirectly from a thermochemical cycle.

$$M^{2+}(g) + 2Cl^-(g) \rightarrow MCl_2(s) \tag{5.6.2}$$

The shape of the lattice-energy curve is essentially the mirror image of the hydration-energy curve in part (a) of Figure **5.6.3**, with only Ca^{2+}, Mn^{2+}, and Zn^{2+} lying on the smooth curve. It is not surprising that the explanation for the deviations from the curve is exactly the same as for the hydration energy data: all the transition-metal dichlorides, except $MnCl_2$ and $ZnCl_2$, are more stable than expected due to CFSE.

Summary

Distorting an octahedral complex by moving opposite ligands away from the metal produces a tetragonal or square planar arrangement, in which interactions with equatorial ligands become stronger. Because none of the d orbitals points directly at the ligands in a tetrahedral complex, these complexes have smaller values of the crystal field splitting energy Δ_t. The crystal field stabilization energy (CFSE) is the additional stabilization of a complex due to placing electrons in the lower-energy set of d orbitals. CFSE explains the unusual curves seen in plots of ionic radii, hydration energies, and lattice energies versus atomic

number. The Jahn–Teller theorem states that a non-linear molecule with a spatially degenerate electronic ground state undergoes a geometrical distortion to remove the degeneracy and lower the overall energy of the system.

5.6: Thermodynamic and Structure Consequences of d orbital splitting is shared under a CC BY-NC-SA 4.0 license and was authored, remixed, and/or curated by LibreTexts.

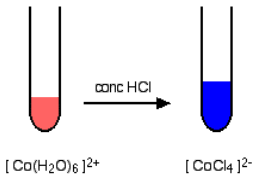
- **Thermodynamics and Structural Consequences of d-Orbital Splitting** is licensed CC BY-NC-SA 4.0.

5.7: Ligand Exchange Reactions and Affinity Determination

This page describes some common ligand exchange (substitution) reactions involving complex metal ions. It assumes that you are familiar with basic ideas about complex ions. A *ligand exchange reaction* involves the substitution of one or more ligands in a complex ion with one or more different ligands.

Replacing aqua with chloro ligands

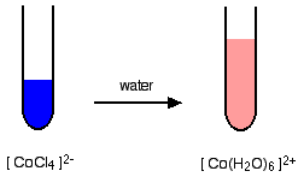
If you add concentrated hydrochloric acid to a solution containing hexaaquacobalt(II) ions (for example, cobalt(II) chloride solution), the solution turns from its original pink color to a dark rich blue. The six aqua molecules are replaced by four chloro ions.



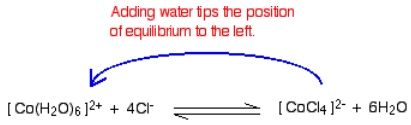
The reaction taking place is reversible.

$$[Co(H_2O)_6]^{2+} + 4\,Cl^- \rightleftharpoons [CoCl_4]^{2-} + 6\,H_2O$$

Concentrated hydrochloric acid is used as the source of chloride ions because it provides a very high concentration compared to what is possible with, say, sodium chloride solution. Concentrated hydrochloric acid has a chloride ion concentration of approximately 10 mol dm^{-3}. The high chloride ion concentration pushes the position of the equilibrium to the right according to Le Chatelier's Principle.

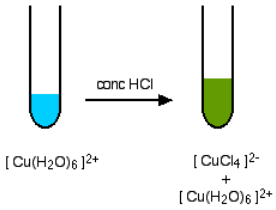


Notice the change in the co-ordination of the cobalt. Chloride ions are bigger than water molecules, and there isn't room to fit six of them around the central cobalt ion. This reaction can be easily reversed by adding water to the solution. Adding water to the right-hand side of the equilibrium has the effect of moving the position of equilibrium to the left. The pink color of the hexaaquacobalt(II) ion is produced again (only paler, of course, because it is more dilute).



Replacing the water in the hexaaquacopper(II) ion

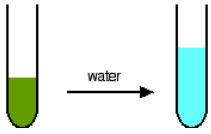
In terms of the chemistry, this is exactly the same as the last example - all that differs are the colors. Unfortunately, these are not quite so straightforward. The color of the tetrachlorocuprate(II) ion is almost always seen mixed with that of the original hexaaqua ion. What you normally see is:



The reaction taking place is reversible, and you get a mixture of colors due to both of the complex ions.

$$[Cu(H_2O)_6]^{2+} \rightleftharpoons [CuCl_4]^{2-} + 6\,H_2O$$

You may find the color of the tetrachlorocuprate(II) ion variously described as olive-green or yellow. Adding water to the green solution, replaces the chloro ligands by water molecules again, and returns the solution to blue.



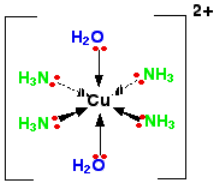
Replacing water molecules by ammonia

Water molecules and ammonia molecules are very similar in size, and so there is no change in co-ordination this time. Unfortunately, the reactions aren't quite so straightforward to describe. Ammonia solution can react with hexaaqua metal ions in two quite distinct ways, because it can act as a base as well as a ligand.

If you add a small amount of ammonia solution you get precipitates of the metal hydroxide - the ammonia is acting as a base. In some cases, these precipitates redissolve when you add more ammonia to give solutions in which a ligand exchange reaction has occurred. In the diagrams below, both steps are shown, but we are only going to consider the chemistry of the overall ligand exchange reaction. The precipitates dissolve because of a complicated series of equilibrium shifts, and we shan't worry about that for the moment.

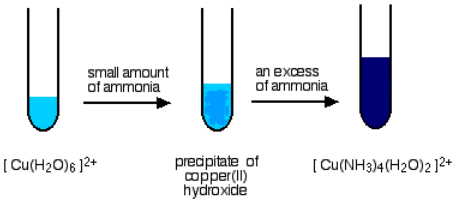
Replacing the water in the hexaaquacopper(II) ion

This is a slightly untypical case, because only four of the six water molecules get replaced to give the tetraamminediaquacopper(II) ion, $[Cu(NH_3)_4(H_2O)_2]^{2+}$.



the tetraamminediaquacopper(II) ion

Notice that the four ammonias all lie in one plane, with the water molecules above and below. What you see in a test tube is:



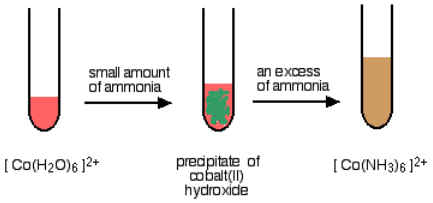
The main equilibrium involved in the ligand exchange reaction is:

$$[Cu(H_2O)_6]^{2+} + 4\,NH_3 \rightleftharpoons [Cu(NH_3)_4(H_2O)_2]^{2+} + 4\,H_2O$$

The color of the deep blue complex is so strong that this reaction is used as a sensitive test for copper(II) ions in solution. Even if you try to reverse the change by adding large amounts of water to the equilibrium, the strength of the deep blue (even highly diluted) always masks the pale blue of the aqua ion.

Replacing the water in the hexaaquacobalt(II) ion

This time, all the water molecules get replaced.



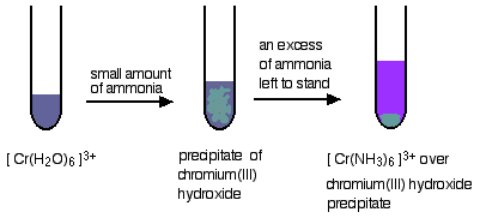
$$[Co(H_2O)_6]^{2+} + 6\,NH_3 \rightleftharpoons [Co(NH_3)_6]^{2+} + 6\,H_2O$$

The straw colored solution formed changes color very rapidly on standing to a deep reddish brown. The hexaamminecobalt(II) ions are oxidised by the air to hexaamminecobalt(III) ions. However, that is a quite separate reaction, and is not a part of the ligand exchange reaction.

Replacing the water in the hexaaquachromium(III) ion

Again, all the agua ligands are replaced by ammine ligands. The difference this time is that the reaction is incomplete. The precipitate has to be left to stand in the presence of excess concentrated ammonia solution for some time to get the fully substituted ammine complex. Even so, you still get left with some unreacted precipitate.

$$[Cr(H_2O)_6\,]^{3+} + 6\,NH_3 \rightleftharpoons [Cr(NH_3)_6]^{3+} + 6\,H_2O$$

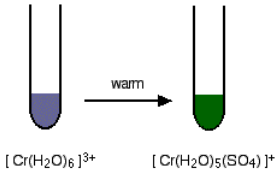


Two more replacements of the water in the hexaaquachromium(III) ion

The color of the hexaaquachromium(III) ion has been shown as a "difficult to describe" violet-blue-grey in all the diagrams above. In practice, when it is produced during a reaction in a test tube, it is often green. A typical example of this is the use of acidified potassium dichromate(VI) as an oxidising agent. Whenever this is used, the orange solution turns green and we nearly always describe the green ion as being $Cr^{3+}_{(aq)}$ - implying the hexaaquachromium(III) ion. That's actually an over-simplification. What happens is that one or more of the ligand water molecules get replaced by a negative ion in the solution - typically sulfate or chloride.

Replacement of the water by sulfate ions

You can do this simply by warming some chromium(III) sulfate solution.



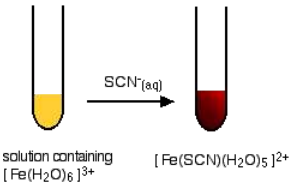
One of the water molecules is replaced by a sulfate ion. Notice the change in the charge on the ion. Two of the positive charges are canceled by the presence of the two negative charges on the sulfate ion.

Replacement of the water by chloride ions

In the presence of chloride ions (for example with chromium(III) chloride), the most commonly observed color is green. This happens when two of the water molecules are replaced by chloride ions to give the tetraaquadichlorochromium(III) ion - $[Cr(H_2O)_4Cl_2]^+$. Once again, notice that replacing water molecules by chloride ions changes the charge on the ion.

A ligand exchange reaction in the test for iron(III) ions

This provides an extremely sensitive test for iron(III) ions in solution. If you add thiocyanate ions, SCN^-, (from, say, sodium or potassium or ammonium thiocyanate solution) to a solution containing iron(III) ions, you get an intense blood red solution containing the ion $[Fe(SCN)(H_2O)_5]^{2+}$.



Contributors and Attributions

- Jim Clark (Chemguide.co.uk)

5.7: Ligand Exchange Reactions and Affinity Determination is shared under a CC BY-NC-SA 4.0 license and was authored, remixed, and/or curated by LibreTexts.

- **Ligand Exchange Reactions (Introduction)** by Jim Clark is licensed CC BY-NC 4.0.

5.8: Ligand Binding Thermodynamics and the Chelate Effect

This page explains what is meant by a stability constant for a complex ion, and goes on to look at how its size is governed in part by the entropy change during a ligand exchange reaction.

Replacing aqua ligands with ammine ligands

If you add ammonia solution to a solution containing hexaaquacopper(II) ions, $[Cu(H_2O)_6]^{2+}$, four of the water molecules are eventually replaced by ammonia molecules to give $[Cu(NH_3)_4(H_2O)_2]^{2+}$. This can be written as an equilibrium reaction to show the overall effect:

$$[Cu(H_2O)_6]^{2+} + 4\,NH_3 \rightleftharpoons [Cu(NH_3)_4(H_2O)_2]^{2+} + 4\,H_2O \tag{5.8.1}$$

In fact, the water molecules get replaced one at a time, and so this is made up of a series of part-reactions:

$$[Cu(H_2O)_6]^{2+} + NH_3 \rightleftharpoons [Cu(NH_3)(H_2O)_5]^{2+} + H_2O \tag{5.8.2}$$

$$[Cu(NH_3)(H_2O)_5]^{2+} + NH_3 \rightleftharpoons [Cu(NH_3)_2(H_2O)_4]^{2+} + H_2O \tag{5.8.3}$$

$$[Cu(NH_3)_2(H_2O)_4]^{2+} + NH_3 \rightleftharpoons [Cu(NH_3)_3(H_2O)_3]^{2+} + H_2O \tag{5.8.4}$$

$$[Cu(NH_3)_3(H_2O)_3]^{2+} + NH_3 \rightleftharpoons [Cu(NH_3)_4(H_2O)_2]^{2+} + H_2O \tag{5.8.5}$$

Although this can look a bit daunting at first sight, all that is happening is that first you have one, then two, then three, then four water molecules in total replaced by four ammine ligands.

Individual stability constants

Let's take a closer look at the first of these equilibria (Equation 5.8.2). Like any other equilibrium, this one has an equilibrium constant, K_c - except that in this case, we call it a stability constant. Because this is the first water molecule to be replaced, we call it K_1 and is given by this expression:

$$K_1 = \frac{[[Cu(NH_3)(H_2O)_5]^{2+}]}{[[Cu(H_2O)_6]^{2+}][NH_3]}$$

There are two points of possible confusion here - one minor, one more important!

- First, the square brackets have changed their meaning! Square brackets are often used to keep everything in a complex ion together and tidy. Here, they have reverted to their other use, which implies concentrations in mol dm^{-3}.
- In order to avoid complete confusion, the square brackets keeping the complexes together have been removed entirely.
- More importantly, if you compare the equilibrium constant expression with the equation, you will see that the water on the right-hand side hasn't been included. That is normal practice with these expressions.
- Because everything is dissolved in water, the water is present as a huge excess. Generating a little bit more during the reaction is going to make no effective difference to the total concentration of the water in terms of moles of water per dm^3.
- The concentration of the water is approximately constant. The equilibrium constant is defined so that you avoid having an extra unnecessary constant in the expression.

With that out of the way, let's go back to where we were - but introduce a value for K_1:

$$[Cu(H_2O)_6]^{2+} + NH_3 \rightleftharpoons [Cu(NH_3)(H_2O)_5]^{2+} + H_2O$$

$$K_1 = \frac{[Cu(NH_3)(H_2O)_5^{2+}]}{[Cu(H_2O)_6^{2+}]\,[NH_3]} = 1.78 \times 10^4 \text{ mol}^{-1} \text{ dm}^3$$

The value of the equilibrium constant is fairly large, suggesting that there is a strong tendency to form the ion containing an ammonia molecule. A high value of a stability constant shows that the ion is easily formed. Each of the other equilibria above also has its own stability constant, K_2, K_3 and K_4. For example, K_2 is given by:

$$[Cu(NH_3)(H_2O)_5]^{2+} + NH_3 \rightleftharpoons [Cu(NH_3)_2(H_2O)_4]^{2+} + H_2O$$

$$K_2 = \frac{[Cu(NH_3)_2(H_2O)_4^{2+}]}{[Cu(NH_3)(H_2O)_5^{2+}]\,[NH_3]}$$
$$= 4.07 \times 10^3 \ \text{mol}^{-1}\,\text{dm}^3$$

The ion with two ammonias is even more stable than the ion with one ammonia. You could keep plugging away at this and come up with the following table of stability constants:

ion	K_n	value (mol^{-1} dm^3)	log K_n
$[Cu(NH_3)(H_2O)_5]^{2+}$	K_1	1.78×10^4	4.25
$[Cu(NH_3)_2(H_2O)_4]^{2+}$	K_2	4.07×10^3	3.61
$[Cu(NH_3)_3(H_2O)_3]^{2+}$	K_3	9.55×10^2	2.98
$[Cu(NH_3)_4(H_2O)_2]^{2+}$	K_4	1.74×10^2	2.24

You will often find these values quoted as log K_1. All this does is tidy the numbers up so that you can see the patterns more easily. The ions keep on getting more stable as you replace up to 4 water molecules, but notice that the equilibrium constants are gradually getting less big as you replace more and more waters. This is common with individual stability constants.

Overall Formation constants

The overall stability constant is simply the equilibrium constant for the total reaction:

$$[Cu(H_2O)_6]^{2+} + 4\,NH_3 \rightleftharpoons [Cu(NH_3)_4(H_2O)_2]^{2+} + 4\,H_2O$$

It is given by this expression:

$$\text{overall } K_{stab} = \frac{[Cu(NH_3)_4(H_2O)_2^{2+}]}{[Cu(H_2O)_6^{2+}]\,[NH_3]^4}$$
$$= 1.20 \times 10^{13} \ \text{mol}^{-4}\,\text{dm}^{12}$$

You can see that overall this is a very large equilibrium constant, implying a high tendency for the ammonias to replace the waters. The "log" value is 13.1. This overall value is found by multiplying together all the individual values of K_1, K_2 and so on. To find out why that works, you will need a big bit of paper and some patience! Write down expressions for all the individual values (the first two are done for you above), and then multiply those expressions together. You will find that all the terms for the intermediate ions cancel out to leave you with the expression for the overall stability constant.

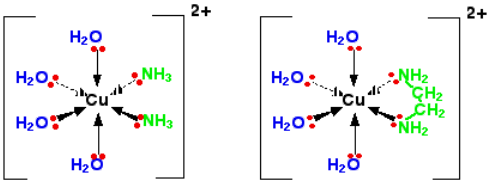
Summary

Whether you are looking at the replacement of individual water molecules or an overall reaction producing the final complex ion, a stability constant is simply the equilibrium constant for the reaction you are looking at. The **larger** the value of the stability constant, the further the reaction lies to the **right**. That implies that complex ions with large stability constants are more stable than ones with smaller ones.

Stability constants tend to be very large numbers. In order to simplify the numbers a "log" scale is often used. Because of the way this works, a difference of 1 in the log value comes from a 10 times difference in the stability constant. A difference of 2 comes from a 100 (in other words, 10^2) times difference in stability constant - and so on.

Stability constants and entropy - the chelate effect

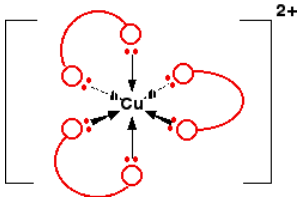
The chelate effect is an effect which happens when you replace water (or other simple ligands) around the central metal ion by multidentate ligands like 1,2-diaminoethane (often abbreviated to "en") or EDTA. Compare what happens if you replace two water molecules around a $[Cu(H_2O)_6]^{2+}$ ion with either 2 ammonia molecules or one molecule of 1,2-diaminoethane.



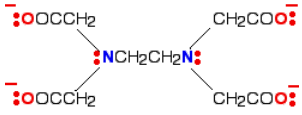
This second structure is known as a chelate from a Greek word meaning a crab's claw. You can picture the copper ion as being nipped by the claw of the 1,2-diaminoethane molecule. Chelates are much more stable than complex ions formed from simple monodentate ligands. The overall stability constants for the two ions are:

ion	log K
$[Cu(NH_3)_2(H_2O)_4]^{2+}$	7.86
$[Cu(H_2O)_4(en)]^{2+}$	10.6

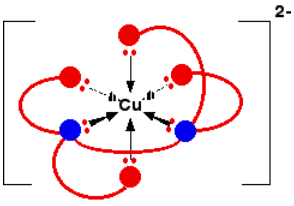
The reaction with the 1,2-diaminoethane could eventually go on to produce a complex ion $[Cu(en)_3]^{2+}$. Simplifying the structure of this:



The overall stability constant for this (as log K) is 18.7. Another copper-based chelate comes from the reaction with EDTA.



the $EDTA^{4-}$ ion



the $[Cu(EDTA)]^{2-}$ ion

This also has a high stability constant - log K is 18.8. However many examples you take, you always find that a chelate (a complex ion involving multidentate ligands) is more stable than ions with only monodentate ligands. This is known as the chelate effect.

The reason for the chelate effect

If you compare the two equilibria below, the one with the 1,2-diaminoethane ("en") has the higher equilibrium (stability) constant (for values, see above).





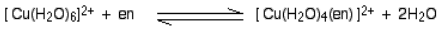
The enthalpy changes of the two reactions are fairly similar. You might expect this because in each case you are breaking two bonds between copper and oxygen atoms and replacing them by two bonds between copper and nitrogen atoms.

If the enthalpy changes are similar, what causes the difference in the extent to which the two reactions happen?

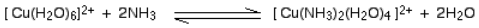
You need to think about the entropy change during each reaction.

Entropy is most easily thought of as a measure of disorder. Any change which increases the amount of disorder increases the tendency of a reaction to happen.

If you look again at the two equiilbria, you might notice that the 1,2-diaminoethane equilibrium does lead to an increase in the entropy. There are only two species on the left-hand side of the equation, but three on the right.



You can obviously get more entropy out of three species than out of only two. Compare that with the other equilibrium. In this case, there is no change in the total number of species before and after reaction, and so no useful contribution to an increase in entropy.



In the case of the complex with EDTA, the increase in entropy is very pronounced.



Here, we are increasing the number of species present from two on the left-hand side to seven on the right. You can get a major amount of increase in disorder by making this change.

Reversing this last change is going to be far more difficult in entropy terms. You would have to move from a highly disordered state to a much more ordered one. That isn't so likely to happen, and so the copper-EDTA complex is very stable.

Summary

Complexes involving multidentate ligands are more stable than those with only monodentate ligands. The underlying reason for this is that each multidentate ligand displaces more than one water molecule. This leads to an increase in the number of species present in the system, and therefore an increase in entropy. An increase in entropy makes the formation of the chelated complex more favorable.

Contributors and Attributions

- Jim Clark (Chemguide.co.uk)

This page titled 5.8: Ligand Binding Thermodynamics and the Chelate Effect is shared under a CC BY-NC 4.0 license and was authored, remixed, and/or curated by Jim Clark.

- **Ligand Exchange Reactions (Thermodynamics)** by Jim Clark is licensed CC BY-NC 4.0.

5.9: Hard and Soft Ligands and Metal Ions

The Hard-Soft Acid-Base concept is a tool for thinking about patterns of Lewis acid-base reactivity. Arland, Chatt, and Davies' observed that *Lewis acids and bases could be classified into two groups based on their propensity to form stable compounds with one another* (*e.g.* acids in a class tend to form more stable adducts with bases in the same class than they did with bases in the other class).[1] Arland, Chatt, and Davies somewhat boringly termed these groups class a and class b but today they are known by Ralph Pearson's name for them. Pearson called the class a acids and bases *hard* and called the class b acids and bases *soft*. These terms reflect the polarizability of the electron cloud, or how "soft" these substance's electron clouds are towards distortion (Figure **5.9.1**). **Soft** acids and bases are relatively polarizable, and **hard** acids and bases are difficult to polarize.

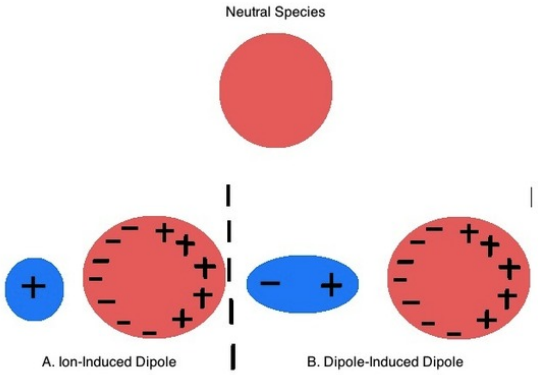


Figure **5.9.1**: Polarizability refers to the ease with which a substance's electron cloud may be distorted under the action of an electric field. Polarizability determines the degree to which a neutral species' electron cloud can be distorted to an induced dipole moment by an ion (as shown on the left) or by a polar molecule (as shown on the right). [CC-BY 4.0, LibreText]

Hard and Soft Classification

Hard Species

Hard acids and bases have a high charge density (highly charged relative to size), and polarization is difficult. Low polarizability is attributed to hard acids being relatively electron-poor and hard bases being relatively electron-rich. Low polarizability is also attributed to the localization of charge on an atom with electron-withdrawing substituents (in the case of a hard acid) or electron-donating substituents (in the case of a hard base). It is also observed that hard acids have high oxidation states or large positive formal charges, while hard bases have low oxidation states or negative formal charges.

For hard acids, which possess few valence electrons, polarization involves distorting core (inner shell) electrons, which are difficult to distort because they are close to the nucleus and experience a high nuclear charge. Hard acids tend to be found towards the left side of the periodic table and involve higher oxidation states and/or electron donating substituents

Soft Species

Soft acids and bases posses many valence electrons and are more readily polarized. Soft acids and bases are more likely to be found towards the middle or right of the periodic table. Soft acids and bases also have little charge density and/or are relatively electron rich. Soft acids are more common to the right of the periodic table and involve lower oxidation states and/or electron donating substituents.

Borderline Species

All hard acids and bases are not equally hard, and all soft acids and bases are not equally soft. There is a graduation in hardness and softness, and there are a number of intermediate acids and bases that do not fit neatly in either category. Figure **5.9.1** classifies each element as a hard, soft, or **borderline** (intermediate) acid or base. Some borderline acids can be considered hard or soft depending on their oxidation state. The higher oxidation state species can be considered hard acids, and the lower oxidation state species can be considered soft acids. Additional representative examples of hard, soft, and borderline bases are shown in Figure Extra close brace or missing open brace and Figure **5.9.3**.

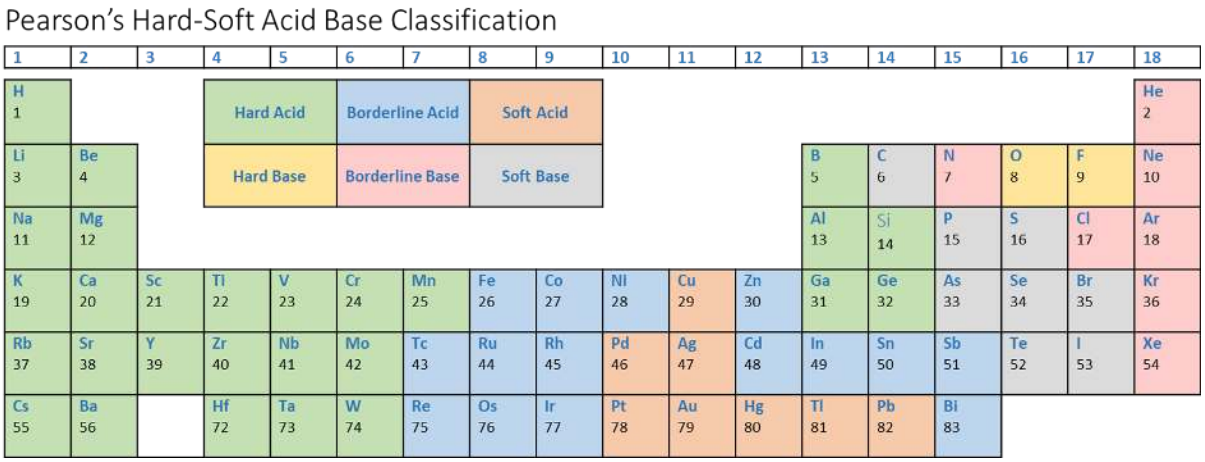


Figure 5.9.1: Pearson's Hard-Soft Acid Base Classification of the Elements (CC-BY-NC-SA; Kathryn A. Newton)

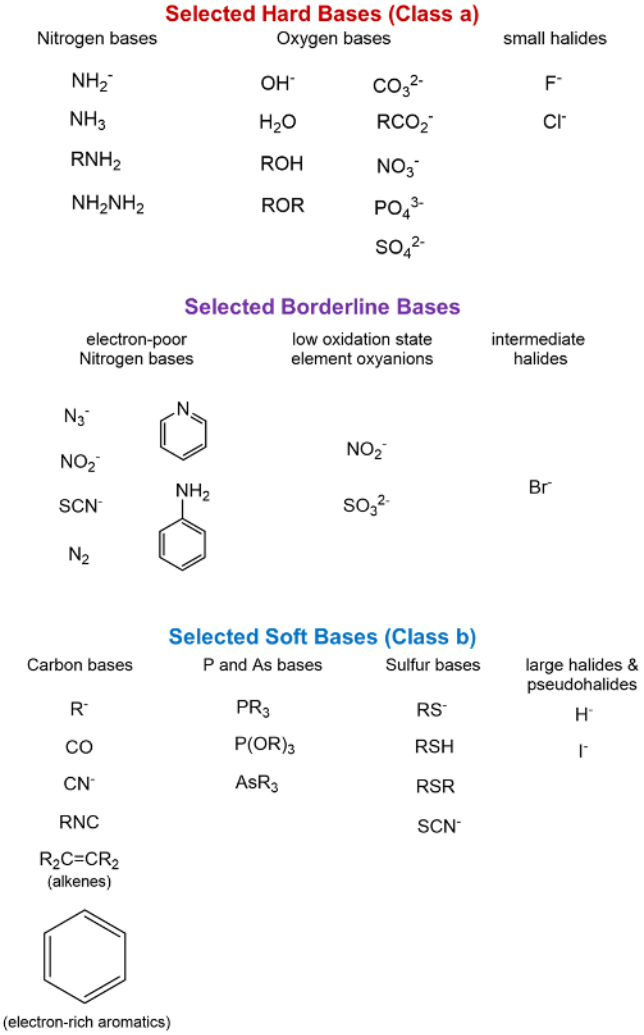


Figure 5.9.2: Representative examples of hard, soft, and borderline bases. (LibreText)

Hard Base	Soft Base	Borderline Base	Hard Acid	Soft Acid	Borderline Acid
NR_3 (R = alkyl group) O^{2-} F^- Cl^-	CO CN^- P S As Se Te I NCS^-	Br^- ^-NCS	Ti^{4+} V^{4+} Cr^{3+}, Cr^{6+} $Mn^{2+}, Mn^{4+}, Mn^{7+}$ Fe^{3+} Co^{3+} Ni^{3+}	Cu^+ M^{n-} (−oxidation state)	Fe^{2+} Co^{2+} Ni^{2+} Cu^{2+}

Figure 5.9.3: HSAB classifcation of selected species. (CC-BY-NC-SA; Kathryn A. Newton)

The Hard-Soft Acid-Base Principle (HSAB Principle)

The **Hard-Soft Acid-Base Concept (HSAB Concept)** explains patterns in Lewis acid-base reactivity as a *like reacts with like* preference. Both thermodynamically and kinetically, hard acids prefer hard bases and soft acids soft bases. Specifically,

- Thermodynamically, hard acids form more stable acid-base complexes with hard bases while soft acids form more stable complexes with soft bases.
- Kinetically, hard acids/electrophiles react more quickly with hard bases/nucleophiles while soft acids/electrophiles react more quickly with soft bases/nucleophiles.

The HSAB principle can predict the equilibrium of Lewis acid-base metathesis and displacement reactions. In a Lewis acid-base **metathesis reaction** the acids and bases swap partners:

$$\mathbf{A_1 : B_1 + A_2 : B_2 \overset{k_1,\, K_{eq}}{\rightleftharpoons} A_1 : B_2 + A_2 : B_1}$$

For example, the equilibrium position of the metathesis reaction between $\mathbf{TlF}$ and $\mathbf{K_2S}$ favors the products:

$$\mathbf{2\,TlF + H_2S \rightleftharpoons Tl_2S + 2\,KF}$$

This is consistent with the HSAB's hard-hard and soft-soft preference.



The HSAB principle also allows for prediction of displacement reactions, in which a Lewis acid or base forms an adduct using a base or acid from an existing Lewis acid-base complex. In these reactions, the displacement of acid or base from the reactant complex may be thought of as a sort of metathesis reaction, one in which in the unbound acid or base switches places with one in the complex. For example, the reaction between $\mathbf{HI}$ and methylmercury cation involves displacement of an iodide from $\mathbf{HI}$ to give $\mathbf{CH_3HgI}$. The position of the equilibrium favors $\mathbf{CH_3HgI}$ since both $\mathbf{CH_3Hg^+}$ and $\mathbf{I^-}$ are soft, while $\mathbf{H^+}$ is a hard acid.

$$\mathbf{HI + HgSCH_3^+ \rightleftharpoons CH_3SHgI + H^+}$$



The hard-hard and soft-soft preferences in Lewis acid-base interactions reflect that:

- The lone pair of a hard base is strongly stabilized electrostatically by a hard acid.
- The lone pair of a soft base is strongly stabilized by forming a covalent bond with a soft acid.

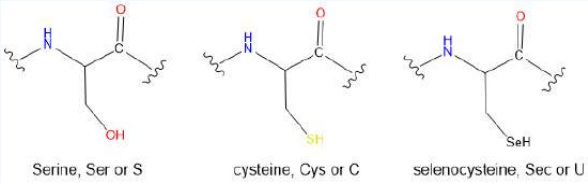
- The lone pair of a hard or soft base is comparatively weakly stabilized by an acid opposite to it in hardness or softness since the overall electrostatic and covalent stabilization of the adduct is comparatively weak.

Problems

Exercise 5.9.1

Rank the acids or bases in each set in increasing order of expected hardness.

a. Cr^{2+} and Cr^{3+}
b. H^+, Cs^+, and Tl^+
c. SCN^- (acting as a base at N) and SCN^- (acting as a base at S)
d. AlF_3, AlH_3, $AlMe_3$
e. The side chains of the following proteinogenic amino acids

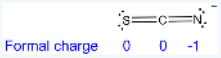


Answer

(a) $Cr^{2+} < Cr^{3+}$ All other things being equal, hardness increases with oxidation state.

(b) $Tl^+ < Cs^+ < H^+$ The order reflects Cs^+ and Tl^+'s larger size relative to H^+ (which doesn't possess any electrons that can be polarized anyway) and that Tl^+ still possesses two valence electrons while Cs^+ possesses none.

(c) SCN^- (acting as a base at S) < SCN^- (acting as a base at N). The order reflects the greater electronegativity of N than S and N's possession of a more negative formal charge of -1.



(d) $AlH_3 < AlMe_3 < AlF_3$. The hardness increases as the substituents on the Lewis acid Al center become less electron donating and more electron withdrawing (and, incidentally, harder bases) as their electronegativity increases in the order H^- < CH_3^- < F^-. Note that the order of electron donating ability for H^- and CH_3^- is the opposite observed for carbocations, for which hyperconjugation plays a larger role.

(e) Sec < Cys < Ser. The hardness increases as the electronegativity of the Lewis base chalcogen increases on going from a selenol to a thiol to an alcohol.

Exercise 5.9.2

Predict the position of equilibrium for the following reaction.

$$Fe_2O_3 + 3\,Ag_2S \rightleftharpoons Fe_2S_3 + 3\,Ag_2O$$

Answer

The equilibrium will favor the reactants (K<1) since the hard-hard and soft-soft interactions in the reactants are more stable than the hard-soft interactions in the products.



Exercise 5.9.3

Predict whether K for the following equilibria will be <<1, ~1, or >>1.

a. $2\,HF + (CH_3Hg)_2S \rightleftharpoons 2\,CH_3HgF + H_2S$
b. $Ag(NH_3)_2^+ + 2\,PH_3 \rightleftharpoons Ag(PH_3)_2^+ + 2\,NH_3$
c. $Ag(PH_3)_2^+ + 2\,H_3B{-}SH_2 \rightleftharpoons 2\,H_3B{-}PH_3 + Ag(SH_2)_2^+$
d. $H_3B{-}NH_3 + F_3B{-}SH_2 \rightleftharpoons H_3B{-}SH_2 + F_3B{-}NH_3$

Answer

a. K< < 1 since the reactant adducts are hard-hard and soft-soft while the products involve hard-soft interactions.

b. K>>1 since the reactant complex, diamine silver(I), is a complex of a hard base, NH_3, with the soft acid, Ag^+, while the product is a complex of the same soft acid with the soft base phosphine.

c. K~1 since all the adducts amongst the reactants and products involve soft acids and bases.

d. K>>1 since BH_3 is a softer acid than BF_3, so it will form a stronger complex with the softer base H_2S while the harder BF_3 forms a stronger complex with the harder base NH_3.

Exercise 5.9.4

Which acid will form the most stable complex with **CO**: BH_3, BF_3, or BMe_3?

Answer

BH_3. Since **CO** forms complexes primarily through its carbon lone pair, it is a soft base and so will form the strongest complex with the softest Lewis acid.

References

1. Ahrland, S.; Chatt, J.; Davies, N. R., The relative affinities of ligand atoms for acceptor molecules and ions. Quarterly Reviews, Chemical Society 1958, 12 (3), 265-276.

2. Pearson, R. G., Hard and Soft Acids and Bases. Journal of the American Chemical Society 1963, 85 (22), 3533-3539.

3. Fleming, I., Molecular orbitals and organic chemical reactions. Reference ed.; Wiley: Hoboken, N.J., 2010.

Notes

* Despite the fruitfulness of this observation, in general it is important to reduce the potential for observer bias by checking observations like these against compounds reported in the chemical literature and databases like the Inorganic Crystal Structure and Cambridge Crystallographic Databases.

** These are very soluble in water, to the point where some solutions are perhaps better described as solutions of water in the halide.

This page titled 5.9: Hard and Soft Ligands and Metal Ions is shared under a CC BY-NC 4.0 license and was authored, remixed, and/or curated by Jim Clark.

- **6.6.2: Hard-Hard and Soft-Soft preferences may be explained and quantified in terms of electrostatic and covalent and electronic stabilization on the stability of Lewis acid-base adducts** by Stephen M. Contakes is licensed CC BY-NC 4.0.

SECTION OVERVIEW

5.10: Potential Isomers of Complex Ions

There are several types of this isomerism frequently encountered in coordination chemistry and the following represents some of them. Isomers that contain the same number of atoms of each kind but differ in which atoms are bonded to one another are called structural isomers, which differ in structure or bond type. For inorganic complexes, there are three types of structural isomers: *ionization*, *coordination*, and *linkage* and two types of stereoisomers: *geometric and optical*.

Structural isomers, as their name implies, differ in their structure or bonding, which are separate from **stereoisomers** that differ in the spatial arrangement of the ligands are attached, but still have the bonding properties. The different chemical formulas in structural isomers are caused either by a difference in what ligands are bonded to the central atoms or how the individual ligands are bonded to the central atoms. When determining a structural isomer, you look at: (1) the ligands that are bonded to the central metal, and (2) which atom of the ligands attach to the central metal. Below is a quick look at the different types of structural isomers. The highlighted ions are the ions that switch or change somehow to make the type of structural isomer it is.

5.10: Potential Isomers of Complex Ions is shared under a CC BY-NC-SA 4.0 license and was authored, remixed, and/or curated by LibreTexts.

CHAPTER OVERVIEW

6: Molecular Orbital Theory

6.1: Overview of Colors from Transition Metal Ions
6.2: Symmetry and Symmetry Operations
6.3: Molecule Shapes (Point Groups)
6.4: Point Group Assignment
6.5: Overview of Classifying Bonding Orbitals in a Molecule
6.6: MO Diagram Construction of CO2
6.7: MO Diagram Construction of H2O
6.8: MO Diagram Construction of NH3
6.9: MO Construction of BF3
6.10: Lewis Acid-Base Dative Bond and MO Diagrams
6.11: MO Diagram for bonding in [M(NH3)6]n+
6.12: MO Diagram for bonding in [M(H2O)6]n+
6.13: Spectrochemical Series for Ligands
6.14: Spectrochemical Series for Metal ions

6: Molecular Orbital Theory is shared under a not declared license and was authored, remixed, and/or curated by LibreTexts.

6.1: Overview of Colors from Transition Metal Ions

The color for a coordination complex can be predicted using the Crystal Field Theory (CFT). The tendency for coordination complexes to display such a wide array of colors is merely coincidental; the d-orbital splitting in coordination complexes results in a gap (**Δ**) that happens to be just the right magnitude to absorb visible light. Because metal complexes can absorb visible light, they display an array of colors. Not only is the color attractive to the eye, it is an indication of the chemical and physical properties of the metal complex. The color (like the magnitude of **Δ**) depends on the identity of the metal ion, the coordination geometry, and the ligand identity. Chemists don't just "look" at color, though - we measure it using electronic absorption spectroscopy. This is usually done in a lab using a UV-visible spectrophotometer.

An example of such a measurement is shown below in Figure **6.1.1** for a Cu(II) complex. The sample appears a pink color to the eye, and when it is measured using a UV-visible spectrometer, it is shown to absorb visible light at approximately 530 nm. The absorption spectrum can indicate the oxidation state of Cu, the ligands bound to the Cu(II) ion, and the coordination geometry. The color of the solution in Figure **6.1.1** is a shade of pink.

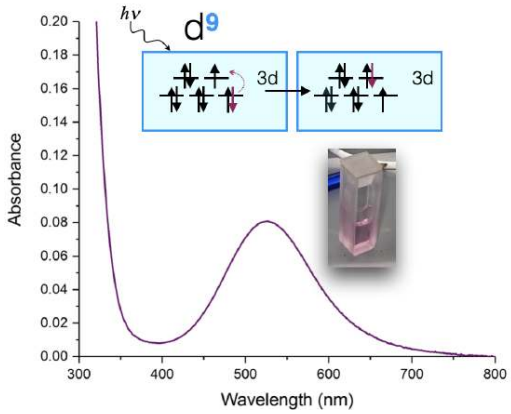


Figure **6.1.1**: A UV-visible spectrum of a Cu(II)-peptide complex. A photo of the sample shows its pink color. The splitting diagram for its approximation as an octahdral complex is shown, where an electronic transition from t_{2g} to e_g is shown. (CC-BY-NC-SA; Kathryn Haas)

The Electromagnetic Spectrum

The electromagnetic spectrum (EM) spectrum is made up of photons of different wavelengths. Photons, unique in displaying the properties of both waves and particles, create visible light and colors in a small portion of the EM spectrum. This visible light portion has wavelengths in approximately the 400-750 nanometer range (a nanometer, "nm," is 10^{-9} meters). Each specific wavelength corresponds to a different color (Figure **6.1.2**), and when all the wavelengths are present, it appears as white light.

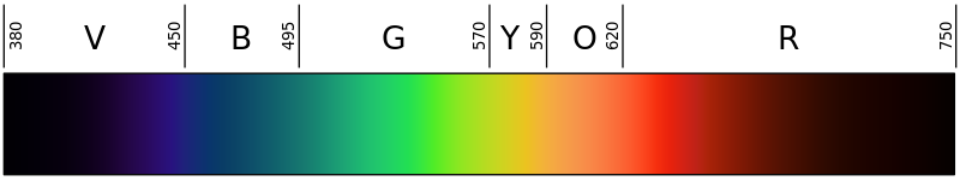


Figure **6.1.2**: A linear representation of the visible light spectrum. (Public Domain; Gringer via Wikipedia)

The wavelength and frequency of a wave are inversely proportional: as one increases, the other decreases; this is a consequence of all light traveling at the same speed.

$$\lambda \propto \nu^{-1}$$

Because of this relationship, blue light has a much higher frequency and more energy than red light.

Perceiving Color

Color is perceived in two ways, through additive mixing, where different colors are made by combining different colors of light, and through subtractive mixing, where different wavelengths of light are taken out so that the light is no longer pure white. For

colors of coordination complexes, subtractive mixing is considered. As shown in Figure **6.1.3**, the idea behind subtractive mixing is that white light (which is made from all the colors mixed together) interacts with an object. The object absorbs some of the light, and then reflects or transmits (or both, depending on the object) the rest of the light, which contacts the eye. The object is perceived as whichever color is not absorbed. In Figure **6.1.3**, white light (simplified as green, red, and blue bands) is shone through a solution. The solution absorbs the red and green wavelengths; however, the blue light is reflected and passes through, so the solution appears blue. This procedure takes place whenever an object displays visible color. If none of the light is absorbed, and all is reflected back off, the object appears white; if all of the light is absorbed, and there is none left to reflect or transmit through, the object appears black.

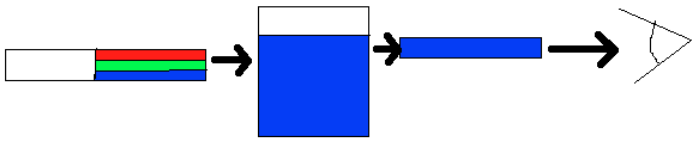
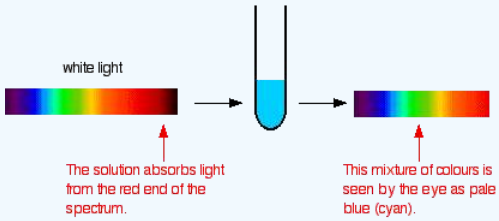


Figure **6.1.3**: Subtractive mixing

Example **6.1.1**: Copper(II) sulfate

If white light (ordinary sunlight, for example) passes through copper(II) sulfate solution, some wavelengths in the light are absorbed by the solution. Copper(II) ions in solution absorb light in the red region of the spectrum. The light which passes through the solution and out the other side will have all the colors in it except for the red. We see this mixture of wavelengths as pale blue (cyan). The diagram gives an impression of what happens if you pass white light through copper(II) sulfate solution.



Working out what color you will see is not easy if you try to do it by imagining "mixing up" the remaining colors. You wouldn't have thought that all the other colors apart from some red would look cyan, for example. Sometimes what you actually see is quite unexpected. Mixing different wavelengths of light doesn't give you the same result as mixing paints or other pigments. You can, however, sometimes get some estimate of the color you would see using the idea of complementary colors.

The absorption spectrum shown above in Figure **6.1.1** is a simple case in which only one absorption band is observed in the visible region of the spectrum. In a simple case like this, the color of a complex can be predicted using a color wheel. When a solution or object absorbs a certain wavelength, we see the complementary color, or the color opposite to the absorbed wavelength on the color wheel in Figure **6.1.4**. In the case of the Cu(II) complex spectrum shown in Figure **6.1.1**, the color of the light absorbed at 530 nm is green, and the predicted color observed is pink. Table **6.1.1** lists the approximate colors of absorption corresponding to wavelengths of light absorbed and gives similar information to that deduced from Figure **6.1.4**.

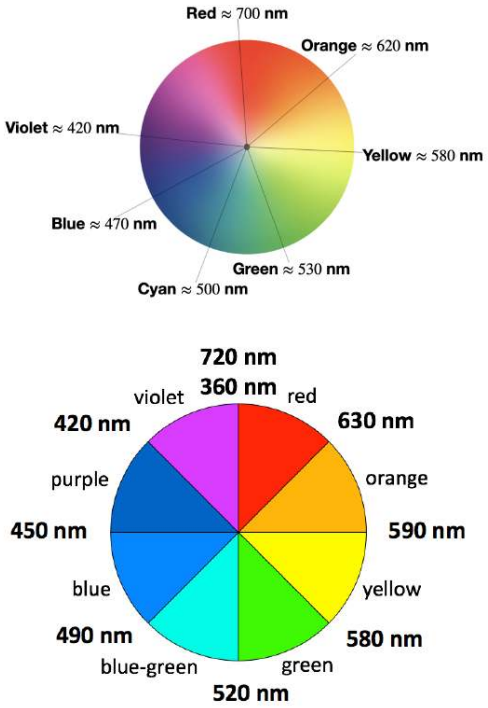


Figure **6.1.4**: Color wheels with wavelengths marked (top: CC-BY-NC-SA; Kathryn Haas)(bottom: CC BY-SA 4.0 International; Tem5psu via source)

Table **6.1.1**: Approximate wavelengths of absorption and their complementary colors observed. * This prediction is limited to simple cases where there is only one absorption band in the visible spectrum.

λ absorbed	E (cm^{-1})	E (eV)	Approximate color absorbed	Predicted color observed (by eye)
> 700 nm	$< 14,000 \frac{1}{cm}$	< 1.77 eV	Infrared	not observable
$\approx 700 - 635$ nm	$\approx 14,300 - 16,000 \frac{1}{cm}$	$\approx 1.77 - 1.95$ eV	Red	Green
$\approx 635 - 590$ nm	$\approx 15,700 - 16,900 \frac{1}{cm}$	$\approx 1.95 - 2.10$ eV	Orange	Blue
$\approx 590 - 560$ nm	$\approx 16,900 - 17,900 \frac{1}{cm}$	$\approx 2.10 - 2.21$ eV	Yellow	Violet
$\approx 560 - 520$ nm	$\approx 17,900 - 19,200 \frac{1}{cm}$	$\approx 2.21 - 2.38$ eV	Green	Red
$\approx 520 - 490$ nm	$\approx 19,200 - 20,400 \frac{1}{cm}$	$\approx 2.38 - 2.53$ eV	Cyan	Red-Orange
$\approx 490 - 450$ nm	$\approx 20,400 - 22,200 \frac{1}{cm}$	$\approx 2.53 - 2.76$ eV	Blue	Orange
$400 - 450$ nm	$\approx 22,200 - 25,000 \frac{1}{cm}$	$\approx 2.76 - 3.10$ eV	Violet	Yellow
<400 nm	$> 25,000 \frac{1}{cm}$	> 3.10 eV	Ultraviolet (UV)	not observable

Colors of Coordination Complexes: Crystal Field Splitting

When ligands attach to a transition metal to form a coordination complex, electrons in the d orbital split into high energy and low energy orbitals. The difference in energy of the two levels is denoted as Δ, and it is a characteristic a property both of the metal and the ligands. This is illustrated in Figure **6.1.5**; the "o" subscript on the Δ indicates that the complex has octahedral geometry.

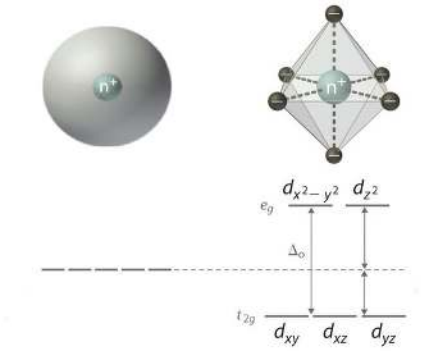


Figure **6.1.5**: d-Orbitals Splitting in an octahedral ligand field. (CC BY-SA-NC; anonymous by request)

If Δ_o is large, and much energy is required to promote electrons into the high energy orbitals, the electrons will instead pair in the lower energy orbitals, resulting in a "low spin" complex (Figure **6.1.6**); however, if Δ_o is small, and it takes little energy to occupy the higher orbitals, the electrons will do so, and remain unpaired (until there are more than five electrons), resulting in a “high spin” complex. Different ligands are associated with either high or low spin —a "strong field" ligand results in a large Δ_o and a low spin configuration, while a "weak field" ligand results in a small Δ_o and a high spin configuration. For more details, see the Crystal Field Theory (CFT) page.

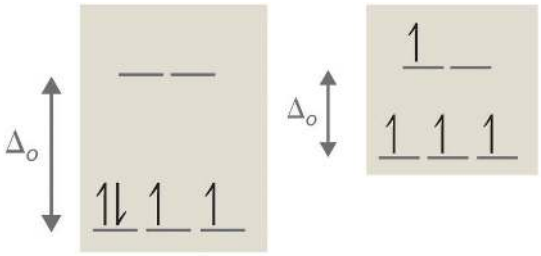


Figure **6.1.6**: (a) Low Spin, Strong Field ($\Delta_o > P$). (b): High Spin, Weak Field ($\Delta_o < P$). (CC BY-SA-NC; anonymous)

A photon equal to the energy difference Δ_o can be absorbed, promoting an electron to the higher energy level. As certain wavelengths are absorbed in this process, subtractive color mixing occurs and the coordination complex solution becomes colored. If the ions have a noble gas configuration, and have no unpaired electrons, the solutions appear colorless; in reality, they still have a measured energy and absorb certain wavelengths of light, but these wavelengths are not in the visible portion of the EM spectrum and no color is perceived by the eye.

In general, a larger Δ indicates that higher energy photons are absorbed, and the solution appears further to the left on the EM spectrum shown in Figure **6.1.2**. This relationship is described in the equation

$$\Delta = \frac{hc}{\lambda}$$

where

- h is Planck's constant ($= 6.626 \times 10^{-34} Js$)
- c is the speed of light ($= 2.998 \times 10^{8} \frac{m}{s}$)
- λ is the wavelength of light absorbed in units of m

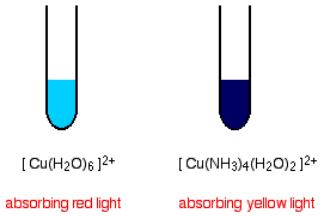
Relating the Colors of Coordination Complexes to the Spectrochemical Series

According to the Crystal Field Theory, ligands that induce smaller CFSE (Δ) values are considered "weak field" and will absorb lower-energy light with longer λ values (ie a "red shift"). Ligands that induce larger CFSE values are considered "strong field" and will absorb higher-energy light with shorter λ values (ie a "blue shift"). Thus, the energy difference, Δ, determines the color of the coordination complex.

The **spectrochemical series**, introduced previously, ranks ligands from weak field/high spin ot strong field/ low spin. It can be used to compare the approximate Δ values of ligands and to predict which wavelengths will be absorbed a complex, and thereby, what color it will appear.

$$\underset{\text{weak-field ligands}}{I^- < Br^- < Cl^- < \underline{S}CN^- < CH_3COO^- < F^- < OH^- < ox^{2-} < ONO^-} < \underset{\text{intermediate-field ligands}}{H_2O < SC\underline{N}^-} < EDTA^{4-} < NH_3 < en < NO_2^- < \underset{\text{strong-field ligands}}{CN^- \approx CO}$$

The greater the CFSE, the more energy that is needed to promote an electron from the lower group of orbitals to the higher ones. In terms of the color of the light absorbed, greater energy corresponds to shorter wavelengths. That means that as the splitting increases, the light absorbed will tend to shift away from the red end of the spectrum towards orange, yellow and so on. There is a fairly clear-cut case in copper(II) chemistry. If you add an excess of ammonia solution to hexaaquacopper(II) ions in solution, the pale blue (cyan) color is replaced by a dark inky blue as some of the water molecules in the complex ion are replaced by ammonia.

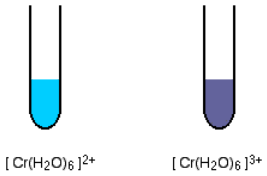


The first complex must be absorbing red light in order to give the complementary color cyan. The second one must be absorbing in the yellow region in order to give the complementary color dark blue. Yellow light has a higher energy than red light. You need that higher energy because ammonia causes more splitting of the d orbitals than water does.

Other Factors

The oxidation state of the metal

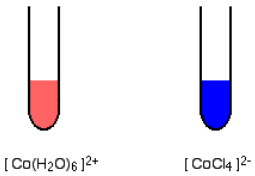
As the oxidation state of the metal increases, so also does the amount of splitting of the d orbitals. Changes of oxidation state therefore change the color of the light absorbed, and so the color of the light you see. Taking another example from chromium chemistry involving only a change of oxidation state (from +2 to +3):



The 2+ ion is almost the same color as the hexaaquacopper(II) ion, and the 3+ ion is the hard-to-describe violet-blue-grey color.

The coordination of the Ion

Splitting is greater if the ion is octahedral than if it is tetrahedral, and therefore the color will change with a change of co-ordination. The problem is that an ion will normally only change co-ordination if you change the ligand - and changing the ligand will change the color as well. Hence, you cannot isolate out the effect of the co-ordination change. For example, a commonly quoted case comes from cobalt(II) chemistry, with the ions $[Co(H_2O)_6]^{2+}$ and $[CoCl_4]^{2-}$.



The difference in the colors is going to be a combination of the effect of the change of ligand, and the change of the number of ligands.

Example 6.1.1

If a solution with a dissolved octahedral complex appears yellow to the eye, what wavelength of light does it absorb? Is this complex expected to be low spin or high spin?

Solution

A solution that looks yellow absorbs light that is violet, which is roughly 410 nm from the color wheel. Since it absorbs high energy, the electrons must be raised to a higher level, and Δ_o is high, so the complex is likely to be low spin.

Example 6.1.2

An octahedral metal complex absorbs light with wavelength 535 nm. What is the crystal field splitting Δ_o for the complex? What color is it to the eye?

Solution

To solve this question, we need to use the equation

$$\Delta_o = \frac{hc}{\lambda}$$

with

- h is Planck's constant and is $6.625 \times 10^{-34} J \cdot s$ and
- c is the speed of light and is $2.998 \times 10^8\, m/s$.

It is also important to remember that 1 nm is equal to 1×10^{-9} meters. With all this information, the final equation looks like this:

$$\Delta_o = \frac{(6.625 \times 10^{-34}\, J \cdot s)(2.998 \times 10^8\, m/s)}{(535nm)\left(\frac{1\, m}{1 \times 10^9\, nm}\right)} = 3.712\, J/molecule$$

It is not necessary to use any equations to solve the second part of the problem. Light that is 535 nm is green, and because green light is absorbed, the complex appears red (refer to Figures **6.1.1** and **6.1.6** for this information).

Note: the fact that the complex is octahedral makes no impact when solving this problem. Although the splitting is different for complexes of different structures, the mechanics of solving the problem are identical.

Example 6.1.3

There are two solutions, one orange and one blue. Both solutions are known to be made up of a cobalt complex; however, one has chloride ions as ligands, while the other has ammonia ligands. Which solution is expected to be orange?

Solution

In order to solve this problem, it is necessary to know the relative strengths of the ligands involved. A sample ligand strength list is given here, but see Crystal Field Splitting for a more complete list:

$$CN^- > en > NH_3 > H_2O > F^- > SCN^- > Cl^-$$

From this information, it is clear that NH_3 is a stronger ligand than Cl^-, which means that the complex involving NH_3 has a greater Δ, and the complex will be low spin. Because of the larger Δ, the electrons absorb higher energy photons, and the solution will have the appearance of a lower energy color. Since orange light is less energetic than blue light, the NH_3 containing solution is predicted to be orange

Example 6.1.4

A *tetrahedral* complex absorbs at 545 nm. What is the respective octahedral crystal field splitting (Δ_o)? What is the color of the complex?

Solution

$$\begin{aligned}\Delta_t &= \frac{hc}{\lambda} \\ &= \frac{(6.626 \times 10^{-34} J \cdot s)(3 \times 10^8 m/s)}{545 \times 10^{-9} m} \\ &= 3.65 \times 10^{-19}\ J\end{aligned}$$

However, the *tetrahedral* splitting (Δ_t) is ~4/9 that of the *octahedral* splitting (Δ_o).

$$\begin{aligned}\Delta_t &= 0.44\Delta_o \\ \Delta_o &= \frac{\Delta_t}{0.44} \\ &= \frac{3.65 \times 10^{-19} J}{0.44} \\ &= 8.30 \times 10^{-18} J\end{aligned}$$

This is the energy needed to promote *one* electron in *one* complex. Often the crystal field splitting is given per mole, which requires this number to be multiplied by Avogadro's Number (6.022×10^{23}).

This complex appears red, since it absorbs in the complementary green color (determined via the color wheel).

Problems

Exercise 6.1.1

What color will a complex be that absorbs light that is 600 nm be?

Answer

Blue. The color absorbed is orange.

Exercise 6.1.2

What color will a complex an octahedral complex appear if it has a Δ_o of $3.75 \times 10^{-19}\ J$?

Answer

It is red. Using $\Delta=hc/\lambda$, $h=6.626*10^{-34}$J*s, $c=2.998*10^8$m/s, wavelength would equal 530 nm. So green is absorbed, and the complementary color of green is red, so red is the color of the complex.

Exercise 6.1.3

Would you expect a violet solution to be high spin or low spin? What about a red solution?

Answer

It would be high spin. The complementary color of violet is yellow, which has a wavelength of 570 nm. For a red solution, the complementary color absorbed is green, with a wavelength of 530 nm, so it would be considered low spin.

? Exercise 6.1.4

There are two solutions, one which is yellow and another which is violet. The solutions are $[Co(H_2O)_6]^{3+}$and $[Co(CN^-)_6]^{3-}$. What are the colors of each solution?

Answer

$[Co(H_2O)_6]^{3+}$ is violet and $[Co(CN^-)_6]^{3-}$ is yellow. Looking at the spectrochemical series, H_2O is a weak field ligand, so it absorbs colors of long wavelengths—in this case, the longer wavelength is yellow, so the color reflected is violet. CN^- is a strong field ligand, so it absorbs colors of shorter wavelengths-in this case, the shorter wavelength is violet, so the color reflected is yellow.

Contributors and Attributions

- Deyu Wang (UCD)

References

- Cox, P. A. Instant Notes Inorganic Chemistry. Second ed. Grand Rapids: Garland, Incorporated, 2004.
- Nassau, Kurt. The Physics and Chemistry of Color : The Fifteen Causes of Color. Second ed. New York: Wiley-Interscience, 2001.
- Petrucci, Ralph H., William S. Harwood, and Geoff E. Herring. General Chemistry : Principles and Modern Applications. Ninth ed. Upper Saddle River: Prentice Hall PTR, 2006.
- Petrucci, Ralph H., Carey Bissonnette, F. Geoffrey Herring, Jeffrey D. Madura. General Chemistry: Principles and Modern Applications. Tenth Ed. Upper Saddle River: Pearson Education, Inc. 2011.

6.1: Overview of Colors from Transition Metal Ions is shared under a CC BY license and was authored, remixed, and/or curated by LibreTexts.

- **Colors of Coordination Complexes** is licensed CC BY 4.0.
- **11.1: Absorption of Light** by Kathryn Haas has no license indicated.
- **Origin of Color in Complex Ions** by Jim Clark is licensed CC BY-NC 4.0.
- **Crystal Field Theory** is licensed CC BY-NC-SA 4.0.

6.2: Symmetry and Symmetry Operations

Symmetry in Chemistry

Symmetry is actually a concept of mathematics and not of chemistry. However, symmetry, and the underlying mathematical theory for symmetry, group theory, are of tremendous importance in chemistry because they can be applied to many chemistry problems. For example it helps us to classify the structures of molecules and crystals, understand chemical bonding, predict vibrational spectra, and determine the optical activity of compounds. We will therefore first discuss the general foundations of symmetry and group theory, and then apply them to chemical problems, in particular chemical bonding.

Let us first find a definition for symmetry. Symmetry is very familiar to us as we associate symmetry with beauty, but very familiar things are not necessarily easy to define scientifically. One common definition is that symmetry is the self-similarity of an object. The more similar parts it has the more symmetric it appears. For example, we would argue that the two wings of the butterfly depicted look similar. If the left wing was very different from the right wing the butterfly would look less symmetric.



Figure 2.1.1 Symmetry depicted through an image of a butterfly (Attribution: Chemlibretexts https://chem.libretexts.org/@api/dek...jpg?revision=2 http://creativecommons.org/licenses/by-nc-sa/3.0/us/)

How can we measure the self-similarity, or symmetry of an object quantitatively? We can do this using the concept of the symmetry operation. It is defined as a movement of an object into an equivalent indistinguishable orientation. The number and kind of symmetry operations that can be carried out defines the symmetry of the object.

Definition: Symmetry Operation

Movement of an object into an equivalent indistinguishable orientation

Symmetry operations are carried out around so-called symmetry elements. A symmetry element is a point, line, or plane about which a symmetry operation is carried out. Let us understand know what symmetry elements and operations exist.

Definition: Symmetry Element

A point, line or plane about which a symmetry operation is carried out

The Identity Operation (*E*)

The most simple operation is the identity operation. It can be denoted by the Schoenflies symbol *E*. Schoenflies symbols are the most common symbols to denote a symmetry operation. The identity operation says that each object is self-similar to itself when you do not move it in any way. This is a trivial statement, but as we will see later, the identity operation is necessary to make the mathematical framework of symmetry, group theory, complete. The identity operation is present in any object. In the example of the depicted snail shell it is the only operation (Fig. 2.1.2).



Figure 2.1.2 Snail shell (Attribution: Petr Kratochvil http://res.publicdomainfiles.com/pdf...8045418010.jpg)

The Proper Rotation Operation

The proper rotation operation is a counter-clockwise rotation about a proper rotational axis by an angle of 360° over an integer number n. After that rotation the object must be indistinguishable from its original form. That means that the object after the rotation must superimpose the original object before the rotation. For example, when n=4, then we rotate around 90°, and after that the object must superimpose its original form. The proper rotational axis is the symmetry element associated with the proper rotation operation. It's Schoenflies symbol is C_n, whereby n is called the order of the rotational axis. A proper rotational operation has the symbol C_n^m, whereby m counts the number of times the operation is carried out. Overall we rotate by and angle of 360°× m/n when we carry out an operation C_n^m. This means that when m=n, then we have rotated around 360° (Fig. 2.1.3). Then all points in the object are at their original position. It is as though we had done nothing with the object. We can also say we have reached the identity *E*. In mathematical form we can say that C_n^n=E. If we rotated one more time, $C_n^{(n+1)}$, then this would be equal to rotating only one time, and thus $C_n^{(n+1)}=C_n^1$. For example if n=4, then rotating four times around 90° will produce the identity. We have rotated around 4 x 90°=360° which is the same a though we had not rotated at all, because all points in the object are in their original position after a 360° rotation. If we rotated 5 times around 90°, it would the same as rotating only one time.

$$C_n^m = 360° \times \frac{m}{n}$$

$$C_n^n = E$$

$$C_n^{n+1} = C_n^1$$

Figure 2.1.3 Properties of the proper rotation operation

If an object has several axes with different order n, then the one with the highest order is called the *principal axis.* If there is more than one axis of the same order, then they get distinguished by primes if they are not conjugate. We will learn about the exact definition of conjugation somewhat later, we can however often see by inspection if two axes are conjugate. This is usually the case when they pass through the object in a equivalent way, and rotate the object in an equivalent way. Axes that pass through less many bonds, get less many primes. This is just a convention, but you have to follow it. An additional rule is that an axis which is in the same position as the principal axis gets the least number of primes. For example, a square planar molecule such as $PtCl_4^{2-}$ has a C_4 principal axis standing perpendicular to the square plane of the molecule. There is an additional C_2 axis where the C_4 axis runs. It is present because one can also rotate around 180°, and not only around 90°. This C_2 axis does not get any prime. You an see that there are four additional C_2 axes, two of them are denoted C_2', and two others are denoted C_2''. You can see that the two axes which only have one prime pass through two Pt-Cl bonds, while the ones that have two primes, do not pass through any bonds. The two C_2' axes are conjugate, meaning that they transform the object in an equivalent way. The two C_2'' axes are also conjugate.

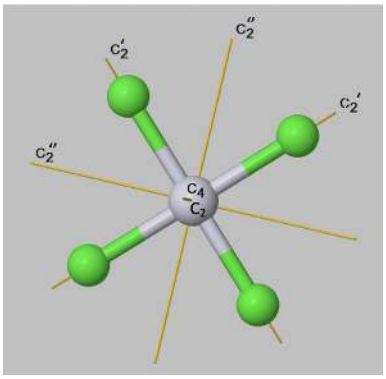


Figure 2.1.4 Proper rotational axes in the $PtCl_4^{2-}$ molecular anion. (Attribution: symotter.org/gallery)

We can now think about how we can write out the axes and their associated proper rotational operations in a systematic way. Let us first look at the symmetry elements, the proper axes: We conventionally write the principal axis first, and then all other axes from their highest to their lowest order. When there are axes of the same order, those with the least number of primes get denoted first, and those with the highest number of primes last. If there are conjugate axes then their number is placed in front of their Schoenflies symbol. For the proper axes of the $PtCl_4^{2-}$ the notation would therefore be: C_4, C_2, $2C_2'$, $2C_2''$. Now let us see how to denote the rotation operations that are associated with these symmetry elements. The notation follows the same rules as for the symmetry elements. In addition, we have to consider that we must not count identical operations twice, we also do not denote the operations that are the same as the identity. For the C_4 axis there are four operations until we reach the identity. C_4^1, C_4^2, C_4^3, and C_4^4. For each of the C_2, C_2', and C_2'' elements there are two operations until the identity is reached. C_2^1, C_2^2, $C_2^{1'}$, $C_2^{2'}$, $C_2^{1''}$, $C_2^{2''}$. The C_4^4, the C_2^2, the $C_2^{2'}$, and the $C_2^{2''}$are the same as the identity and therefore we do not consider them. In addition we can see that the C_4^2 is the same as the C_2^1. This is because the C_4 and the C_2 axes are in the same location, and rotating two times around 90° is the same as rotating one time around 180°. By convention we eliminate the operation associated with the higher order, thus the C_4^2. The overall notation would then be: C_4^1, C_4^3, C_2^1, 2 $C_2^{1'}$ 2 $C_2^{1''}$ (Fig. 2.1.5).

Rotation symmetry operations are: C_4^1, C_4^3, C_2^1, 2 $C_2^{1'}$ 2 $C_2^{1''}$

($C_4^4 = E$, $C_4^2 = C_2^1$, $C_2^2 = E$, $C_2^{2'} = E$, $C_2^{2''} = E$)

Figure 2.1.5 Proper rotation operations in $PtCl_4^{2-}$

The Reflection Operations (σ)

Let us look at reflection operations which are carried out around reflection planes, or mirror planes. Mirror planes have the Schoenflies symbol σ. When we carry out a reflection operation, then we move any point of the object to the other side of the mirror plane. There are two types of mirror planes, so-called horizontal mirror planes and vertical mirror planes. A horizontal mirror plane always stands perpendicular to the principal axis. For example in the depicted BH_3 molecule there is a horizontal mirror plane that stands perpendicular to a C_3 principal axis (Fig. 2.1.6). A horizontal mirror plane has the Schoenflies symbol σ_h.

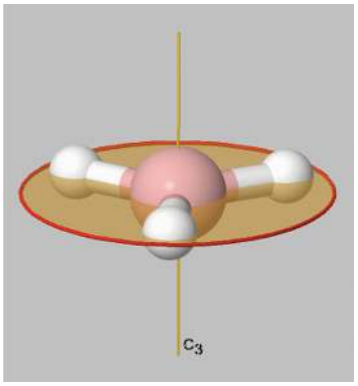


Figure 2.1.6 Visual depiction of the horizontal mirror plane of BH_3, σ_h (Attribution: symotter.org/gallery)

A vertical mirror plane has the property that it contains the principal axis, this means that it is part of the principal axis. It is denoted σ_v. The BH_3 molecule has three vertical axes that pass through the three B-H bonds. You can see that each of them contain

the principal C_3 axis (Fig. 2.1.7). The three vertical mirror planes are conjugate, and therefore they are not distinguished by primes. We can write a coefficient 3 in front of the symbol σ_v to indicate that there are three conjugate vertical mirror planes.

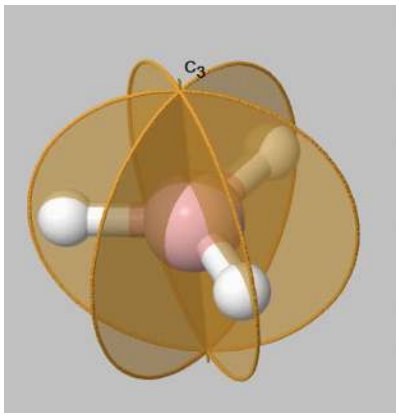


Figure 2.1.7 Visual depiction of the vertical mirror planes of BH_3, 3 σ_v (Attribution: symotter.org/gallery)

Now let us look at how many symmetry operations are associated with a particular mirror plane. Fortunately, things are simple here: There is only one reflection operation associated with one mirror plane. This because reflecting two times at a mirror plane produces the identity E: σ_v^2=E. More generally, when we reflect n times, and n is an even number then this is the same as the identity or, σ_v^n=E (n is even). When n is odd the reflecting n times is the same a reflecting only one time or, $\sigma_v^n=\sigma_v^1$ (n=odd).

The horizontal mirror plane of the BH_3 molecule deserves an additional comment. Carrying out the horizontal reflection does not change the position of any atom. It is important to understand why the operation does exist despite the fact it does not change the position of any atom. The criterion is not whether the position of an atom is changed, but whether the position of the points in the object changes. In the case of the BH_3 molecule the part of the molecule that is located above the mirror plane will be located below the mirror plane after the reflection operation has been carried out. Vice versa any part of the molecule that was formerly below the mirror plane will be located above the mirror plane after the reflection operation has been carried out. For example the lower half of the B atom with be above the mirror plane, and the half above the plane will be below the plane after the execution of the reflection operation.

Like non-conjugate proper rotations are distinguished by primes, also non-conjugate vertical mirror planes must be distinguished by primes. The smaller the number of bonds the vertical mirror plane contains, the larger the number of primes.

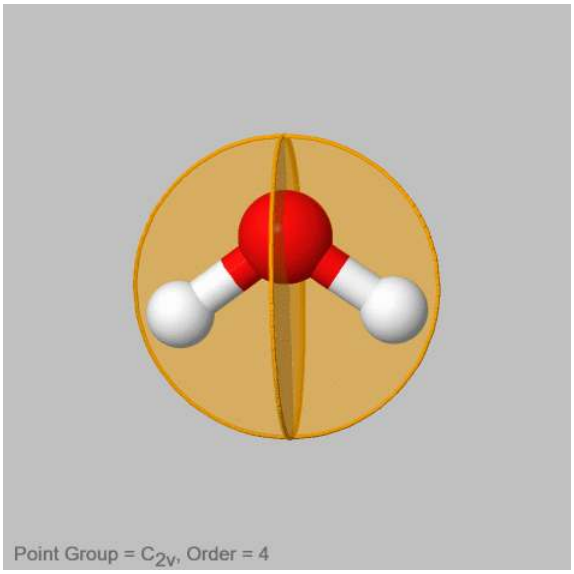


Figure 2.1.8 Non-conjugate vertical mirror planes of H_2O (Attribution: symotter.org/gallery)

For example in the water molecule (Fig. 2.1.8) there are two non-conjugate vertical mirror planes. One contains the two O-H bonds, the other stands perpendicular to the first mirror plane. It is easy to see that these two mirror planes will not move the points

in the atom in an equivalent way, and therefore they are not conjugate. The first mirror plane does not change the position of any atom, while the second one swaps the positions of the two hydrogen atoms. Therefore, the second mirror plane not containing any O-H bonds gets one prime the one that contains the O-H bonds doe not get a prime.

Dihedral Reflection Planes (σ_d)

A special case of a vertical mirror plane is a dihedral mirror plane, denoted σ_d. A dihedral mirror plane bisects the angle between two conjugate C_2 axes.

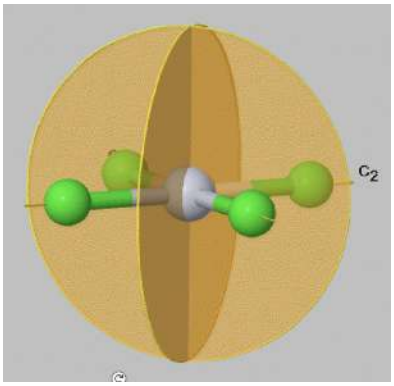


Figure 2.1.9 Dihedral mirror planes of $PtCl_4^{2-}$ (Attribution: symotter.org/gallery)

For example, in the $PtCl_4^{2-}$ anion (FIg. 2.1.9) there are two vertical mirror planes that bisect the angle between the two conjugate C_2 axes that pass through the Pt-Cl bonds. Therefore, these mirror planes are vertical mirror planes σ_d.

The Inversion Operation (*i*)

Let us look next at the inversion operation which is symbolized by a Schoenflies symbol *i*. The symmetry element associated with an inversion, is the inversion center, also called center of symmetry. It is a single point. When an inversion operation is performed, then each point of the object is moved through the inversion center to the other side. Each coordinate in the object (x,y,z) is inverted into the coordinates (-x,-y,-z).

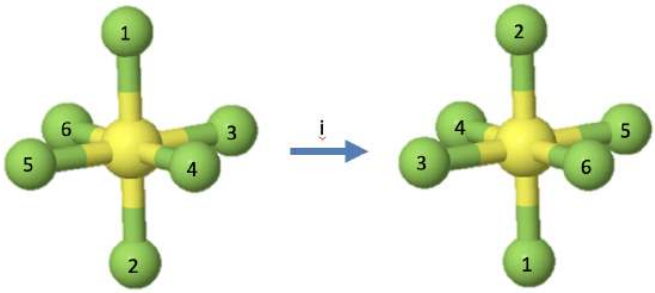


Figure 2.1.10 The inversion operation for SF_6 (Attribution: symotter.org/gallery)

For example, the octahedral molecule SF_6 has an inversion center in the center of the molecule (Fig. 2.1.10). When the inversion operation is carried out, then each fluorine atom is moved through the inversion center to the other side. This means that the fluorine atoms 1 and 2 swap up their positions, the fluorine atoms 3 and 5 swap up their positions, and so do the fluorine atoms 4 and 6. The sulfur atom does not change its position. There is only one inversion operation associated with each inversion center. Inverting two times, or more generally, an integer number of two times produces the identity. Inverting an odd number of times is the same as inverting one time.

The Rotation-Reflection Operation (S_n)

The rotation-reflection operation S_n is the most complex symmetry operation. It is carried out in two steps. First, a rotation around an improper axis is carried out. The angle is determined by the order n of the improper axis, and is 360°/n. This axis is called improper, because the object does not need to superimpose the original object after the rotation. Achieving superposition requires the second step which is the reflection at a mirror plane that stands perpendicular to the improper axis. Only after the second step

the operation is complete. The presence of the rotation-reflection does not require a proper rotational axis or a regular mirror plane σ to exist, however it also do not preclude their existence.

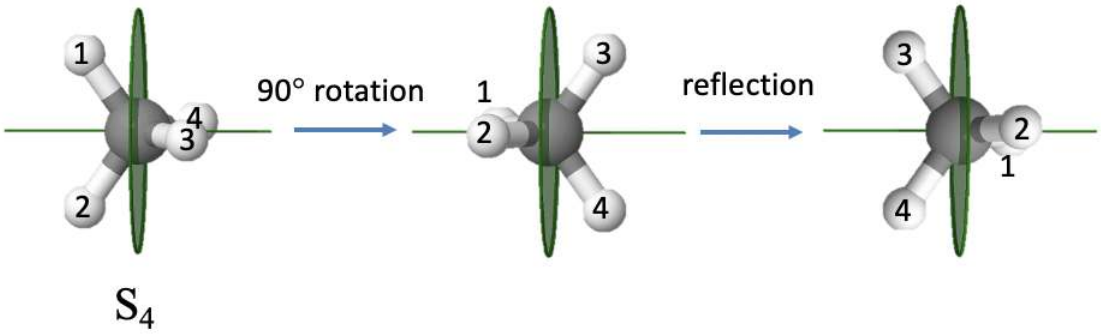


Figure 2.1.11 The improper S_4 rotation for CH_4 (Attribution: symotter.org/gallery)

An example of a molecule with an improper axis is the methane molecule (Fig. 2.1.11). It has an S_4 improper axis. The axis bisects the H-C-H tetrahedral bond angle. The order of the axis is four which requires that we rotate by 90° around this axis. You can see that after we carry out the rotation, the molecule does not superimpose the original molecule. Only after we reflect the rotated molecule at a mirror plane standing perpendicular to the improper axis the molecule superimposes the original molecule.

Properties of the Rotation-Reflection Operation (S_n)

The rotation-reflection has a number of interesting properties. One of the them is that an S_1 operation is the same as a reflection. This is because the order 1 implies a rotation around 360° which produces the identity, and all points within the object are in their original position. This is the same as though we had not rotated at all. This means actually we only did the second step, the reflection, and therefore the S_1 is identical to a "regular" reflection. The second property is that an S_2 operation is the same as an inversion. When you rotate around 180° and then reflect perpendicular to the improper axis of rotation, the positions of the points in the object change exactly the same way as they do when you invert through an inversion center.

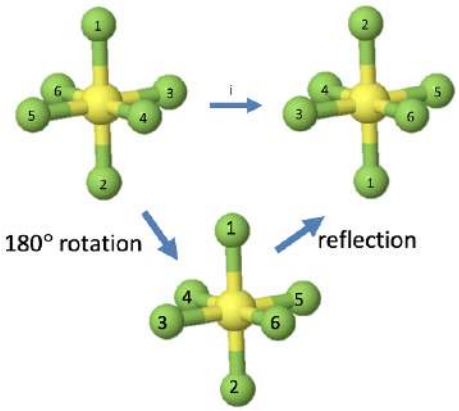


Figure 2.1.12 Rotation-Reflection operations for SF_6 (Attribution: symotter.org/gallery)

Look for example at the SF_6 molecule again (Fig. 2.1.12) which has an inversion center in the center of the atom. We previously saw that when we carry out the inversion, the atoms 1 and 2 swap their position, and so do the atoms 3 and 5, as well as the atoms 4 and 6. Let us carry out the rotation-reflection, and see if the atoms change the same way. Firstly we rotate 180° around an axis that goes through the atoms 1 and 2. This leaves the positions of the atoms 1 and 2 unchanged, but swaps up the positions of the atoms 3 and 5, as well as the atoms 4 and 6. Next we must do a reflection at a plane that stands perpendicular to the improper axis. It is the plane defined by the atoms 3, 4, 5, and 6. Reflection at this plane does not change the positions of the atoms 3, 4, 5, and 6, but it swaps up the positions of the atoms 1 and 2, which lie above and below the plane, respectively. We can see that the positions of the atoms are the same as after the inversion.

The fact that we can express a reflection by an S_1 rotation-reflection, and an inversion by a S_2 rotation-reflection means that the reflection and the inversion are not independent symmetry operations, and we would not need them. The symmetry of an object could be fully described by the identity, proper rotations, and rotation-reflections. However, by convention, we use reflections and

inversions instead of S_1 and S_2, simply because it is easier for the human mind to perform 1-step operations, rather than 2-step operations.

Improper rotations have different properties depending on whether the order of the axis is even or odd. For even orders, the presence of an S_n improper rotational axis implies that there must also be a proper rotational axis with an order n/2. For improper axes of even orders n the identity is produced after n rotation-reflections (Fig. 2.1.13).

$$S_n \text{ with n even} \rightarrow \text{molecule contains } C_{n/2}$$

$$S_n^n = E$$

Figure 2.1.13 Properties of improper rotations with even order *n*

For improper axes of odd order n, carrying out the rotation-reflection n times is the same as carrying out a reflection at a horizontal mirror plane. We need to do the rotation-reflection 2n times to reach the identity (Fig. 2.1.4).

$$S_n \text{ with n odd} \rightarrow \text{molecule contains } C_n \text{ and } \sigma_h$$

$$S_n^n = \sigma_h$$

$$S_n^{2n} = E$$

Figure 2.1.14 Properties of improper axes of odd order *n*

Rotation-Reflections of PF_5 (an example with odd order)

Let us show these properties using two examples. Let us first look at an example with an improper rotation of odd order. The PF_5 molecule has trigonal pyramidal shape with three F atoms in the equatorial plane, and two additional F atoms above and below the plane. The F atoms have been numbered from 1 to 5 as indicated by the subscripts that follow the element symbol (Fig. 2.1.15). The PF_5 has an improper rotational axis S_3 that stands perpendicular to the equatorial plane going through the P-F_1 and P-F_2 bonds. Let us carry out the S_3 symmetry operations step by step and see how the atoms move.

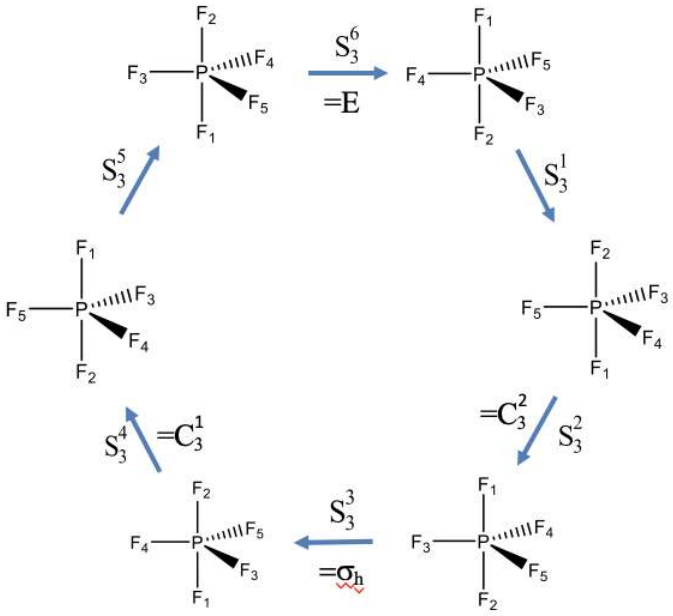


Figure 2.1.15 S_3 symmetry operations for PF_5

We would expect that after we carry out the operation six times the identity will be produced. After three rotation-reflections we would expect that the object has been moved the same way a horizontal mirror plane would do. After the first rotation-reflection the atoms F_1 and F_2 have swapped their positions, and the three F atoms in the equatorial plane have been rotated by 120 degrees counter-clockwise. The F_5 atom now occupies the position of the F_4, the F_4 has been rotated into the position of the F_3, and the F_3 has been moved into the position of the F_5. The second S_3 operation again swaps up the F_2 and F_1 atoms, and rotates the remaining F atoms by 120°. Now the F_5 atoms points toward us, the F_4 atom points away from us, and the F_3 atoms is in the paper plane. Carrying out the operation a third time again swaps the F_1 and F_2 and rotates F_3, F_4, and F_5 counter-clockwise by 120°. Now let us

compare the position of the atoms with the atom positions of the molecule we started with. We see that the position of the equatorial F atoms are same as in the beginning, but the position of the axial F_1 and F_2 atoms have been swapped up. This is equivalent to a reflection at a horizontal mirror plane located within the equatorial plane. This horizontal mirror plane would only swap up the axial F atoms, but would not move the equatorial ones. The S_3^4 operation again swaps up the position of the F_1 and the F_2 atoms, and rotates the equatorial F atoms by 120° counter-clockwise. Now, F_4 points toward us, F_3 points away, and F_5 is in the paper plane. After the fifth rotation-reflection F_1 and F_2 are again swapped so that F_1 is below and F_2 is above the equatorial plane. The atoms F_3, F_4 and F_5 are rotated so that F_3 is in the paper plane, F_5 points toward us, and F_4 points away from us. The sixth rotation-reflection again swaps up F_1 and F_2, and rotates the other F atoms around 120° counter-clockwise. We can now see that the produced molecule is the same as the one we started with, and the identity has been produced.

It is also noteworthy that the S_3^2 and the S_3^4 operation can be expressed by simpler operations, namely C_3^2 and C_3^1 proper rotation operations. We can understand this considering that an S_3^2 operation requires that we reflect two times, and reflecting two times is just like not reflecting at all. So effectively, we only have two rotations around 120° which is equivalent to C_3^2. Similarly, the S_3^4 operation requires to reflect four times, which is the same as not reflecting at all. Thus, effectively, we only rotate four times around 120°. This is the same as rotating only one time around this angle, which is equivalent to a C_3^1 operation.

Using similar considerations, we can also understand why the S_3^3 operation is equivalent to a σ_h. In this case, we rotate 3 x 120° = 360°, and rotating around 360° is the same as not rotating at all. In addition, we carry out a reflection three times. Reflecting an odd number of times is the same as reflecting only one time. Thus overall, we effectively carry out a single reflection only.

Overall, only the S_3^1 and the S_3^5 operations are unique, all others can be expressed by other, simpler operations.

Rotation-Reflections of CH_4 (an example with even order)

Let us illustrate the properties of an improper rotational axis with even order using the example methane (Fig. 2.1.16).

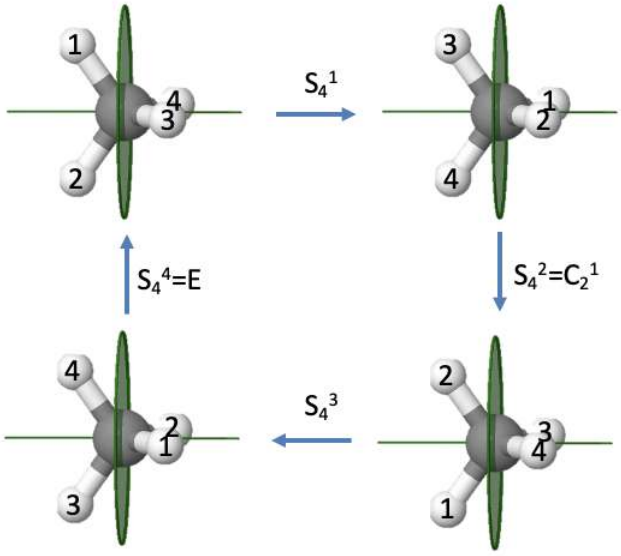


Figure 2.1.16 S_4 symmetry operations for CH_4 (Attribution: symotter.org/gallery)

We previously saw that the methane molecule has an S_4 improper axis. Executing the symmetry operation once moves the H atoms 1 and 2 to the right, whereby atom 1 points to the back and atom 2 points to the front. After the second rotation-reflection the atoms 1 and 2 are reflected back to the left side, but because we have rotated two times by 90° atom 2 points up, and atom 1 points down. Similarly, atoms 3 and 4 are reflected back to the right side, but atom four points toward us and atom 3 points to the back. After three rotation-reflections, the atoms 1 and 2 are again on the right side with atom 2 pointing to the back and atom 1 pointing to the front. Atoms 3 and 4 are on the left with atom 4 pointing up, and atom 3 pointing downward. After the operation is carried out four times, all atoms are back in their original position, meaning the identity has been produced. This is what we expected for an improper rotation of even order. We can see in addition that the S_4^2 operation is the same as an C_2 operation. Rotating two times about 90° is the same as rotating about 180°. Reflecting two times is the same as not reflecting at all. Therefore, effectively, we

only rotated by 180° which is the same as what a C_2^1 operation does. Because an S_4^2 can be expressed by a C_2^1, and an S_4^4 is the same as the identity, only the S_4^1 and the S_4^3 are unique symmetry operations.

The Symmetry of a Molecule

We have now discussed all types of symmetry elements and operations that can exist in an object. Next, let us think about how we can define the overall symmetry of an object. The **overall symmetry** of an object is defined as the sum of all the symmetry operations for this object. If two objects have exactly the same symmetry elements and operations then their symmetry is the same. Using the mathematical language of group theory, the mathematical theory for symmetry, we can say they belong to the same point group. The name point group comes from the fact, that it has at least one invariant point. The number of symmetry operations belonging to a point group is called the order of the point group. Let us see next what different point groups we know and how we can systematically classify them.

Dr. Kai Landskron (Lehigh University). If you like this textbook, please consider to make a donation to support the author's research at Lehigh University: Click Here to Donate.

This page titled 6.2: Symmetry and Symmetry Operations is shared under a CC BY-NC-SA 4.0 license and was authored, remixed, and/or curated by Kai Landskron.

- **2.1: Symmetry Elements and Operations** by Kai Landskron is licensed CC BY 4.0.

6.3: Molecule Shapes (Point Groups)

The Low Symmetry Point Groups

C_1 Point Group

Overall, we divide point groups into three major categories: High symmetry point groups, low symmetry point groups, dihedral point groups, and rotational point groups. Let us begin with the low symmetry point groups. As the name says, these point groups only have few symmetry elements and operations. The point group C_1 is the point group with the lowest symmetry. Molecules that belong to this point group only have the identity as symmetry element.

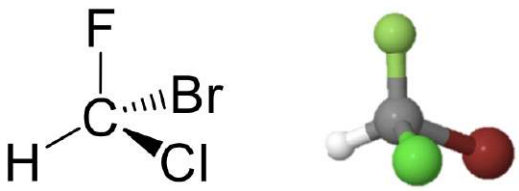


Figure 2.2.1 C_1 point group of bromochlorofluromethane (Attribution: symotter.org/gallery)

An example is the bromochlorofluromethane molecule (Fig. 2.2.1). It has no symmetry element, but the identity. The name C_1 comes from the symmetry element C_1. A C_1 operation is the same as the identity.

C_s Point Group

The point group C_s has a mirror plane in a addition to the identity. An example is the 1,2-bromochloroethene molecule (Fig. 2.2.2).

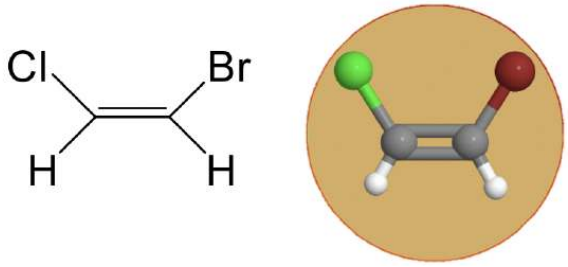


Figure 2.2.2 C_s point group of 1, 2-bromochloroethene (Attribution: symotter.org/gallery)

This is a planar molecule and the mirror plane is within the plane of the molecule. This mirror plane does not move any atoms when the reflection operation is carried out, nonetheless it exists because any point of the molecule above the mirror plane will be found below the mirror plane after the execution of the operation. Vice versa, any point below the mirror plane will be above the mirror plane. This mirror plane does not have a vertical or horizontal mirror plane designation because no proper rotational axes exist.

C_i Point Group

The point group C_i has the inversion as the only symmetry element besides the identity. The point group C_i is sometimes also called S_2 because an S_2 improper rotation-reflection is the same as an inversion. An example is the 1,2-dibromo 1,2-dichloro ethane (Fig. 2.2.3).

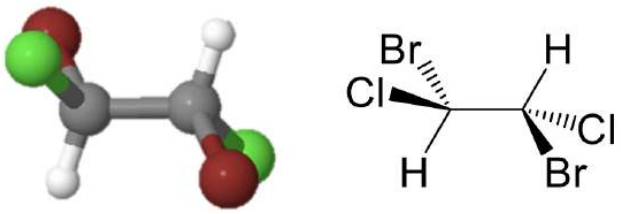


Figure 2.2.3 The C_i point group: 1,2-dibromo 1,2-dichloro ethane (Attribution: symotter.org/gallery)

This molecule looks quite symmetric, but it has inversion center in the middle of the carbon-carbon bond as the only symmetry element. Upon execution of the inversion operation, the two carbons swap up their positions, and so do the two bromine, the two chorine, and the two hydrogen atoms.

The High Symmetry Point Groups

The symmetry elements of the high symmetry point groups can be more easily understood when the properties of platonic solids are understood first. Platonic solids are polyhedra made of regular polygons. In a platonic solid all faces, edges, and vertices (corners) are symmetry-equivalent. We will see that this is a property that can be used to understand the symmetry elements in high symmetry point groups. There are only five possibilities to make platonic solids from regular polygons (Fig. 2.2.4).

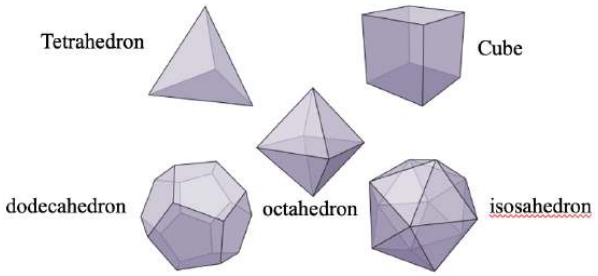


Figure 2.2.4 The platonic solids (Attribution: Drummyfish [CC0] https://commons.wikimedia.org/wiki/F...ransparent.svg)

The first possibility is to construct a tetrahedron from four regular triangles. The second platonic solid is the octahedron made of eight regular triangles. The third possibility is the icosahedron made of twenty triangles. In addition, six squares can be connected to form a cube, and twelve pentagons can be connected to form a dodecahedron. There are no possibilities to connect other regular polygons like hexagons to make a platonic solid.

The icosahedron is the most complex of all platonic solids. If you would like to see and study an icosahedron from the outside and inside, there is one for study on the playground of the Allentown Cedar Beach Park, in Allentown, Pennsylvania.



Figure 2.2.5 Icosahedron at Allentown Cedar Beach Park

The T_d Point Group

The tetrahedron, as well as tetrahedral molecules and anions such as CH_4 and BF_4- belong to the high symmetry point group T_d. Let us find the symmetry elements and symmetry operations that belong to the point group T_d. First, we should not forget the identity operation, E. Next, it is useful to look for the principal axes.

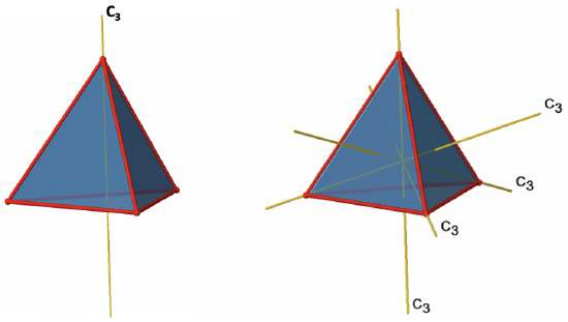


Figure 2.2.6 The C_3 axes in a tetrahedron (Attribution: symotter.org/gallery)

The tetrahedron has four principal C_3 axes (Fig. 2.2.6). It is a property of the high-symmetry point groups that they have more than one principal axis. The C_3 axes go through the vertices of the tetrahedron. Because each C_3 axis goes through one vertex, there are four vertices, and we know that in a platonic solid all vertices are symmetry-equivalent, we can understand that there are four C_3 axes. How many unique C_3 operations are associated with these axes? After three rotations around 120° we reach the identity. Therefore C_3^3=E, and we only need to consider the C_3^1 and the C_3^2 rotation about 120 and 240° respectively. Because there are four C_3 axes, there are four C_3^1 and four C_3^2 operations and eight C_3 operations overall. We can express this by writing the respective numbers as coefficients in front of the Schoenflies symbol for the operations (Fig. 2.2.7).

Symmetry operations: E, $8C_3$

Symmetry operations in detail: E, 4 C_3^1, 4 C_3^2 ($C_3^3 = E$)

Figure 2.2.7 Symmetry operations associated with the C_3 axes in the point group T_d

In addition to the C_3 axes there are C_2 axes (Fig. 2.2.8).

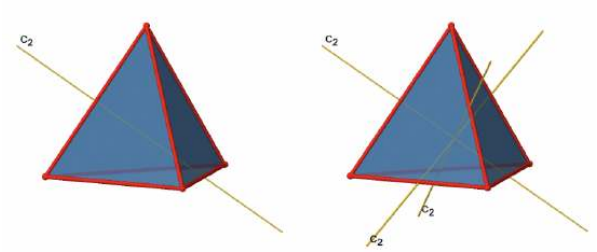


Figure 2.2.8 The C_2 axes in a tetrahedron belonging to the point group T_d (Attribution: symotter.org/gallery)

You can see that a C_2 axis goes through two opposite edges in the tetrahedron. Because a tetrahedron has six edges, and each C_2 axis go through two edges there are 6/2=3 C_2 axes. There is only one C_2 symmetry operation per C_2 axis because we produce the identity already after two rotations. Therefore there are three C_2^1 operations overall (Fig. 2.2.9).

Symmetry operations: $3C_2$

Symmetry operations in detail: 3 C_2^1

Figure 2.2.9 Symmetry operations associated with the C_2 axes in the point group T_d

In addition, the T_d point group has S_4 improper rotation reflections. Like the C_2 axes, they pass through the middle of two opposite edges. This also means that they are superimposing the C_2 axes. Because there are six edges, and two S_4 axes per edge there are 6/2=3 S_4 axes (Fig. 2.2.10).

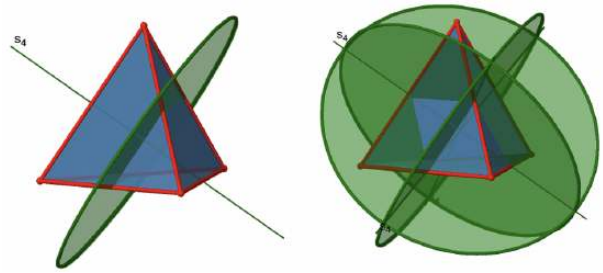


Figure 2.2.10 The S_4 axes in a tetrahedron (Attribution: symotter.org/gallery)

How many operations are associated with these S_4 axes? The order of the axes are even, and therefore we need four S_4 operations to produce the identity. The S_4^2 operation is the same as a C_2^1 operation because reflecting two times is equivalent to not reflecting at all, and rotating two times by 90° is the same as rotating about 180°. Therefore overall, only S_4^1 and S_4^3 operations are unique operations. S_4^2 and S_4^4 can be expressed by the simpler operations C_2^1 and E respectively. Because there are 3 S_4 axes, there are three S_4^1 and three S_4^3 operations. Overall there are six S_4 operations (Fig. 2.2.11).

Symmetry operations: $6S_4$

Symmetry operations in detail: 3 S_4^1, 3 S_4^3

($S_4^4 = E$, $S_4^2 = C_2^1$)

Figure 2.2.11 Symmetry operations associated with the S_4 axes in the point group T_d

There are also mirror planes (Fig. 2.2.11). The planes contain a single edge of the tetrahedron, thereby bisecting the tetrahedron. There a six edges in a tetrahedron, and therefore there are 6/1=6 mirror planes.

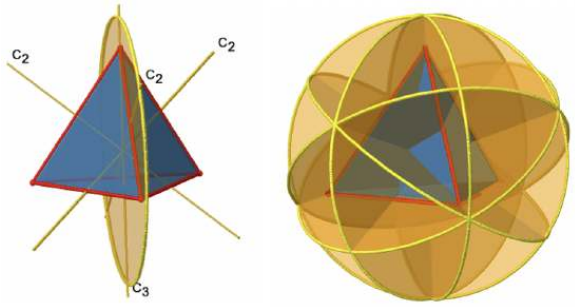


Figure 2.2.12 The mirror planes and C_2 axes in a tetrahedron belonging to the point group T_d (Attribution: symotter.org/gallery)

These planes are dihedral planes because each plane contains a C_3 principal axis and is bisects the angle between two C_2 axes. Overall, there are three C_2 axes and three C_2 operations. There is one reflection operation per mirror plane because reflecting two times produces the identity. Therefore, there are six σ_d reflection operations (Fig. 2.2.12, right and Fig. 2.2.13).

Symmetry operations: $6\sigma_d$

Symmetry operations in detail:6 σ_d

Figure 2.2.13 Reflection operations associated with the σ_d mirror planes in T_d

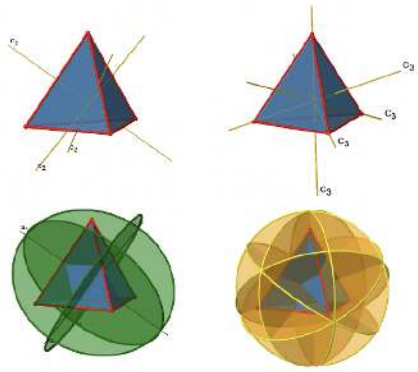


Figure 2.2.14 Summary of symmetry axes and planes in a tetrahedron with the point group T_d (Attribution: symotter.org/gallery)

In sum (Fig.2.2.14 and 2.2.15) we can denote the overall symmetry of the T_d point group the following way: E, $8C_3$, $3C_2$, $6S_4$, $6\sigma_d$. In detail the unique symmetry operations are E, $4C_3^1$, $4C_3^2$, $3C_2^1$, $3S_4^1$, $3S_4^3$, $6\sigma_d$.

Symmetry operations: E, $8C_3$, $3C_2$, $6S_4$, $6\sigma_d$

Symmetry operations in detail: E, 4 C_3^1, 4 C_3^2, 3 C_2^1, 3 S_4^1, 3 S_4^3, 6 σ_d

($C_3^3 = E$, $S_4^4 = E$, $S_4^2 = C_2^1$)

Figure 2.2.15 Summary of the symmetry operations for the point group T_d

The Rotational Subgroup T

The high symmetry point group T is the so-called rotational subgroup of the point group T_d. A rotational subgroup is a point group in which all symmetry operations but the identity and the proper rotations have been removed from a high-symmetry point group. For the point group T this leaves the $4C_3$, the four C_3^2 and the three C_2 operations (Fig. 2.2.17). The S_4 rotation-reflections and the mirror planes have been removed. The point group T is rare.

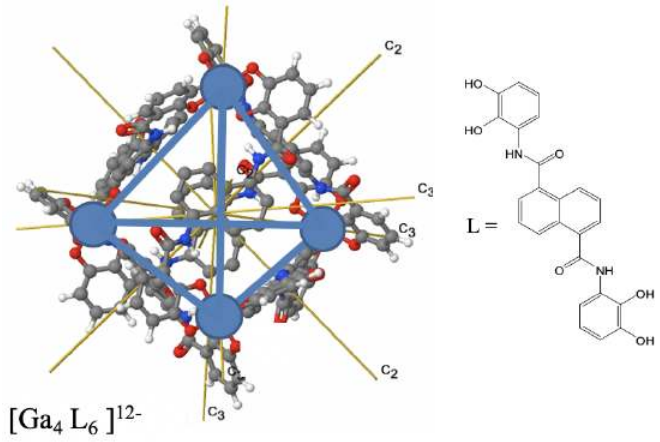


Figure 2.2.16 Symmetry elements in the Ga_4L_6 cage belonging to the point group T (Attribution: symotter.org/gallery)

An example is the depicted Ga_4L_6 cage (Fig. 2.2.16). The Ga atoms occupy the vertices of a tetrahedron, but the point group is not T_d but T because of the shape of the ligands that connect the four Ga atoms.

Symmetry operations: E, $4C_3$, $4C_3^2$, $3C_2$

Figure 2.2.17 Symmetry operations for the Ga_4L_6 cage

The Octahedral Point Group O_h

Another high symmetry point group is the point group O_h. Both the octahedron as well as the cube belong to this point group despite their very different shape (Fig. 2.2.18). Because they belong to the same point group they must have the same symmetry elements and operations. There are many octahedrally shaped molecules, such as the SF_6.

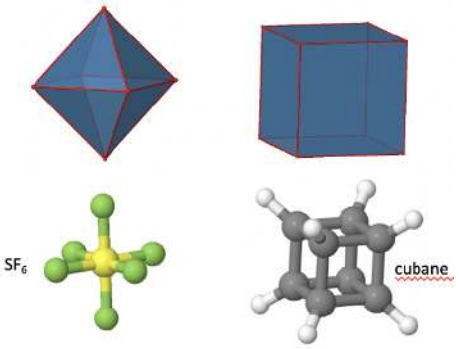


Figure 2.2.18 SF_6 and cubane with cubic and octahedral shape, respectively, belong to the point group O_h (Attribution: symotter.org/gallery)

Molecules with cubic shapes are far less common, because a cubic shape often leads to significant strain in the molecule. An example is cubane C_8H_8. Let us determine the symmetry elements and operations for the point group O_h using the example of the octahedron. If we used the cube, we would get exactly the same results.

There are three C_4 principal axes in the octahedron. They go through two opposite vertices of the octahedron (Fig. 2.2.19). There are three C_4 axes because an octahedron has six vertices which are all symmetry-equivalent because the octahedron is a platonic solid.

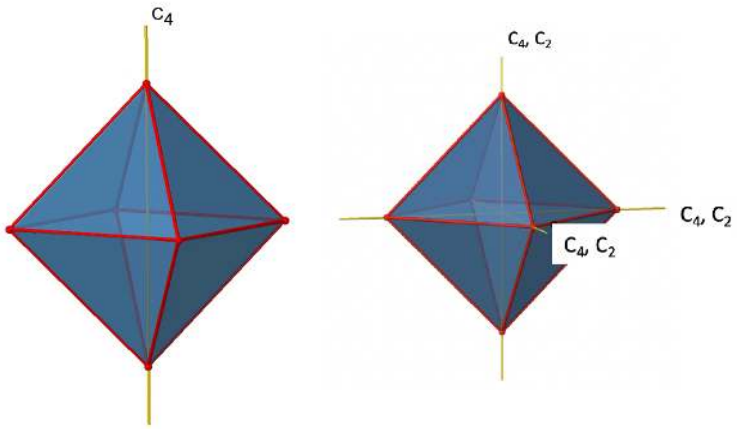


Figure 2.2.19 The C_4 and C_2 axes in the octahedral point group O_h (Attribution: symotter.org/gallery)

We can see that there are also C_2 axes where the C_4 axes run. This is because rotating two times around 90° is the same as rotating around 180°. What are the symmetry operations associated with these symmetry elements? Rotating four times around 90° using the C_4 axes produces the identity. So we have to consider the operations C_4^1, C_4^2, C_4^3 and C_4^4. How many of these are unique? C_4^4 is the same as the identity, so it is not unique, In addition a C_4^2 is identical to a C_2^1, and thus C_4^2 is also not unique, and can be expressed by the simpler operation C_2^1. That leaves the C_4^1 and the C_4^3 as the only unique symmetry operations. Because we have three C_4 axes, there are 2x3=6 C_4 operations, in detail there are $3C_4^1$ and three C_4^3 operations. In addition, there are the three C_2^1 operations belonging the the three C_2 axes (Fig. 2.2.20).

Symmetry elements: E, $3C_4$, 3 C_2

Symmetry operations: E, 6 C_4, 3 C_2
In detail: E, 3 C_4^1, 3 C_4^3
($C_4^2 = C_2^1$, C_4^4 = E)

Figure 2.2.20 C_4 and C_2 symmetry operations in the octahedral point group O_h

In addition, there are four C_3 axes (Fig. 2.2.21). They are going through the center of two opposite triangular faces of the octahedron.

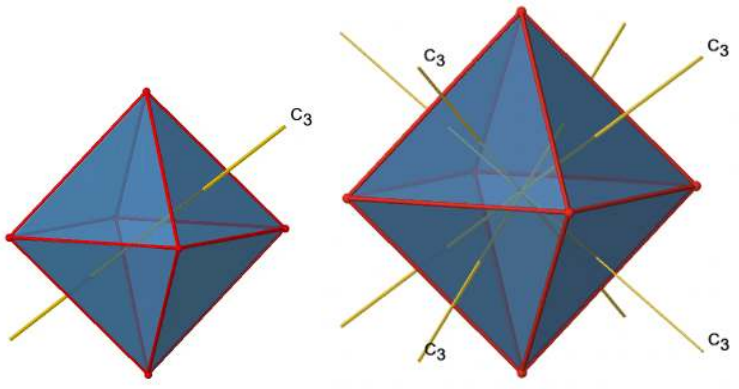


Figure 2.2.21 The C_3 axes in the octahedral point group O_h (Attribution: symotter.org/gallery)

You see above a single C_3 axis, and on the right hand side all four of these axes. How can we understand that there are four axes? An octahedron has overall eight triangular faces, and each C_3 axis goes through two opposite faces, so there are 8/2=4 C_3 axes. Each C_3 axis has the C_3^1 and the C_3^2 as unique symmetry operations. The C_3^3 is the same as the identity. So overall we have 4x2=8 operations, four of them are C_3^1, and four of them are C_3^2 (Fig. 2.2.22).

Symmetry elements: $4C_3$
Symmetry operations: $8\ C_3$
In detail: $4\ C_3^1$, $4\ C_3^2$
$(C_3^3 = E)$

Figure 2.2.22 Symmetry operations of C_3 in the octahedral point group O_h

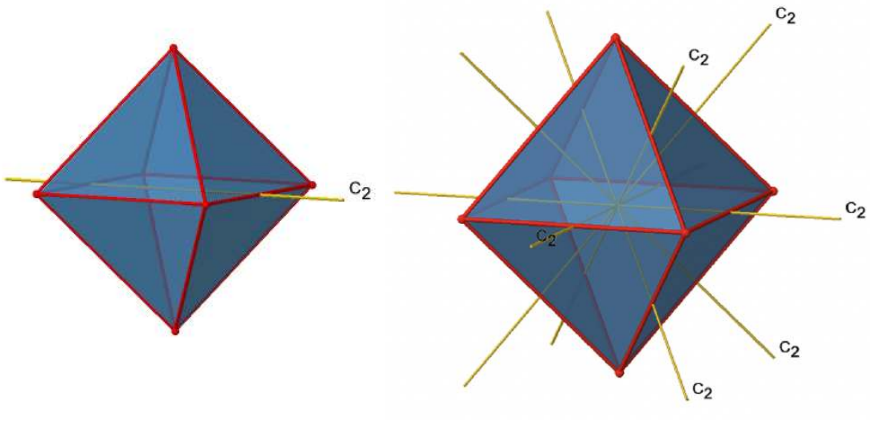


Figure 2.2.23 The C_2' axes in the octahedral point group O_h (Attribution: symotter.org/gallery)

In addition to the C_2 axes that superimpose the C_4 axes, there are C_2' axes which go though two opposite edges of the octahedron (Fig. 2.2.23). How many of them are there? An octahedron has twelve edges, and because each C_2' passes through two edges, there must be 12/2=6 C_2' axes. These axes have primes because they are not conjugate to the C_2 axes that superimpose the C_4 axes. For each C_2' axis there is only the C_2' ^{1} as the unique symmetry operation, and therefore there are overall 6 C_2'^{1} symmetry operations (Fig. 2.2.24).

Symmetry elements: $6\ C_2$'
Symmetry operations: $6\ C_2$'^{1}

Figure 2.2.24 Symmetry operations of C_2' in the octahedral point group O_h

Let us look at the mirror planes next (Fig. 2.2.25). There are horizontal mirror planes that stand perpendicular to the C_4 principle axes. You can see a single one of them below on the left.

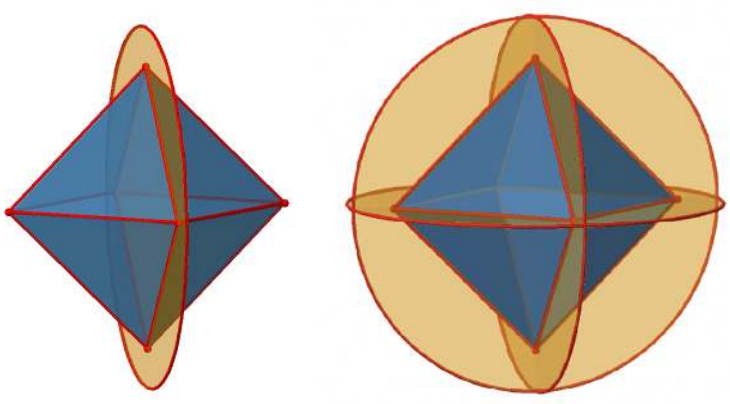


Figure 2.2.25 The horizontal mirror planes in the octahedral point group O_h (Attribution: symotter.org/gallery)

Note that this mirror plane also contains two axes, in addition to the one to which it stands perpendicular. Because it contains two principal C_4 axes, it has also properties of a vertical mirror plane. Nonetheless, we call it a horizontal mirror plane because it stands perpendicular to the third C_4. The horizontal properties trump the vertical ones, so to say. You can see that a single mirror plane contains four edges of the octahedron. Because there are twelve edges, there are 12/4=3 horizontal mirror planes. There is one

mirror plane per principal C_4 axis. There are three horizontal reflection operations because there is always only one reflection operation per mirror plane (Fig. 2.2.26).

Symmetry elements: $3\sigma_h$
Symmetry operations: $3\sigma_h$

Figure 2.2.26 Symmetry operations associated with horizontal mirror planes in the octahedral point group O_h

Next let us look for vertical mirror planes (Fig. 2.2.27). A vertical mirror plane is depicted below on the left.

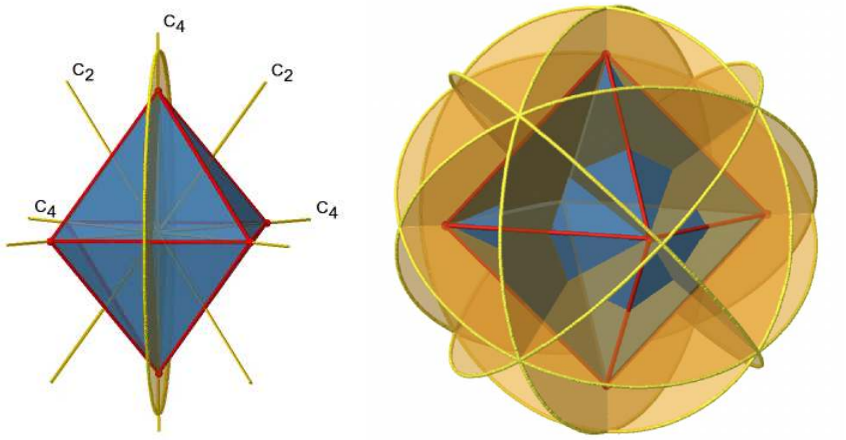


Figure 2.2.27 The vertical mirror planes in the octahedral point group O_h (Attribution: symotter.org/gallery)

You can see that - contrast to the horizontal mirror planes - it does not contain any edges. Rather, it cuts through two opposite edges. You can see that this plane contains a C_4 axis, but it does not stand perpendicular to the other two C_4 axes. Therefore it has only the properties of a vertical mirror plane. You can see however, that the mirror plane bisects the angle between two C_2' axes which also depicted. This makes the vertical mirror planes dihedral mirror planes, σ_d. How may of them do we have? As previously mentioned, each mirror plane cuts through two opposite edges. There are twelve edges in an octahedron, and thus there are 12/2=6 dihedral mirror planes. You can see all of them on the right side of Fig. 2.2.27. Each mirror plane is associated with one reflection operation, therefore there are six dihedral reflection operations (Fig. 2.2.28).

Symmetry elements: $6\ \sigma_d$
Symmetry operations: $6\ \sigma_d$

Figure 2.2.28 Symmetry operations associated with vertical mirror planes in the octahedral point group O_h

Next we can ask if the point group O_h has an inversion center? Yes, there is one in the center of the octahedron (Fig. 2.2.29)!

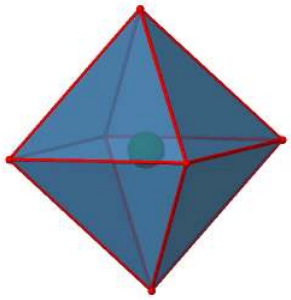


Figure 2.2.29 The inversion center of the octahedral point group O_h (Attribution: symotter.org/gallery)

Each point in the octahedreon can be moved through the inversion center to the other side, and the produced octahedron will superimpose the original one. There is always one inversion operation associated with an inversion center (Fig. 2.2.30).

Symmetry elements: i
Symmetry operations: i

Figure 2.2.30 Symmetry operations associated with the inversion center in the octahedral point group

Next, let us look for rotation-reflections. You can see an S_6 rotation-reflection operation below (Fig. 2.2.31, left).

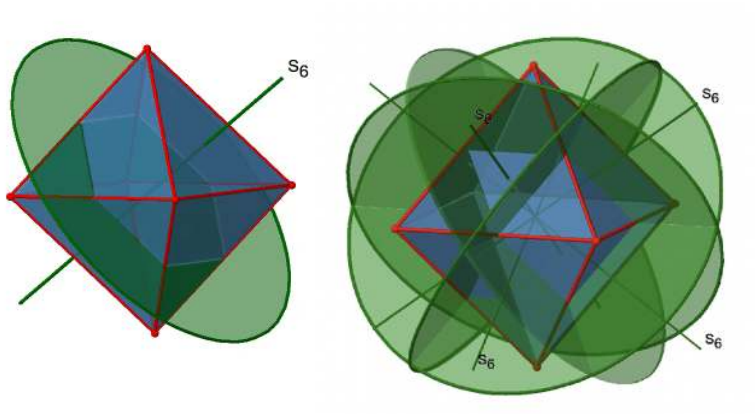


Figure 2.2.31 The S_6 rotation-reflection element of the octahedral point group O_h (Attribution: symotter.org/gallery)

The improper S_6 axis passes though the centers of two opposite triangular faces. One can see that rotation about 60° alone does not make the octahedron superimpose. The reflection at a plane perpendicular to the improper axis is required to achieve superposition. Overall, the rotation-reflection swaps up the position of the two opposite triangular faces. How many S_6 improper axes are there? Since each S_6 passes through two faces, and an octahedron has 8 faces there must be 8/2=4 S_4 axes. You can see all of them above (Fig. 2.2.31, right). Note that they are in the same position as the $4C_3$ axes we previously discussed. How many unique operations are associated with them? For an S_6 axis we need to consider operations from S_6^1 to S_6^6. S_6^6 is the same as the identity so it is not unique. The S_6^2 is the same as a C_3^1 because rotating two times round 60° is the same as rotating around 120°, and reflecting twice is the same as not reflecting at all. Similarly, an S_6^4 is the same as an C_3^2. Rotating four time by 60° is the same as rotating two times by 120° and reflecting four times is the same as not reflecting at all. Further, an S_6^3 is the same as an inversion. After three 60° rotations we have rotated by 180°. If we reflect after that, then this is the same as an S_2^1 operation which is the same as an inversion. Therefore, only the S_6^1 and the S_6^5 operations are unique, all other operations can be expressed by simpler operations (Fig. 2.2.32).

Symmetry elements: 4 S_6
Symmetry operations: 8 S_6
In detail $4S_6^1$, $4S_6^5$
($S_6^2=C_3^1$, $S_6^3=i$, $S_6^4=C_3^2$, $S_6^6=E$)

Figure 2.2.32 Symmetry operations of the rotation-reflection S_6 of the octahedral point group O_h

The octahedron also has S_4 improper axes, and you can see one of them below (Fig. 2.2.33, right).

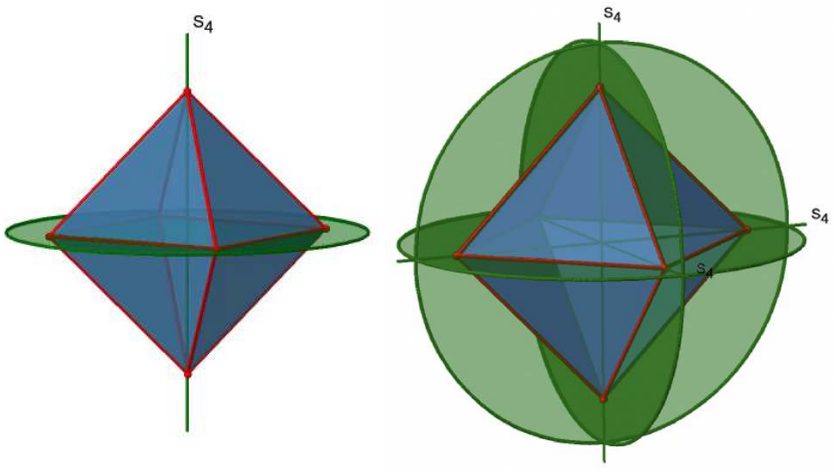


Figure 2.2.33 The S_4 improper axis of the octahedral point group O_h (Attribution: symotter.org/gallery)

It goes through two opposite corners of the octahedron. The S_4 improper axis seemingly does the same as the C_4 axis that goes through the same two opposite vertices, but actually does not. While rotating around 90° already makes the octahedron superimpose with its original form, executing the reflection operation after the rotation swaps up the position of the two vertices, and generally all points of the octahedron above and below the plane, respectively. Overall the S_4 moves the points within the object differently compared to the C_4 which makes it an additional, unique symmetry element. There are overall three S_4 improper axes because the octahedron has six vertices and one S_4 passes through two vertices (Fig. 2.2.34).

Symmetry elements: 3 S_4
Symmetry operations: 6 S_4
In detail: $3S_4^1$, $3S_4^3$
($S_4^2=C_2'$, $S_4^4=E$)

Figure 2.2.34 Symmetry operations associated with the S_4 improper axis of the octahedral point group O_h

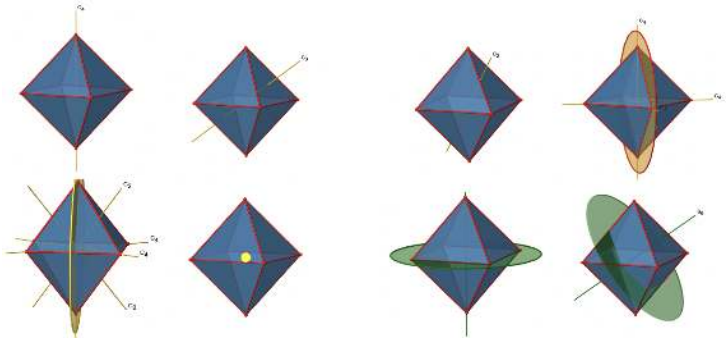


Figure 2.2.35 An overview over all symmetry elements in the octahedral point group O_h (Attribution: symotter.org/gallery)

Here is an overview over all the symmetry elements and operations (Fig. 2.2.35 and 2.2.36). Overall, there are 48 different unique operations that one can perform!

Symmetry elements: E, i, $4S_6$, $4C_3$, $3S_4$, $3C_4$, $6C_2$, $3\,C_2$, $3\sigma_h$, $6\sigma_d$
Symmetry operations: E, i, $8\,S_6$, $8\,C_3$, $6\,S_4$, $6\,C_4$, $6\,C_2$, $3\,C_2$, $3\,\sigma_h$, $6\,\sigma_d$
In detail: E, i, $4\,S_6^1$, $4\,S_6^5$, $4\,C_3^1$, $4\,C_3^2$, $3\,S_4^1$, $3\,S_4^3$, $3\,C_4^1$, $3\,C_4^3$, $6\,C_2$, $3\,C_2$, $3\,\sigma_h$, $6\,\sigma_d$
($S_6^2=C_3^1$, $S_6^3=i$, $S_6^4=C_3^2$, $S_6^6=E$; $C_3^3=E$. $S_4^2=C_2^1$, $S_4^4=E$, $C_4^2=C_2^1$, $C_4^4=E$)

Figure 2.2.36 Summary over all symmetry operations and elements of the octahedral point group O_h

Like the point group T_d , also the point group O_h has a rotational subgroup, named O. It has the identity and the same proper rotations as the point group O_h, but no other symmetry operations (Fig. 2.2.38). An example is the polyoxometalate cluster core shown below (Fig. 2.2.37). Polyoxometalates are cluster anions of the group 5 and 6 elements.

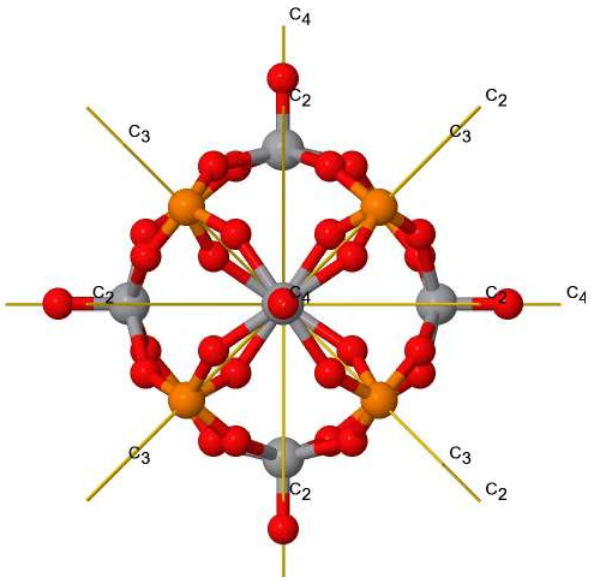


Figure 2.2.37 Proper rotations in a $V_6P_8O_{24}$ polyoxometalate cluster core. The C_3 rotation is animated. (Attribution: symotter.org/gallery)

The point group O is generally rare.

Symmetry elements: E, ~~i, $4S_6$~~, $4C_3$, ~~$3S_4$~~, $3C_4$, $6C_2$, $3\ C_2$, ~~$3\sigma_h$, $6\sigma_d$~~
Symmetry operations: E, ~~i, $8\ S_6$~~, $8\ C_3$, ~~$6\ S_4$~~, $6\ C_4$, $6\ C_2$, $3\ C_2$, ~~$3\ \sigma_h$, $6\ \sigma_d$~~
In detail: E, ~~i, $4\ S_6^1$, $4\ S_6^5$~~, $4\ C_3^1$, $4\ C_3^2$, ~~$3\ S_4^1$, $3\ S_4^3$~~, $3\ C_4^1$, $3\ C_4^3$, $6\ C_2$, $3\ C_2$, ~~$3\ \sigma_h$, $6\ \sigma_d$~~

Figure 2.2.38 Symmetry elements and operations in the point group O (relative to O_h)

Another high symmetry point group is the point group T_h. It can also be derived from the point group O_h. In this case the S_4, the C_4, the C_2', and the σ_d operations are removed from the octahedral symmetry. An example is the hexapyridyl iron (2+) cation (Fig. 2.2.39).

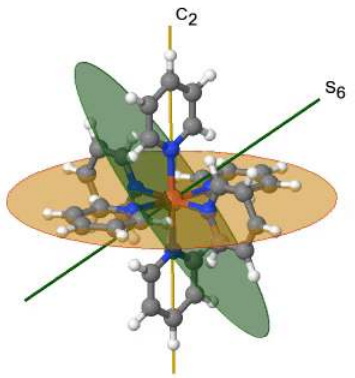


Figure 2.2.39 The hexapyridyl iron (2+) cation and its S_6 and C_2 symmetry elements. An S_6 operation is animated.

You can see that the N-atoms of the pyridyl-ligands surround the Fe atoms octahedrally, but the symmetry is reduced from O_h to T_h because of the planar shape of the pyridyl-ligands. In particular the C_4 symmetry is reduced to C_2. This reduction in symmetry leads to elimination of the S_4, the C_2', and the σ_d symmetry elements (Fig. 2.2.40).

T_h group (symmetry elements: E, i, $4S_6$, $4C_3$, $3C_2$, $3s_h$) can also be considered as a result of reducing **O_h** group symmetry (E, i, $4S_6$, $4C_3$, ~~$3S_4$, $3C_4$, $6C_2$~~, $3\ C_2$, $3\sigma_h$, ~~$6\sigma_d$~~)
by eliminating C_4, S_4 and some C_2 axes and s_d planes

Symmetry operations: i, $8\ S_6$, $8\ C_3$, $3\ C_2$, $3\ \sigma_h$,

Figure 2.2.40 Symmetry operations in $Fe(py)_6^{2+}$ in the point group T_h

The I_h Point Group

The two remaining platonic solids, the icosahedron and the dodecahedron, belong both to the icosahedral point group I_h. This is despite they are made of different polygons (Fig. 2.2.41).

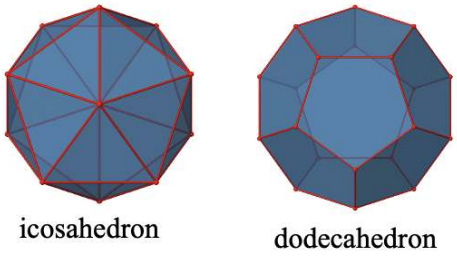


Figure 2.2.41 The icosahedron and dodecahedron of the I_h point group (Attribution: symotter.org/gallery)

Because they belong to the same point group, they have exactly the same symmetry operations. An example for a molecule with icosahedral shape is the molecular anion $B_{12}H_{12}^{2-}$. An example for a molecule with dodecahedral shape is the dodecahedrane $C_{20}H_{20}$.

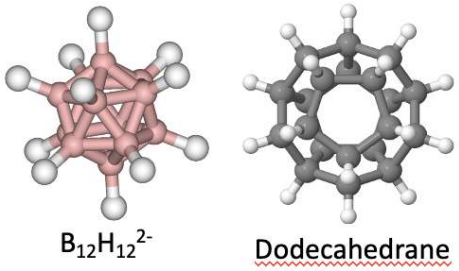


Figure 2.2.42 $B_{12}H_{12}^{2-}$ and the dodecahedrane (Attribution: wikiwand.com https://upload.wikimedia.org/Wikipedia/commons/thumb/9/97/Dodecaborane-3D-balls.png/640px-Dodecaborane-3D-balls.png)

Let us determine the symmetry elements and symmetry operations for the example of the icosahedron. We could also use the dodecahedron, and the results would be the same. The principal axes of the icosahedron are the C_5 axes. You can see one of them, going through the center of the pnetagon comprised of five triangular faces below (Fig. 2.2.43).

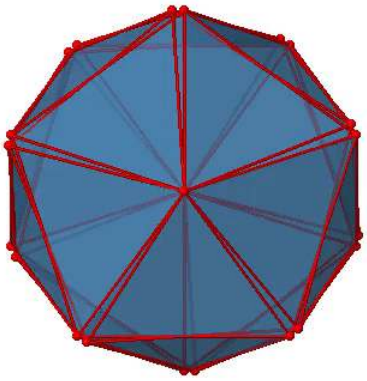


Figure 2.2.43 One of the C_5 axes of the icosahedron stands perpendicular to the paper plane going through the center of a pentagon of the icosahedron (Attribution: symotter.org/gallery)

You can understand that there is a C_5 when considering that there are five triangular faces making a pentagon. The C_5 axis sits in the center of the pentagon. We can see that when we rotate around this C_5 axis, then the produced icosahedron superimposes the original one. The C_5 axis goes through two opposite vertices of the icosahedron. Because an isosahedron has 12 vertices, there must be six C_5 axes overall. You can see all of them below (Fig. 2.2.44).

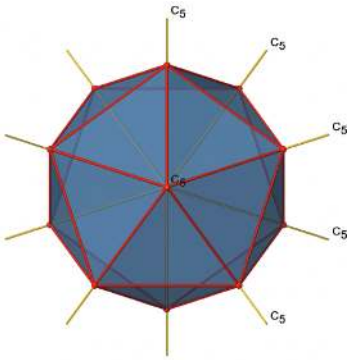


Figure 2.2.44 The C_5 axes of the icosahedron (Attribution: symotter.org/gallery)

There are four unique symmetry operations associated with a single C_5 axis, namely the C_5^1, the C_5^2, the C_5^3, and the C_5^4. The C_5^5 is the same as the identity. Because there are six C_5 axes, there are overall 6x4=24 C_5 symmetry operations (Fig. 2.2.45).

Symmetry elements: 6 C_5
Symmetry operations: 24 C_5
In detail: 6 C_5^1, 6 C_5^2, 6 C_5^3, 6 C_5^4 (C_5^5=E)

Figure 2.2.45 Symmetry operations associated with the C_5 axis of icosahedral point group

In addition, there are C_3 axes. One of them is shown below, and you can see that it passes through the centers of two opposite triangular faces (Fig. 2.2.46).



Figure 2.2.46 One of the C_3 axes of the icosahedral point group (Attribution: symotter.org/gallery)

As one rotates by 120° the atoms on the triangular faces change their position, and the resulting icosahedron superimposes the original one. As the name icosahedron says, there are twenty faces overall.

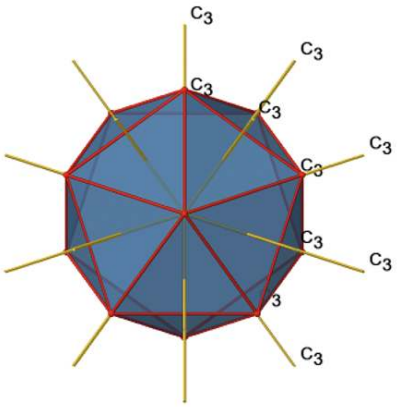


Figure 2.2.47 The C_3 axes of the icosahedral point group (Attribution: symotter.org/gallery)

Because one C_3 passes through two opposite axes, there are 20/2=10 C_3 axes overall (Fig. 2.2.47). Each C_3 axis is associated with two symmetry operations, namely C_3^1, and C_3^2. Thus, there are overall 10x2=20 C_3 symmetry operations.

Symmetry elements: 10 C_3
Symmetry operations: 20 C_3
In detail: 10 C_3^1, 10 C_3^2 (C_3^3=E)

Figure 2.2.48 Symmetry operations of the C_3 axes of the icosahedral point group

There are also C_2 axes (Fig. 2.2.49). They pass through the centers of two opposite edges of the icosahedron. Rotating around the C_2 axis shown makes the icosahedron superimpose.

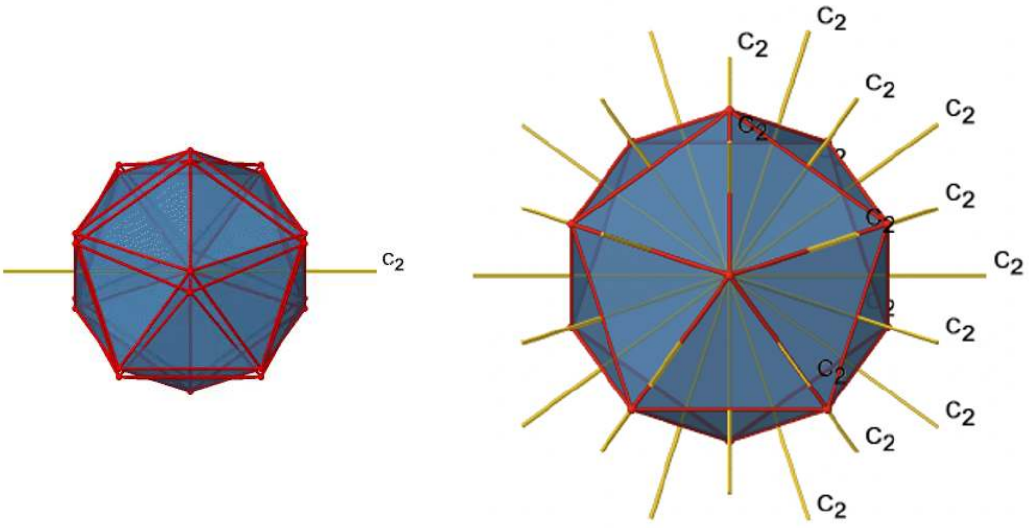


Figure 2.2.49 The C_2 axes of the icosahedral point group (Attribution: symotter.org/gallery)

An isosahedron has overall 30 edges. Because one C_2 axis passes through the centers of two opposite edges, we can understand that there are 30/2=15 C_2 axes. There is one unique C_2 operation per axis, and therefore there are 15 C_2 operations (Fig. 2.2.50).

Symmetry elements: 15 C_2
Symmetry operations: 15 C_2'
In detail: 15 C_2'^{1}

Figure 2.2.50 Symmetry operations associated with the C_2 axes of the icosahedral point group

We have now found all proper rotations. Let us look for mirror planes, next. You can see a mirror plane below (Fig. 2.2.51).

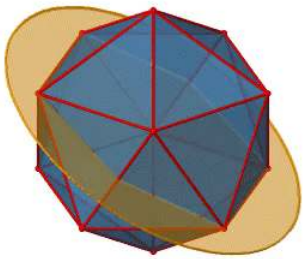


Figure 2.2.51 A mirror plane in the icosahedral point group (Attribution: symotter.org/gallery)

It contains two opposite edges. It also bisects two other edges. An icosahedron has overall 30 edges, therefore there are 30/2=15 mirror planes. You can see all of them below (Fig. 2.2.52 and Fig. 2.2.53)).

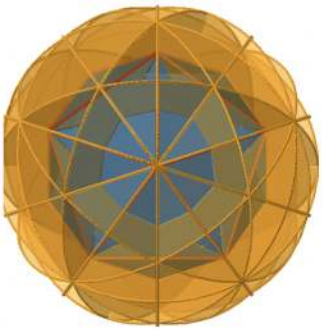


Figure 2.2.52 All the mirror planes in the icosahedral point group (Attribution: symotter.org/gallery)

Symmetry elements: 15 σ
Symmetry operations: 15 σ

Figure 2.2.53 Symmetry operations of the mirror planes in the icosahedral point group

The icosahedron also has an inversion center in the center of the icosahedron (Fig. 2.2.54 and Fig. 2.2.55)).



Figure 2.2.54 The inversion center in the icosahedron (Attribution: symotter.org/gallery)

As we carry out the associated, one symmetry operation, all points in the isosahedron move through the inversion center to the other side.

Symmetry elements: i
Symmetry operations: i

Figure 2.2.55 Symmetry operations of the inversion planes in the icosahedral point group

Let us now look for improper rotations. The improper rotational axes with the highest order are S_{10} axes. They are located in the same position as the C_5 axes, and go through two opposite corners (Fig. 2.2.56).

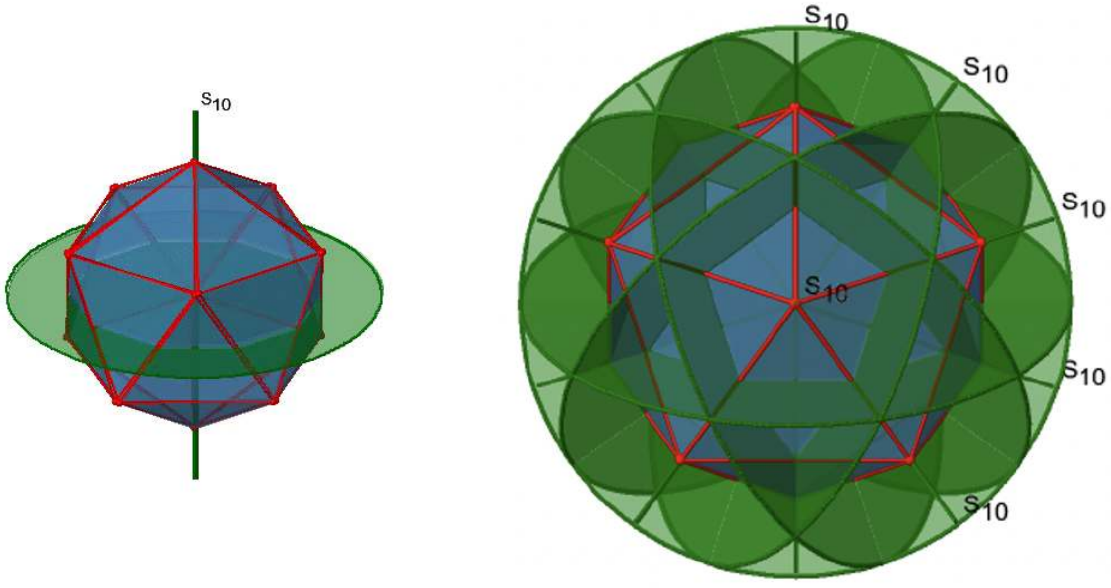


Figure 2.2.56 The S_{10} improper rotational axes in the icosahedral point group (Attribution: symotter.org/gallery)

The S_{10} exists because in an icosahedron there are pairs of co-planar pentagons that are oriented staggered relative to each other. The rotation around 36° brings one pentagon in eclipsed position relative to the other, but superposition is only achieved after the reflection at the mirror plane perpendicular to the rotational axis. Because one S_{10} passes through two opposite vertices, and there

are 12 vertices there are 6 S_{10} improper axes. For each axis there are four unique symmetry operations, the S_{10}^1, the S_{10}^3, the S_{10}^7, and the S_{10}^9. Therefore, there are overall 4x6=24 operations possible (Fig. 2.2.57).

Symmetry elements: 6 S_{10}
Symmetry operations: 24 S_{10}
In detail: 6 S_{10}^1, 6 S_{10}^3, 6 S_{10}^7, 6 S_{10}^9 ($S_{10}^2=C_5^1$, $S_{10}^4=C_5^2$, $S_{10}^5=i$, $S_{10}^6=C_5^3$, $S_{10}^8=C_5^4$)

Figure 2.2.57 Symmetry operations associated with the S_{10} improper rotational axes of the icosahedral point group

Are the lower order improper rotational axes? Yes, there are S_6 axes that pass through the centers of two opposite triangular faces (Fig. 2.2.58). This symmetry element exists because the two triangular faces are in staggered orientation to each other. Rotation alone brings one face in eclipsed orientation relative to the other, but reflection at a mirror plane perpendicular to the axis is required to achieve superposition. The S_6 axes are in the same location as the C_3 axes.

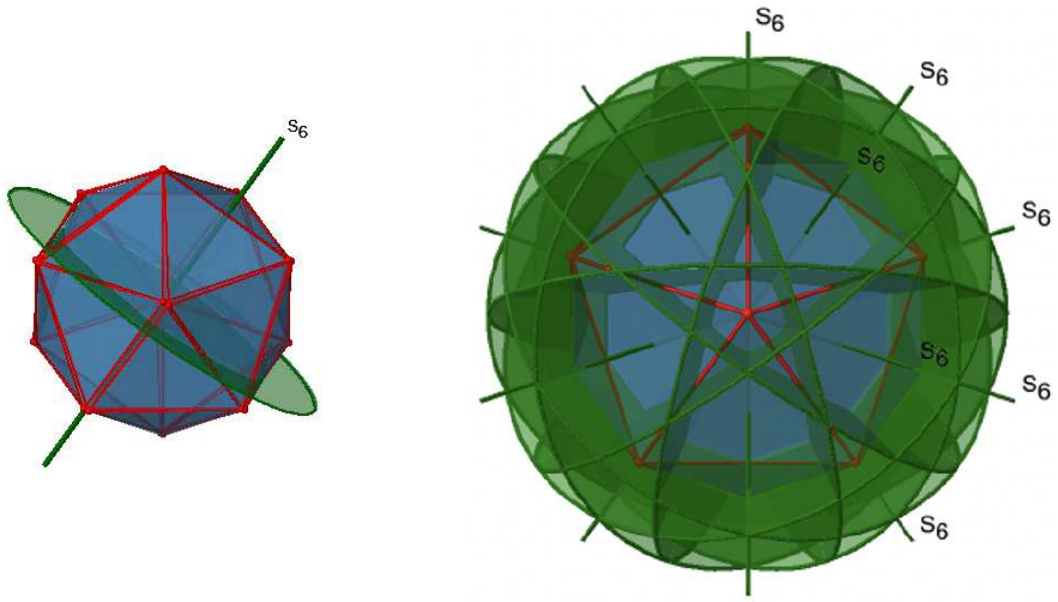


Figure 2.2.58 The S_6 rotation-reflections in the icosahedral point group (Attribution: symotter.org/gallery)

There are 10 S_6 axes because there are twenty faces and one axis passes through two opposite faces. Only the S_6^1 and the S_6^5 operations are unique S_6 operations, all others can be expressed by simpler operations. Therefore there are overall 10 S_6^1+10 S_6^5 = 20 S_6 operations (Fig. 2.2.59).

Symmetry elements: 10 S_6
Symmetry operations: 20 S_6
In detail: 10S_6^1, 10 S_6^5 ($S_6^2=C_3^1$, $S_6^3=i$, $S_6^4=C_3^2$)

Figure 2.2.59 Symmetry operations associated with the S_6 rotation-reflections in the icosahedral point group

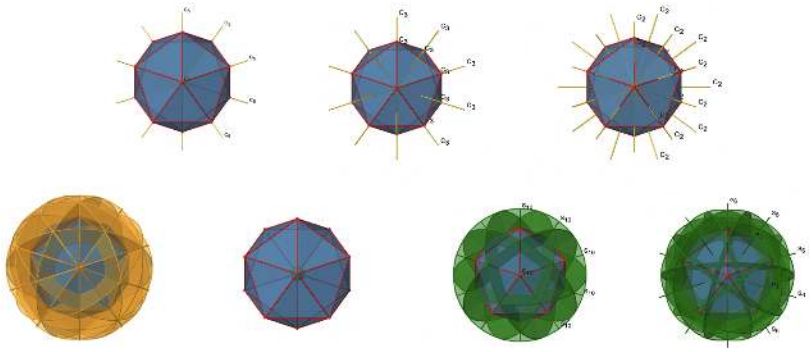


Figure 2.2.60 The symmetry elements of the icosahedral point group (Attribution: symotter.org/gallery)

We have now found all symmetry operations for the I_h symmetry. There are overall 120 operations making the point group I_h the point group with the highest symmetry (Fig. 2.2.60 and Fig. 2.2.61).

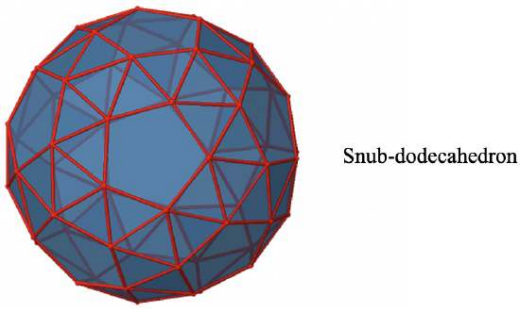
Symmetry elements: E, 6 C_5, 10 C_3, 15 C_2, 15 σ, i, 6 S_{10} , 10 S_6

Symmetry operations: E, 24 C_5, 20 C_3 , 30 C_2', 15 σ, i, 24 S_{10}, 20 S_6

In detail: E, 6 C_5^1, 6 C_5^2, 6 C_5^3, 6 C_5^4, 10 C_3^1, 10 C_3^2, 30 C_2'^{1}, 15 σ, i, 6 S_{10}^1, 6 S_{10}^3, 6 S_{10}^7, 6 S_{10}^9, 10S_6^1, 10 S_6^5

Figure 2.2.61 Summary of the symmetry operations of the icosahedral point group

Also the point group I_h has a rotational subgroup.



Snub-dodecahedron

Figure 2.2.62 The snub-dodecahedron belonging to the point group I (Attribution: symotter.org/gallery)

It is called I. An example of an object with this symmetry is the snub-dodecahedron (Fig. 2.2.62). It has the identity, and all the proper rotation operations of the point group O_h, but the inversion, the rotation-reflections, and the mirror planes are eliminated (Fig. 2.2.63).

Symmetry elements: E, 6 C_5, 10 C_3, 15 C_2, ~~15 σ, i, 6 S_{10} , 10 S_6~~

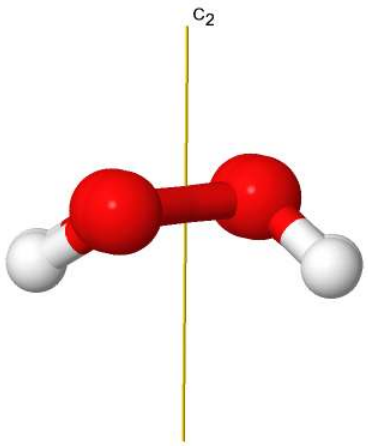
Symmetry operations: E, 24 C_5, 20 C_3 , 30 C_2', ~~15 σ, i, 24 S_{10}, 20 S_6~~

In detail: E, 6 C_5^1, 6 C_5^2, 6 C_5^3, 6 C_5^4, 10 C_3^1, 10 C_3^2, 30 C_2'^{1}, ~~15 σ, i, 6 S_{10}^1, 6 S_{10}^3, 6 S_{10}^7, 6 S_{10}^9, 10S_6^1, 10 S_6^5~~

Figure 2.2.63 Symmetry operations of the icosahedral rotational sub group I (relative to I_h)

Cyclic Point Groups

After having discussed high and low symmetry point groups, let us next look at cyclic point groups. They have the property that they have only a single proper n-fold rotational axis, but no other proper axes. In the most simple case they do not have any additional symmetry element such as mirror planes or rotation-reflections. These point groups are denoted C_n whereby n is the order of the proper axis. An example is the hydrogen peroxide molecule H_2O_2 (Fig. 2.2.64).



Point Group = C_2, Order = 2

Figure 2.2.64 The C_2 rotational axis of hydrogen peroxide

It has a so-called roof-structure due to its non-planarity. One hydrogen atom points toward us, and the other points away from us. This structure is due to the two electron-lone pairs at each sp^3-hybridized oxygen atom. These electron-lone pairs consume somewhat more space than the H atoms, and there is electrostatic repulsion between the electron lone pairs. Therefore, the electron lone pairs at the different oxygen atoms try to achieve the greatest distance from each other. This forces the H-atoms out of the plane, leading to the roof-structure of the hydrogen peroxide. Because the H_2O_2 molecule is not planar, it only has a single C_2 axis, but no other symmetry element besides the identity. The C_2 axis passes through the center of the O-O bond. Execution of the C_2 operation swaps up both the O and the H atoms.

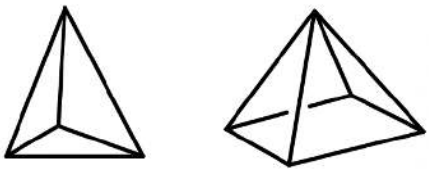
$$C_2 - H_2O_2 \text{ (elements: E, } C_2)$$

Figure 2.2.65 Symmetry elements in the hydrogen peroxide molecule

Definition: Cyclic Groups C_n

Cyclic groups have one rotational axiPyramidal Groups

Another class of groups are the pyramidal groups, denoted C_{nv}. They have n vertical mirror planes containing the principal axis C_n in addition to the principal axis C_n. Generally molecules belonging to pyramidal groups are derived from an n-gonal pyramid. An n-gonal pyramid has an n-gonal polygon as the basis which is capped (Fig. 2.2.66).



N-gonal pyramid

Figure 2.2.66 n-gonal pyramids (n=3,4)

For example a trigonal pyramid has a triangular basis which is capped, a tetragonal pyramid has a square which is capped, and so on. The proper axis associated with a specific pyramid has the order n and goes through the tip of the pyramid and the center of the polygon. An example of a molecule with a trigonal pyramidal shape is the NH_3 (Fig. 2.2.67).

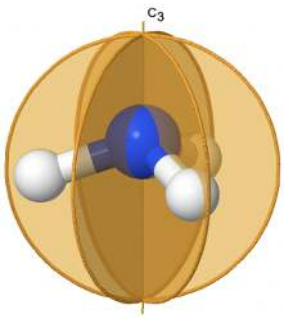


Figure 2.2.67 C_3 axis and vertical mirror planes in NH_3

The three H atoms form the triangular basis of the pyramid, which is capped by the N atom. The NH_3 molecule belongs to the point group C_{3v}. The C_3 axis goes though the N atom which is the tip of the pyramid, and the center of the triangle defined by the H atoms. There are three vertical mirror planes that contain the C_3 axis. Each of them goes through an N-H bond (Fig. 2.2.68).

$$C_{3v} - NH_3 \text{ (elements: E, } C_3, 3\sigma_v)$$

Figure 2.2.68 Symmetry elements in NH_3

Definition: Pyramidal Groups C_{nv}

Pyramidal groups have n vertical plane(s) in addition to the principal axis C_n.

The Linear Group $C_{\infty v}$

A special n-gonal polygon is the cone. A cone can be conceived as an n-gonal pyramid with an infinite number *n* of corners at the base (Fig. 2.2.69).

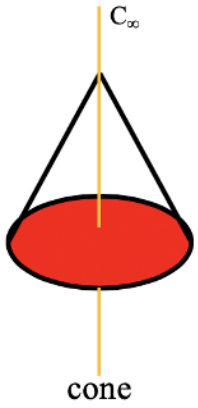


Figure 2.2.69 Cone having a proper rotational axis with infinite order.

In this case the order of the rotational axis that passes through the tip of the cone and the center of the circular basis is infinite. This also means that there is an infinite number of vertical mirror planes that contain the C_∞ axis (Fig. 2.2.71). The point group describing the symmetry of a cone is called the linear point group $C_{\infty v}$. Polar, linear molecules such as CO, HF, N_2O, and HCN belong to this point group. You can see the HCN molecule with its C_∞ axis and its infinite number of vertical mirror planes below (Fig. 2.2.70).

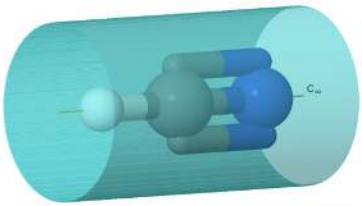


Figure 2.2.70 C_∞ axis of the HCN molecule

The infinite number of mirror planes, shown in blue are forming a cylinder that surround the molecule.

(**elements**: E, C_∞, $\infty\sigma_v$)

Figure 2.2.71 Symmetry elements of polar linear molecules

Definition: Linear group $C_{\infty v}$

The linear group $C_{\infty v}$ has an infinite number of vertical mirror planes containing a C_∞ axis

Reflection Groups

If we add a horizontal mirror plane instead of n vertical mirror planes to a proper rotational axis C_n we arrive at a the reflection point group type C_{nh}. The presence of the horizontal mirror planes also generates an improper axis of the order n. This is because when one can rotate and reflect perpendicular to the rotational axes independently, then it must also be possible to do it in combination. An example of a molecule belong to a reflection group is the trans-difluorodiazene N_2F_2 (Fig. 2.2.72).

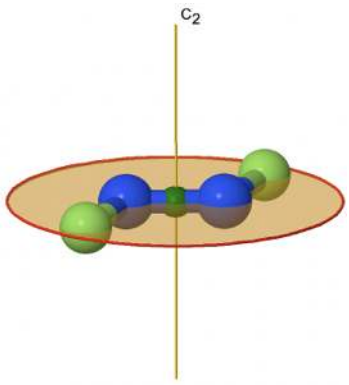


Figure 2.2.72 C_2 axis and horizontal mirror plane in trans-N_2F_2

It is a planar molecule with a C_2 axis going through the middle of the N-N double bond, and standing perpendicular to the plane of the molecule. The horizontal mirror plane stands perpendicular to the C_2 axis, and is within the plane of the molecule. There is an additional inversion center because an S_2 must exist which is the same as an inversion center. The inversion center is in the middle of the N-N bonds. Overall, the molecule has the symmetry C_{2h}.

C_{2h} – *trans*-F-N=N-F (**elements**: E, C_2, *i*, σ_h)

Figure 2.2.73 Symmetry elements in N_2F_2

Definition: Reflection Group C_{nh}

A reflection group has a horizontal plane perpendicular to the principal axis C_n

Dihedral Groups

Dihedral groups are point groups that have n additional C_2 axes that stand perpendicular to the principal axis of the order n. If there are no other symmetry elements, then the point group is of the type D_n.

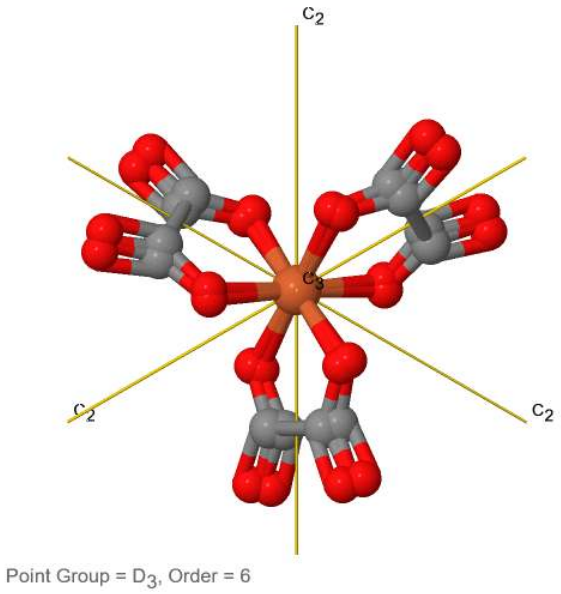


Figure 2.2.74 The tris-oxolato ferrate (3-) ion and its symmetry elements

For example in the point group D_3 there is a C_3 principal axis, and three additional C_2 axes, but no other symmetry element (Fig. 2.2.75). The tris-oxolato ferrate (3-) ion belongs to this point group (Fig. 2.2.75). You can see that the C_3 axis stands perpendicular to the paper plane, and there are three C_2 axes in the paper plane.

D_3 – (**elements**: E, C_3, $3C_2$)

Figure 2.2.75 Symmetry elements in the dihedral group D_3

Definition: Dihedral Groups D_n

In a point group of the type D_n there is a principal axis of order n, n C_2 axes, but no other symmetry elements.

If a horizontal mirror plane is added to the C_n axis and the n C_2 axes we arrive at the prismatic point groups D_{nh} (Fig. 2.2.76). The addition of the horizontal mirror plane generates further symmetry elements namely an S_n and n vertical mirror planes.

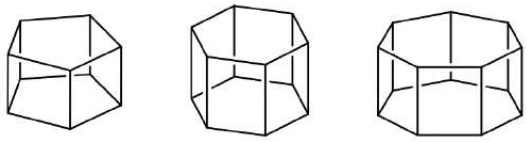


Figure 2.2.76 N-gonal prisms belong to the point group type D_{nh}

Generally, molecules belonging to this point group derive from n-gonal prisms. The order of the principal axis is the same as the number of corners of the polygons the prism are made of.

Definition: Prismatic Groups D_{nh}

In prismatic point groups there is a horizontal mirror plane perpendicular to the principal axis C_n. There are also n C_2 axes.

An example for a molecule belonging to a prismatic point group is PF_5 (Fig. 2.2.77).

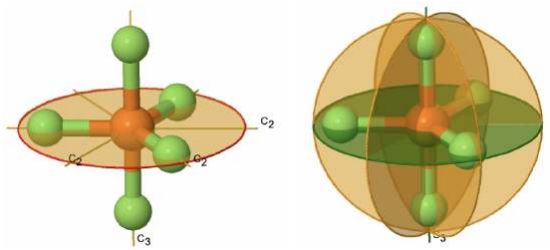


Figure 2.2.77 The PF_5 molecule belonging to the point group D_{3h} and its symmetry elements.

It has a trigonal bipyramidal shape. The C_3 axis goes through the axial F atoms of the molecule, and the three C_2 axes go through the three equatorial F atom. The horizontal mirror plane stands perpendicular to the principal C_3 axis and is located within the equatorial plane of the molecule. In addition, there are the vertical mirror planes that contain the C_3 axis, and go through the three equatorial P-F bonds. There is also an S_3 axis which superimposes the C_3 axis. In sum:

D_{3h} – PF_5 (**elements**: E, C_3, $3C_2$, σ_h, S_3, $3\sigma_v$)

Figure 2.2.78 Symmetry elements of PF_5

A special case of a D_{nh} group is the linear group $D_{\infty h}$. An object that has this symmetry is a cylinder. A cylinder can be conceived as a prism with an infinite number of vertices. Thus, the principal axis that passes through a cylinder has infinite order. Because of the infinite order of the principal axis, there is an infinite number of C_2 axes that stand perpendicular to the principal axis. You can see one such C_2 going though the cylinder (Fig. 2.2.79).

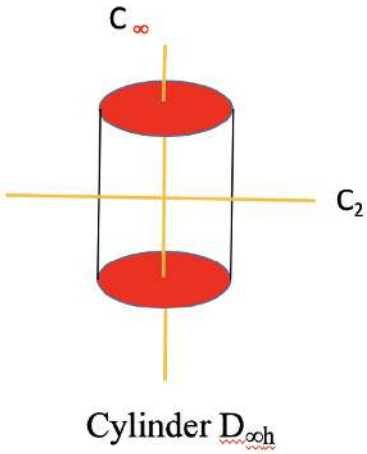


Figure 2.2.79 Cylinder as an example of linear group $D_{\infty h}$

There is now also an improper axis of infinite order, as well as an infinite number of vertical mirror planes. Non-polar linear molecules like H_2, CO_2, and acetylene C_2H_2 belong to the point group $D_{\infty h}$. You can see the C_∞ axis passing through a CO_2 molecule below (Fig. 2.2.80).

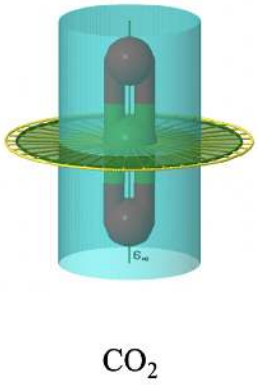


Figure 2.2.80 C_∞ in a CO_2 molecule

You can see the infinite number of vertical mirror planes as a blue cylinder. The infinite number of C_2 axes is shown a yellow lines going around the molecule. In sum:

$$E, C_\infty \infty C_2, \sigma_h, S_\infty, \infty \sigma_v, i$$

Figure 2.2.81 Symmetry elements of linear group $D_{\infty h}$

Definition: Linear Group D_{ooh}

In the point group $D_{\infty h}$ there is an infinite number of n C_2 axes in addition to the principal axis of infinite order, an infinite number of vertical mirror planes, and one horizontal mirror plane.

If we add n vertical mirror planes to the principal axis and the n C_2 axes, we arrive at the point group D_{nd}. The vertical mirror planes are dihedral mirror planes because they bisect the angle between the C_2 axes. An example is the ethane molecule in staggered conformation which has the symmetry D_{3d} (Fig. 2.2.82).

Figure **6.3.1**: Paste Caption Here

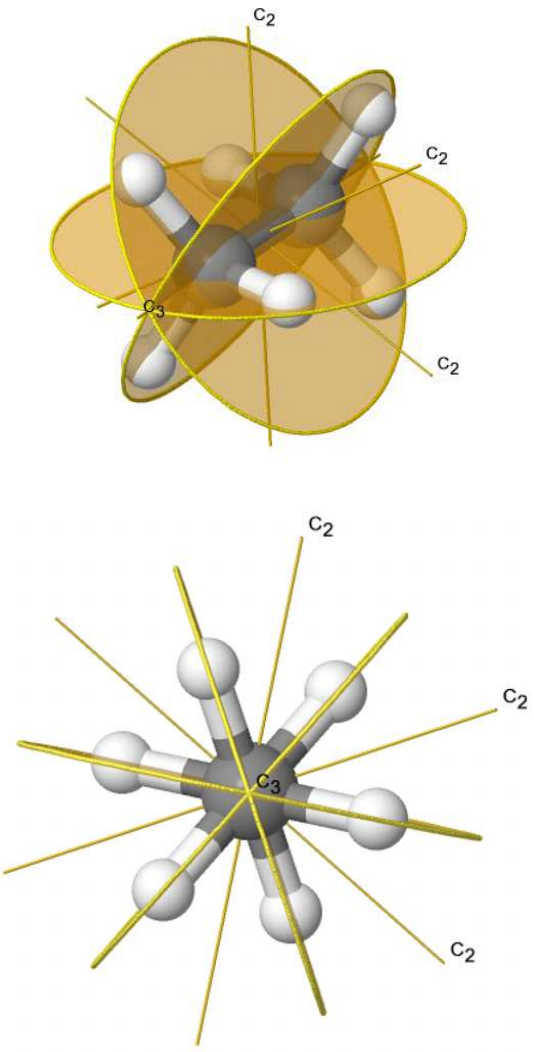


Figure 2.2.82 The ethane molecule in the staggered conformation belongs to the point group type D_{nd}

The C_3 axis goes along the C-C bond, and the $3C_2$ axes pass through the middle of the carbon-carbon bond, and bisect the angle between two hydrogens and one carbon atom. The three dihedral mirror planes pass through the C-H bonds. In addition, the ethane molecule has an S_6 axis, and an inversion center. In sum:

D_{3d} – ethane/staggered (elements: E, C_3, S_6, $3C_2$, 3 σ_d, i)

Figure 2.2.83 Symmetry elements in ethane

Definition: D_{nd}

In this point group type there are n dihedral mirror planes that contain the C_n and bisect the angle between adjacent C_2 axes

Improper Rotational Point Groups

The last class of point groups to be discussed are the improper rotation point groups. The only have one proper rotational axis, and an improper rotational axis that has twice the order of the proper rotational axis (Fig. 2.2.85). There may be an inversion center

present depending on the order of the proper and improper axes. An example the tetramethylcycloocta-tetraene molecule (Fig. 2.2.84).

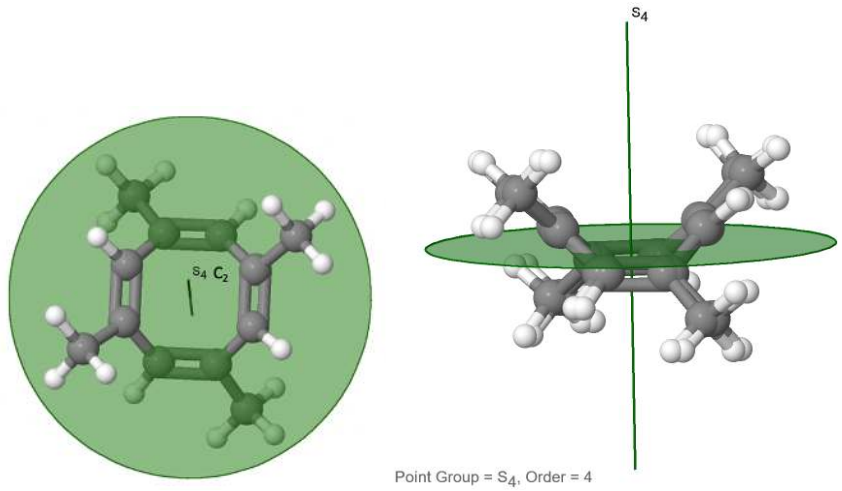


Figure 2.2.84 The S_4 and an C_2 axes of tetramethyl cycloocta-tetraene

It has an S_4 and an C_2 axis as the only symmetry elements besides the identity. Rotating by 90° alone does not superimpose the molecule because two C-C double bonds lie above the plane and two below the plane. In addition, two opposite methyl groups lie above and below the plane respectively. Therefore it needs the additional reflection to achieve superposition. There is also a C_2 axis which is in the same locations as the S_4 axis.

Symmetry elements: E, S_{2n}, C_n

May have inversion center *i*

Figure 2.2.85 Symmetry elements of improper rotational point groups

Guide for the Determination of Point Groups

With the knowledge you have, you can unambiguously identify the point group of a molecule. The key to success is that you are able to see the symmetry elements in the molecule. This takes practice. With enough practice you can identify the point group of a molecule immediately. Until, you can use guides, that you can follow to identify a point group. Such a guide asks systematic questions about the presence or absence of a symmetry element. Depending on whether you answer the question with yes or no you can follow the guide in a particular direction. Eventually, after having answered enough questions the guide will lead you to the respective point group. You can see such a chart below (Fig. 2.2.86).

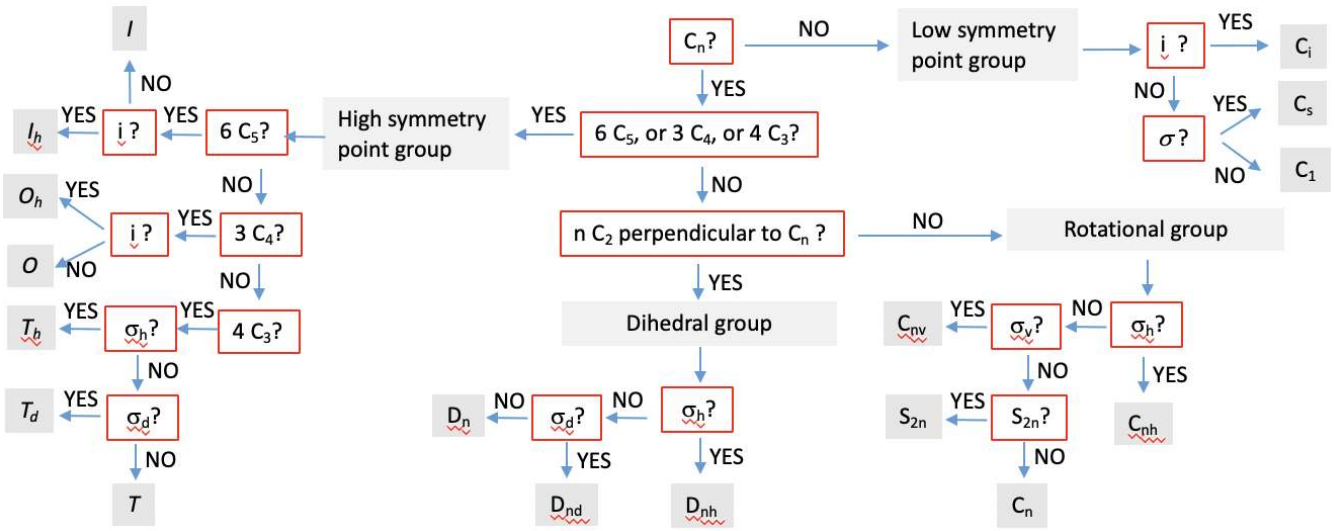


Figure 2.2.86 Guide for determination of point groups

You can first ask if there is at least one C_n present. If not, then the molecule must be in a low symmetry point group. If there is an inversion center, the point group is C_i. If not we can next ask, if there is a mirror plane. If yes it is C_s, and if not the point group is C_1. If a low symmetry point group can be ruled out, then we can ask next, if there is a high symmetry point group. This is the case when there are either $4C_3$, $3C_4$, or $6C_5$ rotational axes present, standing for tetrahedral, octahedral, and icosahedral symmetry, respectively. If there is an inversion center in case a C_5 is present, the point group is I_h. If not, it is I. Similarly, if there are $3C_4$ axes, and an inversion center, the point group must be O_h. If there is no inversion center the point group is O. If there are $4C_3$ axes, the point group must be T type. If there is a horizontal mirror plane in addition, then the point group must be T_h. If not, we can ask next is there are dihedral mirror planes. If yes, the point group is T_d, otherwise it is T. Now we have checked for all high symmetry point groups.

If a high-symmetry point groups can be ruled out, we ask if there are n C_2 axes in addition to the C_n principal axis. If this is so, then we must have a dihedral group of the D type. Next we ask, if there is a horizontal mirror plane. If yes, the point group must be D_{nh}. If not, we ask if there are dihedral mirror planes. If yes, the point group is D_{nd}. If there are no mirror planes at all, then the point group is D_n. If there are no n C_2 axes in addition to the C_n, the the group must be either a rotational group or an improper rotation group. We next ask, if there is a horizontal mirror plane. If yes, then the point group is of the type C_{nh}. If not, we ask if there are vertical mirror planes. If yes, then the point group is C_{nv}. If that is not the case, we ask if there is an S_{2n} in addition to the C_n. If yes, the point group is S_{2n}. If not, it is C_n.

Example: Dibromonaphtalene

Let us practice the point group guide by one example. Let us look at the dibromonaphtalene molecule (Fig. 2.2.87).

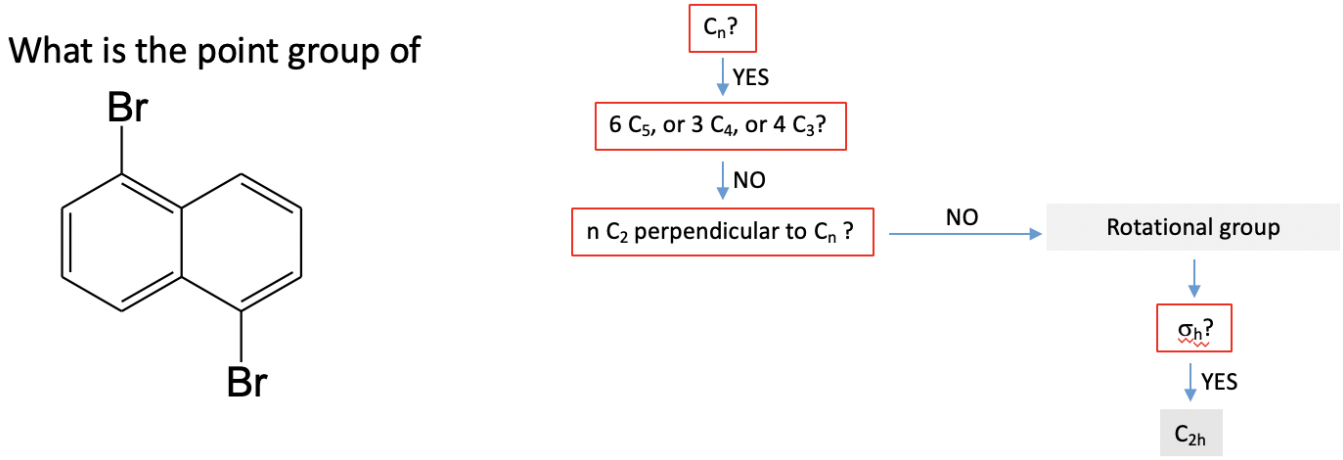


Figure 2.2.87 Guide for determining the point group of dibromonaphtalene

The first question we would ask is: Can you see at least one proper rotational axis? The answer is yes. There is a C_2 proper rotational axis that stands perpendicular to the plane of the molecule and goes through the center of the C-C bond that is shared by the two aromatic rings. Next we ask: Are the $6C_5$, $3C_4$ or $4C_3$ axes? That is clearly not the case, and thus we do not have a high symmetry point group. Next we can think about if the there are $2C_2$ axes in addition to the C_2 axes we already found. The answer is no, so the point group cannot be a dihedral group. Next, we would ask: Is there a horizontal mirror plane. This is indeed the case. There is a horizontal mirror plane in the plane of the molecule. It does not move any atoms around, but as we discussed before, a mirror does not need to do this to exist. This identifies the point group as C_{2h}.

Chiral Point Groups

A chiral point group is a point group that only has proper rotation operations in addition to the identity. This is equivalent to the statement that no improper rotations must exist in a chiral point group. This includes mirror planes and inversion centers because a mirror plane is the same as an S_1, and an inversion center is the same as an S_2. If a molecule belongs to a chiral point group, then it has a mirror image that cannot be superimposed with the original molecule. The two mirror images are called enantiomers. An example is the bromochlorofluoromethane. You can see two enantiomers separated by a dotted line (Fig. 2.2.88).

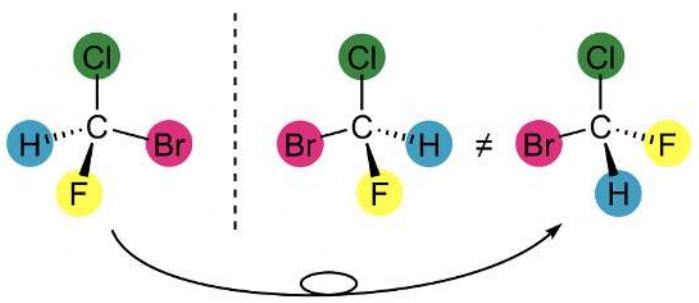


Figure 2.2.88 Chirality in bromochlorofluoromethane

The dotted line represents a mirror plane. Note that this mirror plane is not a mirror plane in the meaning of a symmetry element. You can see that the two molecules to the left and the right of the mirror plane are mirror images respective to each other. The molecules cannot be superimposed meaning that they are enantiomers. Note that the bromochlorofluoromethane molecule on the far right is not an enantiomer to the other two. It the same molecule as the enantiomer on the far left. We only need to rotate clockwise around the C-Cl axis to make the two molecules superimpose meaning that they are the same.

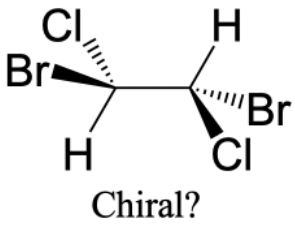


Figure 2.2.89 Dibromodichloroethane

It should be pointed out that the fact that a molecule has a carbon with four different substituents is not sufficient to make it a chiral molecule. The dibromodichloroethane molecule shown above (Fig. 2.2.89) has four different substituents around the carbon atom, but it is not chiral because there is an inversion center in the middle of the C-C bond.

Chiral High Symmetry Point Groups

Chiral groups not necessarily need to have low symmetry, in fact, the high symmetry rotational subgroups I, O, and T are chiral groups because they only have proper axes in addition to the identity (Fig. 2.2.90).

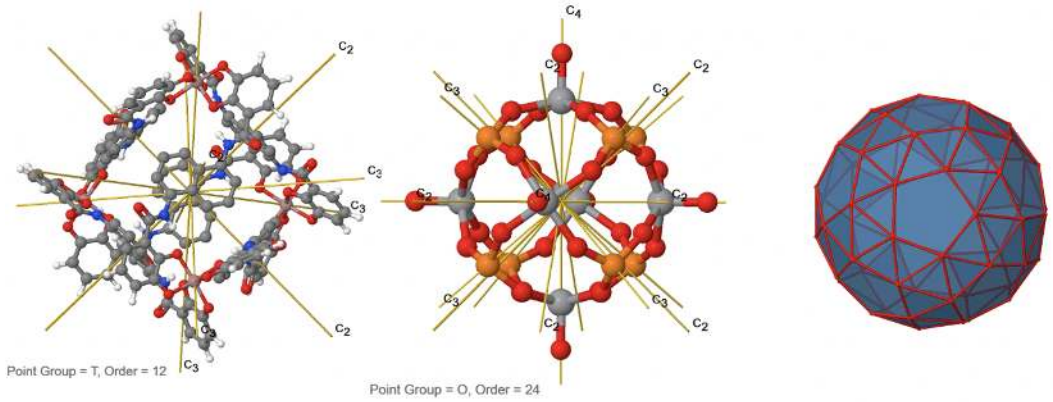


Figure 2.2.90 Objects belonging to chiral high symmetry point groups (T, O, and I from left to right).

Dr. Kai Landskron (Lehigh University). If you like this textbook, please consider to make a donation to support the author's research at Lehigh University: Click Here to Donate.

This page titled 6.3: Molecule Shapes (Point Groups) is shared under a CC BY-NC-SA 4.0 license and was authored, remixed, and/or curated by Kai Landskron.

- **2.2: Point Groups** by Kai Landskron is licensed CC BY 4.0.

6.4: Point Group Assignment

Introduction

A **Point Group** describes all the symmetry operations that can be performed on a molecule that result in a conformation indistinguishable from the original. Point groups are used in Group Theory, the mathematical analysis of groups, to determine properties such as a molecule's molecular orbitals.

Assigning Point Groups

While a point group contains all of the symmetry operations that can be performed on a given molecule, it is not necessary to identify all of these operations to determine the molecule's overall point group. Instead, a molecule's point group can be determined by following a set of steps which analyze the presence (or absence) of particular symmetry elements.

1. Determine if the molecule is of high or low symmetry.
2. If not, find the highest order rotation axis, C_n.
3. Determine if the molecule has any C_2 axes perpendicular to the principal C_n axis. If so, then there are n such C_2 axes, and the molecule is in the D set of point groups. If not, it is in either the C or S set of point groups.
4. Determine if the molecule has a horizontal mirror plane (σ_h) perpendicular to the principal C_n axis. If so, the molecule is either in the C_{nh} or D_{nh} set of point groups.
5. Determine if the molecule has a vertical mirror plane (σ_v) containing the principal C_n axis. If so, the molecule is either in the C_{nv} or D_{nd} set of point groups. If not, and if the molecule has n perpendicular C_2 axes, then it is part of the D_n set of point groups.
6. Determine if there is an improper rotation axis, S_{2n}, collinear with the principal C_n axis. If so, the molecule is in the S_{2n} point group. If not, the molecule is in the C_n point group.

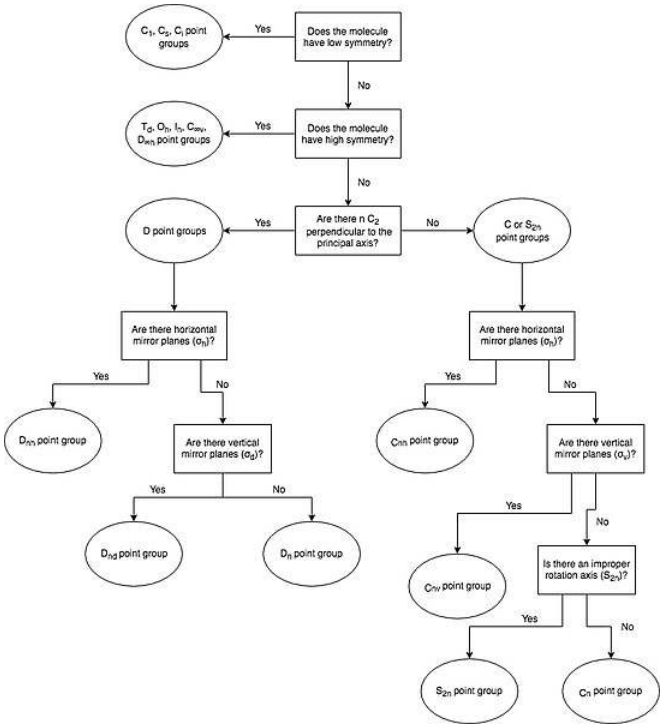


Figure **6.4.1** steps for determining a molecule's overall point group

Example 6.4.1

Find the point group of benzene (C_6H_6).

Solution

1. Highest order rotation axis: C_6

1. Highest order rotation axis: C_6
2. Benzene is neither high or low symmetry
3. There are 6 C_2 axes perpendicular to the principal axis
4. There is a horizontal mirror plane (σ_h)

Benzene is in the D_{6h} point group.

Low Symmetry Point Groups

Low symmetry point groups include the C_1, C_s, and C_i groups

Group	Description	Example
C_1	only the identity operation (E)	CHFClBr
C_s	only the identity operation (E) and one mirror plane	C_2H_2ClBr
C_i	only the identity operation (E) and a center of inversion (i)	$C_2H_2Cl_2Br$

High Symmetry Point Groups

High symmetry point groups include the T_d, O_h, I_h, $C_{\infty v}$, and $D_{\infty h}$ groups. The table below describes their characteristic symmetry operations. The full set of symmetry operations included in the point group is described in the corresponding character table.

Group	Description	Example
$C_{\infty v}$	linear molecule with an infinite number of rotation axes and vertical mirror planes (σ_v)	HBr
$D_{\infty h}$	linear molecule with an infinite number of rotation axes, vertical mirror planes (σ_v), perpendicular C_2 axes, a horizontal mirror plane (σ_h), and an inversion center (i)	CO_2
T_d	typically have tetrahedral geometry, with 4 C_4 axes, 3 C_2 axes, 3 S_4 axes, and 6 dihedral mirror planes (σ_d)	CH_4
O_h	typically have octahedral geometry, with 3 C_4 axes, 4 C_3 axes, and an inversion center (i) as characteristic symmetry operations	SF_6
I_h	typically have an icosahedral structure, with 6 C_5 axes as characteristic symmetry operations	$B_{12}H_{12}^{2-}$

D Groups

The D set of point groups is classified as D_{nh}, D_{nd}, or D_n, where n refers to the principal axis of rotation. Overall, the D groups are characterized by the presence of n C_2 axes perpendicular to the principal C_n axis. Further classification of a molecule in the D groups depends on the presence of horizontal or vertical/dihedral mirror planes.

Group	Description	Example
D_{nh}	n perpendicular C_2 axes, and a horizontal mirror plane (σ_h)	benzene, C_6H_6 is D_{6h}
D_{nd}	n perpendicular C_2 axes, and a vertical mirror plane (σ_v)	propadiene, C_3H_4 is D_{2d}
D_n	n perpendicular C_2 axes, no mirror planes	$[Co(en)_3]^{3+}$ is D_3

C Groups

The C set of point groups is classified as C_{nh}, C_{nv}, or C_n, where n refers to the principal axis of rotation. The C set of groups is characterized by the absence of n C_2 axes perpendicular to the principal C_n axis. Further classification of a molecule in the C groups depends on the presence of horizontal or vertical/dihedral mirror planes.

Group	Description	Example
C_{nh}	horizontal mirror plane (σ_h) perpendicular to the principal C_n axis	boric acid, H_3BO_3, is C_{3h}
C_{nv}	vertical mirror plane (σ_v) containing the principal C_n axis	ammonia, NH_3, is C_{3v}
C_n	no mirror planes	$P(C_6H_5)_3$ is C_3

S Groups

The S set of point groups is classified as S_{2n}, where n refers to the principal axis of rotation. The S set of groups is characterized by the absence of n C_2 axes perpendicular to the principal C_n axis, as well as the absence of horizontal and vertical/dihedral mirror planes. However, there is an improper rotation (or a rotation-reflection) axis collinear with the principal C_n axis.

Group	Description	Example
S_{2n}	improper rotation (or a rotation-reflection) axis collinear with the principal C_n axis	12-crown-4 is S_4

See Also

Symmetry Gallery

This page titled 6.4: Point Group Assignment is shared under a CC BY-NC-SA 4.0 license and was authored, remixed, and/or curated by Wikipedia via source content that was edited to the style and standards of the LibreTexts platform.

- **1.2: Molecular Point Groups** by Wikipedia is licensed CC BY-SA 4.0. Original source: https://en.wikibooks.org/wiki/Advanced_Inorganic_Chemistry.

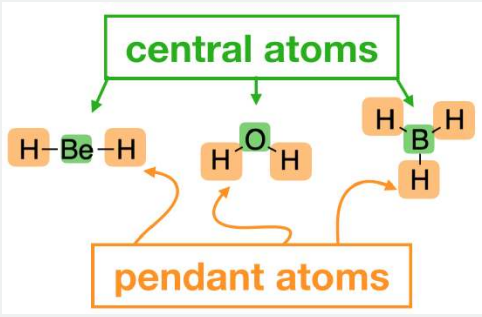
SECTION OVERVIEW

6.5: Overview of Classifying Bonding Orbitals in a Molecule

We can extend the method we used for diatomic molecules to draw the molecular orbitals of more complicated, polyatomic molecules (molecules with more than two atoms). To combine several different atoms in a molecular orbital diagram, we will group orbitals from different atoms into sets that match the symmetry of a central atom. These **group orbitals** are also referred to as **symmetry adapted linear combinations (SALCs)**. We'll use a stepwise approach to do this as summarized below.

Symmetry adapted linear combinations (SALCs)

We need SALCs (aka group orbitals) to draw molecular orbital (MO) diagrams of *polyatomic* molecules. SALCs are groups of orbitals on **pendant atoms**. These groups of orbitals much match the symmetry of valence orbitals on the **central atom** in order to create a productive interaction. When we combine SALCs with the atomic orbitals on the central atom, we can generate a MO diagram that gives us information about the molecule's bonding and electronic states.



Below is a set of steps you can follow to find SALCs and draw a MO Diagram. Each step will be illustrated in detail through the examples in the subsections that follow this page.

1. Find the **point group** of the molecule and assign Cartesian coordinates so that z is the principle axis.
   Sometimes we can simplify things by only looking only at the point group of the relevant orbitals. Only simplify when instructed to do so.*
2. Identify and count the pendant atoms' valence orbitals.
   Is there more than 1 type for each atom (ex. just s, or s and p?) We expect 1 SALC for each ligand orbital.
3. Generate a **reducible representation (Γ)** for the group of pendant atom orbitals using the appropriate character table.
   You have to do this for each set of orbital types. If you only have s orbitals for each ligand, you only need to generate 1 reducible representation. If you have p orbitals, you would generate additional **Γ**'*s for p_x, p_y, and p_z.*
4. Break the **Γ** into its component **irreducible representations** from the character table. Note the symmetry of each irreducible representation, its associated orbitals, and their degeneracy.
5. If you are asked to sketch the shapes of SALCs, determine what they "look like" using one of the following strategies.
   (a) Shortcut: if the reducible representations are listed with s, p, or d orbitals in the character table, just draw them (…and skip steps b-c)
   (b) Systematic method: Draw an expanded character table and draw your molecule with each ligand identified by letters or numbers (*a,b,c...* or *i,j,k...* or *1,2,3...*) Determine where each pendant atom/orbital ends up under each of the operations of your expanded table. Project the values for each irreducible representation onto the chart you created and then add up the values. Positive and negative values are opposite signed orbitals.
6. Draw the MO diagram by combining SALCs with AO's of like symmetry. When drawing SALC energy levels, remember that the more nodal planes in your SALC orbital drawings, the higher the energy or that SALC orbital.

** When we are focused on orbitals, as in the case for finding group orbitals and drawing molecular orbital diagrams, the symmetry of the orbitals are what we are interested in. In the case of high-symmetry point groups, like $D_{\infty h}$ and $C_{\infty v}$ even though the molecule may have a C_∞ axis, the orbitals do not necessarily retain this symmetry element. For example, the p_x orbital would not have a C_∞ axix, but rather a C_2 axis. It is sufficient and useful to substitute D_{2h} for $D_{\infty h}$ and C_{2v} for $C_{\infty v}$ to simplify the problem.*

Curated or created by Kathryn Haas

This page titled 6.5: Overview of Classifying Bonding Orbitals in a Molecule is shared under a CC BY-NC-SA 4.0 license and was authored, remixed, and/or curated by Kathryn Haas.

6.6: MO Diagram Construction of CO2

Construct SALCs and the molecular orbital diagram for CO_2

Carbon dioxide is another linear molecule. This example is slightly more complex than the previous example of the bifluoride anion. While bifluoride had only one valence orbital to consider in its central H atom (the $1s$ orbital), carbon dioxide has a larger central atom, and thus more valence orbitals that will interact with SALCs.

Preliminary Steps

Step 1. Find the point group of the molecule and assign Cartesian coordinates so that z is the principal axis.

The CO_2 molecule is linear and its point group is $D_{\infty h}$. The z axis is collinear with the C_∞ axis. We will use the D_{2h} point group as a substitute since the orbital symmetries are retained in the D_{2h} point group.

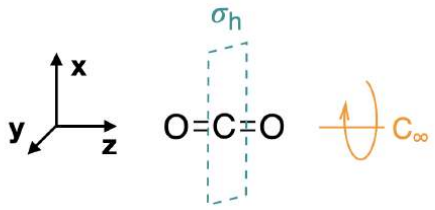


Figure 6.6.1: CO_2 belongs to the $D_{\infty h}$ point group. (CC_BY-NC-SA; Kathryn Haas)

Step 2. Identify and count the pendant atoms' valence orbitals.

Each of the two pendant oxygen atoms has four valence orbitals; $2s$, $2p_x$, $2p_y$, and $2p_z$. Thus, we can expect a total of eight SALCs.

Generate SALCs

The SALCs for CO_2 are identical in shape and symmetry to those described in the previous example for the bifluoride anion. But instead of cutting to the shortcut, we will systematically derive the SALCs here to demonstrate the process.

Step 3. Generate the Γ's

Use the D_{2h} character table to generate four reducible representations ($\Gamma's$); one for each of the four types of pendant atom orbitals (s, p_x, p_y, p_z). For each s orbital, assign a value of 1 if it remains in place during the operation or zero if it moves out of its original place. For each p orbital, assign 1 if there is no change, -1 if it remains in place but is inverted, and 0 if it moves out of its original position. The four Γ's are given below:

D_{2h}	E	$C_2(z)$	$C_2(y)$	$C_2(x)$	i	$\sigma(xy)$	$\sigma(xz)$	$\sigma(yz)$
Γ_{2s}	2	2	0	0	0	0	2	2
Γ_{2p_x}	2	−2	0	0	0	0	2	−2
Γ_{2p_y}	2	−2	0	0	0	0	−2	2
Γ_{2p_z}	2	2	0	0	0	0	2	2

Step 4. Break Γ's into irreducible representations for individual SALCs

Reduce each Γ into its component irreducible representations. There are two strategies that can be used to do this. The quick and easy way is to do it "by inspection", but this only works well for simple cases. The other is by using the systematic approach for breaking a Γ into reducible representations described previously in section 4.4.2 using the following formula:

$$\text{number of } i = \frac{1}{h}\sum(\text{number of operations in class}) \times (\chi_\Gamma) \times (\chi_i) \tag{6.6.1}$$

In other words, the number of irreducible representations of type i is equal to the sum of the number of operations in the class × the character of the Γ_{modes} × the character of i, and that sum is divided by the order of the group (h).

Using either approach results in the following eight irreducible representations ($2A_g + 2B_{1u} + B_{2g} + B_{3u} + B_{3g} + B_{2u}$):

$\mathbf{D_{2h}}$	E	$C_2(z)$	$C_2(y)$	$C_2(x)$	i	$\sigma(xy)$	$\sigma(xz)$	$\sigma(yz)$	
$\mathbf{\Gamma_{2s} = A_g + B_{1u}}$	$\mathbf{\Gamma_{2s}}$	**2**	**2**	**0**	**0**	**0**	**0**	**2**	**2**
	A_g	1	1	1	1	1	1	1	1
	B_{1u}	1	1	−1	−1	−1	−1	1	1
$\mathbf{\Gamma_{2p_x} = B_{2g} + B_{3u}}$	$\mathbf{\Gamma_{2p_x}}$	**2**	**−2**	**0**	**0**	**0**	**0**	**2**	**−2**
	B_{2g}	1	−1	1	−1	1	−1	1	−1
	B_{3u}	1	−1	−1	1	−1	1	1	−1
$\mathbf{\Gamma_{2p_y} = B_{3g} + B_{2u}}$	$\mathbf{\Gamma_{2p_y}}$	**2**	**−2**	**0**	**0**	**0**	**0**	**−2**	**2**
	B_{3g}	1	−1	−1	1	1	−1	−1	1
	B_{2u}	1	−1	1	−1	−1	1	−1	1
$\mathbf{\Gamma_{2p_z} = A_g + B_{1u}}$	$\mathbf{\Gamma_{2p_z}}$	**2**	**2**	**0**	**0**	**0**	**0**	**2**	**2**
	A_g	1	1	1	1	1	1	1	1
	B_{1u}	1	1	−1	−1	−1	−1	1	1

Step 5. Sketch the SALCs

From the systematic process above, you have found the symmetries (the irreducible representations) of all eight SALCs under the D_{2h} point group. To sketch the SALC that corresponds to each irreducible representation, again we use the D_{2h} character table, and specifically the functions listed on the right side columns of the table.

Two A_g SALCs (one from s and one from p_z): The A_g SALCs are each singly degenerate and symmetric with respect to both the principal axis (z) and the inversion center (i) (based on its Mulliken Label). We can look at the functions in the D_{2h} character table that correspond to A_g and see that it is completely symmetric under the group (because the combination of x^2, y^2, z^2 shows that it is totally symmetric). This would be the same symmetry as an s orbital on the central atom. From this information, we know that these SALCs must have symmetry compatible with an s orbital on the central atom, and we can draw the two A_g SALCs shown in Figure **6.6.2**.

Two B_{1u} SALCs (one from s and one from p_z): The Mulliken Label tells us that the B_{1u} SALCs are each antisymmetric with respect to both the principal axis and the inversion center. The function, z, appearing with B_{1u} in the character table tells us that these SALCs have the same symmetry as the z axis, or a p_z orbital on the central atom. From this information, we know that these two SALCs should be compatible with a p_z orbital on the central atom, and we can draw the two B_{1u} SALCs shown in Figure **6.6.2**.

All other SALCs shown below are derived using a strategy similar to the one in the two cases described above.

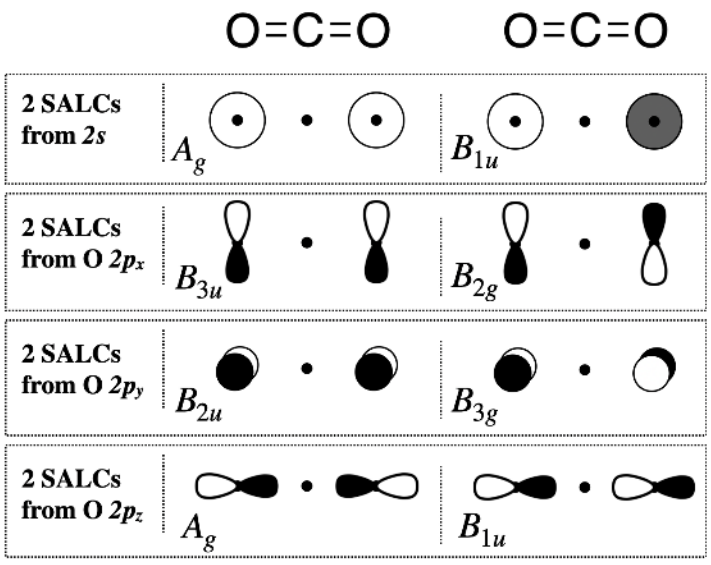


Figure **6.6.2**: SALCs from the valence orbitals of oxygen atoms in CO_2. (CC-BY-NC-SA; Kathryn Haas)

Draw the MO diagram for CO_2

Step 6. Combine SALCs with AO's of like symmetry.

First we identify the valence orbitals on carbon: there are four including $2s$, $2p_x$, $2p_y$, and $2p_z$. Now we identify the symmetry of each using the D_{2h} character table. The symmetry of a central s orbital corresponds to the combination of functions x^2, y^2, and z^2 in the character table; this is A_g. The p_z orbital corresponds to the symmetry of the linear function z in the character table; this is B_{1u}. And so on... The symmetries of the C valence orbitals are listed below.

$$2s = A_g$$
$$2p_x = B_{3u}$$
$$2p_y = B_{2u}$$
$$2p_z = B_{1u}$$

Now that we have identified the symmetries of the eight oxygen SALCs and the four valence orbitals on carbon, we know which atomic orbitals and SALCs may combine based on compatible symmetries. We also need to know the relative orbital energy levels so that we can predict the relative strength of orbital interactions. The orbital ionization energies are listed in Section 5.3.

With knowledge of both orbital symmetries and energies, we can construct the molecular orbital diagram. The carbon atom goes on one side of the diagram while the oxygen SALCs are drawn on the opposite side. Molecular orbitals are drawn in the center column of the diagram:

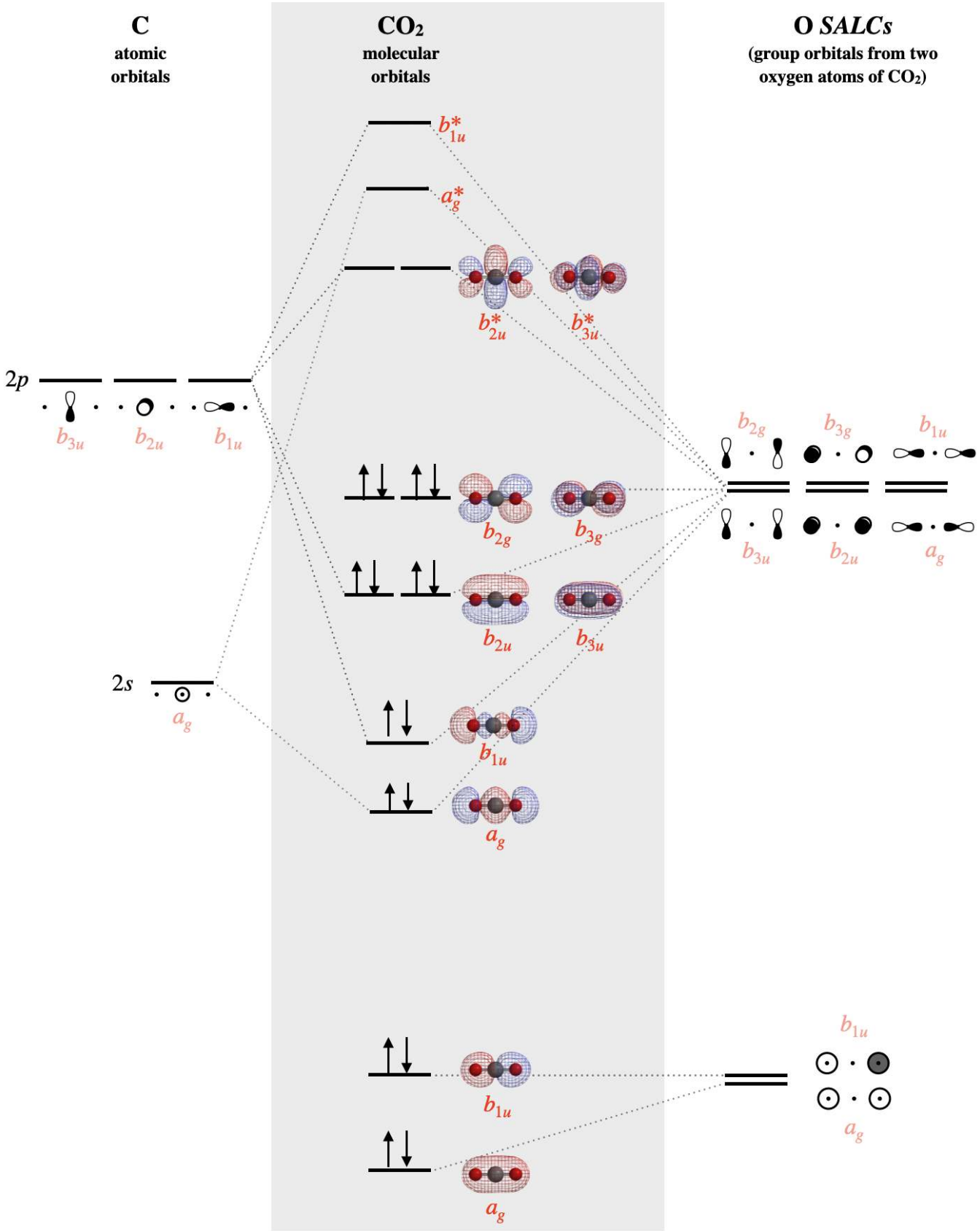


Figure 6.6.3: Molecular orbital diagram for carbon dioxide. (CC-BY-NC-SA; Kathryn Haas)

https://chem.libretexts.org/@go/page/553691

The SALCs on the right side of the diagram above are constructed from groups of either the $2s$ atomic orbitals of oxygen, or the $2p$ atomic orbitals of oxygen. Each SALC will combine with the atomic orbitals of carbon that have compatible symmetry; but the strength of the interaction depends on their relative energies. The individual valence atomic orbitals of oxygen have energies of $-32.36eV$ ($2s$) and $-15.87eV$ ($2p$), while the valence orbitals of carbon have energies of $-19.47eV$ ($2s$) and $-10.66eV$ ($2p$). The $2s$ orbitals of the oxygen are far lower in energy ($-32.36eV$) than all other valence orbitals, and so we should expect that molecular orbitals that are constructed from these oxygen $2s$ will be mostly non-bonding. These mostly non-bonding orbitals are the a_{1g} and b_{1g} orbitals shown at the bottom of Figure 6.6.3. The a_g orbital is lower in energy than the b_{1u} due to slight mixing with other orbitals of a_g symmetry.

The bonding orbitals of CO_2 include two $sigma$ molecular orbitals of a_g and b_{1u} symmetry and two π molecular orbitals of b_{2u} and b_{3u} symmetry. Each of these bonding molecular orbitals possesses a higher-energy antibonding partner. The b_{2g} and b_{3g} SALCs that are formed from oxygen $2p_x$ and $2p_y$ orbitals have no compatible match with carbon valence orbitals; thus they form two b_{2g} and b_{3g} molecular orbitals, which are truly non-bonding and mostly oxygen in character. Still, notice that each orbital is spread across both oxygen atoms at once, and again we see that each non-bonding electron pair in the HOMO is very different in molecular orbital theory compared to Lewis theory. Each non-bonding pair is distributed over both oxygen atoms at once in molecular orbital theory, while in Lewis theory each lone pair is isolated to one atom or to localized bonds attached to that atom.

This page titled 6.6: MO Diagram Construction of CO2 is shared under a CC BY-NC-SA 4.0 license and was authored, remixed, and/or curated by Kathryn Haas.

- **5.4.2: Carbon Dioxide** by Kathryn Haas is licensed CC BY-SA 4.0.

6.7: MO Diagram Construction of H2O

Construct SALCs and the molecular orbital diagram for H_2O.

This is the first example so far that is not a linear molecule. Water is a bent molecule, and so it is important to remember that interactions of pendant ligands are dependent on their positions in space. You should consider the positions of the three atoms in water to be essentially fixed in relation to each other. The process for constructing the molecular orbital diagram *for a non-linear molecule*, like water, is similar to the process for linear molecules. We will walk through the steps below to construct the molecular orbital diagram of water.

Preliminary Steps

Step 1. Find the point group of the molecule and assign Cartesian coordinates so that z is the principal axis.

The H_2O molecule is bent and its point group is C_{2v}. The z axis is collinear with the principal axis, the C_2 axis. There is no need to simplify this problem, as we had done for previous examples. The C_{2v} point group is simple enough.

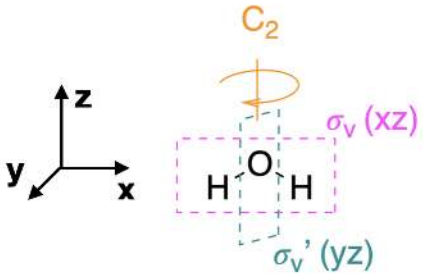


Figure **6.7.1**: The water molecular is in the C_{2v} point group. (CC-BY-NC-SA; Kathryn Haas)

Step 2. Identify and count the pendant atoms' valence orbitals.

Each of the two pendant hydrogen atoms has one valence orbital, the $1s$. Thus, we can expect a total of two SALCs from these two atoms.

Generate SALCs

The SALCs for H_2O are quite simple, yet we will systematically derive the SALCs here to demonstrate the process.

Step 3. Generate the Γ's

Use the C_{2v} character table to generate one reducible representation (Γ); in this case we need only one Γ because there is only one type of valence orbital (the $1s$). For each s orbital, assign a value of 1 if it remains in place during the operation or zero if it moves out of its original place. The Γ is given below:

C_{2v}	E	C_2	$\sigma_v(xz)$	$\sigma'_v(yz)$
Γ_{1s}	2	0	2	0

Step 4. Break Γ's into irreducible representations for individual SALCs

Reduce each Γ into its component irreducible representations. Using either of the processes described previously, we find that the Γ reduces to the two irreducible representations A_1 and B_1 under the C_{2v} point group.

C_{2v}	E	C_2	$\sigma_v(xz)$	$\sigma'_v(yz)$
Γ_{1s}	**2**	**0**	**2**	**0**
A_1	1	1	1	1
B_1	1	−1	1	−1

Step 5. Sketch the SALCs

From the systematic process above, you have found the symmetries (the irreducible representations) of both SALCs under the C_{2v} point group. To sketch the SALC that corresponds to each irreducible representation, again we use the C_{2v} character table, and

specifically the functions listed on the right side columns of the table.

One A_1 SALC: The A_1 SALC is singly degenerate and symmetric with respect to both the principle axis (z) and the inversion center (i) (based on its Mulliken Label). We can look at the functions in the C_{2v} character table that correspond to A_1 and see that it is completely symmetric under the group (because the combination of x^2, y^2, z^2 shows that it is totally symmetric). This would be the same symmetry as an s orbital on the central oxygen atom. From this information, we know that this SALC must have symmetry compatible with an s orbital on the central atom. We can also see from the character table that the z axis, and thus a p_z orbital on oxygen, also possesses A_1 symmetry. This tells us that in addition to being compatible with the oxygen s orbital, it should also be compatible with the oxygen p_z orbital. From this information we can draw the A_1 SALC shown in Figure **6.7.2**. *If it is not obvious how the A_1 sketch in Fig. 6.7.2 is compatible with the s and p_z orbitals of oxygen, inspect the drawings corresponding to molecular orbitals $2a_1$ and $3a_1$ in Fig. 6.7.3.*

One B_1 SALC: The Mulliken Label tells us that the B_1 SALC is singly degenerate and antisymmetric with respect to both the principal axis and the inversion center. The function, x, appearing with B_1 in the character table tells us that this SALC has the same symmetry as the x axis, or a p_x orbital on the central oxygen atom. From this information, we know that this SALC should be compatible with a p_x orbital on the central atom, and we can draw the B_1 SALCs shown in Figure **6.7.2**. *If it is not obvious how the B_1 sketch in Fig. 6.7.2 is compatible with the p_x orbital of oxygen, inspect the drawing corresponding to molecular orbital $1b_1$ in Fig. 6.7.3.*

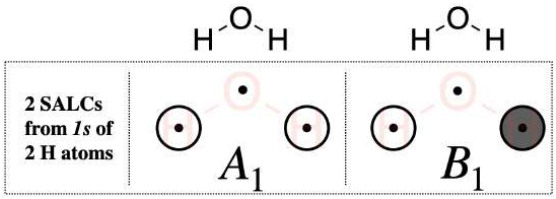


Figure **6.7.2**: Sketch of the A_1 and B_1 hydrogen SALCs of water. (CC-BY-NC-SA; Kathryn Haas)

Not convinced about the sketches of these SALCs? You can convince yourself by putting them to the test. Try the exercise below.

? Exercise 6.7.1

Perform all operations of the C_{2v} point group on the two sketches of H SALCs shown in Figure **6.7.2**, and convince yourself that each sketch does possess the A_1 and B_1 symmetries assigned to them, respectively, under the C_{2v} point group.

Answer

Add texts here. Do not delete this text first.

Draw the MO diagram for H_2O

Step 6. Combine SALCs with AO's of like symmetry.

First we must identify the valence orbitals on the central oxygen: there are four including $2s$, $2p_x$, $2p_y$, and $2p_z$. Now we identify the symmetry of each using the C_{2v} character table. The symmetry of a central $2s$ orbital corresponds to the combination of functions x^2, y^2, and z^2 in the character table; this is A_1. The p_z orbital also corresponds to A_1. And so on... The symmetries of oxygen valence orbitals are listed below.

$$2s = A_1$$
$$2p_x = B_1$$
$$2p_y = B_2$$
$$2p_z = A_1$$

Now that we have identified the symmetries of the two hydrogen SALCs and the four valence orbitals on oxygen, we know which atomic orbitals and SALCs may combine based on compatible symmetries. We also need to know the relative orbital energy levels so that we can predict the relative strength of orbital interactions. The orbital ionization energies are listed in Section 5.3.1.

With knowledge of both orbital symmetries and energies, we can construct the molecular orbital diagram. The valence orbitals of oxygen go on one side of the diagram while the hydrogen group orbitals are drawn on the opposite side. Molecular orbitals are

drawn in the center column of the diagram, as shown in Figure **6.7.3**:

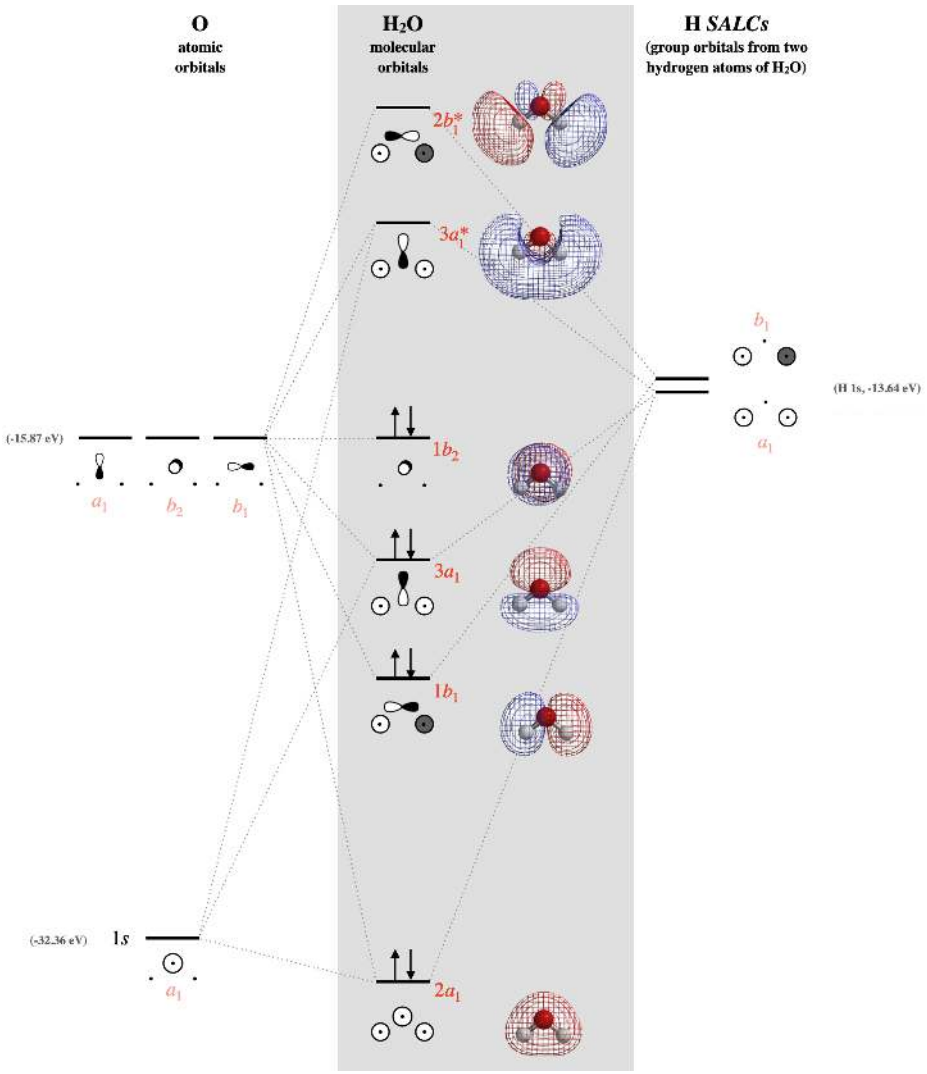


Figure **6.7.3**: The molecular orbital diagram of water. Molecular orbital surfaces calculated using Spartan software. The surface of the $3a_1^*$ orbital has been trimmed. (CC-BY-NC-SA; Kathryn Haas)

Example 6.7.1

In the previous examples shown for the molecular orbital diagrams of the bifluoride anion and carbon dioxide, we discussed differences in the understanding of those molecules from molecular orbital theory compared to Lewis structures. Water contains two lone pairs in its Lewis structure. Compare the predictions about water's lone pairs of electrons and its reactivity based on (1) the combination of elementary models (Lewis, Valence Bond, and Hybridized Orbital theories) and (2) Molecular Orbital theory. Specifically address and explain how the elementary models differ from molecular orbital theory in the following respects:

a. Where are the lone pairs in water?
b. Are the two lone pairs equivalent or are they different?
c. Where are sites on the molecule that will undergo reaction with electrophiles and nucleophiles?

Solution

1) Elementary models: The Lewis structure predicts that two lone pairs are (a) localized on the oxygen atom of water and that (b) both lone pairs are equivalent. The Lewis structure, combined with Valence Bond Theory, would predict that lone pairs occupy two equivalent hybridized sp^3 atomic orbitals on oxygen. (c) Lewis theory would predict that the oxygen lone pairs are

nucleophiles; thus an electrophile would react with the oxygen atom lone pairs. The polarized O-H bond leaves the H atoms as the most electrophilic locations on the water molecule; thus nucleophiles would react at the H atoms of water.

2) Molecular orbital theory: The molecular orbitals predict that (a) the two lone pairs of water are not equivalent, and that (b) each is distributed over the entire molecule. One lone pair is in the truly non-bonding $\mathbf{1}b_2$ orbital (Figure **6.7.3**), which is also the HOMO. There is not another truly non-bonding orbital in the molecule, but the lowest-energy $\mathbf{2}a_1$ orbital could be considered mostly non-bonding due to the large energy difference between it and other valence orbitals. (c) Although the $\mathbf{2}a_1$ orbital can be considered mostly non-bonding, we cannot expect the electrons in $\mathbf{2}a_1$ to react readily, as they are in the lowest-energy molecular orbital. Molecular orbital theory predicts that reactions occur at the HOMO and LUMO orbitals. The HOMO reacts with electrophiles, and in this case, the HOMO is distributed over the top and bottom faces of the molecule, and is centered on the oxygen atom. The LUMO would react with nucleophiles. The LUMO is the orbital labeled $\mathbf{3}a_1^*$ in Figure **6.7.3**, and has a major lobe that is distributed more heavily over the H atoms, and from this we should predict H atoms to be the preferred site of reaction for nucleophiles.

Expressing molecular orbitals in terms of Ψ

The general expression for a molecular orbital, or the linear combination of atomic orbitals (LCAO), was given previously as $\Psi = c_a\psi_a + c_b\psi_b$. In this expression, the wavefunction of two atoms (ψ_a and ψ_b) is combined to form the wavefunction of the molecular orbital. The coefficients c_a and c_b quantify the contribution of each atomic ψ to the molecular Ψ.

$$\Psi = c_a\psi_a + c_b\psi_b$$

In the case of polyatomic orbitals, each LCAO is constructed of atomic orbitals from a central atom and group orbitals (SALCs) from the pendent atoms. In the case of water, the expression above could be modified to give the expression below.

$$\Psi = c_{oxygen}\,(\psi_{oxygen}) + c_{SALCs}\,(N(\psi_{H_a} \pm \psi_{H_b}))$$

N represents the normalizing requirement that was mentioned previously in reference to the requirements for electron wavefunctions and probability functions. The normalizing requirement simply stated is the requirement that the probability of finding the electron in any orbital, including group orbitals, is 1. In general, the value of N for a group orbital is...

$$N = \frac{1}{\sum c_i^2}$$

...where c_i is the coefficient of each unique atomic orbital that contributes to the group. For the hydrogen SALCs of water, there are two atomic orbitals that contribute to equally to each SALC, and so the coefficient on each of the two orbitals is 1. This gives $N = \left(\frac{1}{\sqrt{1^2+1^2}}\right) = \frac{1}{\sqrt{2}}$ for the H SALCs of water.

There are only two hydrogen SALCs: the one in which the hydrogen wavefunctions are added ($N(\psi_{H_a} + \psi_{H_b})$) has A_1 symmetry, and the one in which the hydrogen wavefunctions are subtracted ($N(\psi_{H_a} - \psi_{H_b})$) has B_1 symmetry.

The molecular orbitals from Figure **6.7.3** are expressed below in terms of their LCAO of individual wavefunctions. Yet, note that these expressions are simplifications that ignore orbital mixing. For example, as expressed below, they ignore contributions of oxygen $2s$ to the higher energy moelcular orbitals with A_1 symmetry (the $\mathbf{3}a_1$ and $\mathbf{3}a_1^*$ in Figure **6.7.3**).

MO		*OxygenAO*		*HydrogenSALC*	*Description*
Ψ_{2a_1}	=	$c_{(ox1)}\psi_{(2s)}$	+	$c_{(hy1)}[N(\psi_{H_a} + \psi_{H_b})]$	$c_{(hy1)}$ is positive; bonding, slightly nonbonding
Ψ_{1b_1}	=	$c_{(ox2)}\psi_{(2p_x)}$	+	$c_{(hy2)}[N(\psi_{H_a} - \psi_{H_b})]$	$c_{(hy2)}$ is positive; bonding
Ψ_{3a_1}	=	$c_{(ox3)}\psi_{(2p_z)}$	+	$c_{(hy3)}[N(\psi_{H_a} + \psi_{H_b})]$	$c_{(hy3)}$ is positive; bonding
Ψ_{1b_2}	=	$\psi_{(2p_y)}$			nonbonding
$\Psi^*_{3a_1}$	=	$c_{(ox4)}\psi_{(2p_z)}$	+	$c_{(hy4)}[N(\psi_{H_a} + \psi_{H_b})]$	$c_{(hy4)}$ is negative; antibonding
$\Psi^*_{1b_1}$	=	$c_{(ox5)}\psi_{(2p_x)}$	+	$c_{(hy5)}[N(\psi_{H_a} - \psi_{H_b})]$	$c_{(hy5)}$ is negative; antibonding

This page titled 6.7: MO Diagram Construction of H2O is shared under a CC BY-NC-SA 4.0 license and was authored, remixed, and/or curated by Kathryn Haas.

- **5.4.3: H_2O** is licensed CC BY-SA 4.0.

6.8: MO Diagram Construction of NH3

Construct SALCs and the molecular orbital diagram for NH_3

This is the first example so far that has more than two pendant atoms and the first example in which the molecule has atoms that lie in three dimensions (i.e., it is not flat). Ammonia is a trigonal pyramidal molecule, with three pendant hydrogen atoms. The three-dimensional shape and the odd number of pendant atoms makes this example more complicated than the previous cases of water, carbon dioxide, and bifluoride. In this case, sketching the shapes (step 5) of pendant atom SALCs is less straightforward; rather, an alternative method, the **projection operator method**, is preferred for generating pictorial representations of the SALCs.

As in previous examples, it is important to remember that interactions of pendant ligands are dependent on their positions in three-dimensional space. You should consider the positions of the four atoms in ammonia to be essentially fixed in relation to each other. We will walk through the steps used to construct the molecular orbital diagram of ammonia. The first few steps are the same as you've seen before:

Step 1. Find the point group of the molecule and assign Cartesian coordinates so that z is the principal axis.

The NH_3 molecule is trigonal pyramidal and its point group is C_{3v}. The z axis is collinear with the principal axis, the C_3 axis.

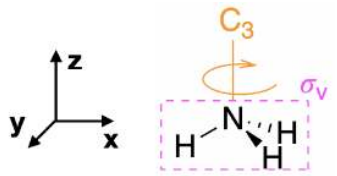


Figure **6.8.1**: The ammonia molecule is in the C_{3v} point group. (CC-BY-NC-SA; Kathryn Haas)

Step 2. Identify and count the pendant atoms' valence orbitals.

Each of the three pendant hydrogen atoms has one valence orbital; the $1s$. Thus, we can expect a total of three SALCs from these three atoms.

Step 3. Generate the Γ's

Use the C_{3v} character table to generate one reducible representation (Γ); in this case we need only one Γ because there is only one type of valence orbital (the $1s$). For each s orbital, assign a value of 1 if it remains in place during the operation or zero if it moves out of its original place. The Γ is given below:

C_{3v}	E	$2C_3$	$3\sigma_v$
Γ_{1s}	3	0	1

Step 4. Break Γ's into irreducible representations for individual SALCs

Reduce each Γ into its component irreducible representations. Using either of the processes described previously, we find that the Γ reduces to the two irreducible representations A_1 and E under the C_{3v} point group.

C_{3v}	E	$2C_3$	$3\sigma_v$
Γ_{1s}	3	0	2
A_1	1	1	1
E	2	−1	0

Notice that we only found TWO irreducible representations. But, in fact we have THREE different SALCs. The E irreducible representation is doubly degenerate, which in this context means that it corresponds to two degenerate SALCs. Thus, we have already found the symmetries of the three SALCs for ammonia: Two of the SALCs are degenerate with E symmetry under the C_{3v} point group, while the third SALC has A_1 symmetry.

Step 5. Sketch the SALCs using the PROJECTION OPERATOR METHOD

From the first four steps (described above), you have found the symmetries (the irreducible representations) of all three SALCs under the C_{3v} point group. To sketch the SALC that corresponds to each irreducible representation, again we use the C_{3v} character

table. But now we will introduce the **projection operator method** to derive the surface representation of each SALC.

Step 5.1: Label the pendent atoms

In the projection operator method, first **label each of the pendant atoms so that we can distinguish identical atoms from one another**; for example, identify the three hydrogen atoms on ammonia as H_a, H_b, and H_c (Figure 6.8.2).

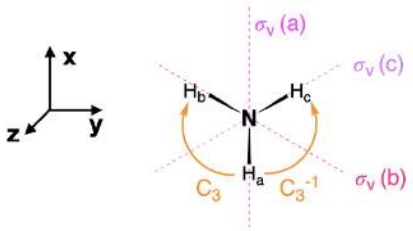


Figure 6.8.2: The three H's in NH_3 are chemically identical, but we can distinguish them using labels for the purpose of applying the projection operator method. In this figure, we have placed the z axis along the principal C_3 axis and placed the x axis colinear with one H. Each of the three H atoms has been labeled as H_a, H_b, or H_c. The σ_v that is coplanar with each H is labeled similarly (a, b, c) to keep account of each individual plane of symmetry. (CC-BY-NC-SA; Kathryn Haas)

Step 5.2: Create an expanded character table with one pendant atom's projected position after each operation

We will **perform each operation of the C_{3v} point group on this labeled molecule** and follow where one of the atoms is projected after the operation is complete. We will arbitrarily choose H_a. For example, upon performing the identity operation, E, the H_a atom is projected onto itself. On the other hand, H_a is projected onto H_b upon a clockwise C_3 rotation (as drawn in Figure 6.8.2). We take into account the result of each operation using an expanded character table (refer to the table below, 6.8.1). In the expanded character table, each operation within each class is written separately (i.e., $2C_3$ is accounted for separately as C_3 and C_3^{-1}).

Table 6.8.1: The expanded character table, and the projection of H_a by each operation is shown below.

C_{3v}	E	C_3	C_3^{-1}	$\sigma_v(a)$	$\sigma_v(b)$	$\sigma_v(c)$
Projection of H_a	H_a	H_b	H_c	H_a	H_c	H_b

(6.8.1)

Step 5.3: Find the contribution of each pendant atom to each SALC

Next, **create a linear combination of the projections for each of the SALCs** (the irreducible representations found in step 4). For each of the irreducible representations, multiply the projection by the respective character of the operation.

$$\text{Contribution of each atom to the SALC } = \sum(\text{Projection of } H_a \times \chi)$$

The linear combination for all irreducible representations of C_3v is shown below.

Table 6.8.2: The symmetry adapted linear combination (SALC) for each irreducible representation of C_3v is shown.

C_{3v}	E	C_3	C_3^{-1}	$\sigma_v(a)$	$\sigma_v(b)$	$\sigma_v(c)$	Linear Combination
Projection of H_a	H_a	H_b	H_c	H_a	H_c	H_b	
A_1	1	1	1	1	1	1	$= 2H_a + 2H_b + 2H_c$
A_2	1	1	1	−1	−1	−1	$= 0$
E	2	−1	−1	0	0	0	$= 2H_a - H_b - H_c$

(6.8.2)

Notice that there are only two irreducible representations that produce SALCs, and these are the same that were found in Step 4, above. This illustrates the fact that only the irreducible representations found through the reduction of the Γ will produce SALCs. We can ignore any irreducible representations that were not found in Step 4. Or, you can check your work in Step 4 by applying the projection operator to any irreducible representations not found in Step 4, and finding that they produce a sum of zero.

Step 5.4: Sketch the SALCs

The meaning of the linear combinations found in Table 6.8.2 is as follows:

- **Sketch the SALC with A_1 symmetry:** The linear combination $2H_a + 2H_b + 2H_c$ indicates all contributions to this SALC are of the same sign (of the wavefunction). Qualitatively, this means there is no node in this SALC. We can take this SALC almost literally to assume that all three H 1s wavefunctions contribute equally to the SALC. We can also use the fact that the A_1 representation possesses the full symmetry of the C_3v point group, is compatible with an s orbital on N, and thus is a totally symmetric SALC.

  Quantitatively, we can apply the normalizing factor, N, for this SALC. The linear combination for the A_1 SALC in Table 6.8.2 shows us that the coefficient for each orbital is 1. Thus, the normalizing factor for the A_1 SALC is $N = \left(\frac{1}{\sqrt{1^2+1^2+1^2}}\right) = \frac{1}{\sqrt{3}}$. This tells us that H_a, H_b, and H_c each contribute $\frac{1}{\sqrt{3}}$ to the normalized A_1 group orbital:

  $$A_1 \text{ group orbital } = \frac{1}{\sqrt{3}}\left[\psi_{H_a} + \psi_{H_b} + \psi_{H_c}\right]$$

  This is shown visually in Figure 6.8.3.
- **Sketch two SALCs with E symmetry:** The linear combination $2H_a - H_b - H_c$ indicates that there are contributions with both positive and negative sign to the wavefunction for each of the E group orbitals. Qualitatively, this tells us that there is a node within each of these two SALCs, and that the total contribution of the positive portion of the wavefunction is equal to the contribution of the negative portion.
  - **Finding the first E SALC:**
    For one of the SALCs, we can take the linear combination from Table 6.8.2 almost literally: The contribution from H_a is equal and opposite to the sum of the contributions from $H_b + H_c$. This would result in a SALC as shown in Figure 6.8.3 (E, left), that would have symmetry of the x axis and that would be compatible with the p_x orbital on N. The node exists in the yz plane and there is an equal contribution of positive and negative parts of the total wavefunction.

    We can also apply the normalizing factor, N, to find this SALC. The linear combination for the E SALC in Table 6.8.2 shows us that the coefficients for orbital contributions are 2, -1, and -1. Thus, the normalizing factor for the first E SALC is $N = \left(\frac{1}{\sqrt{2^2+(-1)^2+(-1)^2}}\right) = \frac{1}{\sqrt{6}}$. This normalized E group orbital is:

    $$\text{First } E \text{ group orbital } = \frac{1}{\sqrt{6}}\left[2\psi_{H_a} - \psi_{H_b} - \psi_{H_c}\right]$$

    This is shown visually in Figure 6.8.3 (E, left).
  - **Finding the second E SALC:**
    The second SALC is less obvious at first glance. We must use clues from the character table to help us determine what it should "look like". Since the E representation transforms as the group, (x, y), we know that one of the SALCs will have the symmetry of the x axis and p_x orbital on the central nitrogen atom, while the other should possess the symmetry of the y axis and be compatible with the p_y orbital on nitrogen. This alone could lead you to the sketch of the second SALC with E symmetry shown in Figure 6.8.3 (E, right). This second E SALC must have a node in the xz plane, and because H_a lies in this node, H_a cannot contribute to this group orbital. Retaining the fact that the positive and negative contributions of the linear combination must be equal, we can arrive at a SALC that has equal but opposite contributions of H_b and H_c, and no contribution by H_c (Figure 6.8.3, right).

    We can also apply the normalizing factor, N, to find this SALC. But we must apply the fact that H_a cannot contribute to the SALC with "y" symmetry. We remove the contribution of H_a, leaving us with coefficients of 0 for H_a and 1 for H_b and H_c. Thus, the normalizing factor for the second E SALC is $N = \left(\frac{1}{\sqrt{0^2+1^2+1^2}}\right) = \frac{1}{\sqrt{2}}$. To this, we must add positive and negative coefficients so that the entire wavefunction of this SALC is normalized. The result for this normalized E group orbital is:

    $$\text{Second } E \text{ group orbital } = \frac{1}{\sqrt{2}}\left[\psi_{H_b} - \psi_{H_c}\right]$$

    This is shown visually in Figure 6.8.3.

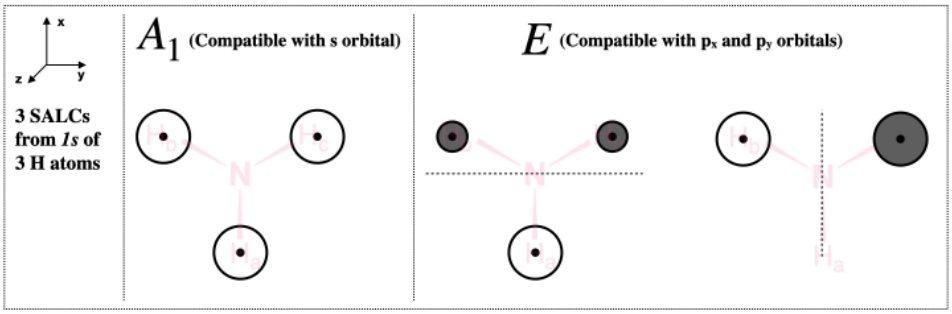


Figure **6.8.3**: Sketches of H SALCs of ammonia from the perspective of the C_3 axiz (z axis). The A_1 SALC is shown at the left, while two degenerate SALCs with E symmetry are shown on the right. Nodes for E group orbitals are shown as dashed lines. (CC-BY-NC-SA; Kathryn Haas)

Step 6. Combine SALCs with AO's of like symmetry to draw the MO diagram for NH_3

First we must identify the valence orbitals on the central nitrogen: there are four including $2s$, $2p_x$, $2p_y$, and $2p_z$. Now we identify the symmetry of each using the C_{3v} character table. The symmetry of a central $2s$ orbital corresponds to the combination of functions x^2, y^2, and z^2 in the character table; this is A_1. The p_z orbital also corresponds to A_1. And so on... The symmetries of nitrogen valence orbitals are listed below.

$$2s = A_1$$
$$(2p_x,\ 2p_y) = E$$
$$2p_z = A_1$$

The next step is to get a sense of the relative energies of valence atomic orbitals for nitrogen and hydrogen, and then construct the molecular orbital diagram. The nitrogen $2s$ orbital is about 12 eV lower in energy than a H $1s$. This difference is an acceptable energy-match for the H orbitals to interact, but would not usually result in a strong interaction. On the other hand, the nitrogen 2p orbitals have an energy very close to the hydrogen 1s, different by only 0.5 eV. Knowledge of the relative energies of the atomic orbitals tells us that, when constructing a diagram, we can place the H SALCs at an energy similar to that of the N $2p$ orbitals, while the N $2s$ is much lower (Figure **6.8.4**).

The $2s$ and $2p_z$ orbitals have A_1 symmetry and can combine with the A_1 SALC. These orbitals will give three molecular orbitals. The $2s$ orbital will not have strong interactions with the other orbitals of A_1 symmetry due to the large energy difference. The $2p_z$ orbital will not have good overlap with the wavefunctions for the three hydrogen orbitals due to their positions in space: The $2p_z$ orbital has half of its angular distribution pointed away from the hydrogen orbitals, and half pointed toward the center of a triangle formed by the three hydrogen atoms. The nitrogen $2s$ and $2p_z$ will combine with the hydrogen SALC of A_1 symmetry to give three molecular orbitals; one low-energy bonding orbital, one mid-energy non-bonding orbital, and one high-energy antibonding orbital. The mid-level non-bonding a_1 molecular orbital is close in energy to, and resembles, the nitrogen $2p_z$ orbital. The lowest energy a_1 molecular orbital will be lower in energy, but be similar to the nitrogen $2s$.

The remaining two $2p$ orbitals are degenerate and possess E symmetry under the C_{3v} point group. Although these orbitals are a good energy match, again, their orientation and positions in space do not allow for good orbital overlap, and their bonding and antibonding interactions are relatively weak compared to what we might otherwise expect from such a good energy match. The e atomic orbitals of nitrogen will combine with the e SALCs to give a set of two degenerate bonding molecular orbitals and a set of two degenerate antibonding orbitals (four total molecular orbitals of e symmetry). The MO diagram for NH_3 is shown in Figure **6.8.4**, with calculated electron density surfaces of each MO shown.

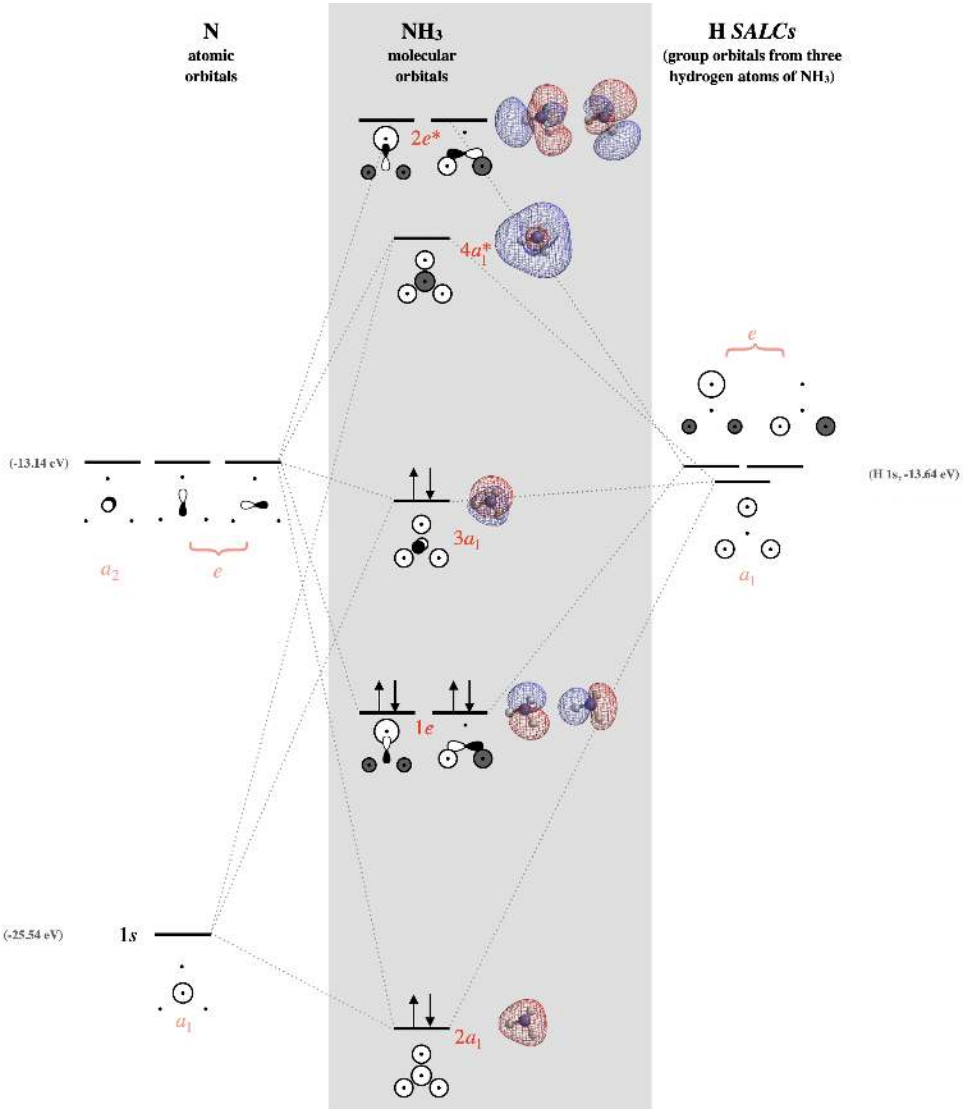


Figure **6.8.4**: The molecular orbital diagram of ammonia. Molecular orbitals surfaces calculated using Spartan software. (CC-BY-NC-SA; Kathryn Haas)

This page titled 6.8: MO Diagram Construction of NH3 is shared under a CC BY-NC-SA 4.0 license and was authored, remixed, and/or curated by Kathryn Haas.

- **5.4.4: NH3** by Kathryn Haas is licensed CC BY-SA 4.0.

6.9: MO Construction of BF3

The case of boron trifluoride (BF_3) is an example of a molecule with one more layer of complexity than the other examples we have seen in previous sections in this chapter. (BF_3) is more complex than previous examples because it is the first case in which there are multiple types of valence orbitals on the pendant atoms. (BF_3) possesses s and p orbitals on *both* the central atom and all of the pendant atoms. We can follow the same steps that we have previously to derive other molecular orbital diagrams; however, there is one important difference: we will treat each type of pendant orbital as an individual set of SALCs.

Step 1. Find the point group of the molecule and assign Cartesian coordinates so that z is the principal axis.

The BH_3 molecule is trigonal planar, and its point group is D_{3h}. The z axis is colinear with the principle axis, the C_3 axis.

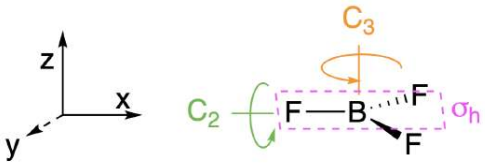


Figure 6.9.1: The molecule is in the D_{3h} point group. (CC-BY-NC-SA; Kathryn Haas)

Step 2. Identify and count the pendant atoms' valence orbitals.

Each of the three pendant fluorine atoms has four valence orbitals: one $2s$ and three $2p$ orbitals. Thus, we can expect a total of twelve SALCs from the three atoms. However, we will treat each type of orbital from the F atoms as its own set; each will have its own set of coordinates, with the y axis along the M-L bond. Thus we expect the following:

- One set of $2s$ SALCs: there is one 2s orbital on each of three atoms. This set will have three SALCs.
- One set of $2p_x$ SALCs: there is one $2p_x$ orbital on each of three atoms. Each of these individual orbitals is perpendicular to the M-L bond and coplanar with the molecule. This set will have three SALCs.
- One set of $2p_y$ SALCs: there is one $2p_y$ orbital on each of three atoms. Each of these individual orbitals is colinear with the M-L bond. This set will have three SALCs.
- One set of $2p_z$ SALCs: there is one $2p_z$ orbital on each of three atoms. Each of these individual orbitals is perpendicular to the M-L bond and parallel with the principal axis of the molecule. This set will have three SALCs.

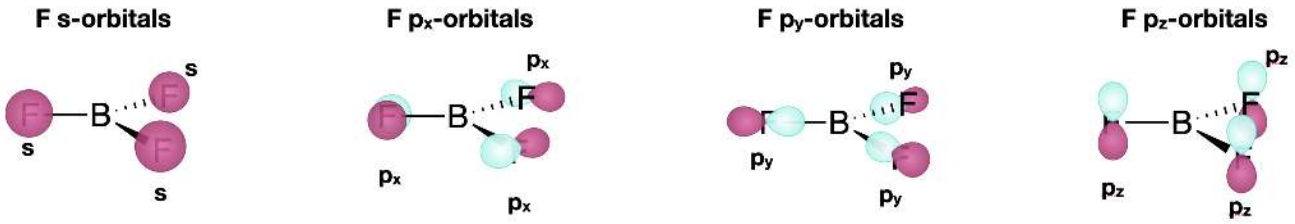


Figure 6.9.2: Individual sets of pendant fluorine atomic orbitals will create separate sets of SALCs. (CC-BY-SA; Kathryn Haas)

Step 3. Generate the Γ's for each set of SALCs

Use the D_{3h} character table to generate one reducible representation (Γ) for each of the four sets of pendant atomic orbitals shown in Figure 6.9.2; in this case we need four Γ because there are four types of valence orbital (the s, p_x, p_y, p_z).

- For the set of s orbitals: perform the operation for each class in the character table. Each s orbital is assigned a value depending on whether it moves or not: assign a value of 1 if it remains in place during the operation, or 0 (zero) if it moves out of its original place.
- for each set of p orbitals: Now there are phases (signs of the wavefunction), so a negative value is possible. Assign a value of 1 to each p orbital if it remains in place and in phase during the operation; assign a -1 if the atom's position remains, while the phase of the orbital is inverted (the positive lobe moves to the position of the negative lobe and vice versa); assign a 0 if it moves out of its original position.

The Γ for each type is given below:

$\mathbf{D_{3h}}$	E	$2C_3$	$3C_2$	σ_h	$2S_3$	$3\sigma_v$
$\mathbf{\Gamma_{2s}}$	3	0	1	3	0	1
$\mathbf{\Gamma_{2p_x}}$	3	0	−1	3	0	−1
$\mathbf{\Gamma_{2p_y}}$	3	0	1	3	0	1
$\mathbf{\Gamma_{2p_z}}$	3	0	−1	−3	0	1

Step 4. Break Γ's into irreducible representations for individual SALCs

Reduce each $\mathbf{\Gamma}$ into its component irreducible representations. Using either of the processes described previously, we find that each of the $\mathbf{\Gamma}$ reduces to two irreducible representations under the $\boldsymbol{D_{3h}}$ point group; in each case one is singly degenerate ($\boldsymbol{A}$) and the other doubly degenerate ($\boldsymbol{E}$). This equates to three SALCs for each $\mathbf{\Gamma}$ (orbital type) and a total of twelve SALCs. This should give us confidence! We were in fact expecting 12 SALCs because we found that there were twelve pendant atomic orbitals to start with.

D_{3h}	E	$2C_3$	$3C_2$	σ_h	$2S_3$	$3\sigma_v$
$\mathbf{\Gamma_{2s}}$	**3**	**0**	**1**	**3**	**0**	**1**
A_1'	1	1	1	1	1	1
E'	2	−1	0	2	−1	0

D_{3h}	E	$2C_3$	$3C_2$	σ_h	$2S_3$	$3\sigma_v$
$\mathbf{\Gamma_{2p_x}}$	**3**	**0**	**−1**	**3**	**0**	**−1**
A_2'	1	1	−1	1	1	−1
E'	2	−1	0	2	−1	0

D_{3h}	E	$2C_3$	$3C_2$	σ_h	$2S_3$	$3\sigma_v$
$\mathbf{\Gamma_{2p_y}}$	**3**	**0**	**1**	**3**	**0**	**1**
A_1'	1	1	1	1	1	1
E'	2	−1	0	2	−1	0

D_{3h}	E	$2C_3$	$3C_2$	σ_h	$2S_3$	$3\sigma_v$
$\mathbf{\Gamma_{2p_z}}$	**3**	**0**	**−1**	**−3**	**0**	**1**
A_2''	1	1	−1	−1	−1	1
E''	2	−1	0	−2	1	0

Step 5: Sketch the SALCs

We'll skip this step for now to make this problem simpler.

Step 6: Draw the MO diagram by combining SALCs with AO's of like symmetry.

We now know the symmetries of different pendant orbital SALCs - and it is helpful if we also know their relative energies, and the energies of the valence orbitals on the central boron atom. We can make predictions based on periodic trends, or we can use a table of ionization energies as a guide. The symmetries of the boron $\boldsymbol{2s}$ and $\boldsymbol{2p}$ orbitals can be found from the $\boldsymbol{D_{3h}}$ character table.

6.9: MO Construction of BF3 is shared under a CC BY-NC-SA 4.0 license and was authored, remixed, and/or curated by LibreTexts.

- **5.4.4: NH_3** by Kathryn Haas is licensed CC BY-SA 4.0.

6.10: Lewis Acid-Base Dative Bond and MO Diagrams

The case of boron trifluoride (BF_3) is an example of a molecule with one more layer of complexity than the other examples we have seen in previous sections in this chapter. (BF_3) is more complex than previous examples because it is the first case in which there are multiple types of valence orbitals on the pendant atoms. (BF_3) possesses s and p orbitals on *both* the central atom and all of the pendant atoms. We can follow the same steps that we have previously to derive other molecular orbital diagrams; however, there is one important difference: we will treat each type of pendant orbital as an individual set of SALCs.

Step 1. Find the point group of the molecule and assign Cartesian coordinates so that z is the principal axis.

The BH_3 molecule is trigonal planar, and its point group is D_{3h}. The z axis is colinear with the principle axis, the C_3 axis.

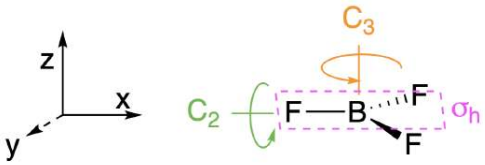


Figure **6.10.1**: The molecule is in the D_{3h} point group. (CC-BY-NC-SA; Kathryn Haas)

Step 2. Identify and count the pendant atoms' valence orbitals.

Each of the three pendant fluorine atoms has four valence orbitals: one $2s$ and three $2p$ orbitals. Thus, we can expect a total of twelve SALCs from the three atoms. However, we will treat each type of orbital from the F atoms as its own set; each will have its own set of coordinates, with the y axis along the M-L bond. Thus we expect the following:

- One set of $2s$ SALCs: there is one 2s orbital on each of three atoms. This set will have three SALCs.
- One set of $2p_x$ SALCs: there is one $2p_x$ orbital on each of three atoms. Each of these individual orbitals is perpendicular to the M-L bond and coplanar with the molecule. This set will have three SALCs.
- One set of $2p_y$ SALCs: there is one $2p_y$ orbital on each of three atoms. Each of these individual orbitals is colinear with the M-L bond. This set will have three SALCs.
- One set of $2p_z$ SALCs: there is one $2p_z$ orbital on each of three atoms. Each of these individual orbitals is perpendicular to the M-L bond and parallel with the principal axis of the molecule. This set will have three SALCs.

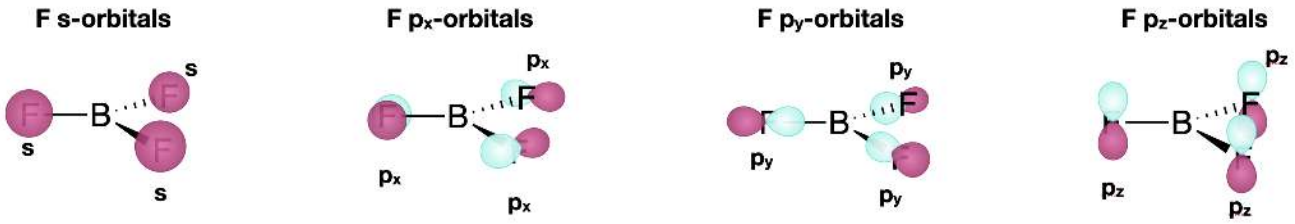


Figure **6.10.2**: Individual sets of pendant fluorine atomic orbitals will create separate sets of SALCs. (CC-BY-SA; Kathryn Haas)

Step 3. Generate the Γ's for each set of SALCs

Use the D_{3h} character table to generate one reducible representation (Γ) for each of the four sets of pendant atomic orbitals shown in Figure **6.10.2**; in this case we need four Γ because there are four types of valence orbital (the s, p_x, p_y, p_z).

- For the set of s orbitals: perform the operation for each class in the character table. Each s orbital is assigned a value depending on whether it moves or not: assign a value of 1 if it remains in place during the operation, or 0 (zero) if it moves out of its original place.
- for each set of p orbitals: Now there are phases (signs of the wavefunction), so a negative value is possible. Assign a value of 1 to each p orbital if it remains in place and in phase during the operation; assign a -1 if the atom's position remains, while the phase of the orbital is inverted (the positive lobe moves to the position of the negative lobe and vice versa); assign a 0 if it moves out of its original position.

The Γ for each type is given below:

$\mathbf{D_{3h}}$	E	$2C_3$	$3C_2$	σ_h	$2S_3$	$3\sigma_v$
$\mathbf{\Gamma_{2s}}$	3	0	1	3	0	1
$\mathbf{\Gamma_{2p_x}}$	3	0	−1	3	0	−1
$\mathbf{\Gamma_{2p_y}}$	3	0	1	3	0	1
$\mathbf{\Gamma_{2p_z}}$	3	0	−1	−3	0	1

Step 4. Break Γ's into irreducible representations for individual SALCs

Reduce each $\mathbf{\Gamma}$ into its component irreducible representations. Using either of the processes described previously, we find that each of the $\mathbf{\Gamma}$ reduces to two irreducible representations under the $\boldsymbol{D_{3h}}$ point group; in each case one is singly degenerate ($\boldsymbol{A}$) and the other doubly degenerate ($\boldsymbol{E}$). This equates to three SALCs for each $\mathbf{\Gamma}$ (orbital type) and a total of twelve SALCs. This should give us confidence! We were in fact expecting 12 SALCs because we found that there were twelve pendant atomic orbitals to start with.

D_{3h}	E	$2C_3$	$3C_2$	σ_h	$2S_3$	$3\sigma_v$
$\mathbf{\Gamma_{2s}}$	**3**	**0**	**1**	**3**	**0**	**1**
A_1'	1	1	1	1	1	1
E'	2	−1	0	2	−1	0

D_{3h}	E	$2C_3$	$3C_2$	σ_h	$2S_3$	$3\sigma_v$
$\mathbf{\Gamma_{2p_x}}$	**3**	**0**	**−1**	**3**	**0**	**−1**
A_2'	1	1	−1	1	1	−1
E'	2	−1	0	2	−1	0

D_{3h}	E	$2C_3$	$3C_2$	σ_h	$2S_3$	$3\sigma_v$
$\mathbf{\Gamma_{2p_y}}$	**3**	**0**	**1**	**3**	**0**	**1**
A_1'	1	1	1	1	1	1
E'	2	−1	0	2	−1	0

D_{3h}	E	$2C_3$	$3C_2$	σ_h	$2S_3$	$3\sigma_v$
$\mathbf{\Gamma_{2p_z}}$	**3**	**0**	**−1**	**−3**	**0**	**1**
A_2''	1	1	−1	−1	−1	1
E''	2	−1	0	−2	1	0

Step 5: Sketch the SALCs

We'll skip this step for now to make this problem simpler.

Step 6: Draw the MO diagram by combining SALCs with AO's of like symmetry.

We now know the symmetries of different pendant orbital SALCs - and it is helpful if we also know their relative energies, and the energies of the valence orbitals on the central boron atom. We can make predictions based on periodic trends, or we can use a table of ionization energies as a guide. The symmetries of the boron $\boldsymbol{2s}$ and $\boldsymbol{2p}$ orbitals can be found from the $\boldsymbol{D_{3h}}$ character table.

6.10: Lewis Acid-Base Dative Bond and MO Diagrams is shared under a CC BY-NC-SA 4.0 license and was authored, remixed, and/or curated by LibreTexts.

- **5.4.4: NH_3** by Kathryn Haas is licensed CC BY-SA 4.0.

6.11: MO Diagram for bonding in [M(NH3)6]n+

Concepts from molecular orbital (MO) theory are useful in understanding the reactivity of coordination compounds. One of the basic ways of applying MO concepts to coordination chemistry is in Ligand Field Theory (LFT). LFT is essentially a version of MO theory that focuses on how the d-orbitals of a metal ion interact with ligand orbitals to create bonding, antibonding, and non-bonding interactions. These interactions result in orbitals that are close in energy to the original d-orbitals of the metal. Due to their similarity to the metal d-orbitals, they are usually referred to as the metal d-orbitals even though they are actually molecular orbitals. The interactions of ligand orbitals with metal d-orbitals results in different splitting of the metal d-orbitals into sets of bonding, antibonding and non-bonding orbitals. In the octahedral case, the splitting of d-orbitals is the same in LFT as we saw previously in CFT. The main difference between the two theories is the explanation of how this splitting is derived. LFT also describes bonding, while CFT can't.

The symmetry of the central metal orbital and that of the ligand group orbitals (aka SALCs, symmetry adapted linear combinations of atomic orbitals) determines the relative eenergies (eg the splitting) of the d-oritals of the metal complex. The symmetry of the SALCs depends on the coordination geometry of the ligands and the specific type of orbitals involved (eg s vs p). For example, ligand s orbitals in a tetrahedral coordination sphere will have a different symmetries and different abilities to interact with the metal d-orbitals than orbitals in an octahedral coordination sphere because they will interact with the different d orbitals in different ways.

> *Ligand Field Theory looks at the effect of donor atoms on the energy of d orbitals in the metal complex.*
>
> *The effect depends on the coordination geometry of the ligands.*

A simple octahedral case

Let's start with an example of six ligand s-orbitals in an octahedral coordination structure. Assume the six ligands all lie along the x, y and z axes and that they interact with the metal using *just* their s orbitals (see Figure 6.11.1).

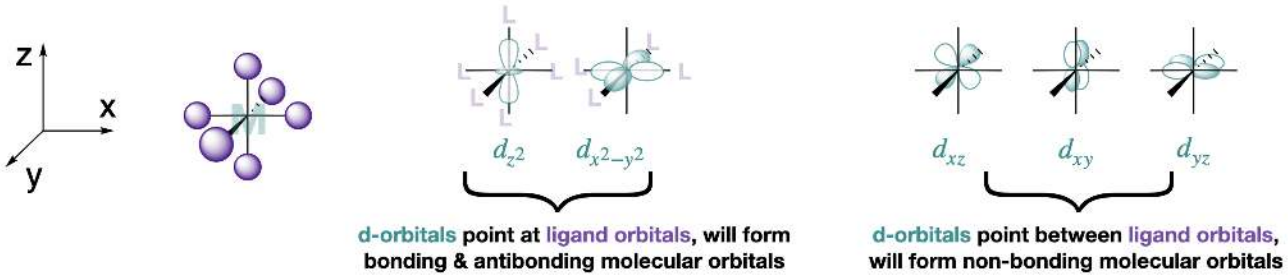


Figure 6.11.1: An octahedral arrangement of ligand s-orbitals (purple) around a central metal (teal). Two of the metal d-orbitals ($d_{x^2-y^2}$ and d_{z^2}) are compatible to bond with ligand s-orbitals, while the other three (d_{xy}, d_{xz}, d_{yz} cannot form productive interactions with ligand s-orbitals (CC-BY-NC-SA; Kathryn Haas).

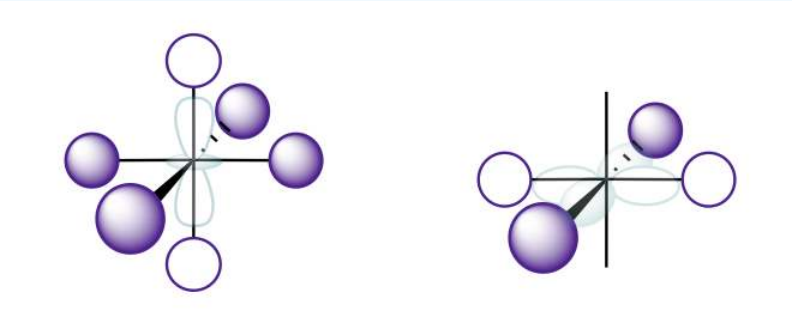
Because the ligand s orbitals lie on the axes, there are two d orbitals that will form productive interactions with these ligands: the $d_{x^2-y^2}$ which has lobes that point directly along the x and y axes, and the d_{z^2}, which has lobes that point along the z axis and along the xy plane. The ligand s orbitals have two SALCs with appropriate symmetry to interact with these two metal d-orbitals. However, the remaining three orbitals, the d_{xy}, d_{xz}, and d_{yz}, cannot form productive interactions with ligand s-orbitals.

Exercise 6.11.1

Sketch the two ligand SALCs that would interact with the d-orbitals, as shown in Figure 6.11.1. What is the symmetry of these SALCs under the octahedral point group?

Answer

The sketches are shown below, where the purple lobes show the group orbital and the teal transparent orbital in the center is the d-orbital with compatible symmetry. These sketches were drawn simply by matching the symmetry of the central metal orbital. A full explanation for how to systematically generate such sketches is described in a previous chapter. The octahedral character table tells us that the (d_{x^2-y^2}\) and d_{z^2} orbitals transform together with e_g symmetry. Thus, the two SALCs sketched below would also transform with e_g symmetry.



The metal $d_{x^2-y^2}$ and d_{z^2} will combine with the e_g SALCs (see exercise above) to form new bonding and antibonding molecular orbitals. A simplified drawing of this interaction, which forms bonding and antibonding molecular orbitals is shown below in Figure **6.11.2**. There are also for other ligand SALCs that will interact with s and p orbitals, but for the moment we're not going to worry about them.

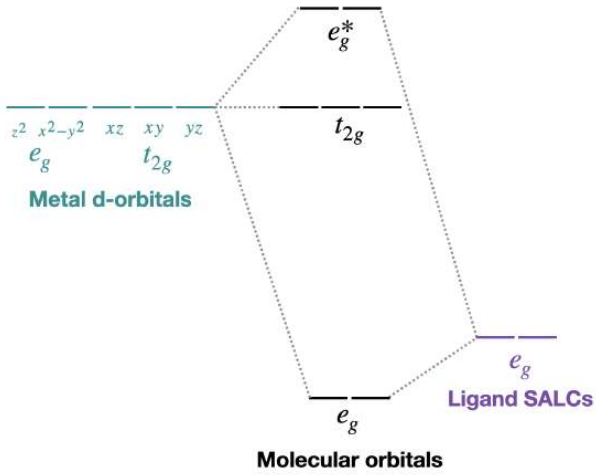


Figure **6.11.2**: Diagram of metal d orbitals (left) and ligand e_g SALCs (right) along with their relative energies. The orbitals in the middle represent the molecular orbitals: there is a set of bonding e_g, a set of antibonding e_g^*, and set of non-bonding t_{2g} orbitals. The metal d-orbitals are considered to be "split" into the t_{2g} and e_g^* molecular orbitals, while the bonding e_g have mostly ligand character (this is all based on relative energies of molecular orbitals compared to metal and ligand atomic orbtials. Energy increases from bottom to top. (CC-BY-NC-SA; Kathryn Haas)

Now, remember that metals usually have d electrons that are much higher in energy than those on typical donor atoms (like oxygen, sulfur, nitrogen or phosphorus). That means the antibonding combinations will be much closer in energy to the original d orbitals, because both are relatively high in energy. The bonding combination will be much closer in energy to the original ligand orbitals, because these ones are all relatively low in energy.

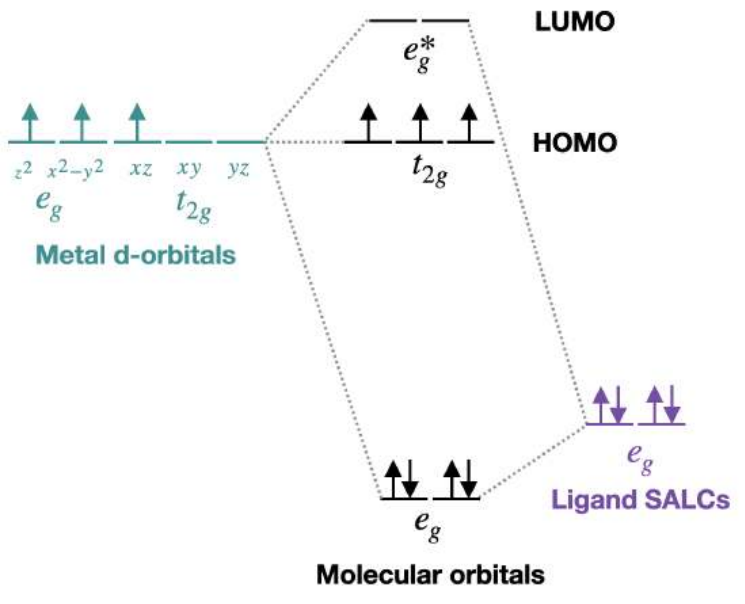
That energetic similarity generally translates into a similarity in shape and location as well. In other words, the antibonding combination between a d orbital and a ligand orbital is a lot like the original d orbital. The bonding combination is more like the original ligand orbital than the original d orbital. Because of those similarities, inorganic chemists often refer to those antibonding orbitals as if they were still the original d orbitals.

Exercise 6.11.1

Use the diagram in Figure **6.11.2**. Fill in the diagram for a d^3 metal complex. Identify the froteir orbtials (the HOMO and the LUMO).

Answer

When filling in electrons to this diagram we assume that each ligand bonds to the metal by donating two electrons; two SALCs results in four ligand electrons to add to the system. The metal has three d orbitals according to the description. The molecular orbitals should then be filled starting with the lowest energy orbitals. The HOMO-LUMO gap is between the t_{2g} non-bonding and e_g^* antibonding orbitals:



Summary for simple octahedral case

- Assume the six ligands all lie along the x, y and z axes.
- The $d_{x^2-y^2}$ and the d_{z^2} orbitals point at the ligands along the axes.
- These two orbitals "become" antibonding orbitals and are thus "raised" relatively high in energy.
- These orbitals are called the "$\mathbf{e_g}$" set of orbitals due to their symmetry under the octahedral point group.

On the other hand, the other three d orbitals, the d_{xy}, d_{xz} and d_{yz}, all lie *between* the donor ligands, rather than hitting them head-on. These orbitals will interact less strongly with the donor electrons.

- The d_{xy}, d_{xz} and d_{yz} orbitals all lie between the bond axes.
- These three orbitals will be changed in energy only a little.
- These orbitals are more like non-bonding orbitals.
- These orbitals are sometimes called the "$\mathbf{t_{2g}}$" set of orbitals.

Remember, only the energy of the *electrons* affects the overall energy of the system. The unoccupied d orbitals are raised in energy, but the occupied orbitals go down in energy (or else stay the same).

Apart from the stabilization of the complex, there is another consequence of this picture. What we are left with is two distinct sets of d energy levels, one lower than the other. That will have an effect on the electron configuration at the metal atom in the complex. In other words, there will be cases where electrons could be paired or unpaired, depending on how these orbitals are occupied.

Take the case of the biologically important iron(II) ion. It has a d^6 valence electron configuration. In less formal parlance of inorganic chemistry, "iron(II) is d^6." In an iron(II) ion all alone in space, all the d orbitals would have the same energy level. We would put one electron in each orbital, and have one left. The left over electron would need to pair up in one of the d orbitals (Notice that, in the chemistry of transition metal *ions*, the valence s and p orbitals are always assumed to be unoccupied).

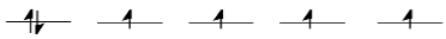


Figure **6.11.5**:

Things are very different in an octahedral complex, like $K_4[Fe(CN)_6]$. In that case, the d orbitals are no longer at the same energy level. There are two possible configurations to consider.

In one case, one electron would go into each of the lower energy d orbitals. A choice would be made for the fourth electron. Does it go into the higher energy d orbital, or does it pair up with one of the lower energy d electrons? The choice depends on how much higher in energy the upper d orbitals are, compared to how much energy it costs to put two electrons in the same d orbital.

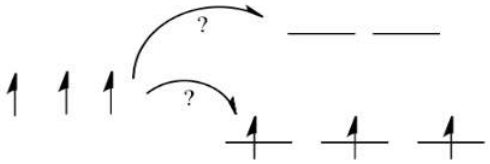


Figure **6.11.6**:

If the "d orbital splitting energy" is pretty low, so that the two sets of d orbitals are still pretty similar in energy, the next electron can go into a higher orbital. Pairing would not be required until the final electron. Overall, that would leave four unpaired electrons, just like in the case of a lone metal ion in space. This is called the "high-spin" case, because electrons can easily go into the higher orbital.

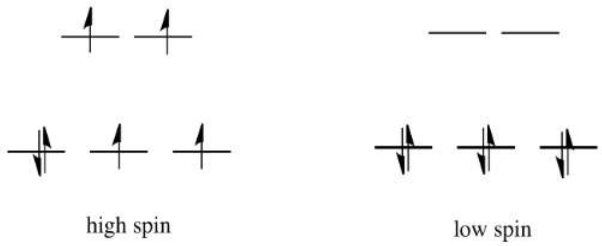


Figure **6.11.7**:

If the d orbital splitting energy is too high, the next electron must pair up in a lower orbital. All three remaining electrons pair up, and so there are no unpaired electrons in the complex. This is called the "low-spin" case, because electrons more easily pair up in the orbital.

So the overall rule is that if the energy to pair up the electrons is greater than the energy needed to get to the next level, the electron will go ahead and occupy the next level.

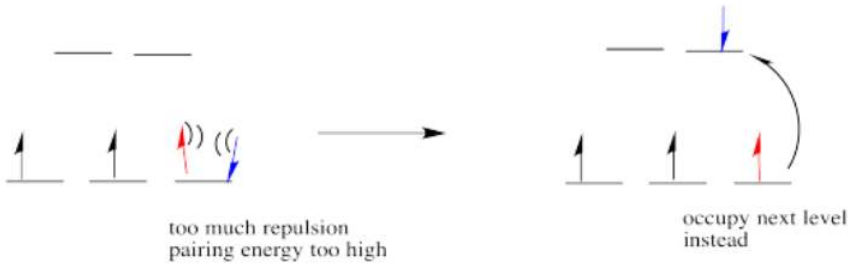


Figure **6.11.8**:

However, if the energy it takes to get to the next level is more than it would cost to pair up, the electrons will just pair up instead.

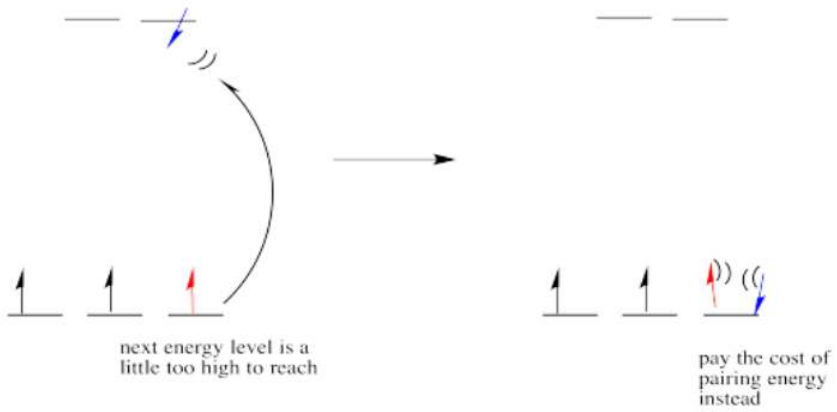


Figure **6.11.9**:

> *The electron configuration can be "high spin" or "low-spin", depending on how large the energy splitting is between the two sets of d orbitals.*

The difference between the high-spin case and the low-spin case is significant because unpaired electrons affect the magnetic properties of a material. The low-spin case would be diamagnetic, resulting in no interaction with a magnetic field. However, the high-spin case would be paramagnetic, and would be attracted to a magnetic field.

It turns out $K_4[Fe(CN)_6]$ is diamagnetic. Thus, it is pretty clear that it is a low-spin complex. The energy difference between the two d orbital levels is relatively large in this case.

In addition to influencing magnetic properties, whether a complex is high- or low-spin also influences reactivity. Compounds with high-energy d electrons are generally more labile, meaning they let go of ligands more easily.

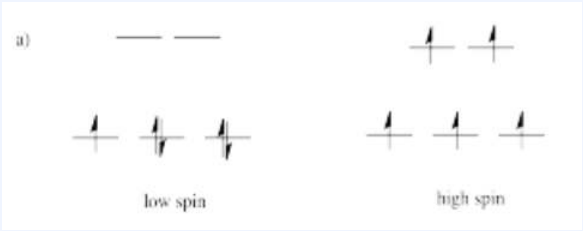
- electron configuration influences magnetic properties
- electron configuration influences lability (how easily ligands are released)

Exercise 6.11.1

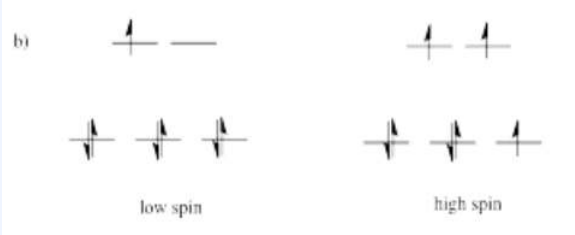
Draw both high spin and low spin d-orbital splitting diagrams for the following ions in an octahedral environment and determine the number of unpaired electrons in each case.

a) Mn^{2+} b) Co^{2+} c) Ni^{2+} d) Cu^{+} e) Fe^{3+} f) Cr^{2+} g) Zn^{2+}

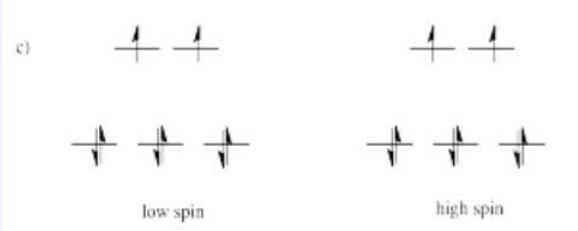
Answer a)



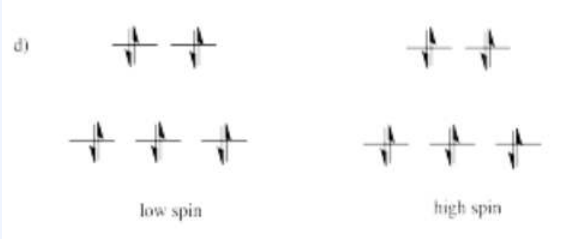
Answer b)



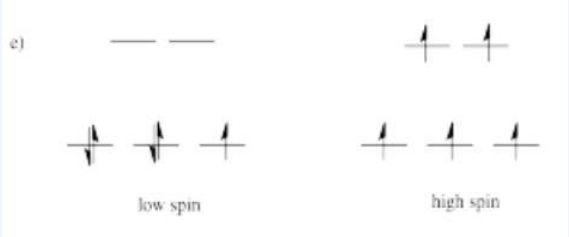
Answer c)



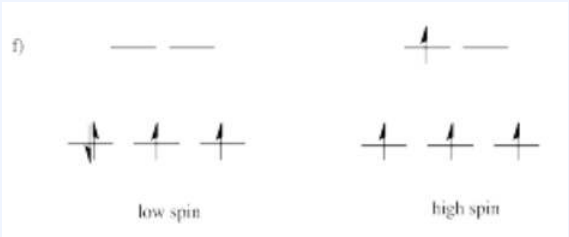
Answer d)



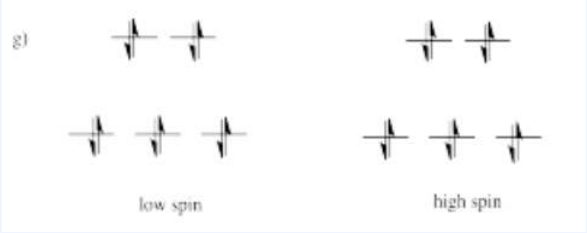
Answer e)



Answer f)



Answer g)



Exercise 6.11.2

The d orbital splitting diagram for a tetrahedral coordination environment is shown below. Given this diagram, and the axes in the accompanying picture, identify which d orbitals are found at which level. In the picture, the metal atom is at the center of the cube, and the circle represent the ligands.

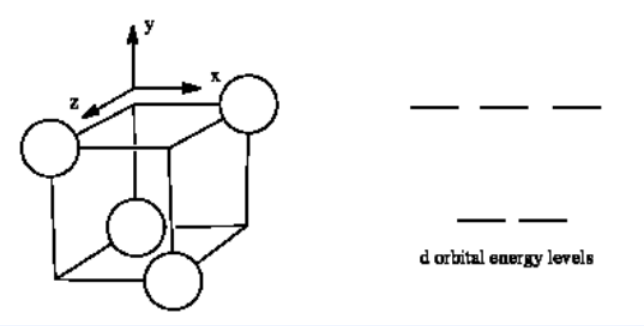
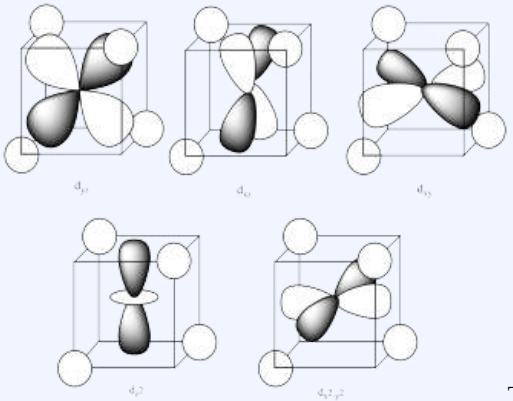


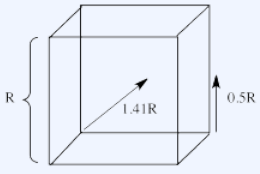
Figure 6.11.17:

Answer

The three orbitals shown above interact a little more strongly with the ligands. The three orbitals shown below interact a little more weakly.



The reason for the difference in the interaction has to do with how close the nearest lobe of a d orbital comes to a ligand. There are really two possible positions: the face of a cube or the edge of a cube. If the ligands are at alternating corners of the cube, then the orbitals pointing at the edges are a little closer than those pointing at the faces of the cube.



$$\sqrt{R^2 + R^2} = 0.5\sqrt{2R^2} = 0.705R$$

Exercise 6.11.3

Typically, the d orbital splitting energy in the tetrahedral case is only about 4/9 as large as the splitting energy in the analogous octahedral case. Explain why it is smaller for the tetrahedral case.

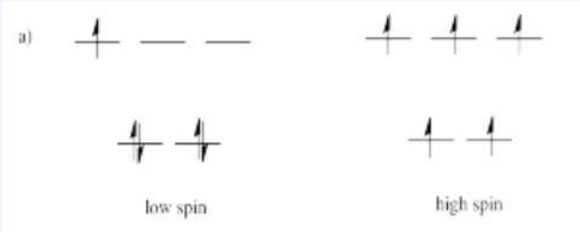
Answer

The ligands do not overlap with the d orbitals as well in tetrahedral complexes as they do in octahedral complexes. Thus, there is a weaker bonding interaction in the tetrahedral case. That means the antibonding orbital involving the d electrons is not raised as high in energy, so the splitting between the two d levels is smaller.

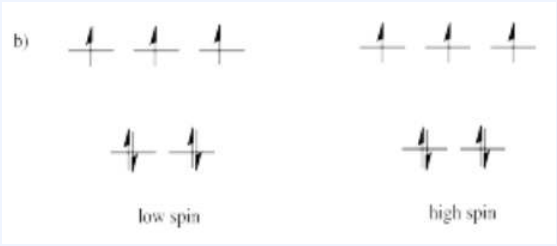
Exercise 6.11.4

Suppose each of the ions in Exercise **6.11.1** (CC8.1) were in tetrahedral, rather than octahedral, coordination environments. Draw the d orbital diagrams for the high spin and the low spin case for each ion.

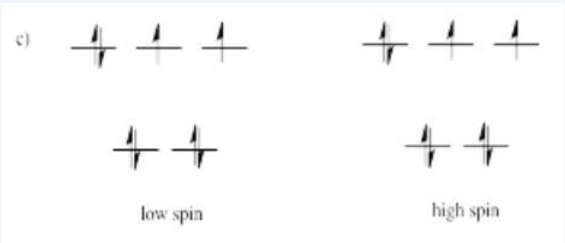
Answer a)



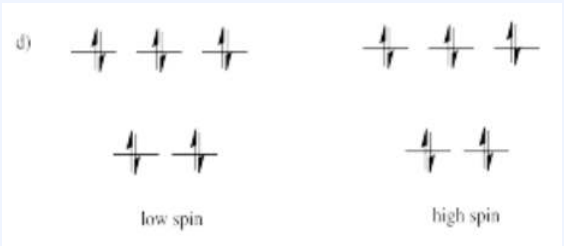
Answer b)



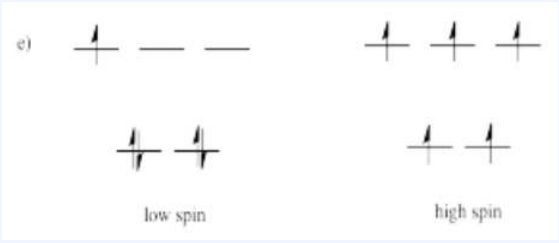
Answer c)



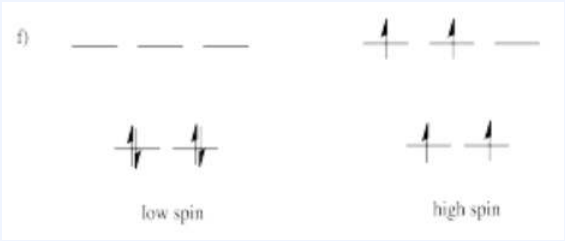
Answer d)



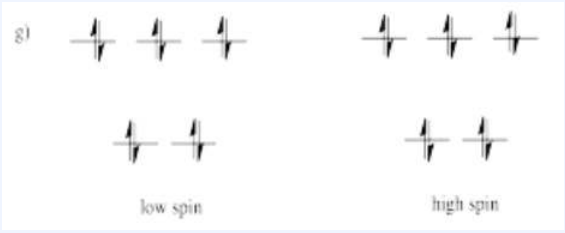
Answer e)



Answer f)



Answer g)



Exercise 6.11.5

Usually, tetrahedral ions are high spin rather than low spin. Explain why.

Answer

Because the d orbital splitting is much smaller in the tetrahedral case, it is likely that the energy required to pair two electrons in the same orbital will be greater than the energy required to promote an electron to the next energy level. In most cases, the complex will be high spin.

Exercise 6.11.6

The d orbital splitting diagram for a square planar environment is shown below. Given this diagram, and the axes in the accompanying picture, identify which d orbitals are found at which level.

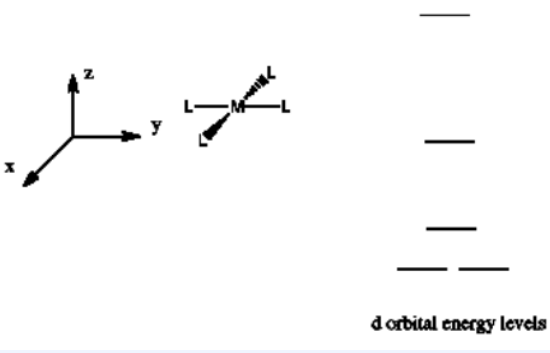
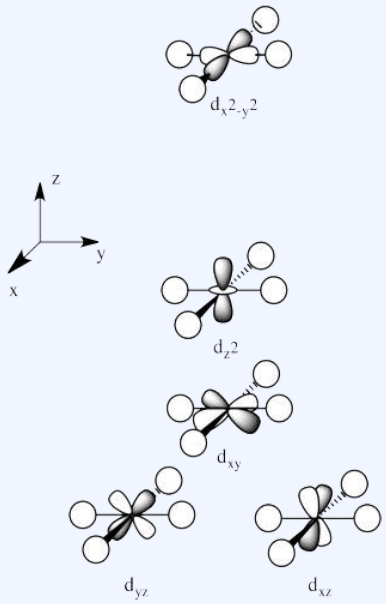


Figure **6.11.18**:

Answer

The orbitals are shown in order of energy.



Attribution

Chris P Schaller, Ph.D., (College of Saint Benedict / Saint John's University)

This page titled 6.11: MO Diagram for bonding in [M(NH3)6]n+ is shared under a CC BY-NC-SA license and was authored, remixed, and/or curated by Kathryn Haas.

6.12: MO Diagram for bonding in [M(H2O)6]n+

Extension of Crystal Field Theory

Experimentally it is known that the nature of the ligand plays an important role in the magnitude of the crystal field splitting in metal complexes and can determine whether a complex is high or low spin. Empirically ligands can be ordered in the spectrochemical series, but using crystal field theory we cannot rationalize where ligands fall in the series. For example, why is the neutral CO one of the strongest field ligands in the series while the anionic halogens are weak field ligands? To understand why ligands behave differently we have to consider how ligand orbitals interact with the metal d orbitals. Ligand field theory is essentially a combination between crystal field theory and molecular orbital theory where we focus only on the orbital overlap between the metal d orbitals and select ligand orbitals (rather than considering all of the valence orbitals on both the metal and ligand)

Metal-Ligand σ Bonding

The bond between a metal and a ligand is primarily a Lewis acid-base interaction where the ligand is a Lewis base and donates a pair of electron to the metal, the Lewis acid. This interaction forms a coordinate covalent bond. As with molecular orbital theory we have to decide how (or if) the ligand lone pairs will overlap with each of the d orbitals, and what type of bonding will be formed In an octahedral complex the ligands and their lone pairs lie along the x, y, and z axes. As shown in Figure **6.12.1**, the two on axis d orbitals ($d_{x^2-y^2}$ and d_{z^2}) have to correct orientation to form sigma bonds with the ligands. With the three off axis d orbitals (d_{xy}, d_{xz}, and d_{yz}) the ligand lone pair overlaps with a node in these orbitals (Figure **6.12.1***c*). This means there is no net overlap and no bonding (or antibonding) molecular orbital can be formed.

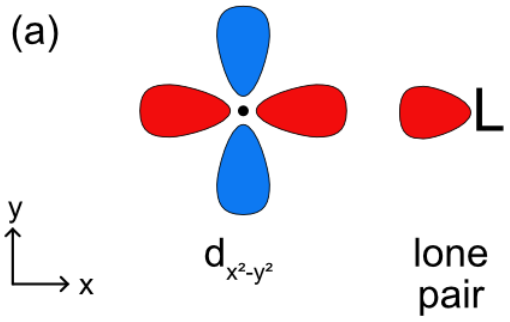


Figure **6.12.1*a***: Overlap between a ligand lone pair orbital and the metal $d_{x^2-y^2}$ orbital to form a sigma bond (CC BY-NC-SA, Catherine McCusker)

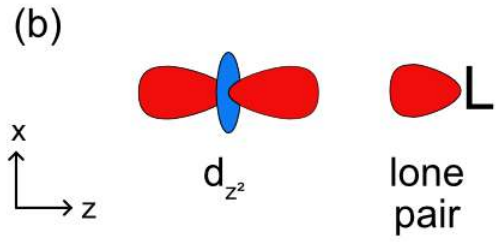


Figure **6.12.1*b***: Overlap between a ligand lone pair orbital and the metal d_{z^2} orbital to form a sigma bond (CC BY-NC-SA, Catherine McCusker)

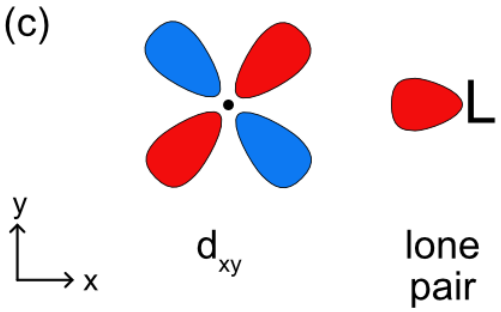


Figure **6.12.1*c***: There is no net overlap between the ligand lone pair orbital and the d_{xy} metal orbital, so this is a non bonding interaction (CC BY-NC-SA, Catherine McCusker)

Knowing this, we can construct a ligand field splitting diagram (a simplified molecular orbital diagram) (Figure **6.12.2**). In the free metal ion all 5 of the d orbitals are degenerate and before they interact with the metal all 6 of the ligand lone pair orbitals are at the same energy as well. Generally, based on electronegativity the ligand lone pair orbitals will be lower in energy than the metal d orbitals. When the ligand lone pairs interact with metal d orbitals the on axis set of d orbitals ($d_{x^2-y^2}$ and d_{z^2}) will form sigma bonding (e_g) and sigma antibonding (e_g*) molecular orbitals. The off axis set of d orbitals are nonbonding and are not stabilized or destabilized by the ligand lone pairs. Unlike a complete molecular orbital diagrams, a ligand field diagram won't necessarily have the same number of molecular orbitals as atomic orbitals becuse not every possible bonding interaction is included (for example, any overlap between the ligand orbitals and the metal s and p orbitals are not included). As in crystal field theory we can define an octahedral ligand field splitting energy (Δ_o), which will be the difference between the two molecular orbitals with the most metal d orbital character. In Figure **6.12.2** the t_{2g} set of d orbitals are nonbonding and therefore 100% metal character. The e_g bonding orbital is closer in energy to the ligand lone pairs and will have a higher % contribution from the ligands, and the e_g* antibonding orbital is closer in energy to the metal d orbitals and will have a higher % contribution from the metal. The relevant energy difference is between the t_{2g} and e_g* orbitals, as highlighted in green in Figure **6.12.2**. The splitting energy will increase as there is a stronger interaction between the metal and ligand orbitals (based on the criteria discussed previously) and the e_g* is more destabilized.

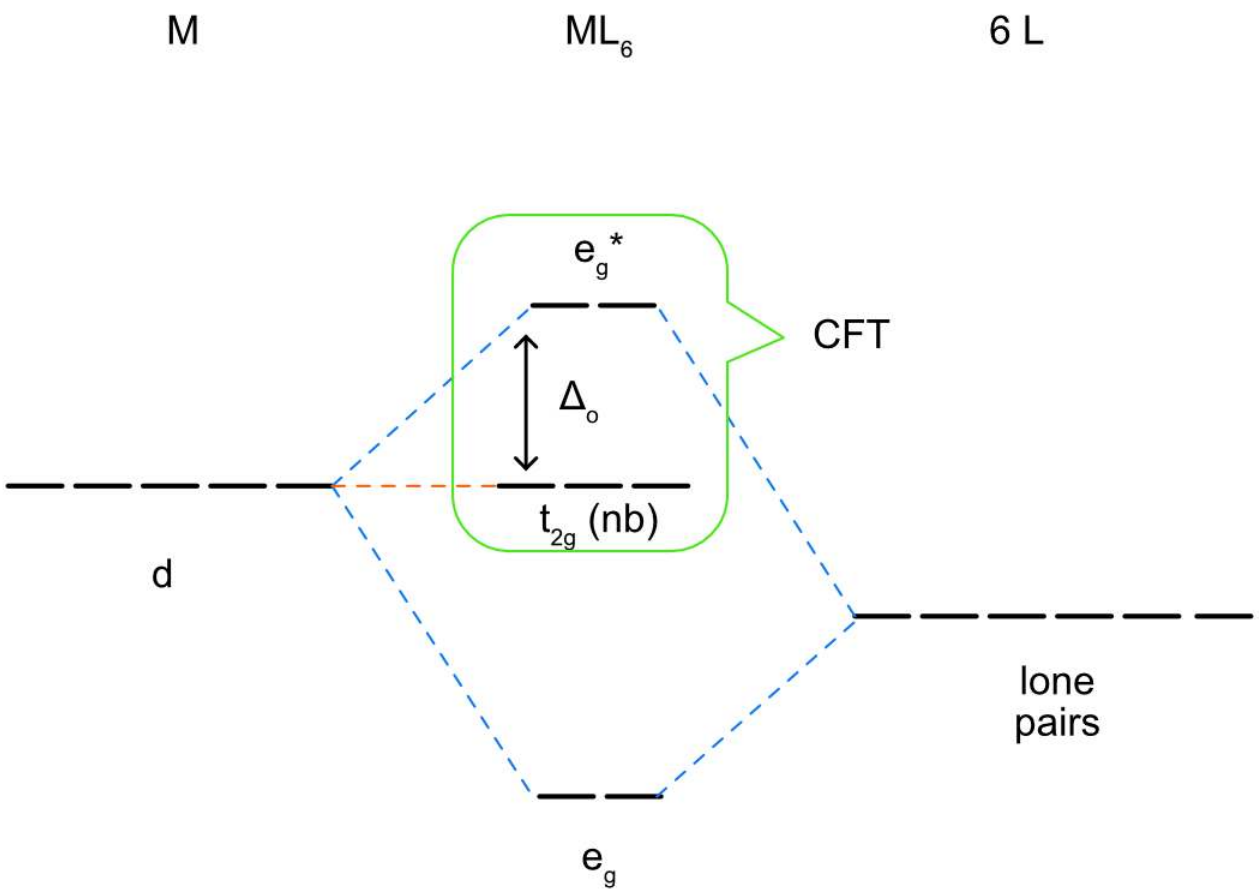


Figure **6.12.2**: Octahedral ligand field splitting diagram for only sigma bonding. The $d_{x^2-y^2}$ and d_{z^2} metal orbitals form sigma bonding (e_g) and antibonding molecular orbitals (e_g*). The d_{xy}, d_{xz}, and d_{yz} orbital are nonbonding (t_{2g} (nb)). The green outline highlights the portion of the diagram that is equivalent to the crystal field splitting diagram. (CC BY-NC-SA; Catherine McCusker)

Metal-Ligand π Bonding

In addition to sigma bonding, some ligands have orbitals available which can form π bonds with metals as well. These could include p orbitals on a single donor atom such as a halogen ion or π bonding or antibonding molecular orbitals on a molecular ligand. To determine how π bonding will change the ligand field splitting picture in Figure **6.12.2**, we will visualize how a ligand p orbital will interact with the metal d orbitals. The $d_{x^2-y^2}$ and d_{z^2} orbitals do not have the correct symmetry to form any type of bond with a ligand p orbital as shown in Figures **6.12.3***a* – *b* The d_{xy}, d_{xz}, and d_{yz} orbitals all have the correct symmetry to form π bonds with a ligand p orbital (Figure **6.12.3***c*).

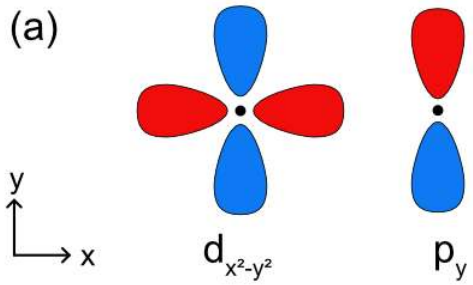


Figure **6.12.3***a*: There is no net overlap between the ligand p orbital and the $d_{x^2-y^2}$ metal orbital, so this is a non bonding interaction (CC BY-NC-SA, Catherine McCusker)

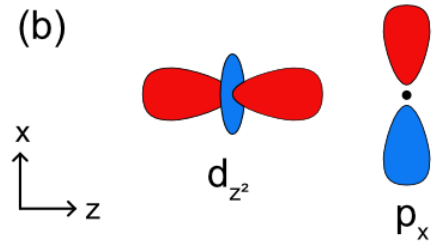


Figure **6.12.3***b*: There is no net overlap between the ligand p orbital and the d_{z^2} metal orbital, so this is a non bonding interaction (CC BY-NC-SA, Catherine McCusker)

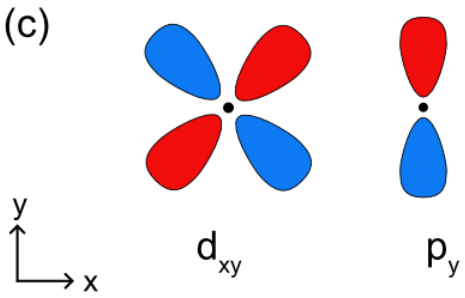


Figure **6.12.3***c*: Overlap between a ligand p orbital and the metal d_{xy} orbital to form a π bond (CC BY-NC-SA, Catherine McCusker)

Unlike metal-ligand σ bonding, where electrons are always donated from the ligand to the metal, electrons in metal-ligand π bonding can be donated from either the metal or the ligand depending on the nature of the orbitals involved. In cases where ligands have empty p or π symmetry orbitals that are close in energy to the metal d orbitals, they can accept electrons from a filled metal orbital. This is also known as π backbonding because the direction of electron donation is opposite of that found in sigma metal ligand bonding. These ligands are called π acceptor ligands. In cases where ligands have filled p or π symmetry orbitals that are close in energy to the metal d orbitals, they can donate electrons to an empty metal orbital. These ligands are called π donor ligands.

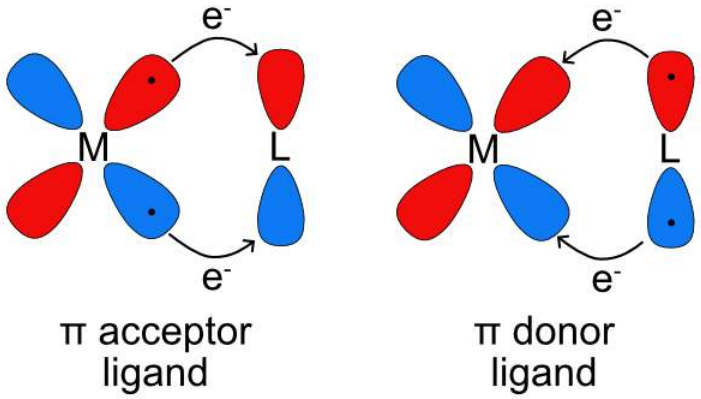


Figure **6.12.4**: Illustration of metal-ligand π bonding with π acceptor and donor ligands. Filled orbitals are represented with black dots. (CC BY-NC-SA, Catherine McCusker)

π Acceptors

Ligands that are π acceptors have empty, low energy π symmetry orbitals available to accept electrons from the metal center. Most often this is a π^* antibonding molecular orbital but it could also be an empty p orbital. Due to the aufbau principle, these empty orbitals will be higher in energy than any filled lone pairs on the ligands and will also generally be higher energy than the metal d orbitals. Similar to multiple bonding in main group compounds π bonding always occurs in combination with sigma bonding so in the ligand field splitting diagram of metal-ligand bonding with a π acceptor ligand the lone pairs for sigma bonding must be included as well as the empty orbitals for π bonding. As seen in Figure **6.12.3**, the $d_{x^2-y^2}$ and d_{z^2} orbitals do not overlap with the ligand p orbitals. The on axis d orbitals will form sigma bonding (e_g) and sigma antibonding (e_g^*) molecular orbitals. Unlike the sigma bonding only diagram, the off axis d orbitals (d_{xy}, d_{xz}, and d_{yz}) overlap with the ligand p orbitals to form π bonding (t_{2g}) and π antibonding (t_{2g}^*) molecular orbitals as seen in Figure **6.12.5**. Rather than being nonbonding, like in the sigma bonding only picture, the metal based t_{2g} molecular orbital is bonding. This increases the energy difference between the t_{2g} and e_g^* and therefore increases Δ_o.

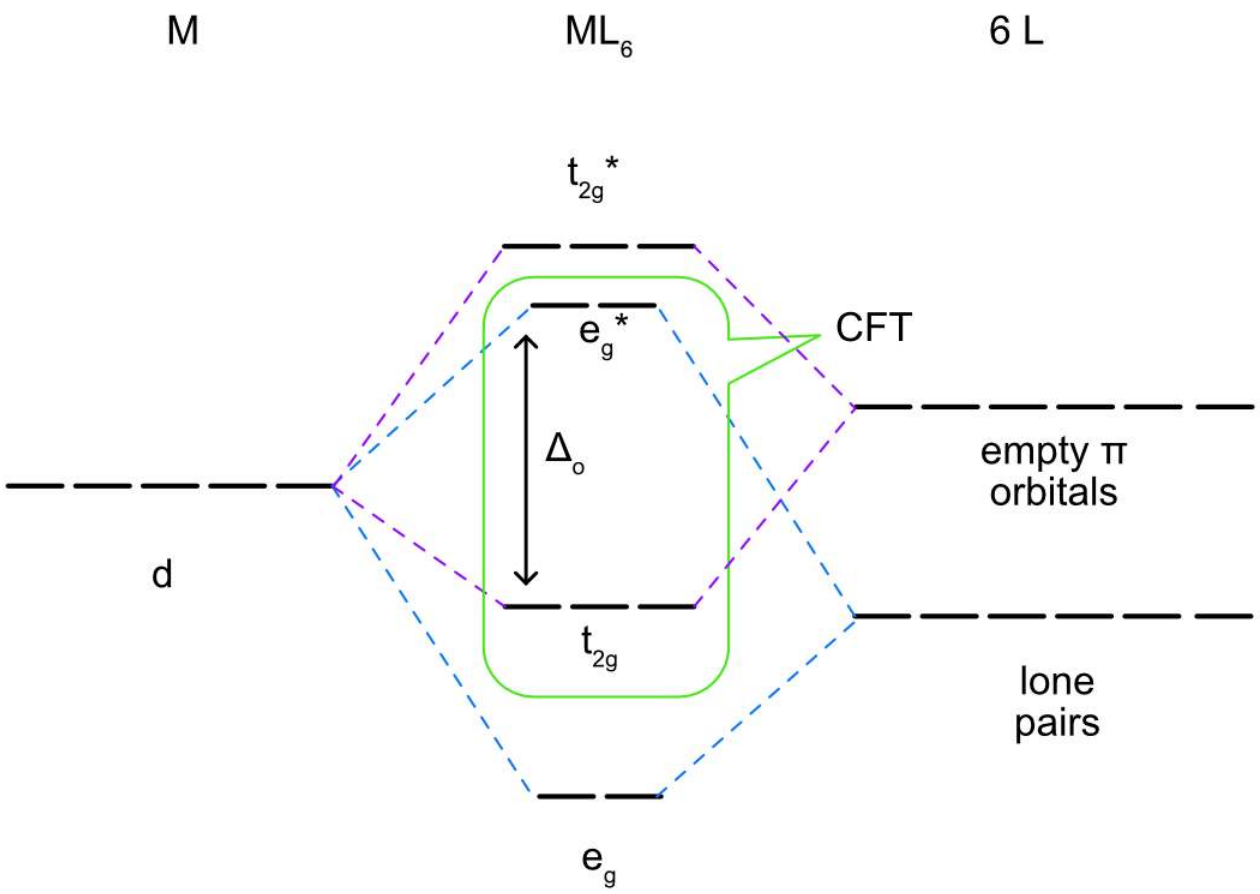


Figure 6.12.5: Octahedral ligand field splitting diagram with a π acceptor ligand. The $d_{x^2-y^2}$ and d_{z^2} metal orbitals form sigma bonding (e_g) and antibonding molecular orbitals (e_g*) with the ligand lone pairs. The d_{xy}, d_{xz}, and d_{yz} orbital form pi bonding (t_{2g}) and pi antibonding molecular orbitals (t_{2g}*) with the empty π symmetry orbitals. The green outline highlights the portion of the diagram that is equivalent to the crystal field splitting diagram. (CC BY-NC-SA; Catherine McCusker)

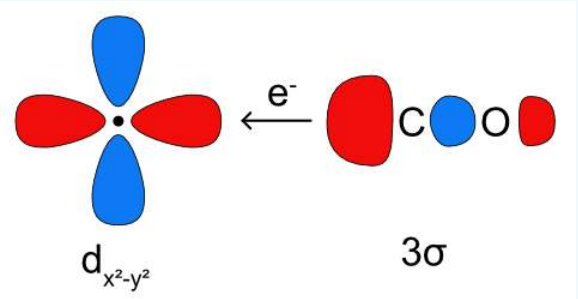
Exercise 6.12.1

Carbon monoxide is one of the most common, and strongest π acceptor ligands in inorganic chemistry. Refer to the molecular orbital diagram of CO and sketch likely metal-ligand orbital interactions for both sigma and pi bonding in a metal-CO complex. Indicate the direction of electron donation in both cases.

Answer

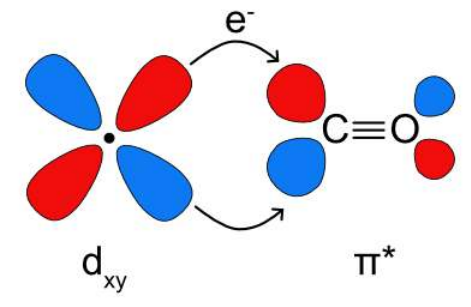
Sigma bonding:

Sigma bonding between a metal ion and a CO ligand involves overlap between the HOMO of CO (3σ) and the metal $d_{x^2-y^2}$ or d_{z^2} orbitals. Electrons are donated from the ligand to the metal.



Pi bonding:

Pi bonding between a metal ion and CO ligand involves overlap between the LUMO of CO (π*) and the metal d_{xy}, d_{xz}, or d_{yz} orbitals. Electrons are donated from the metal to the ligand.



π Donor Ligands

Ligands that are π donors have filled π symmetry orbitals that are high enough in energy to donate electrons to the metal center. Most often this is a filled p orbital, but it could also be a π bonding molecular orbital. As lone pairs are generally the highest occupied orbitals is a molecule, the filled π orbitals will be lower in energy as seen in Figure **6.12.6**. The sigma interaction between the ligand lone pairs and the metal $d_{x^2-y^2}$ and d_{z^2} remain the same as previously described, forming the e_g bonding and e_g* antibonding molecular orbitals. The d_{xy}, d_{xz}, and d_{yz} overlap with the filled π orbitals to form π bonding (t_{2g}) and π antibonding (t_{2g}*) molecular orbitals. The difference between the *pi* acceptor and donor ligands is the energy and character of the t_{2g} and t_{2g}* molecular orbitals. In the π acceptor case above, the t_{2g} orbital is above the e_g and has a higher contribution from the metal and the t_{2g}* is above the e_g* and has a higher contribution from the ligand. In the π donor case the opposite is true. The t_{2g} orbital is below the e_g and has a higher contribution from the ligand and the t_{2g}* is below the e_g* and has a higher contribution from the metal. In this case Δ_o is smaller than in the sigma only picture because the t_{2g} symmetry molecular orbital has gone from nonbonding to antibonding and the energy difference between t_{2g}* and e_g* is smaller.

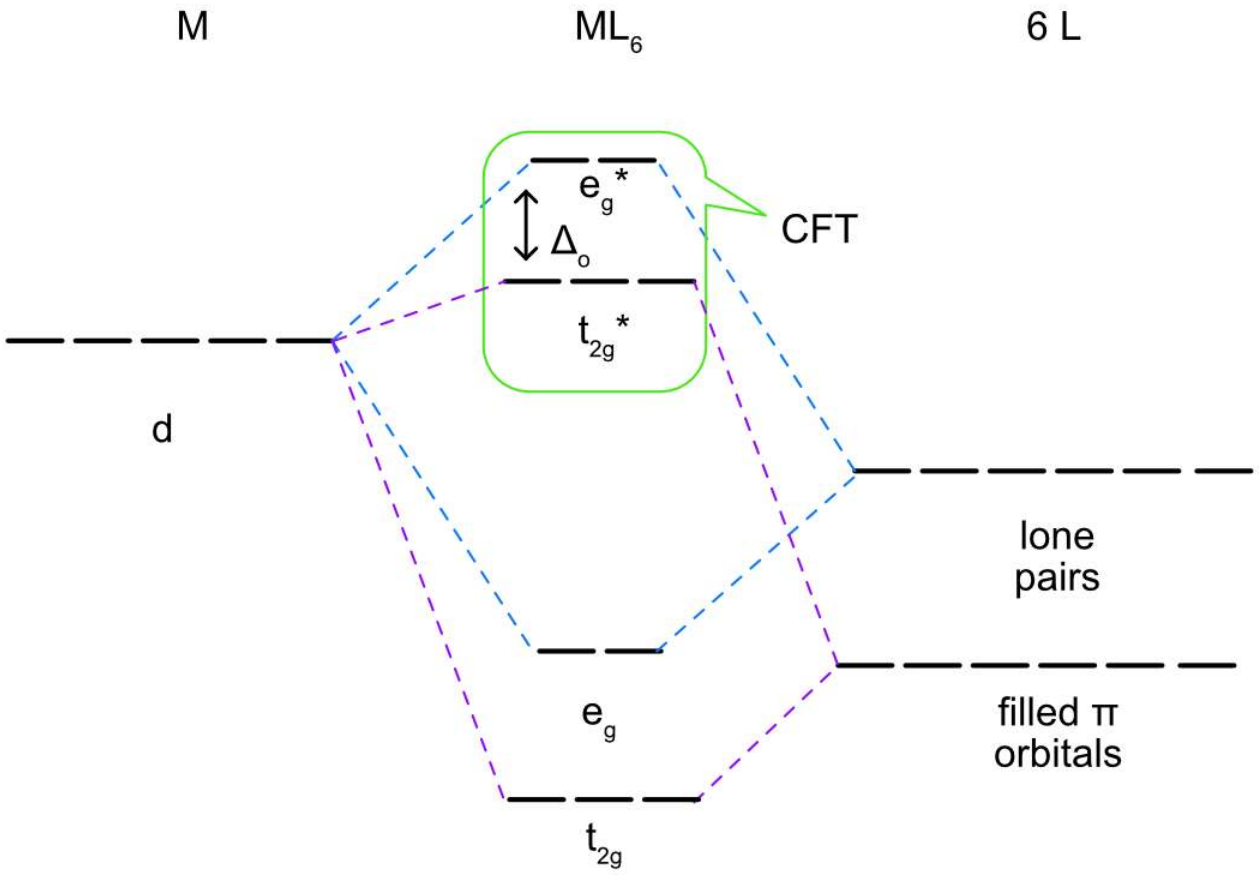


Figure **6.12.6**: Octahedral ligand field splitting diagram with a π donor ligand. The $d_{x^2-y^2}$ and d_{z^2} metal orbitals form sigma bonding (e_g) and antibonding molecular orbitals (e_g*) with the ligand lone pairs. The d_{xy}, d_{xz}, and d_{yz} orbital form pi bonding (t_{2g}) and pi antibonding molecular orbitals (t_{2g}*) with the filled π symmetry orbitals. The green outline highlights the portion of the diagram that is equivalent to the crystal field splitting diagram. (CC BY-NC-SA; Catherine McCusker)

The Spectrochemical Series

As discussed above, crystal field theory alone can't distinguish the behaviors of different ligands or explain why some ligands inherently produce larger splittings than others. Armed with ligand field theory we can now revisit the spectrochemical series and explain why ligands fall where they do within the series.

Strong field ligands

Strong field ligands are ones that produce large splittings between the d orbitals and form low spin complexes. Examples of strong field ligands include CO, CN^-, and NO_2. From a ligand field theory perspective all three of these ligands have strong π bonds (either double or triple bonds) and have empty π* molecular orbitals available for backbonding. Strong field ligands are both sigma donors (all ligands are sigma donors) and π acceptors. π backbonding between a metal and a ligand stabilizes the metal based t_{2g} molecular orbital and increases Δ_o.

Weak field ligands

Weak field ligands are ones that produce small splittings between the d orbitals and form high spin complexes. Examples of weak field ligands include the halogens, OH^- and H_2O. From a ligand field perspective these ions or molecules all have filled orbitals

which can π bond with the metal d orbitals. In the case of the halogens these are filled p orbitals and in the case of OH^- and H_2O these are lone pairs which are perpendicular to the metal-ligand bond. Weak field ligands are both sigma donors and π donors. The π donation from the ligand to the metal destabilizes the metal based t_{2g} molecular orbital and decreases Δ_o.

Intermediate field ligands

Intermediate field ligands produce intermediate splittings between the d orbitals and could form high or low spin complexes. Examples of intermediate field ligands include NH_3 or ethylenediamine (en). From a ligand field perspective these ligands only have a single lone pair available for sigma bonding. All of the other orbitals on nitrogen are used for sigma bonding to the H or C atoms within the molecule. Intermediate ligands are those which are only sigma donors, and are not π donors or π acceptors. In this case the t_{2g} symmetry d orbitals are nonbonding and the Δ_o is determined by the strength of the metal ligand sigma interaction (and amount of destabilization of the e_g* molecular orbital)

This page titled 6.12: MO Diagram for bonding in [M(H2O)6]n+ is shared under a CC BY-NC-SA 4.0 license and was authored, remixed, and/or curated by Catherine McCusker.

- **9.5: Ligand Field Theory** by Catherine McCusker is licensed CC BY-NC-SA 4.0.

6.13: Spectrochemical Series for Ligands

The Nature of the Ligands

Experimentally, it is found that the Δ_o observed for a series of complexes of the same metal ion depends strongly on the nature of the ligands. For a series of chemically similar ligands, the magnitude of Δ_o decreases as the size of the donor atom increases. For example, Δ_o values for halide complexes generally decrease in the order $F^- > Cl^- > Br^- > I-$ because smaller, more localized charges, such as we see for F^-, interact more strongly with the d orbitals of the metal ion. In addition, a small neutral ligand with a highly localized lone pair, such as NH_3, results in significantly larger Δ_o values than might be expected. Because the lone pair points directly at the metal ion, the electron density along the M–L axis is greater than for a spherical anion such as F^-. The experimentally observed order of the crystal field splitting energies produced by different ligands is called the spectrochemical series, shown here in order of decreasing Δ_o:

$$\underset{\text{strong-field ligands}}{CO \approx CN^- > NO_2^-} > en > NH_3 > \underset{\text{intermediate-field ligands}}{SCN^- > H_2O > oxalate^{2-} > OH^- > F} > acetate^- > \underset{\text{weak-field ligands}}{Cl^- > Br^- > I^-}$$

The values of Δ_o listed in Table **6.13.1** illustrate the effects of the charge on the metal ion, the principal quantum number of the metal, and the nature of the ligand.

> *The largest Δ_os are found in complexes of metal ions from the third row of the transition metals with charges of at least +3 and ligands with localized lone pairs of electrons.*

Another factor that plays a key role in whether a transition metal complex is high- or low-spin is the nature of the ligands. The d orbital energy splitting is influenced by how strongly the ligand interacts with the metal. Ligands that interact weakly only produce little change in the d orbital energy levels, whereas ligands that interact strongly produce a larger change in d orbital energy levels. The spectrochemical series is a list of ligands based on the strength of their interaction with metal ions. Ligands are often listed from weaker to stronger ligands, something like this:

$$I^- < Br^- < S^{2-} < SCN^- < Cl^- < NO_3^- < N_3^- < F^- < OH^- < C_2O_4^{2-} < H_2O < NCS^- < CH_3CN < py < NH_3$$

$$< en < bipy < phen < NO_2^- < PPh_3 < CN^- < CO$$

in which py = pyridine; en = ethylenediamine; bipy = 2,2'-bipyridine; phen = 1,10-phenanthroline; SCN means the ligand is bound via sulfur and NCS via nitrogen. The list can vary from one metal ion to another, since some ligands bind preferentially to certain metals (as seen in hard and soft acid and base chemistry).

Exercise 6.13.1

What empirical trends can you see within the spectrochemical series? Are there any factors that make something a stronger field ligand?

Answer

The weaker donors include halides and oxygen donors. Nitrogen atom donors are mostly a little stronger than that. The strongest donors include carbon donors, especially with pi bonds.

The d orbitals that rise in energy in the presence of a ligand can be thought of as forming an antibonding molecular orbital combination with an orbital on the ligand. In addition, there would also be a bonding combination for this interaction. That bonding orbital would be more like the initial ligand orbital. This premise is based on the idea that a ligand orbital is initially lower in energy than the metal orbital, so a bonding combination between these two orbitals is more like the initial ligand orbital, both in energy and location. The d orbital is initially higher in energy than the ligand orbital, so an antibonding combination between these two orbitals is more like the initial d orbital, both in energy and location.

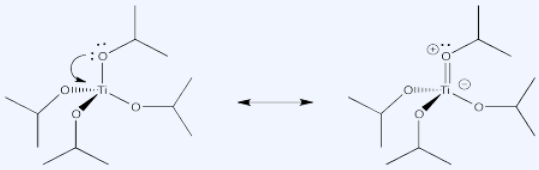
- When orbitals on two different kinds of atoms combine, the antibonding orbital is considered to be more like the orbital that was initially at higher energy.
- In this case, it is still close to a d orbital in energy, location, and shape.

- When orbitals on two different kinds of atoms combine, the bonding orbital is considered to be more like the orbital that was initially at lower energy.

Exercise 6.13.2

Suppose a ligand has more than one lone pair on the donor atom. The donor atom could share an extra pair of electrons with the metal, to form a double bond. This type of interaction is called pi-donation, because a π bond is formed (not to be confused with sigma donation from a π bond, as in alkene binding). Show an example using titanium isopropoxide $Ti(OiPr)_4$.

Answer

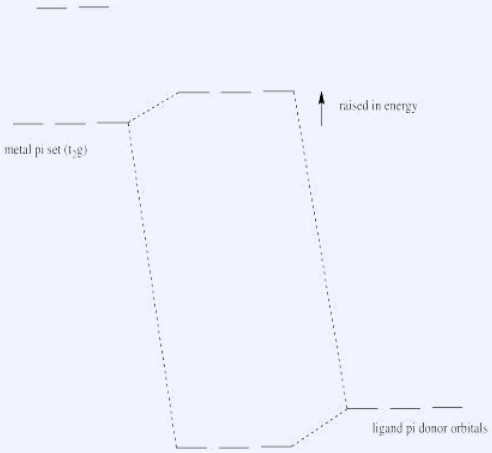


Exercise 6.13.3

In an octahedral environment, three of the d orbitals were not affected by sigma donation from the ligands. Show what happens to the energy level of these d orbitals in the presence of a π donor.

Answer

Pi donation raises the t_{2g} electrons (the d electrons of proper symmetry for pi overlap with the ligands in an octahedral geometry).



Exercise 6.13.4

Some ligands can accept a pair of electrons from the metal. An example is a carbonyl complex, which has a C=O π antibonding orbital that can interact with a d orbital.

a. Show the antibonding orbital on the carbonyl (CO) ligand.
b. Show how a metal d orbital can interact with this orbital.

Exercise 6.13.5

In the previous problem, a lower-energy atomic orbital on the metal interacts with a higher-energy antibonding orbital on the ligand. Show what happens to the energies of these two orbitals when they interact with each other.

Some of the trends we see in the spectrochemical series arise from pi-donating and pi-accepting effects in the ligand. Ligands that have additional lone pairs (other than the one that sigma donates) are π donors. π donors raise the otherwise non-bonding t_{2g} orbitals, because the lone pair on the ligand forms a π bond with the metal. The t_{2g} orbitals and the ligand lone pair orbitals form two new orbitals. The antibonding orbital is closer in energy to the high-energy d orbitals. The bonding orbital is closer in energy to the low-energy ligand orbital.

- π donation raises the t_{2g} set of d orbitals in energy.
- As a result, the d orbital splitting gets smaller.
- Also as a result, a complex with π donation is a little less stable than a complex without π donation.

This type of interaction can be seen in the following pictures (a tetrahedral case).

On the other hand, ligands in which the donor atom is already π bonding to another atom can accept π donation from the metal. This happens by donating an electron pair from a metal t_{2g} orbital into a $\pi*$ orbital on the ligand. In this case, because the $\pi*$ is an antibonding orbital, it is higher in energy than the metal d orbital (or the t_{2g} orbital). The resulting bonding orbital is more like the lower energy metal orbital, whereas the resulting antibonding orbital is more like the higher energy $\pi*$ orbital on the ligand.

- π accepting ligands lower the t_{2g} set of d orbitals in energy.
- As a result, the d orbital splitting gets larger.
- Also as a result, a complex with a π accepting ligand is a little more stable than a complex without a π accepting ligand.

This type of interaction can be seen in the following case (a tetrahedral complex).

The spectrochemical series gets its name because of a shift in a band of the UV-Vis spectrum when two similar complexes are compared that have two different ligands. The effect of the ligand on the d orbital splitting has an effect on the wavelength of light associated with a d orbital (filled) to d orbital (empty) electronic transition. This transition is actually not associated with a major absorption. However, because it often occurs in the region of visible light, it is associated with colored transition metal complexes.

Exercise 6.13.6

Explain what happens to the wavelength of light absorbed for the d-d transition when a chloride ligand on a metal complex is replaced with a hydroxide ligand.

Answer

Because chloride is a weaker ligand than hydroxide, the d orbital splitting gets smaller. A d-d transition would involve less energy, so it would move to longer wavelength (red shift).

Exercise 6.13.7

Predict whether each compound will be square planar or tetrahedral.

a. $[Zn(NH_3)_4]^{2+}$

b. $[NiCl_4]^{2+}$

c. $[Ni(CN)_4]^{2-}$

d. $[Ir(CO)(OH)(PCy_3)_2]^{2+}$; Cy = cyclohexyl

e. $[Ag(dppb)_2]^{+}$; dppb = 1,4-bis(diphenylphosphino)butane

f. $PtCl_2(NH_3)_2$

g. $PdCl_2(NH_3)_2$

h. $[CoCl_4]^{2-}$

i. $Rh(PPh_3)_3Cl$

Answer a)

$[Zn(NH_3)4]^{2+}$ 3d metal, d^{10}, sigma donor ligand → tetrahedral

Answer b)

$[NiCl_4]^{2+}$ 3d metal, d^8, pi donor ligand → tetrahedral

Answer c)

$[Ni(CN)_4]^{2-}$ 3d metal, d^8, pi acceptor ligand → square planar

Answer d)

$[Ir(CO)(OH)(PCy_3)_2]^{2+}$ 5d metal, d^8 → square planar

Answer e)

$[Ag(dppb)_2]^{1+}$ 4d metal, d^{10}, sigma donor ligand → tetrahedral

Answer f)

$[PtCl_2(NH_3)_2]$ 5d metal, d^8 → square planar

Answer g)

$[PdCl_2(NH_3)_2]$ 4d metal, d^8, M^{+2}, sigma donor ligand → square planar

Answer h)

$[CoCl_4]^{2-}$ 3d metal, d^7, sigma donor ligand → tetrahedral

Answer i)

$[Rh(PPh_3)_3Cl]$ 5d metal, d^8 → square planar

Contributors

- Chris P Schaller, Ph.D., (College of Saint Benedict / Saint John's University)

This page titled 6.13: Spectrochemical Series for Ligands is shared under a CC BY-NC-SA 4.0 license and was authored, remixed, and/or curated by Catherine McCusker.

6.14: Spectrochemical Series for Metal ions

The Magnitude of Δ_o

For octahedral complexes, the magnitude of Δ_o dictates whether a complex with four, five, six, or seven d electrons is high spin or low spin, which affects its magnetic properties, structure, and reactivity. Large values of Δ_o (i.e., $\Delta_o > P$) yield a low-spin complex, whereas small values of Δ_o (i.e., $\Delta_o < P$) produce a high-spin complex. As we noted, the magnitude of Δ_o depends on three factors: the charge on the metal ion, the principal quantum number of the metal (and thus its location in the periodic table), and the nature of the ligand. Values of Δ_o for some representative transition-metal complexes are given in Table **6.14.1**.

***Table* 6.14.1:** *Crystal Field Splitting Energies for Some Octahedral (Δ_o)* and Tetrahedral (Δ_t) Transition-Metal Complexes*

Octahedral Complexes	Δ_o (cm^{-1})	Octahedral Complexes	Δ_o (cm^{-1})	Tetrahedral Complexes	Δ_t (cm^{-1})
$[Ti(H_2O)_6]^{3+}$	20,300	$[Fe(CN)_6]^{4-}$	32,800	VCl_4	9010
$[V(H_2O)_6]^{2+}$	12,600	$[Fe(CN)_6]^{3-}$	35,000	$[CoCl_4]^{2-}$	3300
$[V(H_2O)_6]^{3+}$	18,900	$[CoF_6]^{3-}$	13,000	$[CoBr_4]^{2-}$	2900
$[CrCl_6]^{3-}$	13,000	$[Co(H_2O)_6]^{2+}$	9300	$[CoI_4]^{2-}$	2700
$[Cr(H_2O)_6]^{2+}$	13,900	$[Co(H_2O)_6]^{3+}$	27,000		
$[Cr(H_2O)_6]^{3+}$	17,400	$[Co(NH_3)_6]^{3+}$	22,900		
$[Cr(NH_3)_6]^{3+}$	21,500	$[Co(CN)_6]^{3-}$	34,800		
$[Cr(CN)_6]^{3-}$	26,600	$[Ni(H_2O)_6]^{2+}$	8500		
$Cr(CO)_6$	34,150	$[Ni(NH_3)_6]^{2+}$	10,800		
$[MnCl_6]^{4-}$	7500	$[RhCl_6]^{3-}$	20,400		
$[Mn(H_2O)_6]^{2+}$	8500	$[Rh(H_2O)_6]^{3+}$	27,000		
$[MnCl_6]^{3-}$	20,000	$[Rh(NH_3)_6]^{3+}$	34,000		
$[Mn(H_2O)_6]^{3+}$	21,000	$[Rh(CN)_6]^{3-}$	45,500		
$[Fe(H_2O)_6]^{2+}$	10,400	$[IrCl_6]^{3-}$	25,000		
$[Fe(H_2O)_6]^{3+}$	14,300	$[Ir(NH_3)_6]^{3+}$	41,000		

*Energies obtained by spectroscopic measurements are often given in units of wave numbers (cm^{-1}); the wave number is the reciprocal of the wavelength of the corresponding electromagnetic radiation expressed in centimeters: 1 cm^{-1} = 11.96 J/mol.

Source of data: Duward F. Shriver, Peter W. Atkins, and Cooper H. Langford, Inorganic Chemistry, 2nd ed. (New York: W. H. Freeman and Company, 1994).

Charge on the Metal Ion

Increasing the charge on a metal ion has two effects: the radius of the metal ion decreases, and negatively charged ligands are more strongly attracted to the metal. Both factors decrease the metal–ligand distance, which in turn causes the negatively charged ligands

to interact more strongly with the d orbitals. Consequently, the magnitude of Δ_o increases as the charge on the metal ion increases. Typically, Δ_o for a tripositive ion is about 50% greater than for the dipositive ion of the same metal; for example, for $[V(H_2O)_6]^{2+}$, Δ_o = 11,800 cm^{-1}; for $[V(H_2O)_6]^{3+}$, Δ_o = 17,850 cm^{-1}.

Principal Quantum Number of the Metal

For a series of complexes of metals from the same group in the periodic table with the same charge and the same ligands, the magnitude of Δ_o increases with increasing principal quantum number: Δ_o (3d) < Δ_o (4d) < Δ_o (5d). The data for hexaammine complexes of the trivalent Group 9 metals illustrate this point:

$$[Co(NH_3)_6]^{3+}\ \Delta_o = 22{,}900\ cm^{-1}$$
$$[Rh(NH_3)_6]^{3+}\ \Delta_o = 34{,}100\ cm^{-1}$$
$$[Ir(NH_3)_6]^{3+}\ \Delta_o = 40{,}000\ cm^{-1}$$

The increase in Δ_o with increasing principal quantum number is due to the larger radius of valence orbitals down a column. In addition, repulsive ligand–ligand interactions are most important for smaller metal ions. Relatively speaking, this results in shorter M–L distances and stronger d orbital–ligand interactions.

Reasons for Low-spin vs. High-spin: The Effect of the Metal Ion

There are a few factors that determine the magnitude of the d orbital splitting and dictate whether or not an electron can occupy the higher energy set of orbitals instead of pairing up. These factors are based partly on ligand field strength, which is explored on the next page. They also depend on the charge on the metal ion and whether the metal is in the first, second, or third row of the transition metals.

The higher the charge on the metal, the greater the splitting between the d orbital energy levels. For example, Fe(II) is usually high spin. It has a smaller splitting between the lower and higher d orbital levels, so electrons can more easily go to the higher level rather than pair up un the lower level.

On the other hand, Fe(III) is usually low spin. It has a larger splitting between the d levels. In that case, it costs less energy for electrons to pair up in the lower level than to go up to the higher level.

- High-spin versus low-spin cases involve a trade-off between the d orbital splitting energy and the pairing energy.
- 2nd and 3rd row transition metals are usually low spin
- 1st row transition metals are often high spin
- However, 1st row transition metals and be low spin if they are very positive (usually 3+ or greater)

There is a lot going on in metal ions, but we'll take a simplified view of things. Thinking only about electrostatics, we can try to imagine what happens to those electrons when the charge on the metal ion changes.

First we need to know about Coulomb's law. Coulomb's law states that the force of attraction between the electron and the nucleus depends on only two factors: the amount of positive charge in the nucleus, and the distance between the nucleus and the electron.

The greater the charge on the nucleus, the greater the attraction between the electron and the nucleus.

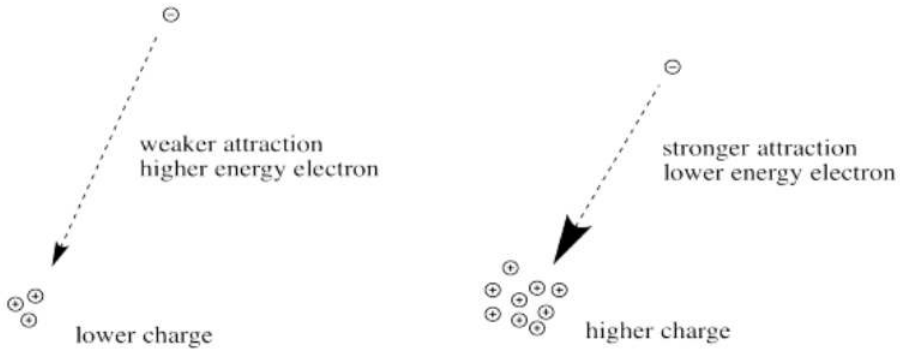


Figure **6.14.10**:

The farther an electron is from the nucleus, the weaker the attraction between the electron and the nucleus.

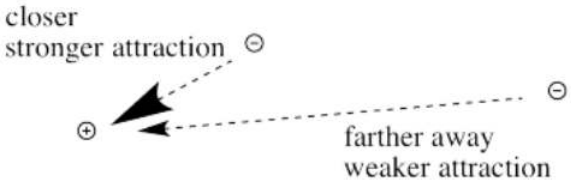


Figure 6.14.11:

Coulomb's law can be used to evaluate the potential energy of the electron. It is one of the factors that determines how high or low those electronic energy levels are that we see in energy level diagrams for atoms, ions and molecules. The energy of the electron varies in a roughly similar way: the greater the charge on the nucleus, the lower the energy of the electron. Also, the closer the electron is to the nucleus, the lower its energy.

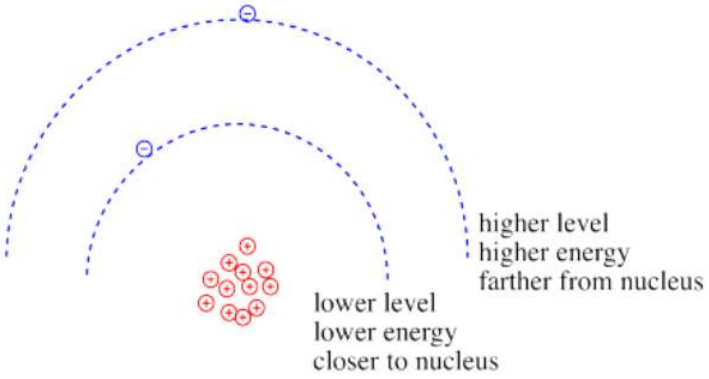


Figure 6.14.12:

Roughly speaking, electrons at higher energy are farther from the nucleus. Electrons at lower energy are closer to the nucleus.

What happens if the charge increases? Maybe a lot more protons are added to the nucleus. Maybe some electrons are lost, so that to the remaining electrons it just *feels like* the charge of the nucleus has increased. Then the electrons should be more attracted to the nucleus. They get a little closer. Their potential energy drops.

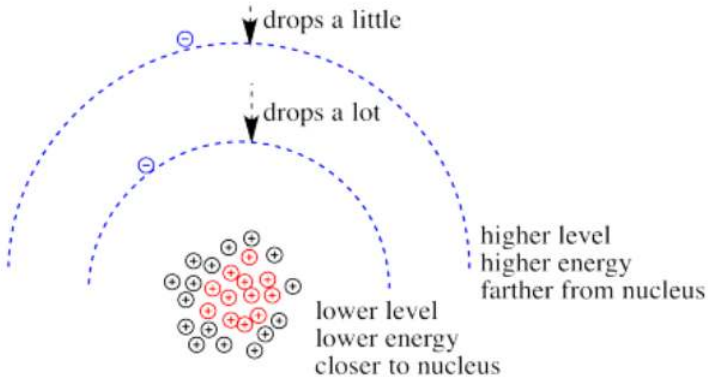


Figure 6.14.13:

Of course, if one electron is closer to the nucleus already, it feels that increase in positive charge more strongly than an electron that is farther away. Consequently it drops further in energy than an electron that is further away.

If we translate that idea into a picture of the d orbital energy levels in an octahedral geometry, it looks like this:

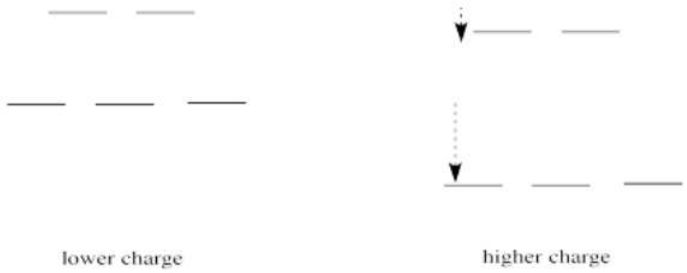


Figure **6.14.14**:

When the charge on the metal ion is increased, both the higher and the lower levels drop in energy. However, the lower level drops more. Thus, the gap between the levels gets wider.

Metals in the second and third row of the periodic table almost never form high-spin complexes. The d orbital energy splitting in these cases is larger than for first row metals. From a very simple point of view, these metals have many more protons in their nuclei than the first row transition metals, dropping that lower set of d electrons lower with respect to the higher set.

That isn't the whole picture for the second and third row transition metals, however. Remember, we are simplifying, and there are factors we won't go into. However, it is important to know that metal-ligand bond strengths are much greater in the second and third row than in the first. We'll look at the whole interaction diagram for an octahedral complex now, including contributions form metal s and p orbitals.

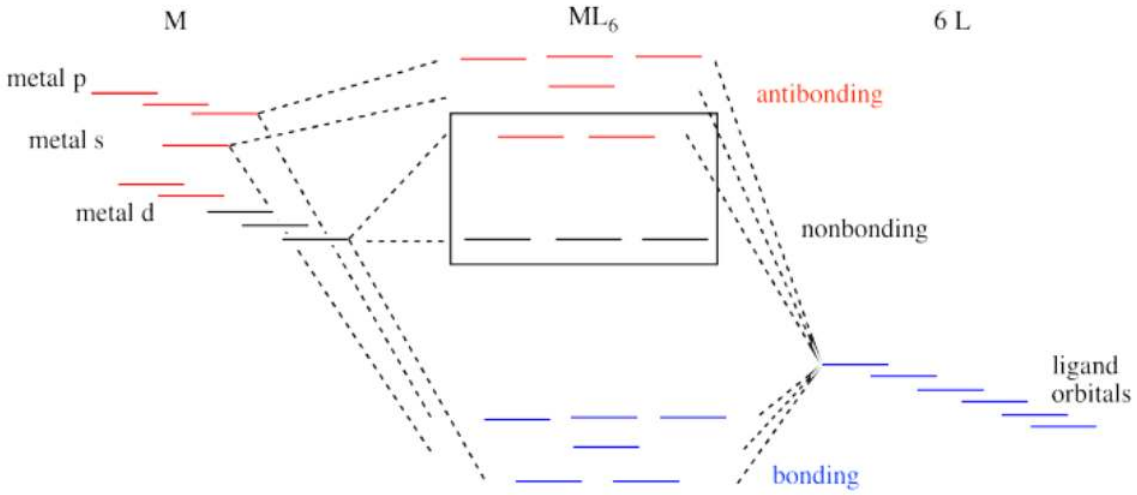


Figure **6.14.15**:

Like all ligand-metal interaction diagrams, the energy levels of the ligands by themselves are shown on one side. The metal's electronic energy levels are shown on the other side. The result of their interaction, a metal-ligand complex, is shown in the middle. The d orbital splitting diagram is shown in a box.

Suppose the diagram above is for a first row transition metal. The diagram for a second or third row metal is similar, but with stronger bonds.

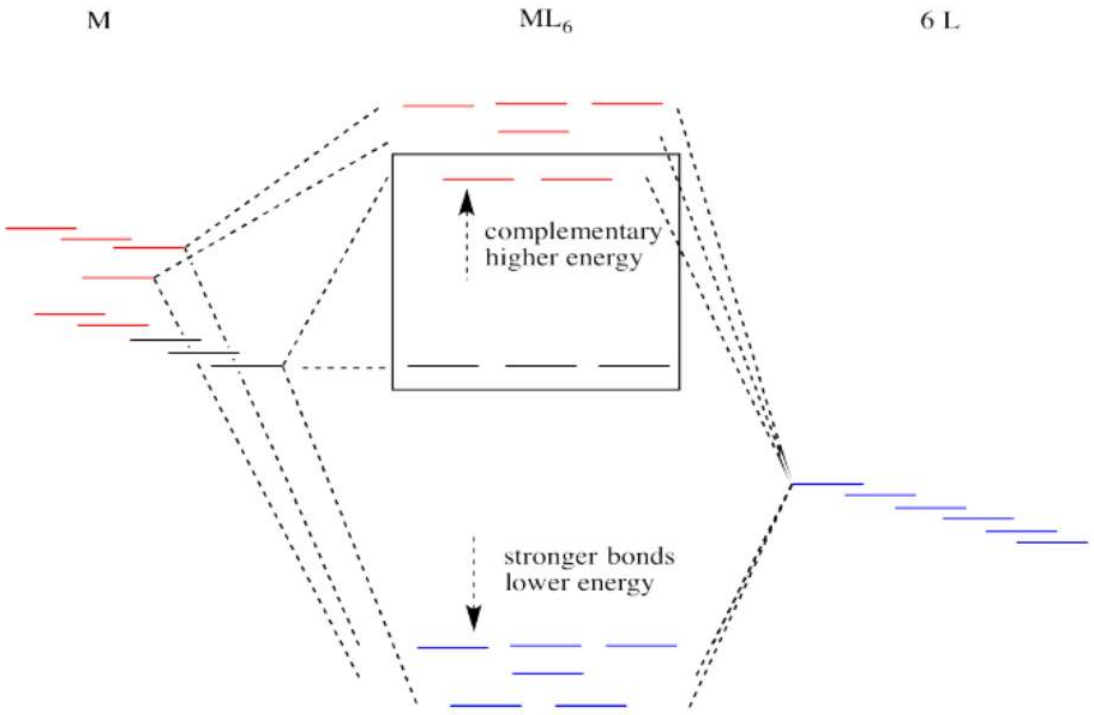


Figure **6.14.16**:

If the bonding interaction is stronger between the metal and ligand, then so is the antibonding interaction. The antibonding levels are bumped higher in energy as the bonding levels sink lower. Generally that's OK, because when the electrons are filled in, they will be found preferentially at the lower levels, not the higher ones. There will be a net lowering of electronic energy.

Why do second and third row transition metals form such strong bonds? Bond strengths are very complicated. In general, there is greater covalency between these metals and their ligands because of increased spatial and energetic overlap. Rather than go into those factors, we'll just think about all those extra protons in the nucleus that are attracting the ligand electrons more strongly.

There is one more important distinction that makes second and third row transition metals low spin. In addition, the pairing energy is lower in these metals because the orbitals are larger. There is more room for two electrons in one orbital, with less repulsion. As a result, electrons are much more likely to pair up than to occupy the next energy level.

- 2nd and 3rd row transition metals have stronger bonds, leading to a larger gap between d orbital levels
- 2nd and 3rd row transition metals have more diffuse orbitals, leading to a lower pairing energy

It is significant that most important transition metal ions in biology are from the first row of the transition block and are pretty labile. That fact plays an important role in the ease of formation and deconstruction of transition-metal containing proteins. In terms of formation, if the metal is more easily released by its previous ligands (either water or some compound that delivers the metal to the site of protein construction), it can form the necessary protein more quickly. However, even if a metal-containing enzyme plays a useful role, it should not be too stable, because we need to be able to regulate the level of protein concentration for optimum activity, or disassemble protein if it becomes damaged. Thus, it is important that the metal ion can be removed easily.

Metal ion properties that effect Δ_o

- **Position on the periodic table (period or shell number)**
  The splitting of the d-orbitals in any ligand field *increases as shell number increases going down the periodic table*. In general, with octahedral ligand fields, the $3d$ metal ions can be either weak-field or strong-field depending on other factors. With octahedral complexes, the $4d$ and larger metal ions are generally strong-field.

- **Oxidation state (charge of the metal ion)**
  As the *metal oxidation state increases, the strength of the field also increases*. The charge on a **3*d*** metal ion can contribute to whether it is weak-field or strong-field (and thus high-spin or low-spin for $d^4 - d^7$ metal ions). In octahedral **3*d*** metals, the +3 metal ions favor stronger-field (and sometimes low spin) complexes. The +2 metal ions in this series favor weaker-field (and usually high spin); but we cannot make a good prediction about this without knowing about the identity of the ligands.

Exercise 6.14.1

Predict whether each compound will be high or low spin.

a. $[Fe(py)_6]^{2+}$

b. $[Fe(H_2O)_6]^{2+}$

c. $[FeBr_6]^{3-}$

d. $[Co(NH_3)_6]^{3+}$

e. $[Cu(NH_3)_6]^{2+}$

f. $[Rh(CO)_6]^{3+}$

g. $[Cr(CO)_6]^{3+}$

h. $[PtCl_6]^{2-}$

Answer a)

$[Fe(py)_6]^{2+}$ 3d metal, M^{+2}, pi acceptor ligand → low spin

Answer b)

$[Fe(H_2O)_6]^{2+}$ 3d metal, M^{+2}, pi donor ligand → high spin

Answer c)

$[FeBr_6]^{3-}$ 3d metal, M^{+3}, pi donor ligand → high spin

Answer d)

$[Co(NH_3)_6]^{3+}$ 3d metal, M^{+3}, sigma donor ligand → low spin

Answer e)

$[Cu(NH_3)_6]^{2+}$ 3d metal, M^{+2}, sigma donor ligand → low spin

Answer f)

$[Rh(CO)_6]^{3+}$ 4d metal, M^{+3} → low spin

Answer g)

$[Cr(CO)_6]^{3+}$ 3d metal, M^{+3}, pi acceptor ligand → low spin

Answer h)

$[PtCl_6]^{2-}$ 5d metal, M^{+4} → low spin

This page titled 6.14: Spectrochemical Series for Metal ions is shared under a CC BY-NC-SA license and was authored, remixed, and/or curated by Kathryn Haas.

CHAPTER OVERVIEW

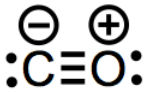
7: Why is Carbon Monoxide Poisonous?

7.1: Pi-Acid Ligands
7.2: [Fe(CO)6]2+ MO Diagram
7.3: Revisit Octahedral Metal Ion Electron Configurations
7.4: Magnetic Moments for Spin State Determination
7.5: LFSE/CFSE Calculations Again
7.6: Spectrochemical Series of Ligands (Again)
7.7: Exchange Inertness of d3, d4(LS), d5(LS), d6(LS), and d8(SQP)
7.8: O2 Reduction, since CO displaces O2
7.9: Bonding in Carbonmonoxy-myoglobin [Fe(CO)]2+
7.10: Active Site of Cytochrome c Oxidase
7.11: Cyanide is also a poison (affinity data)
7.12: Cyanide is also a poison (spectrocopic data)

7: Why is Carbon Monoxide Poisonous? is shared under a not declared license and was authored, remixed, and/or curated by LibreTexts.

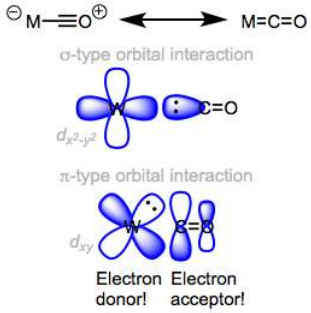
7.1: Pi-Acid Ligands

Carbon monoxide is a simple but fascinating ligand. We have previously noted that carbon monoxide, although a very poor base, is a strong field ligand due to the presence of π backbonding.



General Properties

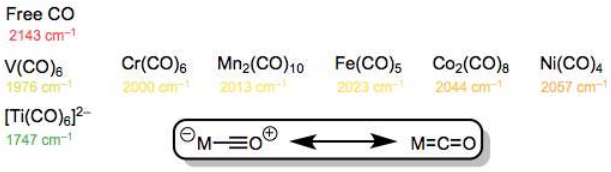
CO is a dative, L-type ligand that does not affect the oxidation state of the metal center upon binding, but does increase the total electron count by two units. We've recently seen that there are really two bonding interactions at play in the carbonyl ligand: a ligand-to-metal n → dσ interaction and a metal-to-ligand dπ → π* interaction. The latter interaction is called backbonding, because the metal donates electron density back to the ligand. To remind myself of the existence of backbonding, I like to use the right-hand resonance structure whenever possible; however, it is important to remember to treat CO as an L-type ligand no matter what resonance form is drawn.



Orbital interactions in M=C=O.

CO is a strong σ-donor (or σ-base) and a good π-acceptor (or π-acid). The properties of ligated CO depend profoundly upon the identity of the metal center. More specifically, the electronic properties of the metal center dictate the importance of backbonding in metal carbonyl complexes. Most bluntly, more electron-rich metal centers are better at backbonding to CO. Why is it important to ascertain the strength of backbonding?

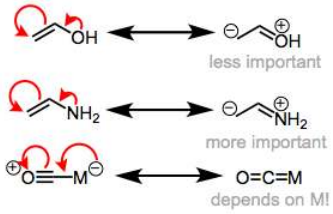
Infrared spectroscopy has famously been used to empirically support the idea of backbonding. The table below arranges some metal carbonyl complexes in "periodic" order and provides the frequency corresponding to the C=O stretching mode. Notice that without exception, every complexed CO has a stretching frequency lower than that of free CO. Backbonding is to blame! The C–O bond order in complexed carbon monoxide is (almost always) lower than that of free CO.



C=O stretching frequencies in metal-carbonyl complexes. Does something seem off here?

The figure above depicts a clear increase in frequency (an increase in C–O bond order) as we move left to right across the periodic table. This finding may seem odd if we consider that the number of d electrons in the neutral metal increases as we move left to right. Shouldn't metal centers with more d electrons be better at backbonding (and more "electron rich")? What's going on here? Recall the periodic trend in orbital energy. As we move left to right, the d orbital energies decrease and the energies of the dπ and π* orbitals separate. As a result, the backbonding orbital interaction becomes worse (remember that strong orbital interactions require well-matched orbital energies) as we move toward the more electronegative late transition metals! We can draw an analogy

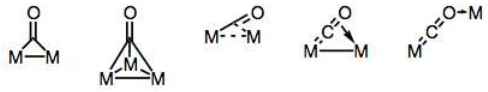
to enamines and enol ethers from organic chemistry. The more electronegative oxygen atom in enol ethers is a worse electron donor than the enamine's nitrogen atom.



The importance of backbonding depends on the electronegativity of the metal and its electron density.

Of course, the contribution of other ligands on the metal center to backbonding cannot be forgotten, either. Logically, electron-donating ligands will tend to make the backbond stronger (they make the metal a better electron donor), while electron-withdrawing ligands will worsen backbonding. Adding electron-rich phosphine ligands to a metal center, for instance, decreases the CO stretching frequency due to improved backbonding.

Carbonyl ligands are famously able to bridge multiple metal centers. Bonding in bridged carbonyl complexes may be either "traditional" or delocalized, depending on the structure of the complex and the bridging mode. The variety of bridging modes stems from the different electron donors and acceptors present on the CO ligand (and the possibility of delocalized bonding). Known bridging modes are shown in the figure below.



Building bridges with carbonyl ligands!

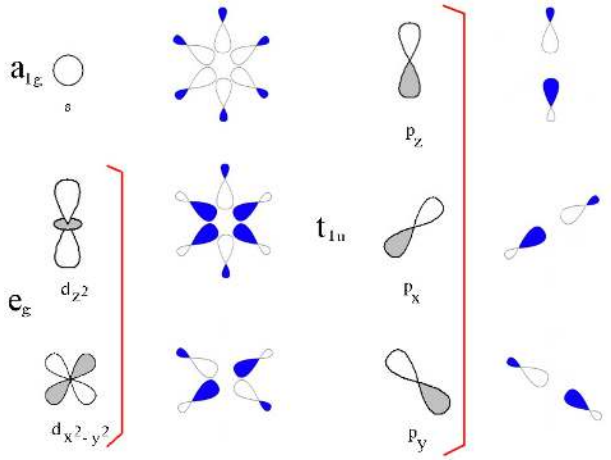
Contributors

- Dr. Michael Evans (Georgia Tech)

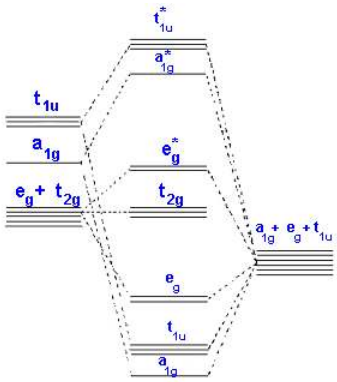
7.1: Pi-Acid Ligands is shared under a CC BY-NC-SA 4.0 license and was authored, remixed, and/or curated by LibreTexts.

7.2: [Fe(CO)6]2+ MO Diagram

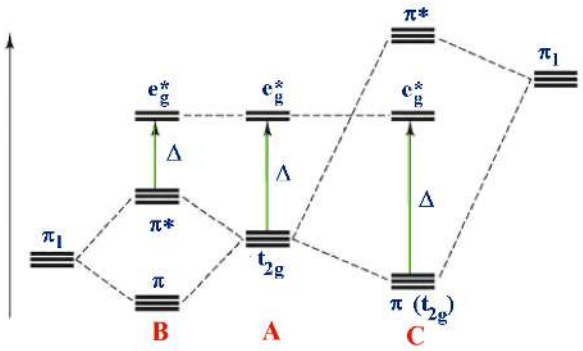
Ligand Field Theory can be considered an extension of Crystal Field Theory such that all levels of covalent interactions can be incorporated into the model. Treatment of the bonding in LFT is generally done using Molecular Orbital Theory. A qualitative approach that can be used for octahedral metal complexes is given in the following 3 diagrams.



In the first diagram, the 3d, 4s and 4p metal ion atomic orbitals are shown together with the ligand group orbitals that would have the correct symmetry to be able to overlap with them. The symmetry adapted linear comination of ligand orbitals are generated by taking 6 sigma orbitals from the ligands, designated as σ_x, σ_{-x}, σ_y, σ_{-y}, σ_z, σ_{-z} and then combining them to make 6 ligand group orbitals. (labelled e_g, a_{1g}, t_{1u})



In the second diagram only sigma bonding is considered and it shows the combination of the metal 3d, 4s and 4p orbitals with OCCUPIED ligand group orbitals (using 1 orbital from each ligand). The result is that that the metal electrons would be fed into t2g and eg* molecular orbitals which is similar to the CFT model except that the eg orbital is now eg*.



For example: B - $[M(II)I_6]^{4-}$ A - $[M(II)(H_2O)_6]^{2+}$ C - $[M(II)(CN)_6]^{4-}$

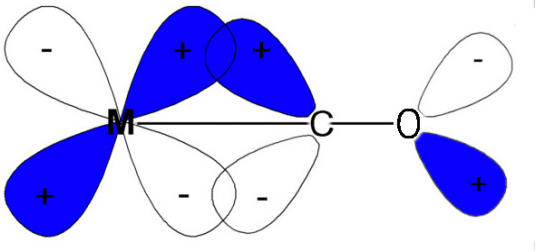
In the third diagram, π (pi) bonding is considered. In general π bonds are weaker than σ (sigma) bonds and so the effect is to modify rather than dramatically alter the description. 2 orbitals from each ligand are combined to give a total of 12 which are subdivided into four sets with three ligand group orbitals in each set. These are labelled t_{1g}, t_{1u}, t_{2g} and t_{2u}. The metal t_{2g} orbital is the most suitable for interaction and this is shown in the 2 cases above.
Case A is the same as above, ignoring π interactions.

- For case B, the ligand π orbitals are full and at lower energy than the metal t_{2g}. This causes a decrease in the size of Δ.
- For case C, the ligand π orbitals are empty and at higher energy than the metal t_{2g}. This causes an increase in the size of Δ.

Returning to the problem of correctly placing ligands in the Spectrochemical series, the halides are examples of case A and groups like CN- and CO are examples of case B. It is possible then to explain the Spectrochemical series once covalent effects are considered.

Some convincing arguments for covalency and effects on Δ come from a study of the IR spectra recorded for simple carbonyl compounds e.g. $M(CO)_6$.

- The CO molecule has a strong triple bond which in the IR gives rise to a strong absorption at ~2140 cm^{-1}. For the series $[Mn(CO)_6]^+$, $[Cr(CO)_6]$ and $[V(CO)_6]^-$, which are isoelectronic, the IR bands for the CO have shifted to 2090, 2000 and 1860 cm^{-1} respectively. Despite the fact that the metals have the same number of electrons (isoelectronic) the frequency of force constant of the CO bond is seen to vary $Mn^+ > Cr > V^-$.
- This can not be explained on an ionic basis but is consistent with the π bonding scheme since the greater the positive charge on the metal, the less readily the metal can delocalize electrons back into the π^* orbitals of the CO group.



Note that the IR values we are dealing with relate to the CO bond and not the M-C so when the CO frequency gets less then it is losing triple bond character and becoming more like a double bond. This is expected if electrons are pushed back from the metal into what were empty π^* antibonding orbitals.

Contributors and Attributions

- Prof. Robert J. Lancashire (The Department of Chemistry, University of the West Indies)

7.2: [Fe(CO)6]2+ MO Diagram is shared under a CC BY-NC-SA 4.0 license and was authored, remixed, and/or curated by LibreTexts.

- **Ligand Field Theory Fundamentals** is licensed CC BY-NC-SA 4.0.

7.3: Revisit Octahedral Metal Ion Electron Configurations

Electronic Structures of Metal Complexes

According to the Aufbau principle, electrons are filled from lower to higher energy orbitals. For the octahedral case, this corresponds to filling the d_{xy}, d_{xz}, and d_{yz} orbitals first. Following Hund's rule, electrons are distributed into orbitals to give the highest number of unpaired electrons. For example, if one had a d^3 complex, there would be three unpaired electrons.

Consider several examples of electronic configurations for octahedral complexes shown in Figure **7.3.1**. The Ti^{3+} ion contains a single d electron, and additional configurations can be obtained as we proceed across the first row of the transition metals by adding a single electron at a time. Additional electrons are placed in the lowest-energy orbital available, while keeping their spins parallel as required by Hund's rule. As shown in Figure **7.3.1**, for d^1–d^3 systems—such as $[Ti(H_2O)_6]^{3+}$, $[V(H_2O)_6]^{3+}$, and $[Cr(H_2O)_6]^{3+}$, respectively—the electrons successively occupy the three degenerate t_{2g} orbitals with their spins parallel, giving one, two, and three unpaired electrons, respectively. We can summarize this for the complex $[Cr(H_2O)_6]^{3+}$, for example, by saying that the chromium ion has a d^3 electron configuration or, more succinctly, Cr^{3+} is a d^3 ion.

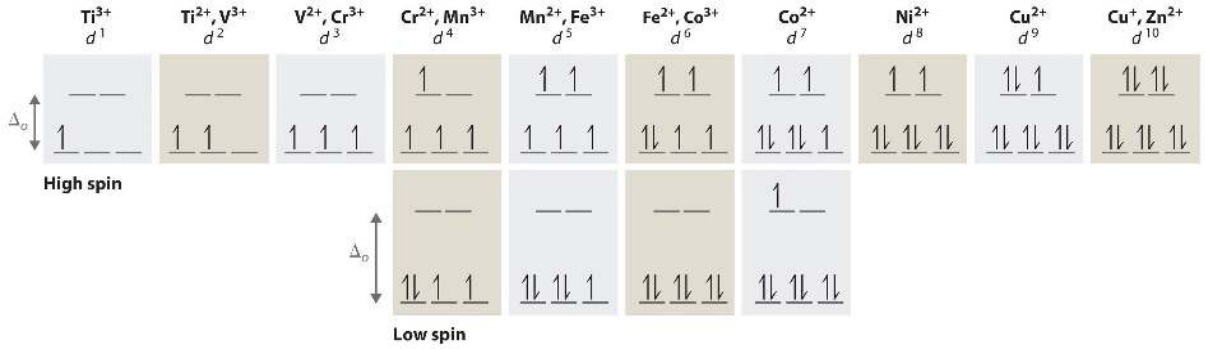


Figure **7.3.1**: The Possible Electron Configurations for Octahedral d^n Transition-Metal Complexes (n = 1–10). Two different configurations are possible for octahedral complexes of metals with d^4, d^5, d^6, and d^7 configurations; the magnitude of Δ_o determines which configuration is observed. (CC BY-SA-NC; anonymous by request)

When we reach the d^4 configuration, there are two possible choices for the fourth electron: it can occupy one of the empty, higher-energy e_g orbitals (d_{z^2} or $d_{x^2-y^2}$) or it can occupy one of the lower-energy, singly-occupied t_{2g} orbitals (d_{xy}, d_{xz}, or d_{yz}). Recall that placing an electron in an already occupied orbital results in electrostatic repulsions that increase the energy of the system; this increase in energy is called the spin-pairing energy (P). If Δ_o is less than P, then the lowest-energy arrangement places the fourth electron in one of the empty e_g orbitals. This configuration maximizes the spin multiplicity. Because this arrangement results in four unpaired electrons, it is called a **high-spin** configuration, and a complex with this electron configuration, such as the $[Cr(H_2O)_6]^{2+}$ ion, is called a high-spin complex. Conversely, if Δ_o is greater than P, then the lowest-energy arrangement places the fourth electron in one of the occupied t_{2g} orbitals. Because this arrangement results in only two unpaired electrons, it is called a **low-spin** configuration, and a complex with this electron configuration, such as the $[Mn(CN)_6]^{3-}$ ion, is called a low-spin complex. Similarly, metal ions with the d^5, d^6, or d^7 electron configurations can be either high spin or low spin, depending on the magnitude of Δ_o.

In contrast, only one arrangement of d electrons is possible for metal ions with d^8–d^{10} electron configurations. For example, the $[Ni(H_2O)_6]^{2+}$ ion is d^8 with two unpaired electrons, the $[Cu(H_2O)_6]^{2+}$ ion is d^9 with one unpaired electron, and the $[Zn(H_2O)_6]^{2+}$ ion is d^{10} with no unpaired electrons.

> *If Δ_o is less than the spin-pairing energy, a high-spin configuration results. Conversely, if Δ_o is greater, a low-spin configuration forms.*

A Note on units

The crystal field splitting energy, Δ_o, may be reported in units of J/mol or wave numbers (cm^{-1}). Typically, energies obtained by spectroscopic measurements are often given wave numbers; the wave number is the reciprocal of the wavelength of the corresponding electromagnetic radiation expressed in centimeters: 1 cm^{-1} = 11.96 J/mol.

Factors That Affect the Magnitude of Δ_o

The magnitude of the crystal field splitting energy, Δ_o, dictates whether a complex with four, five, six, or seven d electrons is high spin or low spin, which affects its magnetic properties, structure, and reactivity. Large values of Δ_o (i.e., Δ_o > P) yield a low-spin complex, whereas small values of Δ_o (i.e., Δ_o < P) produce a high-spin complex. As we noted, the magnitude of Δ_o depends on three factors: the charge on the metal ion, the principal quantum number of the metal (and thus its location in the periodic table), and the nature of the ligand. Values of Δ_o for some representative transition-metal complexes are given in Table **7.3.1**.

Table **7.3.1**: Crystal Field Splitting Energies for Some Octahedral (Δ_o) and Tetrahedral (Δ_t) Transition-Metal Complexes

Octahedral Complexes	Δ_o (cm^{-1})	Octahedral Complexes	Δ_o (cm^{-1})	Tetrahedral Complexes	Δ_t (cm^{-1})
$[Ti(H_2O)_6]^{3+}$	20,300	$[Fe(CN)_6]^{4-}$	32,800	VCl_4	9010
$[V(H_2O)_6]^{2+}$	12,600	$[Fe(CN)_6]^{3-}$	35,000	$[CoCl_4]^{2-}$	3300
$[V(H_2O)_6]^{3+}$	18,900	$[CoF_6]^{3-}$	13,000	$[CoBr_4]^{2-}$	2900
$[CrCl_6]^{3-}$	13,000	$[Co(H_2O)_6]^{2+}$	9300	$[CoI_4]^{2-}$	2700
$[Cr(H_2O)_6]^{2+}$	13,900	$[Co(H_2O)_6]^{3+}$	27,000		
$[Cr(H_2O)_6]^{3+}$	17,400	$[Co(NH_3)_6]^{3+}$	22,900		
$[Cr(NH_3)_6]^{3+}$	21,500	$[Co(CN)_6]^{3-}$	34,800		
$[Cr(CN)_6]^{3-}$	26,600	$[Ni(H_2O)_6]^{2+}$	8500		
$Cr(CO)_6$	34,150	$[Ni(NH_3)_6]^{2+}$	10,800		
$[MnCl_6]^{4-}$	7500	$[RhCl_6]^{3-}$	20,400		
$[Mn(H_2O)_6]^{2+}$	8500	$[Rh(H_2O)_6]^{3+}$	27,000		
$[MnCl_6]^{3-}$	20,000	$[Rh(NH_3)_6]^{3+}$	34,000		
$[Mn(H_2O)_6]^{3+}$	21,000	$[Rh(CN)_6]^{3-}$	45,500		
$[Fe(H_2O)_6]^{2+}$	10,400	$[IrCl_6]^{3-}$	25,000		
$[Fe(H_2O)_6]^{3+}$	14,300	$[Ir(NH_3)_6]^{3+}$	41,000		

Source of data: Duward F. Shriver, Peter W. Atkins, and Cooper H. Langford, Inorganic Chemistry, 2nd ed. (New York: W. H. Freeman and Company, 1994).

Factor 1: Charge on the Metal Ion

Increasing the charge on a metal ion has two effects: the radius of the metal ion decreases, and negatively charged ligands are more strongly attracted to it. Both effects decrease the metal–ligand distance, which in turn causes the negatively charged ligands to interact more strongly with the d-orbitals. Consequently, the magnitude of Δ_o increases as the charge on the metal ion increases. Typically, Δ_o for a +3 ion is about 50% greater than for the +2 ion of the same metal; for example, for $[V(H_2O)_6]^{2+}$, Δ_o = 11,800 cm^{-1}; for $[V(H_2O)_6]^{3+}$, Δ_o = 17,850 cm^{-1}.

Factor 2: Principal Quantum Number of the Metal

For a series of complexes of metals from the same group in the periodic table with the same charge and the same ligands, the magnitude of Δ_o increases with increasing principal quantum number: Δ_o (3d) < Δ_o (4d) < Δ_o (5d). The data for hexaammine complexes of the trivalent Group 9 metals illustrate this point:

$$[Co(NH_3)_6]^{3+}: \Delta_o = 22{,}900\ cm^{-1}$$

$$[Rh(NH_3)_6]^{3+}: \Delta_o = 34{,}100\ cm^{-1}$$

$$[Ir(NH_3)_6]^{3+}: \Delta_o = 40{,}000\ cm^{-1}$$

The increase in Δ_o with increasing principal quantum number is due to the larger radius of valence orbitals down a column. In addition, repulsive ligand–ligand interactions are most important for smaller metal ions. Relatively speaking, this results in shorter M–L distances and stronger d orbital–ligand interactions.

Factor 3: The Nature of the Ligands

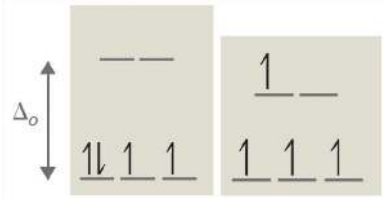


Figure **7.3.2**: Low Spin, Strong Field (Δ_o˃P) High Spin, Weak Field (Δ_o˂P)Splitting for a d^4 complex under a strong field (left) and a weak field (right). The strong field is a low spin complex, while the weak field is a high spin complex.

Experimentally, it is found that the Δ_o observed for a series of complexes of the same metal ion depends strongly on the nature of the ligands. Ligands that cause a transition metal to have a small crystal field splitting, which leads to a high-spin configuration, are called **weak-field**

ligands. Ligands that produce a large crystal field splitting, which leads to a low-spin configuration, are called **strong field ligands** (Figure **7.3.2**).

For a series of chemically similar ligands, the magnitude of Δ_o decreases as the size of the donor atom increases. For example, Δ_o values for halide complexes generally decrease in the order $F^- > Cl^- > Br^- > I-$ because smaller, more localized charges, such as we see for F^-, interact more strongly with the d orbitals of the metal ion.

In addition, a small neutral ligand with a highly localized lone pair, such as NH_3, results in significantly larger Δ_o values than might be expected. Because the lone pair points directly at the metal ion, the electron density along the M–L axis is greater than for a spherical anion such as F^-.

The experimentally observed order of the crystal field splitting energies produced by different ligands is called the spectrochemical series. It is shown here in order of increasing Δ_o:

$$\underset{\text{weak-field ligands}}{I^- < Br^- < Cl^- < \underline{S}CN^- < CH_3COO^- < F^- < OH^- < ox^{2-}} < \underset{\text{intermediate-field ligands}}{ONO^- < H_2O < SC\underline{N}^-}$$
$$< EDTA^{4-} < NH_3 < en < NO_2^- < \underset{\text{strong-field ligands}}{CN^- \approx CO}$$

Note that SCN^- and NO_2- ligands are represented twice in the above spectrochemical series since there are two different Lewis base sites (e.g., free electron pairs to share) on each ligand (e.g., for the SCN^- ligand, the electron pair on the sulfur or the nitrogen can form the coordinate covalent bond to a metal). The specific atom that binds in such ligands is underlined.

> *The largest Δ_o splittings are found in complexes of metal ions from the third row of the transition metals with charges of at least +3 and ligands with localized lone pairs of electrons.*

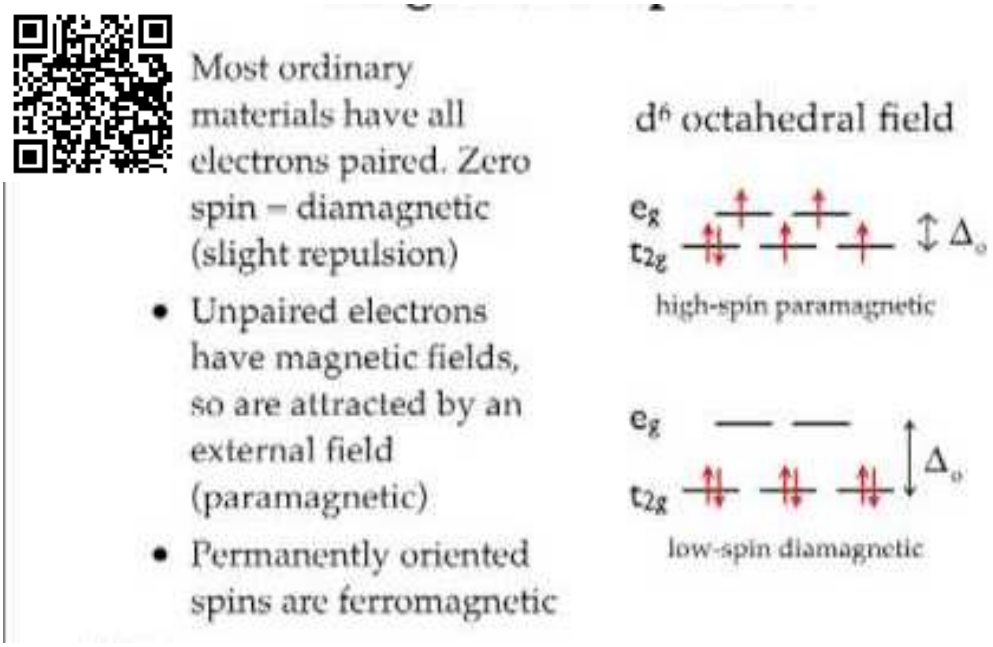
Factor 4: Molecular Geometry

In addition to octahedral complexes, two common geometries observed are that of tetrahedral and square planar. These complexes differ from the octahedral complexes in that the orbital levels are raised in energy due to the interference with electrons from ligands. For the tetrahedral complex, the d_{xy}, d_{xz}, and d_{yz} orbitals are raised in energy while the d_{z^2}, $d_{x^2-y^2}$ orbitals are lowered. For the square planar complexes, there is greatest interaction with the $d_{x^2-y^2}$ orbital and therefore it has higher energy. The next orbital with the greatest interaction is d_{xy}, followed below by d_{z^2}. The orbitals with the lowest energy are the d_{xz} and d_{yz} orbitals. There is a large energy separation between the d_{z^2} orbital and the d_{xz} and d_{yz} orbitals, meaning that the crystal field splitting energy is large. We find that the square planar complexes have the greatest crystal field splitting energy compared to all the other complexes. This means that most square planar complexes are low spin, strong field ligands.

The splitting energy (from highest orbital to lowest orbital) is Δ_{sp} and tends to be larger then Δ_o

$$\Delta_{sp} = 1.74\,\Delta_o \tag{7.3.1}$$

Moreover, Δ_{sp} is also larger than the pairing energy, so the square planar complexes are usually **low spin** complexes.



Example 7.3.1

For the complex, predict its structure, whether it is high spin or low spin, and the number of unpaired electrons present:

$[CoF_6]^{3-}$

Solution

With six ligands, we expect this complex to be octahedral.

The fluoride ion is a small anion with a concentrated negative charge, but compared with ligands with localized lone pairs of electrons, it is weak field. The charge on the metal ion is +3, giving a d^6 electron configuration.

Because of the weak-field ligands, we expect a relatively small Δ_o, making the compound high spin.

In a high-spin octahedral d^6 complex, the first five electrons are placed individually in each of the d orbitals with their spins parallel, and the sixth electron is paired in one of the t_{2g} orbitals, giving four unpaired electrons.

Example 7.3.2

For the complex, predict its structure, whether it is high spin or low spin, and the number of unpaired electrons present:

$[Rh(CO)_2Cl_2]^-$

Solution

This complex has four ligands, so it is either square planar or tetrahedral.

Because rhodium is a second-row transition metal ion with a d^8 electron configuration and CO is a strong-field ligand, the complex is likely to be square planar with a large Δ_o, making it low spin. Because the strongest d-orbital interactions are along the x and y axes, the orbital energies increase in the order $d_{z^2}d_{yz}$, and d_{xz} (these are degenerate); d_{xy}; and $d_{x^2-y^2}$.

The eight electrons occupy the first four of these orbitals, leaving the $d_{x^2-y^2}$. orbital empty. Thus there are no unpaired electrons.

Problems

Exercise 7.3.1

For the complex, predict its structure, whether it is high spin or low spin, and the number of unpaired electrons present.

$[Mn(H_2O)_6]^{2+}$

Answer

octahedral; high spin; five

Exercise 7.3.2

For the complex, predict its structure, whether it is high spin or low spin, and the number of unpaired electrons present.

$[PtCl_4]^{2-}$

Answer

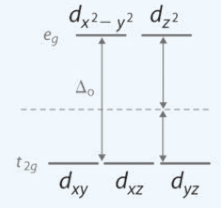
square planar; low spin; no unpaired electrons

Exercise 7.3.3

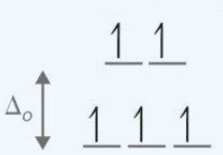
For the complex ion $[Fe(Cl)_6]^{3-}$ determine the number of d electrons for Fe, sketch the d-orbital energy levels and the distribution of d electrons among them, list the number of lone electrons, and label whether the complex is paramagnetic or diamagnetic.

Answer

Step 1: Determine the oxidation state of Fe. Here it is Fe^{3+}. Based on its electron configuration, Fe^{3+} has **5 d-electrons**. Step 2: Determine the geometry of the ion. Here it is an octahedral which means the energy splitting should look like:



Step 3: Determine whether the ligand induces is a strong or weak field spin by looking at the spectrochemical series. Cl^- is a weak field ligand (i.e., it induces high spin complexes). Therefore, electrons fill all orbitals before being paired.



Step four: Count the number of lone electrons. Here, there are **5 electrons**. Step five: The five unpaired electrons means this complex ion is **paramagnetic** (and strongly so).

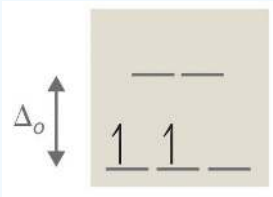
Exercise 7.3.4

For each of the following, sketch the d-orbital energy levels and the distribution of d electrons among them, state the geometry, list the number of d-electrons, list the number of lone electrons, and label whether they are paramagnetic or dimagnetic:

a. $[Ti(H_2O)_6]^{2+}$
b. $[NiCl_4]^{2-}$
c. $[CoF_6]^{3-}$ (also state whether this is low or high spin)
d. $[Co(NH_3)_6]^{3+}$ (also state whether this is low or high spin)
e. True or False: Square Planer complex compounds are usually low spin.

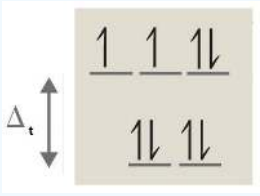
Answer a

octahedral, 2, 2, paramagnetic



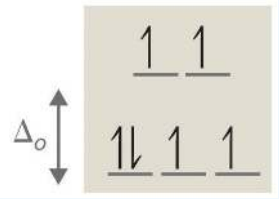
Answer b

tetrahedral, 8, 2, paramagnetic (see Octahedral vs. Tetrahedral Geometries)



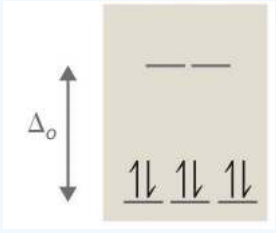
Answer c

octahedral, 6, 4, paramagnetic, high spin



Answer d

octahedral, 6, 0, diamagnetic, low spin



Answer e

True

Summary

Crystal field theory, which assumes that metal–ligand interactions are only electrostatic in nature, explains many important properties of transition-metal complexes, including their colors, magnetism, structures, stability, and reactivity. Crystal field theory (CFT) is a bonding model that explains many properties of transition metals that cannot be explained using valence bond theory. In CFT, complex formation is assumed to be due to electrostatic interactions between a central metal ion and a set of negatively charged ligands or ligand dipoles arranged around the metal ion. Depending on the arrangement of the ligands, the d orbitals split into sets of orbitals with different energies. The difference between the energy levels in an octahedral complex is called the crystal field splitting energy (Δ_o), whose magnitude depends on the charge on the metal ion, the position of the metal in the periodic table, and the nature of the ligands. The spin-pairing energy (P) is the increase in energy that occurs when an electron is added to an already occupied orbital. A high-spin configuration occurs when the Δ_o is less than P, which produces complexes with the maximum number of unpaired electrons possible. Conversely, a low-spin configuration occurs when the Δ_o is greater than P, which produces complexes with the minimum number of unpaired electrons possible. Strong-field ligands interact strongly with the d orbitals of the metal ions and give a large Δ_o, whereas weak-field ligands interact more weakly and give a smaller Δ_o. The colors of transition-metal complexes depend on the environment of the metal ion and can be explained by CFT.

Contributors and Attributions

- Asadullah Awan (UCD), Hong Truong (UCD)
- Prof. Robert J. Lancashire (The Department of Chemistry, University of the West Indies)

7.3: Revisit Octahedral Metal Ion Electron Configurations is shared under a CC BY-NC-SA 4.0 license and was authored, remixed, and/or curated by Kathryn A. Newton, Northern Michigan University.

- **24.5: Bonding in Complex Ions: Crystal Field Theory** is licensed CC BY-NC-SA 4.0.
- **Crystal Field Theory** is licensed CC BY-NC-SA 4.0.

7.4: Magnetic Moments for Spin State Determination

Magnetic moments are often used in conjunction with electronic spectra to gain information about the oxidation number and stereochemistry of the central metal ion in coordination complexes. A common laboratory procedure for the determination of the magnetic moment for a complex is the Gouy method which involves weighing a sample of the complex in the presence and absence of a magnetic field and observing the difference in weight. A template is provided for the calculations involved.

For first row transition metal ions in the free ion state, i.e. isolated ions in a vacuum, all 5 of the 3d orbitals are degenerate.

A simple crystal field theory approach to the bonding in these ions assumes that when they form octahedral complexes, the energy of the d orbitals are no longer degenerate but are split such that two orbitals, the d_{x2-y2} and the d_{z2} (e_g subset) are at higher energy than the d_{xy}, d_{xz}, d_{yz} orbitals (the t_{2g} subset).

For octahedral ions with between 4 and 7 d electrons, this gives rise to 2 possible arrangements called either high spin/weak field or low spin/strong field respectively. The energy gap is dependent on the position of the coordinated ligands in the SPECTROCHEMICAL SERIES.

Note

A good starting point is to assume that all Co(III), d^6 complexes are octahedral and LOW spin, i.e. t_{2g}^6.

In tetrahedral complexes, the energy levels of the orbitals are again split, such that the energy of two orbitals, the $d_{x^2-y^2}$ and the d_{z^2} (e subset) are now at lower energy (more favored) than the remaining three d_{xy}, d_{xz}, d_{yz} (the t_2 subset) which are destabilized.

> *Tetrahedral complexes are ALL high spin since the difference between the 2 subsets of energies of the orbitals is much smaller than is found in octahedral complexes.*

The usual relationship quoted between them is:

$$\Delta_{tet} \approx \frac{4}{9}\Delta_{oct}$$

Square planar complexes are less common than tetrahedral and d^8 e.g. Ni(II), Pd(II), Pt(II), etc, have a strong propensity to form square planar complexes. As with octahedral complexes, the energy gap between the d_{xy} and $d_{x^2-y^2}$ is Δ_{oct} and these are considered strong field / low spin hence they are all diamagnetic, μ=0 Bohr Magneton (B.M.)

The formula used to calculate the spin-only magnetic moment can be written in two forms; the first based on the number of unpaired electrons, n, and the second based on the electron spin quantum number, S. Since for each unpaired electron, $n = 1$ and $S = 1/2$ then the two formulae are clearly related and the answer obtained must be identical.

$$\mu_{so} = \sqrt{n(n+2)}$$

$$\mu_{so} = \sqrt{4S(S+1)}$$

Comparison of calculated spin-only magnetic moments with experimental data for some octahedral complexes

Ion	Config	μ_{so} / B.M.	μ_{obs} / B.M.
Ti(III)	d^1 (t_{2g}^1)	√3 = 1.73	1.6-1.7
V(III)	d^2 (t_{2g}^2)	√8 = 2.83	2.7-2.9
Cr(III)	d^3 (t_{2g}^3)	√15 = 3.88	3.7-3.9
Cr(II)	d^4 high spin (t_{2g}^3 e_g^1)	√24 = 4.90	4.7-4.9
Cr(II)	d^4 low spin (t_{2g}^4)	√8 = 2.83	3.2-3.3
Mn(II)/ Fe(III)	d^5 high spin (t_{2g}^3 e_g^2)	√35 = 5.92	5.6-6.1
Mn(II)/ Fe(III)	d^5 low spin (t_{2g}^5)	√3 = 1.73	1.8-2.1
Fe(II)	d^6 high spin (t_{2g}^4 e_g^2)	√24 = 4.90	5.1-5.7
Co(III)	d^6 low spin (t_{2g}^6)	0	0
Co(II)	d^7 high spin (t_{2g}^5 e_g^2)	√15 = 3.88	4.3-5.2
Co(II)	d^7 low spin (t_{2g}^6 e_g^1)	√3 = 1.73	1.8
Ni(II)	d^8 (t_{2g}^6 e_g^2)	√8 = 2.83	2.9-3.3
Cu(II)	d^9 (t_{2g}^6 e_g^3)	√3 = 1.73	1.7-2.2

Comparison of calculated spin-only magnetic moments with experimental data for some tetahedral complexes

Ion	Config	μ_{so} / B.M.	μ_{obs} / B.M.
Cr(V)	d^1 (e^1)	√3 = 1.73	1.7-1.8
Cr(IV) / Mn(V)	d_2 (e^2)	√8 = 2.83	2.6 - 2.8
Fe(V)	d^3 (e^2 t_2^1)	√15 = 3.88	3.6-3.7
-	d^4 (e^2 t_2^2)	√24 = 4.90	-
Mn(II)	d^5 (e^2 t_2^3)	√35 = 5.92	5.9-6.2
Fe(II)	d^6 (e^3 t_2^3)	√24 = 4.90	5.3-5.5
Co(II)	d^7 (e^4 t_2^3)	√15 = 3.88	4.2-4.8
Ni(II)	d^8 (e^4 t_2^4)	√8 = 2.83	3.7-4.0
Cu(II)	d^9 (e^4 t_2^5)	√3 = 1.73	-

Contributors and Attributions

- Prof. Robert J. Lancashire (The Department of Chemistry, University of the West Indies)

7.4: Magnetic Moments for Spin State Determination is shared under a CC BY-NC-SA 4.0 license and was authored, remixed, and/or curated by LibreTexts.

- **Magnetic Moments of Transition Metals** is licensed CC BY-NC-SA 4.0.

7.5: LFSE/CFSE Calculations Again

The difference in energy between the two sets of d orbitals is called the crystal field splitting energy (Δ_o), where the subscript o stands for octahedral. The magnitude of the splitting depends on the charge on the metal ion, the position of the metal in the periodic table, and the nature of the ligands. Crystal field splitting energy also applies to tetrahedral complexes (Δ_t), where the subscript t standands for tetrahedral. It is important to note that the splitting of the d orbitals in a crystal field does not change the total energy of the five d orbitals. In an octahedral complex, the two e_g orbitals increase in energy by $0.6\Delta_o$, and the three t_{2g} orbitals decrease in energy by $0.4\Delta_o$ (Figure **7.5.1**). Thus the total change in energy is

Misplaced '#'

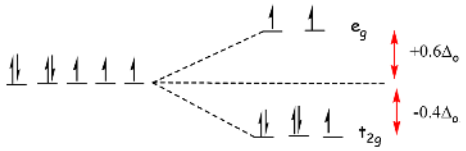


Figure **7.5.1**: Crystal field diagram of an octahedral complex showing the increased energy of the e_g and decreased energy of the t_{2g} orbitals. (LibreText)

> *Crystal field splitting does not change the total energy of the d orbitals.*

Quantifying Crystal Field Stabilization Energy

Recall that stable molecules contain more electrons in the lower-energy (bonding) molecular orbitals in a molecular orbital diagram than in the higher-energy (antibonding) molecular orbitals. If the lower-energy set of d orbitals (the t_{2g} orbitals) is selectively populated by electrons, then the stability of the complex increases relative to the d-orbitals on the free metal ion. For example, the single d electron in a d^1 complex such as $[Ti(H_2O)_6]^{3+}$ is located in one of the t_{2g} orbitals. Consequently, this complex will be more stable than expected on purely electrostatic grounds by $0.4\Delta_o$. The additional stabilization of a metal complex by selective population of the lower-energy d orbitals is called its **crystal field stabilization energy** (CFSE).

The CFSE of a complex can be calculated by multiplying the number of electrons in t_{2g} orbitals by the energy of those orbitals ($-0.4\Delta_o$), multiplying the number of electrons in e_g orbitals by the energy of those orbitals ($+0.6\Delta_o$), and summing the two. Using the high-spin d^7 configuration shown in Figure **7.5.1** as an example:

$$\mathbf{CFSE} = (5 \times -0.4\Delta_o) + (2 \times 0.6\Delta_o) = -0.8\Delta_o \tag{7.5.1}$$

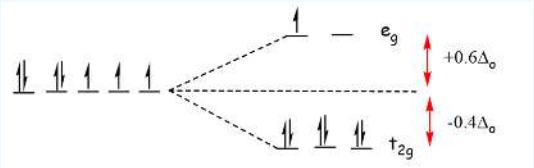
CFSEs are important for two reasons. First, the existence of CFSE nicely accounts for the difference between experimentally measured values for bond energies in metal complexes and values calculated based solely on electrostatic interactions. Second, CFSE represents relatively large amounts of energy (up to several hundred kilojoules per mole), which has important chemical consequences.

Example 7.5.1

What is the Crystal Field Stabilization Energy for a low spin d^7 octahedral complex?

Solution

The splitting pattern and electron configuration for both isotropic and octahedral ligand fields are compared below.



$$\mathbf{CFSE} = (6 \times -0.4\Delta_O) + (1 \times 0.6\Delta_O) = -1.8\Delta_O \tag{7.5.2}$$

Table 7.5.1 gives CFSE values for octahedral complexes with different d electron configurations. The CFSE is highest for low-spin d^6 complexes, which accounts in part for the extraordinarily large number of Co(III) complexes known. The other low-spin configurations also have high CFSEs, as does the d^3 configuration.

Table 7.5.1: CFSEs for Octahedral Complexes with Different Electron Configurations (in Units of Δo)

	High Spin		CFSE (Δ_o)	Low Spin		CFSE (Δ_o)
	t_{2g}	e_g		t_{2g}	e_g	
d^0			0			
d^1	↑		0.4			
d^2	↑ ↑		0.8			
d^3	↑ ↑ ↑		1.2			
d^4	↑ ↑ ↑	↑	0.6	↑↓ ↑ ↑		1.6
d^5	↑ ↑ ↑	↑ ↑	0.0	↑↓ ↑↓ ↑		2.0
d^6	↑↓ ↑ ↑	↑ ↑	0.4	↑↓ ↑↓ ↑↓		2.4
d^7	↑↓ ↑↓ ↑	↑ ↑	0.8	↑↓ ↑↓ ↑↓	↑	1.8
d^8	↑↓ ↑↓ ↑↓	↑ ↑	1.2			
d^9	↑↓ ↑↓ ↑↓	↑↓ ↑	0.6			
d^{10}	↑↓ ↑↓ ↑↓	↑↓ ↑↓	0.0			

> *Octahedral d^3 and d^8 complexes and low-spin d^6, d^5, d^7, and d^4 complexes exhibit large CFSEs.*

Octahedral Preference

Similar CFSE values can be constructed for non-octahedral ligand field geometries. In an octahedral complex, the two e_g orbitals decrease in energy by $0.6\Delta_t$, and the three t_{2g} orbitals increase in energy by $0.4\Delta_t$ (Figure 7.5.2). As for octahedral complexes, the total energy of the d-orbitals in a tetrahedral complex does not change; the total change in energy is

Misplaced '#'

Note: Δ_o and Δ_t represent different units of energy. The tetrahedral crystal field is smaller in energy than the octahedral crystal field, which contributes to the tetrahedral preference for high-spin complexes (Figure 7.5.2). The following conversion may be used for comparing octahedral and tetrahedral complexes that involve same ligands only:

$$\Delta_t \approx \frac{4}{9}\Delta_o \tag{7.5.3}$$

The CFSE for a tetrahedral complex is calculated in Table 7.5.2. These energies can then be compared to the octahedral CFSE to calculate a thermodynamic preference (Enthalpy-wise) for a metal-ligand combination to favor the octahedral geometry. This is quantified via a **Octahedral Site Preference Energy**:

$$OSPE = CFSE_{(oct)} - CFSE_{(tet)}$$

The OSPE quantifies the preference of a complex to exhibit an octahedral geometry vs. a tetrahedral geometry. Figure 7.5.3 compares the CFSE for tetrahedral and octahedral high-spin complexes for each d-electron configuration. From a simple inspection of Figure 7.5.3, the following observations can be made:

- The OSPE is *small* in d^1, d^2, d^5, d^6, d^7 complexes and other factors influence the stability of the complexes including steric factors.

- The OSPE is *large* in d^3 and d^8 complexes which strongly favor octahedral geometries.

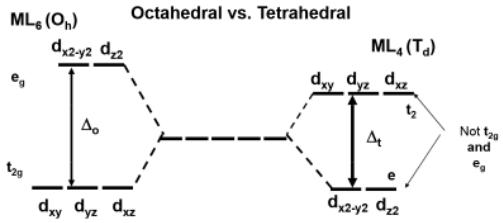


Figure **7.5.2**: A comparison of octahedral and tetrahedral crystal fields. (LibreText)

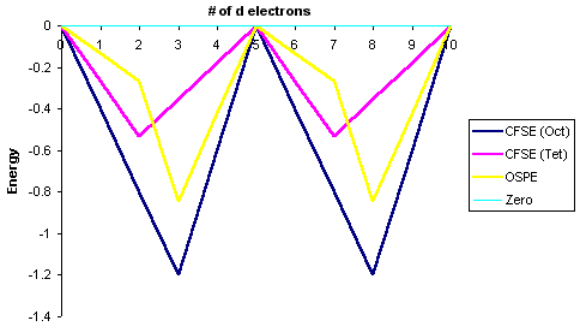


Figure **7.5.1**: Crystal Field Stabilization Energies for both octahedral fields ($CFSE_{oct}$) and tetrahedral fields ($CFSE_{tet}$). Octahedral Site Preference Energies (OSPE) are in yellow. This is for high spin complexes. (LibreText)

Table **7.5.2**: Octahedral Site Preference Energies (OSPE)

Total d-electrons	**CFSE(Octahedral)**		**CFSE(Tetrahedral)**		**OSPE (for high spin complexes)****
	High Spin	Low Spin	Configuration	**Always High Spin***	
d^0	0 Δ_o	0 Δ_o	e^0	0 Δ_t	0 Δ_o
d^1	-2/5 Δ_o	-2/5 Δ_o	e^1	-3/5 Δ_t	-6/45 Δ_o
d^2	-4/5 Δ_o	-4/5 Δ_o	e^2	-6/5 Δ_t	-12/45 Δ_o
d^3	-6/5 Δ_o	-6/5 Δ_o	$e^2t_2^1$	-4/5 Δ_t	-38/45 Δ_o
d^4	-3/5 Δ_o	-8/5 Δ_o + P	$e^2t_2^2$	-2/5 Δ_t	-19/45 Δ_o
d^5	0 Δ_o	-10/5 Δ_o + 2P	$e^2t_2^3$	0 Δ_t	0 Δ_o
d^6	-2/5 Δ_o	-12/5 Δ_o + P	$e^3t_2^3$	-3/5 Δ_t	-6/45 Δ_o
d^7	-4/5 Δ_o	-9/5 Δ_o + P	$e^4t_2^3$	-6/5 Δ_t	-12/45 Δ_o
d^8	-6/5 Δ_o	-6/5 Δ_o	$e^4t_2^4$	-4/5 Δ_t	-38/45 Δ_o
d^9	-3/5 Δ_o	-3/5 Δ_o	$e^4t_2^5$	-2/5 Δ_t	-19/45 Δ_o
d^{10}	0	0	$e^4t_2^6$	0 Δ_t	0 Δ_o

Example 7.5.2

For each complex, predict its structure, whether it is high spin or low spin, and the number of unpaired electrons present.

1. $[Cu(NH_3)_4]^{2+}$
2. $[Ni(CN)_4]^{2-}$

Solution

Because Δ_o is so large for the second- and third-row transition metals, all four-coordinate complexes of these metals are square planar due to the much higher crystal field stabilization energy (CFSE) for square planar versus tetrahedral structures. The only exception is for d^{10} metal ions such as Cd^{2+}, which have zero CFSE and are therefore tetrahedral as predicted by the VSEPR model. Four-coordinate complexes of the first-row transition metals can be either square planar or tetrahedral; the former is favored by strong-field ligands, whereas the latter is favored by weak-field ligands. For example, the $[Ni(CN)_4]^{2-}$ ion is square planar, while the $[NiCl_4]^{2-}$ ion is tetrahedral.

1.

The copper in this complex is a d^9 ion and it has a coordination number of 4. So it is probably either square planar or tetrahedral. To estimate which, we need to fill in the CFT splitting diagrams for each with 9 electrons and ask which has a lower energy. Comparing the square planer (Figure **7.5.1**) splitting diagram with tetrahedral (Figure **7.5.2**), suggests that 9 electrons will have a net lower total energy for square planar (since the $d_{x^2-y^2}$ orbital is high in energy, the others are lower).

For the square planar structure, neither high nor low spin states are possible (only one state) with a single unpaired electron.

2.

The nickle in this complex is a d^8 ion and it has a coordination number of 4. So it is probably either square planar or tetrahedral. To estimate which, we need to fill in the CFT splitting diagrams for each with 8 electrons and ask which has a lower energy. Comparing the square planer (Figure **7.5.1**) splitting diagram with tetrahedral (Figure **7.5.2**), suggests that 8 electrons will have a net lower total energy for square planar (since the $d_{x^2-y^2}$ orbital is high in energy, the others are lower).

For the square planar structure, it is a low spin complex since a high spin requires a lot of energy to promote to the $d_{x^2-y^2}$ orbital. Hence, there are no unpaired electrons.

Example 7.5.3

Which is the preferred configuration for a d^3 metal: tetrahedral or octahedral?

Solution

To answer this, the *Crystal Field Stabilization Energy* has to be calculated for a (d^3 metal in both configurations. The geometry with the greater stabilization will be the preferred geometry.

- For a d^3 *octahedral* configuration, the *Crystal Field Stabilization Energy* is

$$3 \times -0.4\Delta_o = -1.2\Delta_o$$

- For a d^3 *tetrahedral* configuration (assuming high spin), the *Crystal Field Stabilization Energy* is

$$-0.8\Delta_{tet}$$

Remember that because Δ_{tet} is less than half the size of Δ_o, tetrahedral complexes are often high spin. We can now put this in terms of Δ_o (we can make this comparison because we're considering the same metal ion and the same ligand: all that's changing is the geometry)

So for tetrahedral d^3, the Crystal Field Stabilization Energy is:

$$\text{CFSE} = -0.8 \times 4/9\ \Delta_o = -0.355\ \Delta_o.$$

And the difference in Crystal Field Stabilization Energy between the two geometries will be:

$$1.2 - 0.355 = 0.845\ \Delta_{o.}$$

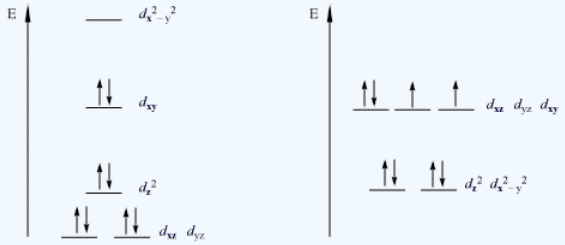
Example 7.5.4

The molecule $[PdCl_4]^{2-}$ is diamagnetic, which indicates a square planar geometry as all eight d-electrons are paired in the lower-energy orbitals. However, $[NiCl_4]^{2-}$ is also d^8 but has two unpaired electrons, indicating a tetrahedral geometry. Why is $[PdCl_4]^{2-}$ square planar if Cl^- is not a strong-field ligand?

Solution

The geometry of the complex changes going from $[NiCl_4]^{2-}$ to $[PdCl_4]^{2-}$. Clearly this cannot be due to any change in the ligand since it is the same in both cases. It is the other factor, the metal, that leads to the difference.

Consider the splitting of the d-orbitals in a generic d^8 complex. If it were to adopt a square planar geometry, the electrons will be stabilized (with respect to a tetrahedral complex) as they are placed in orbitals of lower energy. However, this comes at a cost: two of the electrons, which were originally unpaired in the tetrahedral structure, are now paired in the square-planer structure:



We can label these two factors as ΔE (stabilization derived from occupation of lower-energy orbitals) and P (spin pairing energy) respectively. One can see that:

- If $\Delta E > P$, then the complex will be square planar
- If $\Delta E < P$, then the complex will be tetrahedral.

This is analogous to deciding whether an octahedral complex adopts a high- or low-spin configuration; where the crystal field splitting parameter Δ_o ΔE does above. Unfortunately, unlike Δ_o in octahedral complexes, there is no simple graphical way to represent ΔE on the diagram above since multiple orbitals are changed in energy between the two geometries.

Interpreting the origin of metal-dependent stabilization energies can be tricky. However, we know experimentally that Pd^{2+} has a larger splitting of the d-orbitals and hence a larger ΔE than Ni^{2+} (moreover P is also smaller).

Practically all 4d and 5d d^8 ML_4 complexes adopt a square planar geometry, irrespective if the ligands are strong-field ligand or not. Other examples of such square planar complexes are $[PtCl_4]^{2-}$ and $[AuCl_4]^-$.

Problems

? Exercise 7.5.1

Determine the crystal field stabilization energy (CFSE) in the following octahedral ions:

a. V^{3+}
b. Ni^{2+}
c. Cr^{3+}
d. Zn^{2+}

Answer a

V^{3+} is d^2, with two electrons in the t_{2g} and zero electrons in e_g.

CFSE = $[2(-0.4) + 0(0.6)] \times \Delta_o = -0.8\Delta_o$

Answer b

Ni^{2+} is d^8, with six electrons in t_{2g} and two electrons in e_g.

CFSE = $[6(-0.4) + 2(0.6)] \times \Delta_o = -1.2\Delta_o$

Answer c

Cr^{3+} is d^3, with three electrons in t_{2g} and zero electrons in e_g.

CFSE = $[3(-0.4) + 0(0.6)] \times \Delta_o = -1.2\Delta_o$

Answer d

Zn^{2+} is d^{10}, with six electrons in t_{2g} and four electrons in e_g.

CFSE = $[6(-0.4) + 4(0.6)] \times \Delta_o = 0\Delta_o$.

? Exercise 7.5.2

What are the geometries of the following two complexes?

1. $[AlCl_4]^-$
2. $[Ag(NH_3)_2]^+$

Answer 1

tetrahedral

Answer 2

linear

Contributors and Attributions

- Asadullah Awan (UCD), Hong Truong (UCD)
- Prof. Robert J. Lancashire (The Department of Chemistry, University of the West Indies)

7.5: LFSE/CFSE Calculations Again is shared under a CC BY-NC-SA 4.0 license and was authored, remixed, and/or curated by Kathryn A. Newton, Northern Michigan University.

- **24.5: Bonding in Complex Ions: Crystal Field Theory** is licensed CC BY-NC-SA 4.0.
- **Crystal Field Stabilization Energy** is licensed CC BY-NC-SA 4.0.
- **Non-octahedral Complexes** by Anonymous is licensed CC BY-NC-SA 4.0.
- **Octahedral vs. Tetrahedral Geometries** is licensed CC BY-NC-SA 4.0.
- **Tetrahedral vs. Square Planar Complexes** is licensed CC BY 4.0.
- **10.2.1: Crystal Field Theory** by Chris Schaller is licensed CC BY-NC 4.0.
- **Crystal Field Theory** is licensed CC BY-NC-SA 4.0.

7.6: Spectrochemical Series of Ligands (Again)

The spectrochemical series was determined through an examination of the absorption spectra of a series of octahedral $Co(III)$ complexes by Tsuchida in the 1930's. The position of the d-d absorption band is influenced by the field strength of the ligand, which leads to greater or lesser values of Δ_o. That interaction depends on both the relative energies of the metal and ligand orbitals and the degree of overlap between these orbitals. The closer in energy the two orbitals are to each other, the greater the interaction. Also, the greater the overlap between the two orbitals, the greater the interaction.

Recall that sigma donors simply donate a lone pair to the metal but do not have additional metal-ligand interactions. The classic example is ammonia. The nitrogen in ammonia has only one lone pair to donate and is a simple sigma donor. Ethylenediamine, $NH_2CH_2CH_2NH_2$ (en), is also a sigma donor because it has a single lone pair on each nitrogen atom. The en ligand is a slightly stronger sigma donor than ammonia. The difference is explained by the slightly stronger basicity of en compared to ammonia; the nitrogen lone pairs in en are better donors to both protons and metal ions.

en > NH3 (basicity)

The common pi donors include the halides and some oxygen donors. In these cases, the donor atom has an additional lone pair (or more) which may engage in formation of a pi bond by donation to a metal d orbital. Among the halides, fluoride produces the largest field splitting and iodide the smallest. This trend is also explained in terms of the relative basicity of these halides; fluoride is more basic than bromide. In addition, there is also understood to be better overlap between fluorine's p orbital and the d acceptor of a positively charged metal ion, compared to larger halides such as iodine.

F- > Cl- > Br- > I- (basicity)

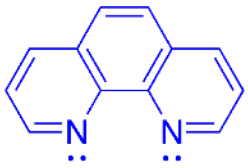
Oxygen donors do not follow this basicity trend. Hydroxide is thought to act as a better pi donor than water, partly because of its negative charge. A carboxylate ligand is not quite as strong a pi donor as hydroxide, probably because its lone pair is delocalized into the carbonyl group.

H20 > RCO2- > HO- (pi donation anion vs neutral)

The pi acceptors include familiar examples such as carbon monoxide (carbonyl ligand) as well as the aromatic phenanthroline.

CO > -CN > phenanthroline > NO2- > SCN-

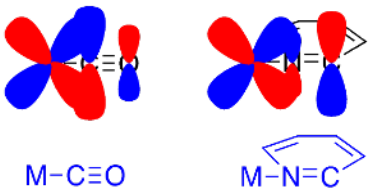
The phenanthroline may be an unfamiliar ligand. It is an aromatic amine, like pyridine. Other aromatic ligands, if they donate through a lone pair such as a phenyl, $C_6H_5^-$, can also be considered pi acceptors. These compounds feature a pi bond that includes the donor atom, so there is a pi* orbital at that position capable of undergoing back-donation from the metal.



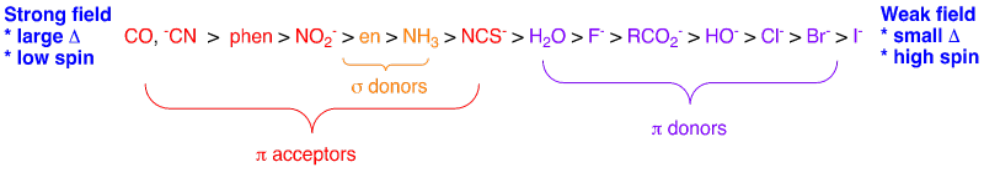
phenanthroline (phen)

Again, there are subtle variations among the field strengths exhibited by these pi acceptors, and there may be several factors contributing to those differences. For example, the cyanide is only slightly weaker field than the isoelectronic carbon monoxide. That small difference may be due to the negative charge on the cyanide rendering it a weaker electron acceptor. On the other hand, phenanthroline is neutral, but it is still a weaker donor than carbon monoxide. That weaker field may be due to the smaller lobe on the nitrogen atom in the pi* orbital in phenanthroline. Because nitrogen is more electronegative than carbon, it makes a greater contribution to the C=N pi bonding orbital than carbon; the opposite is true in the antibonding orbital. Carbon monoxide, in contrast, features a larger lobe on carbon in its pi* orbital. The result is better metal-ligand pi overlap with carbon monoxide than with phenanthroline.

Phosphines are also commonly considered to be pi acceptors, for subtle reasons that have been subject to some debate.1

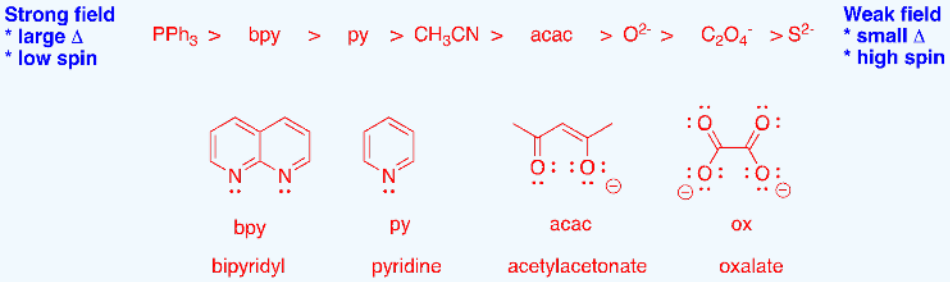


All three of these series can be collated to arrive at a combined list, which is a more complete spectrochemical series. Note that there may be some overlap between the different types of donors. Nevertheless, the overall trend holds: pi acceptors lead to the greatest field splitting on average, whereas di donors lead to the smallest.



Example 7.6.1

Some additional common ligands are displayed according to field strength, below. Classify these ligands as pi donors, sigma donors, or pi acceptors.



Solution

Ph3, based on its structure, appears to be a sigma donor only because it has just one lone pair on the donor atom. However, phosphines tend to behave as pi acceptors; that is, they appear to withdraw some electron density from the metal as indicated by the response of reporter ligands such as CO.

Bpy, py and CH3CN (acetonitrile) all appear to be pi acceptors. Like phen, they behave as weak pi acceptors.

Acac, oxide, oxalate and sulfide are all pi donors. The donor atom in each case has a lone pair in addition to the sigma donor pair.

References

1. Wolczanski, P. T. "Flipping the Oxidation State Formalism: Charge Distribution in Organometallic Complexes as Reported by Carbon Monoxide". *Organometallics* **2017**, *36*, 622-631.

7.6: Spectrochemical Series of Ligands (Again) is shared under a CC BY-NC-SA 4.0 license and was authored, remixed, and/or curated by Kathryn A. Newton, Northern Michigan University.

7.7: Exchange Inertness of d3, d4(LS), d5(LS), d6(LS), and d8(SQP)

Introduction

Kinetics is a branch of chemistry that is concerned with the rates of chemical reactions. In this section, we will discuss the rates of metal-ligand (M-L) substitution reactions.

Let's start with some examples. In the table below are three examples of ligand substitution reactions of hexaaquo metal complexes to form hexaammine complexes. These reactions are nearly identical with the exception of the metal ion. The products are thermodynamically favored in all cases.

Reaction	Rate constant (k)	Labile or Inert
$[Ni(OH_2)]^{2+} + 6NH_3 \rightleftharpoons [Ni(NH_3)_6]^{2+}$	$k = 10^4 s^{-1}$	Labile (happens in < 1 min)
$[Cr(OH_2)]^{3+} + 6NH_3 \rightleftharpoons [Cr(NH_3)_6]^{3+}$	$k = 10^{-3} s^{-1}$	Inert (slow, takes hours)
$[Cu(OH_2)]^{2+} + 6NH_3 \rightleftharpoons [Cu(NH_3)_6]^{2+}$	$k = 10^8 s^{-1}$	Very Labile (happens in seconds)

Definitions

- **Labile** - Metal complexes that undergo "kinetically fast" substitution reactions are **labile**. These reactions usually happen in less than one minute.
- **Inert** - Metal complexes that undergo "kinetically slow" substitution reactions are **inert** or **non-labile**. These reactions usually take hours.
- **Intermediate** - Metal complexes that undergo "kinetically intermediate" substitution reactions are **intermediate**.

A common pitfall is to confuse the meaning of kinetic terms, like *labile* and *inert*, with thermodynamic terms, like *stable* and *unstable*. It is important to distinguish between kinetics and thermodynamics. For example, the complex $[Fe(H_2O)Cl]^{2+}$ has a large formation constant and is thermodynamically stable; yet it is also labile. On the other hand, the complex $[Co(NH_3)_6]^{3+}$ is unstable in acidic aqueous solution and decomposes spontaneously to $[Co(H_2O)_6]^{3+}$; yet it decomposes slowly because it is inert. It is good practice to distinguish between meanings by using terms such as "kinetically labile" or "kinetically inert" and "thermodynamically stable" and "thermodynamically unstable".

Reaction Coordinate Diagrams

One way to visualize chemical reactions is through reaction coordinate diagrams (Figure **7.7.1**). These diagrams illustrate the relative free energy of the reactants and products, when the free energy of the products is lower than the reactants ΔG_{rxn} is negative and the reaction is spontaneous. This is what determines thermodynamic stability. These diagrams also illustrate the changes in free energy as the reaction progresses from reactants to products. In the case of a single step, concerted reaction the reactants go through a higher energy transition state before (potentially) forming products. The free energy difference between the reactants and the transition state is the free energy of activation ($\Delta G^{\ddagger}$), which determines the rate of the reaction. A larger $\Delta G^{\ddagger}$ yields a slower reaction rate because fewer reactants have sufficient energy to form products. In cases where the reaction occurs in 2 steps an intermediate is formed. The step with the largest $\Delta G^{\ddagger}$ will be the slowest, rate determining step. The magnitude of $\Delta G^{\ddagger}$ is what determines kinetic lability.

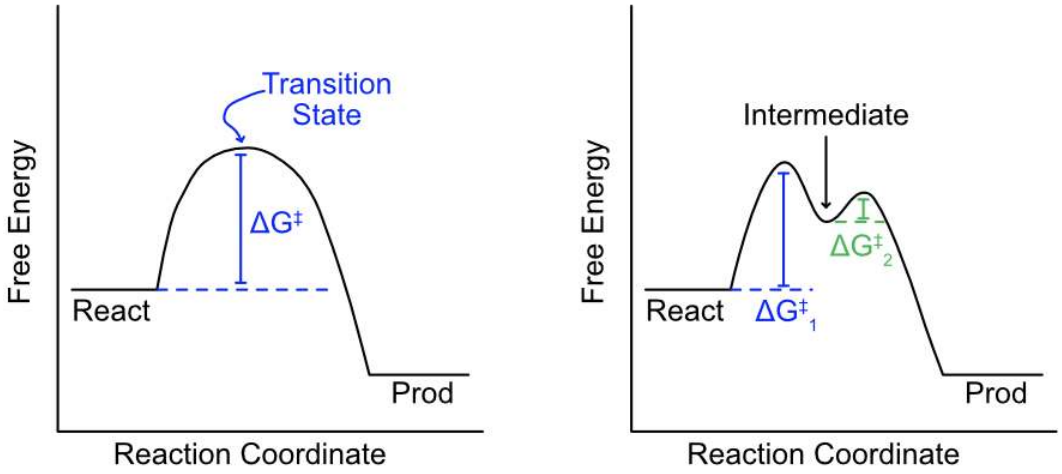


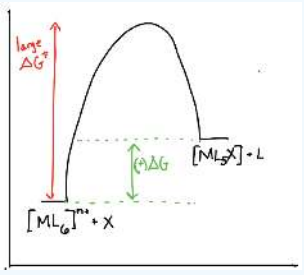
Figure **7.7.1**: Example reaction coordinate diagrams for a single step reaction (left) and a reaction with an intermediate (right). $\Delta G^{\ddagger}$ is the free energy of activation. (CC BY-NC-SA; Catherine McCusker)

Exercise 7.7.1

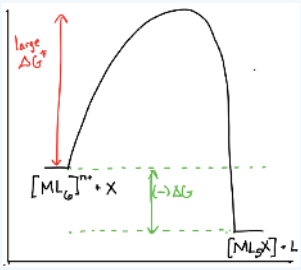
Draw the reaction coordinate diagrams for a reaction of the form $[ML_6]^{n+} + X \rightleftharpoons [ML_5X]^{n+} + L$ in the following scenarios:

a. $[ML_6]^{n+}$ is thermodynamically stable and kinetically inert.
b. $[ML_6]^{n+}$ is thermodynamically unstable and kinetically inert.
c. $[ML_6]^{n+}$ is thermodynamically stable and kinetically labile.
d. $[ML_6]^{n+}$ is thermodynamically unstable and kinetically labile.

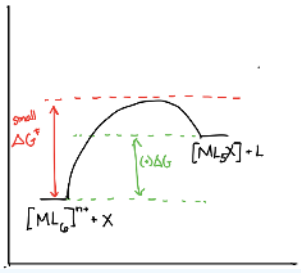
Answer a)



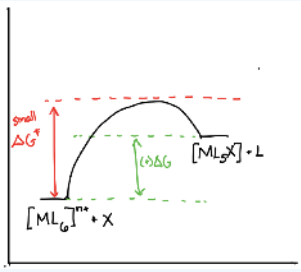
Answer b)



Answer c)



Answer d)



Self Exchange Reactions

$$[ML_5L]^{n+} + L \rightleftharpoons [ML_5L]^{n+} + L \tag{7.7.1}$$

The rate of a chemical reaction depends on both thermodynamic and kinetic factors. One way to isolate the kinetic factors is to study self exchange reactions. In a self exchange reaction the incoming and outgoing ligand are the same and the ΔG_{rxn} of the reaction is 0. In practice this is often done by dissolving hexaaqua metal complexes in isotopically labeled water and monitoring the ligand exchange reaction by NMR. These experiments have found reaction rates for different metals that span more than 12 orders of magnitude as shown in Figure 7.7.2.

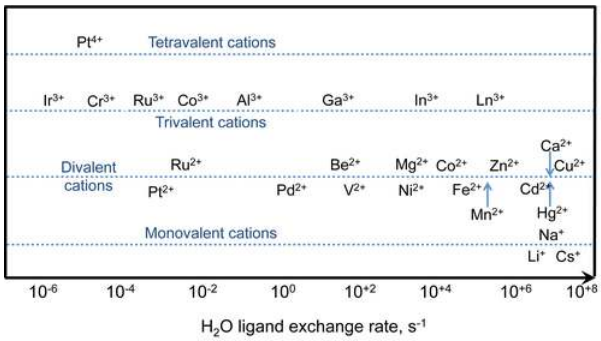


Figure 7.7.2: Water exchange rates measured by NMR for a series of metal ions. (CC BY-SA; Tem5psu via Wikimedia)

Factors that Affect Rates of Substitution Reactions

Some of the factors that affect rates of ligand substitution reactions are those that also affect thermodynamic stability. It is important to remember that kinetic and thermodynamic factors are related, yet separate. The same factors that make a complex stable can also make it more inert. However, it is incorrect to assume that stability is always correlated with reaction rates.

Why are kinetic factors related to thermodynamic stability? For a complex to react or exchange one ligand for another, it must change its geometry to form an intermediate or transition state. For example, inert octahedral complexes often have stable electron configurations. When the reactant electron configuration is particularly stable, it can result in a higher activation energy associated with moving away from the stable configuration.

Factors to consider

1. Electron configuration and LFSE: Electron configurations that place electrons in higher-energy orbitals (particularly antibonding orbitals) result in more labile complexes. As long as there are not electrons in higher-energy orbitals, the lability correlates roughly with LFSE. The more negative the LFSE, the more inert.
2. Size and charge of the metal ion: In general, higher charge density on the metal ion leads to stronger electrostatic attraction between metal and ligand; higher charge density generally correlates with slower rates of ligand substitution.

Taube's Observations of Substitution Rates

Henry Taube (Nobel Prize, 1983) tried to understand lability by comparing the factors that govern bond strengths in ionic complexes to observations about the rates of reaction of coordination complexes. He saw some things that were unsurprising. He also drew some new conclusions based on ligand field theory. Taube observed that many M^{+1} ions are more labile than many M^{+3} ions, in general. That isn't too surprising, since metal ions function as electrophiles or Lewis acids and ligands function as nucleophiles or Lewis bases in forming coordination complexes. In other words, metals with higher charges ought to be stronger Lewis acids, and so they should bind ligands more tightly. However, there were exceptions to that general rule. For example, Taube also observed that Mo^{+5} compounds are more labile than Mo^{+3} compounds. So, there must be more going on here than just the effects of electrostatic attraction.

Another factor that governs ionic bond strengths is the size of the ion. Typically, ions with smaller atomic radii form stronger bonds than ions with larger radii. Taube observed that Al^{3+}, V^{3+}, Fe^{3+} and Ga^{3+} ions are all about the same size. All these ions exchange ligands at about the same rate. That isn't surprising, because they have the same charge and the same radius. However, Cr^{3+} is also about the same size as those ions and it also has the same charge, but it is much less labile. Once again, there are exceptions to our regular expectations based on simple electrostatic considerations. Furthermore, 4d and 5d transition metals (Y→Cd, and Ac→Hg) are much more inert than 3d transition metals (Sc→Zn). This is unexpected when we consider size; the 4d and 5d metals are much larger than the 3d metals. This unexpected behavior tells us that electrostatics alone cannot predict lability.

Exercise 7.7.2

In which compound from each pair would you expect the strongest ionic bonds? Why?

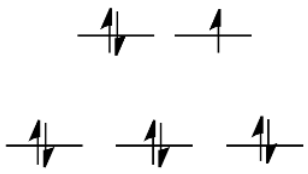
a) LiF vs KBr
b) $CaCl_2$ vs. KCl

Answer a

The ions in LiF are both smaller than in KBr, so the force of attraction between the ions in LiF is greater because of the smaller separation between the charges.

Answer b

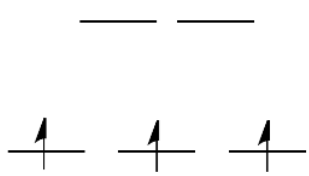
Calcium has a 2+ charge in $CaCl_2$, whereas potassium has only a + charge, so the chloride ions are more strongly attracted to the calcium than to the potassium.



Cu^{2+}

Taube came up with a hypothesis that could explain the seeming contradictory observations described above: *kinetic lability must be affected by d-electron configuration*. This idea forms the basis of Taube's rules about lability. For example, metals like Ni^{2+} and Cu^{2+} are very labile. The d orbital splitting diagrams for those compounds would have d electrons in the e_g set. Remember, the e_g

set arises from interaction with the ligand donor orbitals; this set corresponds to a σ antibonding level. By comparison, V^{2+} is rather inert. The d orbital splitting diagram in this case has electrons in the t_{2g} set, but none in the e_g set. So, having electrons in the higher energy, antibonding e_g level weakens the bond to the ligand, so the ligand can be replaced more easily. In the absence of those higher energy electrons, the bond to the ligand is stronger, and the ligand isn't replaced as easily.



V^{2+}

On the other hand, metals like Ca^{2+}, Sc^{3+} and Ti^{4+} are pretty labile. The d orbital splitting diagrams in those cases are pretty simple: there are no d-electrons at all in these ions. That means having no electrons in these mostly non-bonding levels leaves the complex susceptible to ligand replacement. But it's hard to see why population of an orbital that is mostly non-bonding would have an effect on ligand bond strength. Instead, this factor probably has something to do with the part of ligand substitution that we have ignored so far. Not only does one ligand need to leave, but a second one needs to bond in its place. So, having an empty orbital for the ligand to donate electrons into (or, put another way, not having electrons in the way that may complicate donation from the ligand) makes that part of the reaction easier.

Electron configurations can be generally classified as inert or labile based on crystal field stabilization energy. Configurations with high CFSE will be inert and configurations with low CFSE will be labile. Configurations that are most susceptible to Jahn-Teller distortions will be exceptionally labile, as the elongated bonds will be weaker and those ligands more easily exchanged.

Labile and inert electron configurations

Inert	Labile	Very labile
d^3, ls d^4, ls d^5, ls d^6,	d^1, d^2, hs d^5, hs d^6, hs d^7, d^{10}	hs d^4, d^9

Exercise 7.7.3

Put the metal ions in order of decreasing reaction rate (from labile to inert):

a) Al^{3+}, Na^{+}, Mg^{2+}

b) $Ca^{2+}, Mg^{2+}, Sr^{2+}$

Answer (a)

Most labile to most inert: $Na^{+} > Mg^{2+} > Al^{3+}$

These are metal ions with similar size and varying charge. They are in order of increasing charge and increasing density from left to right.

Answer (b)

Most labile to most inert: $Sr^{2+} > Ca^{2+} > Mg^{2+}$

These metal ions have the same charge, and vary in size. They are in order of decreasing charge and increasing charge density from left to right.

Exercise 7.7.4

Predict whether octahedral complexes of the following metals are labile or inert

a) Co^{3+} (high spin)

b) Co^{3+} (low spin)

c) Fe^{2+} (low spin)

d) Fe^{2+} (high spin)

e) Zn^{2+}

Answer a

hs d^6 labile (electrons in higher energy d orbital set)

Answer b

ls d^6 inert (all electrons in lower energy d orbitals)

Answer c

ls d^6 inert (all electrons in lower energy d orbitals)

Answer d

hs d^5 labile (electrons in higher energy d orbital set, CFSE = 0)

Answer e

d^{10} labile (electrons in higher energy d orbital set, CFSE = 0)

Overall Generalizations for Kinetics

1. s-block metals are very labile, except for those with very high charge density (eg. Mg^{2+} *is inert*)
2. d^{10} metals are labile (eg: Zn^{2+}, Cu^{+}, Hg^{2+})
3. Other ions with a full shell are labile (eg: La^{3+} of f-block)
4. 3d M^{2+}, *when high spin*, are generally labile (eg. Cu^{2+}*is very labile*)
5. 4d and 5d are usually inert due to higher CFSE (low spin, high CFSE)
6. M^{2+} is more labile than the same metal as M^{3+}
7. d^3 and low spin d^6 are inert (eg. Cr^{3+}, Co^{3+}, low spin Fe^{2+})

Attribution

Chris P Schaller, Ph.D., (College of Saint Benedict / Saint John's University)

Curated or created by Kathryn Haas

- Modified by Catherine McCusker (East Tennessee State University)

7.7: Exchange Inertness of d3, d4(LS), d5(LS), d6(LS), and d8(SQP) is shared under a not declared license and was authored, remixed, and/or curated by LibreTexts.

- **10.2: Trends in Kinetic Lability** has no license indicated.

7.8: O2 Reduction, since CO displaces O2

Thermodynamics

The reduction potential for the four-electron reduction of dioxygen (Reaction 5.1) is a measure of the great oxidizing power of the dioxygen molecule.[8] However, the reaction involves the transfer of four electrons, a process that rarely, if ever, occurs in one concerted step, as shown in Reaction (5.2).

$$O_2 \xrightarrow{e^-} O_2^- \xrightarrow{e^-,2H^+} H_2O_2 \xrightarrow{e^-,H^+} H_2O + OH \xrightarrow{e^-,H^+} 2H_2O \tag{5.2}$$

$$\begin{aligned} dioxygen \xrightarrow{e^-} superoxide \xrightarrow{e^-,2H^+} hydrogen\ peroxide \xrightarrow{e^-,H^+} water \\ + hyrdoxyl\ radical \xrightarrow{e^-,H^+} water \end{aligned} \tag{7.8.1}$$

Since most reducing agents can transfer at most one or two electrons at a time to an oxidizing agent, the thermodynamics of the one- and two-electron reductions of dioxygen must be considered in order to understand the overall mechanism.

In aqueous solution, the most common pathway for dioxygen reduction in the absence of any catalyst is one-electron reduction to give superoxide. But this is the least favorable of the reaction steps that make up the full four-electron reduction (see Table 5.1) and requires a moderately strong reducing agent. Thus if only one-electron pathways are available for dioxygen reduction, the low reduction potential for one-electron reduction of O_2 to O_2^- presents a barrier that protects vulnerable species from the full oxidizing power of dioxygen that comes from the subsequent steps. If superoxide is formed (Reaction 5.3), however, it disproportionates quite rapidly in aqueous solution (except at very high pH) to give hydrogen peroxide and dioxygen (Reaction 5.4). The stoichiometry of the overall reaction is therefore that of a net two-electron reduction (Reaction 5.5). It is thus impossible under normal conditions to distinguish one-electron and two-electron reaction pathways for the reduction of dioxygen in aqueous solution on the basis of stoichiometry alone.

$$2O_2 + 2e^- \rightarrow 2O_2^- \tag{5.3}$$

$$2O_2^- + 2H^+ \rightarrow H_2O_2 + O_2 \tag{5.4}$$

$$O_2 + 2e^- + 2H^+ \rightarrow H_2O_2 \tag{5.5}$$

Table 5.1: Standard reduction potentials for dioxygen species in water. a) The standard state used here is unit pressure. If unit activity is used for the standard state of O_2, the redox potentials for reactions of that species must be adjusted by +0.17 V.[8,9]

Reaction		E°, V vs. NHE, pH 7, 25 °C
$O_2 + e^- \rightarrow O_2^-$	(7.8.2)	-0.33[a]
$O_2^- + e^- + 2H^+ \rightarrow H_2O_2$	(7.8.3)	+0.89
$H_2O_2 + e^- + H^+ \rightarrow H_2O + OH$	(7.8.4)	+0.38
$OH + e^- + H^+ \rightarrow H_2O$	(7.8.5)	+2.31
$O_2 + 2e^- + 2H^+ \rightarrow H_2O_2$	(7.8.6)	+0.281[a]
$H_2O_2 + 2e^- + 2H^+ \rightarrow 2H_2O$	(7.8.7)	+1.349
$O_2 + 4H^+ + 4e^- \rightarrow 2H_2O$	(7.8.8)	+0.815[a]

The thermodynamics of dioxygen reactions with organic substrates is also of importance in understanding dioxygen reactivity. The types of reactions that are of particular interest to us here are hydroxylation of aliphatic and aromatic C—H bonds and epoxidation of olefins, since these typical reactions of oxygenase enzymes are ones that investigators are trying to mimic using synthetic reagents. Some of the simpler examples of such reactions (plus the reaction of H_2 for comparison) are given in the reactions in Table 5.2. It is apparent that all these reactions of dioxygen with various organic substrates in Table 5.2 are thermodynamically favorable. However, *direct* reactions of dioxygen with organic substrates in the absence of a catalyst are generally very slow, unless the substrate is a particularly good reducing agent. To understand the sluggishness of dioxygen reactions with organic substrates, we must consider the kinetic barriers to these reactions.

Table 5.2: Examples of hydroxylation and epoxidation reactions.

Reaction	ΔH in kcal/mol	Reference
$CH_{4(g)} + \frac{1}{2}O_{2(g)} \rightarrow CH_3OH_{(g)}$ (7.8.9)	-30	10
$C_6H_{6(g)} + \frac{1}{2}O_{2(g)} \rightarrow C_6H_5OH_{(g)}$ (7.8.10)	-43	11,12
$C_6H_5OH_{(g)} + \frac{1}{2}O_{2(g)} \rightarrow C_6H_5(OH)_{2(g)}$ (7.8.11)	-42	12,13
$C_2H_{4(g)} + \frac{1}{2}O_{2(g)} \rightarrow C_2H_4O_{(g)}$ (7.8.12)	-25	10
$C_5H_5N_{(g)} + \frac{1}{2}O_{2(g)} \rightarrow C_5H_5NO_{(g)}$ (7.8.13)	-13	14
$H_{2(g)} + \frac{1}{2}O_{2(g)} \rightarrow H_2O_{(g)}$ (7.8.14)	-58	10

Kinetics

The principal kinetic barrier to direct reaction of dioxygen with an organic substrate arises from the fact that the ground state of the dioxygen molecule is triplet, i.e., contains two unpaired electrons.[15,16] Typical organic molecules that are representative of biological substrates have singlet ground states, i.e., contain no unpaired electrons, and the products resulting from their oxygenation also have singlet ground states. Reactions between molecules occur in shorter times than the time required for conversions from triplet to singlet spin. Therefore the number of unpaired electrons must remain the same before and after each elementary step of a chemical reaction. For these reasons, we know that it is impossible for Reaction (5.6) to go in one fast, concerted step.

$$\frac{1}{2}\,{}^3O_2 + {}^1X \rightarrow {}^1XO \qquad (5.6)$$

$$\uparrow\uparrow \quad \downarrow\uparrow \qquad \downarrow\uparrow \qquad (7.8.15)$$

The arrows represent electron spins: $\downarrow\uparrow$ represents a singlet molecule with all electron spins paired; $\uparrow\uparrow$ represents a triplet molecule with two unpaired electrons; and $\uparrow$ (which we will see in Reaction 5.13) represents a doublet molecule, also referred to as a free radical, with one unpaired electron. The pathways that do not violate the spin restriction are all costly in energy, resulting in high

activation barriers. For example, the reaction of ground-state triplet dioxygen, i.e.,$^3O_2$, with a singlet substrate to give the excited triplet state of the oxygenated product (Reaction 5.7) is spin-allowed, and one could imagine a mechanism in which this process is followed by a slow spin conversion to a singlet product (Reaction 5.8).

$$\frac{1}{2}\,{}^3O_2 + {}^1X \rightarrow {}^3XO \tag{5.7}$$

$$\uparrow\uparrow \quad \downarrow\uparrow \qquad \uparrow\uparrow \tag{7.8.16}$$

$${}^3XO \xrightarrow{slow} {}^1XO \tag{5.38}$$

$$\uparrow\uparrow \qquad \downarrow\uparrow \tag{7.8.17}$$

But such a reaction pathway would give a high activation barrier, because the excited triplet states of even unsaturated molecules are typically 40-70 kcal/mol less stable than the ground state, and those of saturated hydrocarbons are much higher.[17] Likewise, a pathway in which O_2 is excited to a singlet state that then reacts with the substrate would be spin-allowed (Reactions 5.9 and 5.10). The high reactivity of singlet dioxygen, generated by photochemical or chemical means, is well-documented.[18,19] However, such a pathway for a reaction of dioxygen, which is initially in its ground triplet state, would also require a high activation energy, since the lowest-energy singlet excited state of dioxygen is 22.5 kcal/mol higher in energy than ground-state triplet dioxygen.[15,16]

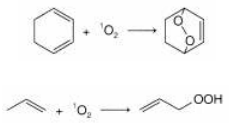
$${}^3O_2 + 22.5\ kcal/mol \rightarrow {}^1O_2 \tag{5.9}$$

$$\uparrow\uparrow \qquad\qquad \downarrow\uparrow \tag{7.8.18}$$

$$\frac{1}{2}\,{}^1O_2 + {}^1X \rightarrow {}^1XO \tag{5.10}$$

$$\downarrow\uparrow \quad \downarrow\uparrow \qquad \downarrow\uparrow \tag{7.8.19}$$

Moreover, the products of typical reactions of singlet-state dioxygen with organic substrates (Reactions 5.11 and 5.12, for example) are quite different in character from the reactions of dioxygen with organic substrates catalyzed by oxygenase enzymes (see Section V):



One pathway for a direct reaction of triplet ground-state dioxygen with a singlet ground-state organic substrate that can occur readily without a catalyst begins with the one-electron oxidation of the substrate by dioxygen. The products of such a reaction would be two doublets, i.e., superoxide and the oneelectron oxidized substrate, each having one unpaired electron (Reaction 5.13). These free radicals can diffuse apart and then recombine with their spins paired (Reaction 5. 14).

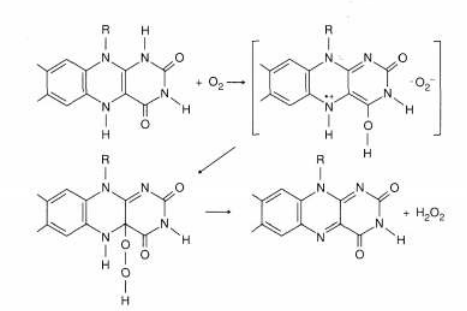
$${}^3O_2 + {}^1X \rightarrow {}^2O_2^- + {}^2X^+ \tag{5.13}$$

$$\uparrow\uparrow \quad \downarrow\uparrow \quad \uparrow \quad \uparrow \tag{7.8.20}$$

$${}^2O_2^- + {}^2X^+ \rightarrow {}^2O_2^- + 2X^+ \rightarrow {}^1XO_2 \tag{5.14}$$

$$\uparrow \quad \uparrow \qquad \uparrow \quad \downarrow \qquad \downarrow\uparrow \tag{7.8.21}$$

Such a mechanism has been shown to occur for the reaction of dioxygen with reduced flavins shown in Reaction (5.15).[20]



However, this pathway requires that the substrate be able to reduce dioxygen to superoxide, a reaction that requires an unusually strong reducing agent (such as a reduced flavin), since dioxygen is not a particularly strong one-electron oxidizing agent (see Table 5.1 and discussion above). Typical organic substrates in enzymatic and nonenzymatic oxygenation reactions usually are not sufficiently strong reducing agents to reduce dioxygen to superoxide; so this pathway is not commonly observed.

The result of these kinetic barriers to dioxygen reactions with most organic molecules is that uncatalyzed reactions of this type are usually quite slow. An exception to this rule is an oxidation pathway known as free-radical autoxidation.

Free-Radical Autoxidation

The term free-radical autoxidation describes a reaction pathway in which dioxygen reacts with an organic substrate to give an oxygenated product in a free-radical chain process that requires an initiator in order to get the chain reaction started.[21] (A free-radical initiator is a compound that yields free radicals readily upon thermal or photochemical decomposition.) The mechanism of free radical autoxidation is as shown in Reactions (5.16) to (5.21).

Initiation: $$X_{2} \rightarrow 2X \cdotp \tag{5.16}$$

$$X\cdot + RH \rightarrow XH + R\cdot \tag{5.17}$$

Propagation: $$R \cdotp + O_{2} \rightarrow ROO \cdotp \tag{5.18}$$

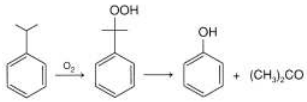
$$\downarrow \quad \uparrow\uparrow \qquad \uparrow \tag{7.8.22}$$

$$ROO\cdot + RH \rightarrow ROOH + R\cdot \tag{5.19}$$

Termination: $$R \cdotp + ROO \cdotp \rightarrow ROOR \tag{5.20}$$

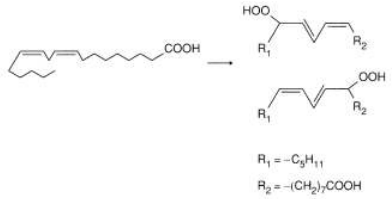
$$2ROO\cdot \rightarrow ROOOOR \rightarrow O_2 + ROOR \tag{5.21}$$

(plus other oxidized products, such as ROOH, ROH, RC(O)R, RC(O)H). This reaction pathway results in oxygenation of a variety of organic substrates, and is not impeded by the spin restriction, because triplet ground-state dioxygen can react with the free radical R• to give a free-radical product ROO•, in a spin-allowed process (Reaction 5.18). It is a chain reaction, since R• is regenerated in Reaction (5.19), and it frequently occurs with long chain lengths prior to the termination steps, resulting in a very efficient pathway for oxygenation of some organic substrates, such as, for example, the oxidation of cumene to give phenol and acetone (Reaction 5.22).[22]



When free-radical autoxidation is used for synthetic purposes, initiators are intentionally added. Common initiators are peroxides and other compounds capable of fragmenting readily into free radicals. Free-radical autoxidation reactions are also frequently observed when no initiator has been intentionally added, because organic substrates frequently contain peroxidic impurities that may act as initiators. Investigators have sometimes been deceived into assuming that a metal-complex catalyzed reaction of dioxygen with an organic substrate occurred by a nonradical mechanism. In such instances, the reactions later proved, upon further study, to be free-radical autoxidations, the role of the metal complex having been to generate the initiating free radicals.

Although often useful for synthesis of oxygenated derivatives of relatively simple hydrocarbons, free-radical autoxidation lacks selectivity and therefore, with more complex substrates, tends to give multiple products. In considering possible mechanisms for biological oxidation reactions used *in vivo* for biosynthesis or energy production, free-radical autoxidation is not an attractive possibility, because such a mechanism requires diffusion of highly reactive free radicals. Such radicals, produced in the cell, will react indiscriminately with vulnerable sites on enzymes, substrates, and other cell components, causing serious damage.[6] In fact, free-radical autoxidation is believed to cause certain deleterious reactions of dioxygen in biological systems, for example the oxidation of lipids in membranes. It is also the process that causes fats and oils to become rancid (Reaction 5.23).[23,24]



How do Enzymes Overcome These Kinetic Barriers?

We see then the reasons that uncatalyzed reactions of dioxygen are usually either slow or unselective. The functions of the metalloenzymes for which dioxygen is a substrate are, therefore, to overcome the kinetic barriers imposed by spin restrictions or unfavorable one-electron reduction pathways, and, for the oxygenase enzymes, to direct the reactions and make them highly specific. It is instructive to consider (1) how these metalloenzymes function to lower the kinetic barriers to dioxygen reactivity, and (2) how the oxygenase enzymes redirect the reactions along different pathways so that very different products are obtained. The first example given below is cytochrome c oxidase. This enzyme catalyzes the four-electron reduction of dioxygen. It overcomes the kinetic barriers to dioxygen reduction by binding dioxygen to two paramagnetic metal ions at the dioxygen binding site, thus overcoming the spin restriction, and by reducing dioxygen in a two-electron step to peroxide, thus bypassing the unfavorable one-electron reduction to form free superoxide. The reaction occurs in a very controlled fashion, so that the energy released by dioxygen reduction can be used to produce ATP. A second example is provided by the catechol dioxygenases, which appear to represent substrate rather than dioxygen activation, and in which dioxygen seems to react with the substrate while it is complexed to the paramagnetic iron center. Another example given below is the monooxygenase enzyme cytochrome PASO, which catalyzes the reaction of dioxygen with organic substrates. It binds dioxygen at the paramagnetic metal ion at its active site, thus overcoming the spin restriction, and then carries out what can be formally described as a multielectron reduction of dioxygen to give a highly reactive high-valent metal-oxo species that has reactivity like that of the hydroxyl radical. Unlike a free hydroxyl radical, however, which would be highly reactive but nonselective, the reaction that occurs at the active site of cytochrome P-450 can be highly selective and stereospecific, because the highly reactive metal-oxo moiety is generated close to a substrate that is bound to the enzyme in such a way that it directs the reactive oxygen atom to the correct position. Thus, metalloenzymes have evolved to bind dioxygen and to increase while controlling its reactivity.

7.8: O2 Reduction, since CO displaces O2 is shared under a CC BY-NC-SA 4.0 license and was authored, remixed, and/or curated by LibreTexts.

7.9: Bonding in Carbonmonoxy-myoglobin [Fe(CO)]2+

As noted above, a variety of other α-donor or π-acceptor ligands will bind to the active sites of biological oxygen carriers.

Carbon Monoxide

As documented in Table 4.2, carbon monoxide (CO) generally binds more strongly to hemoglobin than does dioxygen, hence causing carbon-monoxide poisoning. In addition to being readily available from car exhausts and tobacco smoke to convert oxyhemoglobin to carbonmonoxyhemoglobin, CO is produced in the catabolism of heme molecules.[117] Thus under even the most favorable of conditions, about 3 percent of human hemoglobin is in the carbonmonoxy form. When CO binds to a single metal atom in nonbiological systems, *without exception* it does so through the carbon atom and in a linear manner:[56]

$$Fe—C=O \leftarrow Fe^{II} + {}^{-}C=O^{+} \tag{4.40}$$

Model systems for carbonmonoxy (also called carbonyl) hemoglobin show a geometry similar to that of the Fe—C≡O group, linear or nearly so and essentially perpendicular to the porphyrin plane.[110,118-121] The biochemical literature is littered with reports that this is *not* the geometry adopted by CO in binding to hemoglobins.[122-128] We will return to this topic later in this chapter, since the physiological consequences are potentially important.

Carbon monoxide binds weakly as a σ-donor ligand to four-coordinate cobalt(II) systems.[129] Despite a bout of artifactual excitement,[130] CO has never been observed to bind significantly to five-coordinate Co^{II} systems with a nitrogenous axial base to yield octahedral six-coordinate species.[131] The sulfur analogue thiocarbonyl (CS), although not stable as a free entity, binds very strongly to iron-porphyrin species in a linear manner.[132]

Nitric Oxide

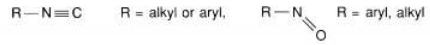
Nitric oxide (NO) binds to hemes even more strongly than CO (and hence O_2),[10] so strongly, in fact, that the Fe—N_{1m} bond is very weak and easily ruptured.[11,111,133] Attachment to the metal is via the nitrogen atom; however, the geometry of attachment is sensitive to the π basicity of the metalloporphyrin, and ranges from linear to strongly bent. In binding to Co^{II} the NO ligand is effectively reduced to NO^{-}, with concomitant oxidation of Co^{II} to Co^{III}.[111]



In much the same way that cobalt-dioxygen systems are paramagnetic ($S = \frac{1}{2}$) and amenable to EPR studies, iron-nitric oxide (also called iron nitrosyl) species are also paramagnetic and isoelectronic with cobalt-dioxygen species. The unpaired spin is localized mostly on the NO group.

Isocyanide and Nitroso Species

In contrast to the dioxygen, carbon-monoxide, and nitric-oxide ligands, the isocyanide and nitroso functions bear an organic tail. Moreover, nitroso ligands are isoelectronic with dioxygen.



Thus, in principle, not only may the steric bulk of the ligand be varied, in order to probe the dimensions[35] of the dioxygen-binding pocket,* but also the σ-donor/π-acceptor properties of the ligands may be varied by appropriate substituents on the aryl ring.

Isocyanide groups may bind to metals in a variety of ways. For 1:1 adducts (Figure 4.19), the isocyanide group is approximately linear, although some flexibility seems to exist in a bis(t-butylisocyanide)iron(Il)tetraphenylporphyrinato complex.[135] For zerovalent metals with much electron density available for donation into ligand π^* orbitals, the isocyanide ligand has been observed to bend at the N atom.[136] One prediction exists that an isocyanide ligand binds in this manner to hemoglobin.[137]

For 1:1 adducts of nitroso ligands, side-on,[138] O-, and N-ligated modes are possible (Figure 4.19). No O-nitroso complexes have been definitively characterized by diffraction methods. For hemoglobin the N-nitroso mode is likely, since this is the mode found

for the nitrosoalkane in Fe(TPP)(amine)(RNO).[139]

To date isocyanide ligands have not achieved their potential as probes of the geometry of the ligand-binding pocket in hemoglobin, partly because we lack structural data on the preferred geometry of attachment of these ligands in a sterically uncongested environment.

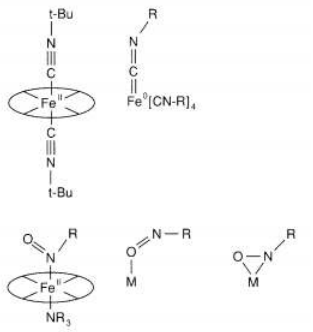


Figure 4.19 - Modes of coordination of isocyanide and nitroso species.

* In fact, this classic experiment of St. George and Pauling established, for the first time and before any crystallographic data were available, that the heme group and the ligand-binding site in hemoglobin reside at least partway inside the protein, rather than on the surface.[134]

7.9: Bonding in Carbonmonoxy-myoglobin [Fe(CO)]2+ is shared under a CC BY-NC-SA 4.0 license and was authored, remixed, and/or curated by LibreTexts.

7.10: Active Site of Cytochrome c Oxidase

The electron transport system (ETS) is an energy production system for aerobic organisms found in the mitochondria of cells. It is the third and final step in cellular respiration, which is the process by which the cell produces energy. When an organism takes in carbohydrate nutrients, they are converted to glucose which can be further broken down through a set of chemical reactions to pyruvate through glycolysis. After glycolysis, this pyruvate molecule is oxidized in the Kreb's cycle which in turn produces ATP and high energy molecules, NADH, and $FADH_2$. Only a few ATP are produced directly from the Kreb's cycle; however the NADH and $FADH_2$ are transported to the ETS where they can be oxidized to produce more ATP (Figure 1).[1]

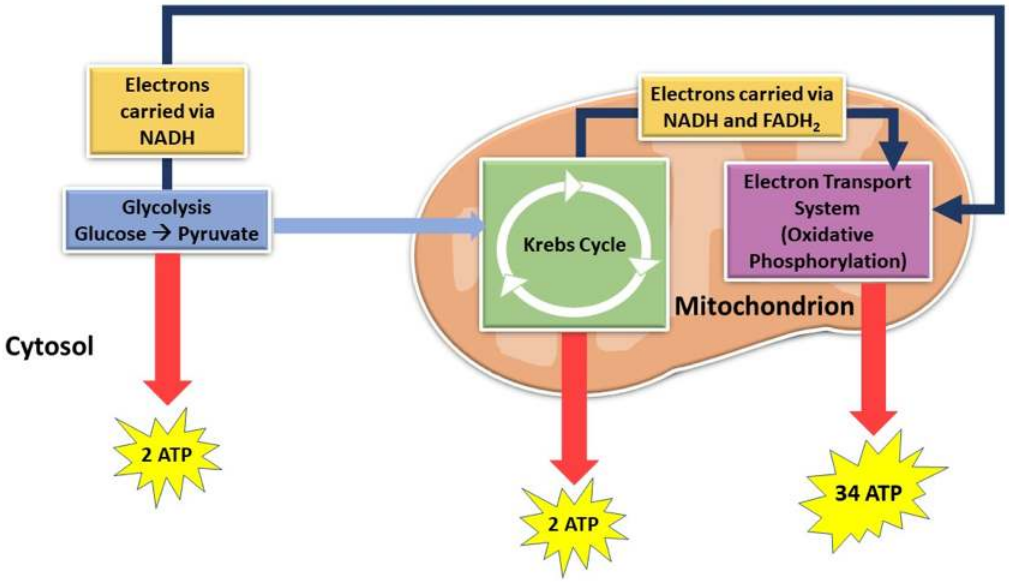


Figure 1. The Process of Cellular Respiration. Cellular respiration is the process used by aerobic organisms to break down sugars to produce energy. The process begins with glycolysis where glucose is broken down into pyruvate producing 2 ATP. Next, the pyruvate moves into the Kreb's cycle in the mitochondria and goes through a series of reactions producing 2 ATP and high energy molecules, NADH and $FADH_2$. These high energy molecules are then transferred to the electron transport system where they are oxidized and start a series of reactions that will ultimately produce 34 ATP.

After the NADH and $FADH_2$ are oxidized to NAD^+ and FAD, the electrons that are removed from NADH and $FADH_2$ and are transported through the four electron transport complexes of the ETS. The movement of electrons provides energy to pump hydrogen ions (H^+) across the inner mitochondrial membrane into the intermembrane space through four complexes.1 The four complexes are NADH-CoQ (ubiquinone reductase), succinate dehydrogenase, cytochrome bc1, and cytochrome oxidase (Figure 2).[2]

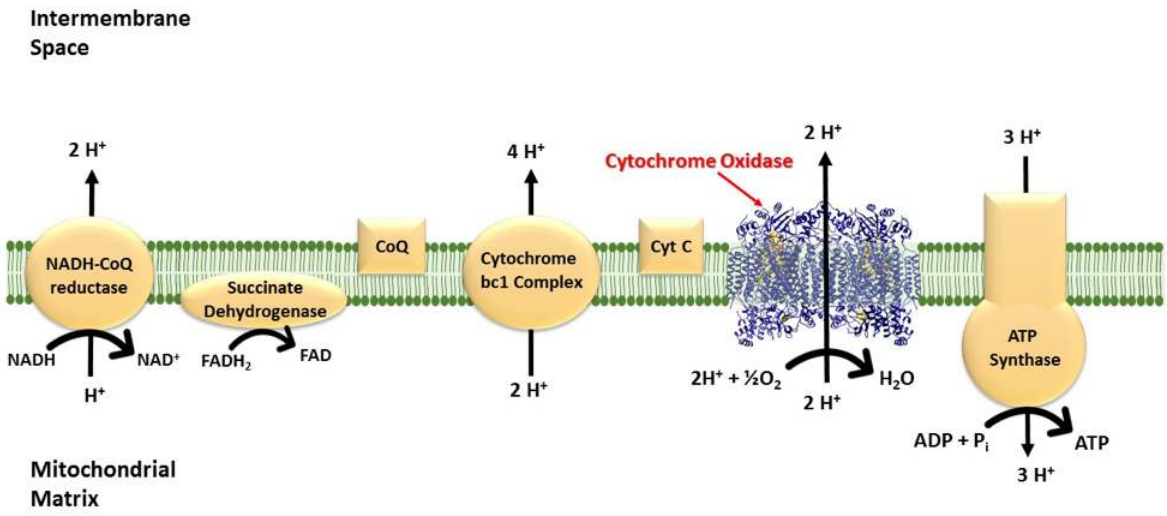


Figure 2. The electron transport system (ETS). The ETS is involved in energy production and occurs in the inner mitochondrial membrane of the mitochondrial matrix. NADH and $FADH_2$ are oxidized allowing electrons to travel through the membrane to the four complexes, NADH-CoQ reductase, succinate dehydrogenase, cytochrome bc1, and cytochrome oxidase (shown in ribbon depiction, PDB 1OCC), pumping H^+ ions across the membrane. The H^+ concentration in the intermembrane space increases and H^+ ions travel through the ATP Synthase to the mitochondrial matrix providing energy to convert ADP to ATP.

The pumping of hydrogen ions through the four complexes stores potential energy by creating a concentration gradient, with higher hydrogen ion concentration in the intermembrane space. This energy is captured as hydrogen ions cross back over to the matrix of the mitochondria, via the ATP synthase, producing energy for the cell in the form of ATP.[1] The hydrogen ion concentration will then increase in the mitochondrial matrix and travel through the three complexes again when another NADH and $FADH_2$ are introduced to the ETS. This process will continue to cycle and produce high numbers of ATP for the cell to use as energy (Figure 2).[1]

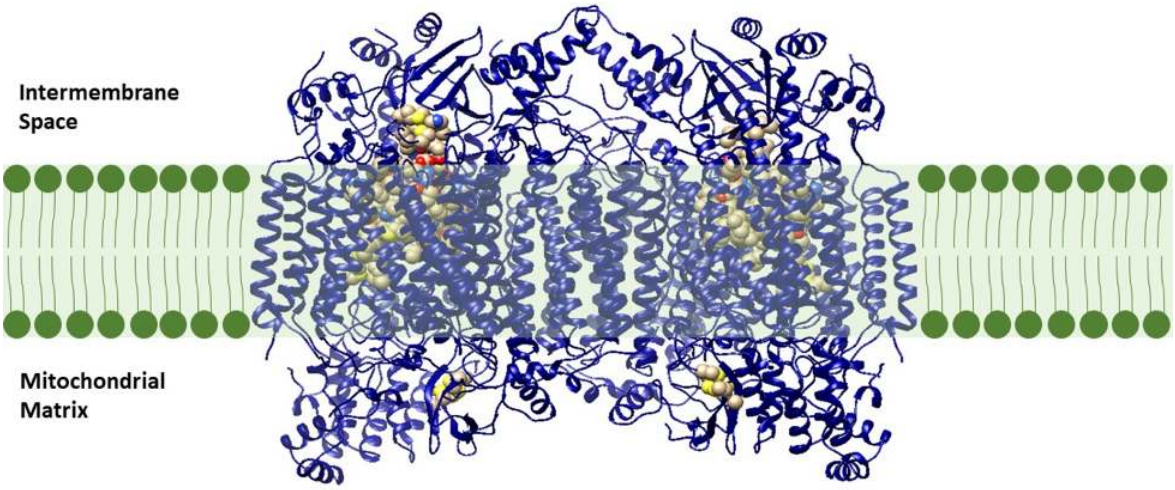


Figure 3. Structure of cytochrome oxidase (1OCC) in the inner mitochondrial membrane. Cytochrome oxidase is a transmembrane protein in the inner mitochondrial membrane. It is a dimer with two identical chemical units containing two hemes,

three coppers, magnesium and a zinc.[2] The protein is shown in ribbon depiction, with atoms of the metal-containing electron transport centers shown in spheres.

Cytochrome oxidase, also known as complex IV, is the terminal, or final, enzyme of the electron transport system (this does not include ATP synthase). Cytochrome oxidase is a transmembrane molecule found in the mitochondria of eukaryotes and in the cellular space of aerobic prokaryotes. This molecule is a proton pump that plays a vital role in producing energy, in the form of ATP, via the ETS (Figure 3). In the last steps of the energy production process, cytochrome oxidase oxidizes the waste products from the end of the energy making process, converting reactive species, H^+ and dioxygen (O_2), to a more stable molecule, water (H_2O). In the absence of cytochrome oxidase, this energetically favorable reaction could be explosive and no energy production would occur.[2] Cytochrome oxidase allows this reaction to occur safely while harnessing energy to form the H^+ ion gradient. This energy produced from the reaction is used to pump H^+ ions from the matrix to the intermembrane space of the mitochondria (Figure 2).[1]

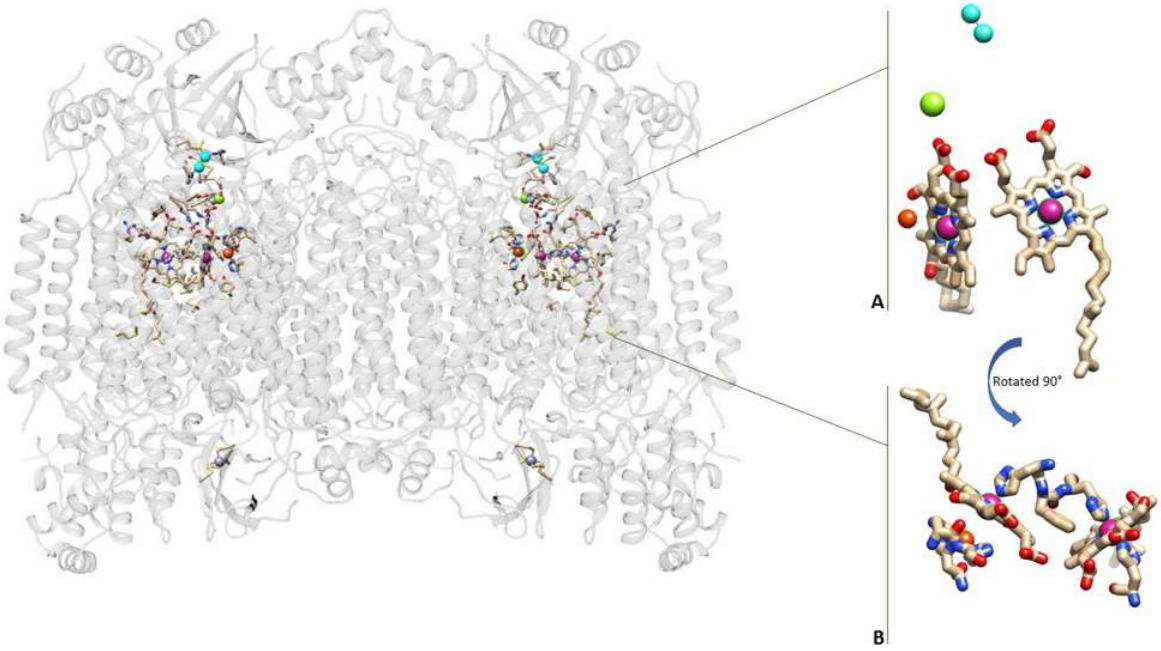


Figure 4. The structure of the metals and their ligands in cytochrome oxidase. This figure shows the two hemes and their irons (purple), two Cu_A (light blue), Cu_B (orange), one magnesium (light green), and one zinc (blue). Cytochrome oxidase is a dimer with its two sets of Cu_A, $heme_a$, $heme_{a3}$, Cu_B, and zinc. The metal complex dimer mirrors one another. Inset A shows a detailed view of Cu_A, magnesium, $heme_a$ (right), $heme_{a3}$ (left), and Cu_B and their spatial relation to one another. Inset B shows $heme_a$ bound to two imidazoles, and $heme_{a3}$ bound to an imidazole. $heme_{a3}$ and Cu_B are close to one another, but do not bind. This space between $heme_{a3}$ and Cu_B is where the oxygen then can bind to the iron. Cu_B is bound to three imidazoles. From PDB 1OCC.

Cytochrome oxidase is a dimer meaning it is made up of two identical proteins. The two proteins in cytochrome oxidase mirror one another. The system uses multiple metals to complete its function including the two irons in the two hemes, three coppers, one magnesium, and one zinc (Figure 4). The irons in the two hemes and the three copper molecules are vital to the success of the enzyme in aerobic respiration.[1]

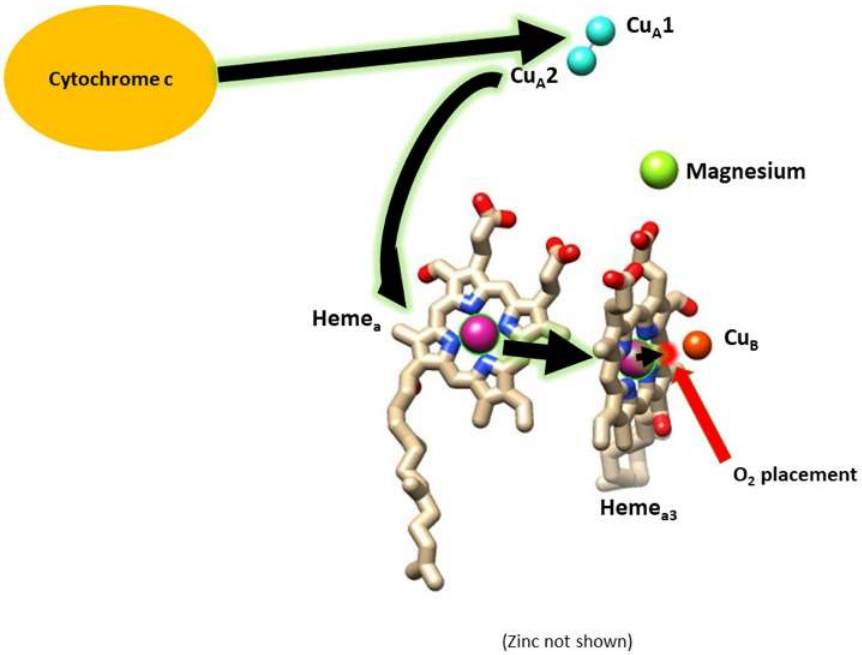


Figure 5. The transfer of electrons from cytochrome c to cytochrome oxidase. This figure shows the transfer of electrons the cytochrome c to the two Cu_A (light blue), to $heme_a$ (purple, left) to $heme_{a3}$ (purple, right), to finally to the oxygen molecule (red sphere). From PDB 1OCC.

---

2 Cu_A molecules function in allowing the electrons to enter the enzyme from cytochrome c.2,3 The electrons travel from the Cu_A molecules to the first heme, also known as $heme_a$. $heme_a$ functions in allowing the electrons to be transferred from Cu_A to the second heme, $heme_{a3}$. The iron in $heme_{a3}$ functions in binding oxygen, with the help of Cu_B. The energy production system selects a heme iron group to bind the oxygen along with the other copper atom and is the location of oxygen reduction (Figure 5).3 The function of magnesium and zinc remains unknown.[4]

$$4e^- + 8H^+ + O_2 \rightarrow 4e^- + 4H^+ + 2H_2O.^{9} \text{ (1)}$$

The overall reduction that occurs in cytochrome oxidase is shown above (Reaction 1). The electron transfers from the electron donor, cytochrome c, to Cu_A to $heme_a$ to $heme_{a3}$ and finally to the electron acceptor, oxygen, are carried out mostly by redox reactions (Figure 5).[3]

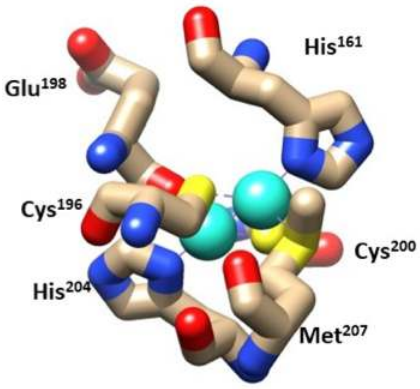


Figure 6. Cu_{A1} and Cu_{A2} with their ligands. This figure shows the two Cu_A (light blue) with their ligands. Cu_{A1} is bound by His^{204}, Cys^{200}, Cys^{196}, and Glu^{198}. Cu_{A2} is bound by His^{161}, Cys^{200}, Cys^{196}, and Met^{207}. From PDB 1OCC.

The electrons travel from cytochrome c to the two Cu_A molecules in the intermembrane space at a fast rate of 70,000 s^{-1} and with an E°' value of 0.27 V.[3,5,6] The Eo', or standard reduction potential, is a value indicating the likelihood a chemical species will be reduced, with a more positive value meaning it is more likely to be reduced. Literature has shown that Cu_A has a mixed oxidation state of I and II (or 1.5 each). Because of this mixed oxidation state when the electrons enter the cytochrome oxidase the charge is shared between the two Cu_A. Only a single electron is transferred from the cytochrome c to the Cu_A.[6] In the cell the environment is different than laboratory conditions, therefore the E°' value would be about +0.05 V.[3]

The two Cu_A molecules are what bring the electrons from the cytochrome c to $heme_a$. They both have tetradentate ligands with a tetrahedron shape.[7] Cu_{A1} is bound by His^{204}, Cys^{200}, Cys^{196}, and Glutamic $acid^{198}$. Cu_{A2} is bound by His^{161}, Cys^{200}, Cys^{196}, and Met^{207}. Both Coppers are bound by Cys^{196} and Cys^{200}, this chelating effect helps stabilize the molecule (Figure 6). The Hard Soft Acid Base (HSAB) theory helps explain the stability of the hemes. HSAB theory characterizes metals as hard, borderline, or soft acids and bases based upon their charge density. HSAB shows that chemical species like to bind with similar species, for example hard acids like to pair with hard bases and borderline acids like to pair with borderline bases. Cu_A applies to the HSAB theory as the copper binds to the imidazole residue on histidine which is borderline for HSAB. The two cysteine and glutamic acid residues that bind with Cu (I) or (II) are soft and hard bases, respectively, for HSAB and may still bind as they are next to borderline. Therefore HSAB may still be a selective method for the Cys and Glu ligands.[3]

As Cu (II) is a d^{10} metal its d orbital is full of electrons. As the d orbital is full the LFSE (ligand field stabilization energy) would be zero. The LFSE is a number that defines the energy of the electrons compared to the average energy of the orbitals. A more negative LFSE indicates lower energy and a more stable complex. As Cu(II) has an LFSE of zero this indicates that the geometry of the metal and its ligands it likely dependent upon sterics. Therefore the tetrahedral geometries of the Cu_{A1} and Cu_{A2} is a result of reducing steric hindrance between the ligands. Cu_{A1} and Cu_{A2} would have an electron count of 17-18. Both coppers each have four ligands with no charge thus having 8 ligand electrons. Copper can have an oxidation state of (I or II), and therefore will have 9-10 d electrons bringing the electron count to 17-18.3

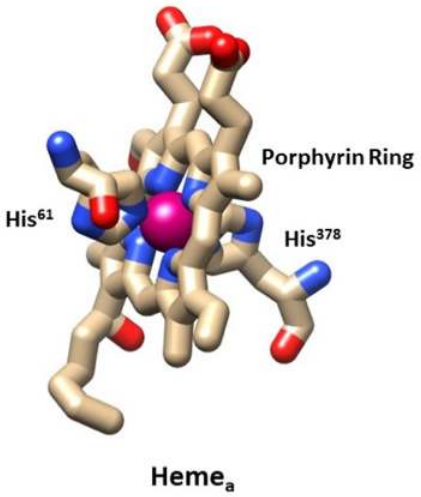


Figure 7. The structure of $heme_a$ and its ligands in cytochrome oxidase. This figure shows the $heme_a$ (purple) in the porphyrin ring and bound by the two histidine ligands, His61 and His378.

After the electrons have entered the cytochrome oxidase from the cytochrome c to the Cu_A molecules they will then transfer to $heme_a$ (Figure 7). This transfer is made possible by 14 covalent bonds and 2 hydrogen bonds spanning 19.5 Å and taking about 20,000 s-1.3 The iron transfers the electrons one at a time and changes from Fe (III) to Fe (II). However, literature shows that the iron only changes its charge about 10-15% as the change in charge is spread over the porphyrin ring decreasing the amount of energy needed.6

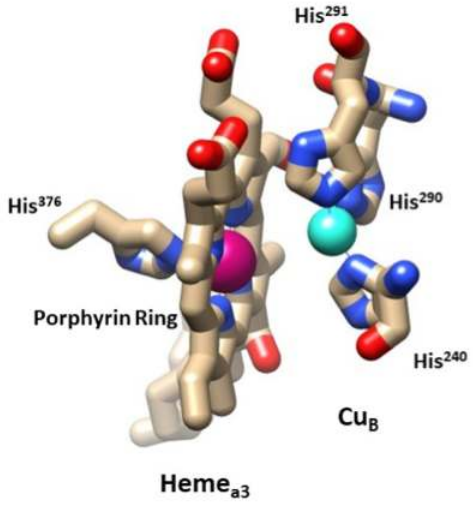


Figure 8. The structure of the heme$_{a3}$ and Cu$_B$ and their ligands in cytochrome oxidase. This figure shows the heme$_{a3}$ (purple) in the porphyrin ring with its histidine ligand and Cu$_B$ (light blue) with its three histidine ligands. Oxygen placement occurs between the heme$_{a3}$ and the Cu$_B$.

Next, the electrons transfer from heme$_a$ to heme$_{a3}$ (Figure 8). The hemes are perpendicular to one another and the edges are located 7 Å apart.[8] How the transfer of electrons from heme$_a$ to heme$_{a3}$ occurs is still not fully understood. Literature shows that electron tunneling stops at heme$_a$, and from heme$_a$ to heme$_{a3}$ the electrons are transferred from the edges of the heme and propelled by protons pumping to the intermembrane space.[6]

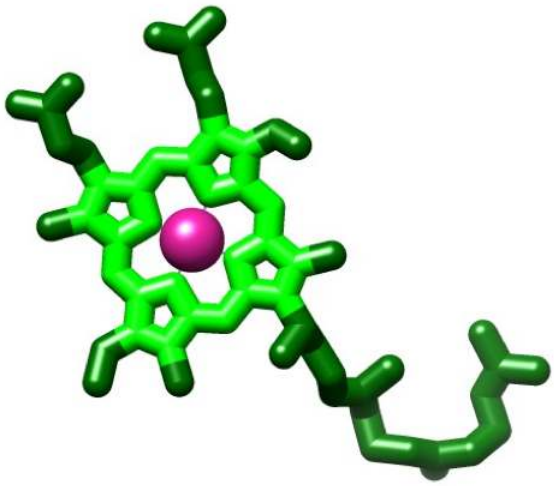


Figure 9. The structure of a porphyrin ring. This figure shows the structure of a porphyrin ring (light green) with its four pyrrole rings and planar geometry. The iron (purple) is in the center of the porphyrin ring and the side groups (dark green) vary depending on the type of heme.

The structure of the heme molecule is a porphyrin ring that is tetradentate chelating of an iron molecule with four nitrogens. Iron can form up to six bonds due to steric constraints that cost the molecule energy by not having enough space for the electrons which repel one another. A porphyrin ring is the building block for heme and is a planar structure composed of four pyrrole rings (Figure 9). Four of the bonds are with the nitrogens of the porphyrin ring, as previously stated, while the fifth coordination site is occupied by an imidazole in histidine, and the sixth coordination site is occupied by another imidazole for heme$_a$, or O_2 for heme$_{a3}$ (Figure 10). Both irons have a planar shape with the heme molecules, but with the addition of their ligands (two imidazole residues for heme$_a$ or an imidazole and an oxygen for heme$_{a3}$) they becomes an octahedral shape.3 The geometry of the hemes can be attributed

to LFSE as the the LFSE equals -0.4 for Fe(II) and -2.0 for Fe(III). This indicates that the geometry of the molecule may be a result of the high stability due to the lower energy of the electrons and their orbitals.[8]

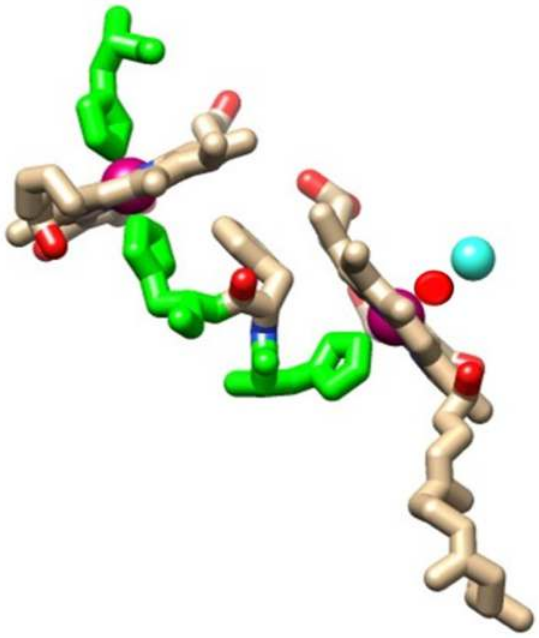


Figure 10. The structure of the metals and their ligands in cytochrome oxidase. This figure shows the two hemes in cytochrome oxidase, $heme_a$ (left) and $heme_{a3}$ (right). $heme_a$ is bound by two imidazoles from Histidines (light green) and $heme_{a3}$ is bound by an imidazole (light green) and an oxygen molecule (red).

Thermodynamic theories are important for ML binding as they provide ideas about the energy needed for breaking bonds and the stability of a molecule. The two hemes in cytochrome oxidase both maintain their stability largely due to their macrocyclic porphyrin ring. This porphyrin ring is made up of 4 pyrroles that bind their nitrogens to the iron. In cytochrome oxidase the iron never needs to leave the hemes and the stability of the porphyrin ring may help the iron stay in its place to properly transfer electrons to oxygen (Figure 10).[9]

The iron does not leave the porphyrin ring for either hemes and the ligands of $heme_a$ remain bound as well. The heme molecules are very stable due to the chelating effect of the porphyrin ring and is relatively inert meaning it holds its metal ion and maintains its planar geometry. The iron in $heme_{a3}$ has an imidazole ligand that remains bound to the iron, but also has a position for oxygen. The oxygen iron bond is broken when electrons are transferred to the oxygen and bound to two H^+ ions.[3] The high lability, or ability of the metal-ligand bond (Fe (II) and O_2) to be broken, is necessary for the water to be released from $heme_{a3}$ and for the cytochrome oxidase to reset for the next set of electrons. The high lability of the Fe (II) is likely a result of the low LFSE value of -0.4. The rate constant is unknown for the iron bound to oxygen. The HSAB theory applies to the iron and the porphyrin ring as Fe (II) and N (in the pyrrole ring) are both classified as having borderline acid character. Like prefers like, indicating that Fe (II) may be using this to select the right ligand to help it bind oxygen, which is hard base for the HSAB theory. The nitrogen in the pyrrole ring is likely a borderline base as it is in a ring structure like pyrimidine and imidazole which are borderline nitrogen containing ring structures as well.[8]

The iron in $heme_a$ transitions between two oxidation states, Fe (III) and Fe (II). The iron $heme_{a3}$ transitions from Fe (II, III, and IV).[10] The two irons in the heme a and a3 both have an electron count of 16-18, as the oxidation state changes. Both irons are bound by four nitrogens from a porphyrin ring, an imidazole nitrogen from His and an O_2 molecule. All of the nitrogen donor atoms are neutral. With six ligands bound to the Fe there would be a total of 12 ligand electrons (6e- x 2=12e-). Knowing that the iron may be missing 2-4 electrons, based on its oxidation state, there remains 4-6 d-electrons giving a total electron count of 16-18 (12 ligand e^- + 4-6 d e^- = 16-18 e^-) (Figure 11). Literature has shown that the iron in $heme_a$ is low spin as it is a 3d metal with a 3+ charge and because it has imidazole ligands that are pi acceptors which are strong field. While the other iron metal center in $heme_{a3}$ is high spin as it is a 3d metal with a 2+ charge.[10,11]

Lastly, the electrons transfer from heme$_{a3}$ to O_2. This transfer is made possible by the iron on the heme$_{a3}$, Cu_B, and a tyrosine. These set of molecules are also known as the bionuclear center (BNC).[3] Once the electron reaches the heme$_{a3}$, Fe(III) becomes Fe (II) and the oxygen binds to the Fe (II). The H^+ ion from the tyrosine ligand of Cu_B transfers to the oxygen bound to Cu_B (I) changing it to Cu_B (II). During this state the Fe (II) double bonds to the oxygen and becomes Fe (IV). The first H^+ and e^- enter the BNC and the H^+ binds to the oxygen on the Cu_B (II). During this step, while the electron places on the tyrosine oxygen the tyrosine oxygen moves to the Cu_B(II) oxygen. Next, the second H^+ and e- set enter with the new H^+ replacing an H^+ on the Cu_B(II) site and the e- placing on the Fe (IV) changing it to Fe (III). The replaced H^+ moves to the Fe (IV). The third set of H^+ and e^- move in with the third H^+ going on the tyrosine oxygen and the electron going on the Cu_B (II) causing it to become Cu_B (I). The final H^+ and e- enter the BNC and place on the Fe (III) causing it to become Fe(II). This stage is also where the two water molecules bound to Fe (III) and Cu_B(I) fall off. The cycle then restarts when oxygen binds to the Fe (II) (Figure 11).[12]

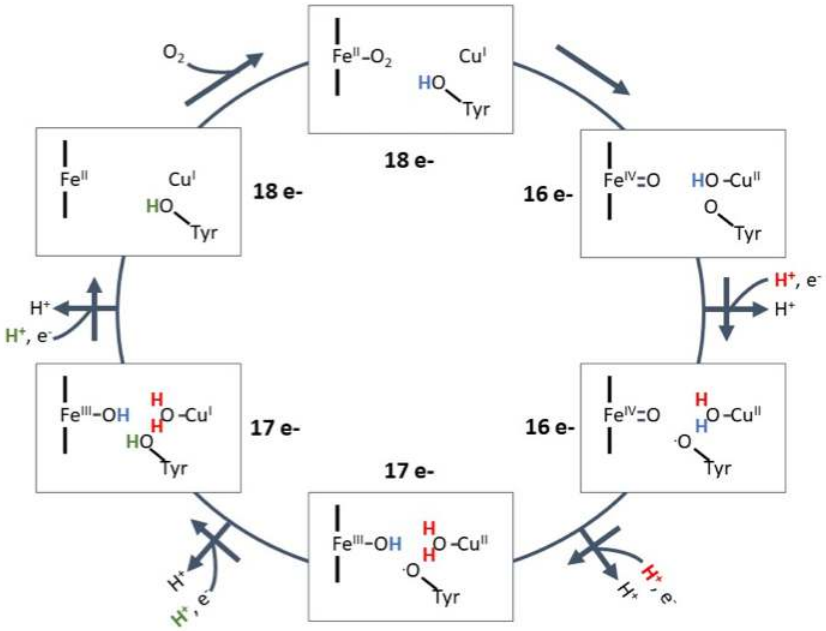


Figure 11. The catalytic cycle of the reaction of O_2 to H_2O in cytochrome oxidase. This figure shows the catalytic cycle that occurs when the oxygen in bound to the Fe (II). The electrons transferred in cytochrome oxidase are brought to the Fe (II) and used to react O_2 and H^+ ions to form water.

Cu_B is vital to the reaction of cytochrome oxidase and has tridentate ligands. All three ligands are imidazole side chains (His^{240}, His^{290}, and His^{291}). With the three imidazole ligands, Cu_B forms a trigonal planar shape and is stabilized by the chelating His^{290} and His^{291} ligands (Figure 8).[3] Similar to the Cu_A ions, Cu_B has an LFSE of 0 and has a trigonal planar geometry due to steric hindrance of the three His ligands. Copper can have an oxidation state of (I) or (II).[10] Cu_B would have an electron count of 14-16. This copper has three imidazole ligands with no charge therefore it has 6 ligand electrons. The HSAB theory also applies to the Cu (II) (Cu_B) center and the 3 imidazole ligands as both are considered borderline acids and bases, respectively, for HSAB and like attracts like, indicating that Cu (II) may be using this to select the right ligands. Cu (I) also occurs and may still be using HSAB to select the imidazole groups as it is close to borderline. Copper can have an oxidation state of +I, or +II, and therefore will have 9-10 d electrons bringing the electron count to 15-16. Cu_B takes on an oxygen and releases it after two H^+ ions are bound to it producing one molecule of water (Figure 11). The rate constant of the O-Cu_B bond is 3.5 x 108 $M^{-1}s^{-1}$ showing that the breaking of the bond is quick as and that it is a weak bond. As previously mentioned, the Cu_B has an LFSE of 0 indicating it is highly labile which correlates with the Cu_B's ability to react quickly with the oxygen.[3]

The reduction potential of the cytochrome oxidase reaction (Reaction 1) is +0.82 V. Beginning with the initial electron donor, cytochrome c, and ending with the final electron acceptor, O_2, we see that the reduction potential went from +0.27 V to +0.82 V. This increase in reduction potential from the electron donor to the electron acceptor makes the overall reactions of cytochrome oxidase spontaneous.[6]

Cytochrome oxidase is a colored protein. Cu_A has absorption bands at about 480 nm, 530 nm, and even one in the infrared spectrum at about 830 nm.[12] Literature has shown that although these absorbances reflect a blue/purple color in the lab, in an intact cytochrome oxidase the hemes hide the Cu_A absorbances with their own absorbances. Cu_A absorptions are charge transfer absorptions as ε>1000 cm-1 (ε=2000 cm^{-1}).[12]

$Heme_a$ has been found to have absorbances at 446 nm and 605 nm. $heme_{a3}$ has absorbances at 441 nm, 611 nm, and 656 nm.[12] The absorbances for both hemes mean the reflected light gives the hemes a reddish/purple color. The absorbances and colors of both hemes have been to found to be likely a result of charge transfers; however no ε value was found in the literature. Cu_B is not colored as it does not have any absorbances in the visual spectrum.[12]

Cytochrome oxidase is a key molecule in aerobic respiration and without a properly functioning enzyme can lead to cell death. The primary disorder associated with cytochrome oxidase is cytochrome oxidase deficiency which is a relatively rare, autosomal recessive disorder.[13] Leigh's Syndrome is a human disease caused by cytochrome oxidase deficiency and its symptoms include poor muscle tone and muscle movement, mental impairment, and lack of growth. These symptoms begin to manifest in infancy and the disorder usually results in death within two to three years of life. Although there is no cure for Leigh's Syndrome, treatment with Vitamin B1 has been shown to help prolong the patient's life. Therefore, cytochrome oxidase is very important to humans and all other aerobic organisms as it is the primary reason we breathe oxygen and is what helps our bodies produce energy to keep us alive.[14]

References

1. Alberts B, Johnson A, Lewis J, et al. 2002. *Molecular Biology of the Cell.*, 4th edition. New York: Garland Science.
2. Goodsell, D. 2000. Cytochrome c Oxidase. *Protein Database* (PDB). (accessed Jan. 23, 2018).
3. Michel, H., Behr, J., Harrenga, A. Kannt, A. 1998. Cytochrome c oxidase: structure and spectroscopy. *Annu. Rev. Biophys. Biomol. Struct.*, 27.
4. Florens L. et al. 1999. The Role of Magnesium and Its Associated Water Channel in Activity and Regulation of Cytochrome *c* Oxidase. *The Phototrophic Prokaryotes*. Springer, Boston, MA.
5. Ludwig, B., Bender, E., Arnold,S., Hüttemann, M., Lee, I., and Kadenbach, B. 1999. Cytochrome c Oxidase and the Regulation of Oxidative Phosphorylation. *Biochemistry*, 38 (46): 15129–15140.
6. Kaila, V. R. I., Verkhovsky, M. I., and Wikstrom, M. 2010. Proton-Coupled Electron Transfer in Cytochrome Oxidase. *Chem. Rev.*, 110: 7062–7081.
7. Youfen Li, Jeong-Soon Park, Jian-Hong Deng, and Yidong Bai. (2006). Cytochrome c oxidase subunit IV is essential for assembly and respiratory function of the enzyme complex. *J Bioenerg Biomembr*, 38 (5-6): 283–291.
8. Carter, K. Palmer, G. 1982. Models of the Two Heme Centers in Cytochrome Oxidase. *The Journal of Biological Chemistry*, 257(22): 13507-13514.
9. Crofts, A. 1994. Cytochrome oxidase: Complex IV. University of Illinois at Urbana-Champaign. Accessed 4 April 2018.
10. Tsukihara, Tomitake, et al. 1996. Structures of metal sites of oxidized bovine heart cytochrome c oxidase at 2.8 angstroms. *Science*, 269: 1136-1144.
11. Kepp, K. 2017. Heme: From quantum spin crossover to oxygen manager of life. *Coordination Chemistry Reviews*, 344: 363-374.
12. Hellwig, P., Soulimane, T., Buse, G., and Mantele, W. 1999. Electrochemical, FTIR, and UV/VIS Spectroscopic Properties of the ba3 Oxidase from *Thermus thermophilus*. *Biochemistry*, 38: 9648-9658.
13. Shoubridge, E. A. 2001. Cytochrome c oxidase deficiency. *American Journal of Medical Genetics*, 106 (1): 46-52.
14. U.S. National Library of Medicine: Genetics Home Reference. (2018, March 6). Leigh Syndrome. Retrieved from https://ghr.nlm.nih.gov/condition/leigh-syndrome.

Contributed by

*This work was originally written by **Allyson Slusser**, Spring 2018: Allyson is currently (as of 2018) a senior biology major at Saint Mary's College in Notre Dame, IN.*

This work was originally edited by Dr. Kathryn Haas (Assistant Professor) and Madison Sendzik (Teaching and Research Assistant) at Saint Mary's College.

7.10: Active Site of Cytochrome c Oxidase is shared under a not declared license and was authored, remixed, and/or curated by LibreTexts.

7.11: Cyanide is also a poison (affinity data)

Formation Constants for Complex Ions

Equilibrium	K_f
$Al^{3+} + 6\,F^- \rightleftharpoons [AlF_6]^{3-}$	7×10^{19}
$Cd^{2+} + 4\,NH_3 \rightleftharpoons [Cd(NH_3)_4]^{2+}$	1.3×10^{7}
$Cd^{2+} + 4\,CN^- \rightleftharpoons [Cd(CN)_4]^{2-}$	3×10^{18}
$Co^{2+} + 6\,NH_3 \rightleftharpoons [Co(NH_3)_6]^{2+}$	1.3×10^{5}
$Co^{3+} + 6\,NH_3 \rightleftharpoons [Co(NH_3)_6]^{3+}$	2.3×10^{33}
$Cu^{+} + 2\,CN \rightleftharpoons [Cu(CN)_2]^-$	1.0×10^{16}
$Cu^{2+} + 4\,NH_3 \rightleftharpoons [Cu(NH_3)_4]^{2+}$	1.7×10^{13}
$Fe^{2+} + 6\,CN^- \rightleftharpoons [Fe(CN)_6]^{4-}$	1.5×10^{35}
$Fe^{3+} + 6\,CN^- \rightleftharpoons [Fe(CN)_6]^{3-}$	2×10^{43}
$Fe^{3+} + 6\,SCN^- \rightleftharpoons [Fe(SCN)_6]^{3-}$	3.2×10^{3}
$Hg^{2+} + 4\,Cl^- \rightleftharpoons [HgCl_4]^{2-}$	1.1×10^{16}
$Ni^{2+} + 6\,NH_3 \rightleftharpoons [Ni(NH_3)_6]^{2+}$	2.0×10^{8}
$Ag^{+} + 2\,Cl^- \rightleftharpoons [AgCl_2]^-$	1.8×10^{5}
$Ag^{+} + 2\,CN^- \rightleftharpoons [Ag(CN)_2]^-$	1×10^{21}
$Ag^{+} + 2\,NH_3 \rightleftharpoons [Ag(NH_3)_2]^+$	1.7×10^{7}
$Zn^{2+} + 4\,CN^- \rightleftharpoons [Zn(CN)_4]^{2-}$	2.1×10^{19}
$Zn^{2+} + 4\,OH^- \rightleftharpoons [Zn(OH)_4]^{2-}$	2×10^{15}
$Fe^{3+} + SCN^- \rightleftharpoons [Fe(SCN)]^{2+}$	8.9×10^{2}
$Ag^{+} + 4\,SCN^- \rightleftharpoons [Ag(SCN)_4]^{3-}$	1.2×10^{10}
$Pb^{2+} + 4\,I^- \rightleftharpoons [PbI_4]^{2-}$	3.0×10^{4}
$Pt^{2+} + 4\,Cl^- \rightleftharpoons [PtCl_4]^{2-}$	1×10^{16}
$Cu^{2+} + 4\,CN \rightleftharpoons [Cu(CN)_4]^{2-}$	1.0×10^{25}
$Co^{2+} + 4\,SCN^- \rightleftharpoons [Co(SCN)_4]^{2-}$	1×10^{3}

This page titled 7.11: Cyanide is also a poison (affinity data) is shared under a CC BY 4.0 license and was authored, remixed, and/or curated by OpenStax via source content that was edited to the style and standards of the LibreTexts platform.

- **22.3: Formation Constants for Complex Ions** by OpenStax is licensed CC BY 4.0. Original source: https://openstax.org/details/books/chemistry-2e.

7.12: Cyanide is also a poison (spectrocopic data)

The magnitude of Δ_o dictates whether a complex with four, five, six, or seven d electrons is high spin or low spin, which affects its magnetic properties, structure, and reactivity. Large values of Δ_o (i.e., $\Delta_o > P$) yield a low-spin complex, whereas small values of Δ_o (i.e., $\Delta_o < P$) produce a high-spin complex. The magnitude of Δ_o depends on three factors: the valence of the metal, the principal quantum number of the metal (and thus its location in the periodic table), and the nature of the ligand(s). Values of Δ_o for some representative transition-metal complexes are given in Table **7.12.1**.

Table **7.12.1**: Crystal Field Splitting Energies for Some Octahedral (Δ_o)* and Tetrahedral (Δ_t) Transition-Metal Complexes

Octahedral Complexes	Δ_o (cm^{-1})	Octahedral Complexes	Δ_o (cm^{-1})	Tetrahedral Complexes	Δ_t (cm^{-1})
$[Ti(H_2O)_6]^{3+}$	20,300	$[Fe(CN)_6]^{4-}$	32,800	VCl_4	9010
$[V(H_2O)_6]^{2+}$	12,600	$[Fe(CN)_6]^{3-}$	35,000	$[CoCl_4]^{2-}$	3300
$[V(H_2O)_6]^{3+}$	18,900	$[CoF_6]^{3-}$	13,000	$[CoBr_4]^{2-}$	2900
$[CrCl_6]^{3-}$	13,000	$[Co(H_2O)_6]^{2+}$	9300	$[CoI_4]^{2-}$	2700
$[Cr(H_2O)_6]^{2+}$	13,900	$[Co(H_2O)_6]^{3+}$	27,000		
$[Cr(H_2O)_6]^{3+}$	17,400	$[Co(NH_3)_6]^{3+}$	22,900		
$[Cr(NH_3)_6]^{3+}$	21,500	$[Co(CN)_6]^{3-}$	34,800		
$[Cr(CN)_6]^{3-}$	26,600	$[Ni(H_2O)_6]^{2+}$	8500		
$Cr(CO)_6$	34,150	$[Ni(NH_3)_6]^{2+}$	10,800		
$[MnCl_6]^{4-}$	7500	$[RhCl_6]^{3-}$	20,400		
$[Mn(H_2O)_6]^{2+}$	8500	$[Rh(H_2O)_6]^{3+}$	27,000		
$[MnCl_6]^{3-}$	20,000	$[Rh(NH_3)_6]^{3+}$	34,000		
$[Mn(H_2O)_6]^{3+}$	21,000	$[Rh(CN)_6]^{3-}$	45,500		
$[Fe(H_2O)_6]^{2+}$	10,400	$[IrCl_6]^{3-}$	25,000		
$[Fe(H_2O)_6]^{3+}$	14,300	$[Ir(NH_3)_6]^{3+}$	41,000		

*Energies obtained by spectroscopic measurements are often given in units of wave numbers (cm^{-1}); the wave number is the reciprocal of the wavelength of the corresponding electromagnetic radiation expressed in centimeters: 1 cm^{-1} = 11.96 J/mol.

Source of data: Duward F. Shriver, Peter W. Atkins, and Cooper H. Langford, Inorganic Chemistry, 2nd ed. (New York: W. H. Freeman and Company, 1994).

Factor 1: Valence of the Metal

Increasing the valence of a metal ion has two effects: the radius of the metal decreases, and ligands are more strongly attracted to it. Both factors decrease the metal–ligand distance, which in turn causes the ligands to interact more strongly with the d-orbitals. Consequently, the magnitude of Δ_o increases as the valence of the metal increases. Typically, Δ_o for a M(III) is about 50% greater than for the M(II) of the same metal; for example, for $[V(H_2O)_6]^{2+}$, Δ_o = 11,800 cm^{-1}; for $[V(H_2O)_6]^{3+}$, Δ_o = 17,850 cm^{-1}.

Factor 2: Principal Quantum Number of the Metal

For a series of complexes of metals from the same group in the periodic table with the same charge and the same ligands, the magnitude of Δ_o increases with increasing principal quantum number: Δ_o (3d) < Δ_o (4d) < Δ_o (5d). The data for hexaammine complexes of the trivalent Group 9 metals illustrate this point:

$$[Co(NH_3)_6]^{3+}: \Delta_o = 22{,}900\ cm^{-1}$$

$$[Rh(NH_3)_6]^{3+}: \Delta_o = 34{,}100\ cm^{-1}$$

$$[Ir(NH_3)_6]^{3+}: \Delta_o = 40{,}000\ cm^{-1}$$

The increase in Δ_o with increasing principal quantum number is due to the larger radius of valence orbitals down a column. In addition, repulsive ligand–ligand interactions are most important for smaller metal ions. Relatively speaking, this results in shorter M–L distances and stronger d orbital–ligand interactions.

Factor 3: The Nature of the Ligands

Experimentally, it is found that the Δ_o observed for a series of complexes of the same metal ion depends strongly on the nature of the ligands. For a series of chemically similar ligands, the magnitude of Δ_o decreases as the size of the donor atom increases. For example, Δ_o values for halide complexes generally decrease in the order F > Cl > Br > I because smaller, more localized charges, such as we see for F, interact more strongly with the d-orbitals of the metal. In addition, a small neutral ligand with a highly localized lone pair, such as NH_3, results in significantly larger Δ_o values than might be expected. Because the lone pair points directly at the metal ion, the electron density along the M–L axis is greater than for a spherical anion such as F. The experimentally observed order of the crystal field splitting energies produced by different ligands is called the spectrochemical series which was presented in a previous section.

7.12: Cyanide is also a poison (spectrocopic data) is shared under a not declared license and was authored, remixed, and/or curated by LibreTexts.

CHAPTER OVERVIEW

8: What Happens "Above The Arrow" in Organic Chemistry

8.1: Metal-Pi System Ligands (e.g. ferrocene)

8.2: 18 Electron Rule

8.3: Organometallic Reaction Types

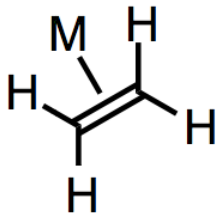
8.4: Organometallic Catalysts

8.5: Suzuki-Miyara Coupling

8: What Happens "Above The Arrow" in Organic Chemistry is shared under a not declared license and was authored, remixed, and/or curated by LibreTexts.

8.1: Metal-Pi System Ligands (e.g. ferrocene)

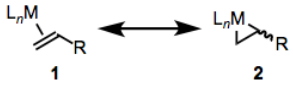
With this post, we finally reach our first class of dative **actor** ligands, **π systems**. In contrast to the **spectator** L-type ligands we've seen so far, π systems most often play an important role in the reactivity of the OM complexes of which they are a part (since they act in reactions, they're called "actors"). π Systems do useful chemistry, not just with the metal center, but also with other ligands and external reagents. Thus, in addition to thinking about how π systems affect the steric and electronic properties of the metal center, we need to start considering the metal's effect on the ligand and how we might expect the ligand to behave as an active participant in reactions. To the extent that structure determines reactivity—a commonly repeated, and extremely powerful maxim in organic chemistry—we can think about possibilities for chemical change without knowing the elementary steps of organometallic chemistry in detail yet.



General Properties

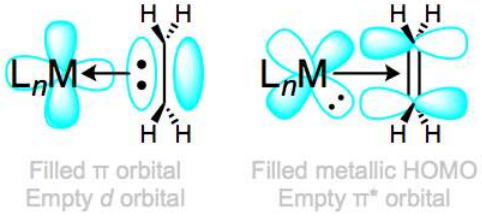
The π bonding orbitals of alkenes, alkynes, carbonyls, and other unsaturated compounds may overlap with dσ orbitals on metal centers. This is the classic ligand HOMO → metal LUMO interaction that we've beaten into the ground over the last few posts. Because of this electron donation from the π system to the metal center, coordinated π systems often act electrophilic, even if the starting alkene was nucleophilic (the **Wacker oxidation** is a classic example; water attacks a palladium-coordinated alkene). The π → dσ orbital interaction is central to the structure and reactivity of π-system complexes.

Then again, a theme of the last three posts has been the importance of orbital interactions with the opposite sense: metal HOMO → ligand LUMO. Like CO, phosphines, and NHCs, π systems are often subject to important backbonding interactions. We'll focus on alkenes here, but these same ideas apply to carbonyls, alkynes, and other unsaturated ligands bound through their π clouds. For alkene ligands, the relative importance of "normal" bonding and backbonding is nicely captured by the relative importance of the two resonance structures in the figure below.



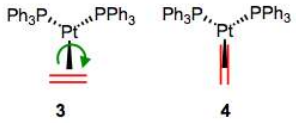
Resonance forms of alkene ligands.

Complexes of weakly backbonding metals, such as the electronegative late metals, are best represented by the traditional dative resonance structure **1**. But complexes of strong backbonders, such as electropositive Ti(II), are often best drawn in the **metallacyclopropane** form **2**. Organic hardliners may have a tough time believing that **1** and **2** are truly resonance forms, but several studies—e.g. of the Kulinkovich cyclopropanation—have shown that independent synthetic routes to metallacyclopropanes and alkene complexes containing the same atoms result in the same compound. Furthermore, bond lengths and angles in the alkene change substantially upon coordination to a strongly backbonding metal. We see an elongation of the C=C bond (consistent with decreased bond order) and some pyramidalization of the alkene carbons (consistent with a change in hybridization from sp2 to sp3). A complete orbital picture of "normal" bonding and backbonding in alkenes is shown in the figure below.



Normal bonding and backbonding in alkene complexes.

Here's an interesting question with stereochemical implications: what is the orientation of the alkene relative to the other ligands? From what we've discussed so far, we can surmise that one face of the alkene must point toward the metal center. Put differently, the bonding axis must be normal to the plane of the alkene. However, this restriction says nothing about rotation about the bonding axis, which spins the alkene ligand like a pinwheel. Is a particular orientation preferred, or can we think about the alkene as a circular smudge over time? The figure below depicts two possible orientations of the alkene ligand in a trigonal planar complex. Other orientations make less sense because they would involve inefficient orbital overlap with the metal's orthogonal d orbitals. Which one is favored?



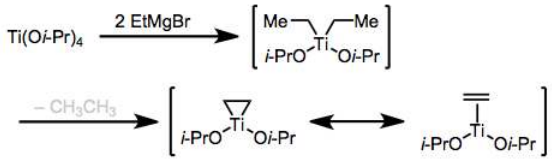
Two limiting cases for alkene orientation in a trigonal planar complex.

First of all, we need to notice that these two complexes are **diastereomeric**. They have different energies as a result, so one must be favored over the other. Naive steric considerations suggest that complex **4** ought to be more stable (in most complexes, steric factors dictate alkene orientation). To dig a little deeper, let's consider any electronic factors that may influence the preferred geometry. We've already seen that electronic factors can overcome steric considerations when it comes to complex geometry! To begin, we need to consider the crystal field orbitals of the complex as a whole. Verify on your own that in this d10, Pt(0) complex, the crystal-field HOMOs are the dxy and dx2–y2 orbitals. Where are these orbitals located in space? In the xy-plane! Only the alkene in **3** can engage in efficient backbonding with the metal center. In cases when the metal is electron rich and/or the alkene is electron poor, complexes like **3** can sometimes be favored in spite of sterics. The thought process here is very similar to the one developed in an earlier post on geometry. However, please note that this situation is fairly rare—steric considerations often either match or dominate electronics where alkenes are concerned.

Synthesis

Alkene and alkyne complexes are most often made via **ligand substitution** reactions, which simply exchange one ligand for another. A nice example of a stable alkene complex synthesized via ligand substitution is [Ir(COD)Cl]2, made from IrCl3 and cyclooctadiene. Similarly, the inimitable Pd2(dba)3 may be prepared from PdCl42– and dibenzylideneacetone (dba). In truth, only a few stable alkene and alkyne complexes find use as organometallic precatalysts and/or catalysts. Substitutions of alkenes for phosphine ligands can be rendered easy, so phosphine precatalysts may be used in reactions that involve intermediate alkene complexes. In addition, unsaturated complexes containing an open coordination site often associate with alkenes and alkynes. Gold(I) chemistry is riddled with examples of this strategy, for example. The unsaturated complexes may be derived from precursors themselves, and the resulting π complexes may be short lived, but that's often the point! Some transformation of the π system is often desired.

I have to mention the metallacyclopropane route to alkene complexes from the Kulinkovich reaction, which is a surprising but awesome transformation. After displacement of two alkoxide ligands on titanium by ethylmagnesium bromide, a process described as either (1) β-hydride elimination followed by reductive elimination, or (2) concerted σ-bond metathesis leads to the liberation of ethane and formation of the alkene complex. The proof that the product is an alkene complex? Other olefins can displace ethylene, and ethylene can come right back in to re-form the product! Ti(II)'s strong backbonding ability almost certainly figures in to the driving force for the ethane-releasing step(s).



Kulinkovich synthesis of alkene complexes. A remarkable loss of ethane!

https://chem.libretexts.org/@go/page/553733

Reactions

The reactivity patterns of alkene and alkyne ligands are remarkably similar to those of carbon monoxide: nucleophilic attack and migratory insertion dominate their chemistry. The important issues of **site selectivity** and **stereoselectivity** come into play when considering alkenes and alkynes, however—the fundamental questions are…

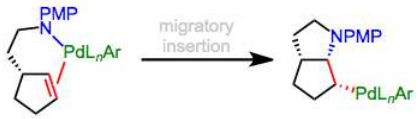
- Which atom gets the nucleophile/migrating group?
- Which atom gets the metal?
- What is the relative orientation of the nucleophile/migrating group and the metal (cis or trans)?

The wide variety of what we might generally call "**atom-metallation**" processes (carbopalladation, carboauration, aminopalladation, oxypalladation, etc.) may involve external nucleophilic addition to the π system, with attachment of the metal to the carbon that was not attacked. The net result is the addition of atom and metal across the π bond, in a trans or anti orientation. The anti orientation results because the nucleophile attacks the face opposite the metal center. A cis orientation of nucleophile and metal is indicative of a migratory insertion pathway (see below). In the example in the following figure, the metal alkyl was converted into a chlorohydrin using copper(II) chloride and LiCl (with stereospecific inversion). Subsequent epoxide formation with NaOH afforded only the cis diastereomer, supporting the trans configuration of the metal alkyl.



Nucleophilic attack on a coordinated alkene or alkyne is always trans, or anti.

Migratory insertion of alkenes and alkynes, like insertions of CO, can be thought of as an internal attack by a nucleophile already coordinated to the metal center. Migratory insertion is the C–C bond-forming step of **olefin polymerization**, and some fascinating studies of this reaction have shown that the alkyl group (the growing polymer chain) migrates to the location of the olefin (not the other way around). Migratory insertion is also important for the **Heck reaction**—in this case, the olefin inserts into a Pd–Csp2 bond. Finally, a large number of metal-catalyzed addition reactions rely on migratory insertion as the key C–X bond-forming step. cis-Aminopalladation is one example.

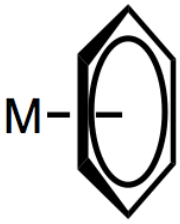


cis-Aminopalladation via migratory insertion. Two new bonds are established with stereospecificity!

Importantly, migratory insertion of alkenes and alkynes into M–X bonds takes place in a syn or cis fashion—the metal and the migrating group (X) end up on the same face of the π system. The site selectivity of migratory insertion may be controlled by either steric factors or the π system's electronics, although the former is more common, I'd say. Electronics are at play in Wacker oxidations of 1-alkenes, for example, which exclusively yield methyl ketones.

Finally, **electrophilic attack** on π systems coordinated to electron-rich metals can also happen, although it's much rarer than nucleophilic attack. Usually these reactions involve coordination of the electrophile to the metal, followed by migratory insertion. We'll hear more about this in a future post on electrophilic attack on coordinated ligands. Coming up next: cyclic π systems!

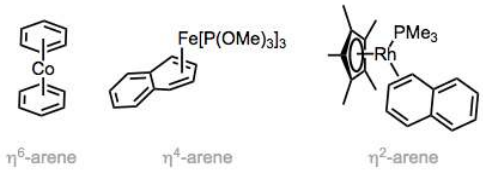
Arene or **aromatic ligands** are the subject of this post, the second in our series on π-system ligands. Arenes are dative, L-type ligands that may serve either as actors or spectators. Arenes commonly bind to metals through more than two atoms, although η2-arene ligands are known. Structurally, most η6-arenes tend to remain planar after binding to metals. Both "normal" bonding and backbonding are possible for arene ligands; however, arenes are stronger electron donors than CO and backbonding is less important for these ligands. The reactivity of arenes changes dramatically upon metal binding, along lines that we would expect for strongly electron-donating ligands. After coordinating to a transition metal, the arene usually becomes a better electrophile (particularly when the metal is electron poor). Thus, metal coordination can enable otherwise difficult **nucleophilic aromatic substitution** reactions.



General Properties

The coordination of an aromatic compound to a metal center through its aromatic π MOs removes electron density from the ring. I'm going to forego an in-depth orbital analysis in this post, because it's honestly not very useful (and overly complex) for arene ligands. π → dσ (normal bonding) and dπ → π* (backbonding) orbital interactions are possible for arene ligands, with the former being much more important, typically. To simplify drawings, you often see chemists draw "toilet-bowl" arenes involving a circle and single central line to represent the π → dσ orbital interaction. Despite the single line, it is often useful to think about arenes as L3-type ligands. For instance, we think of η6-arenes as six-electron donors.

Multiple coordination modes are possible for arene ligands. When all six atoms of a benzene ring are bound to the metal (η6-mode), the ring is flat and C–C bond lengths are slightly longer than those in the free arene. The ring is bent and non-aromatic in η4-mode, so that the four atoms bound to the metal are coplanar while the other π bond is out of the plane. η4-Arene ligands show up in both stable complexes (see the figure below) and reactive intermediates that possess an open coordination site. To generate the latter, the corresponding η6-arene ligand undergoes **ring slippage**—one of the π bonds "slips" off of the metal to create an open coordination site. We'll see ring slippage again in discussions of the aromatic cyclopentadienyl and indenyl ligands.



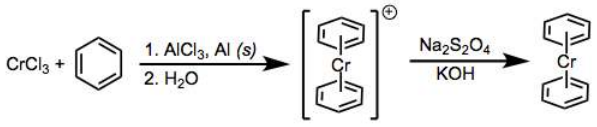
Arene ligands exhibit multiple coordination modes.

Even η2-arene ligands bound through one double bond are known. Coordination of one π bond results in **dearomatization** and makes η2-benzene behave more like butadiene, and furan act more like a vinyl ether. With naphthalene as ligand, there are multiple η2 isomers that could form; the isomer observed is the one that retains aromaticity in the free portion of the ligand. In fact, this result is general for polycyclic aromatic hydrocarbons: binding maximizes aromaticity in the free portion of the ligand. In the linked reference, the authors even observed the coordination of two different rhodium centers to naphthalene—a bridging arene ligand! Other bridging modes include σ, π-binding (the arene is an LX-type ligand, and one C–M bond is covalent, not dative) and L2-type bridging through two distinct π systems (as in biphenyl).

Arene ligands are usually hydrocarbons, not heterocycles. Why? Aromatic heterocycles, such as pyridine, more commonly bind using their basic lone pairs. That said, a few heterocycles form important π complexes. Thiophene is perhaps the most heavily studied, as the desulfurization of thiophene from fossil fuels is an industrially useful process.

Synthesis

There are two common methods for the stoichiometric synthesis of arene "sandwich" complexes, in which a metal is squished between two arenes. Starting from a metal halide, treatment with a Lewis acid and mild reductant rips off the halogen atoms and replaces them with arene ligands. The scope of this method is fairly broad metal-wise.

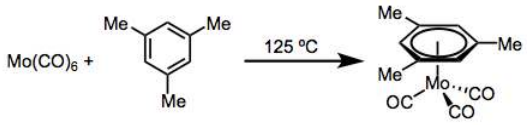


The Fischer-Hafner synthesis. Reduction of metal halides in the presence of arene.

https://chem.libretexts.org/@go/page/553733

A second method, “co-condensation,” involves the simultaneous condensation of metal atom and arene vapor onto a cold (-196 °C) surface.

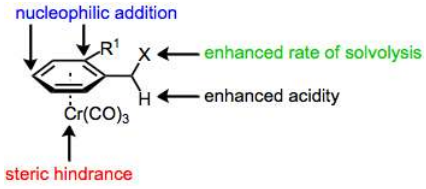
Syntheses of metal arene carbonyl complexes take advantage of the fact that arenes are strongly binding, “chelating” ligands. Infrared spectroscopic studies have shown that a single benzene ligand is a stronger electron donor than three CO ligands—C–O stretching frequencies are lower in metal arene carbonyls than homoleptic metal carbonyls. Since the process is entropically driven, a little heat can get the job done.



Entropically driven synthesis of arene complexes: three molecules for the price of one!

Reactions

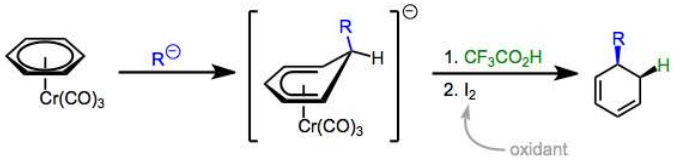
It’s important here to distinguish aromatic X-type ligands from the topic of this post, Ln-type arenes bound only through their π systems. The figure below nicely summarizes the typical behavior of arene ligands coordinated through their π clouds. Although the figure is for chromium carbonyls specifically, other metals apply as well. Note the reactivity of the benzylic position: both cations and anions are stabilized by the metal.



The magic of metal coordination: increased acidity and electrophilicity and steric hindrance.

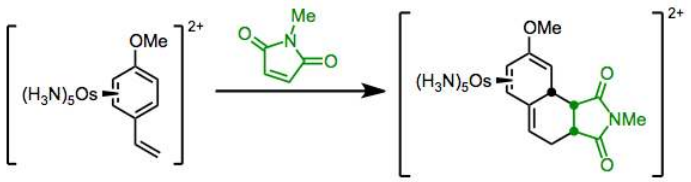
Since the coordination of arenes to metals depletes electron density on the arene, it makes sense that metal-arene complexes should be susceptible to nucleophilic aromatic substitution (NAS). In fact, NAS on metal-coordinated arene ligands has been extensively developed for several different metals. However, all of these NAS methods are stoichiometric because the product ligands are as good as (or better than) the starting ligands at coordinating metal. A stoichiometric amount of another reagent—typically an oxidant—is used to free up the arene. Why are oxidants effective at freeing arene ligands from metal centers? Oxidation worsens the metal’s ability to backbond and consequently decreases the enthalpic advantage of arene binding. Entropy is thus able to take over and release the ligand.

Steric hindrance on the side of the arene bound to the metal is a second important factor to consider. Nucleophilic addition takes place on the face opposite the coordinated metal. If rearomatization through the loss of a leaving group isn’t fast, an electrophile can be introduced after nucleophilic addition, resulting in the cis addition of nucleophile and electrophile across an aromatic π bond. Take that, aromaticity!



Aromaticity takes a beating, thanks to chromium!

We already touched a little on the interesting behavior of η_2-arene complexes, which behave more like their analogues possessing one less double bond. Here’s a nifty example from Harman of a Diels-Alder reaction in which a substituted styrene is the diene. Strike two for aromaticity!



Harman's Os(II) arene chemistry. Styrene is uniquely acting like a diene!

If you're interested in learning more about this fascinating chemistry, check out Harman's review (linked above). The behavior of furan is particularly intriguing.

This brings us to the end of our short series on L-type π-system ligands. However, we'll encounter ligands that bear great similarity to alkenes and arenes in the near future. π Systems that contain an odd number of atoms, unlike π systems we've seen so far, are LnX-type ligands with one covalent M–X bond and n dative bonds. We'll return to this interesting class of ligands after finishing off the dative ligands with metal carbenes and introducing a few simple X-type ligands (hydrides, alkyls, alkoxides, etc.).

This page titled 8.1: Metal-Pi System Ligands (e.g. ferrocene) is shared under a CC BY-NC-SA 4.0 license and was authored, remixed, and/or curated by Michael Evans.

- **2.10: π Systems** by Michael Evans is licensed CC BY-NC-SA 4.0.

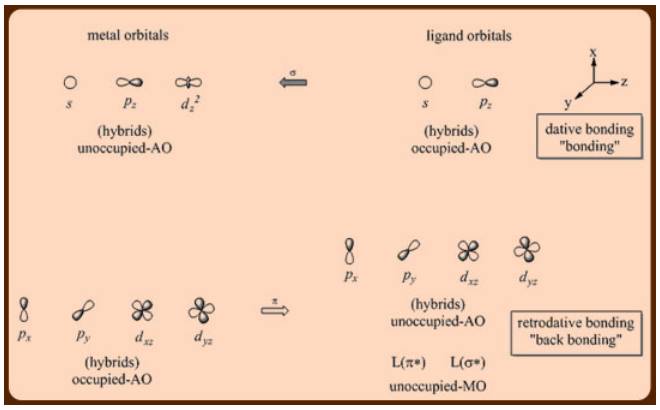
8.2: 18 Electron Rule

Learning Objectives

In this lecture you will learn the following

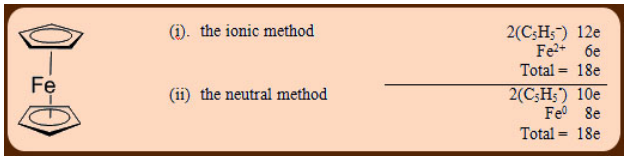
- Have an insight about the stability of the transition metal complexes with respect to their total valence electron count.
- Be aware of the transition metal complexes that obey or do not obey the 18 Valence Electron Rule.
- Have an appreciation of the valence electron count in the transition metal organometallic complexes that arise out of the metal-ligand orbital interactions.

The transition metal organometallic compounds exhibit diverse structural variations that manifest in different chemical properties. Many of these transition metal organometallic compounds are primarily of interest from the prospectives of chemical catalysis. Unlike the main group organometallic compounds, which use mainly *ns* and *np* orbitals in chemical bonding, the transition metal compounds regularly use the $(n-1)d$, *ns* and *np* orbitals for chemical bonding (Figure 1). Partial filling of these orbitals thus render these metal centers both electron donor and electron acceptor abilities, thus allowing them to participate in σ-donor/π-acceptor synergic interactions with donor-acceptor ligands like carbonyls, carbenes, arenes, isonitriles and etc,.

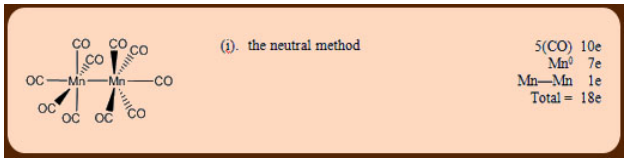


The 18 Valence Electron (18 VE) Rule or The Inert Gas Rule or The Effective Atomic Number (EAN) Rule: The 18-valence electron (VE) rule states that thermodynamically stable transition metal compounds contain 18 valence electrons comprising of the metal *d* electrons plus the electrons supplied by the metal bound ligands. The counting of the 18 valence electrons in transition metal complexes may be obtained by following either of the two methods of electron counting, (*i*). the ionic method and (*ii*). the neutral method. Please note that a metal-metal bond contributes one electron to the total electron count of the metal atom. A bridging ligand donates one electron towards bridging metal atom.

Example 1: Ferrocene $Fe(C_5H_5)_2$



Example 2. $Mn_2(CO)_{10}$



Transition metal organometallic compounds mainly belong to any of the three categories.

a. **Class I** complexes for which the number of valence electrons do not obey the 18 VE rule.

b. **Class II** complexes for which the number of valence electrons do not exceed 18.
c. **Class III** complexes for which the valence electrons exactly obey the 18 VE rule.

The guiding principle which governs the classification of transition metal organometallic compounds is based on the premise that the antibonding orbitals should not be occupied; the nonbonding orbitals may be occupied while the bonding orbitals should be occupied.

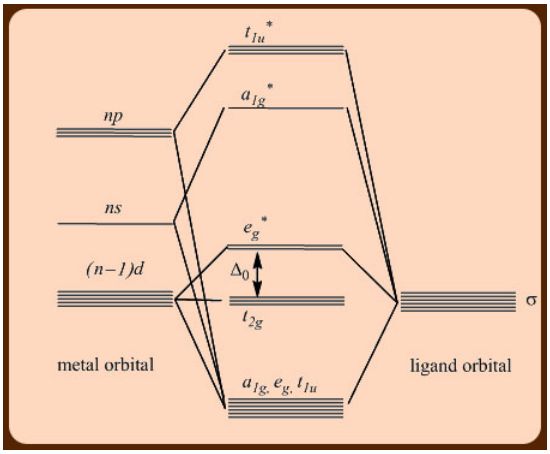


Figure 2. A simplified molecular orbital diagram for an octahedral transition metal complex showing σ−interactions only.

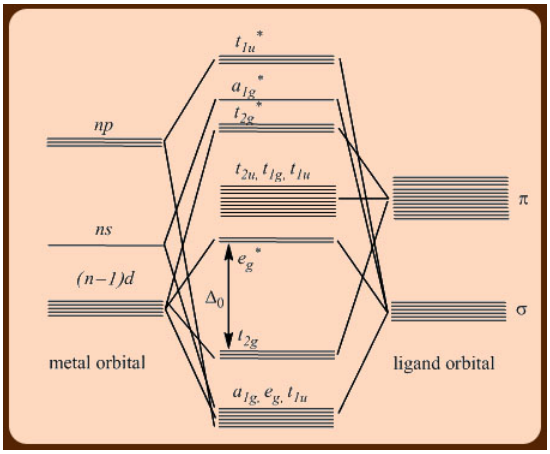


Figure 3. A simplified molecular orbital diagram for an octahedral transition metal complex showing σ−and π−interactions only.

Class I:

In **class I** complexes, the Δ_o splitting is small and often applies to *3d* metals and σ ligands at lower end of the spectrochemical series. In this case the t_{2g} orbital is nonbonding in nature and may be occupied by 0−6 electrons (Figure 2). The e_g* orbital is weakly antibonding and may be occupied by 0−4 electrons. As a consequence, 12−22 valence electron count may be obtained for this class of compounds. Owing to small Δ_{tetr} splitting energy, the tetrahedral transition metal complexes also belongs to this class.

Class II:

In **class II** complexes, the Δ_o splitting is relatively large and is applicable to *4d* and *5d* transition metals having high oxidation state and for σ ligands in the intermediate and upper range of the spectrochemical series. In this case, the t_{2g} orbital is essentially nonbonding in nature and can be filled by 0−6 electrons (Figure 3). The e_g* orbital is strongly antibonding and is not occupied at all. Consequently, the valence shell electron count of these type of complexes would thus be 18 electrons or less.

Class III:

In **class III** complexes, the Δ_o splitting is the largest and is applicable to good σ donor and π acceptor ligands like CO, PF_3, olefins and arenes located at the upper end of the spectrochemical series. The t_{2g}orbital becomes bonding owing to interactions with ligand orbitals and should be occupied by 6 electrons. The e_g* orbital is strongly antibonding and therefore remains unoccupied.

Problems

State the oxidation state of the metal and the total valence electron count of the following species.

1. $V(C_2O_4)_3^{3-}$

Ans: +3 and 14 2. $Mn(acac)_3$ Ans: +3 and 16 3. $W(CN)_8^{3-}$ Ans: +5 and 17 4. $CpMn(CO)_3$ Ans: 0 and 18 5. $Fe_2(CO)_9$ Ans: 0 and 18
Self Assessment test

State the oxidation state of the metal and the total valence electron count of the following species.

1. TiF_6^{2-}

Ans: +4 and 12 2. $Ni(en)_3^{2+}$ Ans: +2 and 20 3. $Cu(NH_3)_6^{2+}$ Ans: +2 and 21 4. $W(CN)_8^{4-}$ Ans: +4 and 18 5. $CH_3Co(CO)_4$ Ans: 0 and 18

Summary

The transition metal complexes may be classified into the following three types. (i). The ones that do not obey the 18 valence electron rule are of class I type (ii). the ones that do not exceed the 18 valence electron rule are of class II and (iii). the ones that strictly follow the 18 valence electron rule. Depending upon the interaction of the metal orbitals with the ligand orbitals and also upon the nature of the ligand position in spectrochemical series, the transition metal organometallic compounds can form into any of the three categories.

The 18-electron rule is used primarily for predicting and rationalizing formulae for stable metal complexes, especially organometallic compounds. The rule is based on the fact that the valence shells of transition metals consist of nine valence orbitals (one s orbital, three p orbitals and five d orbitals), which collectively can accommodate 18 electrons as either bonding or nonbonding electron pairs. This means that, the combination of these nine atomic orbitals with ligand orbitals creates nine molecular orbitals that are either metal-ligand bonding or non-bonding. When a metal complex has 18 valence electrons, it has achieved the same electron configuration as the noble gas in the period. The rule and its exceptions are similar to the application of the octet rule to main group elements.

This rule applies primarily to organometallic compounds, and the 18 electrons come from the 9 available orbitals in d orbital elements (1 s orbital, 3 p orbitals, and 5 d orbitals). The rule is not helpful for complexes of metals that are not transition metals, and interesting or useful transition metal complexes will violate the rule because of the consequences deviating from the rule bears on reactivity. If the molecular transition metal complex has an 18 electron count, it is called **saturated**. This means that additional ligands cannot bind to the transition metal because there are no empty low-energy orbitals for incoming ligands to coordinate. If the molecule has less than 18 electrons, then it is called **unsaturated** and can bind additional ligands.

Electron counting

Two methods are commonly employed for electron counting:

1. Neutral atom method: Metal is taken as in zero oxidation state for counting purpose
2. Oxidation state method: We first arrive at the oxidation state of the metal by considering the number of anionic ligands present and overall charge of the complex

To count electrons in a transition metal compound:

1. Determine the oxidation state of the transition metal and the resulting d-electron count.
   - Identify if there are any overall charges on the molecular complex.
   - Identify the charge of each ligand.
2. Determine the number of electrons from each ligand that are donated to the metal center.
3. Add up the electron counts for the metal and for each ligand.

Typically for most compounds, the electron count should add up to 18 electrons. However, there are many exceptions to the 18 electron rule, just like there are exceptions to the octet rule.

Reactivity

The 18 electron rule allows one to predict the reactivity of a certain compound. The associative mechanism means that there is an addition of a ligand while a dissociative mechanism means that there is a loss of a ligand. When the electron count is less than 18, a molecule will most likely undergo an associative reaction. For example: $(C_2H_4)PdCl_2$

- 16 electron count
- Would it more likely lose a C_2H_4 or gain a CO? Losing a C_2H_4 results in a 14 electron complex while gaining a CO gives an 18 electron complex. From the 18 electron rule, we will expect that the compound will more likely undergo an associative addition of CO.

Example 8.2.1:

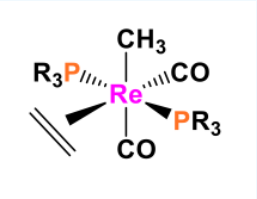


Figure **8.2.1**: Saturated Re metal complex with 18 electron count. (CC SA-BY 4.0; Derrekli)

1. There is no overall charge on the molecule and there is one anionic ligand (CH_3^-)
   - The Re metal must have a positive charge that balances out the anionic ligand charge to equal the 0 overall molecular charge. Since there is a -1 charge contribution from the methyl ligand, the Re metal has a +1 charge.
   - Because the Re metal is in the +1 oxidation state, it is a d^6 electron count. It would have been its regular d^7 electron count if it had a neutral (0) oxidation state.
2. The CH_3^- ligand contributes 2 electrons. Each CO ligand contributes 2 electrons. Each PR_3 ligand contributes 2 electrons. The H2C=CH2 ligand contributes 2 electrons.
3. Adding up the electrons:
   - Re(1): 6 electrons
   - CH_3^-: 2 electrons
   - 2 x CO: 2 x 2 electrons = 4 electrons
   - 2 x PR_3: 2 x 2 electrons = 4 electrons
   - $H_2C=CH_2$: 2 electrons
   - Total: 18 electrons

In this example, the molecular compound has an 18 electron count, which means that all of its orbitals are filled and the compound is stable.

Example 8.2.2: $[M(CO)_7]^+$

The 18 electron rule can also be used to help identify an unknown transition metal in a compound. Take for example $[M(CO)_7]^+$. To find what the unknown transition metal M is, simply work backwards:

1. 18 electrons
2. Each (CO) ligand contributes 2 electrons
   - 7 x 2 electrons = 14 electrons
3. 18 - 14 = 4 electrons
4. d^4
5. M(I) oxidation state
6. The unknown metal M must be V, Vanadium

Example 8.2.3: $[Co(CO)_5]^z$

Similarly to Example 2, the 18 electron rule can also be applied to determine the overall expected charge of an molecule. Take for example $[Co(CO)_5]^z$. To find the unknown charge z:

1. 18 electrons
2. Each CO ligand contributes 2 electrons
    1. 5 x 2 electrons = 10 electrons
3. Co is typically d^9
4. 9 + 10 = 19 electrons
5. To satisfy the 18 electron rule, the $[Co(CO)_5]^z$ compound must have a charge of z = +1.

Ligand Contributions

Below is a list of common organometallic ligands and their respective electron contributions.

Neutral 2e donors	Anionic 2e donors	Anionic 4e donors	Anionic 6e donors
PR_3 (phosphines)	X^- (halide)	$C_3H_5^-$ (allyl)	Cp^- (cyclopentadienyl)
CO (carbonyl)	CH_3^- (methyl)	O^{2-} (oxide)	O^{2-} (oxide)
alkenes	CR_3^- (alkyl)	S^{2-} (sulfide)	
alkynes	Ph^- (phenyl)	NR^{2-} (imide)	
nitriles	H^- (hydride)	CR_2^{2-} (alkylidene)	
	R_nE^- (silyl, germyl, alkoxo, amido etc.)	OR^- (alkoxide, bridging ligand)	
		SR^- (thiolate, bridging ligand)	
		NR_2^- (inorganic amide, bridging ligand)	
		PR_2^- (phosphide, bridging ligand)	

Exceptions

Generally, the early transition metals (group 3 to 5) could have an electron count of 16 or less. Middle transition metals (group 6 to group 8) commonly have 18 electron count while late transition metals (group 9 to group 11) generally have 16 or lower electron count. When a structure has less than an 18 electron count, it is considered electron-deficient or coordinately unsaturated. This means that the compound has empty valence orbitals, making it electrophilic and extremely reactive. If a structure has "too many electrons," that means that not all of the bonds are covalent bonds, and thus some has to be ionic bonds. These bonds are weaker compared to covalent bonds. However, these organometallic compounds that have an electron count greater than 18 are fairly rare.

Summary

The 18-electron rule is similar to the octet rule for main group elements, something you might be more familiar with, and thus it may be useful to bear that in mind. So in a sense, there's not much more to it than "electron bookkeeping".

References

1. Pfenning, Brian (2015). *Principles of Inorganic Chemistry*. Hoboken, New Jersey: John Wiley & Sons, Inc. pp. 629–631. ISBN 9781118973868.

Contributors and Attributions

- Wikipedia (CC-BY-SA-3.0)
- Openstack

8.2: 18 Electron Rule is shared under a CC BY-NC-SA 4.0 license and was authored, remixed, and/or curated by LibreTexts.

- **24.3: The 18-electron Rule** is licensed CC BY-NC-SA 4.0.

8.3: Organometallic Reaction Types

Introduction

In this chapter we will discuss common reactions and catalysis of organometallic compounds. We can classify reactions into two main categories. The first one includes reactions with gain or loss of ligands. You will hear about four reactions that belong to this category: ligand substitution reactions, oxidative additions, reductive eliminations, and nucleophilic displacement. The latter three can involve a change in coordination number while ligand substitution reactions do not.

The second main category are reactions that involve the modification of ligands. There are two reactions you will learn about: The migratory insertion and the β-hydride elimination.

Oxidative Addition Reactions

Let us start with the oxidative addition. How is it defined? An oxidative addition is a reaction in which one or more ligands add to the metal center of a complex and oxidize it. This addition can occur in a cis- or trans-fashion. A cis-addition means that two ligands are added so that they have cis-orientation to each other after the reaction is complete. A trans-addition implies that two new ligands are in opposite, trans-position after they have been added. We can further distinguish between mononuclear and dinuclear additions. Mononuclear addition involves a complex with a single metal. Dinuclear additions are additions to a metal-metal bond. The addition cleaves the metal-metal bond and adds one ligand to each fragment.

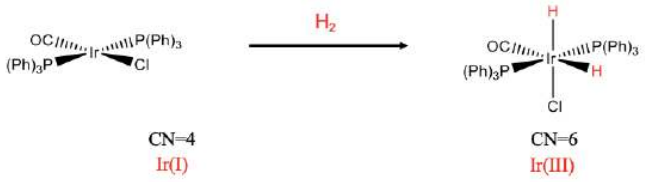


Figure 8.3.1: Mononuclear oxidative cis-addition (Attribution: A. Vedernikov, U Maryland (modified))

Here are a few of examples. The first example is a mononuclear cis-addition (Fig. 8.3.1:). In the reaction we add dihydrogen to a square planar iridium complex. After the reaction there are two additional hydrido ligands, and the coordination number has increased from 4 to 6. We can see that the two hydrido ligands are oriented in cis-fashion relative to each other. We can verify that the addition of the hydrido ligands oxidized the metal by determining the oxidation number of the metal before and after the reaction. There are three neutral ligands and one negatively charged chloro ligand. There is no overall charge at the complex. This means that the oxidation number of Ir is +1. After the reaction, there are the two hydrido ligands that have both a -1 charge. Remember, we get the charge at a ligand by cleaving the metal-ligand bond so that all electrons in the bond get assigned to the ligand. This means the oxidation number must be increased by +2, and is +3 after the reaction.

We can rationalize why the addition occurs in cis-fashion and not in trans-fashion. The two hydrido ligands are the smallest ligands, therefore, steric repulsion is minimized in the complex is minimized when the two hydrido ligands are in cis-position.

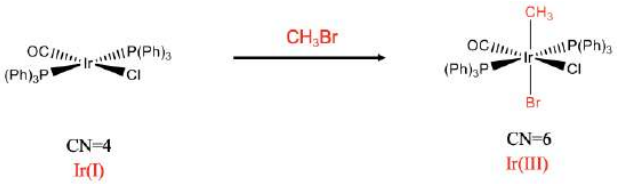


Fig. 8.3.2: Mononuclear oxidative trans-addition (Attribution: A. Vedernikov, U Maryland (modified))

The second example is a mononuclear trans-addition (Fig. 8.3.2:). In this reaction CH_3Br is added to the iridium complex. In this case the two new ligands, a CH_3 and the Br group are in opposite position. Again, the coordination number increases from four to six. We can again verify that an oxidation has occurred by analyzing the oxidation number of Ir. As previously determined, the oxidation number of iridium in the reactant complex is +1. Let us analyze the product complex. The chloro ligand and the bromo ligand have a 1- charge. In addition to that also the CH_3 ligand has a 1- charge assuming that we treat the Ir-C bond as a dative bond. Thus, the oxidation number of Ir must be +3 to give a neutral complex.

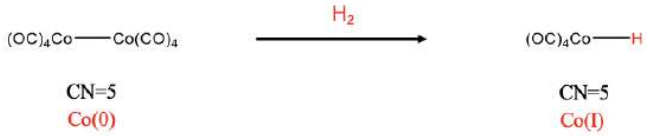


Figure **8.3.3**: Dinuclear addition (Attribution: A. Vedernikov, U Maryland (modified))

The third example is a dinuclear addition (Fig. **8.3.3**:). This addition is neither cis nor trans because it cleaves a metal-metal bond, and the one new ligand is added to each fragment. In the example the Co-Co bond of the dicobalt octacarbonyl gets cleaved upon the reaction with dihydrogen, and two $HCo(CO)_4$ complexes with Co-H bonds form. In this case the coordination number does not increase. Both the reactant and the products have the coordination number 5. We can see that an oxidation of Co has occurred by comparing the oxidation numbers. In the reactant the oxidation number of Co is zero because all CO ligands are neutral and the complex is overall neutral. In the carbonyl hydride product, Co has the oxidation number +1, because the hydrido ligand has a 1-charge.

Oxidative Additions with Intact Ligands

In the previous examples, the ligands that reacted with the complexes lost their integrity. The H-H bond in the H_2 molecule cleaved to form the hydrido ligands, and the C-Br bond in CH_3Br was cleaved to form separate Br and methyl ligands. Not all ligands lose their integrity upon their addition, in particular when they contain multiple bonds. These ligands are called intact ligands. In these cases the bond order within the ligand is reduced, but the number is still greater than zero.

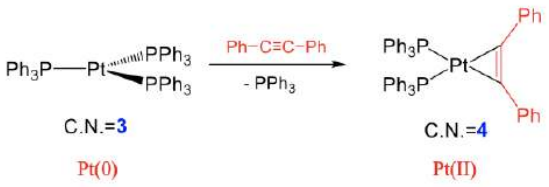


Figure **8.3.4**: Oxidative addition with intact ligands (Attribution: A. Vedernikov, U Maryland (modified))

Examples for intact ligands are are alkenes, alkynes, O_2, etc. In an oxidative addition with an alkyne for example, the alkyne binds side-on to the transition metal under the formation of two metal-C single bonds, and the reduction of the bond order within the alkyne from 3 to 2 (Fig. **8.3.4**:). In the shown reaction, a diphenyl ethine molecule adds to tris(triphenyl phosphine) platinum under the formation of two Pt-C single bonds. The C-C triple bond in the ligand becomes a double bond. This reaction occurs under loss of one of the three triphenyl phosphine ligands. The coordination number at the metal increases from 3 to 4. We can again show that the reaction is oxidative by comparing the oxidation numbers of the metal. In the reactant, Pt has the oxidation number 0 because the three triphenyl phosphine ligands have no charge and the complex has overall no charge. After the reaction, the oxidation number of Pt is +2. This is because when we assign the four electrons of the two Pt-C single bonds to the ligand, the ligand becomes a $(Ph\text{-}C{=}C\text{-}Ph)^{2-}$ ligand with each C atom carrying a 1- charge. Because the product complex is overall neutral, the oxidation number of Pt is +2.

Reductive Elimination Reactions

The reductive elimination reaction is the reverse of the oxidative addition. The reductive elimination can only occur when the two ligands to be eliminated are in cis-position.

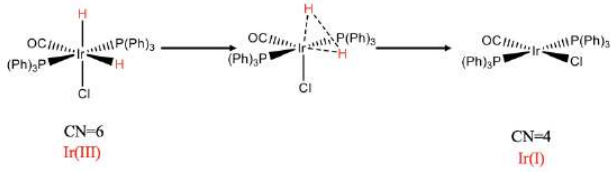


Figure **8.3.5**: Reductive elimination (Attribution: A. Vedernikov, U Maryland.)

For instance the previously discussed oxidative cis-addition of H_2 to the iridium complex is reversible, and the reverse is called the reductive elimination (Fig. **8.3.5**:). The cis-orientation of the two hydrido ligands is necessary to form an H-H bond. The reaction

can be thought of going along a reaction path in which the Ir-H bonds become gradually larger and and the H-H distance gradually smaller until the H_2 molecule is eliminated from the complex.

Catalytic Deuteration of Benzene

Combinations of oxidative additions and reductive eliminations have many applications in the synthesis of organic molecules using an organometallic reactant.

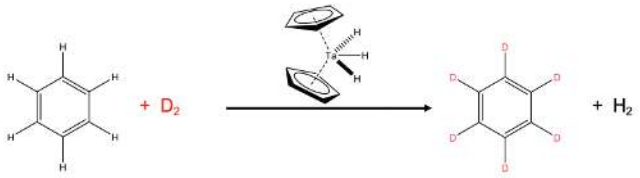


Figure **8.3.6**: Deuteration of benzene

An example is the deuteration of benzene (Fig. **8.3.6**:). Deuterated benzene is an important solvent in NMR spectroscopy. Industrially, the deuteration is done using a dicyclopentadienyltrihydridotantalum(V) catalyst starting out from benzene and D_2. The D_2 is provided in excess to drive the chemical equilibrium to the right side.

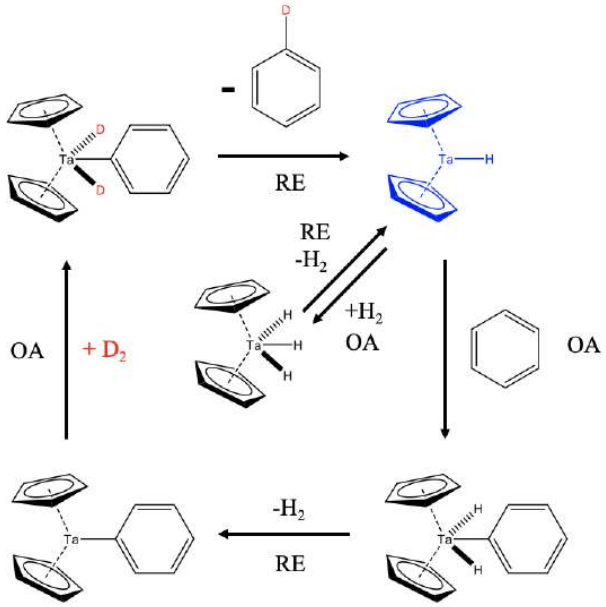


Figure **8.3.7**: Mechanism of the catalytic deuteration of benzene

How does this reaction work mechanistically? This 18e Cp_2TaH_3 is actually a precatalyst that is in chemical equilibrium with H_2 and the 16e dicyclopentadienylhydrido tantalum(III) which is the actual catalyst (Fig. **8.3.7**:). Elimination of H_2 from the Ta(V) catalyst is a reductive elimination (RE) and the re-addition of H_2 to the Ta(III) species an oxidative addition (OA). In the presence of benzene, the Ta(III) species can oxidatively add benzene to form an 18e Ta(V) complex. This complex can reductively eliminate H_2 to form a 16e Cp_2Ta(III)-Ph complex. In the presence of deuterium this complex can add D_2 oxidatively to form an 18e Cp_2D_2Ta(V)-Ph complex. This species can then reductively eliminate a monodeuterated benzene molecule under formation of Cp_2Ta(III)-D. In the presence of enough D_2 this monodeuterated benzene can be further deuterated in subsequent catalytic cycles.

Nucleophilic Displacement Reactions

Another important reaction is the nucleophilic displacement reaction. In these reactions a complex, typically an anion, acts as a nucleophile. The ligand is added, but no electrons are added to the complex. The reactions can be extremely useful for the synthesis of organic compounds. The utility results mostly from the fact that an organic electrophile is turned into a nucleophile.

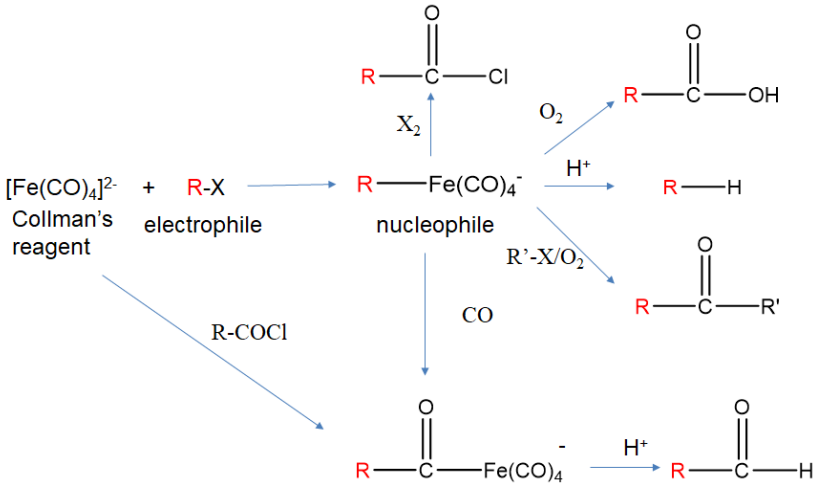


Figure 8.3.8: Examples of nucleophilic displacement reactions

For example, tetracarbonyl ferrate (2-), also known as Collman's reagent reacts with alkyl halides to form alkyl tetracarbonyl ferrate (-) (Fig. 8.3.8:). We can check that the addition of the alkyl group did not add any electrons by counting the electrons before and after the reaction. The $Fe(CO)_4^{2-}$ anion is an 18e complex. Applying the neutral atom method to the electron counting in $[R\text{-}Fe(CO)_4]^-$ means that Fe contributes 8e, the 1- charge adds 1e, the CO ligands 4x2=8 electrons and the alkyl ligand 1e. This gives 8+1+8+1=18 electrons. Also the oxidation number of Fe has not changed upon the addition of the ligand. It is -2 before and after the reaction.

In the alkyltetracarbonyl ferrate (1-) anion, the group R which was formerly an electrophile in R-X, can now act as a nucleophile due to the fact that the Fe-C bond is polarized toward the C-atom. As a nucleophile it can for instance react with protons to form an alkane. It can also react with oxygen to form a carboxylic acid. In the presence of another alkyl halide R'-X it can form a ketone R-C(O)-R'. It can also insert CO into the Fe-C bonding in a so-called migratory insertion reaction, and the reaction product can react with acid to form an aldehyde. With dihalogens X_2 it can form acyl chloride. Collman's reagent cannot only add alkyl halides by also acyl halides to form acyl tetracarbonyl ferrates (-).

Migratory Insertion and Deinsertion (Elimination) Reactions

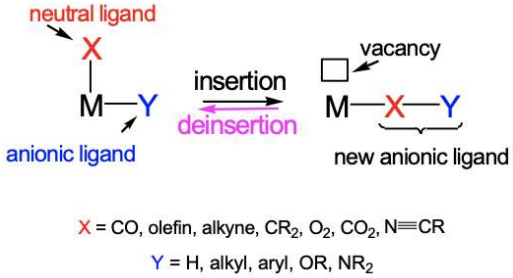


Figure 8.3.9: Migratory insertion (Attribution: A. Vedernikov, U Maryland.)

Our next reaction is the migratory insertion. In a migratory insertion reaction, there is an anionic ligand X and a neutral unsaturated ligand Y in cis-position, and the two ligands couple to form another anionic ligand XY that is attached to the same metal (Fig. 8.3.9:). This produces a vacancy at the metal, meaning a coordination site at the metal which is not occupied by a ligand. In an insertion reaction it is more common that the anionic ligand moves. The reaction is reversible and there is typically a chemical equilibrium. The reverse reaction is called a deinsertion. To drive the chemical equilibrium to the right side one can add the neutral ligand in excess or add a different neutral ligand. The neutral ligand then adds to the vacancy and prevents the reverse reaction. Typical neutral, unsaturated ligands are CO, olefins, alkynes, carbenes, dioxygen, carbon dioxide, and nitriles. Typical anionic ligands are hydrido, alkyl, aryl, alkoxy, and amido-ligands.

Carbonyl Migratory Insertions

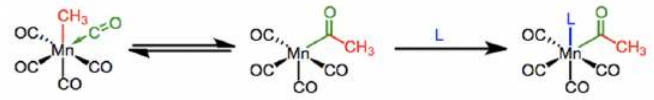


Figure 8.3.10: Carbonyl migratory insertions (Attribution: Michael Evans http://organometallicchem.files.word...8-pm.png?w=700)

One of the most common insertions are carbonyl insertions into alkyl groups like methyl groups (Fig. 8.3.10:). The carbonyl insertion produces an acyl group. To drive the reaction, the reaction can be carried out in the presence of a neutral ligand L like free CO, which occupies the vacant site.

Olefin Insertion and β-Hydride Elimination

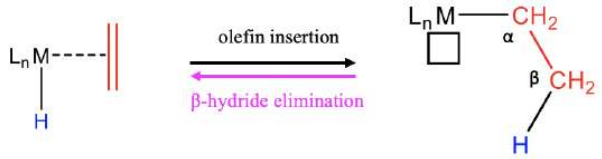


Figure 8.3.11: Olefin insertion and β-hydride elimination

Another very common migratory insertion is the olefin migratory insertion into hydrides (Fig. 8.3.11:). This produces an alkyl group. When the reaction is carried out in the presence of CO which binds to the vacant site, then the reaction is driven to the right side. The reverse of this reaction is the β-hydride elimination. It is called "β"-elimination because of the H-atoms that are attached to the carbon atom in the alkyl chain that is second-closest to the metal are called "β"-hydrogens. The hydrogen atoms that are attached to the carbon which is bound to the carbon bonded to the metal via a metal-carbon bond are called "α"-hydrogens.

Instability of Transition Metal Complexes Caused by β-Hydride Elimination

The β-hydride elimination is responsible for the frequent instability of transition metal alkyl complexes that possess β-hydrogen atoms.

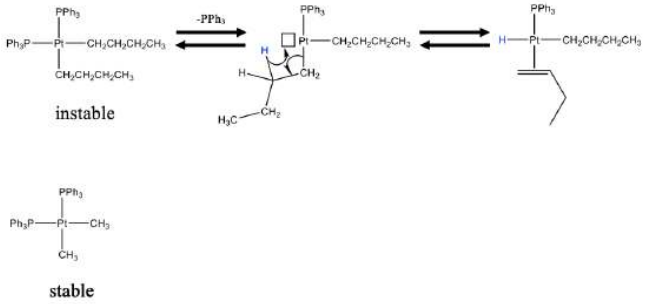


Figure 8.3.12: Instability of transition metal complexes caused by β-hydride elimination (Attribution: A. Vedernikov, U Maryland (modified).)

For example, the depicted dialkyldiphosphine platinum complex is unstable because it has β-hydrogen atoms (Fig. 8.3.12:). Statistically, the complex can lose a phospine complex at a certain rate due to the lability of the Pt-P bond leading to a complex with a vacant site. This complex can then undergo a β-elimination to form an olefin complex. In this case the olefin is a volatile butene molecule which can detach from the metal and leave the system unless the system is hermetically closed. In contrast, the respective methyl complex is stable because it only has α-hydrogens, but not β-hydrogens.

Carbene Migratory Insertion

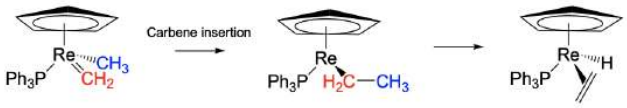


Figure 8.3.13: Carbene migratory insertion (Attribution: A. Vedernikov, U Maryland.)

Migratory insertions are also possible for carbenes. In this case, a CH_2 group bonded to the metal via a M=C double bond plays the role of the neutral, unsaturated ligand. In the shown Re complex the carbene inserts into a Re-CH_3 bond to form an ethyl group.

This ethyl group is unstable because it can undergo β-hydride elimination to form an alkene complex with a hydride ligand.

Dr. Kai Landskron (Lehigh University). If you like this textbook, please consider to make a donation to support the author's research at Lehigh University: Click Here to Donate.

This page titled 8.3: Organometallic Reaction Types is shared under a CC BY 4.0 license and was authored, remixed, and/or curated by Kai Landskron.

- **12.1: Organometallic reactions** by Kai Landskron is licensed CC BY 4.0.

8.4: Organometallic Catalysts

Organometallic Compounds as Hydrogenation Catalysts

Migratory insertions play an important role in catalysis.

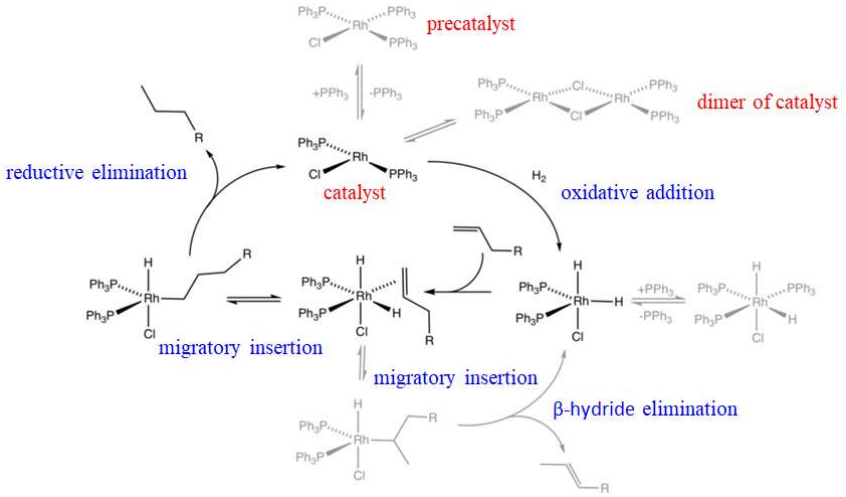


Figure 12.2.2 Mechanism of the Wilkinson hydrogenation catalyst (Attribution: Smokefoot / CC BY-SA (https://creativecommons.org/licenses/by-sa/4.0) https://commons.wikimedia.org/wiki/F...cleJMBrown.png)

For example a Rh-catalyst called the Wilkinson catalyst is an effective hydrogenation catalyst for olefins. The mechanism of the hydrogenation involves a combination of oxidative additions, olefin migratory insertions, and reductive eliminations (Fig. 12.2.2). Wilkinson's catalyst is the square planar chloro tris(triphenylphosphine) rhodium(I) complex. This molecule is actually a precatalyst that becomes the actual catalyst when it statistically loses a triphenylphosphine ligand producing chloro bis(triphenylphosphine) rhodium(I). The loss of this ligand is a reversible reaction, and thus the catalyst is in chemical equilibrium with the precatalyst. The actually catalyst is in a second chemical equilibrium with its dimer. The chloro bis(triphenylphosphine) rhodium(I) catalyst can undergo an oxidative addition in the presence of hydrogen to form a trigonal bipyramidal chlorodihydrido bis(triphenylphosphine) (III) rhodium complex. This species is in chemical equilibrium with an octahedral chlorodihydrido tris(triphenyl phosphine) rhodium(III) species that can form due to the presence of free triphenylphosphine ligands in the system. The trigonal bipyramidal species can then add an olefin that binds side-on to the Rh. Because the olefin is in cis-position to the hydride ligand it can undergo an olefin insertion. The Rh-C bond can either form with the first or the second carbon in the carbon chain of the olefin, giving a linear and a branched alkyl complex, respectively. The branched complex can undergo a β-hydride elimination thereby reforming the trigonal bipyramidal Rh-complex, and an olefin. This reaction is a side-reaction because the branched alkyl complex is sterically more crowded than the linear complex. The linear alkyl Rh complex can undergo a reductive elimination to form the linear alkane and the $RhCl(PPh_3)_2$ catalyst. This completes the catalytic cycle, and a new cycle can start.

Ziegler-Natta Polymerization

Another example of an organometallic catalytic reaction is the Ziegler-Natta olefin polymerization. This reaction is of high industrial importance for the production of olefins like polyethylene. There are both heterogeneous and homogeneous Ziegler-Natta catalysts. The mechanism for the homogeneous catalysts is generally well understood. Homogeneous catalysts are typically metallocene catalysts.

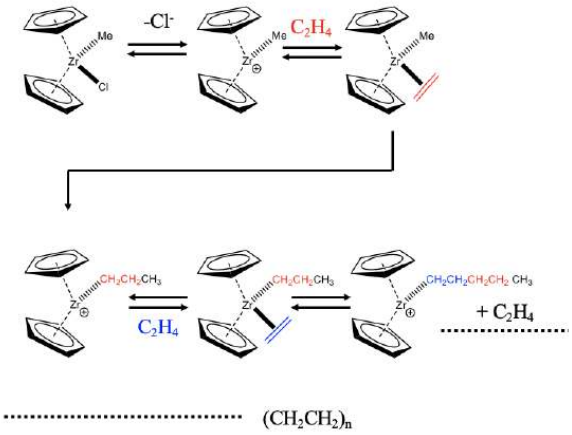


Figure 12.2.3 Zirconium-based Ziegler-Natta catalyst (Attribution: A. Vedernikov, U Maryland (modified).)

An example of a zirconium-based catalyst is shown (Fig. 12.2.3). The catalyst is a coordinatively unsaturated complex cation with two cyclopentadienyl rings and a methyl group. The catalyst is formed from its precatalyst, a neutral molecule with an additional chloro ligand. The catalyst oxidatively adds an olefin like an ethylene molecule to the coordinatively unsaturated site. This step is followed an olefin insertion step that produces a propyl group. The migratory insertion leads to the formation of a vacant site, that can be re-oocupied by another ethylene molecule. This molecule can insert into the propyl chain thereby prolonging the propyl chain to a pentyl chain. The olefin insertion step generates another vacant site that can be reoccupied by a new ethylene molecule. Repeating the catalytic cycle many times eventually leads to polyethylene.

Catalytic Olefin Hydroformylation

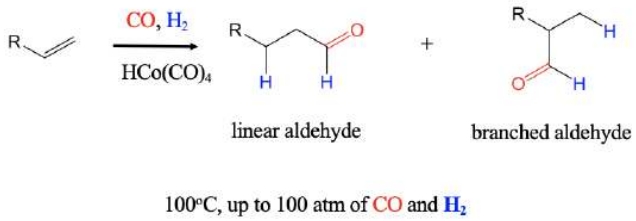


Figure 12.2.4 Catalytic olefin hydroformylation

A further important industrial reaction is the catalytic hydroformylation reaction, also known as oxo-process. It was discovered in 1938 by Otto Roelen at BASF. In the hydroformylation reaction an H atom and a formyl group are added to an alkene to form aldehydes. The reaction can produce both branched an linear aldehydes from terminal alkenes, CO, and H_2 using a carbonyl hydrides such as $HCo(CO)_4$ as a catalyst. The reaction is performed at about 100°C at a pressure of up to 100 atm.

Mechanism of the Catalytic Olefin Hydroformylation by $HCo(CO)_4$

How does the hydroformylation work mechanistically?

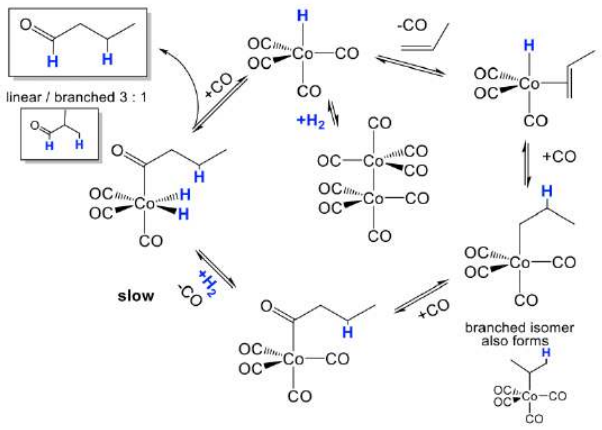


Figure 12.2.5 Mechanism of the catalytic olefin hydroformylation by $HCo(CO)_4$ (Attribution: A. Vedernikov, U Maryland (modified).)

The mechanism is illustrated for the hydroformylation of propene (Fig. 12.2.5). The actual catalyst $HCo(CO)_4$ is first formed from its precatalyst $Co_2(CO)_8$ in the presence of H_2 in a dinuclear oxidative addition reaction. The catalyst can undergo a substitution reaction in which a CO ligand is replaced by the olefin that binds side-on to the cobalt. This species can then undergo a migratory olefin insertion reaction. This leads to a mixture of linear and branched alkyl groups attached to the Co. A new CO ligand can add to the vacant site. The alkyl group can then insert into a carbonyl group in another migratory insert step, and the vacant site can be reoccupied by a new CO molecule. Then, H_2 is added in an oxidative addition. This is the slowest and rate-limiting step in the catalytic cycle. From the addition product the aldehyde can then be eliminated in a reductive elimination reaction. Addition of CO regenerates the catalyst, and the catalytic cycle can begin again.

Hydrocarbonylations

After the hydroformylation, a number of other hydrocarbonylations were developed, and industrially deployed.

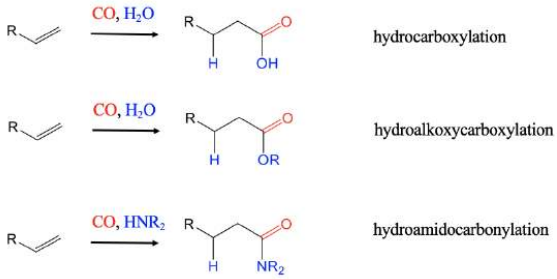


Figure 12.2.6 Hydrocarbonylation reactions

When hydrogen is replaced by H_2O hydrocarboxylations of alkenes lead to carboxylic acids (Fig. 12.2.6). With an alcohol instead of H_2 hydroalkoxycarbonylcations lead to esters. The employment of amines instead of H_2 leads to amides in hydroamidocarbonylation reactions.

The Monsanto Acetic Acid Process

Another carbonylation reaction involving an organometallic catalyst is the Monsanto acetic acid process. It has been introduced by Monsanto in the 1970s for the industrial production of acetic acid from methanol. The reaction involves dual catalysis with HI and $[RhI_2(CO)_2]^-$ as a co-catalysts. How does this reaction work?

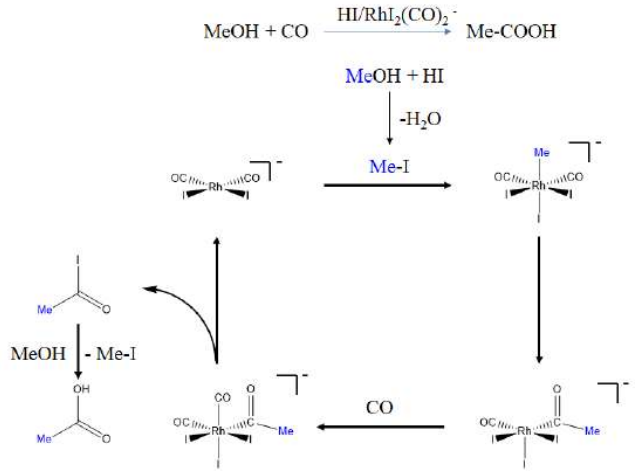


Figure 12.2.7 The catalytic cycle in the Monsanto acetic acid process

In the first step methanol reacts with HI to form methyl iodide. The methyl iodide then reacts with the Rh-catalyst in an oxidative addition reaction in which a methyl and an iodo group are added in trans-fashion to the square-planar Rh-complex to give an octahedral complex. The octahedral complex then undergoes a migratory insertion reaction with CO producing an acyl group and a vacant site. A CO molecule can then add to the vacant site. The acetyl iodide can then be eliminated in a reductive elimination to reform the Rh-catalyst thereby closing the catalytic cycle. The acetyl iodide can then react with methanol to form new methyl iodide and acetic acid. The methyl iodide can start a new catalytic cycle with the Rh-catalyst.

Olefin Metathesis

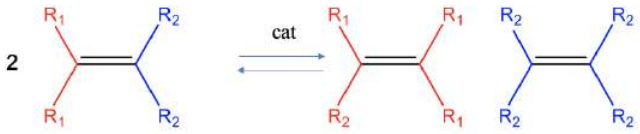


Figure 12.2.8 Olefin metathesis

Olefin metathesis is a reaction which allows to cut and rearrange C=C double bonds in olefins to make new olefins (Fig. 12.2.8). Formally, the carbon-carbon bond of the reactant is cleaved homoleptically and the two carbene fragments are combined in a different way. This reaction is typically an equilibrium reaction, and neither the reactants nor the products are clearly favored. This reaction is catalyzed by molybdenum arylamido carbene complexes or ruthenium carbene complexes.

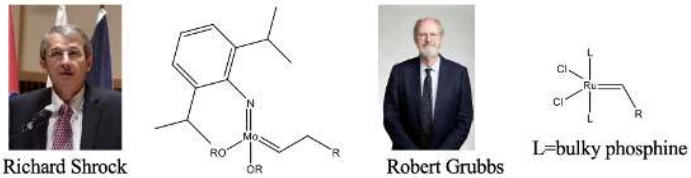


Figure 12.2.9 Shrock catalyst (Attribution: R._Schrock_-_IChO_2012_Opening_Ceremony.JPG: A.mela93derivative work: Materialscientist / CC BY-SA (https://creativecommons.org/licenses/by-sa/3.0) https://commons.wikimedia.org/wiki/F...hrock_2012.jpg) and (Attribution: The Royal Society / CC BY-SA (https://creativecommons.org/licenses/by-sa/3.0) https://commons.wikimedia.org/wiki/F...al_Society.jpg)

The former are called Shrock catalysts, and the latter Grubbs catalysts named after their discoverers Richard Shrock and Robert Grubbs who received the Nobel prize for Chemistry in 2005 (Fig. 12.2.9). The Schrock catalysts are more active, but also very sensitive to air and water. The Grubbs catalysts, while less active, are less sensitive to air and water.

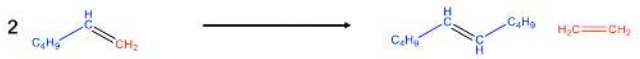


Figure 12.2.10 Regular metathesis

Olefin metathesis often allows for simpler preparation of olefins compared to other methods. Olefin metathesis is particularly powerful when one olefin product is gaseous because then it can be quite easily removed from the chemical equilibrium by purging. This drives the chemical equilibrium to the right side. An example is the preparation of 5-decene from 1-hexene. Cleavage of the C=C double bond in the hexene leads to C_5 and C_1 carbene fragments (Fig. 12.2.10). The two C_1 fragments can combine to form ethylene and the two C_5 fragments combine to 5-decene. The ethylene is volatile and can be purged from the reaction system thereby driving the chemical reaction to the right side.

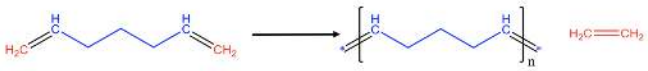


Figure 12.2.11 Acylic diene metathesis (ADMET)

The same principles can also be applied to produce polymers from dienes with two terminal C=C double bonds at the chain ends. This is called acylic diene metathesis (ADMET), Fig. 12.2.11. For instance the cleavage of the two terminal double bonds in a diene with seven C atoms leads to C_1 and C_5 fragments. The C_1 fragments can combine to form ethylene, and the C_5 fragments can combine to make an unsaturated polymer of the type $[CH(CH_2)_3CH]_n$. Again, the reaction can be driven to the right side by removing the gaseous ethylene from the reaction mixture through purging.

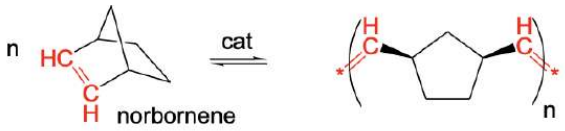


Figure 12.2.12 Ring-opening metathesis polymerization (ROMP)

Another variation of olefin metathesis is ring-opening metathesis polymerization (ROMP). It allows to make polymers from strained cycloolefins, for example norbornene. The reaction driving force is the relief of the strain. Because the strain is removed in the polymer, the chemical equilibrium lies far on the right side. The reaction product in norbornene is a polymer with 5-membered rings that are interconnected by ethylene -CH=CH- units (Fig. 12.2.12).

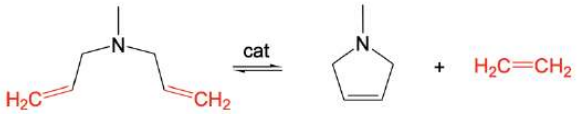


Figure 12.2.13 Ring-closing metathesis (RCM)

The opposite of ROMP is ring-closure metathesis (RCM). RCM allows for the preparation of unstrained rings with C=C double bonds from dienes with C=C double bonds that are five or six carbon atoms apart. This distance is suitable to produce unstrained rings. In the shown example a five-membered ring with a C=C double bond is formed from a diene with terminal C=C double bonds that are five atoms apart.

The Mechanism of Olefin Metathesis

What is the mechanism of olefin metathesis?

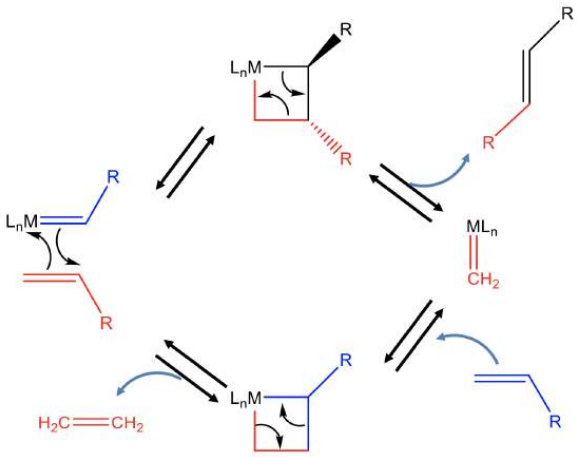


Figure 12.2.14 The mechanism of olefin metathesis

In the first step, the alkene adds to the the carbene fragment of the catalyst in a 2+2 cycloaddition reaction to produce an unstable intermediate with a highly strained four-membered ring (Fig. 12.2.14). This four membered ring can open to produce the first new alkene product R-CH=CH-R and a metal carbene species. This metal carbene can react with another reactant olefin to form another highly stained 4-ring intermediate via a 2+2 cycloaddition reaction. This ring can then reopen again to produce the second alkene metathesis product, in this case ethylene, and the original catalyst. The regenerated catalyst can then start a new catalytic cycle.

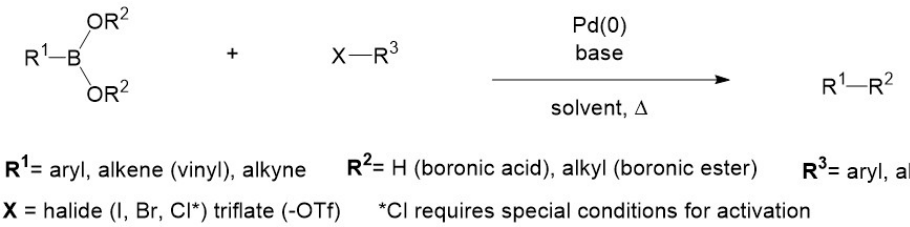
Dr. Kai Landskron (Lehigh University). If you like this textbook, please consider to make a donation to support the author's research at Lehigh University: Click Here to Donate.

This page titled 8.4: Organometallic Catalysts is shared under a CC BY 4.0 license and was authored, remixed, and/or curated by Kai Landskron.

- **12.2: Organometallic Catalysts** by Kai Landskron is licensed CC BY 4.0.

8.5: Suzuki-Miyara Coupling

Suzuki-Miyaura coupling (or Suzuki coupling) is a metal catalyzed reaction, typically with Pd, between an alkenyl (vinyl), aryl, or alkynyl organoborane (boronic acid or boronic ester, or special cases with aryl trifluoroborane) and halide or triflate under basic conditions. This reaction is used to create carbon-carbon bonds to produce conjugated systems of alkenes, styrenes, or biaryl compounds (Scheme 1).



Scheme 1: General reaction scheme of Suzuki cross coupling reaction.

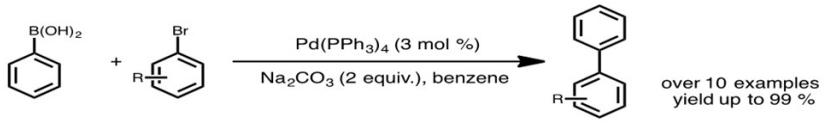
Modified conditions have demonstrated reactivity with less reactive substrates such as alkyl boranes (BR_3) or aryl or alkenyl chlorides by amending the base and ligands employed.

References:

1. Chemler, S. R.; Trauner, D.; Danishefsky, S. J. *Angew. Chem. Int. Ed.*, 2001, *40* , 4544.

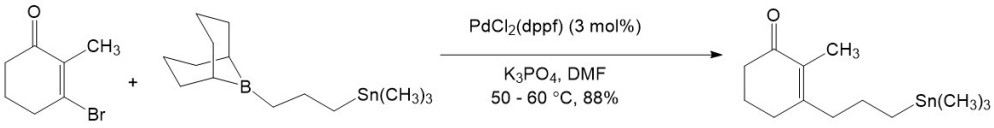
Historical Methods: Forming carbon-carbon bonds via cross coupling reactions

The Suzuki coupling is a pioneering reaction in cross coupling, and has been thoroughly studied since. The first Suzuki-type cross coupling reaction between phenylboronic acid and haloarenes was published by Suzuki and Miyaura in 1981 (Scheme 1).[1] Commonly, Suzuki coupling is compared to Stille coupling seeing that boron has a similar electronegativity to tin, which is used for transmetallation in Stille coupling. Both couplings have a similar reaction scope and proceed via a similar mechanistic cycle.



Scheme 1: Suzuki cross coupling reaction of phenylboronic acid and haloarenes.

Stille cross coupling reactions can form carbon-carbon bonds between alkenyl (vinyl), aryl, or alkynyl halides and an extended scope of organotin alkynes, alkenes, aryl, allyl benzyl, ketones, and alkyl. However, Stille coupling poses several drawbacks seeing that organotin reagents are: (1) highly toxic, (2) costly, and have a (3) lower functional group tolerance, despite Suzuki coupling not being suitable for base sensitive substrates.[2] The example below demonstrates that even under conditions for either a Stille or Suzuki coupling to ensue, primarily Suzuki coupling occurs (Scheme 2).[3]



Scheme 2: Suzuki versus Stille cross coupling reaction.

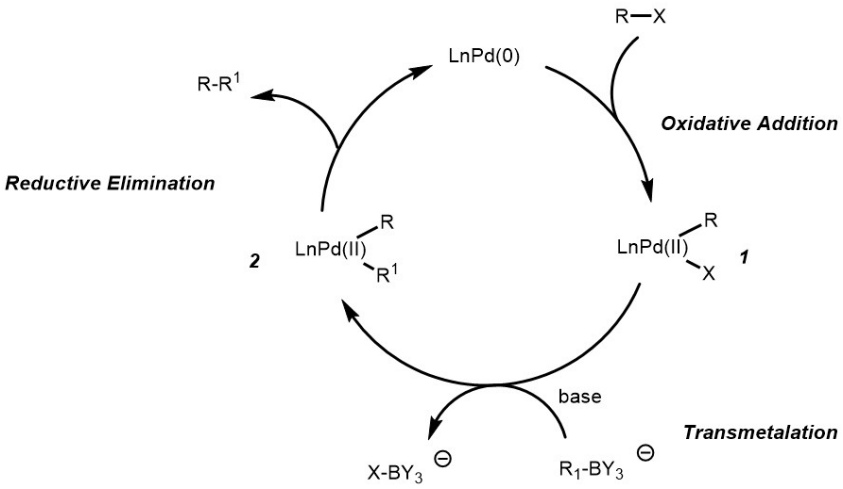
Negishi coupling also demonstrates similar transformations to Suzuki coupling in a comparable substrate scope. It uses organo-zinc for transmetallation. However, Negishi coupling tends to occur in lower yields, with less functional group tolerance, and is water and oxygen sensitive.[1]

References:

1. Miyaura, N.; Yanagi, T.; Suzuki, A. *Synth, Commun*. 1981, *11*, 513.
2. Suzuki, A. *Proc. Jpn. Acad., Ser. B*., 2004, *80*, 8, 359.
3. Ishiyama, T.; Miyaura, N.; Suzuki, A. *Synlett*, 1991, 687.

Reaction Scheme

Suzuki coupling proceeds via three basic steps: oxidative addition, transmetallation, and reductive elimination.



Reaction Mechanism and Mechanistic Studies

The general catalytic cycle for Suzuki cross coupling involves three fundamental steps: *oxidative addition*, *transmetalation*, and *reductive elimination* as demonstrated in Figure 1.[1] The *oxidative addition* of aryl halides to Pd(0) complex is the initial step to give intermediate 1, a Pd(II) species. Under the participation of base, an organoborane compound reacts with intermediate 1 in *transmetalation* to afford intermediate 2. This is followed by *reductive elimination* to give the desired product and regenerate the original Pd(0) species. Depending on different catalytic systems with various catalysts, ligands, and solvents, there are additional processes in the catalytic cycle, including ligand or solvent association and dissociation.[2] Undoubtedly, these three fundamental steps occur since intermediates 1 and 2 have been characterized by isolation[3] or spectroscopic analyses[4].

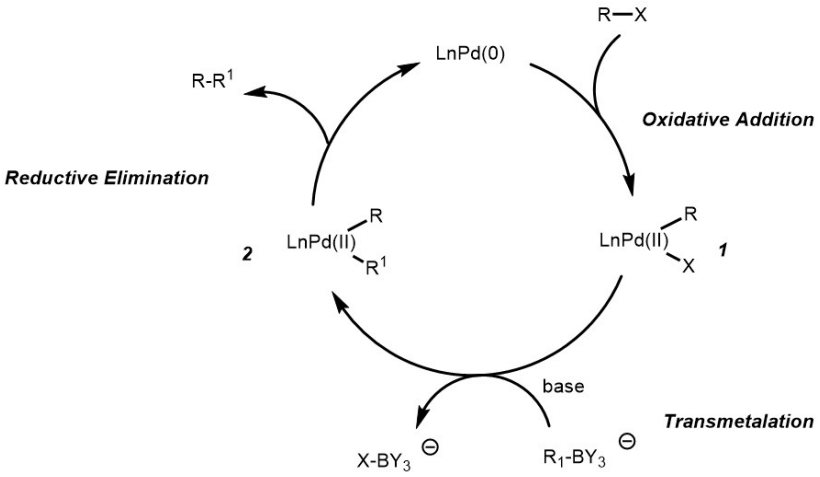


Figure 1: General catalytic cycle for Suzuki cross coupling reaction .

Oxidative addition is the rate determining step in the catalytic cycle and the relative reactivity decreases in the order of I > OTf > Br > Cl.[4a] The oxidative addition involving Pd(0) complexes is a S_N2-type mechanism based on the unambiguous evidence of stereochemical inversion of configuration at alkyl halides carbon.[5] Mechanistic studies have revealed that the apparently simple oxidative addition step consists of four concurrent isomerization pathways from the c*is* isomer, which is initially formed, to the more stable *trans* isomer (Figure 2).[6]

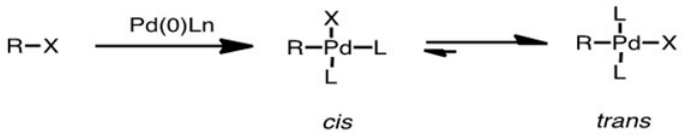


Figure 2: Isomerization from the cis isomer to trans isomer.

Transmetallation is initiated by base to encourage the transfer of the aryl or alkyl group from the organoborane to the Pd complex. The intermediates and stereochemistry of this step were determined by:

1. Low-temperature rapid injection nuclear magnetic resonance (NMR) spectroscopy & kinetic studies have recently revealed three different species containing palladium-oxygen-boron linkages were identified and characterized as the pre-transmetalation intermediates.

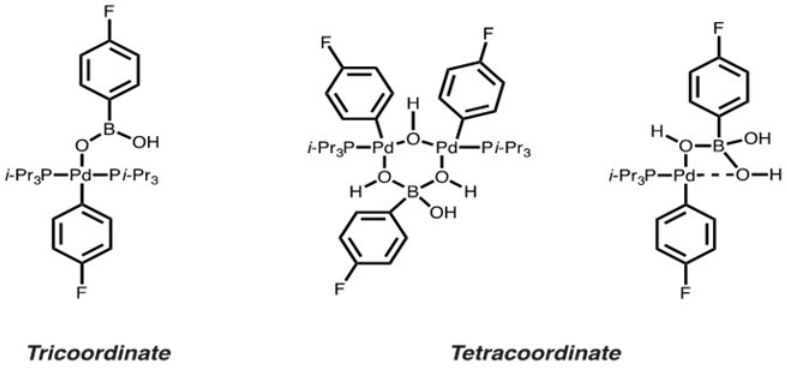


Figure 3: Three key pre-transmetalation intermediates that were identified.

2. Deuterium-labeling experiments demonstrated the retention of stereochemistry in the transmetalation step (*Figure 4*).[8] Here, smaller J-values (approximately 0-7 Hz) correspond to a syn configuration, and larger J-values (8-15 Hz) corresponds to the anti configuration.

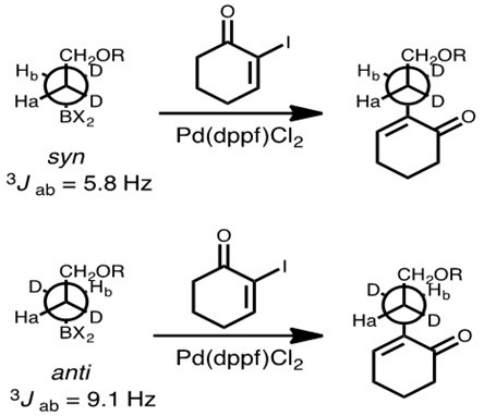


Figure 4: Newman analysis and deuterium-labeling experiment .

Reductive elimination occurs from the *cis* complex, therefore the *trans* complexes isomerizes to *cis* isomer to undergo reductive elimination.[9] The elimination was confirmed to proceed intramolecularly from the *cis* isomer[9] based on:

Kinetic studies showed that reductive elimination obeys first order kinetics, hence the rate and reaction is dependent only on the concentration of the post-transmetallation Pd-complex.

Deuterium labeling demonstrated no cross-coupling product from crossover between two Pd complexes (Figure 5).

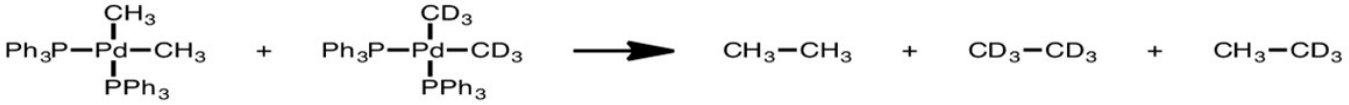


Figure 5: D-labeling experiments for reductive elimination.

References

1. (1) Miyaura, N.; Suzuki, A. *Chem. Rev.*, 1995, *95*, 2457.
2. (2) Barder, T. E.; Walker, S. D.; Martinelli, J. R.; Buchwald, S. L. *J. Am. Chem. Soc.* 2005, *127*, 4685.
3. (3) (a) Fitton, P.; Rick, E.A. *J. Organomet. Chem*. 1971, *28*, 287.
4. (b) Parshall, G. W. *J. Am. Chem. Soc*. 1974, *96*, 2360.
5. (4) Aliprantis, A. O.; Canary, J. W. *J. Am. Chem. Soc.* 1994, *116*, 6985.
6. (5) (a) Lau, K. S. Y.; Stille, J. K. *Acc. Chem. Res*.,1977, *10*, 434.
7. (b) Lau, K. S. Y.; Fries, R. W.; Stille, J. K. *J. Am. Chem. Soc.* 1974, *96*, 5956.
8. (6) Casado, A. L.; Espinet, P. *Organometallics*, 1998, *17*, 954.
9. (7) Thomas, A. A.; Denmark, S. E. *Science*, 2016, *352*, 329.
10. (8) Ridgway, B. H.; Woerpel, K. A. *J. Org. Chem*. 1998, *63*, 458.
11. (9) Gillie, A.; Stille, J. K. *J. Am. Chem. Soc*., 1980, *102*, 4933.

Catalysts

Palladium catalysts are most widely employed in Suzuki coupling. Normally, the active Pd catalyst consist of two parts: precursors (for example: $Pd(OAc)_2$, $Pd_2(dba)_3$, or $Pd(PPh_3)_4$) and ligands. To enhance the reactivity and stability of the catalyst, they were developed to be electron-rich and spatially bulky, which affords a high turnover number (TON) and low loading.[1,2] For example, palladacycles (Figure 4) were developed and exhibit thermal stability, robust reaction times, insensitivity to air and water, low cost, and environmentally friendly.[3,4]

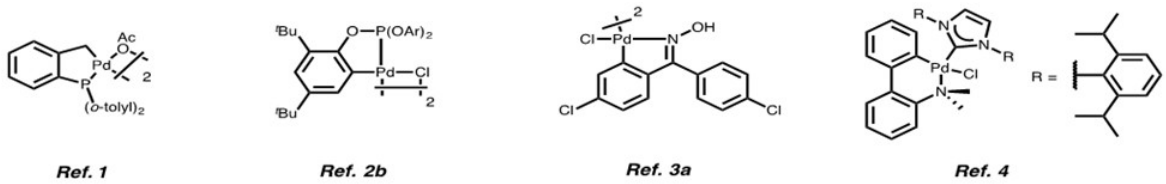


Figure 4: Representative palladacycle catalysts.

In terms of separation and recycling of the catalysts, people have developed polymer-supported heterogeneous catalysis systems for Suzuki coupling reaction.[5] Polymer-supported heterogeneous catalysis have tremendous values in pharmaceutical and industrial synthesis due to the advantage of preventing contamination from the ligand residue in products, fast recovery, and the simple recycling of the catalysts

References

1. (1) Beller, M.; Fischer, H.; Herrmann, W. A.; Ofele, K.; Brossmer, C. *Angew. Chem. Int. Ed.* 1995, *34*, 1848.
2. (2) (a) Welch, S. L.; Bedford, R. B. *Chem. Commun*., 2001, 129.
3. (b) Bedford, R. B. *et al*. *Chem. Eur. J.* 2003, *9*, 3216.
4. (3) (a) Alonso, D. A.; Na´jera, C.; Pacheco, M. C. *J. Org. Chem*. 2002, *67*, 5588.
5. (b) Botella, L.; Na´jera, C. *Angew. Chem. Int. Ed*. 2002, *41*, 179.
6. (4) Navarro, O.; Kelly, R. A.; Nolan, S. P. *J. Am. Chem. Soc*. 2003, *125*, 16194.
7. (5) (a) Kim, J. H.; Kim, J. K.; Shokouhimehr, M.; Lee, Y. S. *J. Org. Chem*. 2005, *70*, 6714.
8. (b) Nishio, R.; Sugiura, M.; Kobayashi, S. *Org. Lett.*, 2005, *7*, 4831.

Suzuki Cross Coupling Reaction Ligand Design

Since the 1980's, Suzuki reactions have been significantly improved, which lends to why the Suzuki reaction is so powerful: the elegant ligand design for Pd catalysts. Ligands are designed with electron-rich and spatially bulky features since electron-rich ligands can facilitate the oxidative addition step, and spatially bulky structures increase the orbital overlapping on the metal which enables reductive elimination.[1] Based on which atom is coordinated with the metal, ligands are categorized as *Phosphine ligands*, *Carbon ligands*, or *Nitrogen ligands*.

Phosphine ligands are the most popular Pd ligands in both the laboratory and industry. PPh_3 was the earliest and most widely use monodentate phosphine ligand[2] in Suzuki reactions. Inspired by the structure of PPh_3, scientists have manipulated substitutions on

the phosphor atom and aromatic ring to tune the different reactivity of the reaction. For example, Fu and other research groups[3] replaced aromatic groups with more electron-rich and bulkier alkyl groups (Figure 1), and the resulting ligands gave high catalytic reactivity on less reactive substrates with lower catalyst loading.

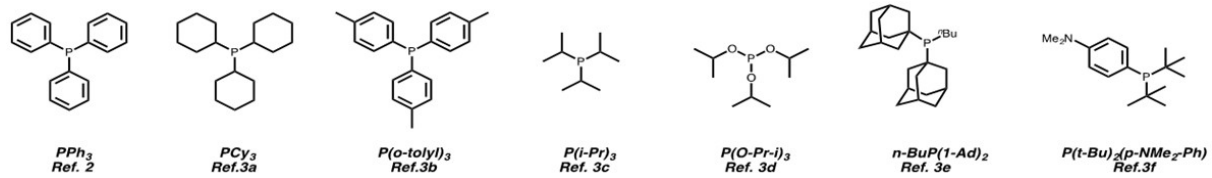


Figure 1: Representative monodentate phosphine ligands.[2,3]

In the late 1990's, Buchwald's group introduced new electronic rich and bulky phosphine ligands based on the frame skeleton of dialkylbiaryl phosphine ligands[4]. Understanding the impact of substitutions on dialkylbiarylphosphines on the efficacy of catalytic reactions, the Buchwald group has synthesized a series of dialkylbiaryl ligands facilitating Palladium-catalyzed C-C, C-N, and C-O bond-forming processes, as well as supporting ligands for other reactions.[4] There are other monodentate phosphine ligands with unique structures, which can also promote Suzuki reaction effectively, for example, monodentate ferrocene phosphine ligands.[5]

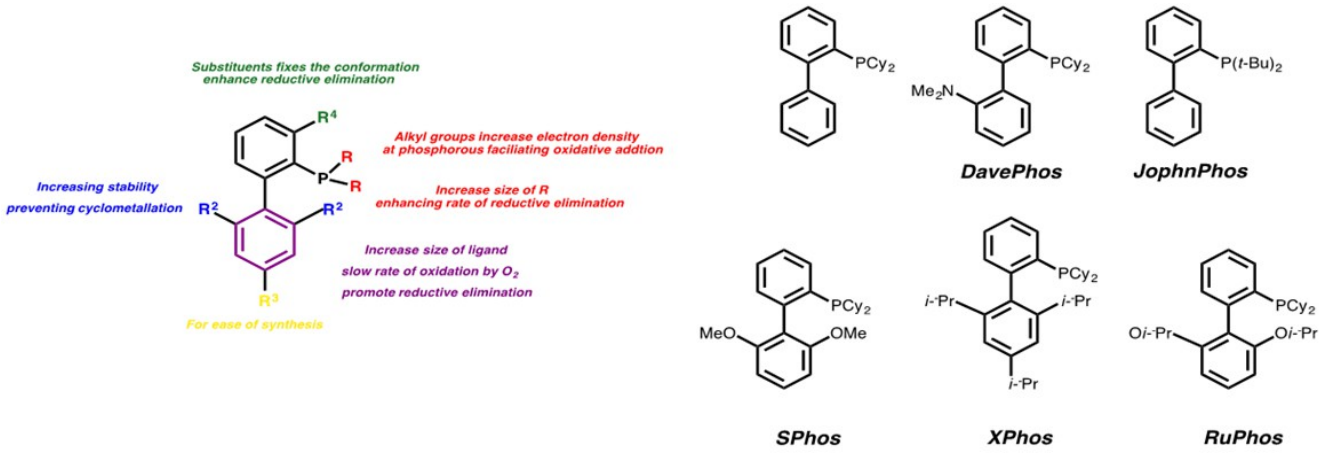


Figure 2: Designing principles and representative dialkylbiaryl ligands from Buchwald group.[4]

Many research groups have also designed and synthesized bidentate phosphine ligands (Figure 3) for the Suzuki reaction, and those ligands showed excellent reactivity on substrates that are generally challenging for monodentate ligands.

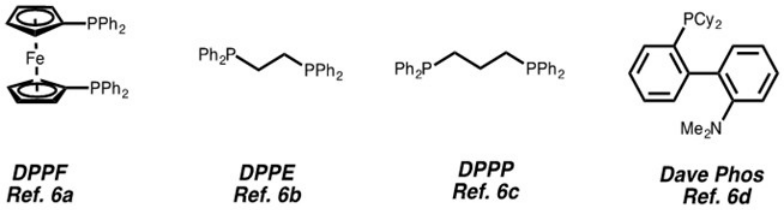


Figure 3: Representative bidentate phosphine ligands.

Carbon & Nitrogen ligands: Carbon ligands mainly comprise carbene[8]- and olefin[9]-type ligands for Suzuki couping. Efficient nitrogen ligands include amines and imines.[9]

References

1. Miyaura, N.; Suzuki, A. *Chem. Rev.*, 1995, *95*, 2457.
2. (a) Zhang, H.; Kwong, F. Y.; Tian, Y.; Chan, K. S. *J. Org. Chem.*, 1998, *63*, 6886.

(b) Sasaki, M.; Fuwa, H.; Ishkawa, M.; Tachibana, K. *Org. Lett.*, 1999, *1*, 1075.

(c) Kim, Y. M.; Yu, S. *J. Am. Chem. Soc*. 2003, *125*, 1696.

(3) (a) Netherton, M. R.; Dia, C.; Neuschutz, K.; Fu, G. C. *J. Am. Soc. Chem*. 2001, *123*, 10099.

(b) Dong, C. G.; Hu, Q. S. *J. Am. Soc. Chem*. 2005, *127*, 10006.

(c) Monteith, M. J. *Spec. Chem. Mag*. 1998, *18*, 436.

(d) Zapf, A.; Beller, M. *Chem. Eur. J*. 2000, *6*, 1830.

(e) Zapf, A.; Ehrentraut, A.; Beller, M. *Angew. Chem. Int. Ed*. 2000, *39*, 4153.

(f) Reider, P. *et al Org. Lett*. 2006, *78*, 1787.

(4) Martin, R.; Buchwald, S. L. *Acc. Chem. Res*., 2008, *41*, 1461.

(5) Liu, S. Y.; Choi, M. J.; Fu, G. C. *Chem. Commun*., 2001, 2408.

(6) (a) Kamatani, A.; Overman, E. *J. Org. Chem*. 1999, *64*, 8743.

(b) De, D.; Krogstad, D. J. *Org. Lett*. 2000, *2*, 879.

(c) Shen, W. *Tetrahedron Lett*. 1997, *38*, 5575.

(d) Old, D. W.; Wolf, J. P.; Buchwald, S. L. *J. Am. Soc. Chem*. 1998, *120*, 9722.

(7) Gstottmayr, C. W.; Bohm, V. P.; Herweck, E.; Grosche, M.; Herrmann, W. A. *Angew. Chem. Int. Ed*. 2002, *41*, 1363.

(8) Kuwano, R.; Yokogi, M. *Org. Lett*. 2005, *7*, 945.

(9) Tao, B.; Boykin, D. W. *J. Org. Chem*., 2004, *69*, 4330.

Suzuki Cross Coupling Reaction Substrate Scope

Electrophilic Partners[1]: The electrophilic partners in Suzuki coupling are: alkenyl, alkynyl, allyl, benzyl, aryl, and alkyl halides or triflates. Aryl halides are activated by electron-withdrawing (EWD) groups in the ortho or para positions or 1-alkenyl halides with EWD groups in the alpha or beta positions. This increases their reactivity in oxidative addition compared to those with electron-donating groups. The order of reactivity of the electrophilic partners based on their leaving groups is:

$$I >> Br > OTf >> Cl > F$$

Chloride electrophiles are the most nonreactive as they are reluctant to participate in oxidative addition. Reactivity with chloride electrophiles has been established by using bulky, electron-donating (electron rich) phosphine ligands on the Pd catalyst and stronger bases to encourage dissociation of Cl.[2]

β- alkyl Suzuki coupling is most successful between hindered electron-rich organoboranes and electron-deficient vinyl or aryl halides or triflates. This counters the trends reported above in that the electrophilic partner would be activated by EWD groups.

Bases[1]: Transmetallation is initiated with base, and it's reactivity varies with solvent.

Strong bases: NaOH, TlOH, and NaOMe perform optimally in THF or H_2O solvent systems

Thallium bases such as TlOH, and its derivatives Tl_2CO_3 and TlOEt, enable cross coupling between alkyl boranes and alkyl halides. It also allows this reaction to proceed at lower temperatures (20 ° C from the usual 50 to 80 ° C). Unfortunately, these bases are air and light sensitive, but are still widely used.[3]

Weak bases: K_2CO_3 and K_3PO_4 perform optimally in DMF

Catalysts: Pd*, Ni, Ru, Fe, Cu

Palladium catalysts are the most widely used for Suzuki coupling and perform best with electron-donating (usually phosphine) ligands.

Nickel catalysts have been recently developed and demonstrate reactivity with inert electrophiles, especially chlorides and unreactive bromides. They have also expanded the electrophile scope to include: aryl fluorides (using a directing group, usually *o*-NO_2), carbamates, sulfamates, esters, phosphate esters and ethers. This is enabled by nickel's variation in oxidation states (Ni^0 à Ni^{2+} and Ni^+ à Ni^{3+}) and increased nucleophilicity due to its small size. Use of Ni in catalysis is favored due to its abundance, and thus low cost.[4]

Boranes: Boronic acids, esters and tri-fluoro derivatives[1,2]

The reactivity of the borane to conduct transmetallation depends on its Lewis acidity. Therefore, EWD substituents increase the reactivity of the borane. The general trend of borane reactivity is:

$ArBF_3 > RB(OH)_2 > RB(OR)_2 >> R_3B$

Alkyl boranes are the least reactive, and rarely participate in transmetallation under standard conditions; however this has been amended with the use of stronger bases.

Selecting a borane for a reaction depends on its compatibility with its electrophile coupling partner and desired borane R group.

References:

1. Chemler, S. R.; Trauner, D.; Danishefsky, S. J. *Angew. Chem. Int. Ed.* 2001, *40* , 4544.
2. Suzuki, A. *Proc. Jpn. Acad., Ser. B.* 2004, *80*, 8, 359.
3. Molander, G. A.; Biolatto, B. *J. Org. Chem.* 2003, *68*, 4302.
4. Han, F. S. *Chem. Soc. Rev.* 2013, *42*, 5270.

Regio- and Stereoselectivity [1,2]

Each step of the catalytic cycle of Suzuki coupling can influence the regio- or stereo- configuration of the product. General rules of regio- and stereoselectivity relative to the substrates are:

Oxidative addition of *alkyl and alkenyl halides* retains the configuration of the electrophilic substrate, however *allylic and benzylic halides* invert this configuration. This step initially produces the *cis* complex which isomerizes to the *trans* complex.

Transmetallation and reductive elimination both retains the regio- and stereochemistry established in oxidative addition.

The borane substrate can also dictate selectivity of the cross coupling product. Often times the reactive borane species is formed *in situ* via hydroboration with 9-BBN. This occurs as a syn addition, and reductive elimination of the product retains the stereochemistry established by the hydroboration. However, reversing the order in which the reagents are added yields the anti addition product, which is also reflected in reductive elimination.

Chiral centers are formed by using chiral borane reagents. These reagents perform asymmetric cross coupling with retention of configuration i.e. (R) boranes yield (R) products, which follows suit for (S) boranes, in >90% enantiomeric excess.[3]

References:

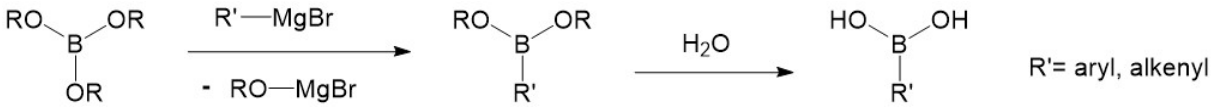
1. Suzuki, A. *Proc. Jpn. Acad., Ser. B.* 2004, *80*, 8, 359.
2. Chemler, S. R.; Trauner, D.; Danishefsky, S. J. *Angew. Chem. Int. Ed.* 2001, *40* , 4544.
3. Rybak, T.; Hall, D. G. *J. Am. Chem. Soc.* 2014, *136*, 6534.

Advantages of Suzuki Coupling

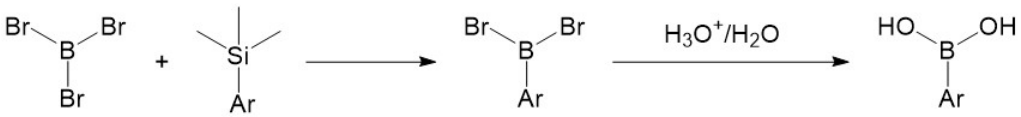
Borane Substrates: Easy to synthesize, stabile, nontoxic, and cost effective[1,2]

The ease of synthesizing boranes provides convenient access to substrates for Suzuki coupling at a low cost and with minimal health risks. The two common methods to synthesize boronic acids are:

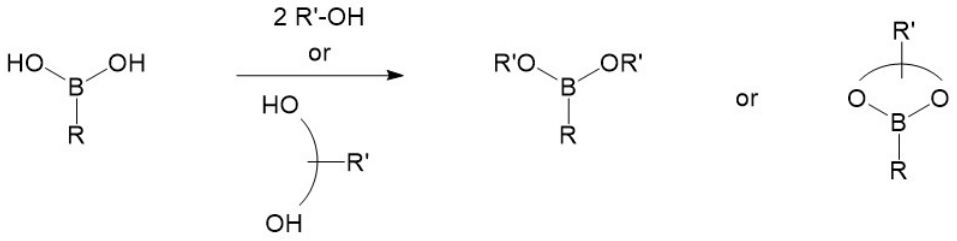
1. React lithium or magnesium Grignard reagents with borate esters, followed by hydrolysis.



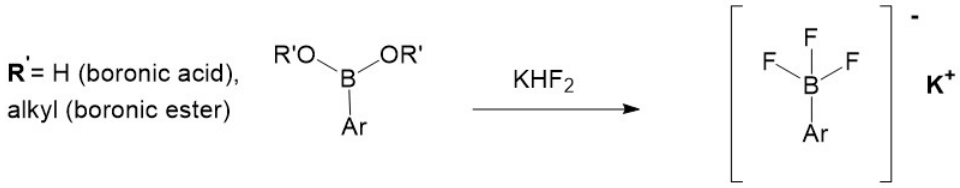
2. React arylsilanes with boron tribromide, followed by acid hydrolysis.



Boronic esters are synthesized from boronic acids using alcohols or diols, especially pinicol.



Aryl trifluoroborates are synthesized by subjecting the corresponding alkyl boronic acid or ester to excess KHF_2. Aryltrifluoroborates possess beneficial characteristics that allow for robust reactivity, easy purified, and reduced protodeboronation, which quenches the borane reagent.[3]



Reaction Conditions: Milder and Greener[1,2,4]

Typically, cross coupling reactions are run in organic conditions; however, Suzuki couplings can be performed in heterogeneous or purely aqueous conditions as organoboranes are water soluble and compatible with water soluble, inorganically supported, ligand-free Pd-catalysts. Boranes are exceptionally nucleophilic, and thus do not require extreme conditions for transmetallation which increases its functional group tolerance. Their high reactivity is also demonstrated in high turnover rates of the Pd catalyst used, which allows for a lower loading.

Organoboranes are nontoxic and stable to extreme heating and exposure to oxygen or water. Consequently, these reagents can be easily used at benchtop, and do not require special equipment or techniques, such as gloveboxes or air-sensitive and dry technique.[1] This reaction has a high atom economy seeing that the byproducts are typically salts and water soluble borane byproducts.[1,4] The lack of interfering byproducts allows for one-pot syntheses to further reduce waste and increase reaction efficiency.[4] These attractive features of organoborane reagents increases its utility and synthetic convenience, and makes Suzuki coupling optimal for large scale and industry synthesis.

References:

1. Suzuki, A. *Proc. Jpn. Acad., Ser. B.* 2004, *80*, 8, 359.
2. Chemler, S. R.; Trauner, D.; Danishefsky, S. J. *Angew. Chem. Int. Ed.* 2001, *40* , 4544.
3. Molander, G. A.; Biolatto, B. *J. Org. Chem.* 2003, *68*, 4302.
4. Paul, S.; Islam, M. M.; Islam, S. M. *RSC Adv.* 2015, *5*, 42193.

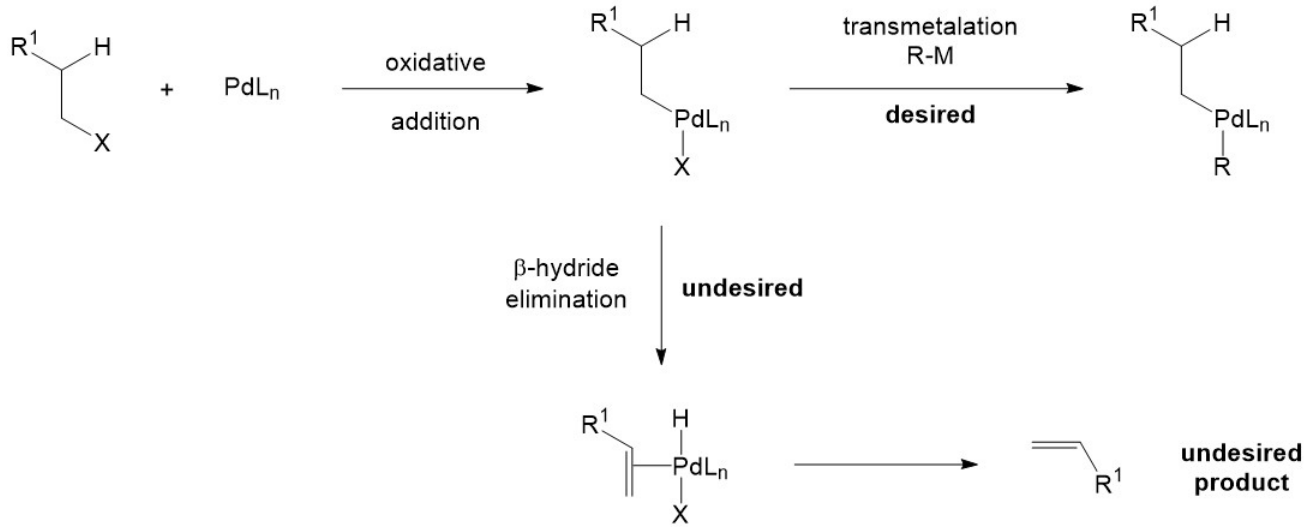
Limitations of Suzuki Coupling:

Issues with reactants:

- Borane substrates commercially available do not encompass all R groups desired
- Borane substrates are generally preinstalled to more complicated substrates synthesized in lab, which is often difficult
- Some alkyl borates (sp^3) and hetero- substrates don't show reactivity[1]
- Chloride substrates react slowly, and with lower yields[1]
- Without base there are many side products[1]

Side reactions:

Beta-hydride elimination competes with reductive elimination, which affords a side product that greatly reduces the yield. This is observed with reactants that have beta-hydrides, most commonly alkyl substrates, but sometimes can be avoided by using Ni catalysts or ligands with larger bite angles.[2]



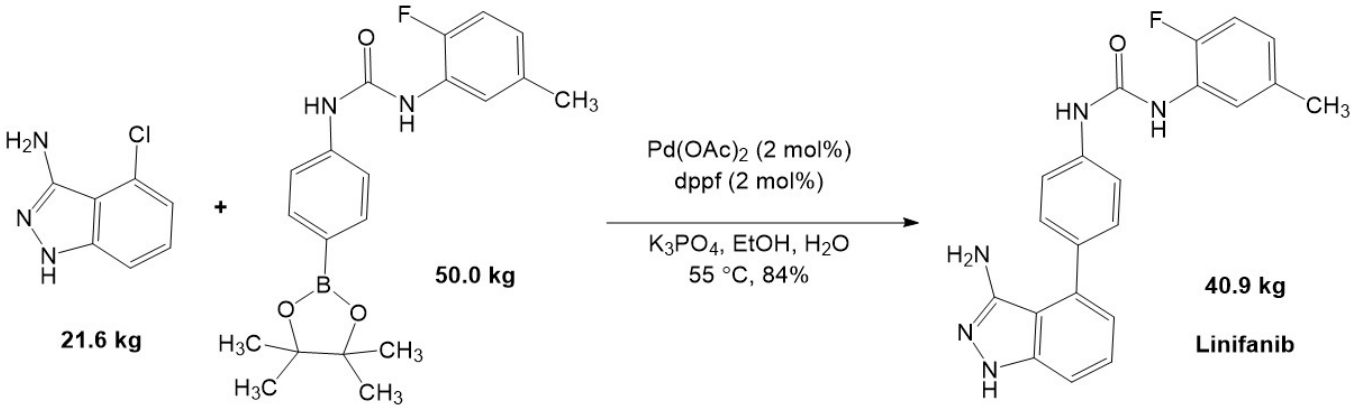
Scheme 1: B-hydride elimination in Suzuki cross coupling reaction.[2]

References:

1. Chemler, S. R.; Trauner, D.; Danishefsky, S. J. *Angew. Chem. Int. Ed.* 2001, *40* , 4544.
2. Netherton, M. R.; Dai, C.; Neuschutz, K.; Fu, G. C. *J. Am. Chem. Soc.* 2001, *123*, 41.

Synthetic Applications:

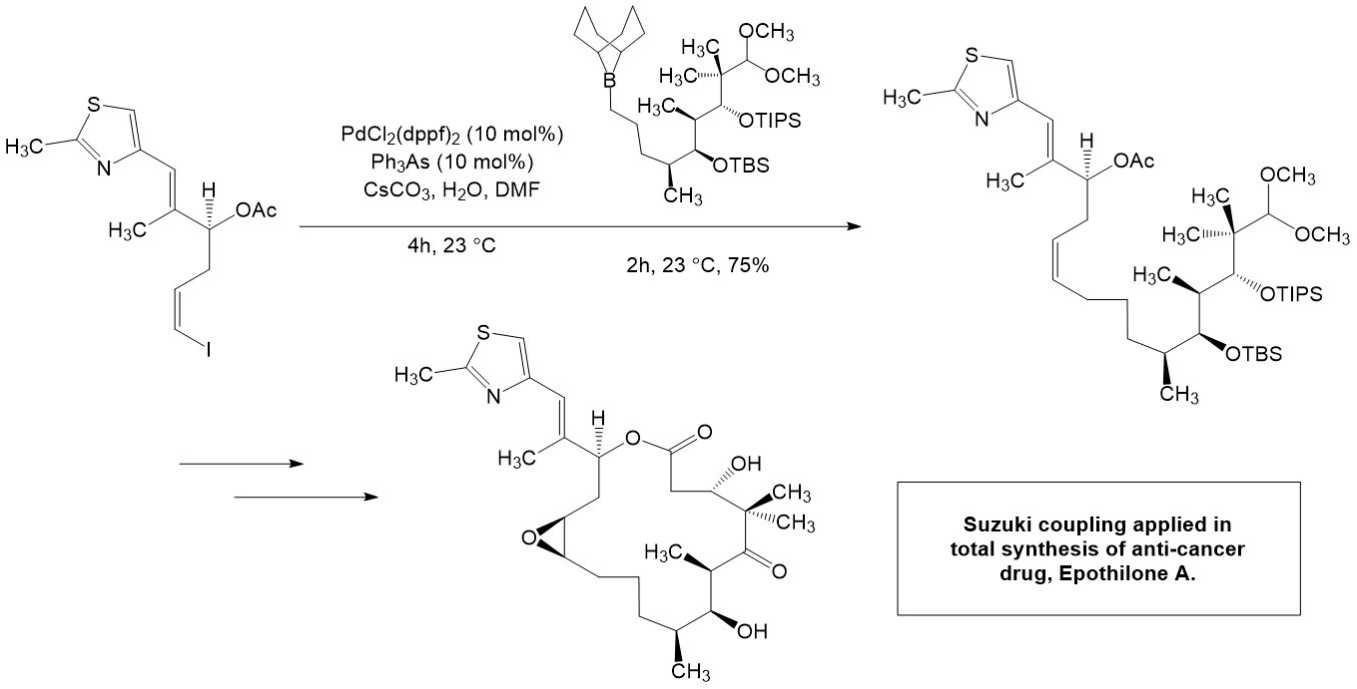
Large-scale, industry synthesis of medicinal drugs[1]



Scheme 1: Suzuki cross coupling reaction to synthesize the drug Linifanib .

Linifanib (Scheme 1) is a tyrosine kinase inhibitor that was FDA approved as an anti-cancer drug that is synthesized on kilogram scale in the presence of different functional groups using Suzuki coupling for its industry production.

Natural products synthesis[2]



Scheme 2: Suzuki cross coupling reaction application: Epothilone total synthesis.

Suzuki coupling in the total synthesis of Epothilone A (Figure 2) was successful in the presence of numerous stereocenters and functional groups.

Polymer synthesis: Suzuki Polycondensation (SPC)[3]

Suzuki coupling has been applied to create polymers of aromatic groups, which yielded the longest conjugated chains. These polymers are categorized by their properties and applications:

(a) Polymers with alkyl or alkoxy chains and (c) Polyelectrolytes: SPC yields poly(*p*-phenylene)'s (PPP's) which are used in LED lights

(b) Amphiphilic PPPs: SPC produces colloidal structures to create rechargeable, solid state lithium batteries

(d) PPP precursors for ladder polymers: currently being developed to apply their thermal, electrical, and optical properties to conducting materials, energy sources, and instrumentation

(e) Polymers with main-chain chirality and (f) Dendronized PPPs: used in organic synthesis of optically pure compounds

(g) Poly(arylene vinylene)'s and poly(arylene ethinylene)'s: Photoluminescence (*PL*) and electroluminescence (*EL*) characteristics for materials and instrumentation

(h) Various polymers: functionalization in synthesis via radical mechanism

References:

1. Meng, D.; Bertinato, P.; Balog, A.; Su, D.; Kamenecka, T.; Sorensen, E. J.; Danishefsky, S., J. *J. Am. Chem. Soc.* 1997, 119, 10073.
2. Kruger, A. W.; Rozema, M. J.; Chu-Kung, A.; Gandarilla, J.; Haight, A. R.; Kotecki, B. J.; Richter, S. M.; Schwartz, A. M.; Wang, Z. *Org. Proc. Res. Dev*. 2009, 13, 1419.
3. Schluter, A. D. *J. Polym. Sci. Part A: Polym. Chem*. 2001, *39*, 1533.

8.5: Suzuki-Miyara Coupling is shared under a CC BY-NC-SA 4.0 license and was authored, remixed, and/or curated by Peiyuan Qu & Amanda Ramdular.

- **Suzuki-Miyaura Coupling** by Amanda Ramdular, Peiyuan Qu is licensed CC BY-NC-SA 4.0.

CHAPTER OVERVIEW

9: Why is Cisplatin "King of the Chemotherapeutic Drugs?"

9.1: Jahn-Teller Distortions

9.2: d8 Low-Spin Preference for Square Planar Geometry

9.3: Trans Effect

9.4: Cisplatin Discovery and Mode of Action

9: Why is Cisplatin "King of the Chemotherapeutic Drugs?" is shared under a not declared license and was authored, remixed, and/or curated by LibreTexts.

9.1: Jahn-Teller Distortions

The Jahn-Teller effect is a geometric distortion of a non-linear molecular system that reduces its symmetry and energy. This distortion is typically observed among octahedral complexes where the two axial bonds can be shorter or longer than those of the equatorial bonds. This effect can also be observed in tetrahedral compounds. This effect is dependent on the electronic state of the system.

Introduction

In 1937, Hermann Jahn and Edward Teller postulated a theorem stating that "stability and degeneracy are not possible simultaneously unless the molecule is a linear one," in regards to its electronic state.[1] This leads to a break in degeneracy which stabilizes the molecule and by consequence, reduces its symmetry. Since 1937, the theorem has been revised which Housecroft and Sharpe have eloquently phrased as "any non-linear molecular system in a degenerate electronic state will be unstable and will undergo distortion to form a system of lower symmetry and lower energy, thereby removing the degeneracy."[2] This is most commonly observed with transition metal octahedral complexes, however, it can be observed in tetrahedral compounds as well.

For a given octahedral complex, the five d atomic orbitals are split into two degenerate sets when constructing a molecular orbital diagram. These are represented by the sets' symmetry labels: t_{2g} (d_{xz}, d_{yz}, d_{xy}) and e_g (d_{z^2} and $d_{x^2-y^2}$). When a molecule possesses a degenerate electronic ground state, it will distort to remove the degeneracy and form a lower energy (and by consequence, lower symmetry) system. The octahedral complex will either elongate or compress the z ligand bonds as shown in Figure **9.1.1** below:

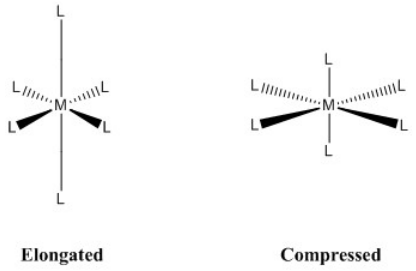


Figure **9.1.1**: Jahn-Teller distortions for an octahedral complex.

When an octahedral complex exhibits elongation, the axial bonds are longer than the equatorial bonds. For a compression, it is the reverse; the equatorial bonds are longer than the axial bonds. Elongation and compression effects are dictated by the amount of overlap between the metal and ligand orbitals. Thus, this distortion varies greatly depending on the type of metal and ligands. In general, the stronger the metal-ligand orbital interactions are, the greater the chance for a Jahn-Teller effect to be observed.

Elongation

Elongation Jahn-Teller distortions occur when the degeneracy is broken by the stabilization (lowering in energy) of the d orbitals with a *z* component, while the orbitals without a *z* component are destabilized (higher in energy) as shown in Figure **9.1.2** below:

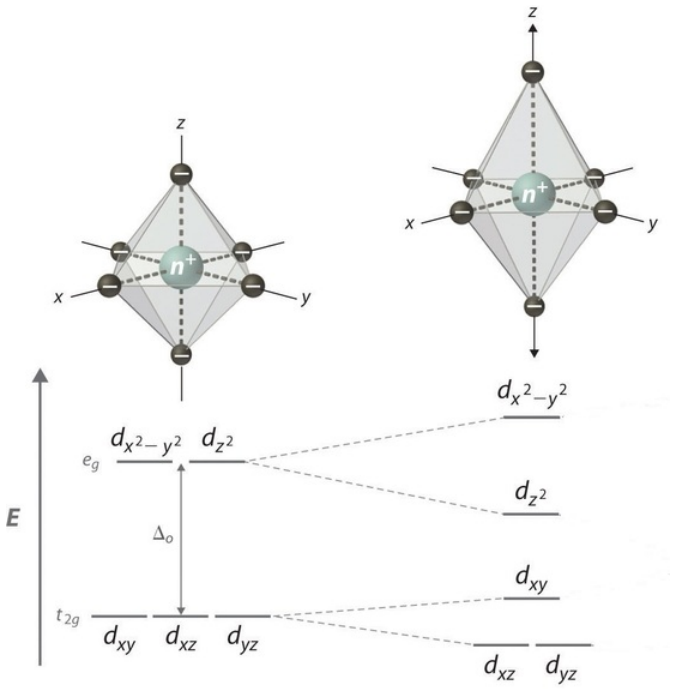


Figure **9.1.2**: Illustration of tetragonal distortion (elongation) for an octahedral complex.

This is due to the d_{xy} and $d_{x^2-y^2}$ orbitals having greater overlap with the ligand orbitals, resulting in the orbitals being higher in energy. Since the $d_{x^2-y^2}$ orbital is antibonding, it is expected to increase in energy due to elongation. The d_{xy} orbital is still nonbonding, but is destabilized due to the interactions. Jahn-Teller elongations are well-documented for copper(II) octahedral compounds. A classic example is that of copper(II) fluoride as shown in Figure **9.1.3**.

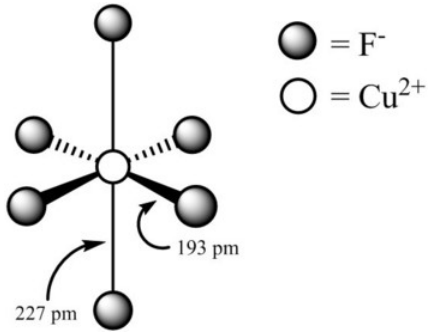


Figure **9.1.3**: Structure of octahedral copper(II) fluoride.[3]

Notice that the two axial bonds are both elongated and the four shorter equatorial bonds are the same length as each other. According the theorem, the orbital degeneracy is eliminated by distortion, making the molecule more stable based on the model presented in Figure **9.1.2**.

Compression

Compression Jahn-Teller distortions occur when the degeneracy is broken by the stabilization (lowering in energy) of the d orbitals *without* a *z* component, while the orbitals with a *z* component are destabilized (higher in energy) as shown in Figure **9.1.4** below:

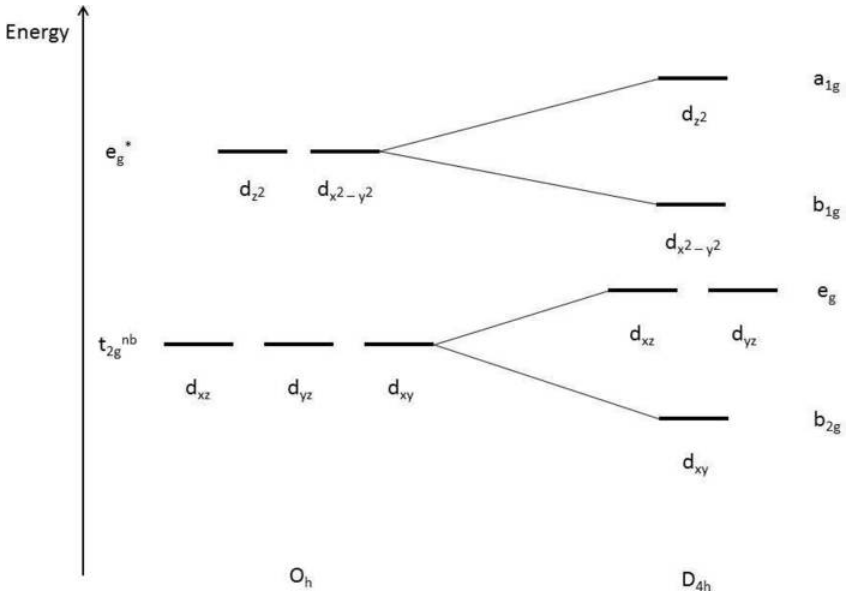


Figure **9.1.4**: Illustration of tetragonal distortion (compression) for an octahedral complex.

This is due to the *z*-component d orbitals having greater overlap with the ligand orbitals, resulting in the orbitals being higher in energy. Since the d_{z^2} orbital is antibonding, it is expected to increase in energy due to compression. The d_{xz} and d_{yz} orbitals are still nonbonding, but are destabilized due to the interactions.

Electronic Configurations

For Jahn-Teller effects to occur in transition metals there must be degeneracy in either the t_{2g} or e_g orbitals. The electronic states of octahedral complexes depend on the number of d-electrons and the splitting energy, **Δ**. When **Δ** is large and is greater than the energy required to pair electrons, electrons pair in t_{2g} before occupying e_g. On the other hand, when ***Delta*** small and is less than the pairing energy, electrons will occupy e_g before pairing in t_{2g}. The **Δ** of an octahedral complex is dictated by the chemical environment (ligand identity), and the identity and charge of the metal ion. If there electron configurations for any d-electron count is different depending on **Δ**, the configuration with more paired electrons is called low spin while the one with more unpaired electrons is called high spin.

The electron configurations diagrams for d1 through d10 with large and small ***δ*** are illustrated in the figures below. Notice that the electron configurations for d^1, d^2, d^3, d^8, d^9, and d^{10} are the same no matter what the magnitude of **Δ**. Low spin and high spin configurations exist only for the electron counts d^4, d^5, d^6, and d^7.

Large Δ

Figure **9.1.5** (below) shows the various electronic configurations for octahedral complexes with large **Δ**, including the low-spin configurations of d^4, d^5, d^6, and d^7:

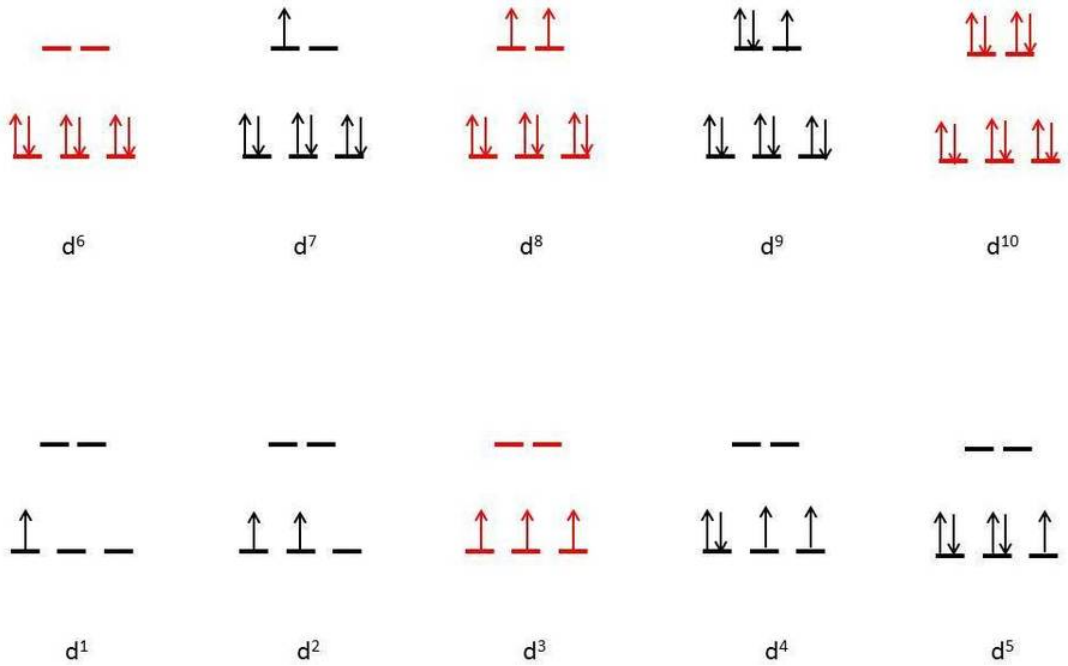


Figure 9.1.5: Electron configuration diagram of octahedral complexes (red indicates no degeneracies possible, thus no Jahn-Teller effects).

The figure illustrates the electron configurations in the case of large **Δ**. The electron configurations highlighted in red (d^3, low spin d^6, d^8, and d^{10}) **do not** exhibit Jahn-Teller distortions. On the other hand d^1, d^2, low spin d^4, low spin d^5, low spin d^7, and d^9, would be expected to exhibit Jhan-Teller distortion. These electronic configurations correspond to a variety of transition metals. Some common examples include Cr^{3+}, Co^{3+}, and Ni^{2+}.

Small Δ

Figure 9.1.6 (below) shows the various electronic configurations for octahedral complexes with small **Δ**, including the high-spin configurations of d^4, d^5, d^6, and d^7::

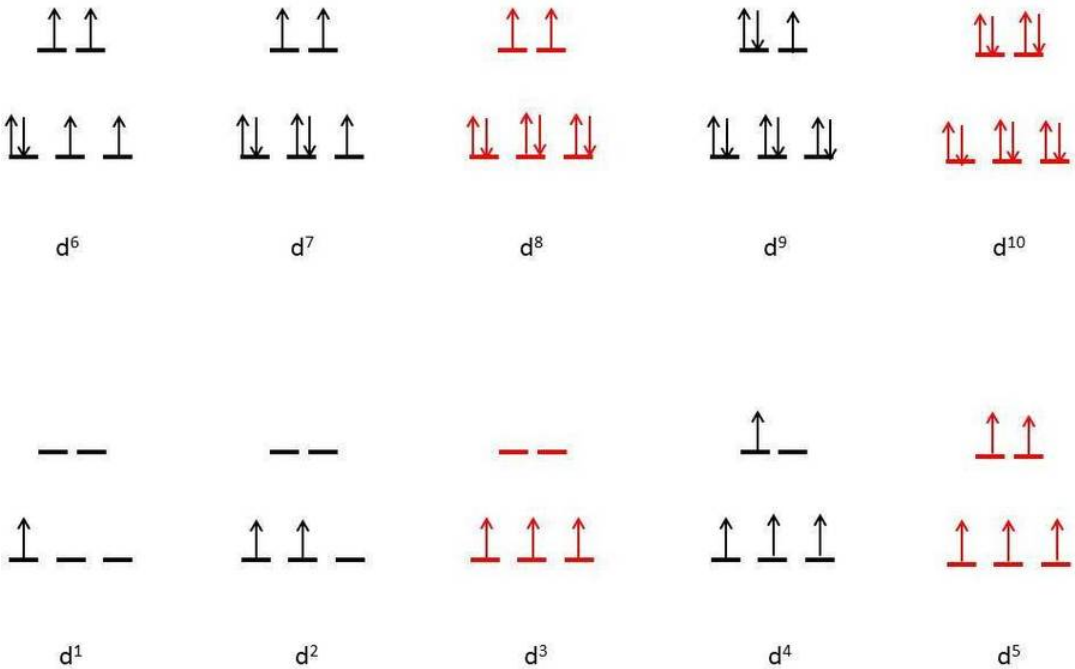


Figure 9.1.6: High spin octahedral coordination diagram (red indicates no degeneracies possible, thus no Jahn-Teller effects).

The figure illustrates the electron configurations in the case of small Δ. The electron configurations highlighted in red (d^3, high spin d^5, d^8, and d^{10}) **do not** exhibit Jahn-Teller distortions. In general, degenerate electronic states occupying the e_g orbital set tend to show stronger Jahn-Teller effects. This is primarily caused by the occupation of these high energy orbitals. Since the system is more stable with a lower energy configuration, the degeneracy of the e_g set is broken, the symmetry is reduced, and occupations at lower energy orbitals occur.

Spectroscopic Observation

Jahn-Teller distortions can be observed using a variety of spectroscopic techniques. In UV-VIS absorption spectroscopy, distortion causes splitting of bands in the spectrum due to a reduction in symmetry (O_h to D_{4h}). Consider a hypothetical molecule with octahedral symmetry showing a single absorption band. If the molecule were to undergo Jahn-Teller distortion, the number of bands would increase as shown in Figure **9.1.7** below:

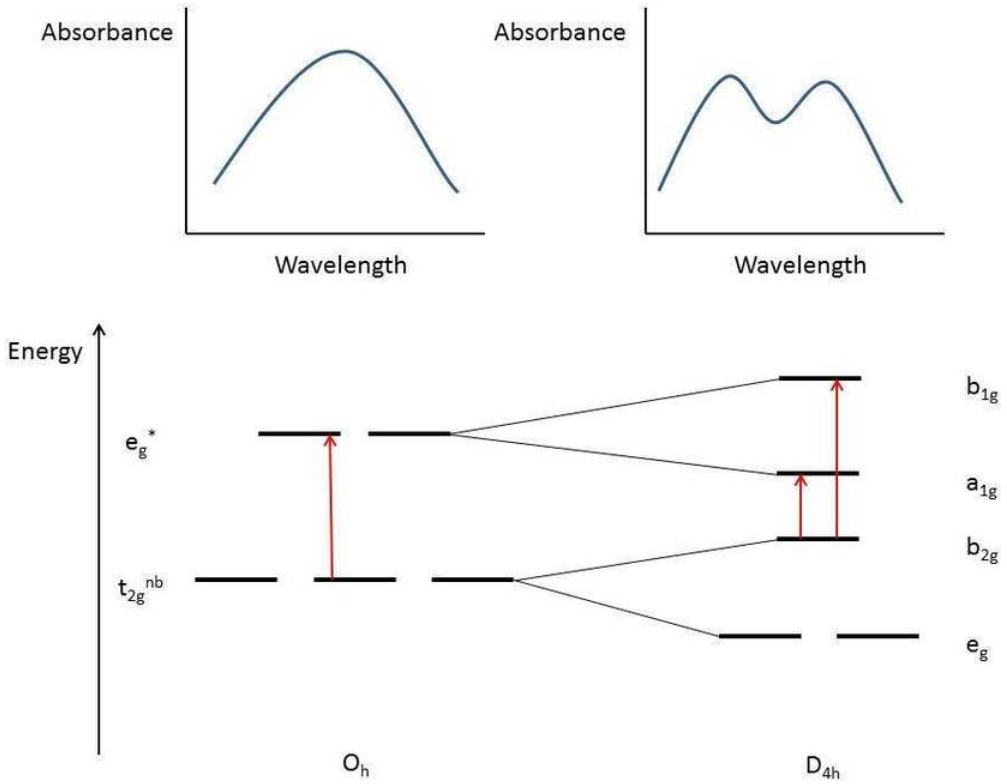


Figure **9.1.7**: Hypothetical absorption spectra of an octahedral molecule (left) and the same molecule with Jahn-Teller elongation (right). The red arrows indicate electronic transitions.

A similar phenomenon can be seen with IR and Raman vibrational spectroscopy. The number of vibrational modes for a molecule can be calculated using the 3n - 6 rule (or 3n - 5 for linear geometry) rule. If a molecule exhibits an O_h symmetry point group, it will have fewer bands than that of a Jahn-Teller distorted molecule with D_{4h} symmetry. Thus, one could observe Jahn-Teller effects through either IR or Raman techniques. This effect can also be observed in EPR experiments as long as there is at least one unpaired electron.

Table **9.1.1**: Examples of Jahn-Teller distorted complexes

$CuBr_2$	4 Br at 240 pm 2 Br at 318 pm
$CuCl_2$	4 Cl at 230 pm 2 Cl at 295 pm
$CuCl_2.2H_2O$	2 O at 193 pm 2 Cl at 228 pm 2 Cl at 295 pm
$CsCuCl_3$	4 Cl at 230 pm 2 Cl at 265 pm
CuF_2	4 F at 193 pm 2 F at 227 pm
$CuSO_4.4NH_3.H_2O$	4 N at 205 pm 1 O at 259 pm 1 O at 337 pm
K_2CuF_4	4 F at 191 pm 2 F at 237 pm
$KCuAlF_6$	2 F at 188 pm 4 F at 220 pm
CrF_2	4 F at 200 pm 2 F at 243 pm
$KCrF_3$	4 F at 214 pm 2 F at 200 pm
MnF_3	2 F at 209 pm 2 F at 191 pm 2 F at 179 pm

The Jahn-Teller Theorem predicts that distortions should occur for *any degenerate state*, including degeneracy of the t_{2g} level, however distortions in bond lengths are much more distinctive when the degenerate electrons are in the e_g level.

References

1. Jahn, H. A.; Teller, E. *Proc. R. Soc. London A*, **1937**, *161*, 220-235. DOI: 10.1098/rspa.1937.0142
2. Housecroft, C.; Sharpe, A. G. *Inorganic Chemistry*. Prentice Hall, 3rd Ed., 2008, p. 644. ISBN: 978-0-13-175553-6
3. Billy, C.; Haendler, H. A. *J. Am. Chem. Soc.*, **1957**, *79*, 1049–1051. DOI: 10.1021/ja01562a011

References

- Janes, R.; Moore, E. A. *Metal-ligand bonding*. The Open University, 2004, p. 23. ISBN 0-85404-979-7
- P.T.Miller, P.G.Lenhert and M.D.Joesten, *Inorg. Chem.*, 11, 2221, 1972.
- J.S.Wood, C.P.Keijzers and R.O.Day, *Acta Crystallogr., Sect.C (Cr. Str. Comm.)*, 40, 404, 1984.
- M.D.Joesten, M.S.Hussain and P.G.Lenhert, *Inorg. Chem.*, 9, 151, 1970.

Practice Questions

1. Why do d^3 complexes not show Jahn-Teller distortions?
2. Does the spin system (high spin v. low spin) of a molecule play a role in Jahn-Teller effects?
3. What spectroscopic method would one utilize in order to observe Jahn-Teller distortions in a diamagnetic molecule?
4. What spectroscopic method(s) would one utilize in order to observe Jahn-Teller distortions in a paramagnetic molecule?
5. Why are Jahn-Teller effects most prevalent in inorganic (transition metal) compounds?

Answers

1. Complexes with d^3 electron configurations do not show Jahn-Teller distortions because there is no ground state degeneracy.
2. Yes. Examining the d^5 electron configuration, one finds that the high spin scenario contains all singly occupied d orbitals (no degeneracy). However, the low spin d^5 electron configuration shows degeneracy, which then leads to possible Jahn-Teller effects.
3. UV-VIS absorption spectroscopy is one of the most common techniques for observing these effects. In general, it is independent of magnetism (diamagnetic v. paramagnetic). Thus, one would see the effect in the spectrum of UV-VIS absorption analysis. Note that EPR requires at least one unpaired electron, and therefore not EPR active.
4. Inorganic, specifically transition metal, complexes are most prevalent in showing Jahn-Teller distortions due to the availability of d orbitals. The most common geometry that the Jahn-Teller effect is observed is in octahedral complexes (see **Figures 2, 4, 5** and **6** above) due to the splitting of d orbitals into two degenerate sets. Due to stabilization, the degeneracies are removed, making a lower symmetry and lower energy molecule.

5. In addition to UV-VIS absorption, one can also employ EPR spectroscopy if a molecule possesses and unpaired electron.

Contributors and Attributions

- Kamran Ghiassi (UC Davis)
- Prof. Robert J. Lancashire (The Department of Chemistry, University of the West Indies)

9.1: Jahn-Teller Distortions is shared under a not declared license and was authored, remixed, and/or curated by LibreTexts.

- **Jahn-Teller Distortions** is licensed CC BY-NC-SA 4.0.

9.2: d8 Low-Spin Preference for Square Planar Geometry

Learning Objectives

- Discuss the d-orbital degeneracy of square planar and tetrahedral metal complexes.

Tetrahedral Geometry

Tetrahedral geometry is a bit harder to visualize than square planar geometry. Tetrahedral geometry is analogous to a pyramid, where each of corners of the pyramid corresponds to a ligand, and the central molecule is in the middle of the pyramid. This geometry also has a coordination number of 4 because it has 4 ligands bound to it. Finally, the bond angle between the ligands is 109.5^{o}. An example of the tetrahedral molecule $\mathbf{CH_4}$, or methane.

In a tetrahedral complex, $\mathbf{\Delta_t}$ is relatively small even with strong-field ligands as there are fewer ligands to bond with. It is rare for the $\mathbf{\Delta_t}$ of tetrahedral complexes to exceed the pairing energy. Usually, electrons will move up to the higher energy orbitals rather than pair. Because of this, *most tetrahedral complexes are high spin.*

Square Planar Complexes

In square planar molecular geometry, a central atom is surrounded by constituent atoms, which form the corners of a square on the same plane. The geometry is prevalent for transition metal complexes with d^8 configuration. This includes Rh(I), Ir(I), Pd(II), Pt(II), and Au(III). Notable examples include the anticancer drugs cisplatin ($\mathbf{PtCl_2(NH_3)_2}$).

A square planar complex also has a coordination number of 4. The structure of the complex differs from tetrahedral because the ligands form a simple square on the x and y axes. Because of this, the crystal field splitting is also different (Figure **9.2.1**). Since there are no ligands along the z-axis in a square planar complex, the repulsion of electrons in the $\boldsymbol{d_{xz}}$, $\boldsymbol{d_{yz}}$, and the $\boldsymbol{d_{z^2}}$ orbitals are considerably lower than that of the octahedral complex (the $\boldsymbol{d_{z^2}}$ orbital is slightly higher in energy to the "doughnut" that lies on the x,y axis). The $\boldsymbol{d_{x^2-y^2}}$ orbital has the most energy, followed by the $\boldsymbol{d_{xy}}$ orbital, which is followed by the remaining orbtails (although $\boldsymbol{d_{z^2}}$ has slightly more energy than the $\boldsymbol{d_{xz}}$ and $\boldsymbol{d_{yz}}$ orbital). This pattern of orbital splitting remains constant throughout all geometries. Whichever orbitals come in direct contact with the ligand fields will have higher energies than orbitals that slide past the ligand field and have more of indirect contact with the ligand fields. So when confused about which geometry leads to which splitting, think about the way the ligand fields interact with the electron orbitals of the central atom.

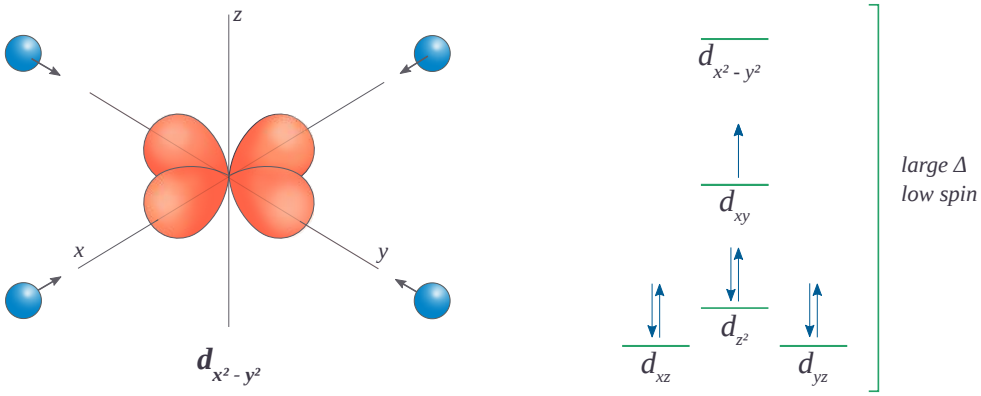


Figure **9.2.1**: In square planar complexes Δ will almost always be large, even with a weak-field ligand. Electrons tend to be paired rather than unpaired because paring energy is usually much less than Δ. Therefore, square planar complexes are usually low spin. (CC BY-SA; Ümit Kaya)

In square planar complexes $\mathbf{\Delta}$ will almost always be large (Figure **9.2.1**), even with a weak-field ligand. Electrons tend to be paired rather than unpaired because paring energy is usually much less than $\mathbf{\Delta}$. Therefore, *square planar complexes are usually low spin.*

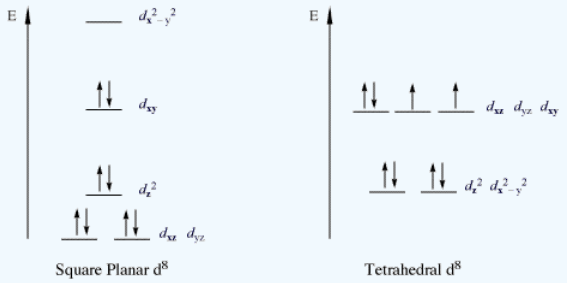
Advanced: $[PdCl_4]^{2-}$ is square planar and $[NiCl_4]^{2-}$ is tetrahedral

The molecule $[PdCl_4]^{2-}$ is diamagnetic, which indicates a square planar geometry as all eight d-electrons are paired in the lower-energy orbitals. However, $[NiCl_4]^{2-}$ is also d^8 but has two unpaired electrons, indicating a tetrahedral geometry. Why is $[PdCl_4]^{2-}$ square planar if Cl^- is not a strong-field ligand?

Solution

The geometry of the complex changes going from $[NiCl_4]^{2-}$ to $[PdCl_4]^{2-}$. Clearly this cannot be due to any change in the ligand since it is the same in both cases. It is the other factor, the metal, that leads to the difference.

Consider the splitting of the d-orbitals in a generic d^8 complex. If it were to adopt a square planar geometry, the electrons will be stabilized (with respect to a tetrahedral complex) as they are placed in orbitals of lower energy. However, this comes at a cost: two of the electrons, which were originally unpaired in the tetrahedral structure, are now paired in the square-planer structure:



Square Planar d^8 Tetrahedral d^8

We can label these two factors as ΔE (stabilization derived from occupation of lower-energy orbitals) and P (spin pairing energy) respectively. One can see that:

- If $\Delta E > P$, then the complex will be square planar
- If $\Delta E < P$, then the complex will be tetrahedral.

This is analogous to deciding whether an octahedral complex adopts a high- or low-spin configuration; where the crystal field splitting parameter Δ_o ΔE does above. Unfortunately, unlike Δ_o in octahedral complexes, there is no simple graphical way to represent ΔE on the diagram above since multiple orbitals are changed in energy between the two geometries.

Interpreting the origin of metal-dependent stabilization energies can be tricky. However, we know experimentally that Pd^{2+} has a larger splitting of the d-orbitals and hence a larger ΔE than Ni^{2+} (moreover P is also smaller).

Practically all 4d and 5d d^8 ML_4 complexes adopt a square planar geometry, irrespective if the ligands are strong-field ligand or not. Other examples of such square planar complexes are $[PtCl_4]^{2-}$ and $[AuCl_4]^-$.

Summary

- In tetrahedral molecular geometry, a central atom is located at the center of four substituents, which form the corners of a tetrahedron.
- Tetrahedral geometry is common for complexes where the metal has d^0 or d^{10}electron configuration.
- The CFT diagram for tetrahedral complexes has $d_{x^2-y^2}$ and d_{z^2} orbitals equally low in energy because they are between the ligand axis and experience little repulsion.
- In square planar molecular geometry, a central atom is surrounded by constituent atoms, which form the corners of a square on the same plane.
- The square planar geometry is prevalent for transition metal complexes with d^8 configuration.
- The CFT diagram for square planar complexes can be derived from octahedral complexes yet the dx2-y2 level is the most destabilized and is left unfilled.

Contributors and Attributions

- Angad Oberoi (UCD), Justin Nuckles (UCD)
- StackExchange (orthocresol)

9.2: d8 Low-Spin Preference for Square Planar Geometry is shared under a CC BY license and was authored, remixed, and/or curated by LibreTexts.

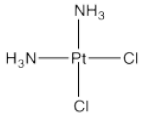
- **Tetrahedral vs. Square Planar Complexes** is licensed CC BY 4.0.

9.3: Trans Effect

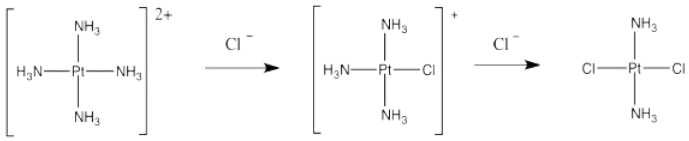
Occasionally in ligand substitution there is a situation in which there are two identical ligands that could be replaced, but two different products would result depending on which ligand left. This situation often happens in square planar complexes, for example. Replacement of one ligand would lead to a *cis* product. Replacement of the other one would lead to a *trans* product.



An important example of this issue is in the synthesis of cis-platin, an antitumour medication frequently used to treat ovarian and testicular cancer.

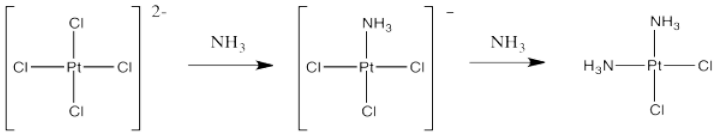


Cis-platin could be made from treatment of tetraammineplatinum(II) with chloride salts. The chloride ion could replace two of the ammonia ligands.



But that doesn't work. That synthesis results in the formation of *trans*-platin, a compound that has all of the nasty side effects of the *cis* isomer but with none of the therapeautic benefit.

If instead you were to start with tetrachloroplatinate salts and treat them with ammonia, you could replace two of the chloride ligands. That works really well, and it provides *cis*-platin, not *trans*-platin.



? Exercise 9.3.1

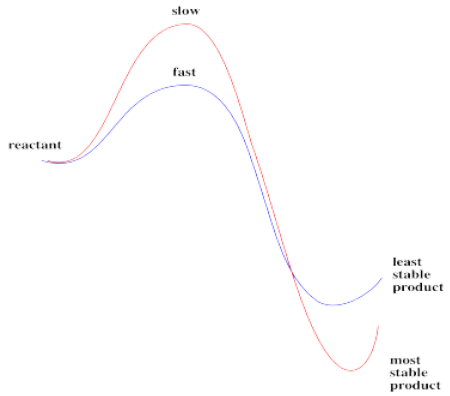
What do you think is the mechanism of substitution of the two reactions above? Why?

Answer

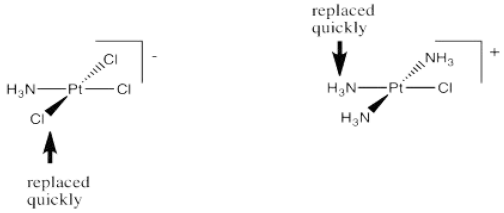
This is probably an associative mechanism because of the square planar geometry.

This reaction, if run under these conditions, is clearly not always under thermodynamic control. Two different products result, depending on how the reaction is done. One of those isomers is probably more stable than the other; if thermodynamics were in charge, it would form the same thing both times.

Instead, there may be an element of kinetic control for at least one of the pathways. A given product might be made, not because it is more stable, but simply because it forms more quickly than the other one.



Take another look at those two reactions. One of the things that they have in common is that the ligand that gets replaced is *trans* to a chloride. It is not *trans* to an ammonia. Maybe the other ligands in the complex can influence how quickly one ligand can leave.



Specifically, the "*trans* effect" is the role of *trans*-ligands in influencing substitution rates in square planar complexes.

The following kinetic data were obtained for substitutions on square planar platinum complexes, in the reaction:

$$trans-(PEt_3)_2PtLCl + py \rightarrow trans-(PEt_3)_2PtLpy^+ + Cl^-$$

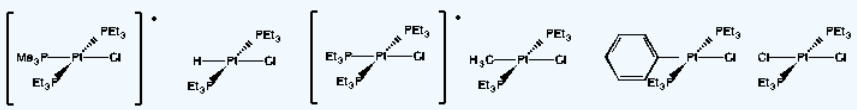
L	k_{obs} (s^{-1})	T, °C
PMe_3	0.20	0
H^-	0.047	0
PEt_3	0.041	0
CH_3^-	6.0×10^{-4}	25
$C_6H_5^-$	1.2×10^{-4}	25
Cl^-	3.5×10^{-6}	25

Ref: Cooper Langford & Harry Gray, *Ligand Substitution Processes*, W.A. Benjamin, NY, 1965, p. 25.

? Exercise 9.3.2

Draw structures for each of the complexes listed in the table.

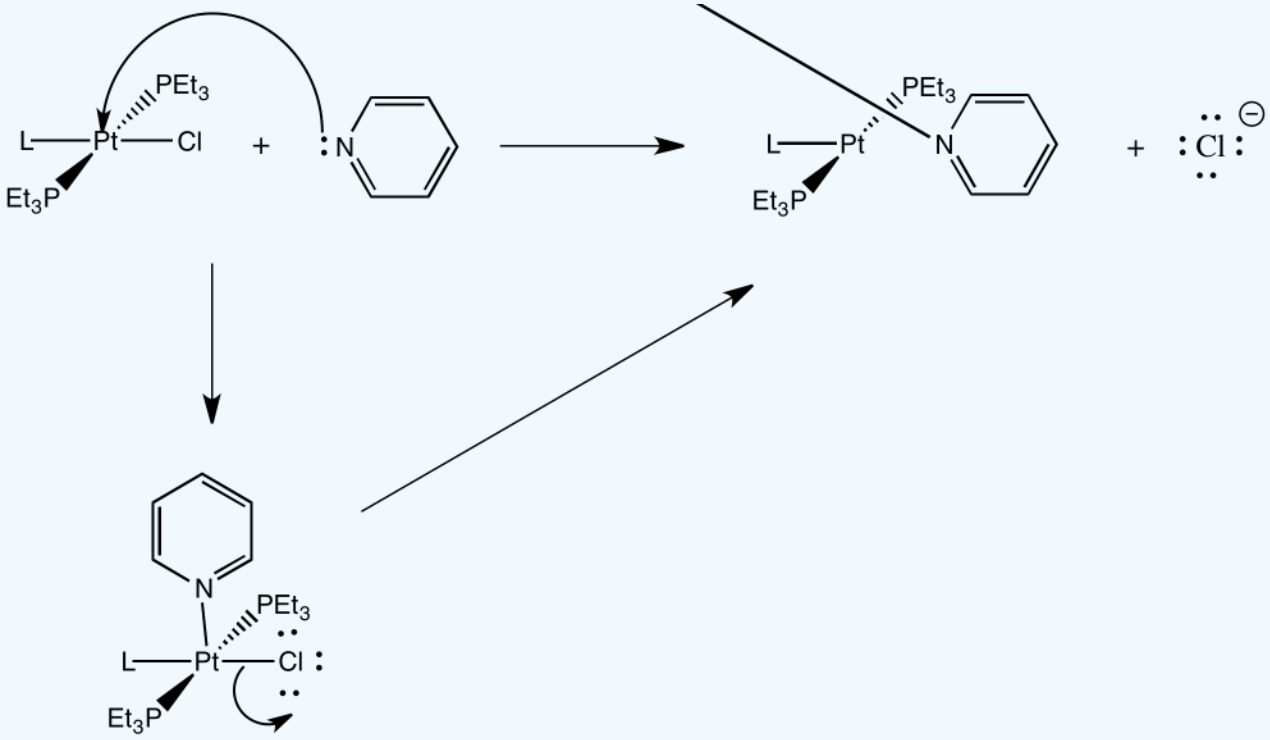
Answer



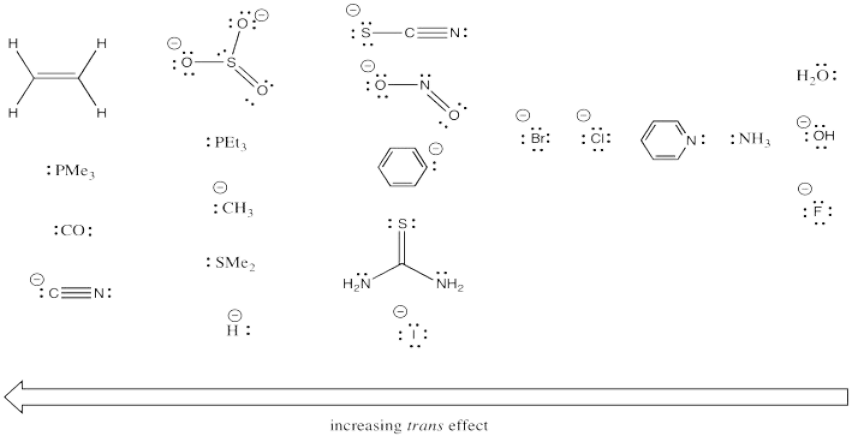
Exercise 9.3.3

Provide a mechanism with arrows for the reaction studied in the table.

Answer



Clearly that *trans* ligand has a dramatic effect on how quickly the chloride can be substituted in the above study. Additional studies like this one have led to some general trends. Below, the ligands on the left have strong *trans*-effects. Ligands *trans* to them are substituted very quickly. The ligands on the right have very modest *trans* effects. Ligands *trans* to them are substituted only slowly.



Exercise 9.3.4

Look for empirical trends in the series of ligands above. Without trying to explain exactly why, find chemically relevant factors that may be responsible for these reactivity trends.

Answer

There is an electronegativity trend: the less electronegative, the greater the *trans* effect (see the halogens, as well as the series O,N,C and also the orders within several pairings: S,P; O,S and N,P).

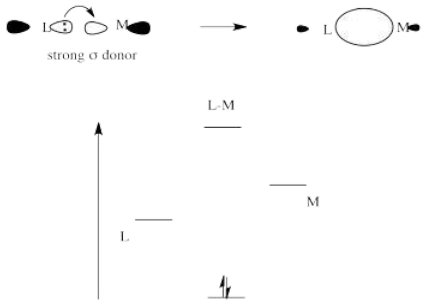
Alternatively, some of the above could be described by a polarizability trend: more polarizable atom, greater *trans* effect (for example, the halogens).

Most of the ligands containing π-bonds have strong *trans* influence (but not all).

Most of the π-donors have a weaker *trans* influence. However, these ligand cover a very broad range in this series.

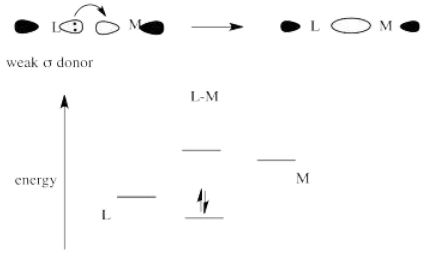
In general, explanations of the trans effect have focused on two separate types of ligands. These are strong sigma donors and strong pi acceptors.

Strong sigma donors donate electrons very effectively to the metal via a sigma bond. Because the ligand trans to this donor would be bonding via donation to the same metal p orbital, there is a competition. The metal p orbital bonds more favorably with the strong sigma donor, and the ligand trans to it is left with a weaker bond.



The strong sigma donor gets good overlap with the metal orbital and the resulting interaction goes down low in energy.

The weak sigma donor gets poorer overlap with the metal orbital and only weak stabilization of the donor electrons.



Place these two choices together, and the metal orbital will engage in a strong bonding interaction with the strong σ-donor. Doing so lowers the electronic energy significantly. It won't interact very much with the weak σ-donor, because doing that won't result in as much lowering of electronic energy. The result is a strong bond on one side of the metal and a weak bond on the other. That weak bond will break easily and that ligand will be replaced easily.



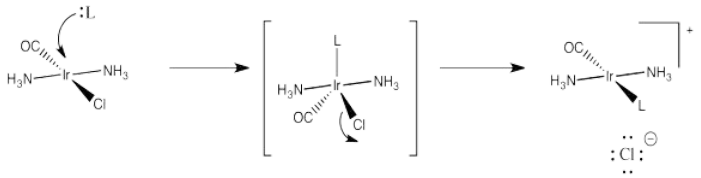
? Exercise 9.3.5

Which of the ligands in the *trans* effect series are probably strong σ-donors? Why?

Answer

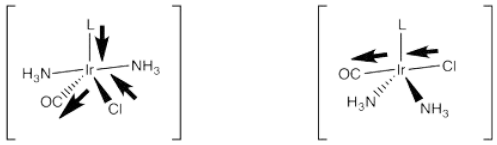
The strongest σ-donors are typically those with more polarizable donor atoms (such as S, P, I) as well as those with less electronegative donor ions such as C^- and H^-.

Strong pi acceptors exert their trans effect in a different way. They are thought to stabilize a particular geometry of the five-coordinate intermediate in substitution of square planar complexes. We haven't worried too much about the geometry of that intermediate, but it is probably trigonal bipyramidal. It would have three ligands in an equatorial plane and two more directly opposite each other, in the axial positions.



Essentially, the incoming ligand pushes two of the ligands down from the square plane to form this trigonal bipyramid. When it comes time for a ligand to leave, it is probably going to be one of these ligands that is already on the move. They are already on a trajectory out of the square plane, anyway.

A strong pi acceptor like CO exerts its *trans* effect by making sure it, along with the ligand opposite it, gets into that equatorial plane. It does that by a stabilizing delocalization that happens when the π-acceptor is in the electron-rich equatorial plane. In that position, it can draw electron density via π-donation from two different donors. If it were in an axial position, it could still delocalize electrons this way, but it would draw most effectively from just one donor rather than two.



favoured

So which of those two ligands is going to keep moving and leave the complex? It certainly won't be the one that is exerting a stabilizing, delocalizing effect on the complex via its strong bonding interactions. It will be the unlucky *trans* ligand that got dragged along with it.

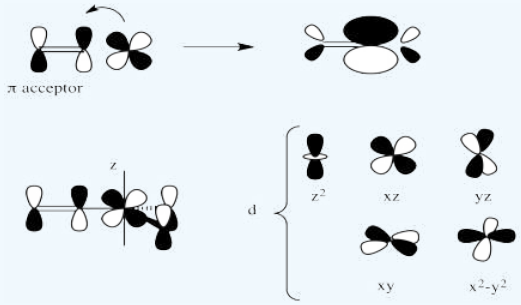
? Exercise 9.3.6

Which of the ligands in the *trans*-effect series are probably strong π-acceptors? Show why.

? Exercise 9.3.7

Draw an orbital picture showing the -delocalization described in the trigonal bipyramidal intermediate. Label the orbitals, assuming the z axis is along the axis of the trigonal bipyramid (i.e. the equatorial plane is the xy plane).

Answer



? Exercise 9.3.8

Substitution of trans ligands in μ-oxo-bis(μ-acetato)diruthenium complexes: Synthesis and kinetic studies. Hussain, Bhatt, Kumar, Thorat, Padhiyar and Shukla, *Inorganica Chemica Acta*, **2009**, *362*, 1101-1108.

Given the structure $[Ru_2O(L)_6(acetate)_2](PF_6)_2$, in which L is a neutral donor,

a) Draw the structure of the counterion, PF_6^-.

b) Provide an account of the valence electron count in the ruthenium coordination complex.

Valence electrons on metal	
Total charge on ligands	
Charge on the metal	
Revised count on metal	
Electrons donated by ligands	
Total electrons on metal in complex	

Data shows that the ligands L are *trans* to the bridging oxo ligand are labile.

c) Use orbital cartoons and words to provide an explanation for this effect.

When water is added to an acetone solution of $[Ru_2O(pyridine)_4(L)_2(acetate)_2](PF_6)_2$, then $[Ru_2O(pyridine)_4(H_2O)_2(acetate)_2](PF_6)_2$ is formed.

d) Draw the product of this reaction.

When pyridine is added to $[Ru_2O(pyridine)_4(H_2O)_2(acetate)_2](PF_6)_2$, then $[Ru_2O(pyridine)_6(acetate)_2](PF_6)_2$ is formed. The following rate constants were observed for this reaction.

[pyridine] mol L^{-1}	k_{obs} s^{-1} (x 10^{-3})
0.005	1.75
0.012	2.53
0.025	9.7
0.049	16.7
0.100	35.2

e) Use the data from this table to determine the order in pyridine. Provide an explanation for your conclusion.

f) Draw a mechanism for the reaction, consistent with the data.

g) Write a rate law for the reaction.

h) The authors studies the same reaction with different ligands instead of pyridine. They observed an increase in rate constants with increasing basicity of the incoming ligands. Provide an explanation for this observation.

Answer a



5 valence electrons - 6 bonds - 0 nonbonding = -1

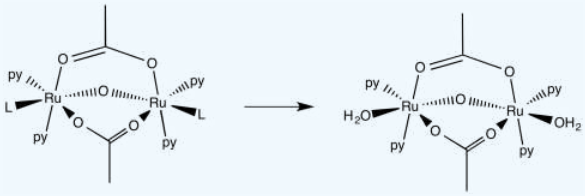
Answer b

Valence electrons on metal	8
Total charge on ligands	-4 (-2 per Ru)
Charge on the metal	+2
Revised count on metal	6
Electrons donated by ligands	12
Total electrons on metal in complex	18

Answer c

The oxo is a strong sigma donor and hogs the orbital with the metal thus leaving very little room for orbital bonding trans to the sigma donor.

Answer d



Answer e

First order. Although there is some amount of error in the data, doubling the pyridine concentration generally results in a doubling of the rate.

Answer f

The mechanism you draw would have to involve a first associative step; because the complex is already 18 electrons, associative interchange is likely.

Answer g

$$Rate = k[ML_n][py]$$

Answer h

Basic ligands have stronger attraction to the metal thus accelerating the reaction.

This page titled 9.3: Trans Effect is shared under a CC BY-NC 3.0 license and was authored, remixed, and/or curated by Chris Schaller via source content that was edited to the style and standards of the LibreTexts platform.

- **3.7: The Trans Effect** by Chris Schaller is licensed CC BY-NC 3.0. Original source: https://employees.csbsju.edu/cschaller/ROBI2.htm.

9.4: Cisplatin Discovery and Mode of Action

Platinum complex drugs commonly used in chemotherapy as anticancer agents. Pt chemotherapeutics make up roughly 50% of all chemotherapeutic drug regimens. Platinum drugs are used in both Pt (II) and Pt(IV) oxidation states. Pt antitumor complexes have at least three components in common:

1. They are electrostatically neutral Pt coordination complexes.
2. They are either square planar Pt(II) compounds or octahedral Pt(IV) compounds with two donor groups that are either primary or secondary amines. These amine ligands are either two *cis* monodentate ligands or one bidentate chelating ligand.
3. They all have two donors groups that act as leaving groups. These donors are either Cl or O, and can be either two monodentate or one bidentate ligand.

Specific examples of both Pt(II) and Pt(IV) drugs will be discussed. Platinum itself is a soft metal, which based on the Hard Soft Acid Base (HSAB) Theory, has a higher affinity to softer ligands which is important in biological systems. It has been hypothesized that Pt drugs use copper transport systems including members of the Ctr family to enter and exit cells.[2] The exact mechanism of this process is still highly debated. Studies have shown that Pt drugs have an affinity towards methionine-rich Ctr1 motifs, which may suggest that Pt(II) has a similar affinity for the sulfur of methionine to that of Cu(I),[2] which is typically transported within the cell by the Ctr family. Pt ions within the drug complex are capable of binding to sulfur on amino acids because Pt is a soft acid and sulfur is a soft base. Pt(IV) complexes do not have the same level of affinity to bind to cysteine and methionine in biological systems as Pt (II) complexes.

Pt(II) Complexes

Common Pt (II) complexes are depicted in the figure below. Cisplatin and oxaliplatin are the most common and effective complexes in chemotherapy. These complexes are all in square planar d^8 configuration. These complexes only have four ligands, which limit the geometries to either square planar or tetrahedral, their splitting diagram is depicted below. Complexes in the square planar position tend to have more Ligand Field Stabilization Energy (LFSE) than those in tetrahedral due to their Δ values which separate their antibonding orbitals from the nonbonding. The Δ value is much higher for d8 complexes in the square planar geometry than those in tetrahedral, which affects the the complex's LFSE. Figures 2 and 3 below depict splitting diagrams for d8 Pt(II), in possible square planar and tetrahedral geometries, respectively. If this system is in a tetrahedral geometry, spin would be an irrelevant factor because Pt(II) is a d8 metal and its electrons must be in the anti-bonding orbitals because the first four electrons occupy the nonbonding orbitals. However, spin is a relevant factor for this system in the case of square planar geometry. In this configuration, the no electrons reside in the x2-y2 anti-bonding orbital because of high LFSE and large Δ value. This stabilizes the complex, which explains the affinity of Pt(II) complexes for square planar geometry. On cisplatin, the two Pt-NH3 bonds are kinetically inert and thermodynamically stable, while the Pt-Cl bonds are semi-labile and can act as leaving groups for nucleophiles. Lability refers to the rate at which the ligands can be replaced with other molecules. Because the Pt-Cl are considered labile, they have a greater ability to act as leaving groups and react with other molecules than non-labile bonds. In cisplatin, the NH3-Pt bonds are not as labile as the Pt-Cl bonds and therefore will not leave the metal complex at the same rate as the Pt-Cl bond would to react with other molecules. This is counterintuitive based on electrostatic theory. The Cl- ligands have a negative charge, which influences the overall charge of the complex. However the -NH3 ligands are neutrally charged and are more inert than the neighboring -Cl- ligands. Typically, this would cause the NH3 ligands to be more labile. But, ligand field theory (LFT) explains that Cl- is both a sigma and pi donor ligand, while NH3 is only a sigma donor ligand. Because Cl- is a sigma and pi donor, its electrons also fill antibonding orbitals when binding to Pt. Since NH3 is only a sigma donor, its electrons do not fill the antibonding orbitals when binding to Pt. Due to the presence of electrons in the antibonding orbitals, the Pt-Cl bonds are not as strong as the Pt-NH3 the Cl- ligands are more labile than NH3. During cisplatin's mechanism of action, the chloride ligands are substituted by water molecules, acting as nucleophiles through a process called aquation, which is important in the drug's efficacy3,4,5.

Cisplatin

Cisplatin $[Pt(II)Cl_2(NH_3)_2]^{2-}$ is one of the most widely used anticancer drugs used especially for testicular and ovarian cancers treatments. This was first discovered in 1965 by biophysicist, Barnett Rosenberg while attempting to investigate effects of electric

fields on cell division with Pt electrodes in a cell growth medium. Instead of the cells dividing properly, they formed filaments while undergoing electrolysis and undergoing subsequent reactions of Pt ions[1].

$$\text{Pt (electrode)} \xrightarrow{\text{electrolysis}} [\text{Pt(IV) Cl}_6]^{2-} \longrightarrow \text{NH}_4{}^{+} \xrightarrow{\text{hv}} [\text{Pt(IV) Cl}_4\ (\text{NH}_3)_2] \tag{9.4.1}$$

The initial product of electrolysis is bacteriostatic and therefore does not promote filamentous growth. Pt in oxidation state (IV) is kinetically inert, low-spin 5d6 and very slow while undergoing reactions. Because of this, Pt(II) was thought to be more effective. Cisplatin, the cis isomer of [Pt(II)Cl2(NH3)2]2- was not bacteriostatic and promoted filamentous growth among the cells, which then in turn, prevented further growth of cancer cells.

Cisplatin in unstable in water, so it is immersed in saline solution to prevent aquation within the body. Saline is a combination of NaCl and water which controls the water levels within the body. If aquation would occur, the water ligands would make the Pt(II) complex very acidic, with pKa values ranging from 5-8. Hydroxyl (-OH) ligands bind and are less reactive because they are more of a strong field ligand than a weak field, like Cl- , the previous ligands. This makes the complex more stable.

The cis conformation of cisplatin affects the distance of the chloro ligands and its drug efficacy as compared to transplatin. The two chloro ligands, the reactive sites, are further apart in transplatin (4.64 A) than cisplatin (3.29 A). This affects how Pt(II) cross-links at DNA sites, which affects its efficacy. Because the Pt ion binds to DNA to stop DNA production, if the Pt ion in transplatin cannot cross-link into DNA because of its ligands, it will not stop DNA production of the cancer cells, or at least not as well as cisplatin. Transplatin reacts very slowly because of the new trans oxygen ligand at its second aquation1.

To promote anticancer activity, the goal is that the Pt ion from the original cisplatin molecule binds to DNA, preventing replication of the cancer cells. After undergoing aquation, the hydroxyl groups leave the Pt ion allowing it to bind to N7 of guanine (G), DNA's major Pt- binding site. The N7 of guanine is one of DNA's major binding site because complexes can easily access this area via the major groove in DNA's B-form6, the most common DNA form. While this is the prefered binding site, cisplatin and other Pt(II) drugs can also bind to N7 of adenine and N3 of cytosine. During cisplatin treatment, cancer cell DNA undergoes 1,2 intrastrand cross-linking of two guanines and sometimes guanine and adenine. The second chloro group undergoes aquation and binds to the second guanine on the DNA strand creating a chelating effect. This cross-linking induced by Cisplatin causes DNA to bend or kink which then causes neighboring proteins to bind to the kinked DNA because they now recognize them as high mobility groups. When this occurs, these newly bound proteins often block these kinks from repair, which halts replication and causes cell apoptosis7. Unfortunately, cisplatin also affects healthy cells as well as cancer cells. Fortunately, healthy cells recognize the damage caused by the kink, where cancer cells do not. This allows enzymes to repair the DNA damage in healthy cells, so they do not undergo apoptosis7. in Figure 4 below shows a Chimera image of a DNA strand within DNA polymerase (ribbons) with the Pt ion, shown in purple, binding to guanine in the DNA strand. The blue atoms bound to the Pt represent the NH3 ligands. Figure 6 shows the same Chimera image, but focused on the binding site between Pt and guanine. The atoms are labeled.

Pt (IV) Complexes

Pt (IV) complexes, commonly referred to as Pt(IV) pro-drugs, are also used as chemotherapeutic agents. These complexes have some benefits over Pt(II) drugs including, they are stable enough to administered orally versus IV, their stability may diminish the side effects caused by Pt(II) drugs, and they may have higher affinity to structural modification via their axial ligands which can enhance their pharmacological properties. Some common Pt(IV) complex drugs are depicted to the right. Pt(IV) complexes differ from Pt(II) complexes in that they have a d6 octahedral geometry with monodentate ligand, except tetraplatin which has one bidentate ligand in addition to the other monodentate ligands. Pt resides in the 5d row of the transition metals. Typically, metals belonging in the 4d and 5d rows of the transition metals have a larger Δ value than those of the 3d metals. This is due to the increase in subshell and size of atoms going down the periodic table. As subshell increases, so does Δ. Another trend to mention is as positive charge on the metal increases, as does Δ. Since the charge on Pt in this system is +4 and it is in the 5d row of the transition metals, I speculate that this system will have a low spin based on the metal ion alone. The splitting diagram of Pt(IV) is depicted below. This image shows the effects of LFSE on the metal. Pt (IV) is low spin with a large Δ value and all electrons residing in the lower energy t2g orbital. This indicates high LFSE which also explains increased bond strength and overall stability of the complex. An increase in LFSE also increases inertness of the system, which decreases lability. The ligands of Pt(IV) will not be as labile as some of Pt(II) due to the difference in LFSE. Pt(II) do not have as much LFSE, therefore, their ligands are more labile and reactive.

Pt(IV) complexes in an octahedral geometry are said to be **substitution-inert**, which makes their interactions and reactions with biological nucleophiles such as cysteine and methionine, very slow. Pt(IV) complexes are considered pro-drugs because they are activated intracellularly in vivo by reduction that makes them act as their square-planar counterparts with the eliminations of their axial ligands.Figure 8 below shows the reduction process. The Pt(IV) complex begins as a Pt(II) complex during synthesis with four ligands in a square planar geometry. The Pt(IV) octahedral configuration is established with the addition of two axial ligands either during a chlorination reaction or an addition reaction with hydrogen peroxide and possible further reactions. When administered orally, Pt(IV) is reduced back to Pt(II) square-planar configuration intracellularly8. Because these complexes can only act as Pt(II) complexes within the cell, where they bind to DNA, they travel throughout the rest of the body as inert Pt(IV) complexes, they may reduce toxicity8.

References

1. Bertini, Ivano; Gray, Harry B.; Stiefel, Edward I.; Valentine, Joan Selverstone. Biological Inorganic Chemistry: Structure and Reactivity, Fifth Edition, W.H. Freeman and Co., New York, 2010.
2. Aresano, Fabio; Losacco, Maurizio; Natile, Giovanni. An Updated View of Cisplatin Transport. 2013. European Journal of Inorganic Chemistry.
3. Johnstone, Timothy C.; Park, Ga Young; Lippard, Stephen J. Understanding Platinum Anticancer Drugs- Phenanthriplatin. Anticancer Res. 34(1): 471-476 Jan 2014.
4. Johnstone, Timothy C.; Lippard, Stephen J. The Chiral Potential of Phenanthriplatin and its Influence On Guanine Binding. Journal of American Chemistry Society. 2014. 136 (5): 2126-2134.
5. Lovejoy, Katherine S.; Serova, Maria; Bieche, Ivan; Emami, Shahin; D'Incalci, Maurizio; Broggini, Massimo; Erba, Eugenio; Gespach, Christain; Cvitkovic, Esteban; Faivre,Sandrine; Raymond, Eric; Lippard, Stephen J. Anticancer Activity of Pyriplatin, a Monofunctional Cationic Platinum (II) Compound, In Human Cancer Cells. Mol Cancer Ther. 2011. 10 (9): 1709-1719.
6. Monaco, PR. A novel major groove binding site in B-form DNA for ethidium cation. J Biomol Struct Dyn. 2007. 25(5):119-25.
7. Reedijk, Jan. Increased understanding of platinum anticancer chemistry. Pure Appl. Chem. 2011. 83 (9): 1709-1719.
8. Wexselblatt, Ezequiel; Gibson, Dan. What do we know about the reduction of Pt(IV) pro-drugs?. Journal of Biochemistry 29 February 2012.

9.4: Cisplatin Discovery and Mode of Action is shared under a not declared license and was authored, remixed, and/or curated by LibreTexts.

Index

A

abbreviated electron configuration
- 1.3.2: Ionization Energy
- 5.2: Electron Configuration of Gas-Phase Metal Ions

absorption energies
- 6: Molecular Orbital Theory

accessibility
- Front Matter

acid ionization constants
- 4.2.1: Trends of Binary Acids

acid strength
- 4.2.1: Trends of Binary Acids

acidity
- 4.2.1: Trends of Binary Acids

acidity and basicity
- 4.2: Arrhenius/Bronsted and Lowry

active electrode
- 3.3: Electrochemical Cells

Alkali Earth
- 1.3.2: Ionization Energy

Alkali Earth Metals
- 1.3.2: Ionization Energy

alkali metals
- 1.3.2: Ionization Energy
- 4.2.1: Trends of Binary Acids

alkaline earth metals
- 4.2.1: Trends of Binary Acids

alkene
- 8.1: Metal-Pi System Ligands (e.g. ferrocene)

ammine ligands
- 5.8: Ligand Binding Thermodynamics and the Chelate Effect
- 5.9: Hard and Soft Ligands and Metal Ions

anode
- 3.3: Electrochemical Cells

antifluorite
- 2.5.2.3: Ionic- Fluorite and Anti-Fluorite

aqua ligands
- 4.3.2: Acidity of Metal Ions in Water
- 5.8: Ligand Binding Thermodynamics and the Chelate Effect
- 5.9: Hard and Soft Ligands and Metal Ions

arene
- 8.1: Metal-Pi System Ligands (e.g. ferrocene)

aromatic
- 8.1: Metal-Pi System Ligands (e.g. ferrocene)

aromatic ligands
- 8.1: Metal-Pi System Ligands (e.g. ferrocene)

Arrhenius acid
- 4.1: Overview

Arrhenius base
- 4.1: Overview

Arrhenius definition
- 4.1: Overview

Arrhenius theory
- 4.2: Arrhenius/Bronsted and Lowry

atomic
- 1: Atomic Properties and Periodicity

atomic orbital
- 1.1.1: Quantum Numbers

atomic radii
- 1.3.2: Ionization Energy

atomic radius
- 1.3.2: Ionization Energy
- 1.3.3: Electron Affinity
- 1.4: Effective Nuclear Charge (Zeff) and Shielding (S); the Reason for Periodicity
- 1.4.3: Zeff Controls "Exceptions" to Periodic Trends

atomization enthalpy
- 2.5.1: Ionic- Measurement of Ionic Bond Strength

Author Bars
- 1.4.1: Slater's Rules

azimuthal quantum number
- 1.1.1: Quantum Numbers

B

balancing redox reactions
- 3: Oxidation and Reduction of Elements

barycenter
- 5.3: Crystal Field Theory, d orbital splitting in presence of ligands

bent
- 2.1.5: Molecule Shape from Valence Shell Electron Repulsion Theory (VSEPR)

beryllium
- 2.1.4: Lewis- Electron-Deficient "Octets" of B and Be

binary acids
- 4: Inorganic Acids and Bases

binary hydrides
- 4.2.1: Trends of Binary Acids

body centered cubic
- 2.4: Structures of Metals and Ionic Compounds

Bohr's equation
- 1.1.3: Representations of Atomic Orbitals

bond angle
- 2.1.5: Molecule Shape from Valence Shell Electron Repulsion Theory (VSEPR)

bond energy
- 4.2.1: Trends of Binary Acids

bond strength
- 4.2.1: Trends of Binary Acids

bonding
- 2: Bonding Theory Overview
- 5: Coordination Chemistry Introduction

Brønsted acids
- 4.2: Arrhenius/Bronsted and Lowry
- 4.2.1: Trends of Binary Acids

Brønsted bases
- 4.2: Arrhenius/Bronsted and Lowry
- 4.2.1: Trends of Binary Acids

Bronsted
- 4: Inorganic Acids and Bases

C

carbon monoxide
- 7: Why is Carbon Monoxide Poisonous?

case sensitivity
- Back Matter

cathode
- 3.3: Electrochemical Cells

cathodic protection
- 3.10: Corrosion

ccp
- 2.5.2.4: Ionic- Zinc Blende (ZnS)

Cell Notation
- 3.3: Electrochemical Cells

cell potential
- 3.3: Electrochemical Cells

character tables
- 6: Molecular Orbital Theory

chelate effect
- 5.8: Ligand Binding Thermodynamics and the Chelate Effect
- 5.9: Hard and Soft Ligands and Metal Ions

chemical reactions
- 4.2: Arrhenius/Bronsted and Lowry

chemistry
- 4.2.1: Trends of Binary Acids

Chemotherapy
- 9.4: Cisplatin Discovery and Mode of Action

cisplatin
- 9: Why is Cisplatin "King of the Chemotherapeutic Drugs?"

clarity
- Back Matter

coding function
- Back Matter

collaboration
- Front Matter

colors
- 6: Molecular Orbital Theory

complex ion
- 5: Coordination Chemistry Introduction

complexes
- 9: Why is Cisplatin "King of the Chemotherapeutic Drugs?"

compression
- 9.1: Jahn-Teller Distortions

concentration cell
- 3.5: Thermodynamic Considerations

conjugate acids and bases
- 4.2: Arrhenius/Bronsted and Lowry

conjugate pairs
- 4: Inorganic Acids and Bases

coordination complex
- 6.1: Overview of Colors from Transition Metal Ions

coordination complexes
- 6: Molecular Orbital Theory
- 6.1: Overview of Colors from Transition Metal Ions

coordination number
- 5: Coordination Chemistry Introduction

corrosion
- 3: Oxidation and Reduction of Elements
- 3.10: Corrosion

covalent
- 2: Bonding Theory Overview

covalent radius
- 1.3.2: Ionization Energy

crystal field orbitals
- 8.1: Metal-Pi System Ligands (e.g. ferrocene)

crystal field stabilization energy
- 5.3: Crystal Field Theory, d orbital splitting in presence of ligands
- 7.7: Exchange Inertness of d3, d4(LS), d5(LS), d6(LS), and d8(SQP)

crystal field theory
5: Coordination Chemistry Introduction
5.3: Crystal Field Theory, d orbital splitting in presence of ligands
5.5: Crystal Field Stabilization Energy
6: Molecular Orbital Theory
6.1: Overview of Colors from Transition Metal Ions
7: Why is Carbon Monoxide Poisonous?
7.5: LFSE/CFSE Calculations Again
7.6: Spectrochemical Series of Ligands (Again)
9: Why is Cisplatin "King of the Chemotherapeutic Drugs?"
crystal structure
2.4: Structures of Metals and Ionic Compounds
cubic closest packing
2.4: Structures of Metals and Ionic Compounds
cubic closet packing
2.5.2.4: Ionic- Zinc Blende (ZnS)
curriculum development
InfoPage
cytochrome c oxidase
7.10: Active Site of Cytochrome c Oxidase

D

D Block Contraction
1.4.3: Zeff Controls "Exceptions" to Periodic Trends
d orbital splitting
5: Coordination Chemistry Introduction
dative
8.1: Metal-Pi System Ligands (e.g. ferrocene)
dative actor ligands
8.1: Metal-Pi System Ligands (e.g. ferrocene)
dearomatization
8.1: Metal-Pi System Ligands (e.g. ferrocene)
definitions
Back Matter
degenerate orbitals
1.1.3: Representations of Atomic Orbitals
density
1: Atomic Properties and Periodicity
diastereomeric
8.1: Metal-Pi System Ligands (e.g. ferrocene)
dipole moment
2.1.5: Molecule Shape from Valence Shell Electron Repulsion Theory (VSEPR)
disproprotionation
3.7: Latimer Diagrams
distortions
9: Why is Cisplatin "King of the Chemotherapeutic Drugs?"
double helix
Back Matter

E

education technology
InfoPage
educators
Front Matter
effective nuclear charge
1.3.2: Ionization Energy
1.4.2: Periodic Trends of Zeff
electrical work
3.5: Thermodynamic Considerations
electrochemical cells
3: Oxidation and Reduction of Elements
electrochemical reactions
3: Oxidation and Reduction of Elements
electromagnetic spectrum
6.1: Overview of Colors from Transition Metal Ions
electron
1: Atomic Properties and Periodicity
2: Bonding Theory Overview
electron affinity
1.3.2: Ionization Energy
1.3.3: Electron Affinity
1.4: Effective Nuclear Charge (Zeff) and Shielding (S); the Reason for Periodicity
electron configuration
5: Coordination Chemistry Introduction
electron configurations
7: Why is Carbon Monoxide Poisonous?
electron density
1.1.3: Representations of Atomic Orbitals
electron spin
1.1.4: Energies of Atomic Orbitals
electronegativity
1.3.2: Ionization Energy
1.3.3: Electron Affinity
1.3.4: Electronegativity --- a molecular property
1.4: Effective Nuclear Charge (Zeff) and Shielding (S); the Reason for Periodicity
4.2.1: Trends of Binary Acids
electronegativity trends
1.3.3: Electron Affinity
1.4: Effective Nuclear Charge (Zeff) and Shielding (S); the Reason for Periodicity
4.2.1: Trends of Binary Acids
electronic configuration
1.2.1: Writing Ground State Electron Configurations
Electronic Configurations
9.1: Jahn-Teller Distortions
electrophilic attack
8.1: Metal-Pi System Ligands (e.g. ferrocene)
elongation
9.1: Jahn-Teller Distortions
energies
1: Atomic Properties and Periodicity
energy
9: Why is Cisplatin "King of the Chemotherapeutic Drugs?"
entry structure
Back Matter
equilibrium
4.2: Arrhenius/Bronsted and Lowry
examples
2: Bonding Theory Overview

F

Face Centered Cubic
2.5.2.1: Ionic- Rock Salt
Faraday's constant
3.5: Thermodynamic Considerations
fcc structure
2.5.2.1: Ionic- Rock Salt
ferrocene
8: What Happens "Above The Arrow" in Organic Chemistry
formal charge
2.1.1: Lewis- Formal Charge
Formation Constants
5.8: Ligand Binding Thermodynamics and the Chelate Effect
5.9: Hard and Soft Ligands and Metal Ions
free
Front Matter
freely available
InfoPage
Frost diagrams
3.8: Frost Diagrams

G

galvanic cell
3.3: Electrochemical Cells
galvanized iron
3.10: Corrosion
genetics
Back Matter
glossary
Back Matter

H

halogens
1.3.2: Ionization Energy
Heck reaction
8.1: Metal-Pi System Ligands (e.g. ferrocene)
heterolytic bond cleavage
4.2.1: Trends of Binary Acids
Hexagonal Closest Packed
2.4: Structures of Metals and Ionic Compounds
high spin
7: Why is Carbon Monoxide Poisonous?
9.1: Jahn-Teller Distortions
higher education
InfoPage
hydride ion
4.2.1: Trends of Binary Acids
hydrogen ion
4: Inorganic Acids and Bases
hydrogen ion transfer
4.2: Arrhenius/Bronsted and Lowry
hydrogen transfer
4.2.1: Trends of Binary Acids
hydron
4.1: Overview
hypervalency
2.1: Covalent- Lewis Octet
hypervalent molecule
2.1.2: Lewis- Expanded Octet
hypovalency
2.1: Covalent- Lewis Octet

I

identity operation
6.2: Symmetry and Symmetry Operations
improper rotation
6.2: Symmetry and Symmetry Operations
inert complex
7.7: Exchange Inertness of d3, d4(LS), d5(LS), d6(LS), and d8(SQP)
inert electrode
3.3: Electrochemical Cells
initiative
Front Matter

intermediate
7.7: Exchange Inertness of d3, d4(LS), d5(LS), d6(LS), and d8(SQP)
ionic salts
4.2.1: Trends of Binary Acids
ionization energy
1.3.2: Ionization Energy
1.3.3: Electron Affinity
1.4: Effective Nuclear Charge (Zeff) and Shielding (S); the Reason for Periodicity
1.4.3: Zeff Controls "Exceptions" to Periodic Trends
ionization potential
1.3.2: Ionization Energy
isomers
5.10: Potential Isomers of Complex Ions

K

Kulinkovich cyclopropanation
8.1: Metal-Pi System Ligands (e.g. ferrocene)

L

labile complex
7.7: Exchange Inertness of d3, d4(LS), d5(LS), d6(LS), and d8(SQP)
Lancashire
9.1: Jahn-Teller Distortions
Lanthanide Contraction
1.4.3: Zeff Controls "Exceptions" to Periodic Trends
Latimer diagrams
3.7: Latimer Diagrams
lattice enthalpy
2.5.1: Ionic- Measurement of Ionic Bond Strength
Lewis
2: Bonding Theory Overview
4: Inorganic Acids and Bases
LibreTexts
Front Matter
InfoPage
ligand
5: Coordination Chemistry Introduction
ligand exchange
5: Coordination Chemistry Introduction
Ligand Exchange Reactions
5.8: Ligand Binding Thermodynamics and the Chelate Effect
5.9: Hard and Soft Ligands and Metal Ions
ligand field theory
6.12: MO Diagram for bonding in [M(H2O)6]n+
6.13: Spectrochemical Series for Ligands
7: Why is Carbon Monoxide Poisonous?
9: Why is Cisplatin "King of the Chemotherapeutic Drugs?"
ligand substitution
8.1: Metal-Pi System Ligands (e.g. ferrocene)
ligands
8: What Happens "Above The Arrow" in Organic Chemistry
linear
2.1.5: Molecule Shape from Valence Shell Electron Repulsion Theory (VSEPR)
low spin
7: Why is Carbon Monoxide Poisonous?
9.1: Jahn-Teller Distortions

M

magnetic moments
7.4: Magnetic Moments for Spin State Determination
magnetic properties
7: Why is Carbon Monoxide Poisonous?
magnetic quantum number
1.1.1: Quantum Numbers
mechanics
1: Atomic Properties and Periodicity
Melting Point
1.3.3: Electron Affinity
1.4: Effective Nuclear Charge (Zeff) and Shielding (S); the Reason for Periodicity
metal hydroxide
4: Inorganic Acids and Bases
metallacyclopropane
8.1: Metal-Pi System Ligands (e.g. ferrocene)
metallic character
1.3.2: Ionization Energy
1.3.3: Electron Affinity
1.4: Effective Nuclear Charge (Zeff) and Shielding (S); the Reason for Periodicity
metalloids
1.3.2: Ionization Energy
molecular
2: Bonding Theory Overview
9: Why is Cisplatin "King of the Chemotherapeutic Drugs?"
molecular orbital theory
7: Why is Carbon Monoxide Poisonous?
molecule polarity
4.2.1: Trends of Binary Acids
molecule shapes
6: Molecular Orbital Theory

N

Nernst equation
3.5: Thermodynamic Considerations
noble gases
1.3.2: Ionization Energy
nonaqueous solvents
4.2: Arrhenius/Bronsted and Lowry
nonmetals
4.2.1: Trends of Binary Acids
nucleophilic aromatic substitution
8.1: Metal-Pi System Ligands (e.g. ferrocene)

O

octahedral
2.1.5: Molecule Shape from Valence Shell Electron Repulsion Theory (VSEPR)
9: Why is Cisplatin "King of the Chemotherapeutic Drugs?"
octahedral metal ion
7: Why is Carbon Monoxide Poisonous?
OER
InfoPage
olefin polymerization
8.1: Metal-Pi System Ligands (e.g. ferrocene)
open education
InfoPage
orbital energy
1.1.3: Representations of Atomic Orbitals
1.1.4: Energies of Atomic Orbitals
orbitals
1: Atomic Properties and Periodicity
organometallic
8: What Happens "Above The Arrow" in Organic Chemistry
overall symmetry
6.2: Symmetry and Symmetry Operations
overview
4: Inorganic Acids and Bases
oxidation
3: Oxidation and Reduction of Elements
Oxidation Potential
1.3.2: Ionization Energy
oxoacids
4.2.2: Trends of Oxyacids
4.2.3: Trends in Metal Hydroxide Basicity/Solubility
oxyacids
4: Inorganic Acids and Bases
4.2.2: Trends of Oxyacids
4.2.3: Trends in Metal Hydroxide Basicity/Solubility

P

pairs
2: Bonding Theory Overview
pauli exclusion principle
1.1.4: Energies of Atomic Orbitals
Pauling's rules
4.2.2: Trends of Oxyacids
4.2.3: Trends in Metal Hydroxide Basicity/Solubility
penetration
1.4.2: Periodic Trends of Zeff
periodic law
1.3.3: Electron Affinity
1.4: Effective Nuclear Charge (Zeff) and Shielding (S); the Reason for Periodicity
periodic table
1.3.2: Ionization Energy
1.3.3: Electron Affinity
1.4: Effective Nuclear Charge (Zeff) and Shielding (S); the Reason for Periodicity
4.2.1: Trends of Binary Acids
periodic trends
1.3.2: Ionization Energy
1.3.3: Electron Affinity
1.4: Effective Nuclear Charge (Zeff) and Shielding (S); the Reason for Periodicity
pi acceptor
6.12: MO Diagram for bonding in [M(H2O)6]n+
6.13: Spectrochemical Series for Ligands
pi donor
6.12: MO Diagram for bonding in [M(H2O)6]n+
6.13: Spectrochemical Series for Ligands
pi system
8.1: Metal-Pi System Ligands (e.g. ferrocene)
pi systems
8.1: Metal-Pi System Ligands (e.g. ferrocene)
point groups
6: Molecular Orbital Theory
Pourbaix diagrams
3.9: Pourbaix Diagrams
principle quantum number
1.1.1: Quantum Numbers
principle shell
1.1.1: Quantum Numbers
probability
1: Atomic Properties and Periodicity

probability density
1.1.3: Representations of Atomic Orbitals
Project
Front Matter
proper rotation
6.2: Symmetry and Symmetry Operations
proton transfer
4.2: Arrhenius/Bronsted and Lowry

Q

quantum
1: Atomic Properties and Periodicity
quantum mechanics
1.1.1: Quantum Numbers

R

reaction coordinate diagram
7.7: Exchange Inertness of d3, d4(LS), d5(LS), d6(LS), and d8(SQP)
Redox Potentials
1.3.2: Ionization Energy
redox reaction
3.1: Redox Reactions
redox reactions
3: Oxidation and Reduction of Elements
reduction
3: Oxidation and Reduction of Elements
reduction potential
1.3.2: Ionization Energy
resonance
2.1.3: Lewis- Resonance
resonance structures
2.1.3: Lewis- Resonance
ring slippage
8.1: Metal-Pi System Ligands (e.g. ferrocene)
rock salt structure
2.5.2.1: Ionic- Rock Salt

S

Sabatier Principle
6.2: Symmetry and Symmetry Operations
sacrificial anode
3.10: Corrosion
Scandide Contraction
1.4.3: Zeff Controls "Exceptions" to Periodic Trends
Schoenflies symbol
6.2: Symmetry and Symmetry Operations
Section 4.1
6.14: Spectrochemical Series for Metal ions
seesaw
2.1.5: Molecule Shape from Valence Shell Electron Repulsion Theory (VSEPR)
shape
2: Bonding Theory Overview
shapes
1: Atomic Properties and Periodicity
shielding
1.4.2: Periodic Trends of Zeff
shielding effect
1.4.3: Zeff Controls "Exceptions" to Periodic Trends
sigma donor
6.12: MO Diagram for bonding in [M(H2O)6]n+
6.13: Spectrochemical Series for Ligands
simple cubic structure
2.4: Structures of Metals and Ionic Compounds
site selectivity
8.1: Metal-Pi System Ligands (e.g. ferrocene)
solubility
4: Inorganic Acids and Bases
spectator
8.1: Metal-Pi System Ligands (e.g. ferrocene)
spectrochemical series
6.1: Overview of Colors from Transition Metal Ions
sphalerite
2.5.2.4: Ionic- Zinc Blende (ZnS)
square pyramidal
2.1.5: Molecule Shape from Valence Shell Electron Repulsion Theory (VSEPR)
stability constant
5: Coordination Chemistry Introduction
Stability Constants
5.8: Ligand Binding Thermodynamics and the Chelate Effect
5.9: Hard and Soft Ligands and Metal Ions
standard cell potential
3.4: Standard Reduction Potentials
standard hydrogen electrode
3.4: Standard Reduction Potentials
standard reduction potential
3.4: Standard Reduction Potentials
standard reduction potentials
3: Oxidation and Reduction of Elements
stereoisomers
5.10: Potential Isomers of Complex Ions
stereoselectivity
8.1: Metal-Pi System Ligands (e.g. ferrocene)
strong and weak acids
4.2: Arrhenius/Bronsted and Lowry
strong field
6.12: MO Diagram for bonding in [M(H2O)6]n+
6.13: Spectrochemical Series for Ligands
structural isomers
5.10: Potential Isomers of Complex Ions
structure
2: Bonding Theory Overview
students
Front Matter
subshell
1.1.1: Quantum Numbers
symmetry
6: Molecular Orbital Theory
9: Why is Cisplatin "King of the Chemotherapeutic Drugs?"
symmetry elements
6.2: Symmetry and Symmetry Operations
symmetry operations
6.2: Symmetry and Symmetry Operations

T

tetrahedral
2.1.5: Molecule Shape from Valence Shell Electron Repulsion Theory (VSEPR)
textbook
Back Matter
textbooks
InfoPage
thermodynamic considerations
3: Oxidation and Reduction of Elements
thermodynamics
5: Coordination Chemistry Introduction
5.8: Ligand Binding Thermodynamics and the Chelate Effect
5.9: Hard and Soft Ligands and Metal Ions
trans effect
9.3: Trans Effect
transition metals
1.3.2: Ionization Energy
6: Molecular Orbital Theory
transition state
7.7: Exchange Inertness of d3, d4(LS), d5(LS), d6(LS), and d8(SQP)
trends
1.3.3: Electron Affinity
1.4: Effective Nuclear Charge (Zeff) and Shielding (S); the Reason for Periodicity
trends in reactivity
3: Oxidation and Reduction of Elements
trigonal bipyramidal
2.1.5: Molecule Shape from Valence Shell Electron Repulsion Theory (VSEPR)
trigonal planar
2.1.5: Molecule Shape from Valence Shell Electron Repulsion Theory (VSEPR)
trigonal pyramidal
2.1.5: Molecule Shape from Valence Shell Electron Repulsion Theory (VSEPR)

V

valence shell electron pair repulsion theory
2.1.5: Molecule Shape from Valence Shell Electron Repulsion Theory (VSEPR)
visible light
6: Molecular Orbital Theory
voltaic cell
3.3: Electrochemical Cells
VSEPR
2: Bonding Theory Overview
2.1.5: Molecule Shape from Valence Shell Electron Repulsion Theory (VSEPR)

W

Wacker oxidation
8.1: Metal-Pi System Ligands (e.g. ferrocene)
wavefunction
1.1.1: Quantum Numbers
wavefunctions
1: Atomic Properties and Periodicity
weak field
6.12: MO Diagram for bonding in [M(H2O)6]n+
6.13: Spectrochemical Series for Ligands

Z

zinc blend structure
2.5.2.4: Ionic- Zinc Blende (ZnS)

Glossary

Sample Word 1 | Sample Definition 1

Detailed Licensing

Many of the pages in this book are re-mixes of open content from other books in the LibreTexts Library. Sometimes sections from several sources are used on the same page and there may be no unique open license. Where there is a conflict, the licensing may appear as *undeclared*. On any page, by toggling AutoAttibution on the Tools menu, you can display the detailed attribution on a paragraph level. Material from different books will be color coded and the source displayed by mousing over the paragraph.

Content in the front and backmatter, directories and similar can be uncopywriteable, being simple listings and these are also shown as *undeclared*.

Overview

Title: Chem 230: Essential Inorganic Chemistry

Webpages: 127

Applicable Restrictions: Noncommercial

All licenses found:

- CC BY-NC-SA 4.0: 69.3% (88 pages)
- Undeclared: 22% (28 pages)
- CC BY 4.0: 4.7% (6 pages)
- CC BY-NC-SA 3.0: 1.6% (2 pages)
- CC BY-NC 4.0: 1.6% (2 pages)
- CC BY-NC 3.0: 0.8% (1 page)

By Page

- Chem 230: Essential Inorganic Chemistry - *Undeclared*
  - Front Matter - *Undeclared*
    - TitlePage - *Undeclared*
    - InfoPage - *Undeclared*
    - Table of Contents - *Undeclared*
    - Licensing - *Undeclared*
  - 1: Atomic Properties and Periodicity - *Undeclared*
    - 1.1: Quantum Mechanics for Orbital Shapes and Energies - *Undeclared*
      - 1.1.1: Quantum Numbers - *CC BY-NC-SA 4.0*
      - 1.1.2: Probability Density and Nodes - *CC BY-NC-SA 4.0*
      - 1.1.3: Representations of Atomic Orbitals - *CC BY-NC-SA 4.0*
      - 1.1.4: Energies of Atomic Orbitals - *CC BY-NC-SA 4.0*
    - 1.2: Ground State Electron Configurations - *Undeclared*
      - 1.2.1: Writing Ground State Electron Configurations - *CC BY-NC-SA 4.0*
      - 1.2.2: Magnetic Properties - *CC BY-NC-SA 4.0*
    - 1.3: Periodic Properties of the Periodic Table - *CC BY-NC-SA 4.0*
      - 1.3.1: Atomic Radius - *CC BY-NC-SA 4.0*
      - 1.3.2: Ionization Energy - *CC BY-NC-SA 4.0*
      - 1.3.3: Electron Affinity - *CC BY-NC-SA 4.0*
      - 1.3.4: Electronegativity --- a molecular property - *CC BY-NC-SA 4.0*
    - 1.4: Effective Nuclear Charge (Zeff) and Shielding (S); the Reason for Periodicity - *CC BY-NC-SA 4.0*
      - 1.4.1: Slater's Rules - *CC BY-NC-SA 4.0*
      - 1.4.2: Periodic Trends of Zeff - *CC BY-NC-SA 4.0*
      - 1.4.3: Zeff Controls "Exceptions" to Periodic Trends - *CC BY-NC-SA 4.0*
  - 2: Bonding Theory Overview - *Undeclared*
    - 2.1: Covalent- Lewis Octet - *CC BY-NC-SA 4.0*
      - 2.1.1: Lewis- Formal Charge - *CC BY-NC-SA 4.0*
      - 2.1.2: Lewis- Expanded Octet - *CC BY-NC-SA 4.0*
      - 2.1.3: Lewis- Resonance - *CC BY-NC-SA 4.0*
      - 2.1.4: Lewis- Electron-Deficient "Octets" of B and Be - *CC BY-NC-SA 4.0*
      - 2.1.5: Molecule Shape from Valence Shell Electron Repulsion Theory (VSEPR) - *CC BY-NC-SA 4.0*
      - 2.1.6: Shape Change from Lone Pairs - *CC BY-NC-SA 4.0*
      - 2.1.7: Shape Change from Double and Triple Bonds - *CC BY-NC-SA 4.0*

- 2.2: Covalent- Molecular Orbital Theory - *CC BY-NC-SA 4.0*
  - 2.2.1: MO- s orbital MOs - *CC BY-NC-SA 4.0*
  - 2.2.2: MO- p orbital MOs - *CC BY-NC-SA 4.0*
  - 2.2.3: MO- d orbital MOs - *CC BY-NC-SA 4.0*
  - 2.2.4: MO- Nonbonding MOs - *CC BY-NC-SA 4.0*
  - 2.2.5: MO- MO Diagram Features - *CC BY-NC-SA 4.0*
  - 2.2.6: MO- MO Diagrams of 1st and 2nd row diatomic molecules - *CC BY-NC-SA 4.0*
  - 2.2.7: MO- MO Diagrams of Heteronuclear Diatomics - *CC BY-NC-SA 4.0*
- 2.3: Metallic- Sea of Electrons and the van Arkel-Ketelaar Triangle - *CC BY-NC-SA 4.0*
- 2.4: Structures of Metals and Ionic Compounds - *CC BY-NC-SA 4.0*
- 2.5: Ionic- Charge and Size Determine Ionic Bonding - *CC BY-NC-SA 4.0*
  - 2.5.1: Ionic- Measurement of Ionic Bond Strength - *CC BY-NC-SA 4.0*
  - 2.5.2: Ionic- Examples of Ionic Structures - *CC BY-NC-SA 4.0*
    - 2.5.2.1: Ionic- Rock Salt - *CC BY-NC-SA 4.0*
    - 2.5.2.2: Ionic- Caesium Chloride (CsCl) - *Undeclared*
    - 2.5.2.3: Ionic- Fluorite and Anti-Fluorite - *CC BY-NC-SA 4.0*
    - 2.5.2.4: Ionic- Zinc Blende (ZnS) - *CC BY-NC-SA 4.0*
  - 2.5.3: Predicting Ionic Structure Type - *CC BY-NC-SA 4.0*

3: Oxidation and Reduction of Elements - *Undeclared*

- 3.1: Redox Reactions - *CC BY-NC-SA 4.0*
- 3.2: Balancing Redox Reactions - *CC BY-NC-SA 4.0*
- 3.3: Electrochemical Cells - *CC BY-NC-SA 4.0*
- 3.4: Standard Reduction Potentials - *CC BY-NC-SA 4.0*
- 3.5: Thermodynamic Considerations - *CC BY-NC-SA 4.0*
- 3.6: General Trends in Reactivity - *CC BY-NC-SA 4.0*
- 3.7: Latimer Diagrams - *CC BY-NC-SA 4.0*
- 3.8: Frost Diagrams - *CC BY-NC-SA 4.0*
- 3.9: Pourbaix Diagrams - *CC BY-NC-SA 4.0*
- 3.10: Corrosion - *CC BY 4.0*

4: Inorganic Acids and Bases - *Undeclared*

- 4.1: Overview - *CC BY-NC-SA 4.0*
- 4.2: Arrhenius/Bronsted and Lowry - *CC BY-NC-SA 4.0*
  - 4.2.1: Trends of Binary Acids - *CC BY-NC-SA 4.0*
  - 4.2.2: Trends of Oxyacids - *CC BY-NC-SA 3.0*
  - 4.2.3: Trends in Metal Hydroxide Basicity/Solubility - *CC BY-NC-SA 3.0*
- 4.3: Lewis Acids and Bases - *CC BY-NC-SA 4.0*
  - 4.3.1: Conjugate Acids of Lewis Bases are Bronsted Acids - *CC BY-NC-SA 4.0*
  - 4.3.2: Acidity of Metal Ions in Water - *CC BY-NC-SA 4.0*
  - 4.3.3: Hard-Soft Designation of Lewis Acids and Bases - *CC BY-NC-SA 4.0*

5: Coordination Chemistry Introduction - *Undeclared*

- 5.1: Ligands - *CC BY-NC-SA 4.0*
- 5.2: Electron Configuration of Gas-Phase Metal Ions - *CC BY-NC-SA 4.0*
- 5.3: Crystal Field Theory, d orbital splitting in presence of ligands - *CC BY-NC-SA 4.0*
- 5.4: Crystal Field Electron Configuration - *CC BY-NC-SA 4.0*
- 5.5: Crystal Field Stabilization Energy - *CC BY-NC-SA 4.0*
- 5.6: Thermodynamic and Structure Consequences of d orbital splitting - *CC BY-NC-SA 4.0*
- 5.7: Ligand Exchange Reactions and Affinity Determination - *CC BY-NC-SA 4.0*
- 5.8: Ligand Binding Thermodynamics and the Chelate Effect - *CC BY-NC 4.0*
- 5.9: Hard and Soft Ligands and Metal Ions - *CC BY-NC 4.0*
- 5.10: Potential Isomers of Complex Ions - *CC BY-NC-SA 4.0*

6: Molecular Orbital Theory - *Undeclared*

- 6.1: Overview of Colors from Transition Metal Ions - *CC BY 4.0*
- 6.2: Symmetry and Symmetry Operations - *CC BY-NC-SA 4.0*
- 6.3: Molecule Shapes (Point Groups) - *CC BY-NC-SA 4.0*
- 6.4: Point Group Assignment - *CC BY-NC-SA 4.0*
- 6.5: Overview of Classifying Bonding Orbitals in a Molecule - *CC BY-NC-SA 4.0*
- 6.6: MO Diagram Construction of CO2 - *CC BY-NC-SA 4.0*
- 6.7: MO Diagram Construction of H2O - *CC BY-NC-SA 4.0*
- 6.8: MO Diagram Construction of NH3 - *CC BY-NC-SA 4.0*
- 6.9: MO Construction of BF3 - *CC BY-NC-SA 4.0*

- 6.10: Lewis Acid-Base Dative Bond and MO Diagrams - *CC BY-NC-SA 4.0*
- 6.11: MO Diagram for bonding in [M(NH3)6]n+ - *CC BY-NC-SA 4.0*
- 6.12: MO Diagram for bonding in [M(H2O)6]n+ - *CC BY-NC-SA 4.0*
- 6.13: Spectrochemical Series for Ligands - *CC BY-NC-SA 4.0*
- 6.14: Spectrochemical Series for Metal ions - *CC BY-NC-SA 4.0*

7: Why is Carbon Monoxide Poisonous? - *Undeclared*

- 7.1: Pi-Acid Ligands - *CC BY-NC-SA 4.0*
- 7.2: [Fe(CO)6]2+ MO Diagram - *CC BY-NC-SA 4.0*
- 7.3: Revisit Octahedral Metal Ion Electron Configurations - *CC BY-NC-SA 4.0*
- 7.4: Magnetic Moments for Spin State Determination - *CC BY-NC-SA 4.0*
- 7.5: LFSE/CFSE Calculations Again - *CC BY-NC-SA 4.0*
- 7.6: Spectrochemical Series of Ligands (Again) - *CC BY-NC-SA 4.0*
- 7.7: Exchange Inertness of d3, d4(LS), d5(LS), d6(LS), and d8(SQP) - *Undeclared*
- 7.8: O2 Reduction, since CO displaces O2 - *CC BY-NC-SA 4.0*
- 7.9: Bonding in Carbonmonoxy-myoglobin [Fe(CO)]2+ - *CC BY-NC-SA 4.0*
- 7.10: Active Site of Cytochrome c Oxidase - *Undeclared*
- 7.11: Cyanide is also a poison (affinity data) - *CC BY 4.0*
- 7.12: Cyanide is also a poison (spectrocopic data) - *Undeclared*

8: What Happens "Above The Arrow" in Organic Chemistry - *Undeclared*

- 8.1: Metal-Pi System Ligands (e.g. ferrocene) - *CC BY-NC-SA 4.0*
- 8.2: 18 Electron Rule - *CC BY-NC-SA 4.0*
- 8.3: Organometallic Reaction Types - *CC BY 4.0*
- 8.4: Organometallic Catalysts - *CC BY 4.0*
- 8.5: Suzuki-Miyara Coupling - *CC BY-NC-SA 4.0*

9: Why is Cisplatin "King of the Chemotherapeutic Drugs?" - *Undeclared*

- 9.1: Jahn-Teller Distortions - *Undeclared*
- 9.2: d8 Low-Spin Preference for Square Planar Geometry - *CC BY 4.0*
- 9.3: Trans Effect - *CC BY-NC 3.0*
- 9.4: Cisplatin Discovery and Mode of Action - *Undeclared*

Back Matter - *Undeclared*

- Index - *Undeclared*
- Glossary - *Undeclared*
- Detailed Licensing - *Undeclared*
- Detailed Licensing - *Undeclared*

Detailed Licensing

Overview

Title: Chem 230: Essential Inorganic Chemistry

Webpages: 127

Applicable Restrictions: Noncommercial

All licenses found:

- CC BY-NC-SA 4.0: 69.3% (88 pages)
- Undeclared: 22% (28 pages)
- CC BY 4.0: 4.7% (6 pages)
- CC BY-NC-SA 3.0: 1.6% (2 pages)
- CC BY-NC 4.0: 1.6% (2 pages)
- CC BY-NC 3.0: 0.8% (1 page)

By Page

- Chem 230: Essential Inorganic Chemistry - *Undeclared*
  - Front Matter - *Undeclared*
    - TitlePage - *Undeclared*
    - InfoPage - *Undeclared*
    - Table of Contents - *Undeclared*
    - Licensing - *Undeclared*
  - 1: Atomic Properties and Periodicity - *Undeclared*
    - 1.1: Quantum Mechanics for Orbital Shapes and Energies - *Undeclared*
      - 1.1.1: Quantum Numbers - *CC BY-NC-SA 4.0*
      - 1.1.2: Probability Density and Nodes - *CC BY-NC-SA 4.0*
      - 1.1.3: Representations of Atomic Orbitals - *CC BY-NC-SA 4.0*
      - 1.1.4: Energies of Atomic Orbitals - *CC BY-NC-SA 4.0*
    - 1.2: Ground State Electron Configurations - *Undeclared*
      - 1.2.1: Writing Ground State Electron Configurations - *CC BY-NC-SA 4.0*
      - 1.2.2: Magnetic Properties - *CC BY-NC-SA 4.0*
    - 1.3: Periodic Properties of the Periodic Table - *CC BY-NC-SA 4.0*
      - 1.3.1: Atomic Radius - *CC BY-NC-SA 4.0*
      - 1.3.2: Ionization Energy - *CC BY-NC-SA 4.0*
      - 1.3.3: Electron Affinity - *CC BY-NC-SA 4.0*
      - 1.3.4: Electronegativity --- a molecular property - *CC BY-NC-SA 4.0*
    - 1.4: Effective Nuclear Charge (Zeff) and Shielding (S); the Reason for Periodicity - *CC BY-NC-SA 4.0*
      - 1.4.1: Slater's Rules - *CC BY-NC-SA 4.0*
      - 1.4.2: Periodic Trends of Zeff - *CC BY-NC-SA 4.0*
      - 1.4.3: Zeff Controls "Exceptions" to Periodic Trends - *CC BY-NC-SA 4.0*
  - 2: Bonding Theory Overview - *Undeclared*
    - 2.1: Covalent- Lewis Octet - *CC BY-NC-SA 4.0*
      - 2.1.1: Lewis- Formal Charge - *CC BY-NC-SA 4.0*
      - 2.1.2: Lewis- Expanded Octet - *CC BY-NC-SA 4.0*
      - 2.1.3: Lewis- Resonance - *CC BY-NC-SA 4.0*
      - 2.1.4: Lewis- Electron-Deficient "Octets" of B and Be - *CC BY-NC-SA 4.0*
      - 2.1.5: Molecule Shape from Valence Shell Electron Repulsion Theory (VSEPR) - *CC BY-NC-SA 4.0*
      - 2.1.6: Shape Change from Lone Pairs - *CC BY-NC-SA 4.0*
      - 2.1.7: Shape Change from Double and Triple Bonds - *CC BY-NC-SA 4.0*
    - 2.2: Covalent- Molecular Orbital Theory - *CC BY-NC-SA 4.0*
      - 2.2.1: MO- s orbital MOs - *CC BY-NC-SA 4.0*
      - 2.2.2: MO- p orbital MOs - *CC BY-NC-SA 4.0*
      - 2.2.3: MO- d orbital MOs - *CC BY-NC-SA 4.0*
      - 2.2.4: MO- Nonbonding MOs - *CC BY-NC-SA 4.0*
      - 2.2.5: MO- MO Diagram Features - *CC BY-NC-SA 4.0*
      - 2.2.6: MO- MO Diagrams of 1st and 2nd row diatomic molecules - *CC BY-NC-SA 4.0*
      - 2.2.7: MO- MO Diagrams of Heteronuclear Diatomics - *CC BY-NC-SA 4.0*

- 2.3: Metallic- Sea of Electrons and the van Arkel-Ketelaar Triangle - *CC BY-NC-SA 4.0*
- 2.4: Structures of Metals and Ionic Compounds - *CC BY-NC-SA 4.0*
- 2.5: Ionic- Charge and Size Determine Ionic Bonding - *CC BY-NC-SA 4.0*
  - 2.5.1: Ionic- Measurement of Ionic Bond Strength - *CC BY-NC-SA 4.0*
  - 2.5.2: Ionic- Examples of Ionic Structures - *CC BY-NC-SA 4.0*
    - 2.5.2.1: Ionic- Rock Salt - *CC BY-NC-SA 4.0*
    - 2.5.2.2: Ionic- Caesium Chloride (CsCl) - *Undeclared*
    - 2.5.2.3: Ionic- Fluorite and Anti-Fluorite - *CC BY-NC-SA 4.0*
    - 2.5.2.4: Ionic- Zinc Blende (ZnS) - *CC BY-NC-SA 4.0*
  - 2.5.3: Predicting Ionic Structure Type - *CC BY-NC-SA 4.0*
- 3: Oxidation and Reduction of Elements - *Undeclared*
  - 3.1: Redox Reactions - *CC BY-NC-SA 4.0*
  - 3.2: Balancing Redox Reactions - *CC BY-NC-SA 4.0*
  - 3.3: Electrochemical Cells - *CC BY-NC-SA 4.0*
  - 3.4: Standard Reduction Potentials - *CC BY-NC-SA 4.0*
  - 3.5: Thermodynamic Considerations - *CC BY-NC-SA 4.0*
  - 3.6: General Trends in Reactivity - *CC BY-NC-SA 4.0*
  - 3.7: Latimer Diagrams - *CC BY-NC-SA 4.0*
  - 3.8: Frost Diagrams - *CC BY-NC-SA 4.0*
  - 3.9: Pourbaix Diagrams - *CC BY-NC-SA 4.0*
  - 3.10: Corrosion - *CC BY 4.0*
- 4: Inorganic Acids and Bases - *Undeclared*
  - 4.1: Overview - *CC BY-NC-SA 4.0*
  - 4.2: Arrhenius/Bronsted and Lowry - *CC BY-NC-SA 4.0*
    - 4.2.1: Trends of Binary Acids - *CC BY-NC-SA 4.0*
    - 4.2.2: Trends of Oxyacids - *CC BY-NC-SA 3.0*
    - 4.2.3: Trends in Metal Hydroxide Basicity/Solubility - *CC BY-NC-SA 3.0*
  - 4.3: Lewis Acids and Bases - *CC BY-NC-SA 4.0*
    - 4.3.1: Conjugate Acids of Lewis Bases are Bronsted Acids - *CC BY-NC-SA 4.0*
    - 4.3.2: Acidity of Metal Ions in Water - *CC BY-NC-SA 4.0*
    - 4.3.3: Hard-Soft Designation of Lewis Acids and Bases - *CC BY-NC-SA 4.0*
- 5: Coordination Chemistry Introduction - *Undeclared*
  - 5.1: Ligands - *CC BY-NC-SA 4.0*
  - 5.2: Electron Configuration of Gas-Phase Metal Ions - *CC BY-NC-SA 4.0*
  - 5.3: Crystal Field Theory, d orbital splitting in presence of ligands - *CC BY-NC-SA 4.0*
  - 5.4: Crystal Field Electron Configuration - *CC BY-NC-SA 4.0*
  - 5.5: Crystal Field Stabilization Energy - *CC BY-NC-SA 4.0*
  - 5.6: Thermodynamic and Structure Consequences of d orbital splitting - *CC BY-NC-SA 4.0*
  - 5.7: Ligand Exchange Reactions and Affinity Determination - *CC BY-NC-SA 4.0*
  - 5.8: Ligand Binding Thermodynamics and the Chelate Effect - *CC BY-NC 4.0*
  - 5.9: Hard and Soft Ligands and Metal Ions - *CC BY-NC 4.0*
  - 5.10: Potential Isomers of Complex Ions - *CC BY-NC-SA 4.0*
- 6: Molecular Orbital Theory - *Undeclared*
  - 6.1: Overview of Colors from Transition Metal Ions - *CC BY 4.0*
  - 6.2: Symmetry and Symmetry Operations - *CC BY-NC-SA 4.0*
  - 6.3: Molecule Shapes (Point Groups) - *CC BY-NC-SA 4.0*
  - 6.4: Point Group Assignment - *CC BY-NC-SA 4.0*
  - 6.5: Overview of Classifying Bonding Orbitals in a Molecule - *CC BY-NC-SA 4.0*
  - 6.6: MO Diagram Construction of CO2 - *CC BY-NC-SA 4.0*
  - 6.7: MO Diagram Construction of H2O - *CC BY-NC-SA 4.0*
  - 6.8: MO Diagram Construction of NH3 - *CC BY-NC-SA 4.0*
  - 6.9: MO Construction of BF3 - *CC BY-NC-SA 4.0*
  - 6.10: Lewis Acid-Base Dative Bond and MO Diagrams - *CC BY-NC-SA 4.0*
  - 6.11: MO Diagram for bonding in [M(NH3)6]n+ - *CC BY-NC-SA 4.0*
  - 6.12: MO Diagram for bonding in [M(H2O)6]n+ - *CC BY-NC-SA 4.0*
  - 6.13: Spectrochemical Series for Ligands - *CC BY-NC-SA 4.0*
  - 6.14: Spectrochemical Series for Metal ions - *CC BY-NC-SA 4.0*
- 7: Why is Carbon Monoxide Poisonous? - *Undeclared*
  - 7.1: Pi-Acid Ligands - *CC BY-NC-SA 4.0*
  - 7.2: [Fe(CO)6]2+ MO Diagram - *CC BY-NC-SA 4.0*

- 7.3: Revisit Octahedral Metal Ion Electron Configurations - *CC BY-NC-SA 4.0*
- 7.4: Magnetic Moments for Spin State Determination - *CC BY-NC-SA 4.0*
- 7.5: LFSE/CFSE Calculations Again - *CC BY-NC-SA 4.0*
- 7.6: Spectrochemical Series of Ligands (Again) - *CC BY-NC-SA 4.0*
- 7.7: Exchange Inertness of d3, d4(LS), d5(LS), d6(LS), and d8(SQP) - *Undeclared*
- 7.8: O2 Reduction, since CO displaces O2 - *CC BY-NC-SA 4.0*
- 7.9: Bonding in Carbonmonoxy-myoglobin [Fe(CO)]2+ - *CC BY-NC-SA 4.0*
- 7.10: Active Site of Cytochrome c Oxidase - *Undeclared*
- 7.11: Cyanide is also a poison (affinity data) - *CC BY 4.0*
- 7.12: Cyanide is also a poison (spectrocopic data) - *Undeclared*

8: What Happens "Above The Arrow" in Organic Chemistry - *Undeclared*

- 8.1: Metal-Pi System Ligands (e.g. ferrocene) - *CC BY-NC-SA 4.0*
- 8.2: 18 Electron Rule - *CC BY-NC-SA 4.0*
- 8.3: Organometallic Reaction Types - *CC BY 4.0*
- 8.4: Organometallic Catalysts - *CC BY 4.0*
- 8.5: Suzuki-Miyara Coupling - *CC BY-NC-SA 4.0*

9: Why is Cisplatin "King of the Chemotherapeutic Drugs?" - *Undeclared*

- 9.1: Jahn-Teller Distortions - *Undeclared*
- 9.2: d8 Low-Spin Preference for Square Planar Geometry - *CC BY 4.0*
- 9.3: Trans Effect - *CC BY-NC 3.0*
- 9.4: Cisplatin Discovery and Mode of Action - *Undeclared*

Back Matter - *Undeclared*

- Index - *Undeclared*
- Glossary - *Undeclared*
- Detailed Licensing - *Undeclared*
- Detailed Licensing - *Undeclared*